ACTA PHYSICA

ACADEMIAE SCIENTIARUM HUNGARICAE

TOMUS XX FASCICULI 1—2

AKADÉMIAI KIADÓ, BUDAPEST

1966

ACTA PHYS. HUNG.

ACTA PHYSICA

A MAGYAR TUDOMÁNYOS AKADÉMIA FIZIKAI KÖZLEMÉNYEI

SZERKESZTŐSÉG ÉS KIADÓHIVATAL: BUDAPEST V., ALKOTMÁNY UTCA 21.

Az *Acta Physica* német, angol, francia és orosz nyelven közöl értekezéseket a fizika tárgyköréből.

Az *Acta Physica* változó terjedelmű füzetekben jelenik meg: több füzet alkot egy kötetet.

A közlésre szánt kéziratok a következő címre küldendők:

Acta Physica, Budapest 502, Postafiók 24.

Ugyanerre a címre küldendő minden szerkesztőségi és kiadóhivatali levelezés.

Az *Acta Physica* előfizetési ára kötetenként belföldre 80 forint, külföldre 110 forint. Megrendelhető a belföld számára az Akadémiai Kiadónál (Budapest V., Alkotmány utca 21. Bankszámla 05-915-111-46), a külföld számára pedig a „Kultúra" Könyv- és Hírlap Külkereskedelmi Vállalatnál (Budapest I., Fő u. 32. Bankszámla 43-790-057-181 sz.), vagy annak külföldi képviseleteinél és bizományosainál.

Die *Acta Physica* veröffentlichen Abhandlungen aus dem Bereich der Physik in deutscher, englischer, französischer und russischer Sprache.

Die *Acta Physica* erscheinen in Heften wechselnden Umfanges. Mehrere Hefte bilden einen Band.

Die zur Veröffentlichung bestimmten Manuskripte sind an folgende Adresse zu richten:

Acta Physica, Budapest 502, Postafiók 24.

An die gleiche Anschrift ist auch jede für die Redaktion und den Verlag bestimmte Korrespondenz zu senden.

Abonnementspreis pro Band: 110 Forint. Bestellbar bei dem Buch- und Zeitungs-Aussenhandels-Unternehmen »Kultúra« (Budapest I., Fő u. 32. Bankkonto Nr. 43-790-057-181) oder bei seinen Auslandsvertretungen und Kommissionären.

EFFECT OF SURFACE DAMAGE ON THE TENDENCY FOR DARKENING OF ZnS SINGLE CRYSTALS

By

P. Sviszt, P. Kovács and M. Farkas-Jahnke

RESEARCH INSTITUTE FOR TECHNICAL PHYSICS OF THE HUNGARIAN ACADEMY OF SCIENCES, BUDAPEST

(Presented by G. Szigeti — Received 13. X. 1964.)

The tendency for darkening of the mechanically abraded and polished, etched and cleaved surfaces of hexagonal ZnS single crystals has been examined simultaneously with electron diffraction studies. The obtained results showed that there is a strong connection between the quality of the crystal surface and the tendency for darkening.

1. Introduction

According to pictures published previously [1] the Zn precipitates produced during the photochemical decomposition of ZnS do not cover homogeneously the surface of the crystal. In the case of most of the crystals the Zn precipitates follow the stacking faults [2] perpendicular to the c-axis, as it was observed microscopically. In the case of a few other crystals not showing any oriented disorder and the surface of which seemed smooth before darkening, the orientation of the precipitated Zn could not be observed.

The question arises whether the orientation of the Zn remains if a layer is removed from such a crystal and the surface so obtained is irradiated. To decide this question a layer has been removed from the surface of crystals with mechanical abrading and polishing, and then they were irradiated in humid air. The study of the darkening of these crystals, however, gave surprising results: even after a 5 hours' irradiation no darkening observable with the naked eye could be seen on the abraded and polished surfaces, whereas if the surface was removed only by etching (without abrading and polishing) the darkening appeared in the same form as on the original crystals.

2. Experimental procedure

The single crystals used for our experiments have been grown from vapour phase in our laboratory [3]. They were prisms of a hexagonal structure. The length of the prisms was 5—6 mm, their diameter 3 mm. The crystals emitted the blue band characteristic for self-activated ZnS-s excited with 365 mm mercury line.

The electron diffraction study of the crystals was carried out with a 80 KV electron beam ($\lambda = 0{,}0417$ Å) in a JRM 6-A type electron microscope. Crystals were attached to the preparate-holder by a mixture of glue and silver colloide. For evaluation the patterns were compared with a transmission electron diffraction pattern of a gold foil made under the same conditions of operation.

The crystals were irradiated in humid air by a 250 W high-pressure mercury lamp fed from a stabilized source without filter. The intensity of the exciting light was approx. 100 mW/cm^2 on the crystal surface. Microphotos were taken by means of a MEF-type Reichert universal microscope.

3. Results

3.1. *Study of the darkening of mechanically abraded and polished and afterwards temperature-treated crystals*

The effect of abrading and polishing on the tendency for darkening of the crystals could be easily cleared. Single crystals suitable for polishing were available. After testing that the crystals chosen for the experiments could be darkened in a relatively short time they were abraded and polished mechanically. Abrading took place with a Naxos-type sand-cloth N° 600. Polishing after the abrading was done with SiC or Al_2O_3. In the latter case the finest fraction was used. Both methods led to the same results.

The result was that the tendency for darkening of the crystals strongly decreased after such treatment. Fig. 1*a* shows an abraded and polished crystal surface. The same surface is given in Fig. 1*b* after a 5 hours' irradiation. In this figure larger and smaller Zn islands can be observed. It must be remarked that the covering of the treated surface with such particles is not a regular phenomenon. In case of the majority of the treated crystal surfaces no or hardly any metal precipitation could be observed after a 5 hours' irradiation.

The reason why we publish the rarely occurring surface picture is that this demostrates better the change of the surface picture after the heat treatment.

Heat treatment was carried out in purified N_2 atmosphere. The time of the heat treatment varied between 30 minutes and one and a half hour at a temperature of 900° C.

Fig. 1*c* shows the same crystal surface after a 1 hour heat treatment at 900° C. In the picture it can be well observed that the surface of the crystal clears after such heat treatment, i.e. a bleaching effect takes place.*

* With this phenomenon and with other forms of the bleaching effect we intend to deal in another paper.

The surface of this heat treated crystal after 10 minutes irradiation is shown in Fig. 1*d*. It can be seen clearly that after the heat treatment the tendency for darkening was noticed after a 10 minutes' irradiation, while a 5 hours' irradiation is not sufficient to produce such darkening (see Fig. 1*b*) after abrading and polishing.

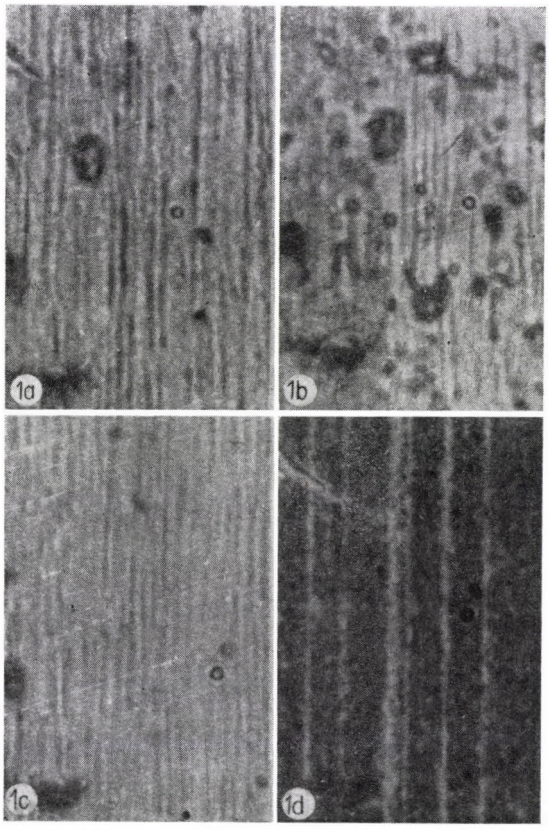

Fig. 1. Microphotograph of the surface of a ZnS single crystal (a) after abrading and polishing (b) after a 5 hours' irradiation, (c) after 1 hour's heat treatment at 900° C, (d) after 10 minutes' irradiation (128 fold magnification)

Parallel with the above experiments the electron diffraction study of the crystals took place too. The systematic examinations showed that the diffraction pattern along a crystal surface hardly changes. This seems very advantageous for the comparison of results as we were unable to make both a diffraction pattern and microscopic picture of the same part of the crystal surface because of technical reasons.

Single crystal spots and Kikuchi lines appeared on the electron diffraction pattern of untreated single crystals indicating that the chosen surfaces

were single crystal faces. Fig. 2*a* shows such a picture. After mechanical abrading and polishing the electron diffraction patterns of the same surfaces showed diffuse Debye-Scherrer rings (Fig. 2*b*). This means that the surface consists of randomly oriented crystal fragments, produced by mechanical treatment.

After a 1 hour heat treatment at 900° C the crystal surface recrystallized and very good single crystal surfaces were formed. This is proved by the appearance of single crystal reflections. An example for this is given in Fig. 2*c*. Since

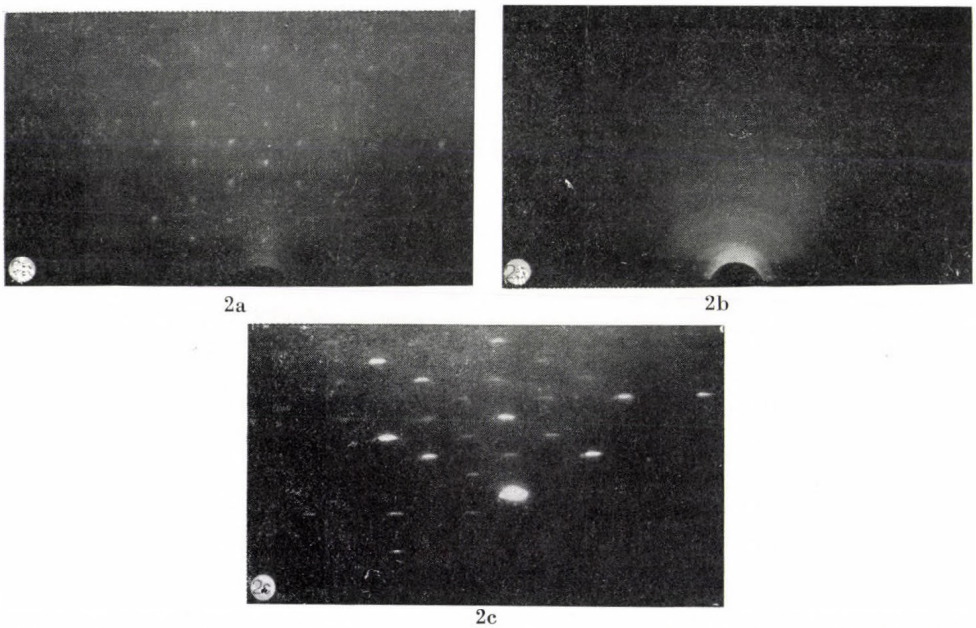

2a 2b

2c

Fig. 2. Electron diffraction pattern of the surface of a ZnS single crystal (a) before, (b) after abrading and polishing, (c) after 1 hour's heat treatment at 900° C

because of abrading and polishing the part of the lattice (directly beneath the fragmented zone) also became slightly deformed [4—5] and during recrystallization the very fine fragmented layer grew to this deformed matrix, so the recrystallized surface layer formed in the course of the heat treatment is also somewhat deformed. Consequently, the single crystal reflections are a little diffuse, too.

3.2. *Study of the darkening of crystals etched after abrading and polishing*

Fig. 3*a* shows the microscopic picture of an abraded and polished crystal surface after a 30 minutes' etching in $H_2SO_4 + H_2O_2$ solution. Irradiating the crystal surface obtained a strong darkening can be observed already after a 20 minutes' irradiation (Fig. 3*b*).

Fig. 4*a* gives the electron diffraction pattern of an abraded and polished crystal surface after etching for 10 minutes. In the photograph it can be easily observed that the single crystal reflections and in some cases even the Kikuchi lines reappear. Besides the single crystal reflections weak Debye-Scherrer rings can also be seen in the picture. This shows that the etching time in the present case was not sufficient for the total removal of the fragmented layer produced

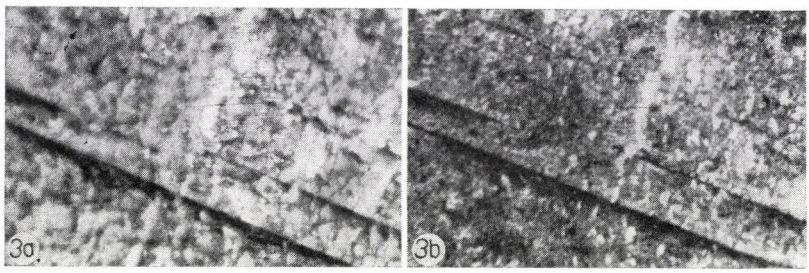

Fig. 3. Microphotograph of an abraded and polished ZnS crystal surface (a) after a 30 minutes' etching, (b) after 20 minutes' irradiation (128 fold magnification)

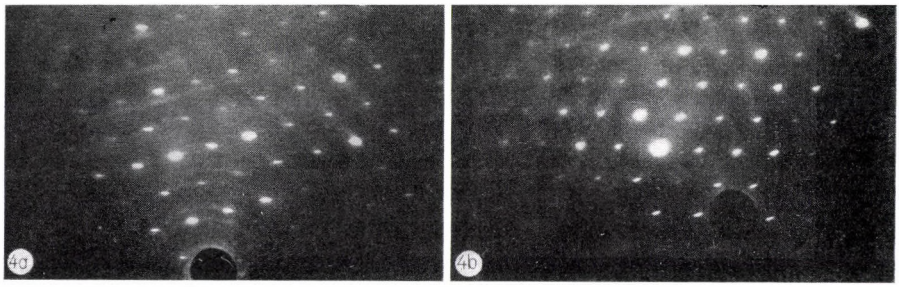

Fig. 4. Electron diffraction pattern of an abraded and polished ZnS single crystal surface (a) after 10 and (b) after 30 minutes' etching

by mechanical treatment. Increasing the time of etching (30 minutes) only single crystal reflections and Kikuchi lines appeared (Fig. 4*b*) i.e. the surface was already a fine single crystal face.

3.3. *Study of the darkening of crystal surfaces produced by cleavage*

As far as the authors know there is no literature concerning the cleavage of ZnS single crystals and the study of surfaces so obtained. This time our aim was not the study of this question either. We only endeavoured to obtain a new surface without greater damages as in the case of mechanical treatment. Hexagonal prisms were used for these experiments, too, the c-axis of which was parallel to the geometrical axis of the crystal. Cleavage took place in the plane of the c-axis. The surfaces obtained were of different qualities. Perfectly

smooth surfaces were produced as well as such on which steps could be observed. These crack steps might be caused either by stresses causing that the cleavage does not work exactly along the respective crystal planes, or by imperfections in the crystal. E.g. it is well known that when an

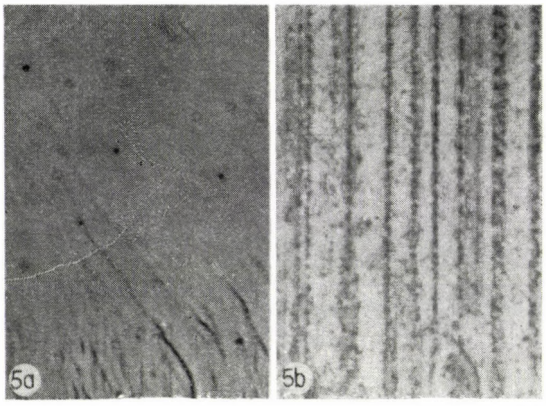

Fig. 5. Microphotograph of a cleavage surface of a ZnS single crystal (a) before irradiation, (b) after 2 minutes' irradiation (256 fold magnification)

Fig. 6. Electron diffraction pattern of a cleavage surface of a ZnS single crystal

otherwise perfect crystal contains screw dislocations intersecting the plane of cleavage a crack on passing along this plane leaves steps on the otherwise smooth cleavage surface [6].

Fig. 5*a* gives a cleavage surface of an average quality before irradiation. After a 2 minutes' irradiation the Zn precipitates are well observable. (Fig. 5*b*) A certain regularity in the position of the precipitates is remarkable. Obviously a decoration of the crystal defects is in question. [7]. In our case precipitation appeared both along the stacking faults, and the broken steps. The for-

mer are always parallel with each other, while the position of the latter relative to each other is different in each crystal.

On electron diffraction patterns of cleaved surfaces ZnS Debye-Scherrer rings were never observed. Only single crystal reflections and Kikuchi lines appeared (Fig. 6). This proves that the freshly cleaved surfaces are very good single crystal faces.

4. Discussion

It is well known that a mechanical treatment of the surface both in the case of metals and semiconductors may lead to an "amorphisation" of the surface layer, i.e. a formation of a layer consisting of extremely small crystallites [8]. As proved by our experiments, a similar layer appears on the surfaces of ZnS single crystals by mechanical treatment. ZnS single crystal faces showing good single crystal reflections in a natural state give no single crystal reflections after mechanical abrading and polishing. The upper layer of the surface is damaged. In this damaged layer there is an outer fragmented zone which consists of randomly oriented crystal fragments.

Since with the appearance of the damaged surface layer the tendency for darkening of the crystals considerably decreased, we have to suppose that the reason for this is just the "amorphisation" of the surface. If a crystal with a damaged layer was heat-treated at 900° C for an hour, i.e. the very fine fragmented outer zone was subjected to recrystallization, the tendency for darkening grew parallel with the appearance of single crystal reflections on the electron diffraction pattern. If the fragmented layer is removed by etching i.e. a new crystalline surface is produced, we again obtain the increase of the tendency for darkening. The new surface appearing by cleavage of the crystals is a very good single crystal surface. In this case no decrease of the tendency for darkening was observed.

Accordingly, the results of our experiments unambiguously led to the conclusion that there is a strong connection between the quality of the ZnS crystal surface and the tendency for darkening.

In the first place one can suppose that the reason for the strong decrease of the tendency for darkening after mechanical treatment is that after polishing abrasive particles remain embedded in the surface. It was recently established conclusively by a radiometric technique [4] that such particles are really present in lapped steel surfaces. But in our case this is not the reason for the decrease of tendency for darkening. This is also justified by the following experiment.

As was seen above (point 3.1), the tendency for darkening which existed before mechanical treatment can be practically restored by 1 hour heat treatment at 900° C. This obviously means that the causes of the decrease of the

tendency for darkening — produced during the mechanical treatment — cease to exist. If we suppose that these causes would be associated with the embedding of the abrasive particles in the surface, then these causes should act after the heat treatment, too, because at the temperature mentioned the Al_2O_3 or SiC does not evaporate from the surface. The following experiment was carried out. A very fine dispersed Al_2O_3 or SiC powder was settled on the original (untreated) as well as the abraded and polished crystal surface, respectively. The quantity of the settled material was so little that its presence was hardly detectable by electron diffraction investigations. After a 1 hour heat treatment in N_2 atmosphere at 900° C, the rings characteristic for Al_2O_3 resp. SiC could be similarly observed on the electron diffraction pattern as before. This shows that the particles settled on the surface before the heat treatment remained really on it after the heat treatment too. In such a way these cannot be responsible for the strong decrease of the tendency for darkening after polishing and the intensive increase of it after heat treatment.

GOBRECHT and KUNZ [9] noticed a slight decrease of the tendency for darkening of ZnS-Cu luminophores when milling them. Unfortunately, these authors did not make parallel structural studies. From other works [10], however, it is known that on the Debye-Scherrer diagram of milled ZnS luminophores the diffraction lines widen and their intensity decreases. At the same time background grows also. All this indicates that after milling strong inner deformations appear in the surface layers of the crystal, i.e. the first step towards the formation of the very fine fragmented surface layer has taken place. Consequently, the tendency for darkening must have decreased also, which has been observed by the authors of [9].

Naturally the above described connection between surface damage and tendency for darkening gives no ansver to the question of why the tendency for darkening decreases with damaging. Further studies are required to clarify this question.

Acknowledgement

The authors are indebted to Dr. G. SZIGETI, for his constant interest in the present work.

REFERENCES

1. P. SVISZT, phys. stat. sol., **4**, 931, 1964.
2. L. T. CHADDERTON, A. G. FITZGERALD and A. D. YOFFE, Phil. Mag., **8**, 167, 1963.
3. P. KOVÁCS and J. SZABÓ, Acta Phys. Hung., **14**, 131, 1962.
4. L. E. SAMUELS, The Surface Chemistry of Metals and Semiconductors, New York—London 1959 (p. 82).
5. T. M. BUCK, The Surface Chemistry of Metals and Semiconductors, New York—London 1959 (p. 107).

6. W. J. Dunning, Physics and Chemistry of the Organic Solid State, New York—London 1963 (p. 411).
7. P. Sviszt and P. Kovács, phys. stat. sol., **9,** K5, 1965.
8. Z. G. Pinsker, Electron Diffraction, London 1953.
9. H. Gobrecht und W. Kunz, Z. Phys., **136,** 21, 1953.
10. *В. Л. Левшин* и *Б. Д. Рыжиков,* Изв. АН СССР сер. физ., **25,** 362, 1961.

ВЛИЯНИЕ ПОВРЕЖДЕНИЯ ПОВЕРХНОСТИ МОНОКРИСТАЛЛОВ ZnS НА ИХ СКЛОННОСТЬ К ПОЧЕРНЕНИЮ

П. ШВИСТ, П. КОВАЧ и М. ФАРКАШ—ЯНКЕ

Р е з ю м е

Исследовалась склонность к почернению гексагональных монокристаллов ZnS с механически шлифованной и поливоранной, расколотой, а также травленной поверхностью. Параллельно было также произведено электроннодифракционное изучение этих поверхностей. Полученные экспериментальные результаты показывают, что имеется тесная связь между качеством поверхности кристаллов и их склонностью к почернению.

APPROXIMATE CALCULATION OF THE TUNNELING FREQUENCIES OF THE PROTON IN THE N—H . . . O HYDROGEN BOND OF THE NUCLEOTIDE BASE PAIRS

By

G. Biczó, J. Ladik

CENTRAL RESEARCH INSTITUTE FOR CHEMISTRY OF THE HUNGARIAN ACADEMY OF SCIENCES
BUDAPEST

and

J. Gergely

COMPUTING CENTRE OF THE HUNGARIAN ACADEMY OF SCIENCES, BUDAPEST

(Presented by G. Schay. — Received 10. XI. 1964)

Using the semiempirical Lippincott—Schroeder method we have calculated the potential function of a N—H . . . O and N—H . . . N hydrogen bond in the nucleotide base pairs. Substituting the obtained N—H . . . O double-well potential into the one-dimensional Schrödinger equation of the proton, we have solved it on a computer by numerical integration. The block diagram of the programme used is given in the Appendix.

With the aid of the energy levels obtained for the proton, following the suggestions of Löwdin, we have calculated the tunneling frequencies of the proton in the different levels. Further, on the basis of a classical estimation we have shown that in the electronic ground state of the system the proton is practically localized in the deeper potential well. The consequences of this fact are discussed from the point of view of the Watson—Crick—Löwdin mutation mechanism.

Introduction

In 1962 Löwdin [1] has raised the very interesting idea that those tautomeric rearrangements of the nucleotide bases which lead to point mutations take place *via* a simultaneous double proton tunneling through the potential barriers of the hydrogen bonds of the nucleotide base pairs. To obtain an estimation for the probability of this tunneling phenomenon it is necessary, as Löwdin has emphasized [1, 2], to calculate the potential function of the hydrogen bonds of the nucleotide base pairs. Namely on the basis of these potential functions, as Löwdin has pointed out [3], it is possible to determine the energy levels of the protons and with the aid of them to make an estimation about the tunneling frequencies.

As a first step in the determination of the mentioned potential functions we have calculated with the aid of the semiempirical Lippincott—Schroeder method [4, 5] the potential functions of the N—H . . .O and N—H . . .N hydrogen bonds of the nucleotide base pairs. For the N—H . . .O hydrogen bond we have solved numerically the one-dimensional Schrödinger-equation of the proton. With the aid of the obtained energy levels it was possible to calculate by numerical integration the tunneling frequencies. Finally we were able to perform a classical estimation for the probabilities to find the protons in the neighbourhood of one of the two minima of the potential function.

Method

According to LIPPINCOTT and SCHROEDER [4, 5] the potential energy function of the proton of a linear X—H . . . Y hydrogen bond can be well approximated with the aid of the expression[1]

$$V(R, r) = D_0(1 - e^{-\alpha}) - D_0^* e^{-\beta} + A\left(e^{-bR} - \frac{R_0}{2R} e^{-bR_0}\right), \tag{1}$$

where

$$\alpha = \frac{n_{(X-H)}(r - r_0)^2}{2r}, \qquad \beta = \frac{n^*(R - r - r_0)^2}{2(R - r)},$$
$$n^* = g n_{(H-Y)}, \qquad D_0^* = \frac{D_{0_{(H-Y)}}}{g}. \tag{2}$$

Here R is the actual X—Y distance and R_0 its value in equilibrium, r is the actual X—H, $r^* = R - r$ the actual H—Y distance (see Fig. 1) and r_0, r_0^* are their values in the equilibrium of the X—H, H—Y bonds, respectively, if the

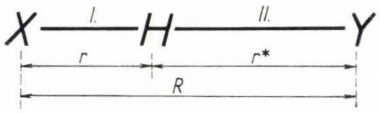

Fig. 1

atoms X and Y *do not* take part in a hydrogen bond. D_0 and $D_{0_{H-Y}}$ are the dissociation energies of the X—H and H—Y bonds, respectively. A suitable value for the universal dimensionless constant g is, according to the detailed calculations of LIPPINCOTT and SCHROEDER [4, 5], 1,45 and 4,80 $Å^{-1}$ for the universal constant b. The values of the constants $n_{(X-H)}$ and $n_{(H-Y)}$ can be determined on the basis of the ionization potentials of the atoms X and H, H and Y, respectively [4, 5].

The value of the constant A can be determined in every case on the basis of the conditions

$$\left.\frac{\partial V(R, r)}{\partial r}\right|_{\substack{r=r_e \\ R=R_0}} = 0, \tag{3}$$

$$\left.\frac{\partial V(R, r)}{\partial R}\right|_{\substack{r=r_e \\ R=R_0}} = 0, \tag{4}$$

[1] As it is easy to see from equation (1), $V(R, r) = 0$ if $r^* = R = \infty$ and $r = r_0$, i.e. atom Y is in the infinity and the proton is in the equilibrium distance of the X—H bond.

where r_e is the equilibrium value of r in the X—H . . .Y *hydrogen bond.* Substituting (1) into (3) we have solved the resulting equation for r_e by successive approximation. Using the obtained values r_e we have determined the appropriate values A for both cases with the aid of equation (4).

We have performed the calculation in both cases for $R = R_0$ and we have used for R_0 in the cases of the hydrogen bonds N—H . . .O and N—H . . .N their average values in the base pairs [6] ($R_0 = 3{,}00$ Å for N—H . . .O and 2,95 Å for N—H . . .N). All the other necessary data have been taken from another paper of SCHROEDER and LIPPINCOTT [7]: $D_{0_{(N-H)}} = 104$ kcal/mole, $D_{0_{(H-O)}} = 118$ kcal/mole, $n_{(N-H)} = 9{,}30$ Å^{-1}, $n_{(H-O)} = 9{,}07$ Å^{-1}, $r_{0_{(N-H)}} = r^*_{0_{(H-N)}} = 1{,}01$ Å, $r^*_{0_{(H-O)}} = 0{,}97$ Å. For both hydrogen bonds we have calculated the function $V(R_0, r)$ in the points [0,75 Å, (0,05 Å), 2,20 Å]. In both cases we have determined the two minima and the maximum of the potential function.

After the calculation of the potential functions we have substituted the function $V(R_0, r)_{(N-H...O)}$ into the SCHRÖDINGER equation of the proton:

$$-\frac{\hbar^2}{2M_p}\frac{d^2\Psi(r)}{dr^2} + V(R_0, r)_{(N-H...O)}\,\Psi(r) = E\Psi(r)\,, \tag{5}$$

where M_p denotes the mass of the proton. Since this equation cannot be solved analytically in the case of a potential function of type (1), we have solved it only numerically with the aid of the M 3 computer of the Computing Centre of the Hungarian Academy of Sciences. The details of this rather time-consuming calculation are given in the Appendix.

As is well known from quantum mechanics the probability of tunneling of a particle with energy ε_i and mass μ through a potential barrier is given in a good approximation by the expression

$$p_{Ti} = k\,\exp\left[-\int_{r_{2i}}^{r_{3i}} 2\sqrt{\frac{2\mu}{\hbar^2}\,(V(r) - \varepsilon_i)}\,dr\right], \tag{6}$$

where the constant k is in the order of 1 [8]. The definition of the limits of integration (r_{2_i} and r_{3_i}) can be seen in Fig. 2.

Substituting into (6) $k = 1$, $\mu = M_p$, $V(r) = V(R_0,\ r)_{(N-H...C)}$ and for the energies E of the different tunneling levels of the proton, obtained from the numerical solution of (5), we have calculated the values p_T belonging to different levels by numerical integration. Further we have calculated for each energy level of the proton the Boltzmann factors $p_{B_i} = \frac{e^{-\frac{\varepsilon_i}{kT}}}{Z}$, where Z denotes the partition function. For T we have taken $37 + 273 = 310^\circ$ K.

Since the numerical solution of equation (5) has provided only stable eigenvalues, but did not provide good eigenfunctions (see the Appendix), we cannot calculate directly from the wave functions the probabilities to find the proton in region I or II (see Fig. 2). Therefore we have made for these

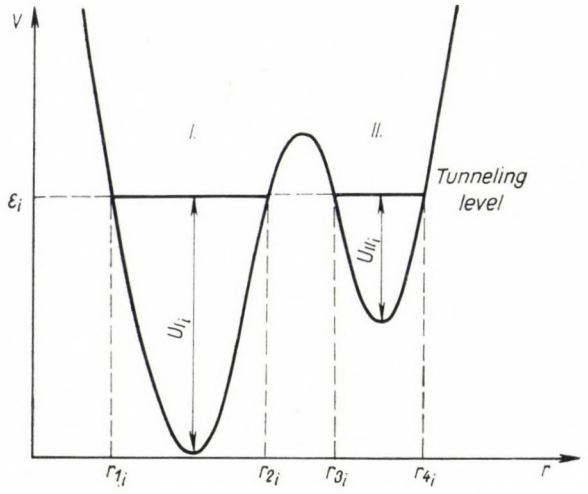

Fig. 2. Tunneling through potential barrier in a double-well potential

probabilities a classical estimation. In a first approximation the potential function in the regions I or II below a given level of the proton can be replaced by the potential function of a harmonic oscillator:

$$V_{I_i} = \frac{1}{2} k_{I_i} r^2 \qquad r_{1_i} \leqslant r \leqslant r_{2_i} ,$$

$$V_{II_i} = \frac{1}{2} k_{II_i} r^2 \qquad r_{3_i} \leqslant r \leqslant r_{4_i} . \tag{7}$$

k_{I_i} and k_{II_i} can be determined from the conditions that V_{I_i} and V_{II_i} have to pass through the points (r_{1_i}, ε_i), (r_{2_i}, ε_i), and through the points (r_{3_i}, ε_i), (r_{4_i}, ε_i), respectively, and further the depth of the potential-wells measured from ε_i is U_{I_i} and U_{II_i}, respectively (see Fig. 2). With the aid of these conditions and of the definitions $d_{I_i} = r_{2_i} - r_{1_i}$ and $d_{II_i} = r_{3_i} - r_{4_i}$ we obtain

$$k_{I_i} = \frac{8U_{I_i}}{d_{I_i}^2} \quad \text{and} \quad k_{II_i} = \frac{8U_{II_i}}{d_{II_i}^2} ,$$

respectively.

Substituting into the expression $\nu = \frac{1}{2\pi}\sqrt{\frac{k}{m}}$ of the oscillators we obtain

$$\nu_{\mathrm{I}_i} = \frac{1}{\pi}\sqrt{\frac{2U_{\mathrm{I}_i}}{md_{\mathrm{I}_i}^2}} \quad \text{and} \quad \nu_{\mathrm{II}_i} = \frac{1}{\pi}\sqrt{\frac{2U_{\mathrm{II}_i}}{md_{\mathrm{II}_i}^2}}. \tag{8}$$

With aid of the latter we can write down immediately the condition of the condition of the stationary equilibrium

$$p_{Ii}\nu_{Ii}p_{Ti}p_{Bi} = p_{IIi}\nu_{IIi}p_{Ti}p_{Bi}.$$

or

$$p_{\mathrm{I}_i} \cdot \frac{1}{\pi}\sqrt{\frac{2U_{\mathrm{I}_i}}{md_{\mathrm{I}_i}^2}} = p_{\mathrm{II}_i} \cdot \frac{1}{\pi}\sqrt{\frac{2U_{\mathrm{II}_i}}{md_{\mathrm{II}_i}^2}}, \tag{9}$$

where p_{I_i} and $p_{\mathrm{II}_i} = 1 - p_{\mathrm{I}_i}$ are the probabilities to find the proton which occupies the i-th level in region I or II, respectively. From equation (9) we obtain

$$p_{\mathrm{I}_i} = \frac{1}{1 + \frac{d_{\mathrm{II}_i}}{d_{\mathrm{I}_i}}\sqrt{\frac{U_{\mathrm{I}_i}}{U_{\mathrm{II}_i}}}}$$

and (10)

$$p_{\mathrm{II}_i} = \frac{1}{1 + \frac{d_{\mathrm{I}_i}}{d_{\mathrm{II}_i}}\sqrt{\frac{U_{\mathrm{II}_i}}{U_{\mathrm{I}_i}}}}.$$

Using the expressions (10) we have calculated p_{I_i} and p_{II_i} for all the tunneling levels of the proton in the N—H . . .O hydrogen bond. Weighting each of these probabilities with the Boltzmann factors p_{B_i} of the appropriate levels we can calculate also the overall probabilities p_{I} and p_{II} to find the proton in region I or II:

$$p_{\mathrm{I}} = \frac{\sum_i p_{\mathrm{I}_i} e^{-\frac{\varepsilon_i}{kT}}}{Z}; \qquad p_{\mathrm{II}} = \frac{\sum_i p_{\mathrm{II}_i} e^{-\frac{\varepsilon_i}{kT}}}{Z}. \tag{11}$$

Results

In Table I we give the calculated values of the potential functions $V_{\mathrm{N-H...O}}$ and $V_{\mathrm{N-H...N}}$. In Table II the extremal values of these potential functions and their positions are given.

Table I

The $V_{N-H...O}$ and $V_{N-H..N}$ potential functions

r Å	$V_{N—H...O}(3{,}00\text{ Å}, r)$ kcal/mole	$V_{N—H...N}(2{,}95\text{ Å}, r)$ kcal/mole
0,75	37,4	37,7
0,80	25,0	25,2
0,85	14,6	14,8
0,90	6,8	6,8
0,95	1,7	1,5
1,00	−0,8	−1,2
1,05	−1,1	−1,7
1,10	0,7	−0,2
1,15	3,8	2,6
1,20	8,0	6,3
1,25	12,7	10,5
1,30	17,6	14,8
1,35	22,2	18,8
1,40	26,2	22,2
1,45	29,5	24,8
1,50	31,8	26,5
1,55	33,0	27,3
1,60	33,1	27,0
1,65	32,0	26,0
1,70	29,9	24,4
1,75	27,0	22,5
1,80	23,6	20,7
1,85	20,0	19,6
1,90	16,8	19,8
1,95	14,5	21,7
2,00	13,8	25,7
2,05	15,3	32,0
2,10	19,4	48,2
2,15	26,4	51,0
2,20	36,1	62,5

Table III summarizes the energy levels of the proton in the N—H . . .O hydrogen bond. The Table contains also the Boltzmann factors p_{B_i}, the tunneling probabilities p_{T_i}, the oscillator frequencies ν_{I_i} approximated by the expression (8) and the probabilities p_{I_i} defined by equation (10). In the last two columns of the Table we find the tunneling frequencies $\nu_{T_i} = \nu_{I_i} p_{T_i} p_{I_i} =$

Table II

The extremal values of the $V_{N-H...O}$ and $V_{N-H...N}$ potential functions

r Å	Min 1,029	Max 1,578	Min 1,993
$V_{N-H...O}$(3,00 Å, r) kcal/mole	−1,226	33,172	13,777
r Å	Min 1,036	Max 1,563	Min 1,871
$V_{N-H...N}$(2,95 Å, r) kcal/mole	−1,738	27,284	19,546

$= \nu_{II_i} p_{T_i} p_{II_i}$, which give how many times a proton in the i-th level crosses the potential barrier in unit time and finally the physically most significant quantities $\nu_{T_i} p_{B_i}$.

Table III

The energy levels of the proton in the N—H . . . O hydrogen bond and the characteristic probabilities and frequencies of the different levels

i	ε_i kcal/mole	p_{B_i}	p_{T_i}	ν_{I_i} sec^{-1}	p_{I_i}	ν_{T_i} sec^{-1}	$\nu_{T_i} p_{B_i}$ sec^{-1}
0	2,163	1,0	0	$9{,}22 \cdot 10^{13}$	1	0	0
1	11,568	$2{,}3 \cdot 10^{-7}$	0	$8{,}84 \cdot 10^{13}$	1	0	0
2	18,045	$6{,}3 \cdot 10^{-12}$	$1{,}8 \cdot 10^{-7}$	$8{,}56 \cdot 10^{13}$	0,521	$7{,}4 \cdot 10^{6}$	$4{,}7 \cdot 10^{-3}$
3	19,430	$6{,}7 \cdot 10^{-13}$	$8{,}8 \cdot 10^{-7}$	$8{,}46 \cdot 10^{13}$	0,516	$3{,}6 \cdot 10^{7}$	$2{,}4 \cdot 10^{-5}$
4	26,028	$1{,}5 \cdot 10^{-17}$	$9{,}3 \cdot 10^{-4}$	$7{,}99 \cdot 10^{13}$	0,515	$3{,}6 \cdot 10^{10}$	$5{,}4 \cdot 10^{-7}$
5	26,553	$6{,}3 \cdot 10^{-18}$	$1{,}6 \cdot 10^{-3}$	$7{,}91 \cdot 10^{13}$	0,515	$6{,}1 \cdot 10^{10}$	$3{,}8 \cdot 10^{-7}$
6	32,019	$8{,}8 \cdot 10^{-22}$	$3{,}4 \cdot 10^{-1}$	$7{,}21 \cdot 10^{13}$	0,511	$1{,}2 \cdot 10^{13}$	$1{,}1 \cdot 10^{-8}$
7	33,167	$1{,}4 \cdot 10^{-22}$	$9{,}9 \cdot 10^{-1}$	$6{,}62 \cdot 10^{13}$	0,501	$3{,}3 \cdot 10^{13}$	$4{,}6 \cdot 10^{-9}$

In Fig. 3 we show the calculated N—H . . .O potential function with the energy levels of the proton. The number at the left side of each level gives the quantities $\nu_{T_i} p_{B_i}$.

We have found for the overall probabilities p_I and p_{II}, which are defined by equations (11), the values $p_I = 1{,}0$ and $p_{II} = 3{,}4 \cdot 10^{-12}$. Finally, it was interesting to calculate the wave length of radiation which is necessary to excite the proton from the ground state (ε_0) to the first tunneling level (ε_2). We have obtained $\lambda = 1{,}8\ \mu$ which falls in the near infrared region.

Comparing the potential functions obtained for the N—H . . .O and N—H . . .N hydrogen bonds (Table I and II) we can see that while the deeper potential wells of the functions are rather similar, there are large differences in the functions in the region of the potential barrier and of the more shallow well. Namely the N—H . . .N function has a smaller barrier and a more shallow second well than the N—H . . .O function. This can be seen, if we take into account that the O atom is more electronegative than the N atom.

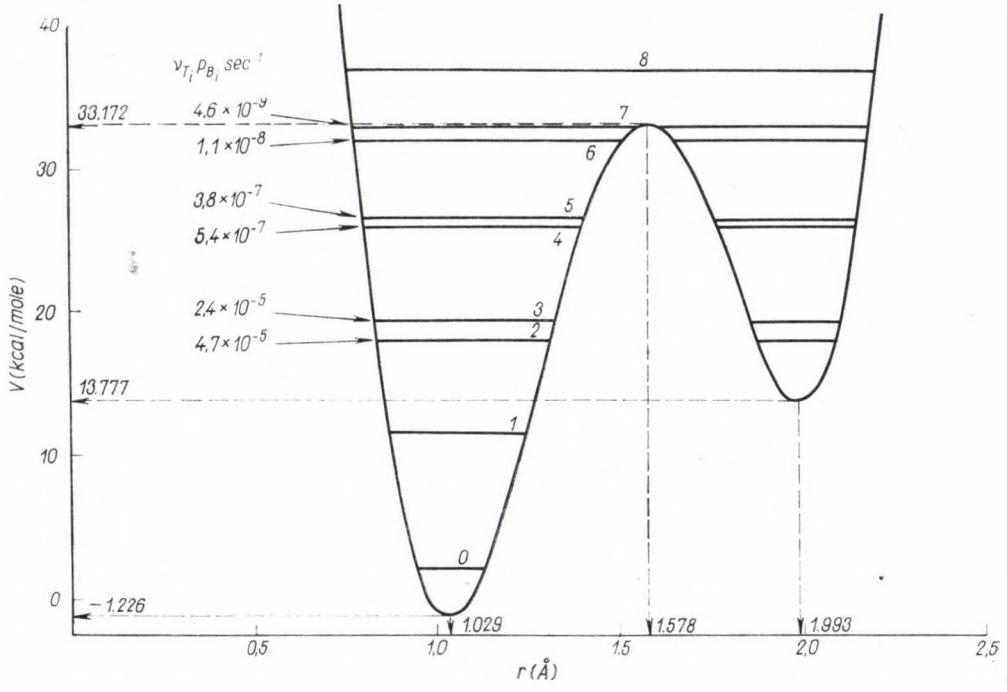

Fig. 3. The potential function of the N—H . . . O hydrogen bond of the nucleotide base pairs and the energy levels of the proton

Discussion

Coming now to Table III we can see that the energy levels of the proton ε_i are placed at a distance of 6—9 kcal/mole from each other until we are below the minimum of the more shallow potential well. Above this we find a splitting of the levels. The two components of these doublets are only 0,5—1,4 kcal/mole far from each other.

The Boltzmann factors p_{B_i} calculated for 37° C show that at this temperature there is a very small probability to have a proton in a state other than the ground state. The tunneling probabilities p_{T_i} increase at the same time in going from the first tunneling level (level 2) to the 7th level, which is very near

to the top of the potential barrier. The oscillator frequencies ν_{I_i} and the probabilities p_{I_i} differ only very slightly in the different levels. Therefore the tunneling frequencies $\nu_{T_i} = p_{I_i}\, \nu_{I_i}\, p_{T_i}$ increase practically in the same measure as the tunneling probabilities p_{T_i} if we are going from the deeper levels to the higher ones. We can see from their values (values between $\sim 10^6$ and $\sim 10^{13}$ sec^{-1}) that if the proton is excited by some means (for instance infrared radiation in the μ wave length region), there will be a rapid oscillation of the proton between the two regions of the double-well potential and the proton can be found approximately with the same probability in the two regions (the values p_{I_i} vary in the tunneling levels between 0,52—0,50).

If the proton can be excited only by the effect of the temperature, however, the Boltzmann factors p_{B_i} become decisive and owing to their exceedingly small values the proton practically will be localized in the deeper well ($p_I = 1{,}0$). Therefore the values $\nu_{T_i}\, p_{B_i}$, i.e. the numbers showing how many times during 1 sec a proton will cross the potential barrier, if it can be excited only by T to a tunneling level, are very small: $\sim 10^{-5}$ sec^{-1}—$\sim 10^{-9}$ sec^{-1}.

We may expect qualitatively the same situation also in the case of the N—H . . .N hydrogen bond. The values ν_{I_i} and p_{I_i} will be in all probability very similar to those found in the N—H . . .O case. Since, however, now the second potential-well is more shallow, we will find tunneling levels higher than in the N—H . . .O case. As a consequence of this and of the fact that the barrier is now smaller the probabilities p_{T_i} and with them the tunneling frequencies ν_{T_i} will now be larger than in the deepest tunneling level of the N—H . . .O hydrogen bond. Because of the Boltzmann factors, however, which are also in all probability very small, we can expect again that the proton, unless it is not excited by radiation or by other means, is localized in the deeper well.

We have to call again attention, however, to the fact as LÖWDIN [3] has pointed out that the shape of the double-well potential function is extremely important from the point of view of all these considerations. A somewhat better approximation of the potential of the N—H . . .N hydrogen bond of the G—C base pair which takes into account also the π electron distribution of this nucleotide base pair has yielded a still more asymmetric double-well potential in the ground electronic state, but the potential function has become rather symmetric in the first excited electronic state of the π electron system [9]. This means that in the excited state there is a much greater probability to find the proton in both regions.

It should be further mentioned that recently independently of our calculations REIN and HARRIS [9a] have calculated the potential function of the same hydrogen bond taking into account the change of the π electron distribution of the base pair and of the 4σ electrons of the hydrogen bond with the position of the proton. Equating the total electronic energy of the system with

the potential energy of the proton they have obtained a less asymmetric double-well potential than we in our previously mentioned [9] approximation. Extending their calculations also to the positive and negative ionized states and to the first excited state, they have calculated the equilibrium constants of the tautomeric rearrangement of the base pair [9b]. Their results show an overall picture similar to ours.

The approximation of the double-well potential should be further improved until it will be possible to arrive at definite tunneling frequencies. Anyway, the qualitative conclusion can be drawn that in the ground electronic state of a base pair, if the proton is also in the ground state, there is a very small probability for the tunneling phenomena. If, however, the electronic system of the base pair is excited or ionized [1, 2], or the proton is excited, there can occur rather large probabilities for the tunneling.

Acknowledgement

We should like to express our gratitude to Professor P.-O. LÖWDIN, who has inspired this work, for many valuable and fruitful discussions and one of us (J. LADIK) for giving him the opportunity to work at different periods in the stimulating atmosphere of his Group. We are further indebted to Mrs. J. GYÜRÜSI for performing some parts of the numerical work on the computer and to Miss A. JESZENÁK for the tedious desk calculations.

Appendix

In the course of the numerical solution of the SCHRÖDINGER equation (5) of the proton the potential function (1) has been used with the appropriate numerical constants of the N—H . . .O hydrogen bond. In atomic units we can write equation (5) in the form

$$\frac{d^2\psi}{dr^2} + 3672\,[E - V(r)]\psi(r) = 0 \tag{A.1}$$

with the function $V(r)$

$$V(r) = C_1 - C_2\left(e^{-\frac{C_3(r-C_4)^2}{r}} + \frac{e^{-\frac{C_5(r-C_6)^2}{C_7-r}}}{C_8}\right), \tag{A.2}$$

where the values of the constants $C_1, \ldots, C_8$ were given numerically. This potential function is, however, because of physical reasons not valid in the neighbourhood of $r = 0$ and $r = C_7 = R_0$. Namely $V(r) \to \infty$, if $r \to 0$ or $r \to R_0$. Since the function (A.2) is equal in the intervals $0 < r < a$ and

$R_0 - a < r < R_0$ in a good approximation to the constant C_1, if we choose the value 0,4 a.u. for a, we have taken in these intervals for $V(r)$ the constant C_1. This is permissible because, according to similar calculations which can be found in the literature [11], the value of the potential can be changed essentially (for instance increased) at the boundaries of the interval without causing significant changes in the eigenvalues.

The task of our calculation was to determine the eigenvalues E_j, i.e. those values E for which $\psi(r)$ satisfies equation (A. 1) in the whole interval $0 < r < R_0$ and fulfils the boundary conditions

$$\psi(0) = \psi(R_0) = 0 \tag{A.3}$$

and the normalization condition

$$\int_0^{R_0} |\psi(r)|^2 \, dr = 1 \,, \tag{A.4}$$

The different wave functions ψ_j which belong to the different eigenvalues E_j are eigenfunctions of equation (A.1).

For the numerical integration of equation (A.1) we have used the RUNGE-KUTTA-MERSON method (see for instance [10]). We have used as starting values

$$\psi(0) = 0 \qquad \text{and} \qquad \left.\frac{d\psi}{dr}\right|_{r=0} = C = 2^{-30}. \tag{A.5}$$

It should be mentioned that for a given value E the solutions obtained for the interval $0 < r < R_0$ are proportional to C, and they will be continuous functions of E.

Let us denote by $Y(E)$ the value of the function $\psi(r)$ obtained for $r = R_0$ for a given value of E and C,

$$Y(E) = \psi(R_0) \,|_{E\,C} \,. \tag{A.6}$$

$Y(E)$ will be of course also a continuous function of E. Our task taken can be reformulated: we have to determine the roots E_j of the equation $Y(E) = 0$, since by the second part of equation (A.3) holds

$$Y(E_j) = 0 \,. \tag{A.7}$$

By the use of the RUNGE-KUTTA-MERSON method we have divided the interval $(0, R_0)$ into 64 parts $\left(R = \frac{R_0}{64}\right)$. In the case of the third eigenvalue

we have used also $R = \frac{R_0}{128}$. We have found deviation between the eigenvalues obtained with the two different values h only in the fifth significant decimal. Similarly we have found that the substitution of C_1 by $4C_1$ for the potential function in the intervals $0 < r < a$ and $R_0 - a < r < R_0$ changes again only the fifth significant decimal of the third eigenvalue. We have performed the integration of the differential equation (A.1) also in the opposite direction (more strictly speaking we have transformed the function $V(r)$ by the transformation $\xi = R_0 - r$. The eigenvalues obtained in this way differ again only in the fifth significant decimals.

Also, according to other much more detailed investigations performed for single-well potential functions [11], we can expect similar stability of the eigenvalues. Therefore in the present case we have not repeated the mentioned investigations in full detail. Further, following LÖWDIN [12] we can estimate the distance between the two lowest energy levels in the harmonic oscillator approximation. In this way we obtain the value of 11 kcal/mole which agrees well with the value of 9,40 kcal/mole obtained from our present calculations. We intend to reinvestigate the problem in a subsequent paper in which we intend to compare the eigenvalues obtained starting from the boundary of the interval with those obtained starting from inside of the interval.

In the calculation we have used a floating point programme, which has worked with a mantissa of 24 bits (7 decimals) and with an exponent of 6 bits (in linear system). The latter corresponds to the orders of magnitude 10^{-9}—-10^{+9}.

It has caused rather serious difficulties that the values of the functions $\psi(r)$ in the interval $0 \leqslant r \leqslant R_0$ differ from each other by many orders of magnitude and they may be multiples of the large permissible number with which the programme is able to work. Therefore in some points of this interval we have divided the functions $\psi(r)$ and $\frac{d\psi}{dr}$ by appropriate constants. (This can be done because equation (A.1) is a homogeneous linear differential equation.)

We have found in some cases for the functions $\psi(R_0, E) \equiv Y(E)$ values as large as 10^{30}. Therefore to find the roots E_j of the equation $Y(E) = 0$, we have linearly interpolated between the positive and negative values of $Y(E)$ in the neighbourhood of the roots. Since we intended to determine the eigenvalues E_j only with a precision of $\varepsilon = 2^{-24} \approx 10^{-7}$, we have continued the successive interpolation only until such positive and negative values $Y(E)$ were found between which the interpolation yielded values E_j in seven decimals.

Since, however, the function $Y(E)$ is an extremely sensitive function of E the values of this function may differ considerably from zero also in the

neighbourhood of the eigenvalues. In some cases they have values $Y(E_j^*) \approx$ $\approx 10^{20}$, where E_j^* is the j-th eigenvalue determined up to 7 decimals. Therefore we were not able to obtain from this calculation reliable eigenfunctions ψ_j.

In Fig. 4 we give a block diagram of the calculation.

Using the programme described we have determined 9 eigenvalues in the energy region mentioned. To be able to obtain reliable eigenfunctions it

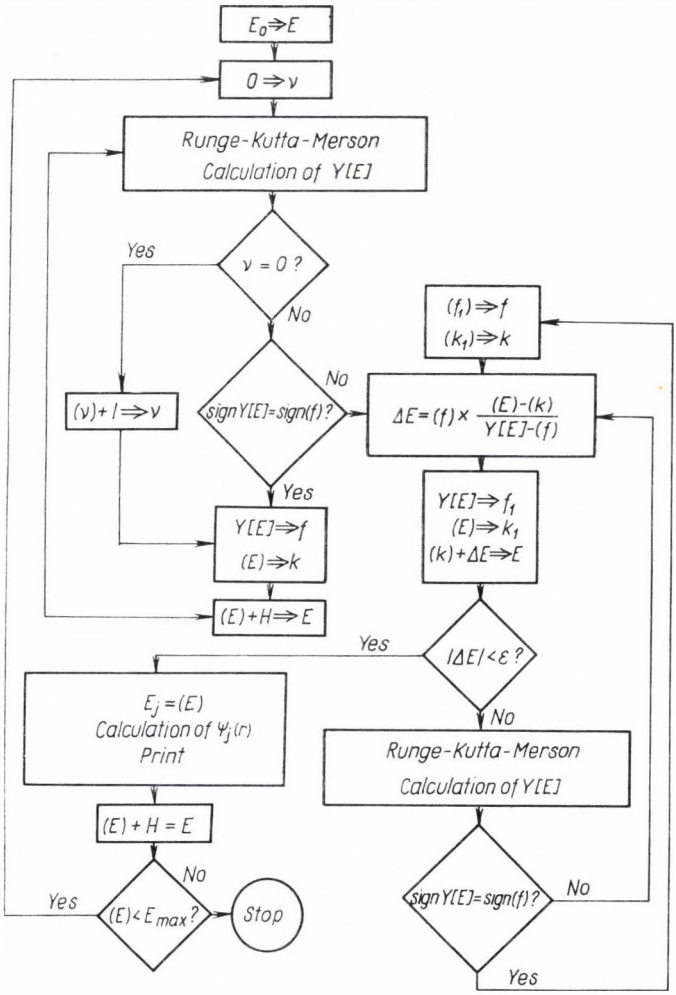

Fig. 4. The block diagram of the numerical integration of the one-dimensional SCHRÖDINGER equation of the proton. E_0 and E_{max}, respectively, mean the limits of the investigated energy region ($E_0 = -1{,}226$ kcal/mole, $E_{max} = 37{,}000$ kcal/mole), H is the length of the energy interval used in the calculation of the function $Y(E)$. The parameter ν may have only the values 0 or 1. $\nu = 0$ for the first calculation of a $Y(E)$ and it has the value $\nu = 1$ for all the subsequent calculations of $Y(E)$ in the neighbourhood of a given eigenvalue. When used the symbol $\Rightarrow$ at the left hand side stands always for a number and at the right hand side for the title of a memory cell. The symbol (k) means, as usual, the content of the cell with title k

would be necessary to use a floating point programme which includes a mantissa with 12—15 decimals and an exponent which gives orders of magnitudes between 10^{-50}—10^{+50}. Since floating point computers with such a word length are not available, this task can be done in all probability only with a floating point programme which uses double word length (one number is placed into two memory cells).

REFERENCES

1. P.-O. Löwdin, Preprint 85, Quantum Chemistry Group, Uppsala University, 1962. P.-O. Löwdin, Rev. Mod. Phys., **35,** 724, 1963.
2. P.-O. Löwdin, Biopolymers, Symposia N° 1, 161, 1964.
3. P.-O. Löwdin, Lectures at the Uppsala Quantum Chemistry Group, 1963.
4. E. R. Lippincott and R. Schroeder, J. Chem. Phys., **23,** 1099, 1955.
5. E. R. Lippincott and R. Schroeder, Hydrogen Bonding, ed. J. Hadzi, Pergamon Press, Oxford, 1959, 361.
6. M. Spencer, Acta Cryst., **12,** 66, 1959.
7. R. Schroeder and E. R. Lippincott, J. Phys. Chem., **61,** 921, 1957.
8. G. Gamow and C. L. Critchfield, Theory of Atomic Nucleus and Nuclear Energy-Sources, Clarendon Press, Oxford, 1949, 162.
9. J. Ladik, Preprint Q. B. 8, Quantum Chemistry Group, Uppsala University, 1963.
9a. R. Rein and F. Harris, J. Chem. Phys., **41,** 3825, 1964.
9b. R. Rein and F. Harris, Science, **146,** 3644, 1964.
10. W. E. Milne, Numerical Solution of Differential Equations, John Wiley Inc., New York, 1957.
11. C. L. Beckel, J. Nakhlen, and I. R. Chowdary, J. Chem. Phys., **40,** 139, 1964.
12. P.-O. Löwdin, Electronic Aspects of Biochemistry, ed. B. Pullmann, Academic Press, New York—London, 1964. 167.

ПРИБЛИЖЕННОЕ ОПРЕДЕЛЕНИЕ ТУННЕЛЬНЫХ ЧАСТОТ ПРОТОНОВ, УЧАСТВУЮЩИХ В ВОДОРОДНОЙ СВЯЗИ N—H . . . O НУКЛЕОТИДНЫХ БАЗИСНЫХ ПАР

Г. БИЦО, Я. ЛАДИК, и Й. ГЕРГЕЛЬ

Р е з ю м е

На основе полуэмпирического метода Липпинкотта—Шредера определяются потенциальные функции водородной связи N—H . . . O и N—H . . . N нуклеотидных базисных пар. Полученный потенциал N—H . . . O с двумя минимумами замещается в одномерное уравнение Шредингера для протона, которое решается численным интегрированием на вычислительной машине.

При помощи вычисленных энергетических уровней протонов, следуя за предложениями Лэвдина, определяются туннельные частоты протонов на отдельных уровнях. Далее, классической оценкой показывается, что электронное основное состояние системы в случае, когда и протон находится в основном состоянии, практически полностью локализуется в окрестности более глубокой потенциальной ямы. Следствия данного факта истолкуются с точки зрения мутационного механизма Уатсона—Крика—Левдина.

ON THE EXAMINATION OF THE HEAT CONDUCTION PHENOMENA OF LOW-PRESSURE GASES

By

G. LAKATOS* and J. BITÓ

INDUSTRIAL RESEARCH INSTITUTE FOR TELECOMMUNICATION TECHNIQUE, BUDAPEST

(Presented by G. Szigeti — Received 26. XI. 1964.)

The authors determine the energy trasferred by heat condution from the cathode of low-pressure gas discharge. They indicate for various gases under given discharge conditions the quantity of energy transmitted from the unit surface area of the cathode by heat conduction of the gas.

1. Introduction

As is well known, the most important result of kinetic gas theory was that the pressure-independence of the internal friction of gases could be demonstrated by its application. At the same time the theory also gave valuable data on the relationships between heat conduction-, diffusion- and internal friction coefficients.

It could be shown that the heat conduction coefficient λ is only the function of the internal friction coefficient η, of the specific heat at constant pressure c_p and of the specific heat at a constant volume c_v, but is independent of the pressure [1]:

$$\lambda = \eta \cdot c_v \,, \tag{1}$$

or considering more exactly the heat transport of the molecules:

$$\lambda = \varepsilon \cdot \eta \cdot c_v, \tag{2}$$

where

$$\varepsilon = \frac{9\gamma - 5}{4} \tag{3}$$

and

$$\gamma = c_p/c_v, \tag{4}$$

generally

$$1 \leq \varepsilon \leq 2{,}5 \,. \tag{5}$$

* At present at the Research Institute for the Electrical Industry.

Later it was established [2] that this holds only if the pressure is higher than that necessary to produce molecular flow. For this reason relationship (1) in practice is only approximately valid [2]. The measurements effectuated until now show that in the domain below 20 mmHg pressure the heat conduction coefficient of gases in general decreases linearly and clearly as a function of the pressure.

The heat conduction phenomena relating to this pressure domain were theoretically deduced in two different ways. KNUDSEN [3] calculated on the basis of the energy transmission mechanism of some molecules impacting against the hot surface, while SMOLUCHOWSKI [4] composed his theory by the application of the idea of the leap of temperature, or that of the "slide-phenomenon" analogous to it. Also, LANGMUIR [5] suggested a method of calculation in case of low pressures, supported by the so-called "layer-theory".

In the course of the following calculation the relationship due to DUSHMAN [6] which clearly describes heat conduction phenomena of low-pressure gases is applied, where the heat energy W transferred is given by the relation

$$W = \frac{2\pi \cdot a \cdot l \cdot \lambda_t \cdot \Delta T}{a \cdot ln[r/a]}, \tag{6}$$

W being the heat energy transferred (watt),
l the length of the hot wire (cm),
a the diameter of the hot wire (cm),
ΔT the arising temperature difference (°C),
λ_t the heat conduction coefficient of the gas ($W \cdot \mathrm{cm}^{-1}\ \mathrm{degree}^{-1}$),
$r\gamma$ the internal radius of the discharge tube (cm).

The value of the heat conduction coefficient λ_t can be given for each gas by averaging, starting from the heat conduction coefficient of the gas in question measured at 0° C and 760 mmHg. The temperature dependence of λ_t, e.g. for argon gas is given by relation (6)

$$\lambda_t = 1{,}470 \cdot 10^{-5} \frac{T^{1/2}}{1 + \frac{142}{T}}, \tag{7}$$

where T is the measured temperature in °C.

2. Conditions of examination and results

If the above relationships are known the heat conduction coefficients of the various gases can be given for the pressure domain within 2—3 mmHg examined here and for the temperature in question.

The use of the calculation methods described above enable a determination of the heat conduction energy losses occurring at the low-pressure gas discharge tube-cathodes. This is of fundamental importance in the establishment of the energy balance of the cathodes. Namely, in determining the energy balance of the cathodes three considerable possibilities of energy-losses have to be considered: the processes of heat conduction, those of radiation and the heat transport by electron emission (7). When examining heat conduction phenomena, the heat conduction processes occurring in the gas of the discharge count are most important, while the heat quantity conducted by the metallic electrodes and glass surfaces are generally comparatively negligible.

In order to be able to take into account the appropriate temperature distribution also, when indicating the heat conduction energy losses occurring in gases, the calculations are to be made by means of the integrated average of relation (7), where the integration comprises the complete range or the fall in temperature.

Relation (7) can be expressed in the form of

$$\lambda_t = 1{,}470 \cdot 10^{-5} \frac{T^{3/2}}{142 + T}, \tag{8}$$

from which the required integrated average λ is:

$$\lambda = \frac{1{,}470 \cdot 10^{-5}}{T_2 - T_1} \left[2/3\, T^{3/2} - 2 \cdot 142 \cdot T^{1/2} + 2(142)^{3/2} \cdot \tanh \left(\frac{T}{142} \right)^{1/2} \right]_{T_1}^{T_2}, \tag{9}$$

where T_1 is the lower limit of the temperature difference zone (°C), T_2 the upper limit of the temperature difference zone (°C).

The calculations were made for argon at 3 mmHg, argon at 2,75 mmHg, neon at 1,94 mmHg and for a mixture of 20% argon and 80% neon at 2,00 mmHg. In this period a local glow-discharge takes place between the two metallic electrodes. During the glow-period the measurement of the temperature of the cathodes of the argon-filled discharge tubes ranged from 930 to 980°C, depending on the extent of the load current and the cathode coil. The observed cathode temperature of the discharge tube filled with pure neon was 1250°C during the glow-period.

The heat conduction coefficients varied between the magnitudes of 10^{-4} to 10^{-5} watt/cm °C and, according to expectations, the heat conduction coefficient of neon was about one order of magnitude higher than that of argon. This points to the fact that the employment of neon is advisable when relatively greater heat quantities have to be transferred by heat conduction.

Substituting the values of the heat conduction coefficients obtained into relation (6), the quantity of energy transferred from the cathode by heat con-

duction can be determined. This was the aim of the experiment. The transferred energy quantities relative to the unit surface of the cathodes obtained are indicated in Table 1.

Table 1

	a	*b*	*c*	*d*
Gas filling	argon	argon	neon	argon 20% + neon 80%
Pressure (mmHg)	3,00	2,75	1,94	2,00
Glow current (mA)	460	670	840	760
Glow performance (W)	4,0	6,6	12,4	9,0
Energy transferred by heat conduction (W/cm^2)	3,46	3,80	18,15	12,00

As can be seen from Table 1, the energy transferred by heat conduction is the highest for gas discharge tubes filled with pure neon, as expected. When evaluating the data of Table 1 it should be remembered that the cathodes of the tubes of type *a*, were not identical with those of the tubes of types *b*, *c*, and *d* either in size or surface area. The cathodes of types *b*, *c*, and *d* were of similar construction.

Applying the calculations explained above, the authors determined the energy balance of the respective cathodes under different discharge conditions, during the glow period [7]. The results obtained agreed well with the data found in another way and with those published in the literature. The agreement of the data obtained otherwise with those obtained as above is shown in Table 2.

Table 2

	a	*b*	*c*	*d*
Gas filling	argon	argon	neon	argon 20% + neon 80%
Pressure (mmHg)	3,00	2,75	1,94	2,00
Energy leaving by heat conduction (W/cm^2), calculated in the manner described here	3,46	3,80	18,15	12,00
Energy transported by heat conduction (W/cm^2), calculated from the energy-balance	3,90	4,05	19,00	12,7

REFERENCES

1. A. Eucken, Physik. Z., **14,** 324, 1913.
2. B. C. Dickins, Proc. Roy. Soc. London, **A 143,** 417, 1934.
3. M. Knudsen, Ann. Phys., **31,** 205, 1910.
4. M. von Smoluchowski, Ann. Phys., **35,** 983, 1911.
5. I. Langmuir, Phys. Rev., **34,** 401, 1912.
6. S. Dushman, Scientific Foundation of Vacuum Technique, John Wiley, New York, 1949.
7. G. Lakatos and J. Bitó, Acta Technica, 1964. In the press.

ОБ ИССЛЕДОВАНИИ ЯВЛЕНИЙ ТЕПЛОПРОВОДНОСТИ ГАЗОВ ПРИ НИЗКОМ ДАВЛЕНИИ

ДЬ. ЛАКАТОШ и Я. БИТО

Р е з ю м е

Авторами определяется энергия, уносимая от катода газового разряда при низком давлении теплопроводностью. Вычисляется отданное единицей площади катода количество энергии, обусловленное теплопроводностью газа, в случае разных газов при тех же условиях разряда.

STACKING FAULTS IN HEXAGONAL ZnS RODS AND NEEDLES

By

E. LENDVAY and P. KOVÁCS

RESEARCH INSTITUTE FOR TECHNICAL PHYSICS OF THE HUNGARIAN ACADEMY OF SCIENCES, BUDAPEST

(Presented by G. Szigeti. — Received 18. XII. 1964)

The present paper deals with the investigation of stacking faults in hexagonal ZnS rods and needles. Some possible models are presented for dislocations in wurtzite lattice and the formation of certain crystal-regions without striations and birefrigence bands. The description of the macro- and microlamellar structure in ZnS, appearing in the direction perpendicular to the c-axis is given.

1. Introduction

Interest in ZnS crystals is centred mainly on their luminescent and photoconductive properties. Nowadays both microcrystalline ZnS and single crystals are studied, but it must be noted that the basic research has shifted from microcrystals to that of single crystals of ZnS. This is in close connection with the fact that part of the phenomena appearing in ZnS, — especially electroluminescence — show a strong anisotropy in different crystallographical directions.

Natural cubic (F 43 m) and hexagonal (C 5 mc) ZnS crystals are generally almost perfect structurally but they often contain impurities in rather high concentration, (appr. 5—10%) so that the luminescent and semiconductive properties of the material are completely killed. Several methods have been described for the preparation of artificial ZnS crystals (see e.g. [1, 2]). The chemical purity of these synthetic crystals is generally sufficient but their structural qualities are worse than those of natural crystals. The synthetic crystals often have a polytype character containing a mixture of three-layer (cubic) and two-layer (hexagonal) modifications.

The study of the structure "purity" of ZnS crystals in luminescent research is as important as that of chemical purity. A number of phenomena indicates that besides point defects other imperfections have also a decisive role especially in electroluminescence. One of these phenomena is the (1010)-oriented lighting lines on the basal plane of ZnS rods [3, 4]. A similar localized character appears in the photovoltage and photoconduction effects, etc.

In this paper we shall deal with the stacking faults in hexagonal rods and needles. They are the most common type of faults in ZnS, therefore they have a decisive role in the physical properties of the material.

2. Stacking faults in ZnS rods and needles

The crystals examined were prepared in our laboratory. Some remarks in connection with this work are already discussed in a previous paper [5]. In [5] the question of flux has already been mentioned. Very good results were obtained with $SrCl_2$, but a great quantity of Sr was built into the ZnS lattice. The study of electroluminescence requires high purity, therefore we use HCl as flux at present. With this method we succeeded to produce rather pure crystals of sufficient size emitting the blue band characteristic of selfactivated ZnS excited with the 365 nm Hg line.

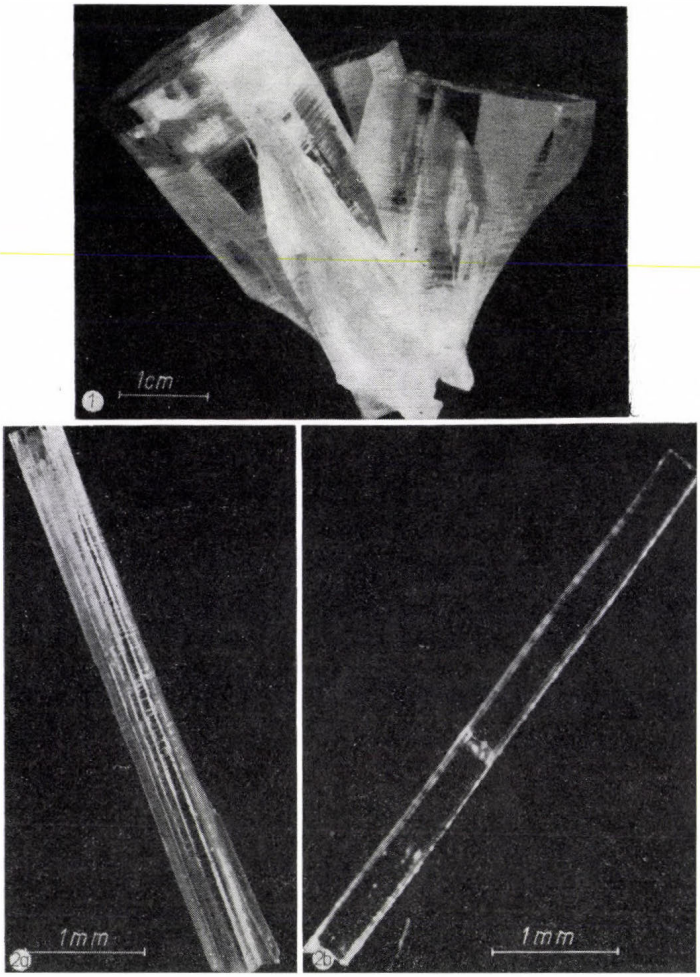

Fig. 1. Adjacently developed hexagonal ZnS rods. The crystals have nearly perfect basal planes

Fig. 2. Birefringence bands on habit faces of ZnS needles in polarized light. a — crystal with high band density, b — needle with only few birefringence bands

These crystals generally show strong birefringence bands in polarized light. In some cases these bands can be observed along the whole crystal (e.g. in case of thick rods) in other cases they can be found only in a certain region of crystals. On the prism-faces of the thick rods (see e.g. Fig. 1) there are often macroscopic glide effects that can be observed by the naked eye. For needles the phenomenon usually can be seen well only in polarized light and crystals containing only a few birefrigence bands are very rare. Fig. 2 shows two needles, on one of them very few optical disorders can be seen. The other needle shows the usual inhomogeneous behaviour in polarized light. It can be observed by interferometric methods that the latter crystal has crystal

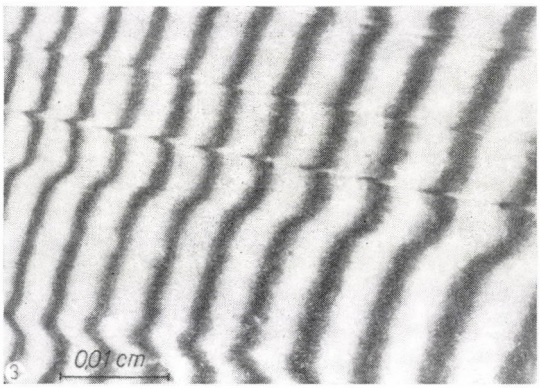

Fig. 3. The interferometric picture of a habit face of ZnS needle. The microphotograph was made with Nomarski interferometer in sodium light

domains on the prism faces slipped in a plane perpendicular to the c-axis (see Fig. 3). It is very probable that such faults are produced by the built-in wurtzite lamellae in the sphalerite matrix [6].

The loss of the original sequence may possibly be due to several kinds of causes, namely the real sequence of the structure can be interrupted during growth by the process itself. BROPHY and SAMELSON have described that crystals grown at temperatures above 1240 °C already have a reversed pseudocubic structure [7].

As the growth from vapour phase usually takes place above the transition point of ZnS [1, 2], the rate of cooling also strongly influences the real structure of the crystals. During a slow cooling the whole crystal or certain crystal regions transform into the cubic arrangement. It is probable that the slipped layers mentioned (see e.g. in Fig. 1) were also produced by these processes. The fitting of the two structures gives no difficulty as both contain the same type of layers. E.g. in Fig. 4 a cubic-hexagonal-cubic domain is represented. On rapid cooling the hexagonal structure may freeze and stresses due to non-

planar isothermal surfaces produce a high dislocation density in the surface region [8, 9]. This again leads to a mixed structure caused by the stacking faults in the crystal [10].

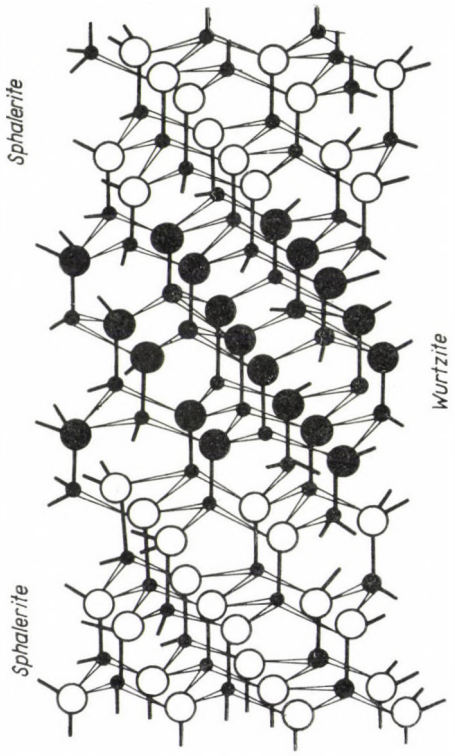

Fig. 4. The fitting model of the sphalerite-wurtzite domains in ZnS lattice

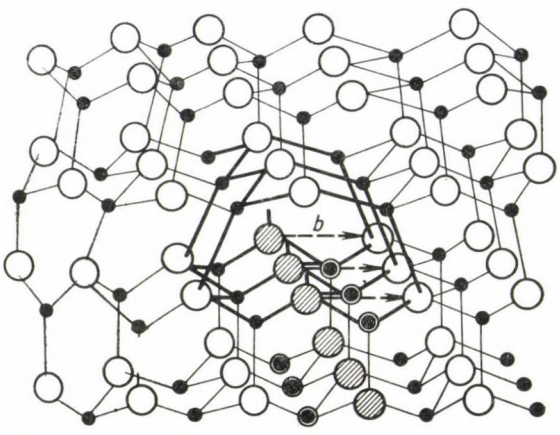

Fig. 5. The model of an edge-dislocation in wurtzite lattice. The atoms belonging to the extra-half plane are denoted by ◎, ▨ resp. Heavy lines denote the strongly disturbed region of the lattice, "b" is the corresponding shear vector

In ZnS the stacking faults generally appear perpendicular to the c-axis, in the basal plane. These are the so called "b" faults [10]. In the case of "b" faults the normal hexagonal sequence is disturbed and three or more layers in the lattice follow one another in the sequence characteristic for the cubic structure. (ABCABC... or other combinations of the three different layers.) This means that in the disturbed regions beside the (0001) planes there are crystallographical directions in which the nearest neighbourhoods can be connected with straight lines. This is impossible in a perfect hexagonal lattice.

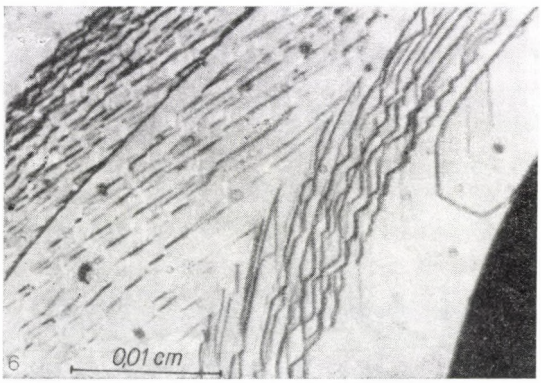

Fig. 6. Slipped lamellar structure around the basal-plane of a ZnS rod. The microphotograph was made with Nomarski interference-contrast setup

In hexagonal crystals the dislocations formed can be deduced from the READ models [9]. Fig. 5 shows a possible structure of an edge dislocation in wurtzite. This dislocation may split into partials. These isolated partials and the associated wide stacking faults can be directly observed by transmission electron microscopy [10]. The same applies to the so called "p" faults which can be found in the prism-planes of ZnS [10]. For thick rods and needles this latter type of fault is of secondary importance.

Glides can be observed microscopically in given directions apart from electron microscopical detection. When looking from the top of the crystal with the same areas hexagonal, slipped lamellae can be seen. In Fig. 6 a crystal is shown covered with high indexed top planes. Along the edges a "valley" and a "wall" can be seen built from such slipped lamellae. On both the inner sides of the valley and the top of wall the individual layers and the boundaries of each lamella can easily be observed. The lamella boundaries produce a special kind of kink structure and certain growth layers on the surface are oriented in the same manner.

The role of the effects mentioned increases for thick rods, where the rapid inhomogeneous cooling of the surface leads to strong stresses in the

surface regions. It is very probable that the appearance of the high dislocation density near the surface, similarly to the case of CdS crystals [11, 12], is caused by the processes mentioned. On the habit faces of such crystals macroscopic deformations are visible. (See e.g. Fig. 1). In Fig. 7 one habit face of

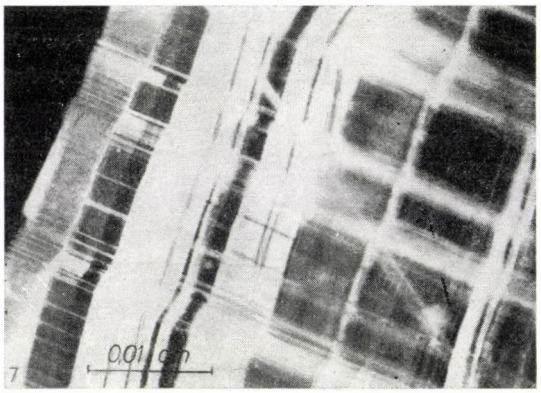

Fig. 7. The birefringence band structure on the prism-face of a ZnS rod in polarized light

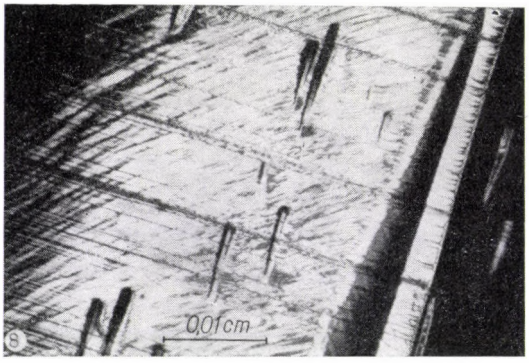

Fig. 8. The etching picture on a high indexed habit face of ZnS crystal. The microphotograph was made with Nomarski interference contrast setup

such thick crystal is shown in polarized light. It is very interesting that on the face a strong proportion in the basal plane can be detected. This is very rare in the case of needles, but in the case of rods it can often be found. At the crystal edge very thin lamellas jutting from the crystal are visible. These thin lamellas can also be seen in Fig. 3. It is characteristic for these types of crystals that their X-ray patterns show a strongly mixed cubic-hexagonal character. In the case of needles cooling more rapidly and homogeneously than the rdos we generally cannot detect such structure.

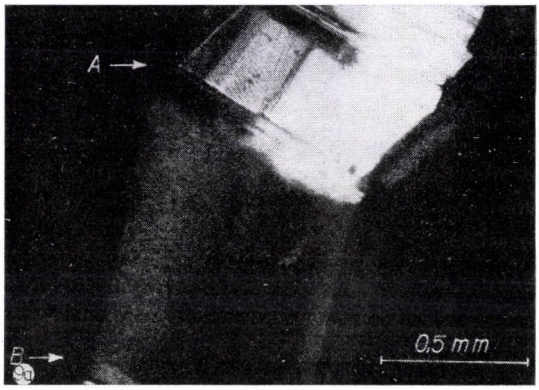

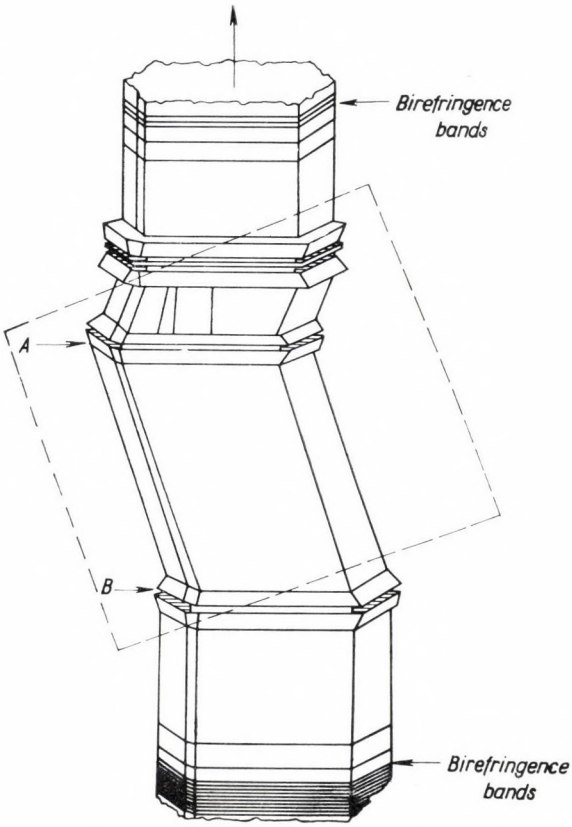

9b

Fig. 9. a — Etched ZnS crystal containing bend planes. b — Drawing of the crystal. The microphotograph was made from the surrounded region of the crystal

The etching picture of the habit faces of crystals containing only a few faults is also more simple. Fig. 8 shows a habit face etched with HCl vapor at high temperature. It can be seen that the investigated face is probably high indexed. In a low concentration there are etching figures emerging parallel with the c-axis. The very fine striations in the direction of basal plane mark the boundaries between the microlamellas in the crystal. Apart from the fine structure on the face there are deep etched striations, too. Within a certain region each lamella has approximately the same width. It is remarkable that the etching develops a structure which makes an angle of 45° with the basal plane. It is probably due to the faults forming at lower temperatures in the cubic arrangement of lattice.

Sometimes among the crystals one can find crystals with macroregions without striations and birefringence bands i.e. without stacking faults. The most interesting example of this kind of crystals is represented by Fig. 9. Fig. 9/a shows the middle part of an etched ZnS prism of medium thickness (appr. 1 mm) in polarized light. It is clearly observable that the crystal region between A and B contains no etched striations, etch-pits and birefrigence bands. The section A—B is limited by very interesting and characteristic crystal regions the orientation of which differs from that of A—B. These crystal regions are separated by "rings". These are features separating the upper and lower parts of the crystal as well as the parallel oriented but slipped regions. (See Fig. 9/b.) Such crystals are very common and it seems probable that the origin of these crystals is connected with the dislocation motion. In the case of hexagonal metals it is well known that if the temperature is high enough during or after a mechanical deformation (bending) a polygonization occurs. As a result of this process the dislocation density decreases strongly and the dislocations form a sub-boundary by rearrangement and annihilation. This effect has been observed in hexagonal metals deformed at high temperature by bending. During the process the dislocations leave their glide planes by climbing and annihilate one another until the density corresponding to the COTTRELL equation remains only [8, 13]. This arrangement produces a sub-boundary of the tilt-type. If the temperature is low and the climb motion of edge dislocations is impossible, the so called "kink" appears.

As in the process of ZnS growth there are many types of causes producing local bending (stresses caused by non-isothermal cooling, the influence of the adjacently grown crystals on each other, etc.) the formation of bend-planes and sub-boundaries of the type mentioned in hexagonal ZnS is quite possible. This is also proved by the annihilation of edge-dislocations in the region A—B and X-ray diagrams showing the purest cubic structure in the region A—B [14]. Presumably the symmetrical rings are a consequence of the high dislocation density around the limiting sub-boundaries, but this has to be proved by further experiments.

The clear ZnS crystal regions mentioned are very important, because the study of the role of dislocations in electroluminescence requires crystals with low dislocation density. In our further experiments we shall try to clarify this with the help of similar ZnS crystals.

3. Acknowledgement

Our grateful thanks are due to Prof. G. Szigeti for many stimulating discussions and encouragement, and to Mrs. T. Sellei, Mr. P. Lőrik and Miss A. Barényi for their assistance.

REFERENCES

1. H. K. Henisch, Electroluminescence. Pergamon Press, Oxford, 1962.
2. H. F. Ivey, Electroluminescence and Related Effects. Academic Press, New York, 1963.
3. J. L. Gillson et al., Luminescence of Organic and Inorganic Materials. Ed. H. Kallmann and M. Spruch. John Wiley and Sons. New York, 1962.
4. P. Zalm, Thesis. Univ. of Amsterdam, 1956.
5. P. Kovács and J. Szabó, Acta Phys. Hung., **14,** 131, 1962.
6. H. Samelson, J. Appl. Phys., **32,** 309, 1961.
7. H. Samelson and V. A. Brophy, J. Electrochem. Soc., **108,** 150, 1961.
8. H. G. van Bueren, Imperfections in Crystals. North-Holland Publishing Co., Amsterdam, 1960.
9. W. T. Read, Dislocations in Crystals. McGraw Hill, New York, 1933.
10. S. Amelinckx, phys. stat. solidi, **2,** 1660, 1962.
11. J. Woods, Brit. J. Appl. Phys., **11,** 296, 1960.
12. D. C. Reynolds and S. J. Czyzak, J. Appl. Phys., **31,** 94, 1960.
13. A. H. Cottrell, Dislocations and Plastic Flow of Crystals. The Clarendon Press, Oxford, 1956.
14. E. Lendvay, M. Farkas-Jahnke and P. Kovács (to be published).

УПЛОТНЕНИЕ ДЕФЕКТОВ В ПАЛОЧНЫХ И ИГОЛЬЧАТЫХ КРИСТАЛЛАХ ГЕКСАГОНАЛЬНОГО ZnS

Э. ЛЕНДВАИ и П. КОВАЧ

Р е з ю м е

В настоящей работе исследуется уплотнение дефектов в палочных и игольчатых кристаллах гексагонального ZnS. Показываются некоторые из возможных моделей для дислокации в решетке ZnS без линейчатых полос двойного лучепреломления. Дается описание макро- и микрослойной структуры ZnS, появляющейся в направлении, перпендикулярном к c — оси.

THEORY OF CONGRUENCE IN GRAVITATIONAL FIELDS. I.

RED SHIFT AND GEODESICS FROM THE SAME THEOREM

By

M. SÜVEGES

RESEARCH GROUP FOR THEORETICAL PHYSICS OF THE HUNGARIAN ACADEMY OF SCIENCES, BUDAPEST

(Presented by A. Kónya. — Received 28. XII. 1964)

A theorem on parallelism is proved. Roughly speaking, the theorem states that physical quantities are congruent under Levi—Civita transport in Riemannian spaces. The three crucial tests of general relativity are deduced from the theorem.

Introduction

It is a prominent feature of a gravitational field that it is possible to introduce coordinate systems which are Euclidean at a prescribed point. Suppose now that we introduce a system which is Euclidean at a point P and define in this system an ennuple K_P of orthogonal basis vectors at P. Suppose we do the same at an other point Q by means of an other coordinate transformation. In the two local Cartesian systems K_P and K_Q natural laws are supposed to be described by equations of the same form in their respective local coordinates. It now seems reasonable to put the following problems: Is there any transformation connecting K_P and K_Q and if there is how it looks like. We will try to give a solution on the assumption that gravitational fields are described by (four dimensional) Riemannian manifolds.

To get a rough idea about the nature of the problem consider first the case when P and Q are infinitely near to each other and start out by analysing a simple physical situation.

Suppose we fixed a metric by some means or other once and for all. In the space defined by the metric we are allowed to manipulate freely with empty coordinate transformations. Let us introduce a coordinate system x' which is Euclidean at the point P'. This can be done for any arbitrary point and can be thought of as a transformation to a freely falling box at P' of sufficiently small dimensions. Fix a system $K_{P'}$ of orthogonal unit vectors in the tangent space at P' and give it a parallel displacement (in the sequel parallel displacement will be simply described as transport) along an infinitesimal vector dx' which has end point Q'. We get a system $K_{Q'}$ of axes at Q'. Now space is Euclidean even at Q', at least to first order in dx', and transport is an ordinary parallel displacement in an Euclidean space, at least in this

approximation. If we imagine some physical quantity written first in system $K_{P'}$, then in $K_{Q'}$, then congruence under ordinary transport can be defined as follows. Take a quantity, for example a contravariant vector $u'^{a}(P')$ (for simplicity we shall always work with vectors but more general quantities can be treated similarly by taking appropriate bases in the tangent spaces at the points considered), the components of which are referred to $K_{P'}$. We first transport $K_{P'}$ to $K_{Q'}$ and if we perform the same transformation on $u'^{a}(P')$ then congruence under transport means that the quantity $u'^{a}(Q')$ at Q' has the same numerical value with respect to $K_{Q'}$ as $u'^{a}(P')$ at P' had with respect to $K_{P'}$. We shall simply say that $u'^{a}(P')$ and $u'^{a}(Q')$ are congruent under transport along dx'. Moreover transport is defined in this case by the differential equation

$$du'^{a} = 0\,, \quad (u'^{a}(Q') = u'^{a}(P') + \ldots) \tag{1}$$

at least in a first approximation, since the Christoffel symbols vanish at P'.

Now we know, at least it is commonly assumed, that physical quantities are congruent under transport in a Euclidean space and our point is that this state of affairs should be independent of the coordinates chosen in the Riemannian manifold. If this is to be the case, then if we go over from the geodesic to some other coordinate system x by means of an empty coordinate transformation then ordinary transport should be replaced by its covariant generalisation, the Levi-Civita transport, and quantities should still be congruent under this new transport. Roughly speaking, from congruence under transport in a Euclidean space would follow congruence under Levi-Civita transports in a Riemannian manifold as a consequence of the postulate of covariance.

However, difficulties immediately arise in connection with the above rough argument.

The first is that the parallel transport in the geodesic system is the ordinary one only as far as terms of higher than first order can be neglected in equ. (1), or what amounts to the same the metric tensor at Q' is Euclidean only to the same approximation.

A second objection can be raised in connection with the meaning of the word covariant. Under the pretext of working covariantly we in fact say that a physical quantity u^{a} is congruent under a transformation defined by the differential equation

$$du^{\alpha} + \Gamma^{\alpha}_{\beta\gamma}\, dx^{\beta}\, u^{\gamma} = 0\,, \tag{2}$$

because this equation is the covariant generalisation of the differential equation

$$du^{\alpha} = 0\,. \tag{3}$$

Such a generalisation might be satisfactory for a mathematician but not quite so for a physicist since the transformations defined by these two equations are quite different and the postulate of covariance would really mean the postulate of congruence under a new physical transformation. Hence to be correct we must prove that from congruence defined by (3) follows congruence defined by (2) without a priori using the mathematical concept of the generalised transport in Riemannian spaces.

These difficulties can be resolved, and in fact the solution to our initial problem provided, with the help of the Fermi theorem according to which coordinate systems can be introduced which are Euclidean along any curve given a priori.

A theorem on congruence

In fact, it is easy to see that there is an intimate relationship between parallel transport and the possibility of introducing coordinate systems which are Euclidean along any prescribed curve. Consider first the special case when the curve is a not-null geodesic.

The argument for null geodesics can be carried through in a similar way by taking special parameters along the geodesics.

We want to describe the following situation. A small space laboratory is put on a geodesic C from a point P. In the laboratory there is a small object, such as an elementary particle, under observation. Define an ennuple of orthogonal unit vectors K, comoving with the object. The ennuple and the object are put on C with the same initial conditions as the laboratory.

Suppose an observer is making measurements on a quantity u'^a attached to the object. At point P' he finds some value $u'^a(P')$ with respect to his system of unit vectors $K(P')$ at P'. At another point Q' on his geodesic he will find the same numerical value when he refers his measurements to his comoving system $K(Q')$ at that point. This is the expression of the fact that he finds u'^a congruent under transport along the time axis in the ordinary sense.

To describe the situation we start by taking an ennuple of unit vectors* $u^a_a(P)$ at P, referred to natural bases in the tangent space at P, in some coordinate system x. If we transport the ennuple by Levi-Civita transport along C we get an ennuple $u^a_a(\sigma)$ of unit vectors in each tangent space along C, where σ is the length of arc of the geodesic. The fourth vector is supposed to be the tangent to C at each point of C. Take an arbitrary vector $u^a(P)$ referred to

* Latin indices label vectors and also refer to coordinate and tensor components in Fermi coordinates.

natural bases in the tangent space at P and give it Levi-Civita transport along C. We obtain a vector field $u^a(\sigma)$ along C and obviously we have

$$u^a(\sigma) = N^a u_a^a(\sigma), \tag{4}$$
$$(g_{\alpha\beta} u_a^\alpha u_b^\beta = \mathrm{diag}[111 - 1]),$$

where the components N^a of $u^a(\sigma)$ on the ennuple $u_a^a(\sigma)$ are constant all along C since lengths and angles are preserved by Levi-Civita transport.

Consider the geodesic C_s in the hyperplane perpendicular to the tangent to C issuing from a point of C of parameter σ, with the initial conditions for the tangent $\frac{dx^a}{ds}$ to C_s

$$\left(\frac{dx^a}{ds}\right)_\sigma = u^a(\sigma) = N^a u_a^a(\sigma).$$

Here s is the length of arc of C_s ($s = 0$ at C). A point x^a on C_s is obtained by expanding along C_s. With the aid of the geodesic equation defining C_s and equations obtained from it by differentiation we get (1)

$$x^a = \varphi^a(\sigma) + u_a^a(\sigma)(N^a s) + \ldots, \tag{5}$$

where $\varphi^a(\sigma)$ defines C in system x and terms of higher than first order in $(N^a s)$ are not written out. If we introduce a new coordinate system x' defined by

$$x'^k = N^k s, \quad x'^4 = \sigma \quad (k = 1, 2, 3), \tag{6}$$

then Levi-Civita proves [1] (in fact this is the way Levi-Civita proves the Fermi theorem) that in the new coordinates the metric tensor is Euclidean at all points of C'

$$(g'_{ab})_{C'} = \mathrm{diag}\,[111 - 1], \qquad (\Gamma'^a_{bc})_{C'} = 0, \tag{7}$$

all along C'. It is also proved there that the transformed vectors u'^b_a are the (unit) tangent vectors to the new coordinate curves. In fact they can be taken as systems of natural basis vectors in the tangent spaces at each point of C' in the new coordinates. Moreover we have all along C

$$\left(\frac{\partial x^\alpha}{\partial x'^a}\right)_C = u_a^\alpha(\sigma), \qquad \left(\frac{\partial x'^a}{\partial x^\alpha}\right)_C = u_a^a(\sigma), \tag{8}$$

where Latin indices on u_a^a are raised and lowered by means of $(g'_{ab})_{C'} = \mathrm{diag}\,[111 - 1]$, the metric tensor along C in the Fermi coordinates, and

$$u_a^a u_b^a = \delta_b^a, \qquad u_b^a u_\beta^b = \delta_\beta^a.$$

The constructed system x' is clearly suitable to describe the situation of the observer making local measurements in the space craft. He has only to identify his local Cartesian basis vectors with the transformed vectors u'^b_a of u^a_a, all along his world line C'. In system x' these are unit vectors in the ordinary sense and they satisfy the differential equations of ordinary transport

$$(du'^b_a)_{C'} = 0 \tag{9}$$

exactly since $(\Gamma'^a_{bc})_{C'} = 0$ at every point of C'.

Consider now the vector $u^a(\sigma)$ given by (4) attached to the object, in the original coordinate system x, which is transported along C by Levi-Civita transport. Clearly, it will be numerical constant N^a in system x' with respect to the Cartesian systems defined by the observer along his world line* since

$$u'^a = \left(\frac{\partial x'^a}{\partial x^a}\right)_C u^a(\sigma) = N^a = u^a_a\, u^a(\sigma) \tag{10}$$

and it will satisfy the ordinary transport equation

$$(du'^a)_{C'} = 0 \tag{11}$$

exactly along C'.

This is the exact mathematical description of the fact that the observer in the freely falling space craft finds the vector unchanged, i.e. congruent under ordinary transport along his proper time σ, with respect to his comoving local Cartesian system.

This is obviously true exactly on C', and with this the first difficulty mentioned before is disposed of.

Let us now turn to the second and forget everything about the mathematical concept of transport in a Riemannian manifold. Suppose we find a coordinate system x' for which the metric is Euclidean along C' and $(\Gamma'^a_{bc})_{C'} = 0$ and introduce a set of ennuples of unit vectors u'^b_a along C' which are obtained from each other by ordinary transport defined by (9). A quantity u'^a which is congruent under ordinary transport satisfies the differential equation (11) and we ask what are the corresponding differential equations satisfied by u^a in any other coordinate system x. Let us suppose we find in system x a vector field u^a along C, referred to natural bases in the tangent spaces at points of C, such that its transformed field u'^a in x' is constant along C', i.e. that it is congruent in the ordinary sense along C' in system x'.

* It should be noted that the components u'^a of u^a in the Fermi system along C' are identical with the components N^a of u^a in the anholonomic system defined in x by the transported ennuples u^a_a along C as can be seen from (10).

We have

$$u'^a = \left(\frac{\partial x'^a}{\partial x^\alpha}\right)_C u^\alpha \tag{12}$$

and since

$$u'^a(P') = u'^a(Q')$$

for any two points P' and Q' on C' it follows that

$$u^\alpha(Q) = \left(\frac{\partial x^\alpha}{\partial x'^b}\right)_Q \left(\frac{\partial x'^b}{\partial x^\beta}\right)_P u^\beta(P) . \tag{13}$$

Let us now fix the point P, differentiate along C and eliminate the constant $\left(\frac{\partial x'^b}{\partial x^\beta}\right)_P u^\beta(P)$. We obtain

$$du^\alpha(Q) = d\left(\frac{\partial x^\alpha}{\partial x'^b}\right)_Q \left(\frac{\partial x'^b}{\partial x^\beta}\right)_Q u^\beta(Q) . \tag{14}$$

Because $(\Gamma'^a_{bc})_{C'} = 0$ we obtain from the transformation properties of the Christoffel symbols that

$$\left[d\left(\frac{\partial x^\alpha}{\partial x'^b}\right)\frac{\partial x'^b}{\partial x^\beta}\right]_C = -\left[\Gamma^\alpha_{\gamma\beta}\, dx^\gamma\right]_C , \tag{15}$$

where dx^α is tangent to the geodesic. Hence equ. (14) is identical with the transport equation

$$du^\alpha + \Gamma^\alpha_{\beta\gamma}(C)\, dx^\gamma\, u^\beta = 0 . \tag{16}$$

It is an easy matter to prove that the $u^\alpha_a(\sigma)$ satisfy equations of the same form in coordinates x. Since angles and lengths are conserved under Levi-Civita transport the components of the vector u^α with respect to the ennuples $u^\alpha_a(\sigma)$ are constant all along C.

It has now been proved without a priori using the mathematical concept of Levi-Civita transport that from congruence under ordinary transport in Euclidean space follows congruence under transformations defined by the differential equations (16), at least in the geodetic case. Hence also the second difficulty mentioned is resolved in this case.

The generalisation of the above argument for arbitrary curves is not difficult and proceeds along similar lines by taking an ennuple of unit vectors in the tangent space to the manifold at some point of the curve and transporting it along the curve etc.

Further, we were always considering congruence of vectors instead of general quantities. However, the generalisation to more general quantities can easily be done by taking appropriate bases in the tangent spaces at different points of the manifold.

The final conclusion of the argument can be condensed into the definition and theorem.

Definition. A quantity $\xi(P)$ at a point P referred to some basis, defined in the tangent space at P, and a quantity $\xi(Q)$ at a point Q are said to be congruent under Levi-Civita transport along a curve C connecting P and Q, if they are numerically identical when $\xi(Q)$ is referred to a basis, defined in the tangent space at Q, obtained from the basis at P by Levi-Civita transport along C.

Since the Fermi theorem holds we have proved the following theorem.

Theorem. A quantity $\xi(P)$ defined in the tangent space at a point P and a quantity $\xi(Q)$ defined in the tangent space at a point Q are congruent under Levi-Civita transport along an arbitrary curve C connecting P and Q.

In this sense two bases, defined in the tangent spaces at two different points, which are obtained from each other by Levi-Civita transport along any curve connecting the points might be said to be physically equivalent.

Of course, the theorem is valid as far as gravitational fields can be described by Riemannian manifolds and physical quantities are congruent under ordinary transport in Euclidean space.

Because of the fundamental importance of transport we enumerate some well known properties of the solutions of the equations

$$\frac{d\xi^\alpha}{d\sigma} + \Gamma^\alpha_{\beta\gamma}\frac{dx^\beta}{d\sigma}\xi^\gamma = 0, \tag{17}$$

where $x^\alpha = x^\alpha(\sigma)$, $(b < \sigma < c)$ is any parameterized curve and the functions $x^\alpha(\sigma)$ are of class 1. Equations (17) have a unique set of solutions $\xi^1(\sigma), \ldots, \xi^n(\sigma)$ satisfying the initial conditions $\xi^\alpha(\sigma_0) = \xi^\alpha_0$ with ξ^α_0 arbitrary and σ_0 any number in the segment $b < \sigma < c$. The solutions are linear in the initial constants and are of the form

$$\xi^\alpha(\sigma) = a^\alpha_\beta(\sigma, \sigma_0)\xi^\beta(\sigma_0)\,. \tag{18}$$

This defines a linear homogeneous transformation $\xi^\alpha(\sigma_0) \to \xi^\alpha(\sigma)$ from the tangent space at the point $x^\alpha(\sigma_0)$ to the tangent space at $x^\alpha(\sigma)$. This holds in a certain maximum segment $b' < \sigma < c'$. Further, each of the transformations (18) is an isometric mapping, i.e. leaves the fundamental quadratic form invariant, from one tangent space to another and these transformations constitute a pseudo-group.

Red shift and geodesics

The experimental consequencies of the Theorem could be divided into what might be called local and global. Local consequencies could be checked by experiments performed in the tangent space at any point of the manifold, global ones by comparing physical quantities in the tangent spaces at different points. The three crucial tests of general relativity are of the global type and we first turn to these.

Take first the geodesics. The Theorem says that quantities at two different points P and Q are congruent (in the sense of the Definition) under Levi-Civita transport along any curve C connecting P and Q. Pick out that curve C for which the tangent to the curve is $u'^{\alpha} = \{0, 0, 0, \text{const}\}$ in the Fermi coordinates all along C. All quantities will then be congruent under ordinary transport in the Fermi system. Accordingly, they are obtained from each other by a transformation of Levi-Civita transport in any coordinate system. In particular this must be the case for the tangent vector u^{α} to C. However, the transport equation for u^{α} is just the differential equation defining the geodesic. The same can be said of null-geodesics and thus the geodesic hypothesis follows from the theorem.

To see what about red shift consider the Schwarzschild exterior solution* and take a curve C defined by $dx^{\alpha} = \{dr, 0, 0, 0\}$ connecting two points P and Q. According to the Theorem a vector field is congruent under Levi-Civita transport from point to point along C and the vector $\xi^{\alpha}(Q)$ at Q is obtained from the vector $\xi^{\alpha}(P)$ at P by a transformation defined by equation (17). If we put the Christoffel symbols for the Schwarzschild metric (of signature $+2$) into (17) together with dx^{α} which defines the curve, we obtain the set

$$
\begin{aligned}
d\xi^1 &= \left(1 - \frac{2m}{r}\right)^{-1} \frac{m}{r^2}\, dr\, \xi^1 , \\
d\xi^2 &= -\frac{dr}{r}\, \xi^2 , \\
d\xi^3 &= -\frac{dr}{r}\, \xi^3 , \\
d\xi^4 &= -\left(1 - \frac{2m}{r}\right)^{-1} \frac{m}{r^2}\, dr\, \xi^4 .
\end{aligned}
\tag{19}
$$

* Obviously, the theorem is valid for any Riemannian manifold and is independent of the validity of the Einstein equations. If one likes one may take the Schwarzschild solution as an empirical finding.

These are separate total differential equations and the integrals are easily found to be

$$\xi^1\left(1-\frac{2m}{r}\right)^{-\frac{1}{2}}=\text{const.},\quad r\xi^2=\text{const.},$$
$$r\xi^3=\text{const.},\quad \xi^4\left(1-\frac{2m}{r}\right)^{\frac{1}{2}}=\text{const.} \tag{20}$$

The matrix of the transformation

$$\xi^\alpha(r_2)=a^\alpha_\beta(r_2\,r_1)\,\xi^\beta(r_1) \tag{21}$$

is given by

$$a^\alpha_\beta(r_2\,r_1)=\text{diag}\left[\left(\frac{1-\frac{2m}{r_1}}{1-\frac{2m}{r_2}}\right)^{-\frac{1}{2}},\frac{r_1}{r_2},\frac{r_1}{r_2},\left(\frac{1-\frac{2m}{r_1}}{1-\frac{2m}{r_2}}\right)^{\frac{1}{2}}\right]. \tag{22}$$

Identify now the vector $\xi^\alpha(C)$ with the coordinate differentials in the tangent spaces at the corresponding points. Then the meaning of the transformation of the second and third component is clear. It simply says that the distance $d=r\xi^2=rd\Theta$ perpendicular to r is constant and is independent of r. The same is true for $r\xi^3=rd\Phi$. The transformations of the first and fourth components are identical with the formulas for the comparison of distances and time differentials in general relativity.

The interpretation of these results is as follows. In the tangent space at any point $P(r)$ local geometry, and thus behaviour of measuring rods etc., is determined by the constant metric tensor $g_{\alpha\beta}(P)$ at that point. Obviously, $g_{\alpha\beta}$ varies from point to point. Since, however, every physical quantity must be congruent under Levi-Civita transport along r so must the metric tensor. Indeed, it is easy to see with the aid of (22) that

$$g_{\alpha\beta}(r_2)=a^{\cdot\cdot}_\alpha(r_2,r_1)\,a^\delta_\beta(r_2,r_1)\,g_{\delta\gamma}(r_1) \tag{23}$$

and this must be so since $g_{\alpha\beta}$ satisfies the Levi-Civita transport equations identically which is a remarkable fact.

It is easy to verify that the transformations (21) satisfy the pseudo-group property and that $ds^2(r_1)=ds^2(r_2)$, i.e. they leave the fundamental quadratic form invariant.

However, before working out other consequencies of the Theorem we now have to face a problem. This is that Levi-Civita transport between two points depends on the curve we choose between the points. What will happen

if we choose curves different from what we actually chose. For example let us take any curve defined by $dx^a = \{dx^a, 0\}$, $(a = 1, 2, 3)$ and substitute into (17) together with the Christoffel symbols for the Schwarzschild solution. We obtain the set

$$d\xi^k + \Gamma^k_{ij}\, \xi^i\, dx^j = 0\,, \quad (i, j, k = 1, 2, 3)\,, \tag{24}$$

$$d\xi^4 + \left(1 - \frac{2m}{r}\right)^{-1} \frac{m}{r^2} dr\, \xi^4 = 0\,, \tag{25}$$

i.e. the time component separates out and depends only on r and is independent of the curve chosen. Thus there is no trouble as far as present day experimental evidence goes. However, the transformations of the space components do depend on the curves chosen and we have to face the fact that, in general, Levi-Civita transport between two points is not a unique operation. We are going to deal with this problem in a following paper.

REFERENCE

1. T. Levi-Civita, Math. Ann., **97**, 299, 1926—1927.

ТЕОРИЯ ТОЖДЕСТВА В ГРАВИТАЦИОННОМ ПОЛЕ I КРАСНОЕ СМЕЩЕНИЕ И ГЕОДЕЗИЯ В ДАННОЙ ТЕОРИИ

М. ШЮВЕГЕШ

Резюме

Доказывается теорема параллелизма. Грубо говоря, теорема устанавливает, что физические величины тождественны транспорту Лэви—Чивита в пространстве Риманна. Из теоремы выводятся три основные доказательства общей теории относительности.

THEORY OF CONGRUENCE IN GRAVITATIONAL FIELDS. II.

THE POSSIBLE COSMOLOGICAL ORIGIN OF THE GROUP $L^{\uparrow}_{+}$

By

M. SÜVEGES

RESEARCH GROUP FOR THEORETICAL PHYSICS OF THE HUNGARIAN ACADEMY OF SCIENCES, BUDAPEST

(Presented by A. Kónya. — Received 28. XII. 1964)

A corollary to the Theorem proved in the previous paper states that local coordinate systems, defined in the tangent space at any point of the Riemannian manifold, that are obtained from each other by transformations of the holonomy group at that point are physically equivalent. With the aid of this corollary it is proved that if the Universe is a non-vacuum Einstein manifold of signature $+2$, then the six-dimensional orthochronous proper Lorentz group $L^{\uparrow}_{+}$ is a good local symmetry group in the tangent space at any point of the Universe. Conversely, if $L^{\uparrow}_{+}$, or at least a subgroup of it, is a good local group then the Universe cannot be flat.

Introduction

In the previous paper [1] (I) a theorem on congruence in gravitational fields was proved on the assumption that gravitational fields are Riemannian manifolds. The theorem, roughly speaking, states that local coordinate systems, defined in the tangent spaces at two different points of the manifold that are obtained from each other by Levi-Civita transport (LCt) along some curve C connecting the points are physically equivalent. It was shown there that the three classical tests of general relativity follow from the theorem. It would, of course, be straightforward to work out other experimental consequencies of the Theorem.

However, a well-known fact was also pointed out in I, namely, that LCt between two points is not a unique operation, but the result of the transport depends on the curve we happen to choose between the points. At first sight this seems to be an unpleasant implication of the Theorem and in this paper we are going to work out some of its general physical consequencies.

Congruence under the holonomy group

In fact apart from the conceptual difficulty involved in the many-valuedness of LCt there is a practical one which will be clear from the following example.

Suppose we want to compare two identical objects, such as elementary particles, situated at two different points x and y of the manifold V_n. We pro-

ceed as follows. Consider the objects brought together at x. Choose a curve $C_1(xy)$ connecting x and y and bring one of the objects to point y along $C_1(xy)$. Consider some quantity $\xi(C_1)$ (a quantity might be a null quantity such as a differential equation) attached to the object moved along $C_1(xy)$. The Theorem in I states that $\xi(x)$ and $\xi(y)$ are congruent (in the sense of the Definition, I) under LCt along $C_1(xy)$ and, they are obtained from each other by the transformation defined by LCt along $C_1(xy)$ (in which case we write $\xi(x) \overset{t(C_1)}{=\!=} \xi(y)$). In this sense two local systems K_x and $K_y(1)$ in the tangent spaces at x and y, respectively, such that $K_x \overset{t(C_1)}{=\!=} K_y(1)$ are physically equivalent.

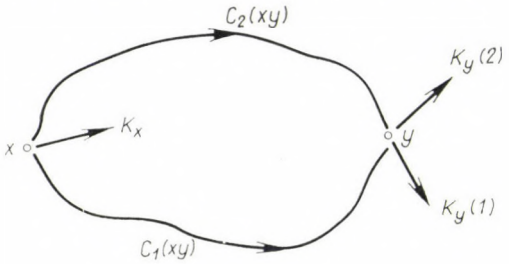

Fig. 1

If we choose another curve $C_2(xy)$ between x and y by transport we have $K_x \overset{t(C_2)}{=\!=} K_y(2)$. However, $K_y(2)$ will in general be different from $K_y(1)$.

In fact to determine all possible local systems K_y at y which are equivalent to K_x we ought to integrate the transport equations along all possible curves connecting x and y. Obviously this is a quite impossible mathematical task in this primitive form. However, we can get around this problem in the following way.

Suppose we denote the transformation defined by LCt along $C_1(xy)$ by the same expression $C_1(xy)$ as the curve itself. Then the equivalent system $K_y(1)$ at y can be written symbolically as

$$K_y(1) = C_1(xy)\, K_x\,. \tag{1}$$

Consider now the other curve $C_2(xy)$ connecting x and y (see the Figure, where only one vector in each system K is shown for simplicity).

The system $K_y(2) \overset{t(C_2)}{=\!=} K_x$ equivalent to K_x along $C_2(xy)$ is obtained by the transformation

$$K_y(2) = C_2(xy) K_x. \tag{2}$$

However, $K_y(2)$ can be obtained in a different way. If we transport $K_y(1)$ along $C_1(xy)$ in the opposite direction we obtain

$$K_x = C_1(xy)^{-1} K_y(1)\,.$$

where $C_1(xy)^{-1}$ is the transformation, and the curve, inverse to $C_1(xy)$. If now we transport K_x so obtained along $C_2(xy)$ we obtain $K_y(2)$ from $K_y(1)$ by means of (2)

$$K_y(2) = C_2(xy)C_1(xy)^{-1}K_y(1)\,, \tag{3}$$

where $C_2(xy)C_1(xy)^{-1}$ is now the transformation along the closed curve $C_2(xy)C_1(xy)^{-1}$ through y. Since LCt conserves lengths this is a rotation in the tangent space at y. If we take a third curve $C_3(xy)$ we can repeat the argument with $C_3(xy)$, $K_y(3)$ and $C_2(xy)$, $K_y(2)$ then with $C_4(xy)$, $K_y(4)$ and $C_3(xy)$, $K_y(3)$ etc. In other words, if we obtain a system $K_y(1)$ such that $K_y(1) \overset{t(C_1)}{=\!=} K_x$ by integrating the transport equations along any curve $C_1(xy)$ then other equivalent systems $K_y(2)$, $K_y(3)$, . . . at y are obtained from $K_y(1)$ by means of some rotations at y. This suggests that there might be a relationship between rotations in the tangent spaces at points of the manifold and LCt along curves between different points. In fact let us consider the following more general case.

Choose an arbitrary point y in the manifold and define in the tangent space at that point a local system K_y. Take an arbitrary closed curve $C_1(y)$ through the point y and give K_y a LCt along $C_1(y)$. After describing the closed curve we have at y another system $K_y(1)$ equivalent to K_y given by

$$K_y(1) = C_1(y)K_y\,. \tag{4}$$

It is proved by the mathematicians that the transformations (4) for all possible choices of $C_1(y)$ form a group, the holonomy group (hg) Ψ_y of the manifold.

The Theorem of I is valid for any curve, in particular for any closed curve. Apply then the Theorem to all possible closed curves through y. If congruence is defined by the Definition in I, we obtain the trivial corollary to the Theorem of I.

Corollary. Physical quantities, defined in the tangent space at an arbitrary point of the manifold, are congruent under transformations of the holonomy group at that point.

In the sense of the definition of congruence it might then be said that any two local systems, defined in the tangent space at an arbitrary point of the manifold, that are obtained from each other by a transformation of the holonomy group are physically equivalent.

To see the potential physical meaning of this corollary let us consider a physical object, such as an elementary particle, at a point y and take it along all possible closed curves through y in the manifold. The Theorem says that every physical quantity (also null quantities such as the differential equations of physics) attached to the object will suffer LCt along the curves and through this LCt the object will pick up, picturesquely speaking, on its

way informations about the properties of the manifold as a whole. After describing all possible curves the object at point y will remember the structure of the manifold and the information about the manifold will be stored in the holonomy group at that point. In other words, the global structure of the manifold determines a local structure in the tangent space at every point by means of the local symmetry group, the holonomy group at that point.

Thus the fact that LCt between two points is not a unique operation is now seen to be far from unpleasant. On the contrary, it opens up fascinating possibilities since it provides a connection between local symmetries and the global structure of the manifold.

Incidentally, the integration problem mentioned can also be resolved by means of the holonomy group Ψ_y. Namely one has only to integrate the transport equation along any one curve $C_1(xy)$ connecting x and y to obtain $K_y(1)$, then all other equivalent systems K_y at y are obtained from $K_y(1)$ by transformations of Ψ_y. In other words all transformations consist of a linear homogeneous transformation which leaves lengths, but not necessarily the metric tensor, invariant followed by transformations of the holonomy group Ψ_y. Thus the integration problem is reduced to that of determining the holonomy group.

We are now going to present some mathematical properties of holonomy groups, associated with the Levi-Civita connection, in Riemannian manifolds and, also, try to draw some immediate physical consequences of the Corollary.

Some general experimental consequences

An important consequence can be obtained by considering the holonomy groups Ψ_x and Ψ_y at two different points x and y. If $C(y)$ is a closed curve at point y and the corresponding transformation of Ψ_y is also denoted by $C(y)$, we may construct a closed curve $C(x)$ at point x by going first from x to y along some curve C, then along $C(y)$ and back to x along C^{-1}. If C is the transformation along C we get for the whole transformation $C^{-1}C(y)C$ and this must be a transformation of Ψ_x. This means that Ψ_x and Ψ_y are isomorphic and there is in fact only one holonomy group for the manifold. Even more, it is easy to see that if Ψ_x and Ψ_y are described with respect to two local bases at x and y, respectively, that can be obtained from each other by LCt along C the transformations are numerically identical.

Now the global structure of the manifold V_n determines a local symmetry group at every point of V_n defined by the holonomy group Ψ_x and in this way a physical object at x, such as an elementary particle, is provided with a structure defined by Ψ_x for every x of V_n. By considering the above property of Ψ_x we are lead to extend the notion of congruence of quantities attached

to the object to that of structures. In fact the above property of Ψ_x says that two structures at points x and y are congruent in the sense that Ψ_x and Ψ_y defining them are numerically identical when they are referred to local systems at x and y which are obtained from each other by LCt along some curve. We have thus the result that the local structure, at least that defined by Ψ_x, of a physical object is independent of the point in the manifold.

Important consequences of the Corollary can be obtained by considering the properties of the holonomy group Ψ_x at one point x (for the definitions and proofs of the theorems see Chapitre III in LICHNEROWICZ [2]).

We first define a subgroup $\sigma_x(V_n)$, the restricted holonomy group of Ψ_x. $\sigma_x(V_n)$ consists of all transformations along all possible closed curves through x which are homotopic to zero.

Theorem 1. The restricted holonomy group $\sigma_x(V_n)$ coincides with the arc-wise connected component of the identity in the holonomy group $\Psi_x(V_n)$.

We define the local holonomy group σ_x^* as follows. Consider all open connex neighbourhoods U in V_n containing x. The set σ_x^* in $\sigma_x(V_n)$ defined by

$$\sigma_x^* = \bigcap_{x \ni U} \sigma_x(U)$$

is a subgroup of $\sigma_x(V_n)$ since it is the intersection of subgroups $\sigma_x(U)$ of $\sigma_x(V_n)$.

Theorem 2. The local holonomy group σ_x^* is a connected Lie group and there exists a neighbourhood $U(x)$ of the point x such that σ_x^* coincides with the corresponding restricted holonomy group $\sigma_x[U(x)]$.

Theorem 3. Every element of $\sigma_x(V_n)$ is finite product of elements deduced from elements of σ_y^* $(y \in V_n)$ by transport along the curves joining y to x.

Theorem 4. Given a special neighbourhood U of x_0 such that $\sigma_{x_0}^* = \sigma_{x_0}(U)$ the Lie algebra of the local holonomy group $\sigma_{x_0}^*$ is the algebra obtained from the tensors

$$R^{\alpha}_{\beta\gamma\mu} V^{\gamma} W^{\mu} \tag{5}$$

($R^{\alpha}_{\beta\gamma\mu}$ is the curvature tensor) at x by transport along the curves joining x_0 to x.

One can deduce from Theorems 3 and 4 that the Lie algebra of the restricted holonomy group $\sigma_x(V_n)$ is obtained from the elements deduced from the tensors (5) at x by transport along the curves joining x_0 to x.

Corollary 4. For a linear connexion of zero curvature the restricted holonomy group is reduced to the identity.

We now define the infinitesimal holonomy group σ_x' at x for a manifold of class C^{∞}. The Lie algebra $d\sigma_x'$ of σ_x' is given by the $\frac{\alpha}{\beta}$—domain of the curvature

tensor and its covariant derivatives

$$R^{\alpha}_{\beta\gamma\delta}, \; R^{\alpha}_{\beta\gamma\delta;\varepsilon}, \; R^{\alpha}_{\beta\gamma\delta;\varepsilon\varrho}, \ldots$$

Theorem 5. For any arbitrary vectors V^{λ}, W^{μ}, $u_1^{\nu_1}$, $u_2^{\nu_2}$, ... $u_k^{\nu_k}$ ... at a point x the tensors at x

$$[R^{\alpha}_{\beta\lambda\mu} V^{\lambda} W^{\mu}], \ldots \; [u_1^{\gamma_1} u_2^{\gamma_2} \ldots u_k^{\gamma_k} R^{\alpha}_{\beta\lambda\mu;\,\gamma_1\gamma_2\ldots\gamma_k} V^{\lambda} W^{\mu}], \ldots \tag{6}$$

define elements of the Lie algebra $d\sigma_x^*$ of the local holonomy group σ_x^*.

It is also proved that the elements (6) for $k = 0, 1, \ldots$ define a Lie subalgebra $d\sigma_x'$ of $d\sigma_x^*$.

From the theorems it is seen that the infinitesimal holonomy group σ_x' is a subgroup of the restricted group σ_x and thus also of the complete hg Ψ_x.

We are now able to deduce some physical consequences of the Corollary.

Consider first the case when there is no additional restriction, such as on signature etc., imposed on the manifold V_n. We have immediately a consequence which is independent of the detailed nature of Ψ_x.

From Theorems 3 and 4 and Corollary 4 it follows that the curvature of every non-flat manifold V_n determines a local symmetry group defined by the restricted hg σ_x at every point of the manifold. Conversely, if σ_x, or at least a subgroup of it, is found to be a good group locally then the manifold cannot be flat.

We now inquire about the explicit nature of Ψ_x in a V_n. Since LCt conserves the fundamental quadratic form and the metric tensor is a covariant constant,* Ψ_x is an orthogonal group in the tangent space at x. If we refer Ψ_x to an orthonormal ennuple at x (which is equivalent to the introduction of a coordinate system which is geodesic at x, see I) it is seen that Ψ_x is a subgroup of the orthogonal group $O(n)$ and σ_x is a subgroup of $SO(n)$. To specify Ψ_x further we have to make special assumptions about the manifold.

We now require that V_n should be of dimension 4 and of signature $(+++-)$. By introducing a coordinate system in V_n which is geodesic at x, it is easy to see that Ψ_x is a subgroup of the homogeneous Lorentz group L. And since σ_x is defined by closed curves at x homotopic to zero, the restricted *hg* σ_x is a subgroup of the homogeneous orthochronous proper Lorentz group $L_+^{\uparrow}$. And this is independent of any field equations. To specify σ_x further the straightforward way would be to take interesting manifolds and work out explicitly the holonomy groups. However, the metric tensor is usually expected to satisfy some field equations and it is more interesting to see whether

* A quantity is covariant constant if it satisfies the transport equations identically, independently of the curves chosen, or what amounts to the same, it is a numerical constant under transformations of the hg Ψ_x.

there exists a connection between the structure of the field equations and the structure of the holonomy group. Suppose now that the Einstein equations are valid. Then gravitational fields are Einstein manifolds and the classification of Einstein manifolds by means of subgroups of the hg, initiated by PETROV [3] (Weyl tensor) and developed further by SCHELL [4] (infinitesimal hg) and others (for references see e.g. BEIGLBÖCK [7]) is pertinent. From the work of these authors it is seen that, as is expected, the dimensionality of at least the local symmetry group $L_+^\uparrow$ has no absolute meaning but is, in general, different for different manifolds.

However, instead of discussing any particular manifold we discuss a more general problem. Suppose the Universe is an Einstein space of signature $(+2)$. Since the Universe is not empty we might safely suppose that it is a non-vacuum Einstein space. Then the local symmetry group σ_x is a subgroup of $L_+^\uparrow$ and we ask about its dimensionality. We have the theorem of BEIGLBÖCK [7] (Satz 3).

Theorem. A manifold V_n with $R_{\nu\mu} \sim g_{\nu\mu}$ and $R \neq 0$ has always a six-dimensional infinitesimal holonomy group σ_a'.

Consequently, if the Universe is a non-vacuum Einstein manifold of signature $(+2)$ then the local symmetry group σ_x, subgroup of Ψ_x, is the six-dimensional homogeneous orthochronous proper Lorentz group $L_+^\uparrow$ in the tangent space at each point of the Universe. Conversely, if the Universe is of signature $(+2)$ and if the six-dimensional $L_+^\uparrow$, or at least a subgroup of it, is found to be a good local symmetry group then, by Corollary 4, the Universe cannot be flat, independently of any field equations. Moreover, the Einstein equations are not in contradiction with dimension six for $L_+^\uparrow$.

This establishes then a connection between the structure of the Universe and the structure of elementary particles via the holonomy group. In fact it is obvious that, under the assumptions made, the group $L_+^\uparrow$ is nothing but a local manifestation of the structure of the Universe at large and is far from being a property of flat space. On the contrary in a flat space σ_x would be the identity and the very existence of $L_+^\uparrow$ is due to the fact that the Universe is curved. Indeed, it might be said that if the Einstein equations are valid then at least the $L_+^\uparrow$-properties of elementary particles are determined by the stucture of the Universe.

This example shows how cosmology and elementary particle physics may help each other. If the manifold describing the Universe is found observationally then its hg can be calculated which, in turn, must be a local symmetry group. Conversely, if a local symmetry group is found which is the hg of a manifold, then the metric tensor of the manifold can be calculated. We refer on this point to GOLDBERG and KERR [5], CAHEN and DEBEVER [6] and BEIGLBÖCK [7] who show how to get, at least in some cases, the metrics of a V_n with a given σ_x.

Summary

The basic ideas of a theory of congruence in gravitational fields have been presented in the previous paper (I) and here. The main content of the theory is condensed in a theorem proved in I. Some immediate physical consequences were shown to follow from the Theorem almost on inspection. These are the three classical tests of general relativity, the congruence of local structures at different points in a gravitational field and the cosmological origin of $L_+^\uparrow$. Obviously, many more experimental consequences of the Theorem can be calculated and work is going on in this direction.

The author is grateful to Professor P. GOMBÁS for giving him the opportunity to work on the problems presented here and in paper I.

REFERENCES

1. MÁTÉ SÜVEGES, Acta Phys. Hung., **20**, 41, 1965.
2. A. LICHNEROWICZ, Théorie globale des connexions et des groupes d'holonomie, Roma, 1955.
3. A. Z. PETROV, Sci. Not. Kazan State Univ., **110**, 55, 1950.
4. J. F. SCHELL, J. Math. Phys., **2**, No. 2, 1961.
5. J. N. GOLDBERG and R. P. KERR, J. Math. Phys., **2**, No. 3, 1961.
6. N. CAHEN et R. DEBEVER, Bull. Cl. Sci. Acad. Roy. Belg., Ser. V, **47**, 6, 1962.
7. W. BEIGLBÖCK, Z. Physik, **179**, 148, 1964.

ТЕОРИЯ ТОЖДЕСТВА В ГРАВИТАЦИОННОМ ПОЛЕ, II
ВОЗМОЖНОСТЬ КОСМОЛОГИЧЕСКОГО НАЧАЛА В ГРУППЕ $L_+^\uparrow$

М. ШЮВЕГЕШ

Резюме

Доказанная в предыдущей статье теорема устанавливает, что локальные координатные системы, определенные в тангенциальном пространстве в любой точке множества Римана, полученного одно из другого путем преобразования голономной группы в данной точке, физически эквивалентны. При помощи данного следствия доказывается, что если вселенная является невакуумным множеством Эйнштейна, тогда соответствующая шестимерная группа Лоренца L является правильной симметричной группой в тангенциальном пространстве в любой точке вселенной. Наоборот, если L, или хоть её одна подгруппа, является правильной группой, то вселенная не может быть плоской.

ON THE PHYSICAL SIGNIFICANCE OF THE RETARDED AND ADVANCED POTENTIALS

By

L. JÁNOSSY

CENTRAL RESEARCH INSTITUTE FOR PHYSICS, BUDAPEST

(Received 29. XII. 1964)

The role of the retarded and advanced potentials in the solutions of MAXWELL's equations are discussed. It is pointed out that the solutions can be represented as a superposition of retarded solutions and "wandering waves" the latter having no sources. If the possibility of the existence of wandering waves is excluded it may be suggested that only those particular solutions of MAXWELL's equations occur in nature that can be represented with the help of retarded potentials. It is pointed out that the latter assumption leads to the conclusion that electromagnetic processes are irreversible.

Retarded potentials

§ 1. MAXWELL's equations can be written in the form (see also [1]):

$$\left.\begin{aligned} \operatorname{rot}\mathbf{E} &= -\frac{1}{c}\dot{\mathbf{B}}, && \text{(a)}\\ \operatorname{rot}\mathbf{B} &= \frac{1}{c}\dot{\mathbf{E}} + 4\pi\mathbf{i}_{\text{eff}}, && \text{(b)}\\ \operatorname{div}\mathbf{B} &= 0, && \text{(c)}\\ \operatorname{div}\mathbf{E} &= 4\pi\varrho_{\text{eff}}, && \text{(d)} \end{aligned}\right\} \tag{1}$$

where

$$\left.\begin{aligned} \mathbf{i}_{\text{eff}} &= \mathbf{i} + \frac{1}{c}\dot{\mathbf{P}} + \operatorname{rot}\mathbf{M}, && \text{(a)}\\ \varrho_{\text{eff}} &= \varrho - \operatorname{div}\mathbf{P}, && \text{(b)} \end{aligned}\right\} \tag{2}$$

$\mathbf{i}$ and ϱ are current and charge densities of the "true currents" and "true charges". $\mathbf{i}_{\text{eff}}$ and ϱ_{eff} are the source densities including the currents and charge densities accompanying polarization.

The eqs. (1a) and (1b) determine the changes of $\mathbf{E}$ and $\mathbf{B}$ for a given initial condition. The relations (1c,d), if satisfied at $t = 0$ by the initial condition, will remain satisfied at any other time, as can be shown easily provided the source densities obey the continuity relation

$$\operatorname{div}\mathbf{i}_{\text{eff}} + \frac{1}{c}\frac{\partial\varrho_{\text{eff}}}{\partial t} = 0. \tag{3}$$

§ 2. The field strengths **E** and **B** can be expressed in terms of potentials **A** and Φ in the following manner:

$$\mathbf{E} = -\operatorname{grad}\Phi - \frac{1}{c}\frac{\partial \mathbf{A}}{\partial t}, \qquad \text{(a)}$$
$$\mathbf{B} = \operatorname{rot}\mathbf{A}. \qquad \text{(b)} \tag{4}$$

We note that when the values of **E** and **B** are given at a time $t = 0$ it is always possible to find potentials **A** and Φ which describe the given field **E**, **B** at that instant.

Indeed, giving an initial condition for an instant $t = 0$ we may write

$$\mathbf{A}(\mathbf{r}, 0) = \mathbf{a}(\mathbf{r}) \quad \text{and} \quad \left(\frac{\partial \mathbf{A}(\mathbf{r}, t)}{\partial t}\right)_{t=0} = \dot{\mathbf{a}}(\mathbf{r}), \tag{5}$$

and we can prescribe $\mathbf{a}(\mathbf{r})$ and $\dot{\mathbf{a}}(\mathbf{r})$ independently of each other. If we choose

$$\Phi(\mathbf{r}, 0) = \varphi(\mathbf{r}) \tag{6}$$

arbitrarily, we may put

$$\dot{\mathbf{a}}(\mathbf{r}) = c(\mathbf{E}(\mathbf{r}, 0) + \operatorname{grad}\varphi(\mathbf{r})), \tag{7}$$

and thus satisfy (4a). Supposing further $\mathbf{B}(\mathbf{r}, 0) = \mathbf{B}_0(\mathbf{r})$ we find from (4b)

$$\mathbf{a}(\mathbf{r}) = \frac{1}{4\pi}\operatorname{rot}\int \frac{\mathbf{B}_0(\mathbf{r}+\mathbf{R})}{R}\, d^3\mathbf{R} + \operatorname{grad}\psi(\mathbf{r}), \tag{8}$$

where ψ can be chosen arbitrarily.

We see thus that a field distribution

$$\mathbf{E}(\mathbf{r}, 0) = \mathbf{E}_0(\mathbf{r}), \quad \mathbf{B}(\mathbf{r}, 0) = \mathbf{B}_0(\mathbf{r}) \tag{8a}$$

existing for $t = 0$ can be expressed in the form (4a), (4b) in terms of suitably chosen potentials. In any case $\mathbf{E}_0(\mathbf{r})$ and $\mathbf{B}_0(\mathbf{r})$ have to satisfy

$$\operatorname{div}\mathbf{B}_0(\mathbf{r}) = 0, \quad \operatorname{div}\mathbf{E}_0(\mathbf{r}) = 4\pi\varrho_{\text{eff}}(\mathbf{r}, 0). \tag{8b}$$

The potentials **A**, Φ and the time derivative $\dot{\mathbf{A}}$ at $t = 0$ must be chosen according to the relations (5)—(8). The initial conditions for the potentials are not uniquely determined as the relations (5)—(8) contain two functions $\varphi(\mathbf{r})$ and $\psi(\mathbf{r})$ which can be chosen arbitrarily.

§ 3. Inserting (4a) and (4b), respectively, into (1a) we find identities. Inserting (4a, b) into the remaining equation (1b) and (1d) we find that MAX-

WELL's equations will be satisfied by the field strengths **E**, **B** as expressed through potentials in the form (4a, b), provided the potentials obey the following system of equations:

$$\left.\begin{aligned} \nabla^2 \mathbf{A} - \frac{1}{c^2}\ddot{\mathbf{A}} &= -4\pi \mathbf{i}_{\text{eff}}\,, \quad \text{(a)} \\ \nabla^2 \Phi - \frac{1}{c^2}\ddot{\Phi} &= -4\pi \varrho_{\text{eff}}\,, \quad \text{(b)} \\ \operatorname{div} \mathbf{A} + \frac{1}{c}\dot{\Phi} &= 0\,. \qquad \text{(c)} \end{aligned}\right\} \tag{9}$$

We note that (9a—c) are sufficient conditions for the potentials to obey, in the sense that field strengths derived according to (4) form potentials obeying (9) which in their turn obey MAXWELL's equations (1).

§ 4. The relations (9a, b, c) are not independent of each other. Taking the div of the first equation and adding the time derivative of the second multiplied by 1/c to the former, we obtain with the help of (c) the continuity relation (3). We see thus that the relations (9a, b, c) together can only then be satisfied if the source densities on the right-hand side obey the continuity relation.

Furthermore, integrating (9a) twice with respect to t we find

$$\mathbf{A}(\mathbf{r}, t) = \mathbf{a}(\mathbf{r}) + t\dot{\mathbf{a}}(\mathbf{r}) + c^2 \int_0^t \int_0^t (\nabla^2 \mathbf{A} + 4\pi\, \mathbf{i}_{\text{eff}})\, dt'^2\,, \tag{10}$$

where $\mathbf{a}(\mathbf{r})$ and $\dot{\mathbf{a}}(\mathbf{r})$ define the initial condition for $\mathbf{A}(\mathbf{r}, t)$. From the relation (10) we can obtain $\mathbf{A}(\mathbf{r}, t)$ for any value of $t \neq 0$ if $\mathbf{a}(\mathbf{r})$ and $\dot{\mathbf{a}}(\mathbf{r})$ are given, e.g. by integrating in small steps.

Inserting the values of $\mathbf{A}(\mathbf{r}, t)$ obtained from (10) into (9c) we can obtain Φ for any value of t by integration. We find thus

$$\Phi(\mathbf{r}, t) = \varphi(\mathbf{r}) - c \int_0^t \operatorname{div} \mathbf{A}\, dt'\,. \tag{11}$$

Inserting (11) into (9b) and using the integrated continuity relation, i.e.

$$\varrho_{\text{eff}}(\mathbf{r}, t) = \varrho_0(\mathbf{r}) - c \int_0^t \operatorname{div} \mathbf{i}_{\text{eff}}\, dt'\,,$$

we find as the result of a short calculation

$$\nabla^2 \varphi(\mathbf{r}) = -4\pi \varrho_0(\mathbf{r})\,. \tag{12}$$

If (12) is to be valid for the whole of space then $\varphi(\mathbf{r})$ can be determined (apart from an additive constant) uniquely. We have

$$\varphi(\mathbf{r}) = \int \frac{\varrho_0(\mathbf{r}+\mathbf{R})}{R}\, d^3\mathbf{R}\,. \tag{13}$$

From (13) it follows that

$$\varphi \to 0 \quad \text{for} \quad \mathbf{r} \to \infty\,, \tag{14}$$

and we shall always suppose this condition to be valid. We see therefore that the system (9), (14), if we prescribe an initial condition of the type (5)—(8) for the potentials, admits exactly of one set of solution. Taking together this result with those of § 2 we see that the eqs. (9) may be uniquely solved, the solution corresponding to a field with a given initial condition

$$\mathbf{E}(\mathbf{r}, t) = \mathbf{E}_0(\mathbf{r})\,, \quad \mathbf{B}(\mathbf{r}, t) = \mathbf{B}_0(\mathbf{r})\,.$$

The above initial condition must be, of course, in accord with (1c) and (1d), further the source densities must obey the continuity relation.

§ 5. A particular solution of the wave eqs. (9) can be obtained in terms of the retarded potentials, i.e.

$$\mathbf{A}_{\text{ret}}(\mathbf{r}, t) = \int \frac{\mathbf{i}_{\text{eff}}(\mathbf{r}+\mathbf{R}, t')}{R}\, d^3\mathbf{R}\,, \tag{15a}$$

$$\Phi_{\text{ret}}(\mathbf{r}, t) = \int \frac{\varrho_{\text{eff}}(\mathbf{r}+\mathbf{R}, t')}{R}\, d^3\mathbf{R}\,, \tag{15b}$$

with

$$t' = t - \frac{R}{c}\,. \tag{15c}$$

Inserting equations (15) into (9) we find that the potentials expressed by (15- satisfy indeed the wave equations. The equations give thus a particular solu) tion of (9). As $\mathbf{A}_{\text{ret}}$ and Φ_{ret} are exactly determined by the expressions (15) in terms of the source densities these expressions cannot be made to satisfy an arbitrary initial condition.

When inserting (15) into (9) there appears some formal difficulty since the right-hand expressions (15) have singularities for $R = 0$ and are thus improper integrals. The integrals should be interpreted as being given by the proper integrals which are obtained when introducing polar coordinates, i.e. eq. (15) must be understood to signify

$$\mathbf{A}(\mathbf{r}, t) = \int_0^{2\pi} d\varphi \int_0^{\pi} \sin\vartheta\, d\vartheta \int_0^{\infty} R\, \mathbf{i}_{\text{eff}}(\mathbf{r}+\mathbf{R}, t')\, dR\,.$$

The integrand of the latter integral is regular. See also [1].

The general solution of (9) can be obtained by adding to (15) solutions of the homogeneous wave equations

$$\left.\begin{aligned} \nabla^2 \mathbf{A}_0 - \frac{1}{c^2} \ddot{\mathbf{A}}_0 = 0 \,, \\ \nabla^2 \Phi_0 - \frac{1}{c^2} \ddot{\Phi}_0 = 0 \,, \\ \operatorname{div} \mathbf{A}_0 + \frac{1}{c} \dot{\Phi}_0 = 0 \,. \end{aligned}\right\} \tag{16}$$

The system (16) admits solutions satisfying an arbitrary initial condition for the field as can be seen from the considerations of § 3 inserting there $\mathbf{i}_{\text{eff}} = 0$ and $\varrho_{\text{eff}} = 0$. Thus adding to the solutions (15) a suitable solution of (16) solutions of (9) satisfying an initial condition of the form (8a, b) for the field **E, B** can be obtained.

§ 6. The physical interpretation of the solutions of MAXWELL's equations, when putting

$$\mathbf{A} = \mathbf{A}_{\text{ret}} + \mathbf{A}_0 \,,$$

$$\Phi = \Phi_{\text{ret}} + \Phi_0 \,,$$

can be summarized as follows. The field **E, B** consists of two parts, i.e.

$$\mathbf{E} = \mathbf{E}_{\text{ret}} + \mathbf{E}_h \,, \quad \mathbf{B} = \mathbf{B}_{\text{ret}} + \mathbf{B}_h \,,$$

where the suffices "ret" and "h" refer to the parts obtained from the retarded potentials and the potentials obeying the homogeneous wave equations.

The retarded field $\mathbf{E}_{\text{ret}}$, $\mathbf{B}_{\text{ret}}$ is produced by the retarded action of charges ϱ_{eff} and currents $\mathbf{i}_{\text{eff}}$. I.e. the action of a charge $\varrho_{\text{eff}}(\mathbf{r}', t')$ which is at the time t' in a point $\mathbf{r}'$ is felt in a distant point $\mathbf{r}$ at a time $t = t' + |\mathbf{r} - \mathbf{r}'|/c$, thus the action of the charge and similarly the action of the currents spread with a velocity c.

§ 7. As far as the solutions of MAXWELL's equations are concerned the retarded field may be super-imposed by a homogeneous field which acts upon charges and currents and which, however, has no sources. The latter fields can be described as consisting of "wandering waves" travelling through space which have not been produced by sources, and they can therefore be taken to be part of the world just as are elementary particles or atoms.

It must be noted that such wandering waves once they fall upon matter excite atoms and thus induce these to emit radiation of the retarded type

thereby losing energy. Therefore, even if wandering waves exist they gradually diminish like e.g. radioactive material diminishes.

It is a question of observation whether wandering waves do or do not exist in nature. It may be noted that whenever we observe electromagnetic waves coming e.g. from the universe, we immediately look for the sources of these waves and thus automatically assume that they are of the retarded type.

It does not seem to be a far-fetched hypothesis that such wandering waves do not exist in nature. If we suppose this then we conclude that *Maxwell's equations give only necessary conditions for the motion of electromagnetic waves, but that only those particular solutions which can be expressed by retarded potentials are realized in nature.*

Advanced potentials

§ 8. Particular solutions of the wave equations can also be obtained in the form

$$\mathbf{A}_{\mathrm{adv}}(\mathbf{r}, t) = \int \frac{\mathbf{i}_{\mathrm{eff}}(\mathbf{r} + \mathbf{R}, t'')}{R} d^3\,\mathbf{R}\,, \tag{17a}$$

$$\Phi_{\mathrm{adv}}(\mathbf{r}, t) = \int \frac{\varrho_{\mathrm{eff}}(\mathbf{r} + \mathbf{R}, t'')}{R} d^3\,\mathbf{R} \tag{17b}$$

with

$$t' = t + R/c\,. \tag{17c}$$

The potentials obtained by the equations (17) satisfy also the wave equations (9), they obey initial conditions which are different from those which are obeyed by the solutions (15).

As both (15) and (17) are linear in the source densities we see that suitable linear combinations of (15) and (17) give also solutions of the wave equations.

Denoting by $\mathbf{A}_{\mathrm{ret}}\{\mathbf{i}'\}$ the potential obtained from (15a) by inserting $\mathbf{i}_{\mathrm{eff}} = \mathbf{i}'$ and similarly by $\mathbf{A}_{\mathrm{adv}}\{\mathbf{i}''\}$ that obtained from (17a) when putting $\mathbf{i}_{\mathrm{eff}} = \mathbf{i}''$, we see easily that

$$\mathbf{A}\{\mathbf{i}' + \mathbf{i}''\} = \mathbf{A}_{\mathrm{ret}}\{\mathbf{i}'\} + \mathbf{A}_{\mathrm{adv}}\{\mathbf{i}''\} \tag{18}$$

is a mixed potential which satisfies the wave equations if the current density $\mathbf{i}_{\mathrm{eff}} = \mathbf{i}' + \mathbf{i}''$.

Similarly, the mixed scalar potential

$$\Phi\{\varrho' + \varrho''\} = \Phi_{\mathrm{ret}}\{\varrho'\} + \Phi_{\mathrm{adv}}\{\varrho''\} \tag{19}$$

satisfies (9) for $\varrho_{\text{eff}} = \varrho' + \varrho''$.

By splitting the effective densities $\mathbf{i}_{\text{eff}}$, ϱ_{eff} in various ways into components $\mathbf{i}'$, ϱ' and $\mathbf{i}''$, ϱ'' solutions of (9) can be obtained satisfying various initial conditions. Thus it seems that the system (9) with a given initial condition can be satisfied with the help of suitable mixed potentials.

§ 9. The advanced potentials and therefore also the mixed potentials seem void of physical significance. The advanced potentials appear to describe the state of the field in a point $\mathbf{r}$ at a time t from the distribution of currents and charges at later times $t'' > t$.

Because of this some authors believe the potentials to be merely mathematical expressions which facilitate solving the wave equations, but which are without particular physical significance.

We do not agree with this view but wish to point out that a mixed solution of the wave equations can be written in the form

$$\begin{aligned} \mathbf{A}\{\mathbf{i}_{\text{eff}}\} &= \mathbf{A}_{\text{ret}}\{\mathbf{i}'\} + \mathbf{A}_{\text{adv}}\{\mathbf{i}''\}, \\ \Phi\{\varrho_{\text{eff}}\} &= \Phi_{\text{ret}}\{\varrho'\} + \Phi_{\text{adv}}\{\varrho''\} \end{aligned} \tag{20}$$

with $\mathbf{i}_{\text{eff}} = \mathbf{i}' + \mathbf{i}''$, $\varrho_{\text{eff}} = \varrho' + \varrho''$.
Considering (18) and (19) we can also write in place of (20)

$$\begin{aligned} \mathbf{A}\{\mathbf{i}_{\text{eff}}\} &= \mathbf{A}_{\text{ret}}\{\mathbf{i}_{\text{eff}}\} + \left(\mathbf{A}_{\text{ret}}\{\mathbf{i}' - \mathbf{i}_{\text{eff}}\} + \mathbf{A}_{\text{adv}}\{\mathbf{i}_{\text{eff}} - \mathbf{i}'\}\right), \\ \Phi\{\varrho_{\text{eff}}\} &= \Phi_{\text{ret}}\{\varrho_{\text{eff}}\} + \left(\Phi_{\text{ret}}\{\varrho' - \varrho_{\text{eff}}\} + \Phi_{\text{adv}}\{\varrho_{\text{eff}} - \varrho'\}\right). \end{aligned} \tag{21}$$

The expressions in the large brackets on the right-hand side of (21) give potentials which satisfy the homogeneous wave equations (16). Thus decomposing the mixed potentials in the fashion (21) we see that these can be understood as corresponding to the retarded field of the existing sources $\mathbf{i}_{\text{eff}}$, ϱ_{eff} superposed by the potentials of "wandering waves".

Thus, as far as we admit the existence of wandering waves, the mixed solutions when written in the form (21) obtain a simple physical significance.

§ 10. Comparing (15) and (17) we see that processes which have to be described by pure advanced potentials can also be taken as the time reversal of processes described by retarded potentials. If it is true that in nature only the retarded solutions occur then we see that processes containing electromagnetic radiation are irreversible in the sense that the processes reversed in time do not occur.

This is quite plausible when considering in particular electromagnetic processes. E.g. as the process reversed to that of the expansion of spherical waves emitted by an atom we have spherical waves contracting into an atom. The latter process cannot reasonably be supposed to occur.

Similarly, collisions between elementary particles which lead to emission of radiation are essentially irreversible, since in the reversed collision one would have to expect radiation to arrive out of space just in time to be absorbed by the colliding particles in order to ensure the "reversed collision".

It seems thus that electromagnetic phenomena are essentially irreversible in time. The reversed forms of real processes may satisfy Maxwell's equations, but they are of the type which are represented by advanced potentials only and thus cannot be supposed to occur.

Of course, with the help of wandering waves the reversal of a process might occur, as can be seen from relation (21). However, in this fashion such a reverse process could only occur with "heavenly help" — i.e. a long time before the process starts, waves which happen to be just suitable to produce the reverse effect would already have had to start from far distant points.

The probability of such an accidental reversal of a process must be taken to be negligibly small. Therefore, even if we do not exclude wandering waves we have to conclude that as a rule electromagnetic processes are irreversible in spite of the symmetry in time of Maxwell's equations.

REFERENCES

1. L. JÁNOSSY, Acta Phys. Hung., **20**, 59, 1966.

ФИЗИЧЕСКИЙ СМЫСЛ РЕТАРДИРОВАННОГО И УСОВЕРШЕНСТВОВАННОГО ПОТЕНЦИАЛОВ

Л. ЯНОШИ

Р е з ю м е

Истолкуется роль ретардированного и усовершенствованного потенциалов в решении уравнений Максвелла. Показывается, что решения могут представляться в виде наложения ретардированных решений и «бегущей волны», не имеющей источников. Если исключить возможность существования бегущих волн, то получается, что в природе наблюдаются лишь те частные решения уравнений Максвелла, которые представляются ретардированными потенциалами. Показывается далее, что из последнего предположения вытекает необратимость электромагнитных процессов.

REMARK ON SOME ASPECTS OF MAXWELL'S EQUATIONS

By

L. JÁNOSSY

CENTRAL RESEARCH INSTITUTE FOR PHYSICS, BUDAPEST

(Received 29. XII. 1964)

MAXWELL's equations are written in a form containing only **E** and **B** and the electric and magnetic polarizations. It is shown that expressions somewhat deviating from the usual ones can be obtained for the energy density and the POYNTING vector, if one separates carefully electromagnetic and non-electromagnetic sources of energy. The question of the ponderomotive force is discussed and it is shown that the state of a complicated physical system cannot be described by giving the value of its total energy and momentum and therefore no generally valid expression for the ponderomotive force can be given. All the same in any given case, when the mechanical properties of the system are taken into account, its behaviour can be understood.

I

The effective currents and charges

§ 1. Although MAXWELL's theory gives a complete and consistent description of electromagnetic phenomena, certain questions remain which have been giving rise to many discussions e.g. in Hungary GY. MARX—G. GYÖRGYI [1], G. GYÖRGYI [2], and J. SÁROSI [3]. Here we shall make some remarks upon the role of the field strengths **E**, **H** and the displacements **D**, **B** and also on the question of the so-called ponderomotive force.

§ 2. The electric field of a polarized dielectric can be described as that of electric dipoles inside the medium. The electric field strength **E** in a point **r** outside the dielectric is given by the relation

$$\mathbf{E} = -\operatorname{grad} \Phi \,, \tag{1a}$$

with

$$\Phi(\mathbf{r}) = -\int \frac{\operatorname{div} \mathbf{P}(\mathbf{r}+\mathbf{R})}{R}\, d^3\mathbf{R} \,, \tag{1b}$$

where we have introduced the variable $\mathbf{R} = \mathbf{r}' - \mathbf{r}$, $\mathbf{r}'$ representing coordinates of points inside the medium, and $\mathbf{P}(\mathbf{r}')$ the polarization vector. The integration is to be taken over the whole of the dielectric.

Sometimes a surface integral is added to the right-hand side of (1b) which takes care of the charges appearing on the surface of the dielectric.

We omit this integral supposing the polarization vector $\mathbf{P}(\mathbf{r}')$ to be a continuous function of $\mathbf{r}'$ and to change from its value inside the dielectric to zero in a thin surface layer.

It follows from (1a) and (1b) that the field outside the dielectric may also be regarded as due to charges with a density distribution

$$\varrho_P = -\operatorname{div} \mathbf{P}\,, \tag{1c}$$

where ϱ_P is the so-called Poisson charge.

§ 3. If $\mathbf{r}$ is a point inside the dielectric the right-hand expression of (1b) is an improper integral having a singularity for $\mathbf{R} = 0$. The latter integral can be replaced by a proper integral by introducing polar coordinates, i.e. we may write:

$$\int \frac{\operatorname{div} \mathbf{P}(\mathbf{r}+\mathbf{R})}{R}\, d^3\mathbf{R} = \int_0^{2\pi} d\varphi \int_0^{\pi} \sin\vartheta\, d\vartheta \int_0^{\infty} \operatorname{div} \mathbf{P}(\mathbf{r}+\mathbf{R})\, R dR\,. \tag{2}$$

It should be noted that to postulate (2) amounts to making an explicit assumption about the field acting inside the dielectric. Mathematically, other interpretations of the improper integral giving the field inside the dielectric are also possible. It is, however, not on the strength of mathematical reasoning but on that of experiment, that one has to decide which expression gives the field inside the dielectric correctly.

Usually it is supposed that the force upon a charge inside a dielectric is given by $e\mathbf{E}$. In principle, this statement may be tested experimentally, however, we do not think that at present there exists explicit evidence confirming it.

§ 4. The magnetic field produced by a magnetically polarized medium can be represented in analogy to (1a, 1b) in the following way:

$$\mathbf{H} = -\operatorname{grad} \Omega \tag{3a}$$

with

$$\Omega(\mathbf{r}) = -\int \frac{\operatorname{div} \mathbf{M}(\mathbf{R}+\mathbf{r})}{R}\, d^3\mathbf{R}\,, \tag{3b}$$

where $\mathbf{M}(\mathbf{r}')$ is the magnetic polarization in the point $\mathbf{r}'$. For a point $\mathbf{r}$ outside the magnetized body we can also write

$$\mathbf{H} = \operatorname{rot} \mathbf{A}\,, \tag{4a}$$

$$\mathbf{A}(\mathbf{r}) = \int \frac{\operatorname{rot} \mathbf{M}(\mathbf{R}+\mathbf{r})}{R}\, d^3\mathbf{R}\,. \tag{4b}$$

For points outside the magnetized medium the integrals (3b, 4b) are regular; for such points it can be shown, that (3a, b) lead to the same values for the field **H** as (4a, b). Indeed, applying the operation rot to (4b) and interchanging the integration with the operation rot we find, remembering the relation

$$\text{rot rot} = \text{grad div} - \nabla^2,$$

from (4a)

$$\mathbf{H} = \text{grad} \int \frac{\text{div}\, \mathbf{M}(\mathbf{R}+\mathbf{r})}{R}\, d^3\mathbf{R} - \int \frac{\nabla^2 \mathbf{M}(\mathbf{R}+\mathbf{r})}{R}\, d^3\mathbf{R}\,. \tag{5}$$

In the second term the operator ∇^2 is supposed to operate upon **r**. However, as **M** is a function of $\mathbf{R}+\mathbf{r}$ it can also be taken to operate on **R** without changing the value of the integral. In the latter case we find, integrating by parts and supposing that $\mathbf{M}(\mathbf{r}') = 0$ if $\mathbf{r}'$ is a point on the surface of the medium,

$$\int \frac{\nabla^2 \mathbf{M}(\mathbf{R}+\mathbf{r})}{R}\, d^3\mathbf{R} = \int \mathbf{M}(\mathbf{R}+\mathbf{r})\, \nabla^2 \left(\frac{1}{R}\right) d^3\mathbf{R}\,.$$

However, if **r** corresponds to a point outside the medium, i.e. $\mathbf{M}(\mathbf{r}') = 0$, then the integral is restricted to values $R > 0$ and we can take $\nabla^2\left(\frac{1}{R}\right) = 0$, thus the second term of (5) vanishes and we see that in this case (4a, b) is identical with (3a, b).

The expressions (4a, b) show, that the magnetic field outside the magnetized medium may also be regarded as due to currents which produce a vector potential $\mathbf{A}(\mathbf{r})$ and have a density

$$\mathbf{i}_M = \text{rot}\, \mathbf{M}\,. \tag{6}$$

We see thus that the field outside a magnetized medium can be represented purely mathematically by either a suitable magnetic charge density $-\text{div}\, \mathbf{M}$, or alternatively by a suitable current density $\mathbf{i}_M = \text{rot}\, \mathbf{M}$.

The question arises whether it is the current density or the magnetic charge density that correctly gives the field *inside* the medium.

This field when calculated from (4a, b) may be denoted by **B** and when obtained from (3a, b) by **H**. From (5) we verify (using a representation in terms of polar coordinates whenever we meet with improper integrals) that

$$\mathbf{B} = \mathbf{H} + 4\pi\mathbf{M}\,. \tag{7}$$

§ 5. Relations (3a, b) and (4a, b) when applied to the inside of the medium represent different transitions from discrete dipoles to the continuous dipole distribution — mathematically both transitions are equally possible, —

and only by experiment can it be decided which of the transitions gives the correct expression for the field strength.

From the observation of cosmic rays traversing permanent magnets and from that of neutrons passing through magnetized matter it seems to follow, that the force acting upon particles passing through a magnet is correctly described by **B**.

§ 6. It should be noted that in a medium which is in the process of being polarized electrically, the motion of the Poisson charges gives rise to convection currents of density

$$\mathbf{i}_P = \frac{1}{c}\dot{\mathbf{P}}, \tag{8}$$

where the dot (·) represents differentiation with respect to time. Thus the field arising from the electric and magnetic polarization of a medium may be regarded as produced by sources constituted of a charge density ϱ_P and a current density $\mathbf{i}_P + \mathbf{i}_M$. If we add to these the true charge densities ϱ and the densities $\mathbf{i}$ of the true currents, we find for the total sources of an electromagnetic field:

$$\begin{aligned} \varrho_{\text{eff}} &= \varrho - \operatorname{div}\mathbf{P}, \\ \mathbf{i}_{\text{eff}} &= \mathbf{i} + \frac{1}{c}\dot{\mathbf{P}} + \operatorname{rot}\mathbf{M}. \end{aligned} \tag{9}$$

It can easily be seen from (9) that the effective current and charge densities obey the continuity equation

$$\operatorname{div}\mathbf{i}_{\text{eff}} + \frac{1}{c}\frac{\partial\varrho_{\text{eff}}}{\partial t} = 0. \tag{9a}$$

§ 7. MAXWELL's equations can thus be written in the following form:

$$\left.\begin{aligned} \operatorname{rot}\mathbf{E} &= -\frac{1}{c}\dot{\mathbf{B}}, && \text{(a)} \\ \operatorname{rot}\mathbf{B} &= \frac{1}{c}\dot{\mathbf{E}} + 4\pi\,\mathbf{i}_{\text{eff}}, && \text{(b)} \\ \operatorname{div}\mathbf{E} &= 4\pi\,\varrho_{\text{eff}}, && \text{(c)} \\ \operatorname{div}\mathbf{B} &= 0. && \text{(d)} \end{aligned}\right\} \tag{10}$$

We see that the equations (10a—d) contain only **E**, **B** and the effective source densities ϱ_{eff} and $\mathbf{i}_{\text{eff}}$ which are produced not only by the true charges and currents, but also by those appearing inside the atoms of the polarized material.

It seems satisfactory that in the form (9) and (10) in which we have written MAXWELL's equations, the equations describing the electromagnetic field [eqs. (10)] are separated from those [eqs. (9)] which involve the properties of the material upon which the field acts.

II

Energy and momentum considerations

§ 8. Multiplying (10a) by $-\mathbf{B}$ and (10b) by $\mathbf{E}$ and adding the equations thus obtained, we find the following relation:

$$\operatorname{div} \mathcal{S} + \frac{\partial u}{\partial t} + c\, \mathbf{E}\, \mathbf{i}_{\text{eff}} = 0\,, \tag{11a}$$

where we have put

$$\mathcal{S} = \frac{c}{4\pi} (\mathbf{E} \times \mathbf{B})\,, \tag{11b}$$

$$u = \frac{1}{8\pi} (\mathbf{E}^2 + \mathbf{B}^2)\,. \tag{11c}$$

We suggest that (11a, b, c) represent the conservation law of the purely electromagnetic part of the energy. Thus we suggest that $\mathcal{S}$ (which has a form similar to that of the Poynting vector) represents the flow of energy and u the density of energy. The usual expression

$$\operatorname{div} \mathcal{S}' + \frac{\partial u'}{\partial t} + c\, \mathbf{E}\mathbf{i} = 0\,, \tag{12a}$$

where

$$\mathcal{S}' = \frac{c}{4\pi} (\mathbf{E} \times \mathbf{H})\,, \tag{12b}$$

$$\dot{u}' = \frac{1}{4\pi} (\mathbf{E}\dot{\mathbf{D}} + \mathbf{H}\dot{\mathbf{B}})\,, \quad \text{with } \mathbf{D} = \mathbf{E} + 4\pi\, \mathbf{P} \tag{12c}$$

contains mathematically the same relation as (11a, b, c). We note that unless ε and μ are constant in time, $\dot{u}'$ is not a total time differential and cannot be integrated without the explicit knowledge of the details of the polarization processes.

We shall discuss further below the different physical implications contained in the relations (11) and (12).

§ 9. Multiplying vectorially (10a) from the left by **E** and similarly (10b) by **B** we obtain with the notations (11b, c), making use of well-known vector relations

$$\mathrm{Div}\,\mathfrak{T} + \frac{1}{c^2}\dot{\mathscr{P}} + \mathbf{f}_{\mathrm{eff}} = 0\,, \tag{13a}$$

where

$$\mathbf{f}_{\mathrm{eff}} = \mathbf{E}\,\varrho_{\mathrm{eff}} + \mathbf{i}_{\mathrm{eff}} \times \mathbf{B}\,, \tag{13b}$$

$$\mathfrak{T} = -\frac{1}{4\pi}(\mathbf{E} \circ \mathbf{E} + \mathbf{B} \circ \mathbf{B}) + \mathbf{1}\,u\,. \tag{13c}$$

The relations (13a, b, c) can be most easily understood as describing the exchange of momentum between the field and the matter. Indeed, $\mathbf{f}_{\mathrm{eff}}$ is the density of force excerted by the field. $\mathbf{f}_{\mathrm{eff}}$ has two parts:

$$\mathbf{f}_{\mathrm{eff}} = \mathbf{f} + \mathbf{f}_P\,, \tag{14}$$

where

$$\mathbf{f} = \varrho\mathbf{E} + \mathbf{i} \times \mathbf{B}\,, \tag{14a}$$

is the density of the Lorentz force exerted upon the charge and the currents traversing the matter and

$$\mathbf{f}_P = \varrho_P\,\mathbf{E} + (\mathbf{i}_P + \mathbf{i}_M) \times \mathbf{B}\,,$$

is the density of force excerted upon the atoms. $\mathbf{f}_P$ represents the action of the outside field upon the currents and the charge inside the individual atoms. Suppose that

$$\frac{1}{c}\mathscr{P} = \mathbf{G} \tag{15}$$

gives the momentum density of the field and that the tensor $\mathfrak{T}$ represents the density of flow of momentum. (13a) can then be understood to mean that the electromagnetic momentum flowing into a certain volume there produces partly an increase of electromagnetic momentum at a rate of $\frac{1}{c}\dot{\mathscr{P}}$ and partly transfers momentum to the matter contained in that volume. The total rate of transfer of electromagnetic momentum to other forms of momenta has a density $\mathbf{f}_{\mathrm{eff}}$. This transferred momentum is partly taken up by the atoms and partly by the true currents and charges.

III

Non-electromagnetic contributions to energy and momentum density

§ 10. The relations (11) and (13) describing the flow of energy and momentum are mathematically equivalent to the relations used usually, we have only grouped the terms in an unusual way. We presently discuss the significance of the difference between our expressions and those usually used.

1. If $\varepsilon =$ constant, the electric part of the energy is usually taken as $u'_{\mathrm{el}} = \frac{1}{8\pi}\mathbf{ED}$. We use instead $u_{\mathrm{el}} = \frac{1}{8\pi}\mathbf{E}^2$ the difference between the two expressions being given by

$$u'_{\mathrm{el}} - u_{\mathrm{el}} = \frac{1}{2}\mathbf{E}\,\mathbf{P}\,.$$

More generally, when ε may depend on $\mathbf{E}$ or other quantities, we have

$$u'_{\mathrm{el}} - u_{\mathrm{el}} = \int_0^{\mathbf{P}} \mathbf{E}\,d\,\mathbf{P}\,. \tag{16a}$$

The above expressions give the density of work done by the electric field. This work appears as *mechanical* or *elastic* energy which is stored in the dipoles. Thus the quantity u'_{el} includes, apart from the purely electric energy density, also the density of mechanical energy which is stored in the polarized atoms. $u_{\mathrm{el}} = \frac{1}{8\pi}\mathbf{E}^2$ does not include this energy density, therefore it can be taken as purely electric energy.

That energy of the amount given by (16a) is really stored in a polarized dipole can also be seen when remembering that a polarized dipole once the outside field is switched off starts to oscillate and emits the energy stored according to (16a) in the form of electromagnetic radiation.

2. The magnetic density of energy is usually written as

$$u'_{\mathrm{magn}} = \frac{1}{4\pi}\int \mathbf{H}\,d\mathbf{B}\,,$$

thus we find writing $u_{\mathrm{magn}} = \frac{1}{8\pi}\mathbf{B}^2 = \frac{1}{4\pi}\int \mathbf{B}\,d\mathbf{B}$

$$u'_{\mathrm{magn}} - u_{\mathrm{magn}} = -\int \mathbf{M}d\,\mathbf{B}\,. \tag{16b}$$

The difference between the two expressions for the magnetic energy density as given in (16b) corresponds to non-magnetic energy as can be seen from the following consideration.

If we polarize a medium by turning its magnetic dipoles into the direction of the external magnetic field, we gain energy as the magnetic field itself produces torques on the dipoles which try to turn these into the direction of the field. However, while the dipoles are adjusted into the direction of the field, currents are induced inside the atoms which try to diminish the magnetic moments of the dipoles. In the process of polarization these currents have to be overcome by some outside source and the energy must be taken up from the source so as to maintain the dipole moments. This results in a transfer of energy from some non-magnetic form of energy to magnetic field energy and thus the total increase of energy in the process of polarization is less, than the increase of purely magnetic energy, the difference being given by (16b).

In order to illustrate the above consideration on hand of a macroscopic model we remember that a solenoid carrying current, when placed into a magnetic field, will try to turn in such a way that its own field becomes parallel to the external field. However, while the solenoid moves the outside field induces currents in it opposing the current which already flows and therefore the EMF acting on the solenoid has to do work in order to compensate the induced currents and to keep the magnetic moment of the solenoid constant. Taking the energy balance of the whole process we find that there is an increase of purely magnetic energy accompanied by some decrease of, say chemical energy, which was used to maintain the current in the solenoid.

The reduction of non-magnetic energy in the process of polarization can also be illustrated as follows. Consider atoms carrying dipole moments as rigid bodies rotating round an axis. The turning of such rotating atoms into the direction of an outside magnetic field require work to be done in order to maintain the rotation of the atoms. Thus mechanical energy is transformed into magnetic energy equal to the difference $u'_{\text{magn}} - u_{\text{magn}}$.

We see thus that u represents the density of purely electromagnetic energy, while u' represents electromagnetic energy mixed with other forms of energy stored in the atoms.

3. The POYNTING vector is usually written in the form

$$\mathcal{P}' = \frac{c}{4\pi}(\mathbf{E} \times \mathbf{H}). \tag{17}$$

The difference

$$\mathcal{P}_M = \mathcal{P}' - \mathcal{P} = -c(\mathbf{E} \times \mathbf{M}) \tag{17a}$$

corresponds to the flow of density $u_M = u' - u$ of mechanical energy induced by the electromagnetic field, which is carried by the dipoles while interacting with the field.

It is interesting to note, that such a flow may occur even if $\mathbf{E}$, $\mathbf{M} = \text{const.}$, thus in a state where the dipoles do not move and do not change their polarization.

§ 11. So as to see more clearly the nature of the flow $\mathscr{P}_M$ we note that

$$\operatorname{div} \mathscr{P}_M = - c \operatorname{div} (\mathbf{E} \times \mathbf{M}) = c(\mathbf{E} \operatorname{rot} \mathbf{M} - \mathbf{M} \operatorname{rot} \mathbf{E}) .$$

With the help of (10) and (6) the right-hand expression can be rewritten and we find

$$\operatorname{div} \mathscr{P}_M = c \, \mathbf{E} \, \mathbf{i}_M + \mathbf{M}\dot{\mathbf{B}} . \tag{18}$$

The second term of (18) gives the flow carried by the magnetic dipoles in the process of their adjustment. There is no term in (18) corresponding to the motion of the electric dipoles. The reason for this is that

$$\mathbf{E} \, \mathbf{i}_P - \frac{1}{c} \mathbf{E}\dot{\mathbf{P}} = 0 , \tag{19}$$

thus (18) may also be written

$$\operatorname{div} \mathscr{P}_M = c \, \mathbf{E}(\mathbf{i}_M + \mathbf{i}_P) + \mathbf{M}\dot{\mathbf{B}} - \mathbf{E}\dot{\mathbf{P}} . \tag{20}$$

We may therefore include the energy transfer carried by electric dipoles in the right-hand side of (18); however, this does not contribute to $\operatorname{div} \mathscr{P}_M$.

The work done by the electric field on the Poisson charges ϱ_M appears on the spot as potential energy and this type of energy transfer does not contribute to the flow of energy.

§ 12. The first term in the right-hand expression of (18) shows that mechanical energy is deposited at a constant rate when the field is constant in time and space.

The mechanism of the latter flow can be illustrated when considering the following schematic model.

As the model of a dipole consider a charged rigid body rotating freely with a constant angular velocity $\boldsymbol{\omega}$. Suppose at the centre of gravity of the system a point charge which neutralizes the system as a whole.

If such a dipole is brought into a homogeneous electric field $\mathbf{E}$ the direction of which is perpendicular to $\boldsymbol{\omega}$ we find that the electric force tries to accelerate one side of the rotating body and to decelerate the other (see Fig. 1). The inner forces keeping the rotating body together, maintain the uniform rotation. In this way the electric force transfers energy to the parts which have a component of velocity parallel to $\mathbf{E}$ and takes up energy from the other parts. Thus there is a steady flow of elastic energy across the system. The direction of flow is perpendicular to both $\mathbf{E}$ and $\boldsymbol{\omega}$ and its value is given quantitatively by (17a).

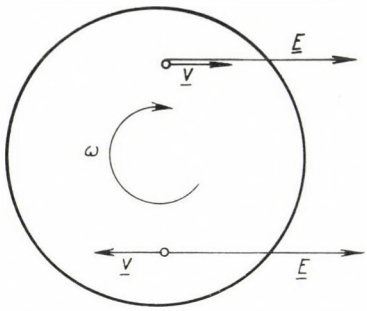

Model of magnetic dipole

Fig. 1

IV

The ponderomotive forces

§ 13. We have thus shown how the purely electromagnetic energy, the energy flow and the momentum of a system can be described and separated from the contributions of mechanical or elastic energy and momentum contained in the material.

The densities u', $\mathscr{P}'$ and $\mathbf{G}'$ contain thus apart from the electromagnetic densities also contributions of a different nature.

The reason why the quantities u', $\mathscr{P}'$ and $\mathbf{G}'$ were originally introduced into the theory and not the quantities u, $\mathscr{P}$ and $\mathbf{G}$ is that at the time when the theory was worked out one tried to describe the *total* energy and the *total* momentum of systems.

Such attempts must, however, fail unless one is satisfied with an oversimplified model of matter. The energy and momentum of real matter under the influence of an electromagnetic field is determined by many factors and cannot be described without a detailed analysis of the physical properties of the material involved. We note that apart from the electromagnetic and the elastic energy a real physical system contains also heat and chemical energy and other forms of energy.

Among other effects an electromagnetic field produces complicated elastic stresses in a mechanical system and changes its elastic energy in a complicated way. In this way e.g. electrostriction and the magnetostriction also contribute to the total energy.

§ 14. In BECKER's text-book [4] the MAXWELL tensor is extended by terms giving the electrostriction. This is done in an attempt to complete the expressions for energy and momentum density. However, the term given by

BECKER accounts only for one of the many contributions of non-electromagnetic energy and momentum.

We think that a satisfactory description is obtained from the beginning if we limit ourselves to the purely electromagnetic part of energy and momentum, i.e. if we use u, $\mathcal{P}$ and $\mathbf{G}$. We must be aware when doing so that for the description of the interaction with matter the non-electromagnetic properties of the interacting material have to be taken into account separately. The connection between electromagnetic and other properties of the material is introduced by giving the dependence of the polarization vectors $\mathbf{P}$ and $\mathbf{M}$ on the electromagnetic field and the state of the matter. The connections $\mathbf{P} = \varkappa\mathbf{E}$ and $\mathbf{M} = \frac{\chi}{\mu}\mathbf{B}$ must be regarded as very rough approximations.

§ 15. We are now in a position to give a simple answer to the question: "which is the expression that gives the correct value for the ponderomotive force a field excerts upon matter?"

We note, that the term ponderomotive force is not very clear in itself. It was introduced at a time when one tried to formulate general laws for matter as such, with as little regard as possible to the real and varying properties of material systems.

The energy and momentum transferred by radiation to a closed physical system are described by relations (11) and (13) which in the integral form can also be written in the following way:

$$\left.\begin{aligned} -\int \mathcal{P}\, d\mathbf{S} &= \frac{d}{dt}\int u dV + c\int \mathbf{E}\, i_{\text{eff}}\, dV\ , \quad \text{(a)} \\ -\int \mathfrak{T}\, d\mathbf{S} &= \frac{d}{dt}\int \mathbf{G} dV + \int \mathbf{f}_{\text{eff}}\, dV\ . \qquad \text{(b)} \end{aligned}\right\} \tag{21}$$

Relation (21a) shows that part of the electromagnetic energy flowing into a surface $\mathbf{S}$ produces there electromagnetic energy of density u, the remaining part of it being transferred into other types of energy at a rate of $\mathbf{E}\,\mathbf{i}_{\text{eff}}$. The latter energy appears in two parts: $\mathbf{E}\,\mathbf{i}$ is the work done on real currents and charges, while the rest is transferred to the atom of the system.

Similarly (21b) shows that the total momentum flow $\mathfrak{T}$ through the surface $\mathbf{S}$ remains partly in the form of electromagnetic momentum with a density $\mathbf{G}$, the rest being transferred to the matter. The transferred part can again be divided into one part which is taken up by the currents and the rest which is taken up by the atoms of the system.

§ 16. We see thus clearly what happens to the energy and the momentum flowing through the surfaces S into the system occupying the volume V.

The "ponderomotive force" might be defined as the rate of increase of the momentum of the system. However, such a description is purely formal

and it does not help to clarify e.g. the behaviour of a mechanical system in a collision.

We may e.g. try to determine the momentum of a system by letting it collide with a solid wall, measuring the recoil of the wall.

The result of such a collision depends very much on the internal properties of the colliding systems. It depends also on the mode of the collision, i.e. whether the various types of momenta contained in the system all take part in the collision or not.

If the colliding system is in the solid state, then it is likely that the momenta of its atoms will be transferred to the wall. It is, however, an open question (and depends on the details of the collision process) whether the momentum carried by the currents flowing inside the colliding system is or is not transferred in the collision. Further the electromagnetic waves contained in the colliding body might themselves be reflected on the wall, but they may also penetrate into the wall according to circumstances. We see therefore that it is impossible to foretell on general grounds (without going into the details of the collision) what the result of the collision will be.

To illustrate the problem, we consider a box which contains a number of loose bodies and which collides with a wall. In the first instant the momentum transfer in such a collision will be only that of the box itself, as the bodies inside will continue to move owing to their inertia. These bodies will, however, transfer their momentum when striking the front wall of the box from the inside. — Whether their momentum is then transferred to the wall depends on whether this secondary collision takes place soon enough after the first impact.

A material system containing atoms, currents and radiation may be compared with such a box. It is futile to try to define its momentum as if it was a "mass point". A description that fully accounts for the actual state of such a system must give the distribution of its momentum over its various parts and in particular over its atoms and further the distribution of the currents and the radiation contained in it.

Under clearly specified circumstances the behaviour of the system as a whole can be described by some integral over the mentioned distributions. There is no law giving "the momentum of the system" regardless of the connection in which this momentum is to act.

The ponderomotive force was introduced in an attempt to give an expression for the change of momentum of a physical system under the influence of radiation. However, once we realize that the behaviour of a system cannot be characterized simply by one momentum vector we see that the concept of the ponderomotive force is an oversimplified one. When considering a real process it is necessary to determine the detailed form of the energy and momentum transfer between the various components of the body. Only by

taking into account their physical properties can we determine what will happen to the body under the influence of the electromagnetic field.

V

A remark on the Poynting vector

§ 17. The POYNTING vector seems to us to give the flow of density of energy in any electromagnetic field. Sometimes it is stated that the POYNTING vector has only meaning in those parts of space where div $\mathcal{P} \neq 0$, i.e. where a real exchange of energy takes place.

We venture to suggest that $\mathcal{P}$ always gives the density of flow of energy, even if this flow happens to be a stationary one with div $\mathcal{P} = 0$.

Consider e.g. the crossed fields of a charge and a permanent magnet. In the latter field $\mathbf{E} \times \mathbf{B}$ does not vanish and we expect the energy to flow steadily in a stationary fashion. We think this picture gives a good description of the real state of affairs.

We note that as long as the charge and the magnet giving rise to the crossed field are widely separated, the POYNTING vector has only negligible values and there is practically no flow of energy. If the magnet is brought into the vicinity of the charge, the energy of the field is redistributed during this motion, and the energy flow starts. Once the magnet has reached its final position the energy has reached a state of stationary flow and through inertia this state persists further as long as the charge and the magnet remains in this position.

REFERENCES

1. G. MARX and G. GYÖRGYI, Acta Phys. Hung., **3**, 213, 1954.
2. G. GYÖRGYI, Magy. Fiz. Folyóirat, **5**, 187, 1957.
3. J. SÁROSI, Magy. Fiz. Folyóirat, **12**, 439, 1964.
4. M. ABRAHAM and R. BECKER, Classical Theory of Electricity and Magnetism, Translation from the German, B. G. Teubner, Leipzig, 1932.

ЗАМЕЧАНИЕ О НЕКОТОРЫХ ПОЛОЖЕНИЙ УРАВНЕНИЙ МАКСВЕЛЛА

Л. ЯНОШИ

Р е з ю м е

Уравнения Максвелла написаны в форме, содержащей только **E**, **B**, и электрическую и магнитную поляризаций. Показывается, что для плотности энергии и вектора Пойнтинга можно вывести выражения, в некоторой степени отличающиеся от обыкновенных, если произвести тщательное разделение источников электромагнитного и неэлектромагнитного происхождения. Дискутируется вопрос пондеродвижущей силы и найдено, что сложные физические системы не могут быть описаны заданием их полной энергии и количества движения, и, таким образом, нет возможности для составления общего с точки зрения его действительности выражения для пондеродвижущей силы. Несмотря на это, принимая во внимание все механические свойства системы, поведение ее может быть понято.

ON THE REPRESENTATION OF THE LORENTZ DEFORMATION

By

L. JÁNOSSY

CENTRAL RESEARCH INSTITUTE FOR PHYSICS, BUDAPEST

(Received 29. XII. 1964)

It is shown that with the help of the eigenvalues of LORENTZ matrices LORENTZ transformations can be brought into a standard form. Using this standard form we find that any LORENTZ deformation appears, relative to a suitable system of reference, as an acceleration in a fixed direction, and a rotation through a fixed angle around the direction of acceleration.

§ 1. In a number of papers [1—4] we have dealt with the physical interpretation of the LORENTZ transformation. In the course of the analysis a problem arose with which we want to deal in the present paper.

Using the terminology explained formerly we may denote events and also physical systems by Gothic letters and use Latin symbols for their representation relative to some system of reference. Thus we denote an event by $\mathfrak{E}$ and its representation relative to a system of coordinates K by

$$E = K(\mathfrak{E}) ,$$

where E stands short for a four-component vector $\mathbf{x}$,

$$\mathbf{x} = \mathbf{r}, t .$$

We shall make use of LORENTZ systems of reference only. Such a system is an inertial system in which the measures of coordinates and clocks are adjusted by means of light signals, these adjustments being such that light appears to be propagated isotropically relative to the system of reference when this is expressed in the coordinates thus adjusted.

More precisely, the LORENTZ system can be characterized in the following manner. Consider two events $\mathfrak{E}_1$ and $\mathfrak{E}_2$, where $\mathfrak{E}_1$ should be the start of a light signal from a point P_1 and $\mathfrak{E}_2$ its arrival in a point P_2. The coordinates of these events relative to a system K may be written

$$\mathbf{x}_1 = \mathbf{r}_1, t_1 \qquad \mathbf{x}_2 = \mathbf{r}_2, t_2 .$$

The system K is a LORENTZ system if for any values of $\mathbf{r}_1$ and $\mathbf{r}_2$ we have

$$\xi \Gamma \xi = 0 , \tag{1}$$

where $\xi = \mathbf{x}_2 - \mathbf{x}_1$ and Γ is the matrix with elements

$$\Gamma_{\nu\mu} = \begin{cases} 1 & \text{if} \quad \nu = \mu = 1, 2, 3 \\ 0 & \text{if} \quad \nu \neq \mu \\ -c^2 & \text{if} \quad \nu = \mu = 4. \end{cases} \tag{2}$$

§ 2. The representations of an event relative to different systems of reference are connected by LORENTZ transformations, thus if $\mathbf{x}'$ is the representation of $\mathfrak{E}_1$ relative to K' and $\mathbf{x}$ that relative to K we have

$$\mathbf{x}' = \Lambda\mathbf{x} + \lambda\,, \tag{3}$$

where Λ is a LORENTZ matrix obeying the relation

$$\tilde{\Lambda}\,\Gamma\,\Lambda = \Theta\,\Gamma\,, \quad \Theta \neq 0\,, \tag{4}$$

or the equivalent relation

$$\Lambda^{-1} = \Theta^{-1}\,\Gamma^{-1}\,\tilde{\Lambda}\,\Gamma \tag{5}$$

and λ is a quantity with four constant components.

Instead of (3) we can also write

$$\mathbf{x}' = \mathfrak{L}_{\mathbf{p}}\,(\mathbf{x})\,. \tag{6}$$

$\mathfrak{L}_{\mathbf{p}}$ is the LORENTZ transformation leading from the coordinates relative to K to those relative to K', the suffix $\mathbf{p}$ specifying the particular Lorentz transformation. Thus the suffix $\mathbf{p}$ is a parameter with eleven components and it contains also one sign; we may write more explicitly

$$\mathbf{p} = \Theta, \mathbf{O}, \mathbf{v}, \boldsymbol{\lambda}, \varepsilon \text{ with } \Theta > 0, \quad |\,\mathbf{v}\,| < c, \quad \varepsilon = \pm 1, \tag{7}$$

where $\mathbf{O}$ is an orthogonal matrix obeying

$$\tilde{\mathbf{O}}\,\mathbf{O} = \mathbf{1}\,. \tag{8}$$

$\mathbf{v}$ is a vector with three components (giving the velocity of K' relative to K in measures of K), λ contains the four inhomogeneous terms of (3) and $\varepsilon = \Lambda_{44}/|\,\Lambda_{44}\,|$ defines the convention of time measure in K' relative to that in K. $\Theta > 0$ gives the ratio of units of time and length in K relative to those in K'.

The set of transformations with parameters $\mathbf{p}$ form a group and are also called improper LORENTZ transformations. The proper LORENTZ transformations are a subgroup of these transformations with parameters

$$\mathbf{q} = \mathbf{O},\ \mathbf{v},\ \lambda, \tag{9}$$

with the restrictions

$$\Theta = 1, \quad \det \mathbf{O} = +1, \quad |v| < c, \quad \varepsilon = +1. \tag{9a}$$

§ 3. Consider a physical system of some kind, it may be denoted by $\mathfrak{P}$. The system may consist of a number of points $\mathfrak{P}_1, \mathfrak{P}_2, \ldots, \mathfrak{P}_N$ moving under the influence of inner and outer forces.

The representation of $\mathfrak{P}$ relative to K a be written

$$\mathbf{P} = K(\mathfrak{P}),$$

where $\mathbf{P}$ consists of points $P_1, P_2, \ldots, P_N$ with coordinate vectors at the time t

$$\mathbf{r}_n(t), \qquad n = 1, 2, \ldots, N$$

in measures of K.

The representation

$$\mathbf{P}' = K'(\mathfrak{P})$$

of $\mathfrak{P}$ relative to K' can be obtained from that relative to K by a LORENTZ transformation. Thus the coordinate vector $\mathbf{r}'_n(t')$ of P'_n relative to K' at the time t' (in measures of K') is found to be

$$\mathbf{r}^*_n(t') = \mathbf{L}\mathbf{r}_n(t_n) + \mathbf{u}' t_n + \mathbf{l}, \tag{10a}$$

where the values of t_n have to be chosen so as to satisfy

$$t' = \mathbf{u}\,\mathbf{r}_n(t_n) + B\,t_n + t_0\,. \tag{10b}$$

Here we have expressed Λ and λ in the following manner

$$\Lambda = \begin{pmatrix} \mathbf{L} & \mathbf{u}' \\ \mathbf{u} & B \end{pmatrix}, \quad \lambda = \mathbf{l}, t_0 \tag{10c}$$

and $\mathbf{L}$ is a third-order matrix, $\mathbf{u}$, $\mathbf{u}'$, $\mathbf{l}$ are three-component vectors and B, t_0 scalars. The t_n, $n = 1, 2, \ldots, N$ can be regarded as auxiliary quantities.

§ 4. The transformation (10a, b, c) can be given also a different meaning. Writing

with
$$\left.\begin{aligned} \mathbf{r}^*_n(t) &= \mathbf{L}\mathbf{r}_n(t_n) + \mathbf{u}' t_n + \mathbf{l}, \\ t &= \mathbf{u}\,\mathbf{r}_n(t_n) + Bt_n + t_0 \end{aligned}\right\} \tag{11}$$

we may regard the $\mathbf{r}^*_n$ as the coordinate vectors relative to K of points P^*_n at the time t (relative to K).

Thus $\mathbf{P}^*$ is the representation in K of a system $\mathfrak{P}^*$ in K and we may write

$$\mathbf{P} = K(\mathfrak{P}), \qquad \mathbf{P}^* = K(\mathfrak{P}^*), \tag{12}$$

and we call $\mathfrak{P}^*$ the *Lorentz deformed system* $\mathfrak{P}$. In place of (11) we shall also write

$$\mathbf{P}^* = L_{\mathfrak{q}}(\mathbf{P}), \tag{13}$$

where $L_{\mathfrak{q}}$ stands for the transformation (11). We use the symbol L in place of $\mathfrak{L}$ to denote that the transformation does not lead from one system of reference to another, but that it signifies a change of one physical system into another (all measures taken relative to one system of reference K only).

We have written $\mathfrak{q}$ for the suffix of L because we shall consider only deformations corresponding to proper LORENTZ transformations, thus we restrict the value of $\mathfrak{q}$ according to (9a). For the transition between LORENTZ systems of reference we may use both proper and improper transformations. We may thus use for coordinate transformations all those with two parameters as given by (7).

§ 5. The representations of $\mathfrak{P}$ and $\mathfrak{P}^*$ relative to a system K' can be written

$$\left.\begin{aligned} \mathbf{P}' &= K'(\mathfrak{P}) = \mathfrak{L}_p(\mathbf{P}), \\ \mathbf{P}^{*\prime} &= K'(\mathfrak{P}^*) = \mathfrak{L}_p(\mathbf{P}^*). \end{aligned}\right\} \tag{14}$$

From (13) and (14) we find also

$$\mathbf{P}^{*\prime} = L_{\mathfrak{q}'}(\mathbf{P}) \tag{15}$$

with

$$L_{\mathfrak{q}'} = \mathfrak{L}_{\mathfrak{p}} L_{\mathfrak{q}} \mathfrak{L}_{\mathfrak{p}}^{-1}, \tag{16}$$

where $L_{\mathfrak{q}'}$ is the LORENTZ transformation which is obtained as the superposition of three LORENTZ transformations.

From (15) we conclude that *the representations* $\mathbf{P}'$ *and* $\mathbf{P}^{*\prime}$ *of* $\mathfrak{P}$ *and* $\mathfrak{P}^*$ *are connected through a Lorentz transformation in any system of reference, provided they are connected by a Lorentz transformation in at least one system of reference.*

We may thus write instead of (13) more generally

$$\mathfrak{P}^* = L_{\mathfrak{q}}(\mathfrak{P}), \tag{17}$$

where $\mathfrak{q}$ characterizes the LORENTZ deformation itself and $\mathfrak{q}$ can be represented in various systems of reference as

$$K(\mathfrak{q}) = \mathfrak{q}, \quad K'(\mathfrak{q}) = \mathfrak{q}', \ldots, \text{etc.}$$

§ 6. The problem we want to deal with in this paper is to determine the set of LORENTZ transformations which appear as the representations of a given LORENTZ deformation $L_{\mathfrak{q}}$ if we consider all possible LORENTZ systems of reference.

Consider thus two representations $L_{\mathfrak{q}}$ and $L_{\mathfrak{q}'}$ of $L_{\mathfrak{q}}$. We have

$$L_{\mathfrak{q}'} = \mathfrak{L}_{\mathfrak{p}} L_{\mathfrak{q}} \mathfrak{L}_{\mathfrak{p}}^{-1} . \tag{18}$$

Writing (18) more explicitly, we see from (3) and (6) that (18) gives no restriction as to the inhomogeneous part of the transformation $\mathbf{L}_{\mathfrak{q}'}$. Denoting the LORENTZ matrices corresponding to the transformations in (18) by $\Lambda_{\mathfrak{q}'}$ $\Lambda_{\mathfrak{q}}$ and $\Lambda_{\mathfrak{p}}$ we may thus write in place of (18)

$$\Lambda_{\mathfrak{q}'} = \Lambda_{\mathfrak{p}} \Lambda_{\mathfrak{q}} \Lambda_{\mathfrak{p}}^{-1} . \tag{19}$$

From (19) we verify easily that $\Lambda_{\mathfrak{q}'}$ defines a proper LORENTZ transformation if $\Lambda_{\mathfrak{q}}$ does so, no matter whether $\Lambda_{\mathfrak{p}}$ defines a proper or improper LORENTZ transformation. We see thus, that *we can restrict the Lorentz deformations to those represented by proper Lorentz transformations without restricting the systems of reference to those connected by proper Lorentz transformations only.*

§ 7. With the help of a suitable matrix $\mathbf{S}$ we can transform $\Lambda_{\mathfrak{q}'}$ into diagonal form, we have

$$\mathbf{S}^{-1} \Lambda_{\mathfrak{q}'} \mathbf{S} = \mathbf{D} \quad = \text{diagonal matrix.} \tag{20}$$

We shall also write

$$D_{\nu\mu} = \delta_{\nu\mu} D_{\nu} ,$$

where D_{ν} are the eigenvalues of $\Lambda_{\mathfrak{q}'}$. Comparing (19) and (20) we see that the D_{ν} are also the eigenvalues of $\Lambda_{\mathfrak{q}}$. We conclude, that *two Lorentz matrices* $\Lambda_{\mathfrak{q}}$ *and* $\Lambda_{\mathfrak{q}'}$ *can only then represent the same Lorentz deformation if they possess the same eigenvalues.*

§ 8. We prove the reverse of the above statement also to be true. This means that if two LORENTZ matrices $\Lambda_{\mathfrak{q}}$ and $\Lambda_{\mathfrak{q}'}$ possess the same eigenvalues then there exist such LORENTZ systems of reference K and K' relative to which $\Lambda_{\mathfrak{q}}$ and $\Lambda_{\mathfrak{q}'}$ represent the deformation $\mathfrak{q}$.

So as to prove the above statement we write down as a first step the secular equation for a LORENTZ matrix $\Lambda_{\mathfrak{q}}$, thus

$$\det (\Lambda_{\mathfrak{q}} - D_{\nu} \mathbf{1}) = 0, \qquad \nu = 1, 2, 3, 4. \tag{21}$$

Explicitly written we find, remembering that $\det \Lambda_{\mathfrak{q}} = 1$

$$x^4 - \text{spur}\, \Lambda_{\mathfrak{q}}^{-1} x^3 + c_2 x^2 - \text{spur}\, \Lambda_{\mathfrak{q}} x + 1 = 0 \tag{22}$$

for

$$x = D_\nu, \qquad \nu = 1, 2, 3, 4,$$

where c_2 is a function of the elements of Λ_q. From (5) we see that

$$\text{spur } \Lambda_q^{-1} = \text{spur } \Lambda_q ,$$

therefore the equation (22) is symmetric and the four solutions D_ν contain pairs of reciprocal values. We may write

$$D_1 = \frac{1}{D_2} = a, \qquad D_3 = \frac{1}{D_4} = b , \tag{23}$$

where

$$a, b \neq 0.$$

Consider a particular transformation with the matrix

$$\Lambda_{\varphi v} = \begin{pmatrix} \cos\varphi & -\sin\varphi & 0 & 0 \\ \sin\varphi & \cos\varphi & 0 & 0 \\ 0 & 0 & B & -Bv \\ 0 & 0 & -Bv/c^2 & B \end{pmatrix}, \tag{24a}$$

$$B = \frac{1}{\sqrt[+]{1 - v^2/c^2}} .$$

We find that in this particular case the eigenvalues are given as

$$D_1 = e^{i\varphi}, \quad D_2 = e^{-i\varphi}, \quad D_3 = \sqrt[+]{\frac{c - v}{c + v}}, \quad D_4 = \sqrt[+]{\frac{c + v}{c - v}}, \tag{24b}$$

in accord with (23).

§ 9. From (20) we find that a Lorentz matrix Λ_q with eigenvalues D_ν can always be written in the form

$$\Lambda_q = \mathbf{S}\,\mathbf{D}\,\mathbf{S}^{-1} . \tag{25}$$

Comparing (25) with (4) we find for $\Theta = 1$, that the matrix $\mathbf{S}$ has to fulfil the following condition

$$\tilde{\mathbf{S}}^{-1}\,\mathbf{D}\,\tilde{\mathbf{S}}\,\Gamma\,\mathbf{S}\,\mathbf{D}\,\mathbf{S}^{-1} = \Gamma . \tag{26}$$

Writing further

$$\tilde{\mathbf{S}}\,\Gamma\,\mathbf{S} = \Omega \tag{27}$$

we may also write after multiplying (26) from the left by $\widetilde{\mathbf{S}}$ and from the right by $\mathbf{S}$

$$\mathbf{D}\,\Omega\mathbf{D} = \Omega. \tag{28}$$

The $\nu - \mu$th element of (28) reads

$$D_\nu\,\Omega_{\nu\mu}\,D_\mu = \Omega_{\nu\mu}\,,$$

and so

$$\Omega_{\nu\mu} = 0 \quad \text{if} \quad D_\nu\,D_\mu \neq 1.$$

Furthermore taking the transposed of (27) we see that $\Omega = \widetilde{\Omega}$ and $\det \Omega \neq 0$, thus Ω must be of the form

$$\Omega = \begin{pmatrix} 0 & A & 0 & 0 \\ A & 0 & 0 & 0 \\ 0 & 0 & 0 & B \\ 0 & 0 & B & 0 \end{pmatrix} \quad A,\, B \neq 0. \tag{29}$$

§ 10. We note that to every LORENTZ matrix Λ_q with eigenvalues given by $\mathbf{D}$ there exist matrices $\mathbf{S}$ satisfying (25). Since Λ_q is a LORENTZ matrix the matrices $\mathbf{S}$ satisfy also (27) and (29).

However, if a matrix $\mathbf{S}$ satisfies (25) then any matrix

$$\mathbf{S}' = \mathbf{S}\,\mathbf{F}$$

also satisfies (25) provided $\mathbf{F}$ is a diagonal matrix with non-vanishing diagonal elements.

If S satisfies (27) then we have

$$\widetilde{\mathbf{S}}'\,\Gamma\,\mathbf{S}' = \mathbf{F}^{-1}\,\Omega\,\mathbf{F} = \Omega'\,.$$

By a suitable choice of $\mathbf{F}$ we can achieve that Ω' reduces to

$$\Omega' = \Omega_0 = \begin{pmatrix} 0 & 1 & 0 & 0 \\ 1 & 0 & 0 & 0 \\ 0 & 0 & 0 & 1 \\ 0 & 0 & 1 & 0 \end{pmatrix}.$$

Thus writing $\mathbf{S}$ in place of $\mathbf{S}'$ we can always find for a given Λ_q a matrix $\mathbf{S}$ such that

$$\widetilde{\mathbf{S}}\,\Gamma\,\mathbf{S} = \Omega_0\,. \tag{30}$$

Considering two matrices Λ_q and $\Lambda_{q'}$ with equal eigenvalues, we can find matrices **S** and **T** such that

$$\Lambda_q = \mathbf{S}\,\mathbf{D}\,\mathbf{S}^{-1}, \qquad \Lambda_{q'} = \mathbf{T}\,\mathbf{D}\,\mathbf{T}^{-1}, \tag{31}$$

and

$$\widetilde{\mathbf{S}}\,\Gamma\,\mathbf{S} = \widetilde{\mathbf{T}}\,\Gamma\,\mathbf{T} = \Omega_0 . \tag{32}$$

From the relation (32) we find

$$(\mathbf{T}\,\mathbf{S}^{-1})\,\Gamma(\mathbf{T}\,\mathbf{S}^{-1}) = \Gamma ,$$

we may therefore write

$$\mathbf{T}\,\mathbf{S}^{-1} = \Lambda_p , \tag{33}$$

where Λ_p is a LORENTZ matrix.

From (31) and (33) we find further

$$\Lambda_{q'} = \Lambda_p\,\Lambda_q\,\Lambda_p^{-1} . \tag{34}$$

We see therefore that any two matrices Λ_q and $\Lambda_{q'}$ which possess the same eigenvalues can be transformed into each other by a similarity transformation (34), they can therefore be regarded as representations of one matrix Λ_q and so we have proved the statement made in § 8.

§ 11. It is interesting to construct explicitly the matrices **S** and also to give a standard form of matrices Λ_q with given eigenvalues. For this purpose we introduce the matrix ω with complex elements as follows:

$$\omega = \frac{1}{2}\begin{pmatrix} 1+i & 1-i \\ 1-i & 1+i \end{pmatrix}.$$

We have $\omega^2 = \begin{pmatrix} 0 & 1 \\ 1 & 0 \end{pmatrix}$ and

$$\Omega_0^{1/2} = \begin{pmatrix} \omega & 0 \\ 0 & \omega \end{pmatrix}$$

and so (30) is satisfied by $\mathbf{S} = \mathbf{S}_0$ with

$$\mathbf{S}_0 = \Gamma^{-1/2}\,\Omega^{1/2}, \quad \widetilde{\mathbf{S}}_0 = \Omega^{1/2}\,\Gamma^{-1/2}, \tag{35}$$

$$\mathbf{S} = \Lambda_p\,\mathbf{S}_0 . \tag{36}$$

All the matrices of the form

$$\Lambda_{q'} = \Lambda_p\,\mathbf{S}_0\,\mathbf{D}\,\mathbf{S}_0^{-1}\,\Lambda_p^{-1} \tag{37}$$

are therefore LORENTZ matrices with the same eigenvalues D_ν.

So as to see the significance of (37) more clearly we introduce the diagonal matrix with elements as given by (24b) for **D**. We find

$$\mathbf{S}_0 \mathbf{D} \mathbf{S}_0^{-1} = \Lambda_{\varphi v}, \tag{38}$$

i.e. the matrix on the right-hand side is the LORENTZ matrix of the particular form (24a). From (38) and (37) we see that all the LORENTZ matrices

$$\Lambda_{\mathfrak{q}} = \Lambda_{\mathfrak{p}} \Lambda_{\varphi v} \Lambda_{\mathfrak{p}}^{-1} \tag{39}$$

have the same eigenvalues, namely those given by (24b). Thus all the LORENTZ matrices with the eigenvalues (24b) can be brought into the form (39), where $\Lambda_{\varphi v}$ is given by (24c).

§ 12. From the considerations above we see that the matrix $\Lambda_{\varphi v}$ gives a standard form of the matrices belonging to transformations with the same eigenvalues.

Physically this means that in this way any LORENTZ deformation can be characterized essentially by two quantities, i.e. by a velocity v by which the system is accelerated while suffering the deformation, and an angle φ through which it is turned around an axis pointing into the direction of **v**.

Apart from this the deformation consists of a parallel displacement and a constant change of phase, both described by the inhomogeneous terms λ of the transformation.

Disregarding the inhomogeneous part of the transformation, we see that each LORENTZ deformation represented relative to a suitable system of reference appears in the form (24a) and may then be characterized by the quantities v and φ.

§ 13. The question remains whether the transformations which contain the same absolute values of φ and v, but where the sign of either or both these quantities differ, can be obtained as the representation of the same deformation? As the result of a simple analysis one concludes that coordinate transformations $\mathfrak{L}_{\mathfrak{p}}$ which correspond to proper LORENTZ transformations cannot produce such a change of representation, i.e. all the transformations derived from $\Lambda_{\varphi,v}$ will differ from those derived from $\Lambda_{\varphi,-v}$. However, introducing a coordinate system by means of a suitable improper LORENTZ transformation we may obtain a representation of $\Lambda_{\varphi,-v}$ equal to $\Lambda_{\varphi,v}$. From this it follows that the representations of $\Lambda_{\mathfrak{q}} \neq 1$ and $\Lambda_{\mathfrak{q}}^{-1}$ differ if they are taken relative to systems of reference connected by proper LORENTZ transformations. However, $\Lambda_{\mathfrak{q}}$ may be equal to $\Lambda_{\mathfrak{q}}^{-1}$ (i.e. to a suitable representation of $\Lambda_{\mathfrak{q}}^{-1}$) if the systems of reference K and K' are connected by an improper LORENTZ transformation.

REFERENCES

1. L. JÁNOSSY, Acta Phys. Hung., **1,** 391, 1952; Ann. d. Phys., **11,** 293, 1953.
2. L. JÁNOSSY, Uszp. Fiz. Nauk., **62,** 149, 1957.
3. L. JÁNOSSY, Preprint of the Central Res. Inst. of Phys. of the Hung. Acad. Sci., Budapest, 1960 (in English); Vopr. Filoz., **8,** 101; **9,** 89, 1961 (in Russian); Filoz. Szle, **6,** 153, 1962 (in Hungarian).
4. L. JÁNOSSY, Acta Phys. Hung., **17,** 421, 1964.
5. L. JÁNOSSY and T. ELEK: „A relativitáselmélet filozófiai problémái", Akadémiai Kiadó, Budapest, 1963. (in Hungarian)

О ПРЕДСТАВЛЕНИИ ДЕФОРМАЦИИ ЛОРЕНЦА

Л. ЯНОШИ

Р е з ю м е

Показывается, что при помощи собственных значений матрицы Лоренца преобразования Лоренца сводятся к стандартной форме. Применением данной формы найдено, что любая из деформаций Лоренца, по отношению к соответствующей системе, проявляется как ускорение в определенном направлении и как вращение с определенной угловой скоростью вокруг направления ускорения.

ON THE ANOMALOUS MULTIPLET SPLITTING OF THE TRIPLET TERMS OF THE TiO MOLECULE

By

R. TŐRÖS

DEPARTMENT OF ATOMIC PHYSICS, POLYTECHNICAL UNIVERSITY, BUDAPEST

(Presented by I. Kovács. — Received 12. I. 1965)

It will be shown that the anomalous triplet splitting of the $C^3\Pi - X^3\Pi$ and $A^3\Delta - X^3\Pi$, (1,0) bands of the TiO molecule is due — similarly to the splitting of the (0,0) bands — to an anomalous triplet splitting of both the upper and the lower terms. The anomalous triplet splittings can be explained in terms of spin-orbit and spin-spin interactions. The accurate value of the multiplet splitting constant A has been determined for the level $v = 1$ of the states $C^3\Pi$ and $A^3\Delta$.

1. Introduction

The (1,0), (0,0) and (0,1) transitions of the $C^3\Pi - X^3\Pi$ and $A^3\Delta - X^3\Pi$ bands of the TiO molecule have been photographed by CHRISTY [1] and PHILLIPS [2], and deviations from the normal splitting of the band have been observed. The triplet formulae accounting for the anomalous triplet splitting valid for Hund's cases a) and b) as well as for the intermediate cases has been derived by KOVÁCS [3], [4], [5]. By using these formulae the accurate value of the multiplet splitting constant A can also be determined. The value of the multiplet splitting constant has been determined for the state $C^3\Pi$ by BUDÓ [6] from the results of CHRISTY. He obtained the value $A = 88$ cm^{-1} for the levels $v = 0$ and $v = 1$. PHILLIPS has obtained the value $A = 105$ cm^{-1} for the levels $v = 0$ and $v = 1$ of the $A^3\Delta$ state, making thereby the remark that the result is only an approximate one. PHILLIPS believes that the deviation is due to vibrational perturbation.

KOVÁCS has shown [7] that the deviation can be explained by taking into account the spin-spin and the spin-orbit interaction. KOVÁCS carried out the analysis for the $A^3\Delta - X^3\Pi$ and $C^3\Pi - X^3\Pi$ (0,0) band of the TiO molecule. In the present paper the calculations will be performed for the (1,0) transitions of the same bands.

2. The transition $A^3\Delta - X^3\Pi$

We have determined from the experimental wave number data the normal splitting of the upper state from the relation

$$\begin{aligned} \Delta F'_{31}(I) = Q_3(I) - Q_1(I) + \Delta F''_{31}(I) = R_3(I-1) - R_1(I-1) + \\ + \Delta F''_{31}(I-1) = P_3(I+1) - P_1(I+1) + \Delta F''_{31}(I+1), \end{aligned} \tag{1}$$

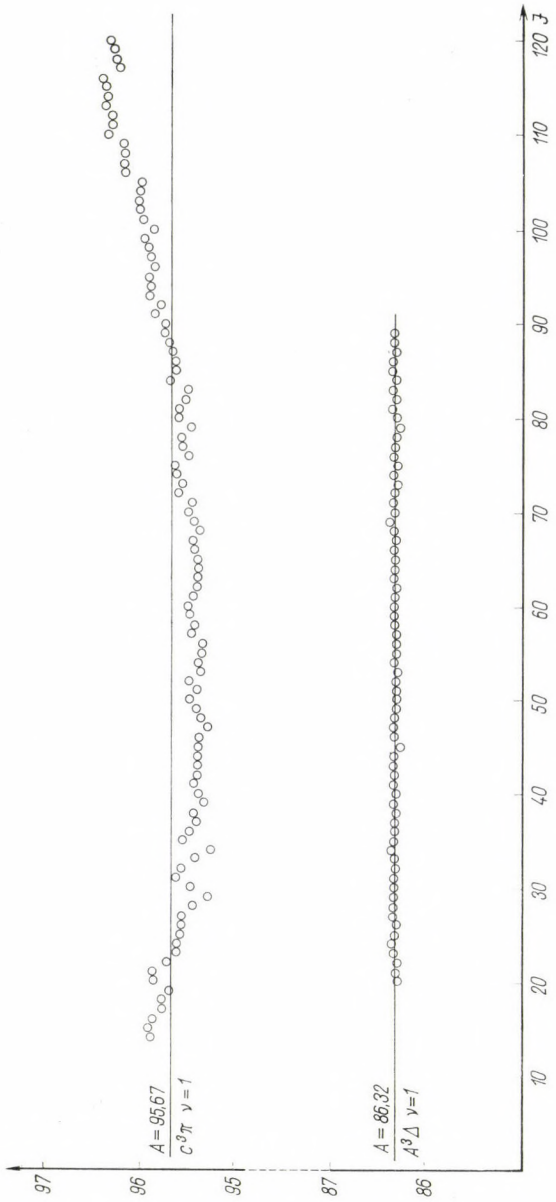

Fig. 1. The constant A as a function of I

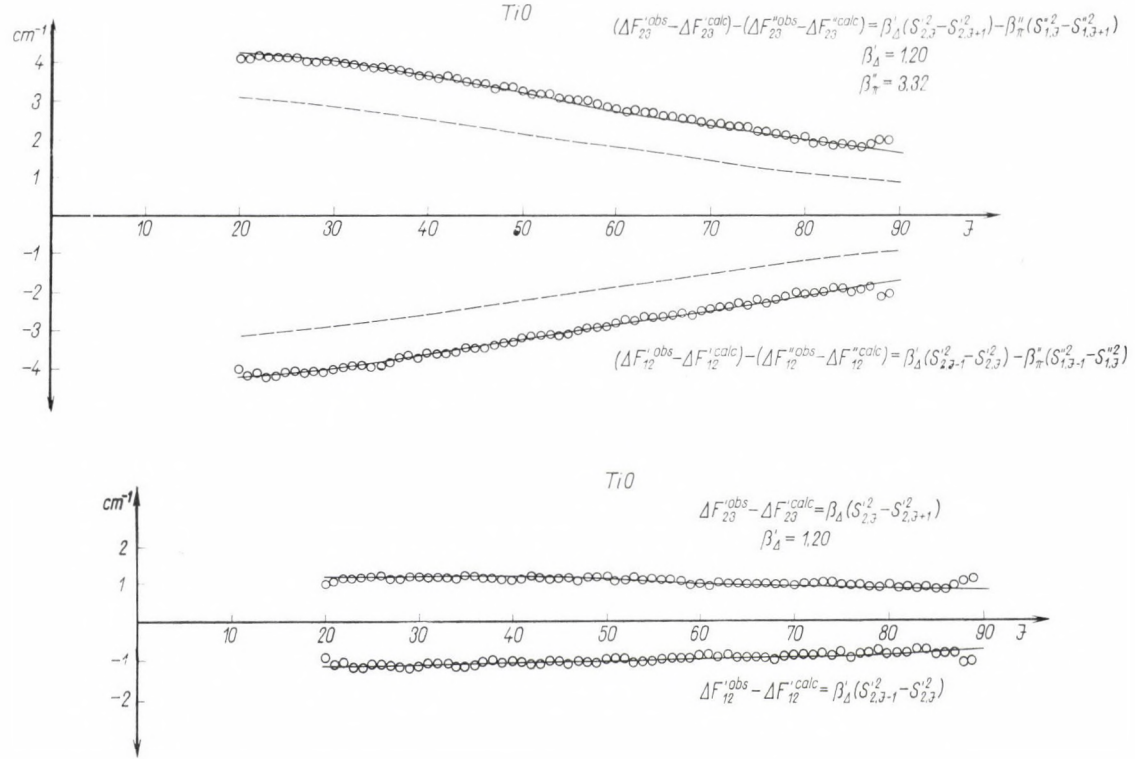

Figs. 2., 2a. The anomalous multiplet splitting of the transition $A^3\Lambda - X^3\Pi$

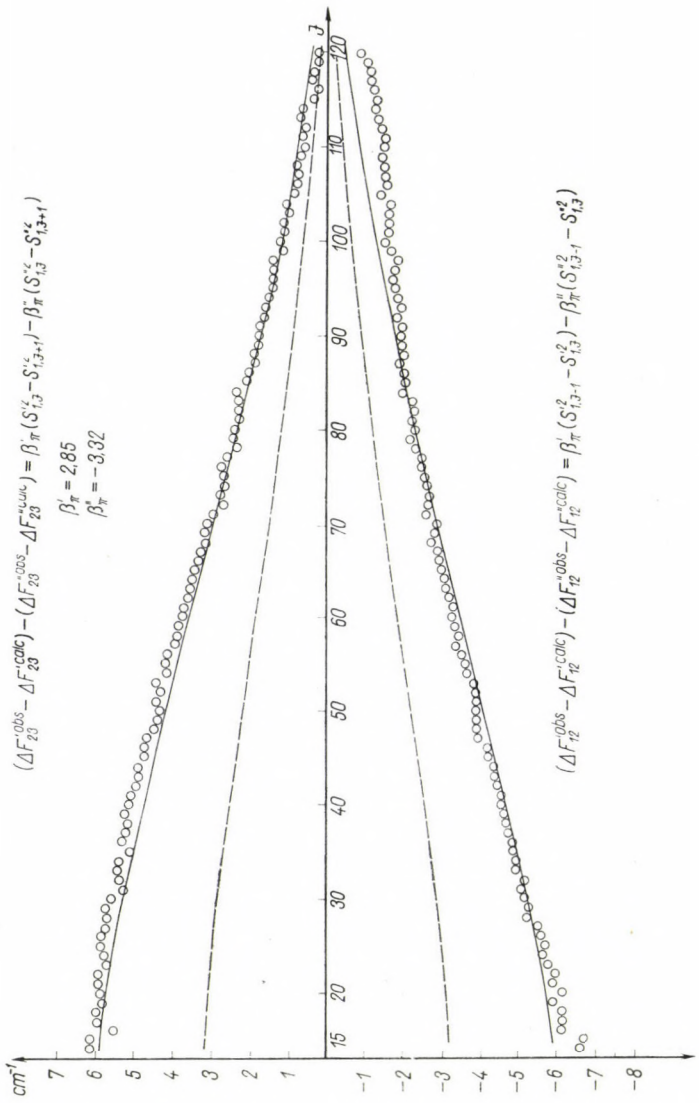
$(\Delta F_{23}^{'obs} - \Delta F_{23}^{'calc}) - (\Delta F_{23}^{''obs} - \Delta F_{23}^{''calc}) = \beta_\pi' (S_{1,3}'^2 - S_{1,3+1}'^2) - \beta_\pi'' (S_{1,3}'^2 - S_{1,3+1}'^2)$
$\beta_\pi' = 2{,}85$
$\beta_\pi'' = -3{,}32$
$(\Delta F_{12}^{'obs} - \Delta F_{12}^{'calc}) - (\Delta F_{12}^{''obs} - \Delta F_{12}^{''calc}) = \beta_\pi' (S_{1,3-1}^2 - S_{1,3}^2) - \beta_\pi'' (S_{1,3-1}^2 - S_{1,3}^2)$
cm⁻¹
J

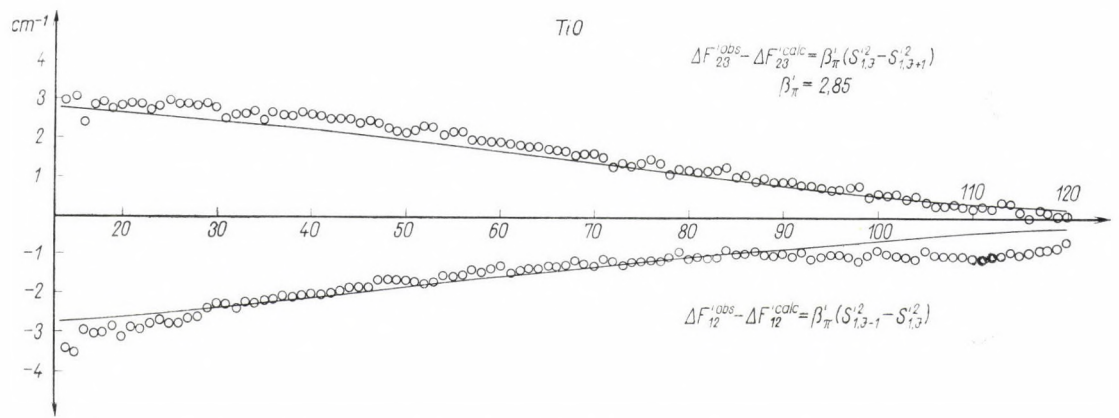

Figs. 3., 3a. The anomalous multiplet splitting of the transition $C^3\Pi - X^3\Pi$

where $\Delta F''_{31}(I)$ has been calculated from the data of the lower state by the triplet formula. (For $v'' = 0$ $B'' = 0{,}5340$ cm^{-1}, $D'' = -6{,}1 \cdot 10^{-7}$ cm^{-1}, $A'' = 100$ cm^{-1}.)

The constants of the upper state have been calculated from the approximate relation [7]

$$\left(\frac{1}{4B}\right)^2 \{\Delta F'_{31} + \gamma'(2I+1) - D'[(I+1)^2(I+2)^2 - (I-1)^2 I^2]\}^2 = \\ = (Y'-2)^2 - \frac{11}{2} + I(I+1)\,. \tag{2}$$

The quantities Y', A' and γ' are listed in the Table. The values of A for different values of I are presented in Fig. 1.

Anomalous splitting is also found by using the obtained value of A' which is more accurate than that used previously. We have determined the anomalous splitting for the lower and upper states from the expressions [7]

$$[\Delta F'^{\text{obs}}_{12} - \Delta F'^{\text{calc}}_{12}] - [\Delta F''^{\text{obs}}_{12} - \Delta F''^{\text{calc}}_{12}] = \\ = \beta'_A (S'^2_{2,I-1} - S'^2_{2,I}) - \beta''_\pi (S''^2_{1,I-1} - S''^2_{1,I})\,, \tag{3}$$

$$[\Delta F'^{\text{obs}}_{23} - \Delta F'^{\text{calc}}_{23}] - [\Delta F''^{\text{obs}}_{23} - \Delta F''^{\text{calc}}_{23}] = \\ = \beta'_A (S'^2_{2,I} - S'^2_{2,I+1}) - \beta''_\pi (S''^2_{1,I} - S''^2_{1,I+1})\,. \tag{4}$$

The notation used in these formulae is explained below. For the case of the Δ-term

$$S_{2,I-1} = -\frac{(I-2)(I+2)}{\sqrt{C_1(I)}}\,; \quad S_{2,I} = \frac{Y-2}{\sqrt{C_2(I)}}\,; \\ S_{2,I+1} = \frac{(I-1)(I+3)}{\sqrt{C_3(I)}}\,, \tag{5}$$

$$\left.\begin{aligned} C_1(I) &= 2Y(Y-4)(I-1)(I+2) + (2I+1)(I-2)I(I+2)\,, \\ C_2(I) &= Y(Y-4) + I(I+1)\,, \\ C_3(I) &= 2Y(Y-4)(I-2)(I+3) + (2I+1)(I-1)(I+1)(I+3) \end{aligned}\right\} \tag{6}$$

and for the case of the Π-terms

$$S_{1,I-1} = -\frac{\sqrt{2}(I^2-1)}{\sqrt{C_1(I)}}\,; \quad S_{1,I} = \frac{Y-2}{\sqrt{C_2(I)}}\,; \quad S_{1,I+1} = \frac{\sqrt{2}\,I(I+1)}{\sqrt{C_3(I)}}\,, \tag{5a}$$

$$\left.\begin{aligned} C_1(I) &= Y(Y-4)I(I+1) + 2(2I+1)(I-1)I(I+1)\,, \\ C_2(I) &= Y(Y-4) + 4I(I+1)\,, \\ C_3(I) &= Y(Y-4)(I-1)(I+2) + 2(2I+1)I(I+1)(I+2)\,. \end{aligned}\right\} \tag{6a}$$

β_Δ and β_π are the anomalous splitting constants, the appropriate choice of which makes possible the interpretation of the experimental data.[1] (Figs. 2 and 2a.)

3. The transition $C_3\,\Pi - X^3\,\Pi$

After determining the quantities $Y = A/B$ and γ we have calculated the normal triplet splitting in a similar way as before. The deviations of the calculated and the experimental data are now given by the formulae (cf. [1])

$$[\Delta F'^{\,\mathrm{obs}}_{12} - \Delta F'^{\,\mathrm{calc}}_{12}] - [\Delta F''^{\,\mathrm{obs}}_{12} - \Delta F''^{\,\mathrm{calc}}_{12}] = \\ = \beta'_\pi (S'^2_{1,I-1} - S'^2_{1,I}) - \beta''_\pi (S''^2_{1,I-1} - S''^2_{1,I}) \tag{7}$$

$$[\Delta F'^{\,\mathrm{obs}}_{23} - \Delta F'^{\,\mathrm{calc}}_{23}] - [\Delta F''^{\,\mathrm{obs}}_{23} - \Delta F''^{\,\mathrm{calc}}_{23}] = \\ - \beta'_\pi (S'^2_{1,I} - S'^2_{1,I+1}) - \beta''_\pi (S''^2_{1,I} - S''^2_{1,I+1})\,, \tag{8}$$

and they are presented in the Figs. 3 and 3a.[1]

The values obtained for β''_π are given in the Table.

Table

	v	A	Y	γ	ρ
$C^3\,\Pi$	1	95,67	197,22	−0,0417	+2,85
$A^3\,\Delta$	1	86,32	171,74	—	+1,20
$X^3\,\Pi$	0	100,00	188,00	—	−3,32

4. Acknowledgement

I should like to express my thanks to Professor Dr. I. Kovács for calling my attention to the problem and supporting my work.

[1] It should be noted that in accordance with the results of [7] we have obtained the value $\beta''_\pi = -3{,}32$. Therefore the fact that the two curves of the Figure can be reproduced simultaneously by the choice of one single parameter (β'_π) is a strong argument in support of the correctness of the assumptions on which formulae (3) and (4) based.

REFERENCES

1. A. Christy, Phys. Rev., **33**, 701, 1929.
2. J. G. Phillips, The Astrophysical J., **114**, 151, 1951.
3. I. Kovács, Acta Phys. Hung., **12**, 67, 1960.
4. I. Kovács, Acta Phys. Hung., **13**, 303, 1961.
5. I. Kovács, Can. J. of Phys., **42**, 2180, 1964.
6. A. Budó, Z. Phys., **98**, 437, 1936.
7. I. Kovács, Acta Phys. Hung., to be published.

ОБ АНОМАЛЬНОМ МУЛЬТИПЛЕТНОМ РАСЩЕПЛЕНИИ ТРИПЛЕТНЫХ ТЕРМОВ МОЛЕКУЛЫ TiO

Р. ТЭРЭШ

Резюме

Показывается, что аномальное триплетное расщепление полосных систем $C^3\Pi - X^3\Pi$ и $A^3\Delta - X^3\Pi$ (1,0) молекулы **TiO** — соответственно аномальному расщеплению полосных систем (0,0) — сводится к аномальному триплетному расщеплению, наблюдаемому как на низших, так и на высших термах. Аномальные триплетные расщепления истолкуются с принятием во внимание спин-орбитального и спин-спинового взаимодействий. На уровне $v = 1$ вычисляются точные значения постоянных мультиплетного расщепления A в состояниях $C^3\Pi$ и $A^3\Delta$.

THE PUMPING THEORY OF DIFFUSION PUMPS

By

G. Tóth

PHYSICAL INSTITUTE, UNIVERSITY FOR TECHNICAL SCIENCES, BUDAPEST

(Presented by A. Kónya. — Received 19. I. 1965)

Theories on the pumping effect of diffusion pumps assume an ideal gas transport by the jet, and so the diffusion seems to be essential in the performance of pumps. To attain correct numerical results secondary effects are supposed. Other theories try to examine the pumping effect on the ground of the collisions between gas and vapour molecules, but with the help of the "mean-free-path" theory, which is not very easy to survey in this case, and not quite of universal validity. This paper tries to handle the pumping effect with the aid of the kinetic theory of nonuniform gases. On this ground an equation is obtained, which will be solved for an ideal case. Thus it will be possible to understand the pumping effect in a deeper manner, to verify the experimental results and to critically evaluate previous theories.

1. Introduction

The diffusion pump is one of the most important instruments to produce high-vacuum. Great advantage is its comparatively simple apparatus, robustness, its easy handling and economy.

Diffusion pumps have been developed over the past fifty years. In spite of this the theory of pump performance is not satisfactory. So diffusion pumps are designed and constructed with trial methods.

The sketch of a diffusion pump is shown in Fig. 1. Mercury or oil of high molecular weight are boiled in the boiler (a) and the vapour streams at high speed across the nozzle (c) into the pump chamber. Gas molecules having entered the pump from the container to be evacuated across inlet (e) interact with the vapour molecules and by the vapour beam pass downwards towards the forepressure outlet and on the forepressure side (f) the backing pump exhausts them across (h). (For brevity the vapour of the pumping fluid will be called "vapour" and the material to be removed "gas", remarking, that the diffusion pump is suitable to remove vapours.)

2. Experimental results

Essential characteristics of pump performance are: forepressure tolerance, pumping speed and ultimate vacuum. (Recently the backstreaming has been taken into account in pump performance, but this paper studies only

the working principle of diffusion pumps, and the backstreaming can be neglected in this respect.)

The vapour pressure in the boiler is of the order of mmhg. To obtain a suitable jet one needs a forepressure under certain threshold. This threshold can be characterized by the forepressure tolerance.

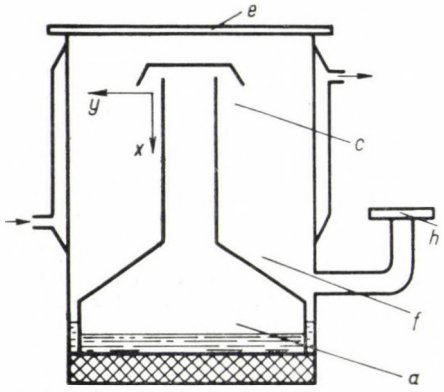

Fig. 1. Single-stage diffusion pump

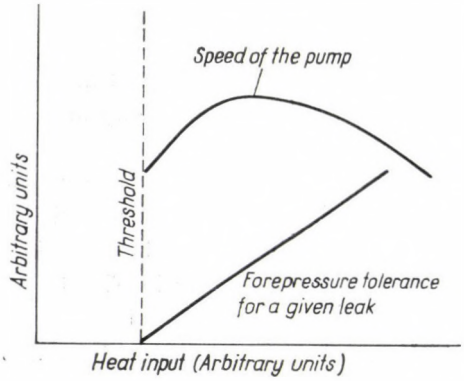

Fig. 2. Effect of change in heat input on performance of diffusion pump

Forepressure tolerance is specified as the forepressure at which the inlet pressure increases 10 per cent at maximal throughput. The decrease of the forepressure tolerance with decreasing heat input at the boiler was found experimentally (Fig. 2).

Diffusion pumps are able to sustain certain pressure drop between the pump inlet and forepressure outlet. Accordingly the inlet pressure depends on the forepressure (Fig. 3).

The ultimate pressure is the smallest pressure attainable by a pump. Practically the vapour pressure of the pumping fluid in the given circumstances will be the ultimate pressure because of the pump ability to hold

a great pressure ratio, so a low forepressure. In practice thus baffles or cold traps are needed. The ultimate pressure and pressure ratio are shown in Fig. 4 for helium and nitrogen. According to former and the latest experiments the pressure ratio and so the attainable ultimate pressure are worse for gases of low molecular weight [2], [6], [14], [18]. To increase the pressure ratio a multi-stage pump is applied.

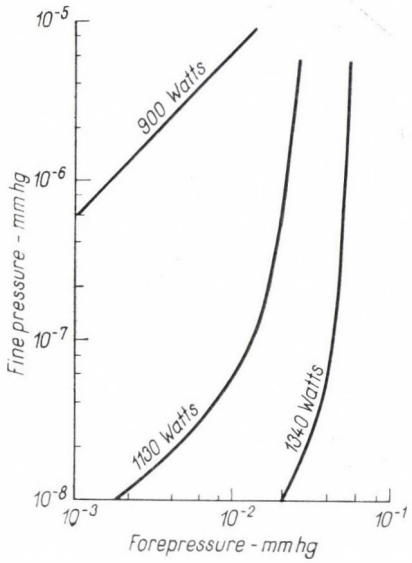

Fig. 3. Forepressure tolerance characteristics for different heater power with oil diffusion pump DO-501 for hydrogen [14]

A significant characteristic of diffusion pumps is the speed defined by $S = Q/P$, where Q is the quantity of molecules streaming across the pump inlet per second, and P is the pressure at the same place. Because of using always a known gas at a given temperature Q can be given in the form $Q = PV$, so $S = V$, namely, the volume of gas streaming across the pump inlet per second [23].

The speed of a pump depends on the heat input (Fig. 2). The speed, because of being independent of pressure in a wide pressure range, (Fig. 5), is a characteristic of the pump at the smallest pressures as well. The peculiar pressure range is affected by the heat input and the nozzle cross section (Fig. 6). The speed of a pump in given circumstances depends on the molecular weight of gases to be removed. There is a wide discrepancy in the data of literature in this respect. GIBSON [9] obtained for hydrogen the one third of the speed of air. SETLOW [18] obtained the speed of air for hydrogen but only at high heat input; at normal heat input he measured only $\frac{1}{3}$ to $\frac{1}{4}$ of the

speed of air. NOELLER [14] and HENDERSON [10] obtained twice the speed of air for hydrogen using baffles and liquid nitrogen refrigerations at the high vacuum side. FLUCKE [5] found in his measurements an increase of the speed

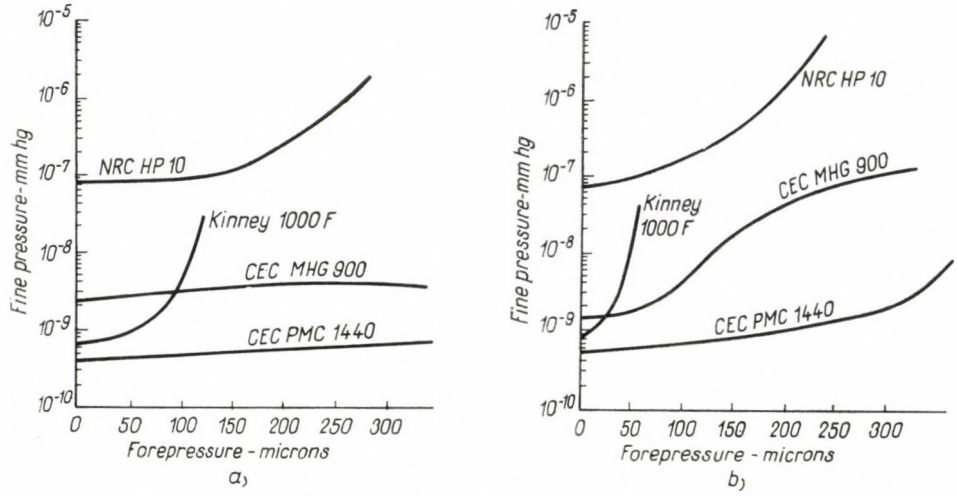

Fig. 4. a) Forepressure tolerance characteristics for nitrogen; *b)* Forepressure tolerance characteristics for helium [10]

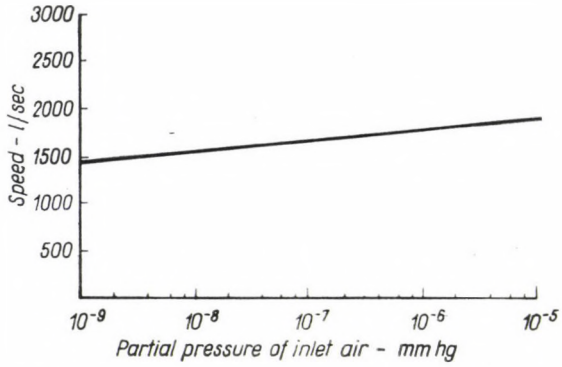

Fig. 5. Speed of oil diffusion pump DO-8001 with baffle and cold trap, pumping air [14]

at the rate $1/M^{1/2}$, where M is the molecular weight: in the experiments he used liquid air refrigeration at the high vacuum side. According to DAYTON [2] the rate of speeds for hydrogen and air for a pump may be various, depending on the design of pump the pumping fluid, the heat input and the fore pump capacity.

Pumps of different sizes have different speeds. The efficiency of a pump is estimated by the Ho-coefficient. The Ho-coefficient or speed factor is

defined as the ratio of the speed measured at the inlet to the nozzle chamber to the ideal speed as calculated by the kinetic theory for the pump mouth. The ideal speed is identical with the speed of the perfect vacuum.

In the pressure region of diffusion pumps the behaviour of gases is molecular, thus the quantity of molecules streaming in a given direction per second per cm^2 is $\frac{1}{4} nc$ by kinetic theory; where n is the number of molecules per cm^3, c is the mean-speed. In the case of perfect vacuum there is streaming only towards the perfect vacuum, so the speed of the perfect vacuum at 20 °C is

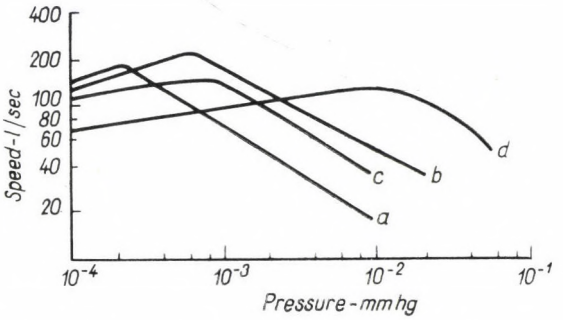

Fig. 6. a) The width of the gap of the nozzle is small, the heat input is small; *b)* The width of the gap of the nozzle is small, the heat input is high; *c)* The width of the gap of the nozzle is high, the heat input is small; *d)* The width of the gap of the nozzle is high, the heat input is high [1]

11,7 lit per sec per cm^2 for air and 44 lit per sec cm^2 for hydrogen. This quantity is called the conductance of the pump orifice per cm^2 for the given gas.

The Ho-coefficient of a well-designed pump is about 0,5. MILLERON [13] found that the attainable Ho-coefficient for gases of low molecular weight might not be as high as for air.

3. Theories treating pump performance

Earlier theories [7], [8], [11], [12], [15], [16], [20], [24] accept the diffusion as working principle of the pump. In GAEDE's pump (Fig. 7) the diffusion occurs in tube AB. In modern pumps, according to [11], [12], [20], [24], the gas diffuses into the vapour beam at plane D (Fig. 8). This supposition made it possible to understand why the pump speed is constant in a wide pressure range and why the pump speeds are different for different gases.

This assumption on diffusion, however, means a gas transport limited only by the opening of the pump, which does not depend on the vapour jet.

To attain reasonably acceptable numerical results secondary effects are assumed (for example back diffusion).

To understand the role of the jet, more accurate investigation is needed. JAECKEL [11], [12] assumes backstreaming vapour molecules in the jet (Fig. 9), so he gets more exact speed results than before. NOELLER [15], [16] examines

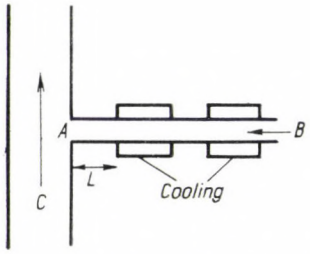

Fig. 7. Vacuum pumping by diffusion principle according to GAEDE

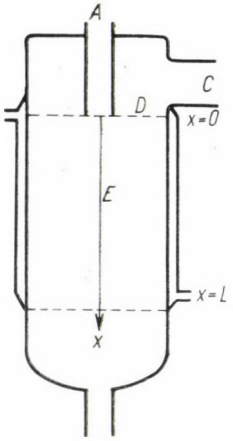

Fig. 8. Single-stage diffusion pump

the jet by the theory of gasdynamics, establishes the formation of shock waves owing to supersonic vapour flow. By this he can interpret the speed curve of diffusion pumps and the difference between diffusion and jet pumps as well.

The above theories assume that the diffusion occurs at the mouth of the pump. This assumption, however, may be argued against on the basis that the diffusion phenomena are created by the constant motion of the molecules; thus considering the motion of a single gas molecule it may not be decided whether it takes place among vapour molecules possessing also a beam speed

in addition to thermal agitation, or it is influenced only by molecules of thermal agitation; and so "diffusion" occurs all over the pump chamber.

Thus it seems, it would be better to treat this problem on the ground of the motion and collision of gas and vapour molecules by kinetic theory. This was attempted recently [1], [3], [4], [17], but on the basis of not very well-founded assumptions. Therefore the results of these theories contradict in some respects the experimental data (for example the ultimate vacuum is,

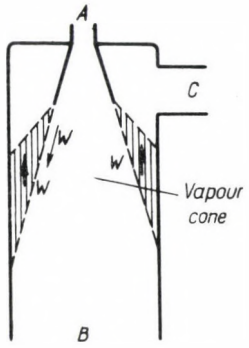

Fig. 9. Single-stage diffusion pump

better for gases of low molecular weight according to [4]), or they are empirical rather than theoretical results.

4. The working mechanism by kinetic theory

It is an obvious assumption that the suction effect of the diffusion pump is due to collisions between gas and vapour molecules. Molecules possess an irregular molecular motion and collide with each other. Their speeds after collision are determined by the speed before the collision, the mass of the molecules and the sort of the collision. Thus diffusion in this case means the penetration of gas molecules due to their thermal agitation into a space filled with other gas. It is evident that the intensity of the penetration is influenced by the impacts with the molecules of the other gas.

If the velocity-distribution of the gas molecules in the container to be evacuated is a Maxwell one, the mean molecular velocity is zero and no gas stream exists.

At the mouth of the pump the gas molecules having thermal agitation enter the vapour of the pumping fluid possessing a stream velocity besides thermal agitation and collide with them. The mixture of gas and vapour molecules is in constant motion all over the pump chamber. Different velo-

cities and collisions of molecules exist. Thus it may be stated that the gas enters the vapour jet at every place x, not only at $x = 0$ (Fig. 8), as in the previous theories. This interaction of gas and vapour molecules causes the gas to flow to the forepressure side, well known from experiment. It may be supposed that the interaction influences the velocity distribution of the gas and accordingly gas flow is obtained in a given direction.

The working mechanism of the suction may be described as follows: the Maxwell velocity distribution of the gas alters due to collisions between gas and vapour molecules, therefore a gas flow toward the forepressure side will exist.

In the following the gas flow in the pump chamber per unit cross section area and time will be determined by means of kinetic theory [21], [25].

The investigations will be done on the ground of a pump model shown in Fig. 1.

Accross the nozzle (c) a vapour beam of high speed streams into the pump chamber. The velocity and density of the vapour depend upon x and y. Gas molecules enter the pump chamber across the pump mouth (e), interact with the vapour molecules and accordingly they are driven to the forepressure side (f).

The interaction will not be treated for single molecules, but the encounters of gas and vapour molecules per unit volume and time at x will be investigated. The velocity component of the vapour may be supposed not to cause any gas transport in the direction y, it only influences the density distribution of the gas.

Suppose that the gas has a velocity distribution function $f_1 = f_1(\mathbf{v}_1, x)$. If it were known, the gas flow across unit cross-section and in unit time at x could be determined as

$$i = \int \mathbf{v}_{1x} f_1 \, dv_1 \,. \tag{1}$$

Certainly f_1 is not a Maxwell velocity distribution function because the interaction with the vapour alters the Maxwell distribution, and exactly this process results in the pumping effect.

Although f_1 is not known, expression [1] may be determined from the Boltzmann equation:

$$\frac{\partial}{\partial t} f_1 + \mathbf{v} \frac{\partial}{\partial \mathbf{r}} f_1 + \frac{1}{m} \frac{\partial}{\partial \mathbf{v}} (\mathbf{F} f_1) = \left[\frac{\partial f_1}{\partial t} \right]_{\text{coll}} . \tag{2}$$

Equation (2) will be more simple in our case because the force action is negligible, and the problem is one-dimensional and independent of time. Therefore:

$$v_{1x} \frac{\partial}{\partial x} f_1 = \left[\frac{\partial f_1}{\partial t} \right]_{\text{coll}} . \tag{3}$$

Let us expand f_1 into infinite series [21], [25]:

$$f_1 = f_1^{(0)} + f_1^{(1)} + \dots .$$

Define

$$\int f_1 \, d\mathbf{v}_1 = \int f_1^{(0)} d\mathbf{v}_1 = n_1 ,$$

$$\int v_1^2 f_1 \, d\mathbf{v}_1 = \int v_1^2 f_1^{(0)} \, d\mathbf{v}_1 ,$$

so

$$f_1^{(0)} = A_1 \, n_1 \exp \left(-\beta_1^2 \, v_1^2\right) ,$$

where

$$A_1 = \frac{\beta_1^3}{\pi^{3/2}} , \quad \beta_1^2 = \frac{M_1}{2RT} . \tag{4}$$

R is the universal gas constant, M_1 is the molecular weight, $n_1 = n_1(x)$ the number density of the gas; T is the temperature.

The problem will be solved in second approximation taking only $f_1^{(1)}$ into consideration. $f_1^{(1)}$ may be expressed as [21]

$$f_1^{(1)} = c v_{1x} [\exp \left(-\beta_1^2 \, v_1^2\right) ,$$

where $c = c(x)$ is independent of the velocity.

The velocity distribution of the vapour is considered in first approximation and we assume that every vapour molecule has a mean speed or beam speed $v_0 = v_0(x)$ besides thermal agitation. Owing to this:

$$f_2 = A_2 \, n_2 \exp \left[-\beta_2^2 \, (v_2 - v_0)^2\right] ,$$

where β_2 and A_2 have the same meaning as in [4]: $n_2 = n_2(x)$ is the number density of the vapour.

On the left-hand side of (3) the term $f_1^{(1)}$ can be dropped in comparison with $f_1^{(0)}$. Equation (3) multiplied by v_{1x} and integrated over all velocity space yields

$$\frac{1}{2\beta_1^2} \frac{dn_1}{dx} = \int v_{1x} \left[\frac{\partial}{\partial t} f_1\right]_{\text{coll}} d\boldsymbol{v}_1 = \left[\frac{\partial i}{\partial t}\right]_{\text{coll}} . \tag{5}$$

The collision term is considered by examining how the impacts affect the gas flow. In the evaluation of the right-hand side of (5) the influence of collisions only with vapour molecules must be taken into consideration because collisions of the gas molecules with each other can have no effect upon the momentum of the whole gas.

Let the mass of a gas molecule be m_1, its velocity $\mathbf{v}_1$, m_2 and $\mathbf{v}_2$ the respective values for a vapour molecule, $\mathbf{w}$ their relative velocity and $\mathbf{u}$ the velocity of their common center of mass. Then

$$\mathbf{u} = \mu_1 \mathbf{v}_1 + \mu_2 \mathbf{v}_2 , \quad \mathbf{w} = \mathbf{v}_1 - \mathbf{v}_2 ,$$

$$\mu_1 = \frac{m_1}{m_1 + m_2} , \qquad \mu_2 = \frac{m_2}{m_1 + m_2} .$$

The mean value of the change in gas flow in a single collision is [25]:

$$\Delta i = -\mu_2 w_x (1 - \cos \Theta) ,$$

where Θ is the angle with which the relative velocity deviates due to collision.

The total change in gas flow due to all collisions in a second is

$$\left[\frac{\partial i}{\partial t}\right]_{\text{coll}} = -2\pi \int_{-\infty}^{+\infty} \int_{0}^{\pi} \int w \mu_2 w_x (1 - \cos \Theta) G f_1 f_2 \sin \Theta \, d\Theta \, d\mathbf{v}_1 \, d\mathbf{v}_2 , \tag{6}$$

where G is the scattering coefficient. Assuming a hard elastic sphere interaction, G is given by

$$G = \pi \left(\frac{\sigma_1 + \sigma_2}{2}\right)^2 ,$$

where σ_1 and σ_2 are the diameters of the molecules.

To evaluate integral (6) the variables are changed from $\mathbf{v}_1$, $\mathbf{v}_2$ to $\mathbf{u}$ and $\mathbf{w}$, and it is assumed that the gas and vapour has the same temperature. This last assumption has no influence on i, because the equalization of temperatures of gas and vapour affects only the thermal agitation of molecules and a transport is not affected.

After computing integral (6) the function $c(x)$ in $f_1^{(1)}$ may be determined from (5), and thus the gas flow may be determined in second approximation from (1).

$$i = -\frac{dn_1}{dx} \frac{v_0 \varphi_1(z)}{G n_2} + v_0 \varphi_2(z) n_1 , \tag{7}$$

$$\varphi_1(z) = \frac{z \exp(z^2)}{[4z^3 - 2z + \sqrt{\pi}\, \Phi(z) \exp(z^2)(1 + 4z^4)] 4 \sqrt{\pi}} ,$$

$$\varphi_2(z) = \frac{4z^3 + 2z + \sqrt{\pi}\, \Phi(z) \exp(z^2)(4z^4 + 4z^2 - 1)}{2[4z^3 - 2z + \sqrt{\pi}\, \Phi(z) \exp(z^2)(1 + 4z^4)]} ,$$

$$z = \beta_2 v_0 \sqrt{\mu_1} , \quad \Phi(z) = \int_0^z \exp(-x^2) \, dx .$$

The numerical values of $\varphi_1(z)$ and $\varphi_2(z)$ at different beam speeds of vapour for hydrogen and air are shown in Table I. The necessary numerical data were taken from [1], [22], [24].

From (7) the intensity of the gas flow i may be determined, if the velocity and density distributions of the vapour are known. Computing i is difficult because φ_1 and φ_2 depend upon x.

5. Calculation for an ideal pump

Qualitative statements may be made if (7) is solved for the simple case when the velocity and density of the vapour is constant, independent of x.

The ultimate pressure of the pump is obtained by integrating (7) in the case of $i = 0$:

$$\frac{n}{n_0} = \exp\left[G n_2 \frac{\varphi_2}{\varphi_1} L\right] = \exp[a], \tag{8}$$

where n_0 is the number density of the gas at $x = 0$ (assuming that the x component of the beam velocity of vapour is zero at this point), n is the number density at the forepressure side.

The gas at the forepressure side may be assumed to have a Maxwell distribution because at this place the effect of collisions with vapour molecules is neglected, thus the pressure P there is proportional to the number density: $P = kn$.

The number density n_0 of the gas at $x = 0$ may be considered to be the same as the number density in the container to be evacuated, because the change in number density from the container to the pump mouth is negligible when compared with the change from $x = 0$ to the forepressure side. (Obviously the number density of the gas decreases toward the pump inlet because of the vapour molecules being there in thermal agitation, and so the gas must diffuse through it into the pump.) Assume that the pressure in the container is proportional to the number density $n_0 : p_0 = kn_0$, so

$$\frac{n}{n_0} \approx \frac{P}{P_0}. \tag{9}$$

We use data from [1] and assume that the speed of the vapour is constant and equal to that at the mouth of the nozzle, furthermore that a mean vapour density exists and that the speed of the vapour beam is exactly the speed of sound. Taking $L = 1$ cm, we obtain 2 and 27 for the numerical value of (9) in case of hydrogen and air, respectively.

Consider the specific pumping speed obtained with the previous assumption.

Integrating equ. (7), since i is constant (independent of x) and according to (21) the specific speed is

$$s = \frac{i}{n_0'} = \frac{v_0 \varphi_2}{\exp(a) - 1}\left[\exp(a) - \frac{n'}{n_0'}\right], \tag{10}$$

where n' and n_0' are the gas number densities at the forepressure side and in the container (in this case n_0' is also approximately the same as the density at $x = 0$ because $n' \gg n_0'$).

We obtain from (21) that

$$\exp(a) = \frac{n}{n_0} = \frac{p}{p_0} \gg 1, \tag{11}$$

so

$$s = v_0 \varphi_2 \left(1 - \frac{n'}{n_0'} \middle| \frac{n}{n_0}\right). \tag{12}$$

The Table shows that $\varphi_2 \approx 1$. In the working range of diffusion pumps the rate of fore and fine pressures, namely the pressure ratio in a wide pressure range is negligible to that obtained from (9) for the case of the ultimate pressure:

$$\frac{n'}{n_0'} \ll \frac{n}{n_0}.$$

Thus

$$s \approx v_0.$$

Therefore in this approximation the specific pumping speed is approximately equal to the beam speed of vapour at the mouth of the nozzle. According to data obtained from [1], [22] this speed is about $2 \cdot 10^4$ to $6{,}8.10^4$ cm/sec, so the specific speed is about 20—68 lit/cm^2 sec. Evidently the pump mouth is not considered in this speed, therefore the true speed is

$$s' = \frac{1}{\frac{1}{s} + \frac{1}{s_0}}, \tag{13}$$

where s_0 is the specific conductance of the pump orifice. The pump orifice means the tube from $x = 0$ to the container to be evacuated. The value of s_0 for a short tube is 11,6 lit/sec for air and 43 lit/sec for hydrogen at 20 C°. The conductance may be smaller due to vapour molecules above the jet having only thermal agitation and the gas molecules must diffuse through them from the container to the pump.

These numerical results show that the former solution of equ. (7) is of optimal value. Apart from this, useful qualitative results are obtained from the ideal case.

Expression (8) gives a smaller compression capacity for gases of low molecular weight than for high ones.

Increasing the density of the vapour increases essentially the compression capacity; increasing the beam speed has a role in increasing φ_2/φ_1, which also increases the compression capacity.

These results allow us to interpret the experimental data.

The Ho-coefficient for this ideal pump is smaller for hydrogen than for air unless the speed of the vapour is twice as great as the speed of sound.

The number of air molecules pumped by such an ideal pump is determined by the diffusion of air molecules across the pump orifice (see equ. (13) and the value of s_0 and s for air). Therefore such an ideal pump may be called "diffusion pump" only for air. In the case of hydrogen the ideal pump having less then sonic vapour speeds is a "vapour pump", since now the role of the jet is essential due to the rate of s_0 and s in (13).

6. Results for real diffusion pumps

It is possible to obtain qualitative results for the performance of real diffusion pumps from the theory and calculations previously performed.

Since a sufficiently low forepressure is needed for forming a suitable jet, diffusion pumps work below a certain forepressure. The decrease of the fine pressure also makes a change in the jet [15], [2]. To obtain an optimum jet a low fine pressure is necessary. (Further decreasing the fine pressure probably does not alter the jet essentially.) Reaching this condition the pump achieves a maximum specific speed. Thus the growing parts of the speed functions obtained by experiments may be interpreted with the change of the velocity and density distribution of the jet. With full knowledge of the distribution function of the vapour jet at any fine and forepressure values it should be possible to determine the speed by equ. (7). Once having this optimum jet the speed will be constant in a pressure range for which the bracket expression in (12) is about one. This circumstance exists for a wide pressure range if the ultimate pressure of the given pump is very small. Modern pumps can reach a very low ultimate pressure and, accordingly, their speeds are constant in a wide pressure range (Fig. 5). This pressure range is narrower for H_2 than for air. Near the ultimate pressure the speed decreases. (In the term "ultimate pressure" the effect of the vapour pressure of the pumping fluid is not included.)

Therefore to attain a comparatively high specific speed multi-stage pumps are required, especially in the case of light gases. In multi-stage pumps

the existing pressure drop in one stage is small compared to the compression capacity of the stage.

It is evident that a high compression capacity does not assure a high specific speed, only makes it constant for a wide pressure range. In the case of gases of low molecular weight the compression ratio necessary for obtaining an optimum jet and the compression capacity of the jet may be of the same order, thus increasing the compression capacity is needed.

Equ. (8) shows that this is attainable by increasing the jet density. But an indefinite increase of the jet density is impossible because the number of the vapour molecules coming into the pump mouth increases and they hinder the motion of the gas molecules into the pump so the speed of the pump decreases. This reasoning fits in with the experimental facts (Fig. 6).

There certainly exists an optimum jet density. A higher density already hinders the motion of the gas molecules but a lower one does not exert a suitable compression capacity.

Values of specific speeds published in the literature are very different. The reasons for this, beside the difference in pump constructions and testing procedures, are the experimental circumstances. Using cooled baffles and refrigeration traps the speed for gases of low molecular weight is higher than for air, because the speed is determined by the conductance of the pump mouth in this case [see equ. (13)], and it is higher for gases of low molecular weight. If the conductance of the pump mouth is much smaller than the suction capacity of the pump, the rate of speeds for hydrogen and air is 3,8, according to the rate of conductances of the pump mouth for the gases in question. If the conductance of the pump mouth and the suction capacity of the pump are of the same order but the latter is higher, different values for the rate of speeds for hydrogen and air should be attained but the speed for air would be higher. If there are no cooled baffles or refrigeration traps and the jet is not convenient the speed for hydrogen would be lower than for air since, as it was shown, if the compression capacity of the pump is not satisfactory it is much lower for gases of low molecular weight and the speed decreases.

Using cooled baffles and refrigeration traps the speed of a pump will be constant for a wider pressure range because the diffusion stream across these obstacles is independent of pressure. Their conductances are much smaller than the suction capacity of the pump, thus according to (13) these smaller conductances determine the speed of the pump.

7. Conclusions

From the above theoretical reasoning it is easy to understand why some research workers believe that diffusion is dominant in the operation of pumps. In the original pump of GAEDE the conductance of the pump mouth was

Table I

Hydrogen — Mercury $\mu_1 = 0{,}01$					Air — Mercury $\mu_1 = 0{,}127$			
$\beta_2 r_0$	z	$\varphi_1(z)$	$\varphi_2(z)$	φ_2/φ_1	z	$\varphi_1(z)$	$\varphi_2(z)$	φ_2/φ_1
0,91	0,0091	0,33	1,23	3,73	0,12	0,081	1,03	12,7
1,00	0,010	0,26	1,00	3,85	0,13	0,070	0,96	13,8
1,2	0,012	0,23	1,01	4,39	0,15	0,057	0,95	16,8
1,4	0,014	0,19	1,01	5,33	0,18	0,047	0,92	19,8
1,5	0,015	0,18	1,02	5,67	0,19	0,043	0,91	21,3
1,6	0,016	0,16	1,02	6,38	0,20	0,039	0,90	22,9
1,8	0,018	0,14	1,00	7,14	0,23	0,035	0,88	25,3
2,0	0,020	0,13	0,99	7,62	0,25	0,029	0,86	29,7
2,2	0,022	0,12	0,99	8,25	0,28	0,025	0,83	33,0
2,4	0,024	0,11	0,98	8,91	0,30	0,022	0,81	36,7
2,6	0,026	0,10	0,98	9,80	0,33	0,019	0,79	40,5
2,8	0,028	0,091	0,98	10,90	0,36	0,017	0,78	45,1
3,0	0,030	0,085	0,97	12,14	0,38	0,015	0,76	49,0
3,4	0,034	0,072	0,96	13,25	0,43	0,013	0,72	57,6

very small, being capillary; in the performance of modern pumps cooled baffles and traps are employed to prevent backstreaming and the conductance of the pump mouth decreases by this fact; the conductance is always higher for gases of low molecular weight.

From our previous discussions it is clear that there is no real fundamental principle to design a pump having a Ho-coefficient of the same value for hydrogen as for air.

It is apparent from the idealized model that while the compression capacity is very high, the specific speed is comparatively small. Thus it may be expected for the development of pumps the favouring of types having high compression ratio stages. However, an essential increase in specific pump speed or Ho-coefficient is impossible; otherwise it has no importance due to cooled baffles and traps.

Besides qualitative results quantitative ones may be obtained if some more detailed knowledge existed about the density and velocity distribution of the jet and its alteration.

The vapour stream from the boiler to the nozzle may be studied by thermodynamics and this was already attempted [19]. The vapour jet after leaving the nozzle may be determined with the aid of gasdynamics or kinetic theory and then numerical results may be obtained with the help of equ. (7).

Perhaps it is possible to repeat the previous procedure for the mixture of a gas and a vapour but it seems to be too complicated as yet.

The complete solution of the problem should make it possible to determine the optimum jet for a pressure range, the cross sections of nozzle and pump chamber and the necessary boiler input. Thus the design of pumps should be based on theoretical grounds instead of purely experimental ones.

REFERENCES

1. P. ALEXANDER, J. Sci. Instr., **23,** 11, 1946.
2. B. B. DAYTON, Rev. Sci. Instr., **19,** 793, 1948.
3. N. FLORESCU, Vacuum, **4,** 30, 1954.
4. N. FLORESCU, Vacuum, **10,** 250, 1960.
5. D. FLUKE, Rev. Sci. Instr., **19,** 665, 1948.
6. A. FUJINAGA, T. HANASAKA and H. TOTTORI, Vac. Symp., 390, 1962.
7. W. GAEDE, Ann. Phys., **46,** 357, 1915.
8. W. GAEDE, T. techn. Phys., **4,** 337, 1923.
9. R. J. GIBSON, Rev. Sci. Instr., **19,** 276, 1948.
10. W. G. HENDERSON, J. T. MARK and C. S. GEIGER, Vac. Symp., 170, 1959.
11. R. JAECKEL, Z. Naturforsch., **2A,** 666, 1947.
12. M. MATRICON, J. Phys. Rad., **3,** 127, 1932.
13. N. MILLERON, Vacuum, **13,** 255, 1963.
14. H. G. NOELLER, G. REICH and W. BÄCHLER, Vac. Symp., 72, 1959.
15. H. G. NOELLER, Z. Angew. Phys., **7,** 218, 1955.
16. H. G. NOELLER, Vacuum, **5,** 59, 1955.
17. L. RIDDIFORD and R. F. COE, J. Sci. Instr., **31,** 33, 1954.
18. R. B. SETLOW, J. Sci. Instr., **19,** 533, 1948.
19. H. R. SMITH, Vac. Symp., 140, 1959.
20. L. WERTENSTEIN, Proc. Cambr. phil. Soc., **23,** 578, 1927.
21. S. CHAPMAN and T. G. COWLING, The Mathematical Theory of Nonuniform Gases, Cambridge University Press, London.
22. S. DUSHMAN: Scientific Foundations of Vacuumtechnique, Budapest, 1959 (in Hungarian).
23. A. GUTHRIE and R. K. WAKERLING, Vacuum Equipment and Technique, McGraw-Hill, New York, 1949.
24. R. JAECKEL, Kleinste Drucke, Springer Verlag, Berlin, 1950.
25. E. H. KENNARD, Kinetic Theory of Gases, McGraw-Hill, New York, 1938.

ТЕОРИЯ ВСАСЫВАНИЯ ДИФФУЗИОННЫХ НАСОСОВ

Г. ТОВТ

Резюме

В теориях по механизму всасывания диффузионных насосов предполагается идеальная переносная способность газа в струях, истекающих из сопла высоковакуумного насоса и, таким образом, кажется, что диффузия играет главную роль в работе насосов. С целью получения правильных численных результатов в этих теориях предполагается наличие вторичных эффектов. В других теориях работы насосов эффект всасывания истолкуется на основе удара между молекулами газа и пара, но с помощью теории «свободного пробега», которая довольно громоздка и не достаточно общая. В данной работе сделана попытка для объяснения эффекта всасывания на основе кинетической теории неоднородных газов. Выводится уравнение, которое решается в одном идеальном случае. Это дает возможность для более глубокого понимания эффекта всасывания, истолкования экспериментальных результатов и критической оценки предшествующих теорий.

TWO SUBGROUPS OF THE LORENTZ GROUP AND THEIR PHYSICAL SIGNIFICANCE

By

L. JÁNOSSY

CENTRAL RESEARCH INSTITUTE FOR PHYSICS
BUDAPEST

(Received 12. II. 1965)

It is shown that the LORENTZ group can be represented as the product of two subgroups. The one subgroup is connected with rotation, the other with translation. The results of the negative relativistic experiments, like the MICHELSON—MORLEY experiment, are connected with the invariance of laws with respect to the rotational subgroup, while the positive relativistic effects, like the change of mass with velocity, are connected with the invariance with respect to the translational subgroup.

§ 1. The LORENTZ transformation can be written*

$$\mathbf{x}' = \mathscr{L}(\mathbf{x}) = \Lambda^{(\mathbf{p})}\,\mathbf{x} + \lambda\,, \tag{1}$$

where Λ is a fourth order matrix obeying

$$\tilde{\Lambda}^{(\mathbf{p})}\,\Gamma\Lambda^{(\mathbf{p})} = \Theta\,\Gamma \tag{2}$$

with $\Theta > 0\,,\quad \Gamma_{\nu\mu} = \delta_{\nu\mu}\,\gamma_\nu\,,\quad \gamma_1 = \gamma_2 = \gamma_3 = 1,\quad \gamma_4 = -\,c^2\,.$

The index $\mathbf{p}$ stands for the parameters of the transformation. The proper LORENTZ transformations are further restricted as follows:

$$\Theta = 1,\quad \det\Lambda^{(\mathbf{p})} = +\,1,\quad \Lambda^{(\mathbf{p})}_{44} > 0\,. \tag{3}$$

The matrix $\Lambda^{(\mathbf{p})}$ which we shall call a LORENTZ matrix depends on six parameters, explicitly it can be written in the following way:

$$\Lambda^{(\mathbf{p})} = \begin{pmatrix} \mathbf{L} & \mathbf{v}B \\ -\,\mathbf{v}'\,B/c^2 & B \end{pmatrix}, \tag{4}$$

where $\mathbf{v} = v_1, v_2, v_3$ is a three-component vector with the dimension of a velocity; further

$$\left.\begin{aligned} \mathbf{L} &= \mathbf{0} - (B-1)\,(\mathbf{v}' \circ \mathbf{v})/v^2\,, \\ B &= \frac{1}{\sqrt{1 - v^2/c^2}}\,,\quad \mathbf{v}' = -\,\mathbf{0}\mathbf{v}, \end{aligned}\right\} \tag{5}$$

* For notation see [1].

and $\mathbf{O}$ is an orthogonal matrix, thus $\mathbf{O}\widetilde{\mathbf{O}} = \mathbf{1}$. The relation (5) contains six parameters, i.e. the three components of $\mathbf{v}$ and three parameters in terms of which the orthogonal transformation $\mathbf{O}$ can be expressed.

It can be seen easily that the matrix Λ as given by (4) and (5) obeys indeed (2) and (3) and it can also be shown that any matrix obeying (2) and (3), i.e. any proper LORENTZ matrix, can be brought into the form (4), (5).

The matrix $\Lambda^{(\mathfrak{p})}$ can also be written

$$\Lambda^{(\mathfrak{p})} = \mathbf{O}^{(4)}\,\Lambda_{\mathbf{v}}\,, \tag{6}$$

where

$$\mathbf{O}^{(4)} = \begin{pmatrix} \mathbf{O} & 0 \\ 0 & 1 \end{pmatrix}, \tag{6a}$$

$$\Lambda_{\mathbf{v}} = \begin{pmatrix} \mathbf{V} & \mathbf{v}B \\ \mathbf{v}B/c^2 & B \end{pmatrix} \quad \text{and} \quad \mathbf{V} = 1 + (B-1)\,(\mathbf{v}\circ\mathbf{v})/v^2\,. \tag{6b}$$

Thus any LORENTZ matrix can be written as the product of an orthogonal transformation matrix of the type $\mathbf{O}^{(4)}$ and a transformation matrix of the type $\Lambda_{\mathbf{v}}$ which does not change the directions of the axes but changes the translational velocity of the system of reference by an amount $\mathbf{v}$.

§ 2. The LORENTZ matrix (4) can be taken as part of a coordinate transformation (1); this transformation leads from a system K to a system K' which moves with a velocity $\mathbf{v}'$ relative to K, the orthogonal matrix defining the directions of the axes of K' relative to K.

Alternatively, a transformation of the form (1) can be taken to describe a LORENTZ deformation. Indeed, consider a physical system $\mathfrak{Q}$. Another system $\mathfrak{Q}^*$ can be produced by replacing the points $\mathfrak{P}_1, \mathfrak{P}_2, \ldots, \mathfrak{P}_n$ of $\mathfrak{Q}$ by points $\mathfrak{P}_1^*, \mathfrak{P}_2^*, \ldots, \mathfrak{P}_n^*$ making up $\mathfrak{Q}^*$.

Written more explicitly, at the time t the point $\mathfrak{P}_n$ may have coordinates $\mathbf{r}_n(t)$, at a time t^* the corresponding point $\mathfrak{P}_n^*$ then has coordinates $\mathbf{r}_n^*(t^*)$, so that

$$\mathbf{r}_n^*(t^*),\, t^* = \mathbf{x}_n^*\,,$$

and

$$\mathbf{x}_n^* = L_{\mathbf{q}}(\mathbf{x}_n) = \Lambda_{\mathbf{q}}\,\mathbf{x}_n + \lambda\,. \tag{7}$$

In the above consideration $\mathbf{x}_n$ and $\mathbf{x}_n^*$ are the (four-component) coordinates of the points of $\mathfrak{Q}$ and $\mathfrak{Q}^*$ both taken relative to one system of coordinates, K.

We have written $\Lambda_{\mathbf{q}}$ in place of $\Lambda^{(\mathfrak{p})}$ to signify that we are considering a transformation that refers to one particular system of reference, K, and describes the change $\mathfrak{Q}\to\mathfrak{Q}^*$ in terms of the coordinates relative to this system of reference. Thus $\Lambda_{\mathbf{q}}$ is the homogeneous part of the transformation (7) which

represents a deformation in terms of coordinates relative to K. Λ_q is a tensor and we shall call it the *deformation tensor.*

We may also write symbolically

$$\mathfrak{Q}^* = L_q(\mathfrak{Q}) \tag{7a}$$

and the representation of (7a) relative to K can be written in the form (7). The representation of (7a) relative to another system of coordinates, K', can be written

$$\mathbf{x}_n^{*\prime} = \Lambda_{q'} \mathbf{x}_n' + \lambda' , \tag{8}$$

where

$$\left.\begin{aligned} \mathbf{x}_n^{*\prime} &= \Lambda^{(p)} \mathbf{x}_n^* + \lambda , \\ \mathbf{x}_n' &= \Lambda^{(p)} \mathbf{x}_n + \lambda , \end{aligned}\right\} \tag{9}$$

and $\Lambda^{(p)}$ is the homogeneous part of the transformation leading from K to K'. From (8) and (9) it follows, that

$$\Lambda_{q'} = \Lambda^{(p)} \Lambda_q \Lambda^{(p)-1} . \tag{10}$$

Thus Λ_q, $\Lambda_{q'}$, . . . are the representations of the deformation tensor Λ_q relative to systems of reference K, K', . . .

From (10) it follows that the representations of a deformation tensor Λ_q are all proper LORENTZ matrices if one of the representations is a proper LORENTZ matrix, regardless of whether or not the matrices $\Lambda^{(p)}$ are proper LORENTZ matrices.

§ 3. The representations of a deformation tensor corresponding to the deformation $\mathfrak{Q} \to \mathfrak{Q}^*$ in different systems of reference are given by matrices that are connected by relations of the form (10). From (10) it may be seen that the representations Λ_q, $\Lambda_{q'}$, . . . of Λ_q are matrices with the same eigenvalues. It was shown elsewhere [2], that the eigenvalues of a LORENTZ matrix can be written

$$e^{i\varphi} , \quad e^{-i\varphi} , \quad \sqrt{\frac{c+v}{c-v}} , \quad \sqrt{\frac{c-v}{c+v}} , \tag{11}$$

i.e. the eigenvalues are characterized by an angle φ and a velocity v. A LORENTZ matrix can be brought into a standard form, this means, that in a suitable representation a matrix Λ_q with eigenvalues (11) obtains the form

$$\Lambda_{q_0} = \begin{pmatrix} \cos\varphi & \sin\varphi & 0 & 0 \\ -\sin\varphi & \cos\varphi & 0 & 0 \\ 0 & 0 & B & Bv \\ 0 & 0 & Bv/c^2 & B \end{pmatrix} . \tag{12}$$

The deformation tensor represented by (12) describes turning through an angle φ around the x_3-axis and acceleration by an amount v in the direction of the x_3-axis.

§ 4. We note that the transformation eq. (6a) has the eigenvalues

$$e^{i\varphi},\ e^{-i\varphi},\ 1,\ 1. \tag{13}$$

(We remark that the eigenvalues of the third order orthogonal matrix $\mathbf{O}$ are $e^{i\varphi}$, $e^{-i\varphi}$, 1.)

The representations of $\mathbf{O}^{(4)}$ relative to various systems of reference will in general not appear in the form (6a). However, all the representations of $\mathbf{O}^{(4)}$ have eigenvalues of the form (13).

By $\mathbf{O}^{(4)}$ we may denote not only the deformation tensors that appear in the form (6a) but all the deformation tensors with eigenvalues of the form (13). We may call these deformations *rotational* deformations. We see from (13) that the product of two rotational deformation tensors is also a rotational deformation tensor. It can thus be concluded that the rotational deformations form a subgroup of the LORENTZ group.

Similarly, the eigenvalues of the deformation tensors Λ_v are found to be

$$1, 1, \sqrt{\frac{c+v}{c-v}}, \sqrt{\frac{c-v}{c+v}}. \tag{14}$$

It follows from the form of the eigenvalues (14) that the product of two matrices with such eigenvalues has also eigenvalues of similar type and therefore the matrices Λ_v form also a subgroup of the LORENTZ group.

§ 5. We see thus that the proper Lorentz group can be built up of two subgroups: one subgroup with elements of the rotational type $\mathbf{O}^{(4)}$, another subgroup with elements of the translational type Λ_v. The elements of the proper Lorentz group can be represented as the products of a rotational element with a translational element.

In order to make this representation unique, we may use the following convention. Of a given Lorentz matrix Λ_q with eigenvalues (11) we determine the normal representation (12) and from this normal form we define the splitting of Λ_q into its two components as follows. Let $\Lambda^{(p)}$ denote the coordinate transformation from the system of reference in which Λ_q appears in the normal form (12) into the system K relative to which we wish to represent Λ_q. We have thus

$$\Lambda_q = \Lambda^{(p)}\,\Lambda_{q_0}\,\Lambda^{(p)-1}, \tag{15}$$

and also

$$\Lambda_q = \mathbf{O}^{(4)}\,\Lambda_v, \tag{15a}$$

with

$$\mathbf{O}^{(4)} = \Lambda^{(\mathfrak{p})}\, \mathbf{O}_{\varphi}^{(4)}\, \Lambda^{(\mathfrak{p})-1}\,, \quad \Lambda_{\mathfrak{v}} = \Lambda^{(\mathfrak{p})}\, \Lambda_{\mathfrak{v}}\, \Lambda^{(\mathfrak{p})-1} \tag{15b}$$

and

$$\mathbf{O}_{\varphi}^{(4)} = \begin{pmatrix} \cos\varphi & \sin\varphi & 0 & 0 \\ -\sin\varphi & \cos\varphi & 0 & 0 \\ 0 & 0 & 1 & 0 \\ 0 & 0 & 0 & 1 \end{pmatrix},$$

$$\Lambda_{\mathfrak{v}} = \begin{pmatrix} 1 & 0 & 0 & 0 \\ 0 & 1 & 0 & 0 \\ 0 & 0 & B & Bv \\ 0 & 0 & Bv/c^2 & B \end{pmatrix}, \tag{15c}$$

Relations (15), (15a), (15b), (15c) give a unique procedure for the splitting up of a deformation tensor into its rotational and translational parts.

As $\mathbf{O}_{\varphi}^{(4)}$ and $\Lambda_{\mathfrak{v}}$ are commutative, their transforms $\mathbf{O}^{(4)}$ and $\Lambda_{\mathfrak{v}}$ are also commutative and we find

$$\Lambda_{\mathfrak{q}} = \mathbf{O}^{(4)}\, \Lambda_{\mathfrak{v}} = \Lambda_{\mathfrak{v}}\, \mathbf{O}^{(4)}\,.$$

We see therefore that any element of the Lorentz group can be split into the product of an element of the rotational group and an element of the translational group in a manner in which the factors are commutative.

§ 6. We may make here the following interesting remark on the connection of this splitting up of the Lorentz group with physical phenomena. The theory of relativity is based partly on the negative results of certain experiments like the MICHELSON—MORLEY or the TROUTON—NOBLE experiment. In these negative experiments an arrangement is turned round and no apparent effect is observed.

The turning round of an apparatus corresponds to a LORENTZ deformation of the rotational type. The negative outcome of these experiments can be predicted from the LORENTZ invariance of the laws of nature. However, if the laws of nature were invariant only with respect to the rotational subgroup of the LORENTZ transformation this would be sufficient to account for the negative results of these experiments.

There exist further the so-called positive relativistic effects, like the change of mass with velocity or the perpendicular DOPPLER effect. The latter effects can be understood by supposing that the laws of nature are invariant with respect to the translational group.

We see thus that the invariance of the laws of nature with respect of the two subgroups of the LORENTZ group manifests itself in two distinct groups of experiments. Taking these groups of experiments together, we come to

conclude that the laws of nature are invariant against both the translational and the rotational subgroup, and therefore against the whole proper LORENTZ group, as the elements of the whole group can be formed as products of the elements taken from the two subgroups.

From the experimental point of view it may be added that the first type of experiments, i.e. the negative experiments, has been carried out with very great precision, therefore the invariance against the rotational group is very precisely established experimentally.

The experiments concerning the change of mass with velocity are not very accurate (see e.g. [3]) howerer, very good evidence for the invariance with respect to the translational sub-group was obtained by D. C. CHAMPEREY, G. R. ISAAK and A. M. KHAN [4] with the help of the Mössbeuer effect. These measurements seem to be the most precise carried out so far supporting LORENTZ invariance.

Thus the measusements of CHAMPENEY et al. together with the older measurements of the Michelson type provide good evidence for the invariance with respect to both sub-groups and therefore provide evidence for the invariance with respect to the whole group of proper LORENTZ transformations.

REFERENCES

1. L. JÁNOSSY, Acta Phys. Hung., **20,** 81, 1966.
2. L. JÁNOSSY, Acta Phys. Polonica, **27,** 61, 1965,
3. P. FARAGÓ and L. JÁNOSSY, Nuovo Cim., **5,** 1411, 1957.
4. D. C. CHAMPENEY, G. R. ISAAK and A. M. KHAN, Physics Letters, **7,** 241, 1963.

ДВЕ ПОДГРУППЫ ГРУППЫ ЛОРЕНЦА И ИХ ФИЗИЧЕСКИЙ СМЫСЛ

Л. ЯНОШИ

Резюме

В работе показывается возможность представления группы Лоренца в виде произведения двух подгрупп. Первая из подгрупп связана с ротацией, другая — с трансляцией. Отрицательный результат опытов по теории относительности — например опыта Майкельсона—Морли — связан с инвариантностью законов, относящихся к подгруппе вращения, а положительный результат опытов по теории относительности — например, зависимоть массы от скорости тела — связан с инвариантностью по отношению трансляционной подгруппы.

EXPERIMENTAL ERRORS AND THE INTERPRETATION OF COMMON LEAD ISOTOPE ABUNDANCES IN LEAD ORES

By

A. KOVÁCH

INSTITUTE OF NUCLEAR RESEARCH OF THE HUNGARIAN ACADEMY OF SCIENCES, DEBRECEN

(Presented by A. Szalay. — Received 22. II. 1965)

Experimental error sources, giving rise to incorrect model ages according to the HOLMES—HOUTERMANS model are discussed. Special attention is paid to the apparent age anomalies caused by the inadequate resolution of the mass spectrometer.

Introduction

Since the discovery of the variability and time dependence of the isotopic constitution of common lead by NIER et al. in 1938 [1], several models have been worked out for the interpretation of common lead isotopic abundances [2]. Since the parent system of any common lead ore usually cannot be associated with some known geochemical system, there is a rather free scope in constructing various models, based on various principles having equally the appearance of truth, and using experimentally determined isotopic constitution data for settling the free parameters of a given model. As our knowledge of the primary sources of lead are very insufficient, the main check on the adequacy of one or another model is their internal consistency in case of using a group of experimental data other than that applied in the course of the construction of the given model itself.

The individual models can be roughly divided into single-stage and multistage ones, considering the behaviour in time of the parent system assumed. On the other hand, with respect to the space behaviour of the parent system, they can be classified as homogeneous and heterogeneous models, the latter allowing local variations in the U/Pb ratio of the parent system.

Though nowadays it is the general opinion that in the case of each lead occurrence a special model is the best to work out, great use has been made up to now of the single-stage heterogeneous model developed by HOLMES [3] and HOUTERMANS [4] (H—H model). We do not intend to discuss here the basic principles of this model, in this respect we refer to the literature already cited [2]. We should like, however, to describe briefly the general features of it.

According to the H—H model the development of lead isotope abundances can be described by the following equations

$$x = x_0 + \alpha V(e^{\lambda t} - e^{\lambda t}), \tag{1}$$

$$y = y_0 + V(e^{\lambda' t} - e^{\lambda' t}), \tag{2}$$

$$z = z_0 + V(e^{\lambda'' t} - e^{\lambda'' t}). \tag{3}$$

The symbols used in equation (1) — (3) are defined in Table 1.

Dividing equ. (2) by equ. (1) a simple relation between the isotopic constitution and age can be obtained

$$\frac{y - y_0}{x - x_0} = \frac{1}{\alpha} \frac{e^{\lambda' t_0} - e^{\lambda' t}}{e^{\lambda t_0} - e^{\lambda t}}. \tag{4}$$

Equation (4) means that if the isotopic ratio y is plotted against the ratio x, points representing ores with different isotopic composition but having the same age should lie along straight lines starting from the point represented by the coordinates x_0, y_0. The slopes of these straight lines (isochrones) are determined by the absolute age only.

Table 1

Symbols and constants used throughout this work

Isotope abundance ratio	Present ($t = 0$)	At time t	Primeval value ($t = t_0$)
Pb^{206}/Pb^{204}		x	x_0
Pb^{207}/Pb^{204}		y	y_0
Pb^{208}/Pb^{204}		z	z_0
U^{238}/Pb^{204}	αV	$\alpha V e^{\lambda t}$	$\alpha V e^{\lambda t_0}$
U^{235}/Pb^{204}	V	$V e^{\lambda' t}$	$V e^{\lambda' t_0}$
Th^{232}/Pb^{204}	W	$W e^{\lambda'' t}$	$W e^{\lambda'' t_0}$

$\lambda = \lambda(U^{238}) = 0{,}1537 \cdot 10^{-9}\, y^{-1}$ $\quad x_0 = 9{,}50$

$\lambda' = \lambda(U^{235}) = 0{,}9722 \cdot 10^{-9}\, y^{-1}$ $\quad y_0 = 10{,}36$ $\quad \alpha = 137{,}8$

$\lambda'' = \lambda(Th^{232}) = 0{,}0499 \cdot 10^{-9}\, y^{-1}$ $\quad z_0 = 29{,}49$

Equations (1) and (2) are parametric representations of the so-called "isotope development lines" of the same graph. The point corresponding to the isotopic composition of a given lead sample, developing in a closed system represented by a fixed value of V, is changing his position with time along such a development line in the H—H diagram. (See Fig. 1.)

This means that a given lead sample can be unambiguously characterized either by the pair of the values x and y, or by the values V and t, the former called the "milieu index" and the latter the "model age". It is obvious that

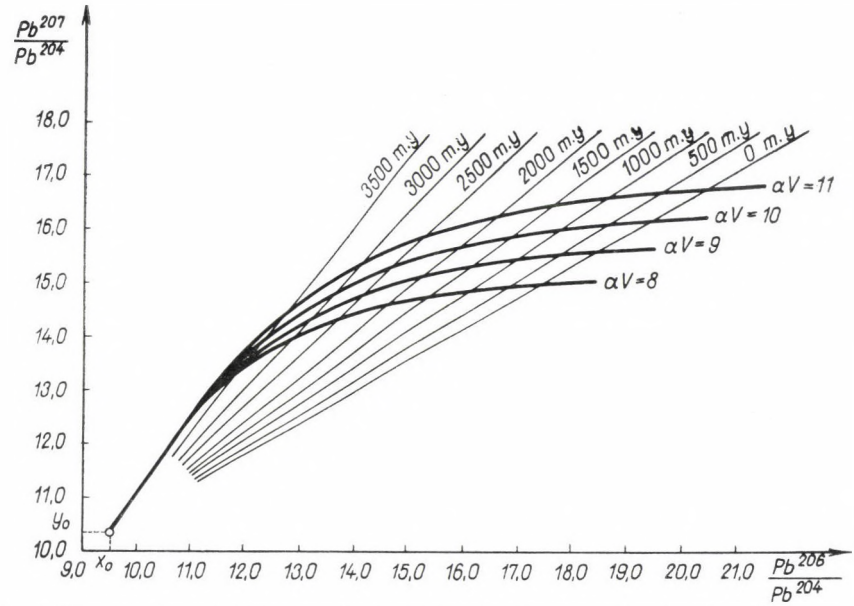

Fig. 1. The relationship between the isotopic abundances of lead and model ages according to the HOLMES—HOUTERMANS model

errors in the determination of the isotopic data have an influence on the value of "model age" determined this way, as well as on the value of the "milieu-index".

Sources of errors in the determination of lead isotope abundances

There are two main sources of errors in investigating the isotopic constitution of lead: statistical errors arising in the course of the measurement of the individual peak heights (or peak height ratios) and errors being due to the inadequate resolution of the mass analysing system.

Statistical errors are well known and lead isotope abundance data are usually given together with their statistical variances. The analysis of errors due to incorrect resolution is, however, neglected, though in some cases it succeeded in proving the influence of this effect on the final data. In this respect we should like to refer to the work of RUSSELL and others [5] correcting the data given by ASHWATNARAYANA [6] on the basis of the thorough re-evaluation of the original mass spectrograms and taking into account the effect of the poor resolution of the mass spectrometer too; as well as to

the work done at Vancouver University aiming at the re-examination of some previously investigated material with improved techniques [7].

The importance of this question is supported by the fact that most of the lead isotope abundance data (especially data used as an experimental basis in the elaboration of lead isotope abundance models) were obtained with mass spectrometers having intermediate resolution characteristics. The mass peaks used in the mass spectrometry of lead (Pb^+, PbS^+, PbI^+, $Pb(CH_3)_4^+$) lie in the upper part of the mass scale of these instruments and thus to obtain reasonable accuracy the highest resolution available with these instruments is to be achieved.

Influence of resolution to lead isotope abundance data

In the course of scanning a mass spectrogram peak heights are measured at the output of the analysing system. As a result of several factors not discussed in detail here, the mass spectrum does not consist of sharp maxima at the individual mass numbers, but the peaks are broadened to an extent characterized by the resolving power of the instrument and thus they possibly can — more or less — contribute in intensity to the neighbouring peaks too.

If the relative difference in the mass numbers is low, we can say that the peak shape is determined by instrumental effects only. This means that a "reduced peak shape function" $f(\mu - \mu_0)$ can be constructed characterizing the peak shape with no respect to the height of it and being normalized at mass number $\mu = \mu_0$ to unity. If the measured peak height at mass number μ_0 is I_0, the contribution of this peak to the intensity measured at mass number μ will thus be $I = I_0 \cdot f(\mu - \mu_0)$.

If we assume that the individual peaks contribute only to the intensity of the neighbouring peaks (i.e. $f(\mu - \mu_0) = 0$ if $|\mu - \mu_0| > 1$), in the case of lead the measured peak intensities $I_\mu^{(m)}$ and the "real" intensities I_μ will satisfy

$$I_{204}^{(m)} = I_{204}\,, \tag{5}$$

$$I_{206}^{(m)} = I_{206} + I_{207} \cdot f(-1)\,, \tag{6}$$

$$I_{207}^{(m)} = I_{207} + I_{208} \cdot f(-1) + I_{206} \cdot f(+1)\,, \tag{7}$$

$$I_{208}^{(m)} = I_{208} + I_{207} \cdot f(+1)\,. \tag{8}$$

Assuming — in a rough approximation — that the peaks are of symmetrical shape, i.e. $f(-1) = f(+1) = a$; the isotope abundance ratios with respect to the abundance of the Pb^{204} isotope can be given as follows:

$$x^{(m)} = x + a \cdot y, \tag{9}$$

$$y^{(m)} = y + a\,(x + z)\,, \tag{10}$$

$$z^{(m)} = z + a \cdot y\,. \tag{11}$$

From equations (9)—(11) the following expressions can be simply derived:

$$\frac{y^{(m)} - y}{x^{(m)} - x} = \frac{x + z}{y}, \tag{12}$$

$$\frac{z^{(m)} - z}{x^{(m)} - x} = 1. \tag{13}$$

This means that in the case of a symmetrical peak shape if we determine the isotopic composition of a given sample under different resolution conditions, the measured values will lie along straight lines in the x, y diagram, as well as in the z, x diagram, the slope of this in the former being determined by the real isotope ratios only. In the z, x diagram the line of displacement inclines by 45° to the coordinate axes independently of the age of the sample.

From the viewpoint of the H—H model it is of obvious importance to examine, how far measurements carried out under inappropriate resolution conditions can influence the position of the measured points in the $x - y$ diagram with respect to the isochrones, i.e. how far this effect can influence the value of the model age obtained.

The discussion of this problem is rendered more difficult by the fact that the basic assumptions of the H—H model do not give a well-defined relation between all the three Pb isotope ratios even with fixed t. Fixing the parameter V results in a definite relation between the values x and y, but the value z depends still on the Th/Pb ratio. We chose therefore in calculating displacements in the H—H diagram the quantity V as a parameter, the value of the parameter W being fixed by the relation $W/V = 3{,}77$. This ratio is the same as found by RUSSELL et al. [8] for "conformable" leads, and corresponds to the approximate ratio of the geochemical abundances of Th and U as well. Since uranium and thorium are very similar in their geochemical character, no variation in the Th/U ratio was found reasonable to compute with, all the more because a two-parameter treatment would make the survey of this problem superfluously involved.

In Fig. 2 the slopes of displacement lines are shown according to equ. (12) with the U^{238}/Pb^{204} value as parameter, as function of absolute age. In Fig. 3 for comparison, the slopes of isochrones are also shown.

As one can see the isochrone slope varies with age between the limits 0,59 and 1,75 while the displacement slopes vary between 3,10 and 3,75, according to the age and the value of the U^{238}/Pb^{204} ratio. Of course, variations in the Th/U ratio would rather strongly influence the slope of the displacement lines, but since only minute displacements in the H—H diagram are to be expected, we found it reasonable to use an average displacement slope for each t in our calculations.

As a result of this simple approximation we can count in practice with a linear shift of the H—H isochrones. Since the slopes of the displacement lines are always greater than the isochrone slopes, even in the case of a parent system highly depleted in thorium, the resulting model age will be always higher than the true one, i.e. measurements carried out under inappropriate resolution conditions give rise to apparent B-type anomalies.

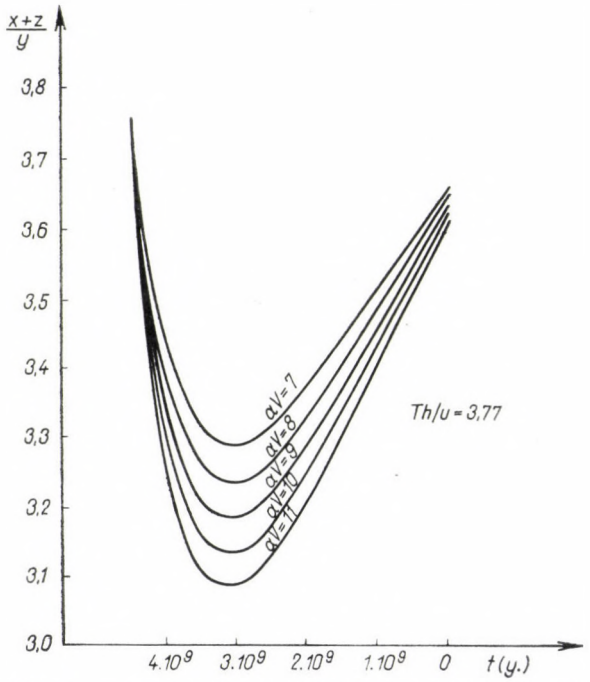

Fig. 2. Relationships between the slopes of displacements of points in the H—H diagram as a result of incorrect resolution and the parameters of the HOLMES—HOUTERMANS model

In Fig. 4 the displacement of the isochrones in the H—H diagram is shown assuming a symmetrical peak shape with a reduced peak contribution factor $f(\pm 1) = 0{,}005$. In general one can state that if the individual peaks contribute by $1\,{}^0/_{00}$ of their intensity to that of the neighbouring peaks, the resulting model age for paleozoic and younger leads would be high by about 50 m. y., the value of the milieu index appearing by about 1% higher than the real one. In the case of old precambrian ores the resulting age value does not markedly differ from the real model age, e.g. in the case of an ore 3000 m. y. old the shift would be about 20 m. y., but the milieu index would be high by about 2.5%. Stating this, we should like to emphasize that a $0{,}5-1\,{}^0/_{00}$ cross-contribution of neighbouring peaks is a very realistic estimation in the case of common analytical mass spectrometers.

Summarizing the preceding discussion the conclusion can be drawn that if the model age of a given lead sample is to be determined with an accuracy of ± 10 m. y., then it should be assured that the contribution of the neigh-

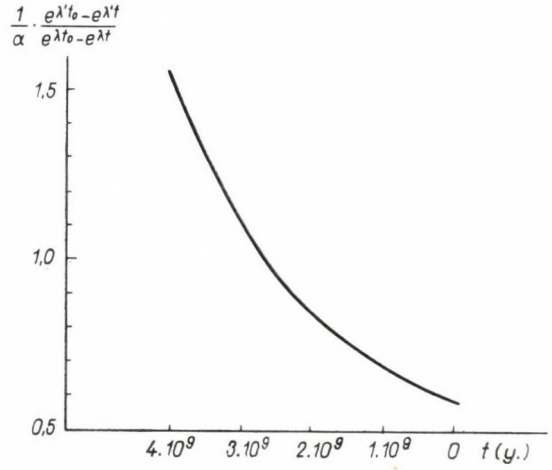

Fig. 3. Isochrone slopes of the HOLMES—HOUTERMANS model

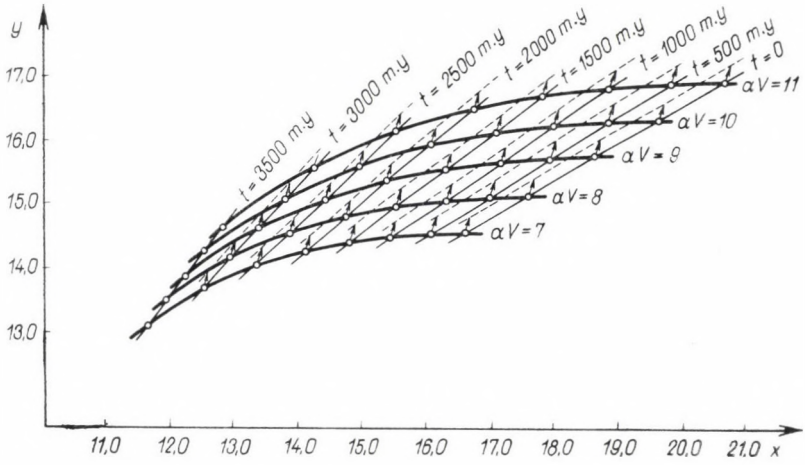

Fig. 4. Displacement of the HOLMES—HOUTERMANS isochrones as a result of incorrect resolution of the mass spectrometer. A symmetrical peak shape and a reduced peak contribution factor $f(\pm 1) = 0{,}005$ is assumed

bouring peaks to each other in intensity should be less than $0{,}2\ ^0/_{00}$, otherwise the age shifting effect of modest resolution must be taken into consideration.

We should like to note, however, that a symmetrical peak shape is to be expected in an ideal case only. In practice — as a consequence of scattering processes occurring in the vacuum chamber of the mass spectrometer

and causing a negatively skewed distribution of ion kinetic energies — asymmetric peak shapes occur with a broadening of the peak "tail" towards the seemingly smaller mass numbers.

This means that in equations (5)—(8) $f(-1) > f(+1)$ and thus foreign contribution to the peak intensities arise mainly from peaks of greater mass numbers. In such a case the following relation can be derived from equations (5)—(8):

$$\frac{y^{(m)} - y}{x^{(m)} - x} = \frac{z}{y} + \frac{x}{y}\,\frac{f(+1)}{f(-1)} < \frac{x+z}{y}\,. \tag{14}$$

In a limiting case we have $f(+1) = 0$, and so the following limits can be given for the displacement slope in case of an asymmetric peak shape:

$$\frac{z}{y} \leqq \frac{y^{(m)} - y}{x^{(m)} - x} \leqq \frac{x+z}{y}\,. \tag{15}$$

The quantity z/y varies within the limits 2,1 — 2,8, the exact value depending on the age of the sample and on the choice of the model parameters. This justifies also our previous statement that the displacement slopes are always greater than the isochrone slopes and that it is reasonable to compute with an average displacement slope.

The numerical demands on the resolving power of the mass spectrometer as previously given are thus only limiting values, but they change only slightly if we calculate with an asymmetric peak shape.

We should like to emphasize that in the preceding discussion we did not touch the question of the overall validity of the H—H model; our calculations presume the perfect validity of it and deal only with apparent deviations caused by instrumental effects.

Statistical and other errors

The variations of the isotopic ratios x, y and z are composed of the variations of the peak intensities measured for the individual lead isotopic peaks in the mass spectrogram. As the abundance of the Pb^{204} isotope is by far the smallest (in case of common leads usually 1,2—1,8%) the errors of the relative abundances are predominantly determined by the variation of the measured Pb^{204} peak intensity and thus the quantities x, y and z are usually correlated to a considerable extent. Since the variations of the Pb^{206} and Pb^{207} intensities are of the same order, this correlation leads to the development of elliptical deviation patterns in the x, y diagram, with the great axis inclining by about 45° to the coordinate axes, the centre of this deviation pattern supplying the most probable values for the quantities x and y. Erratic

age values originating from statistical errors are — in a statistical manner — equally distributed between B-type and J-type anomalies, but B-type anomalies are in the case of leads younger than 2700 m. y. connected with a seemingly high, and J-type anomalies with seemingly low values of the milieu index. In the case of leads older than about 2700 m. y. the situation becomes reversed.

In some types of mass spectrometers systematic errors can arise from the presence of Hg^{204} background in the instrument, interfering with the Pb^{204} intensity, especially if the measurements are carried out on the atomic ions. One should note, however, that disturbing background due to Hg^{204} can occur even at higher mass numbers, for example in the region of the PbI^+ ions as a consequence of the following reaction:

$$PbI^+ + Hg^{204} \rightleftharpoons Pb + Hg^{204}I^+$$

the product of which reaction contributes to the intensity measured at mass number 331 for the $Pb^{204}I^+$ ion.

Erratically high Pb^{204} abundances measured in the presence of a Hg background result in the displacement of the points in the $x-y$ diagram in the 45° direction and give rise to the development of apparent B-type anomalies. Of course, if we take into account the background due to mercury, this effect does not play a role, but it enlarges the uncertainty of the determination of the Pb^{204} abundance.

The individual error sources dealt with in this report usually appear together, and thus can give rise to rather complicated deviation patterns in the H—H diagram. In the following we should like to demonstrate the above mentioned effects in a practical case.

A practical case

The author of this report has recently published some experimental data on the lead isotopic constitution of the lead ores of the Velence Mountains, Hungary [9]. The rather great scatter of the experimental points in the $x-y$ diagram rendered it probable that, in spite of the acceptable deviations of the individual measurements, they are burdened by some errors being superior to the statistical ones. To clear up this question all samples have been remeasured with improved techniques. The results are plotted in Fig. 5 where results of the first set of measurements as given in [9] are shown by circles and the replicate data by full dots.

It is conspicuous that in the case of the repeated measurements the statistical errors could be highly reduced, resulting primarily in the increased

accuracy of the Pb^{204} determination. The ratio of the main axes of the dispersion ellipses is about 1 : 3,5; indicating an improvement of this order in the relative accuracy of the Pb^{204} determinations, while the accuracies of the Pb^{206} and Pb^{207} determinations are improved by a factor of about 2.

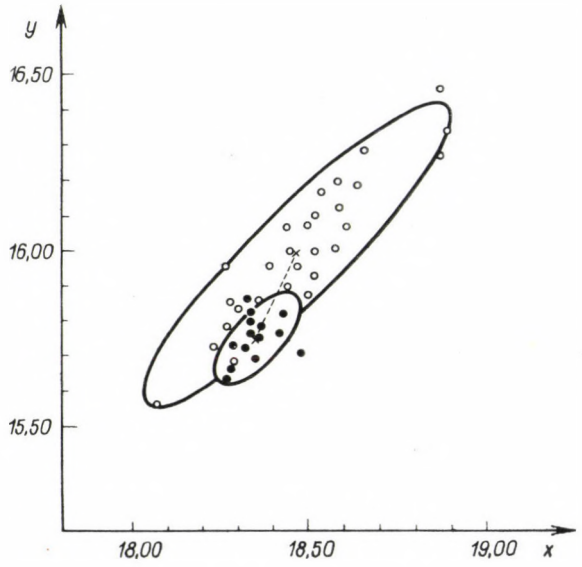

Fig. 5. Isotopic constitution of lead ores of the Velence Mountains, Hungary, according to two sets of measurements. Results as given in [9] are shown by circles, dots represent replicate data determined with improved techniques

Fig. 5 strikingly shows that the resolution of the instrument was not sufficient during the first measurements. The average isotope abundance values of the two sets of measurements differ significantly from each other, and the slope of the straight line to the two central points is $1{,}95 \pm 1{,}0$ the error being calculated from the deviation of the two average points. This steepness corresponds within the limits of error to the displacement slope which may be calculated on the basis of the discussions of this report.

For the very reason of the approximative nature of the general statements made in this report more elaborate conclusions concerning this special case cannot be drawn, but, by all means, the presence of additional errors originating from the inadequate mass resolution could be stated without any doubt, and thus the H—H model ages given in the previous report [9] turn out to be high to some extent.

Detailed data on the replicate measurements will be published in a separate report.

REFERENCES

1. A. O. C. Nier, Phys. Rev., **55,** 153, 1939.
2. R. D. Russell and R. M. Farquhar, Lead Isotopes in Geology, Intersci. Publ. Inc., N. Y. — London, 1960.
3. A. Holmes, Nature, **157,** 680, 1946.
4. F. G. Houtermans, Naturwiss., **6,** 185, 1946.
5. R. D. Russell et al., Nature, **194,** 565, 1962.
6. U. Ashwatnarayana, Nature, **193,** 470, 1962.
7. R. D. Russell, Researches on Lead Isotope Abundances in Earth Science and Meteoritics, ed. by J. Geiss and E. D. Goldberg, N. Holland Publ. Co., Amsterdam, 1963, p. 44.
8. R. D. Russell and R. M. Farquhar, Geochim. et Cosmochim. Acta, **19,** 41, 1960.
9. A. Kovách, MTA III. Oszt. Közl., **13,** 239, 1963.

ЭКСПЕРИМЕНТАЛЬНЫЕ ОШИБКИ И ИНТЕРПРЕТАЦИЯ ИЗОТОПНОГО СОСТАВА ОБЫКНОВЕННОГО СВИНЦА

А. КОВАЧ

Р е з ю м е

Рассматриваются источники экспериментальных ошибок, приводящиеся к неправильным модельным возрастам по модели Голмса и Гутерманса. Особое внимание уделяется на кажущиеся аномалии возрастов, вызванные неудовлетворительным разрешением масс-спектрометра.

STUDY OF THE MULTIPLE SCATTERING CONSTANT IN EMULSION AT GREAT CELL LENGTHS

By

G. Bozóki, É. Gombosi, L. Jenik, E. Nagy and M. Sahini*

CENTRAL RESEARCH INSTITUTE OF PHYSICS, BUDAPEST

(Presented by L. Jánossy. — Received 9. III. 1965)

The dependence of the multiple scattering constant (K) on cell length is studied in the interval of 0,5 cm $\leq t \leq$ 10 cm by means of two different methods. By the "coordinate method" the average value of K is found to be $K = 30{,}2 \pm 0{,}6$ in the cell length interval of 0,5 cm $\leq t \leq$ 3 cm. When the effect of spurious scattering is taken into account this value decreases to $27{,}1 \pm 1{,}2$. The "angular dispersion" method yields $K = 30{,}2 \pm 2{,}5$ for the cell length interval of 3 cm $\leq t \leq$ 10 cm. It is found that the spurious scattering depends on the cell length as $d_{sp} = at^n$ where $a = (6{,}84 \pm 1{,}33) \cdot 10^{-3}$ and $n = 1{,}22 \pm 0{,}17$ in the cell length interval of 0,2 cm $\leq t \leq$ 3 cm.

1. Introduction

Multiple Coulomb scattering of high energy particles in emulsion at great cell length ($t \geq 1$ cm) has been studied recently by several authors [1—7]. Some of them found that the scattering constant K for such cell lengths is constant and smaller than the theoretically expected saturation value, others obtained results, which showed that K has a decreasing tendency with increasing cell length. Such an effect — if it exists — is very important not only from the point of view of the theory of multipl Coulomb scattering but also for the determination of the momentum of high energy particles. Therefore it seemed to be worth while to continue our earlier investigations [6].

In the investigation reported here the dependence of the scattering constant on cell length was determined from $t = 0{,}5$ cm up to $t = 10$ cm by two different methods.

In the interval of 0,5 cm $\leq t \leq$ 3 cm, the "coordinate method" [8] of multiple scattering measurements and for higher cell lengths the "angular dispersion method"** [5, 6] were used. At $t = 3$ cm, K was determined by both methods to check their consistency.

The present measurements permitted also investigation of the spurious scattering as a function of cell length.

* On leave from the Institute of Atomic Physics, Bucharest.

** This method is analogous to the "tangent" or "angular" method of multiple scattering measurements.

2. Discussion of the methods of measurement

2.1. The scattering constant can be calculated in the case of the coordinate method from the well-known formula:

$$K = \frac{0{,}513 \cdot p\beta \cdot \bar{d}_c}{t^{3/2}} \tag{1}$$

with the approximation $\bar{d}_{sp} \ll \bar{d}_c$. Here $\bar{d}_c$ and $\bar{d}_{sp}$ are quantities calculated from the second differences of the coordinate values of the track measured and refer to multiple Coulomb scattering and spurious scattering, respectively. (d, t and $p\beta$ are expressed in μ, $100\,\mu$ and MeV/c, respectively.) The value of the scattering constant thus obtained is larger than or at most equal to the true value of K. The less the spurious scattering can be neglected as compared with the Coulomb scattering, the greater is this deviation. Measurements were made e.g. by [4] in two regions of a plate, where in the first region the spurious scattering was small, while in the second it was large. The scattering constant was found to be in the "good region" $K = (28{,}0 \pm 2{,}2)$ and in the "bad region" $K = (42{,}1 \pm 3{,}6)$. It is obvious that the method described above is rather sensitive to the spurious scattering in the emulsion plate.

2.2. In the case of the "angular dispersion" method [5], the lateral angular distribution is measured in two or more strips perpendicular to the direction of the beam. When the distance t of the strips from one another is measured in units of $100\,\mu$, the scattering constant can be determined from the following formula:

$$K_t = \frac{(|\bar{\vartheta}|\bar{\vartheta}_t|^2 - {}_0|^2)^{1/2}}{1{,}225 \cdot t^{1/2}}\, p\beta\,. \tag{2}^*$$

Here $|\bar{\vartheta}_t|^2 = \sum_{i=1}^{N} \vartheta_{t,i}^2/N$ and $|\bar{\vartheta}_0|^2 = \sum_{i=1}^{N} \vartheta_{0,i}^2/N$, where, $\vartheta_{0,i}$ and $\vartheta_{t,i}$ are the projected angles (in degrees) between the i-th measured track and the average direction of the beam in the first strip ($t = 0$), and the strip at a distance t, respectively.

The contributions of the various noises (grain, stage, reading noise) to the Coulomb scattering angle are the same in each strip. Thus by this method the effect of all noises can be eliminated. However, the effect of small-angle diffraction scattering has to be taken into account. (See the Appendix.)

* The average scattering angles measured by the "coordinate" method are calculated from those measured by the "angular" or "tangent" method, by multiplying the latter by a factor of 1,225 [8].

3. Experimental results

3.1. *Measurement with the coordinate method*

3.1.1. Measurements were carried out on tracks of π^--mesons of momentum (17,2 $\pm$ 0,2) GeV/c in Ilford G5 emulsion plates of size 14,5 cm $\times$ 23,5 cm $\times$ 0,06 cm by means of a Koristka R4 microscope with an objective of 55 $\times$ magnification.

Tracks of a total length of about 10 m were measured with a basic cell length of $t = 0{,}5$ cm and a further total length of about 3 m track with smaller cell lengths ($t = 50\ \mu \div 0{,}5$ cm). The sections of tracks lying inside a region of about 30 μ from the top or the bottom of the plates were omitted from the measurement.

The tracks were so aligned that they stayed within the eyepiece scale ($\sim 50\,\mu$) over the entire (roughly 10 cm) movement of the stage.

The average of the measured second differences may be written as the sum of certain averaged quantities relating to the Coulomb scattering, the spurious scattering and other noises in the following way:

$$D_m^2 = d_c^2 + d_{sp}^2 + d_n^2 .$$

The value of the total noise was found to be (0,150 $\pm$ 0,003) μ when a cell-length of 50 μ was used.

The distributions of the absolute values of the second differences for cell lengths $t = 0{,}5;\ 1;\ 2$ and 3 cm after cut off at $|D_m| = 4\,|\overline{D_m}|$ and normalization to the total number of second differences are shown together with the corresponding normal distribution in Fig. 1. Due to the cut off 2,7; 1,9; 0,8 and 0.9 per cent of the total number of second differences were omitted when plotting the various curves. A χ^2-test analysis showed that the cut off distributions can be well approximated by normal distributions up to the highest cell length measured.

3.1.2. The mean values of the second differences corrected for the constant noise (d_m) after cut off and plotted versus cell length are shown in Fig. 2a (open circles). The theoretical curve obtained for d_c with values of $K(t)$ calculated by VOYVODIC and PICKUP [9] who took into account the finite size of the nucleus, is also reproduced in the same figure. Because of the effect of spurious scattering one should expect the experimental values to be large or at most equal to the corresponding values of d_c.

The present results are not in contradiction with the above expectation. The largest — but not significant — deviations in the "bad" direction between the experimental points and the theoretical curve are at cell lengths of $t = 2{,}5$ and 3 cm.

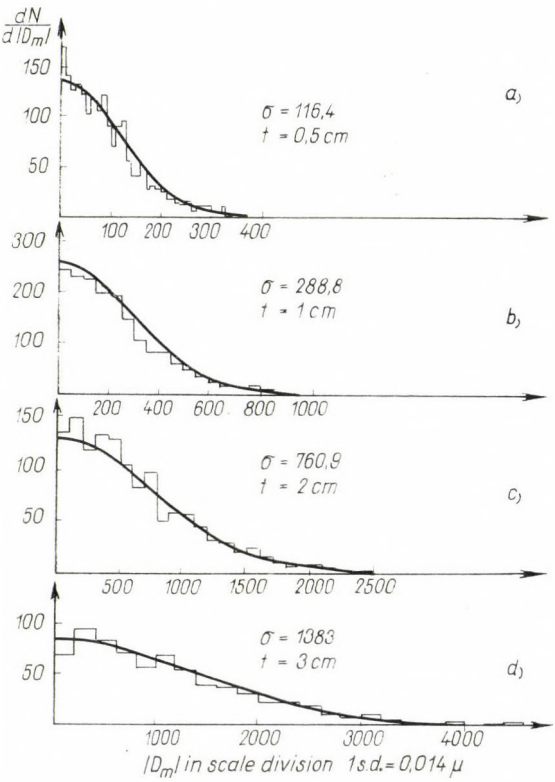

Fig. 1. Distributions of second differences (D_m) for cell lengths a) $t = 0{,}5$ cm, b) $t = 1$ cm c) $t = 2$ cm and d) $t = 3$ cm

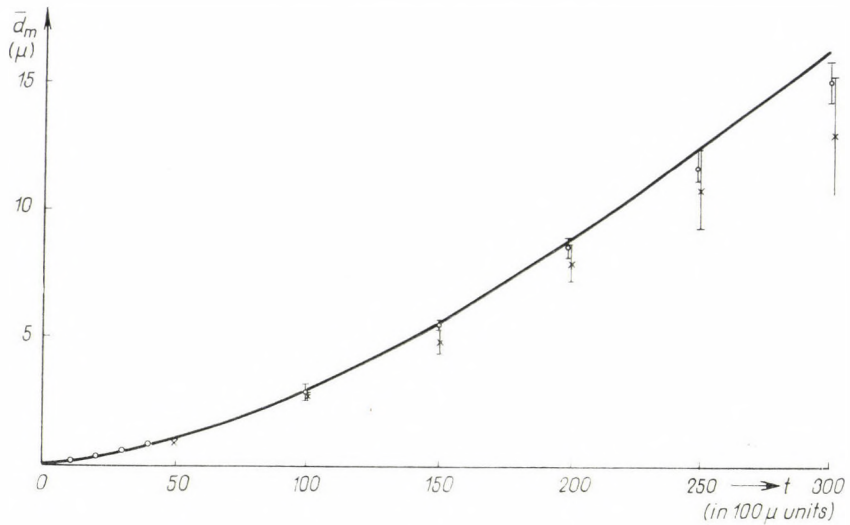

Fig. 2a

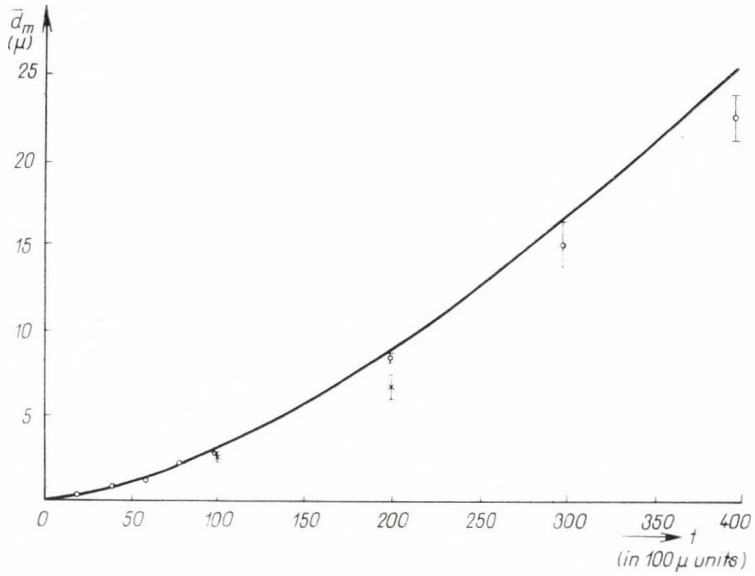

Fig. 2b

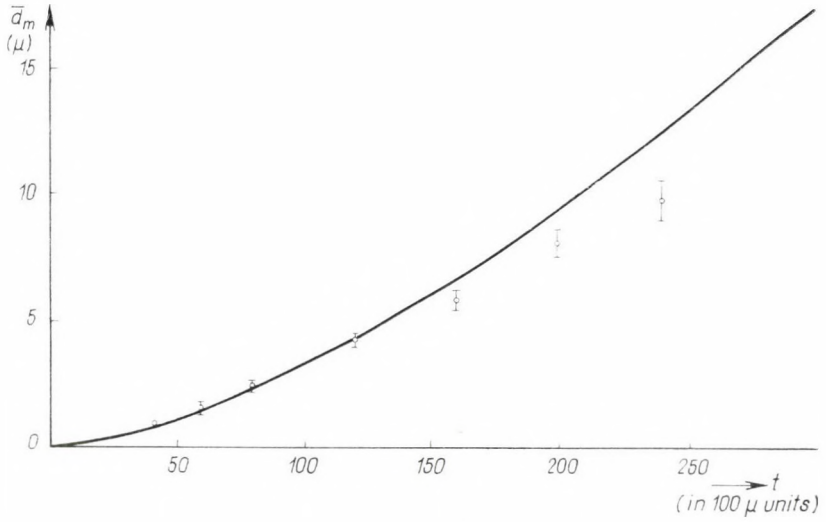

Fig. 2c

Fig. 2. Variation of d_m with t. a) present experiment (17,2 GeV/c π^-). The points marked by ⊼ correspond to second differences corrected for spurious scattering
b) YASH PAL et al. ⊼ and A. A. KAMAL et al. ⊼ (17,2 GeV/c π^-)
c) A. HOSSAIN et al. (16,2 GeV/c/π^-). The continuous curves show the variation of d_c at given energy calculated with a K-value obtained by VOYVODIC and PICKUP by taking into account the finite size of the nucleus [9]

For comparison the values obtained by other authors for 16,2 GeV [1], 17,2 GeV [3, 4] π^--mesons are plotted together with the theoretical d_c-curve corresponding to these energies in Figs. 2b—c. One may see that in most of the cases the deviations are larger and more pronounced than in the present case. It has to be emphasized, however, that the fact that in consequence of the effect of spurious scattering there does not seem to be disagreement between the experimental and the theoretical values, does not imply the non-existence of such a disagreement.

3.1.3. In the present investigations we have used the method of ČASNIKOV et al. [10] which does not require knowledge of K. By this method, the value of $\bar{d}_c$ and $\bar{d}_{sp}$ can be obtained from the measured second ($\bar{d}_m$) and third ($d_{m,3}$) differences. Introducing the notations

$$\varrho = \frac{\bar{d}_{m,3}}{\bar{d}_m}, \quad \varrho_c = \frac{\bar{d}_{c,3}}{\bar{d}_c} = \sqrt{\frac{3}{2}} \quad \text{and} \quad \varrho_{sp} = \frac{\bar{d}_{p,3}}{\bar{d}_{sp}}$$

we have

$$d_c = \bar{d}_m \sqrt{\frac{\varrho^2 - \varrho_{sp}^2}{\varrho_c^2 - \varrho_{sp}^2}}; \tag{3}$$

$$\bar{d}_{sp} = \bar{d}_m \sqrt{\frac{\varrho_c^2 - \varrho^2}{\varrho_c^2 - \varrho_{sp}}}. \tag{4}$$

The values of $\bar{d}_c$ obtained from equ. (3) with $\varrho_{sp}^2 = \frac{10}{3}$* are plotted in Fig. 2a (crossed points). It can be seen, that all the experimental points for $t \geq 1$ cm lie under the theoretical curve, i.e. the deviation is more pronounced than in the first case (see 3.1.2) despite of the greater statistical error of the individual values.

The values of $\bar{d}_{sp}$ obtained from eq. (4) for different cell lengths are plotted in Fig. 3. From this it may be seen that the spurious scattering does not show any saturation (or break down) tendency with increasing cell length as obtained in certain cases by some authors [11—13] for cell lengths $t \geq 1$ cm. The discrepancy may be due to the fact that in the methods applied by those authors** K had to be known.

* This assumption is supported by the fact, that experimental values very close to $\varrho_{sp}^2 \approx \varrho_n^2 = \frac{10}{3}$ were obtained by ČASNIKOV et al. with the formula given in ref. [10]:

$$\varrho_{sp}^2 = \left[\left(\frac{t_2}{t_1}\right)^3 d_{m,3}(t_1) - d_{m,3}^2(t_2)\right] \Big/ \left[\left(\frac{t_2}{t_1}\right)^3 d_m^2(t_1) - d_m^2(t_2)\right],$$

where t_1 and t_2 represent two different cell lengths.

** Except A. ADITYA et al. [12] who used relative scattering measurements for the determination of the spurious scattering.

According to the present measurements the dependence of the spurious scattering on the cell length is given by a power law:

$$\bar{d}_{sp} = a \cdot t^n \tag{5}$$

with $n = 1{,}22 \pm 0{,}17$ and $a = (6{,}84 \pm 1{,}3) \cdot 10^{-3}$ obtained by means of the method of least squares. These values are in a good agreement with the date listed in Table V in the paper of JONES and KALBACH [13] and with the results of MARZARI-CHIESA and WATAGHIN [14].

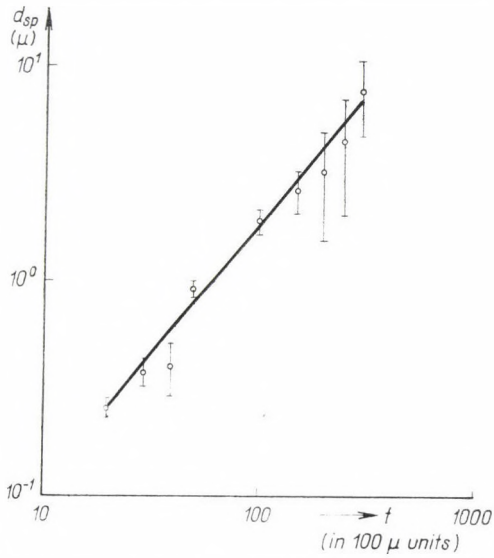

Fig. 3. Dependence of spurious scattering on cell length

Table I

t (100 μ)	K if $\bar{d}_{sp} \ll \bar{d}_c$	K corr.
50	$31{,}8 \pm 1{,}7$*	$27{,}5 \pm 2{,}0$
100	$30{,}4 \pm 2{,}0$	$27{,}1 \pm 2{,}2$
150	$30{,}1 \pm 1{,}1$	$26{,}3 \pm 2{,}7$
200	$30{,}0 \pm 1{,}2$	$27{,}8 \pm 4{,}4$
250	$29{,}5 \pm 1{,}7$	$27{,}2 \pm 4.0$
300	$28{,}7 \pm 1{,}7$	

The ϱ-values were also calculated and plotted vs. the cell length (Fig. 4a). For comparison the results of [3—4] and [10] are also presented (Figs. 4b—d).

* This value is higher than expected because the assumption $\bar{d}_{sp} \ll \bar{d}_c$ does not hold at this cell length.

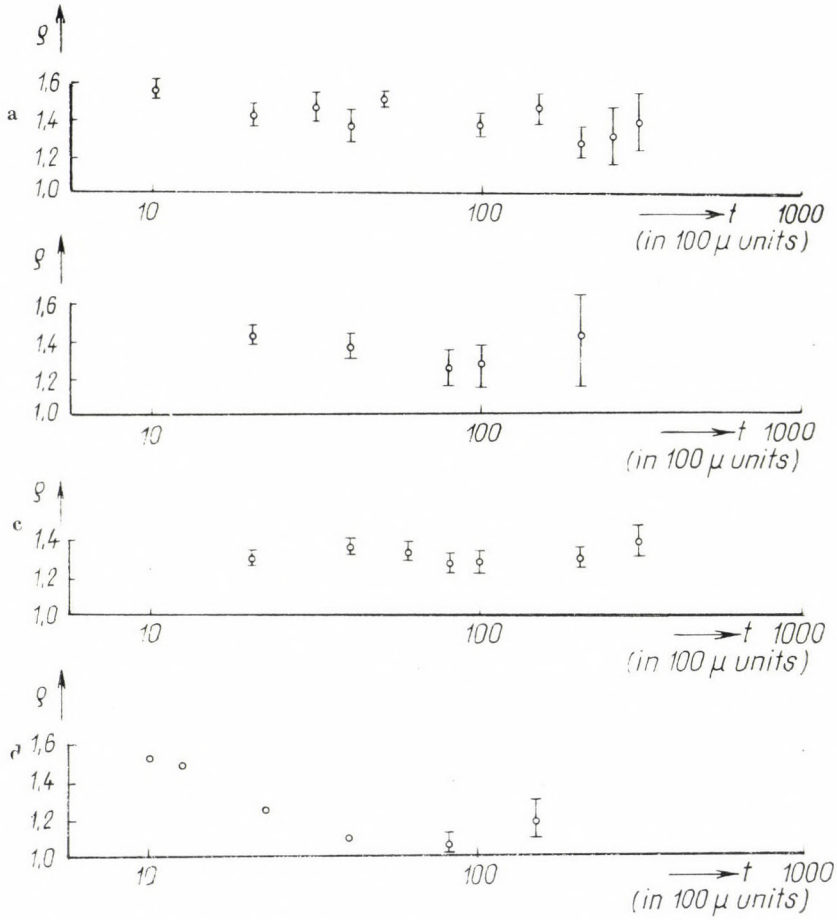

Fig. 4. Variation of ϱ vs. t. a) present experiment, b) YASH PAL et al., c) A. A. KAMAL et al., d) ČASNIKOV et al.

The ϱ-values measured by [10] depend significantly on cell length* while other authors have not found such a dependence.

The average of the ϱ-values in our measurements and in refs. [3, 4, 10] are $1{,}45 \pm 0{,}02$; $1{,}38 \pm 0{,}04$; $1{,}35 \pm 0{,}02$ and $1{,}60 \pm 0{,}01$, respectively. All of them are significantly larger than $\varrho_c = \sqrt{\frac{3}{2}} = 1{,}225$ predicted theoretically for multiple Coulomb scattering.

The values of the scattering constant calculated on the assumption $\bar{d}_{sp} \ll \bar{d}_c$ and with values obtained from eq. (3) are listed in Table I, respectively.

* The ϱ-values in Fig. 4a—c were calculated from the second and third differences corrected for the constant noise, while those in Fig. 4d were calculated from the uncorrected data. This difference, however, does not explain the significant dependence on cell length since for large t ($t \gtrsim 0{,}1$ cm) the noise becomes negligible as compared to the measured value.

3.2. *Measurement with the angular dispersion method*

3.2.1. Measurements were carried out in the same region of the emulsion plates as in the former case by means of a Koristka MS2 microscope with an objective of 55× magnification. The plate was placed on the stage in such a way that the angle between the direction of stage motion and the average direction of the pion beam ($\bar{\alpha}$) was about zero. In order to include only primary particles only those tracks were measured where the projected angles between the tracks and the average direction of the beam were smaller than 1°.

In three strips, at distances 1,8; 4,8 and 11,8 cm from the edge of the plate (the second and third strip, respectively, being at $t = 3$ and $t = 10$ cm from the first one), about 1000 tracks were measured. At the end points of each strip (1000 μ wide) the ordinates of the tracks were measured and thus the values of tg α_i directly obtained. Then the angle $\vartheta_i = \alpha_i - \bar{\alpha}$ between the direction of the i-th track and the average beam direction was calculated. (The reading error of each angle was $\sim$0,15 m rad.)

In order to eliminate the possible background due to single Coulomb scatterings, knock-on electrons and secondaries from inelastic nuclear interactions, a cut off was applied at $|\vartheta_i| = 4\,|\overline{\vartheta}|$. In this way the same background "events" were eliminated as in the case of the coordinate method.* In the first, second and third strips 0,6%, 1,5%, and 0,6% of the total number of tracks were omitted, respectively.

The average angle and the variance $\sigma = \sqrt{\frac{\pi}{2}}\,|\overline{\vartheta_t}|$ of the corresponding normal distributions before and after applying cut off are listed in Table II for different cell lengths.

Table II

$\frac{t}{(100\mu)}$	$\lvert\vartheta_i\rvert$ (m. rad)		σ_t (m. rad)	
	before	after	before	after
	cut off			
0	(1,54 ± 0,04)	(1,51 ± 0,04)	(1,93 ± 0,04)	(1,89 ± 0,04)
300	(1,78 ± 0,04)	(1,69 ± 0,04)	(2,22 ± 0,05)	(2,12 ± 0,05)
1000	(2,15 ± 0,05)	(2,10 ± 0,05)	(2,69 ± 0,06)	(2,63 ± 0,06)

* In the case of two normal distributions with variance σ_c and σ_a respectively, "events" having identical probability are omitted if both distributions are cut off at $|\vartheta_c| = \varkappa\,\sigma_c$ and $|\vartheta_a| = \varkappa\,\sigma_a$ respectively (where $\varkappa$ is an arbitrarily chosen constant, having the same value in both cases).

The statistical errors were calculated from the formulae:

$$\delta\,|\overline{\vartheta_t}|/|\overline{\vartheta_t}| = (1{,}14/2(N_t - 1))^{1/2} \text{ and } \delta\,\sigma_t/\sigma_t = (2(N_t - 1))^{1/2},$$

where N_t is the total number of angles measured.

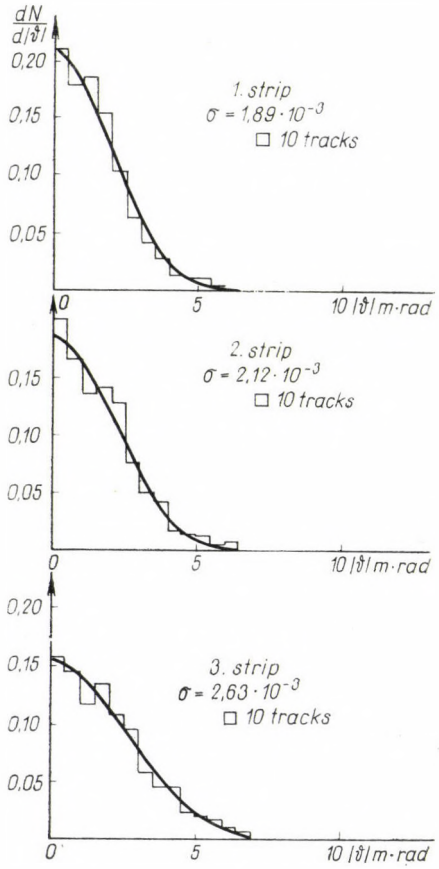

Fig. 5. Distributions of $|\vartheta_{t,i}|$ obtained in the first, second and third strip

3.2.2. The angular distributions (after cut-off) are shown together with the corresponding normal distributions in Fig. 5. The distributions are normalized to 1. A χ^2-test shows that the experimental distributions can be well approximated by normal ones.

For the calculation of the scattering constant one has to use eq. [2]. This relation, however, holds only if multiple Coulomb scattering is present. Taking into account the contribution of the small-angle diffraction scattering, $|\overline{\vartheta_{t,\mathrm{corr}}}|^2 = (|\overline{\vartheta_t}|^2 - \langle|\vartheta_{t,\mathrm{nucl.}}|\rangle^2)$ has to be written in eq. (2) instead

of $|\overline{\vartheta_t}|^2$. (For the calculation of $\langle\vartheta_{t,\text{nucl.}}|\rangle^2$ see the Appendix.) With this eq. (2) may be rewritten in the form

$$\overline{|\vartheta_{t,\text{corr}}|^2} = \overline{|\vartheta_0|^2} + \alpha t, \quad \text{where} \quad \alpha = \left(\frac{1{,}225}{p\beta} K\right)^2. \tag{6}$$

In Fig. 6 $|\overline{\vartheta_{t,\text{corr}}}|^2$ is plotted vs. cell length. The experimental points yield a straight line, indicating the constancy of K in this interval. When using

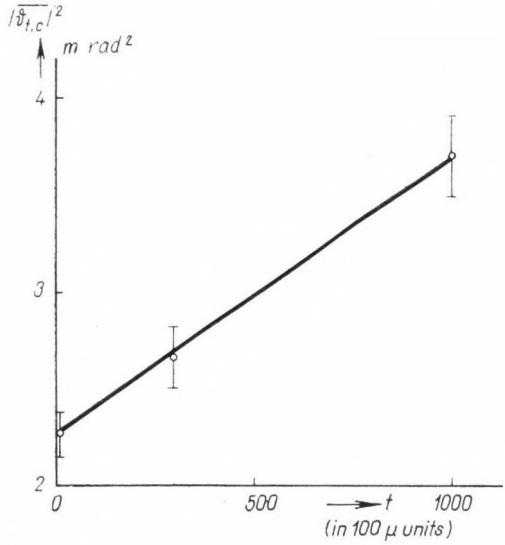

Fig. 6. Variation of $|\vartheta_{t,c}|^2$ vs. t. The continuous line was calculated using the method of least squares

the method of the least squares, the value of α and that of K can be calculated. K was found to be

$$\overline{K} = 30{,}2 \pm 2{,}5.$$

4. Discussion and conclusions

4.1. It is apparent from Table I that in the interval of 0,5 cm $\leq t \leq$ 3 cm the K-values show a small, but in no way significant dependence on cell length, and can be well approximated by a constant: $\overline{K} = 30{,}2 \pm 0{,}6$. With the "angular dispersion-method" $\overline{K} = 30{,}2 \pm 2{,}5$ was obtained from $t = 3$ cm up to $t = 10$ cm, which is in agreement with the above value. If one corrects for spurious scattering one finds, in the same interval, the dependence of the K-values on cell length to be weaker (see Table I), and the average value of K to be $27{,}1 \pm 1{,}2$. Therefore it seems necessary to correct for the effect of

Table III

Values of the

Cell length t (cm)	Expected values	Meas									
		[11]	[8]	[9]	[10]	[10]	present paper		[12]	[9]	[10]
0,1	27,3	28,2 ± 1.0						[1]	30,6 ± 0.9	[4]	
0,15	27,7	27,9 ± 1.4									
0,2	28,3	28,6 ± 1.7			28,8 ± 0.4				30,1 ± 1.2	29,9 ± 0.9	
0,3	28,6								30,9 ± 1.7		
0,4	28,9				27,8 ± 0.5	29,0 ± 1.8			31,0 ± 2.1	30,2 ± 1.5	30,6 ± 1.2
0,5	29,2						31,8 ± 1.7	27,5 ± 2.0	31,3 ± 2.3		
0,6	29,4				28,1 ± 0.7				32,2 ± 2.9		
0,8	29,8			30,5 ± 1.7	27,8 ± 0.7				29,8 ± 3.4	29,0 ± 2.6	
1,0	30,1			26,9 ± 1.7	28,9 ± 1.0		30.4 ± 2.0	27,1 ± 2.2			
1,5	30,6						30,1 ± 1.1	26,3 ± 2.7			
2,0	30,9		26,6 ± 1.2	23,2 ± 2.6	29,3 ± 0.8		30,0 ± 1.2	27,8 ± 4.4			
2,5	31,2						29,5 ± 1.7	27,2 ± 4.0			
3,0	31,2		25,4 ± 1.8		27,2 ± 1.1		28,7 ± 1.7				
4,0	31,2				27,6 ± 1.6						
5,0	31,2										
6,0	31,2										
7,0	31,2										
7,2	31,2										
8,0	31,2										
9,5	31,2										
10,0	31,2										
Mean value	K	28,2 ± 0.7	26,3 ± 1.0	27,7 ± 1.1	28,3 ± 0.2		30,1 ± 0.6	27,1 ± 1.2	30,6 ± 0.6	29,9 ± 0.8	

Method applied	Coordinate				
	cut off with replacement	without cut off	using cut off		
Measurements	on single tracks		by rel. scattering	on single tracks	by relative scattering
Particle: Type	π				
Particle: Energy (GeV)	4,5	16,2	17		6,2

[1] corrected for d_{sp}

[2], [3] } corrected for small angle diffraction scattering

[4] These values have to be multiplied by a factor of 27/24 see ref. [12]

scattering constant

ured by

[10]	[10]	[13]	[8]	[2]	present	[2]	[3]	[6]	[6]	[6]
		4			2		3			
31,8 ± 1,9	28,0 ± 2,2	30,4 ± 1,0								
			27,5 ± 2,5					31,2 ± 2,7	30,0 ± 1,7	
								28,6 ± 2,5	27,6 ± 1,6	
				30,3 ± 0,7				27,1 ± 2,4	27,3 ± 1,6	
								28,1 ± 2,5		
						30,4 ± 0,9		28,3 ± 2,6		
								26,5 ± 2,5		
							29,4 ± 2,0			
								27,4 ± 2,7		
								28,5 ± 2,8		
					30,2 ± 2,5			28,2 ± 0,9	28,2 ± 0,9	31,5 ± 1,7

		Angular dispersion				γ dispersion	
without cut off		cut off					
	on single tracks	on single tracks				on single tracks	
p	μ	π		p		p	μ
27	8	0.3	17	6	9	27	8

spurious scattering at smaller cell lengths where its relative contribution to the total average scattering is larger than at larger cell lengths.

Similar results were obtained by KAMAL et al. [4] using the "coordinate method", by CHEMEL et al. [5] and two of the authors [6] applying the "angular dispersion method" and by ADITYA [7] using a treatment analogous to the "angular dispersion method".

In Table III K-values are listed which were measured for different energies in the 0,1 cm $\leq t \leq$ 10 cm cell length interval. Dividing the pion and proton data into two parts with respect to the cell lengths, 0,1 cm $\leq t \leq$ $\leq$ 1 cm and 1 cm $\leq t \leq$ 10 cm, the weighted averages of the K-values over the first, second and the total cell length intervals are:* 28,9 $\pm$ 0,2; 29,3 $\pm$ 0,3 and 29,0 $\pm$ 0,2, respectively.

The above results suggest that — for nuclear-active particles independently of their energies —

a) K is constant at cell lengths $t \geq$ 0,1 cm, and

b) smaller than expected from the theory of VOYVODIC and PICKUP, even if the influence of the spurious scattering is taken into account.

The above effect may be due to the fact that

1. either the experimental method used for determining K is not adequate at such great cell lengths or

2. the statistical theory of multiple Coulomb scattering needs some modification.

The fact that the different methods give the same result (within the experimental error) speaks against the first possibility.

We are indebted to Dr. E. FENYVES for helpful discussions.

Appendix

Calculation of $\langle|\vartheta|\rangle^2$ *in case of small angle diffraction scattering of pions on emulsion nuclei*

Let us introduce the following notations and definitions:

1. N_1 be the number of nuclei of type i per cm^3 in the emulsion,

2. A_1 the mass-number of nuclei of type i,

3. $1/\lambda_i = N_i \bar{\sigma}_i = N_i 2\pi \int_0^{\theta_l} \frac{d\sigma_i}{d\theta} \sin\theta \, d\theta$, is the inverse value of the mean free path for diffraction scattering, and $\bar{\sigma}_i$ the corresponding total cross section;

4. $$\frac{d\sigma_i}{d\theta} \sin\theta \; d\theta = \left(\frac{k_i^* \sigma_t}{4\pi}\right)^2 A_i^{4/3} q_i e^{-\frac{(k^*_i R_0 \Theta)^2}{4} q_i (1+A^{2/3}_i)} \sin\theta \, d\theta \qquad (A1)$$

* In these averages the results written in the 2nd and 3rd columns are not included.

is the differential angular distribution of pions scattered on nuclei of type i, where θ is the solid angle of scattering, the θ_i the limiting polar angle, k_i^* is the wave number of the incoming pion in the CMS of the pion and nucleus of type i.

$R_0 A_i^{1/3}$ is the interaction radius of a nucleus of type i, σ_t can be expressed in terms of R_0 as follows: $\sigma_t = R_0^2 \pi$ (for the present calculation: $R_0 = 1{,}25$ fermi, i.e. $\sigma_t = 49$ m barn), $q_i = \dfrac{2P_0 + A_i}{P_0 + A_i}$ is a factor which transforms the angles from the LS to the CMS according to the expression:

$$\theta_{\mathrm{CMS}}\, d\,\theta_{\mathrm{CMS}} = q_i\, \theta_{\mathrm{LS}} d\,\theta_{\mathrm{LS}}\,.$$

($P_0 = 17{,}2$ GeV/c is the momentum of the incoming pion in the LS). Eq.(A1) can be normalized to 1 in the interval $0 \leq \theta \leq \theta_l$ as follows:

$$W_i(\theta)\, d\theta = 2\pi\, \frac{\dfrac{d\sigma_i}{d\vartheta} \sin\theta}{\bar{\sigma}_i}\, d\,\theta\,. \qquad (A2)$$

Let us now investigate the angular distribution of the pion beam when this is parallel to the longer edge of the plate at a depth t in the emulsion.

The normalized angular distribution of diffraction scattering is given by:

$$p(\theta, t)\, d\theta = \frac{1}{\sum\limits_i N_i A_i^{2/3}} \sum_i \left\{ N_i A_i^{2/3} \left[\left(1 - \frac{t}{\lambda_i} \right) \delta(\theta)\, d\theta + \frac{t}{\lambda_i} W_i(\theta)\, d\theta \right] \right\} \qquad (A3)$$

and the square of the expected absolute value of the projected scattering angle by:

$$\langle |\vartheta| \rangle^2 = \frac{\pi}{4} \int_0^{\theta_l} \theta^2\, p(\theta, t)\, d\theta\,. \qquad (A4)$$

After integration and putting $\sin\theta \approx \theta$, one obtains:

$$\langle |\vartheta| \rangle^2 = \frac{\sigma_t^2}{4R_0^4}\, \frac{1}{\sum\limits_i N_i A_i^{2/3}}\, \Sigma \left[N_i^2 A_i^2\, \frac{1 - \Delta(x_{0i})}{k_i^*\, q_i\, (1 + A_i^{2/3})} \right] \cdot t = b(t)t\,, \qquad (A5)^*$$

where

$$\Delta(x_{0i}) = (1 + x_{0i}^2) e^{-x_{0i}^2} \text{ and } x_{0i}^2 = \frac{(k_i^*\, R_0\, \theta_i)^2}{4}\, q_i\, (1 + A_i^{2/3})\,.$$

* Here the relation $\theta^2 = \vartheta^2 + \Phi^2$ between solid angle, projected angle and dip angle (Φ) is used.

$b(t)$ is a slowly varying function of t. This dependence is due the fact that for different cell lengths the cut off was made at different projected angles. The values obtained for $b(t)$ are given in Table IV.

Table IV

t (100μ)	$b(t)$ [m. rad]^2/100μ
300	$6{,}27 \cdot 10^{-4}$
1000	$7{,}25 \cdot 10^{-4}$

The ratio of the inelastic to the elastic scattering cross section for π-nucleus interaction was calculated in the $0 \leq \vartheta \leq \vartheta_l$ angular interval as:

$$\frac{\sigma_{\text{inel.}}}{\sigma_{\text{el.}}} \approx 0{,}06 .$$

This result means that no correction is necessary for the effect of the secondary particles emitted at small angles in inelastic processes.

REFERENCES

1. A. Hossain, M. F. Votruba and A. Wataghin, Nuovo Cimento, **22,** 308, 1961.
2. A. Hossain, M. F. Votruba, A. Wataghin and D. Evans, Nuovo Cimento, **22,** 861, 1961.
3. Yash Pal and A. K. Roy, Nuovo Cimento, **27,** 960, 1963.
4. A. A. Kamal, G. K. Rao and Y. V. Rao, preprint.
5. B. Chemel and Tsai-Chu, Comptes Rendus, **249,** 1494, 1959.
6. G. Bozóki and E. Gombosi, Pribory i Technika Experimenta, **6,** 61, 1963.
7. Prem. K. Aditya, Nuovo Cimento, **31,** 473, 1964.
8. C. F. Powell, P. M. Fowler and P. H. Perkins, The Study of Elementary Particles by the Photographic Method, Pergamon Press 1959, p. 114.
9. L. Voyvodic and E. Pickup, Phys. Rev., **85,** 91, 1952.
10. J. Ja. Časnikov, Z. V. Anzon, Z. S. Takibaev and J. S. Streljecov, ZETP, **45,** 29, 1963.
11. F. W. Fisher and J. J. Lord, Nuovo Cimento, **11,** 44, 1959.
12. P. K. Aditya, V. S. Bhatia and P. M. Sood, Nuovo Cimento, **29,** 577, 1963.
13. J. J. Jones and R. M. Kalbach, Nuovo Cimento, **31,** 10, 1964.
14. A. Marzari-Chiesa and A. Wataghin, Suppl. Nuovo Cimento, **26,** Serie 10, 279, 1962.
15. F. A. Brisbout, C. Dahanayake, A. Engler, P. H. Fowler and P. B. Jones, Nuovo Cimento, **3,** 1400, 1956.
16. S. Biswas, N. D. Prasad and S. Mitra, Proc. Ind. Acad. Sci., **46 A,** 167, 1957.
17. P. K. Aditya, V. S. Bhatia and P. M. Sood, Rep. on nuclear emulsion technique with special reference to measurement of high momenta; Bombay, p. 34, Nov. 1961.

ИЗУЧЕНИЕ ПОСТОЯННОЙ МНОГОКРАТКОГО РАССЕЯНИЯ В ЭМУЛЬСИИ ПРИ БОЛЬШИХ РАЗМЕРАХ ЯЧЕЕК

Г. БОЗОКИ, Э. ГОМБОШИ, Л. ЕНИК, Э. НАДЬ и М. ШАГИНИ

Резюме

Изучается зависимость постоянной многократкого рассеяния (K) от размера ячейки двумя различными методами в интервале 0,5 см $\leq t \leq$ 10 см. «Координационным методом» для среднего значения постоянной K при размере ячейки в интервале $0{,}5 \leq t \leq 3$ см получено значение $K = 30{,}2 \pm 0{,}6$. Если принять во внимание эффект ложного рассеяния, то значение постоянной уменьшается до $27{,}1 \pm 1{,}2$. Метод «угловой дисперсии» результирует $K = 30{,}2 \pm 2{,}5$ для размера ячейки в интервале 3 см $\leq t \leq$ 10 см. Найдено, что ложное рассеяние зависит от размера ячейки согласно соотношению $d_{SD} = at^n$, где $a = (6{,}84 \pm 1{,}33) \cdot 10^{-3}$ и $n = 1{,}22 \pm 0{,}17$ в интервале 0,2 см $\leq t \leq$ 3 см.

ÜBER DIE ENERGIEVERTEILUNG DER ELEKTRONEN IM STATISTISCHEN ATOM

Von

P. GOMBÁS

PHYSIKALISCHES INSTITUT DER UNIVERSITÄT FÜR TECHNISCHE WISSENSCHAFTEN
BUDAPEST

(Eingegangen: 15. III. 1965)

Für die Energieverteilung der Elektronen statistisch behandelter Atome werden Formeln hergeleitet und zwar sowohl für den Fall einer globalen Behandlung der Elektronen, als auch für den Fall, dass die Elektronen im Atom in Gruppen mit gleicher Nebenquantenzahl unterteilt sind. Die Resultate für die Energieverteilung der Elektronen werden im Falle des K-und Hg-Atoms mit den aus den Hartreeschen Tabellen berechneten Verteilungen verglichen, wobei sich zeigt, dass die statistischen Verteilungsfunktionen über die wellenmechanischen Verteilungen sehr gut hinwegmitteln. Weiterhin werden mit den statistischen Energieverteilungen der Elektronen Energiemittelwerte von Elektronen in Atomen berechnet. Für diese ist die Übereinstimmung mit den wellenmechanischen Resultaten weniger gut. Die im § 2 und § 3 gewonnenen Resultate können auf beliebige statistisch behandelte Systeme erweitert werden.

§ 1. Einleitung und Zusammenfassung

Es ist einigermassen überraschend, dass das sehr naheliegende Problem: die Bestimmung der Energieverteilung der Elektronen im statistischen Atom bis jetzt nicht näher untersucht wurde. Dies wollen wir in der vorliegenden Arbeit nachholen und zwar bestimmen wir zunächst die Energieverteilung der Elektronen im statistischen Atom und zwar sowohl für den Fall einer globalen Behandlung (d. h. keinerlei Unterteilung der Elektronen in Gruppen), sowie auch für den Fall, dass die Elektronen des Atoms in Gruppen mit gleicher Nebenquantenzahl unterteilt sind. Diese werden dann für die Atome K und Hg mit den entsprechenden wellenmechanischen Verteilungen verglichen. Weiterhin werden die Formeln für die Energieverteilung zur Berechnung von Mittelwerten der Elektronenenergie im Atom herangezogen. Die im §2 und §3 hergeleiteten Resultate kann man auf beliebige statistisch behandelte Systeme verallgemeinern.

§ 2. Berechnung der Energieverteilung der Elektronen im Thomas—Fermischen Atom

Wir gehen von der Energie ε eines Elektrons im Atom am Ort $\mathfrak{r}$ aus, das sich im Potential V befindet und das einen Impuls vom Betrag p besitzt. Man hat dann

$$\frac{p^2}{2m} - Ve = \varepsilon\,, \tag{1}$$

wo m die Masse des Elektrons und e die positive Elementarladung bezeichnet. Hieraus folgt für den Impulsbetrag

$$p = [2m(\varepsilon + Ve)]^{1/2}. \tag{2}$$

Mit diesem Ausdruck ergibt sich für die Anzahl dn der Elektronen pro Volumeneinheit, deren Impulsbetrag zwischen p und $p + dp$, bzw. deren Energie zwischen ε und $\varepsilon + d\varepsilon$ liegt in bekannter Weise[1]

$$dn = \frac{8\pi}{h^3} p^2 \, dp = \frac{4\pi(2m)^{3/2}}{h^3} (\varepsilon + Ve)^{1/2} d\varepsilon \,, \tag{3}$$

wobei wir mit h die Plancksche Konstante bezeichneten. Hieraus erhält man durch Integration für die Anzahl der Elektronen im Atom, deren Energie zwischen ε und $\varepsilon + d\varepsilon$ fällt

$$dN = \frac{4\pi(2m)^{3/2}}{h^3} d\varepsilon \int (\varepsilon + Ve)^{1/2} dv \,, \tag{4}$$

wo dv das Volumenelement bezeichnet und das Integral nur auf solche Gebiete auszudehnen ist, für welche der Ausdruck unter der Wurzel im Integranden $\geqq 0$ ist. Wenn wir — wie wir dies im folgenden durchweg tun wollen — eine kugelsymmetrische Potentialverteilung im Atom voraussetzen, so können wir für dN schreiben

$$dN = \frac{16\pi^2 (2m)^{3/2}}{h^3} d\varepsilon \int (\varepsilon + Ve)^{1/2} r^2 \, dr \,, \tag{5}$$

wo r die Entfernung vom Kern bezeichnet.

Mit diesen Formeln lässt sich durch Integration nach ε sofort die Anzahl $n(\varepsilon)$ der Elektronen pro Volumeneinheit, bzw. die Anzahl $N(\varepsilon)$ der Elektronen im ganzen Atom angeben, deren Energie zwischen der tiefsten Energie ε_0 und einer beliebigen Energie ε liegt. Diese tiefste Energie des Elektrons ergibt sich, wenn die kinetische Energie gleich 0 wird, wenn also die gesamte Energie mit der potentiellen Energie am Ort r identisch ist. Man hat also

$$\varepsilon_0 = -eV \tag{6}$$

und erhält für $n(\varepsilon)$ und $N(\varepsilon)$

$$n(\varepsilon) = \frac{8\pi(2m)^{3/2}}{3h^3} (\varepsilon + Ve)^{3/2} \,, \tag{7}$$

$$N(\varepsilon) = \frac{32\pi^2 (2m)^{3/2}}{3h^3} \int (\varepsilon + Ve)^{3/2} r^2 \, dr \,, \tag{8}$$

[1] Man vgl. z. B. P. GOMBÁS, Die statistische Theorie des Atoms und ihre Anwendungen, S. 6, Springer, Wien, 1949.

wo die Integration nach r nur auf den Bereich auszudehnen ist, für welchen im Integranden der Ausdruck unter der Wurzel $\geqq 0$ ist.

Hieraus ergibt sich sofort die Anzahl der Elektronen, deren Energie zwischen ε_1 und ε_2 liegt, für die Volumeneinheit und für das ganze Atom, und zwar erhält man, falls $\varepsilon_2 > \varepsilon_1$ ist, für die Volumeneinheit $n(\varepsilon_2) - n(\varepsilon_1)$ und für das ganze Atom $N(\varepsilon_2) - N(\varepsilon_1)$.

Wir wollen im folgenden zunächst das Thomas—Fermische Modell zugrunde legen und unsere Verteilungsformeln in den Thomas—Fermischen Variablen x und φ ausdrücken, die folgenderweise definiert sind[2]

$$x = \frac{r}{\mu}, \tag{9}$$

$$\varphi = \frac{r}{Ze^2}(Ve + \varepsilon_\mu), \tag{10}$$

wo $\varepsilon_\mu = -V_0 e$ die höchstmögliche Energie eines Elektrons und V_0 das höchste Potential im Thomas—Fermischen Atom darstellt, weiterhin μ die Thomas—Fermische Längeneinheit

$$\mu = \frac{1}{4}\left(\frac{9\pi^2}{2Z}\right)^{1/3} a_0 = \frac{0{,}8853}{Z^{1/3}} a_0 \tag{11}$$

bezeichnet; Z ist die Ordnungszahl und a_0 der erste Bohrsche Wasserstoffradius. Wenn wir statt der Energie ε die dimensionslose Variable

$$u = \frac{\mu}{Ze^2}\varepsilon \tag{12}$$

einführen, d. h. ε in der Einheit Ze^2/μ ausdrücken, so ergibt sich

$$dn(u,x) = \frac{3}{2}\frac{Z}{4\pi\mu^3}\left(\frac{\varphi}{x} + u - u_\mu\right)^{1/2} du, \tag{13}$$

$$n(u,x) = \frac{Z}{4\pi\mu^3}\left(\frac{\varphi}{x} + u - u_\mu\right)^{3/2}, \tag{14}$$

$$dN(u) = \frac{3}{2} Z\, du \int\left(\frac{\varphi}{x} + u - u_\mu\right)^{1/2} x^2\, dx, \tag{15}$$

$$N(u) = Z\int\left(\frac{\varphi}{x} + u - u_\mu\right)^{3/2} x^2\, dx, \tag{16}$$

wo

$$u_\mu = \frac{\mu}{Ze^2}\varepsilon_\mu \tag{17}$$

gesetzt wurde.

[2] Man vgl. z. B. P. Gombás, l. c., S. 40.

Für neutrale Atome, mit denen wir uns im folgenden vorwiegend befassen, ist[3] $\varepsilon_\mu = 0$ und somit auch $u_\mu = 0$. Für neutrale Atome setzen wir statt φ das Symbol φ_0.

Die Verteilungsfunktion $dn(u, x)/du$, d. h. die Besetzungsdichte der Energieniveaus, sowie die Verteilungsfunktion $n(u, x)$, d. h. die Anzahl der Elektronen, deren Energie $\leqq u$ ist, beziehen sich auf einen beliebigen Abstand x vom Kern. Diese Verteilungen sind also Funktionen von u und x; sie haben natürlich nur in den Gebieten einen Sinn, in welchen der Ausdruck unter der Wurzel $\geqq 0$ ist. In den Figuren 1 und 2 sind diese Verteilungen für neutrale Atome bei einigen festgehaltenen u-Werten als Funktionen von x dargestellt. Die Verteilungsfunktionen $dN(u)/du$, d. h. die Besetzungsdichte der Elektronen sowie $N(u)$ die Anzahl der Elektronen des Atoms, deren Energie $\leqq u$ ist, sind Funktionen von u. Diese Verteilungsfunktionen sind ebenfalls für neutrale Atome in den Figuren 3 und 4 dargestellt.

Die Funktion $N(u)$ haben wir für die neutralen Atome K und Hg mit den $N(u)$-Werten verglichen, die man mit der Methode des »self-consistent field« erhält.[4] Aus dieser Methode ergibt sich naturgemäss für $N(u)$ kein glatter sondern ein stufenweise abfallender Verlauf. Wie aus den Figuren 5 und 6 zu sehen ist, gibt unsere Funktion $N(u)$ einen guten Mittelwert der wellenmechanischen stufenweise abfallenden Kurve.

Es sei noch bemerkt, dass natürlich $n(u_\mu, x)$ mit der Elektronendichte $\varrho(x)$ am Ort x identisch ist, d. h.

$$n(u_\mu, x) = \varrho(x) \tag{18}$$

ist und ferner

$$N(u_\mu) = N \tag{19}$$

die Anzahl der Elektronen im Atom darstellt.

§ 3. Berechnung von Energiemittelwerten im Thomas—Fermischen Atom

Wir wollen zunächst den Mittelwert $\bar{\varepsilon}(x)$ der Energie eines Elektrons an einem bestimmten Ort x im Atom bestimmen. $\bar{\varepsilon}(x)$ definieren wir folgendermassen

$$\bar{\varepsilon}(x) = \frac{1}{\varrho} \int_{\varepsilon_0}^{\varepsilon_\mu} \varepsilon \, dn \,. \tag{20}$$

[3] P. GOMBÁS, l. c., S. 38.

[4] Für K: D. R. HARTREE u. W. HARTREE, Proc. Roy. Soc. London (A) **166**, 450, 1938; für Hg: D. R. HARTREE, Phys. Rev. **46**, 738, 1934 und D. R. HARTREE u. W. HARTREE, Proc. Roy. Soc. London (A) **149**, 210, 1935.

Wenn man hier dn aus (3) einsetzt und berücksichtigt, dass $\varepsilon_0 = -V_0 e$ ist, so erhält man nach einfacher Rechnung

$$\bar{\varepsilon}(x) = \frac{8\pi(2m)^{3/2}}{3h^3} \frac{1}{\varrho} \left[\varepsilon_\mu - \frac{2}{5}(Ve + \varepsilon_\mu) \right] (Ve + \varepsilon_\mu)^{3/2} . \tag{21}$$

Mit Rücksicht auf die Thomas—Fermische Beziehung[5]

$$\frac{5}{3} \varkappa_k \varrho^{2/3} = Ve + \varepsilon_\mu , \tag{22}$$

wo $\varkappa_k$ die Konstante

$$\varkappa_k = \frac{3}{10} \frac{(3\pi^2)^{2/3} h^2}{4\pi^2 m} = \frac{3}{10} (3\pi^2)^{4/3} e^2 a_0 \tag{23}$$

bezeichnet, ergibt sich hieraus das Resultat

$$\bar{\varepsilon}(x) = -\frac{2}{5} Ve + \frac{3}{5} \varepsilon_\mu = -\frac{2}{5} \frac{Ze^2}{\mu} \frac{\varphi}{x} + \frac{Ze^2}{\mu} u_\mu , \tag{24}$$

das man auch unmittelbar aus (22) erhalten kann, wenn man in Betracht zieht, dass $\varkappa_k \varrho^{2/3}$ die mittlere kinetische Energie eines Elektrons darstellt.[6]

Die mittlere Energie $\bar{\varepsilon}_A$ eines Elektrons bezogen auf das ganze Atom erhält man nun in der Weise, dass man $\bar{\varepsilon}(x)$ auf das ganze Atom mittelt, d. h.

$$\bar{\varepsilon}_A = \frac{1}{N} \int \bar{\varepsilon} \varrho \, dv \tag{25}$$

setzt. Nach Einsetzen von $\bar{\varepsilon}(x)$ aus (24) ergibt sich[7]

$$\bar{\varepsilon}_A = \frac{2}{7} \frac{Z}{N} V_e(0) e + \frac{9}{7} \varepsilon_\mu , \tag{26}$$

wo $V_e(r)$ das Potential der Elektronenwolke bezeichnet. Für $V_e(0)$ gilt der Ausdruck[8]

$$V_e(0) e = \frac{Ze^2}{\mu} \varphi'(0) - \varepsilon_\mu , \tag{27}$$

[5] Man vgl. z. B. P. GOMBÁS, l. c., S. 34.
[6] Man vgl. z. B. P. GOMBÁS, l. c., S. 7.
[7] Bezüglich der Integration vgl. man P. GOMBÁS, l. c., S. 62.
[8] P. GOMBÁS, l. c., S. 62.

womit man aus (26)

$$\bar{\varepsilon}_A = \frac{2}{7}\frac{Z^2 e^2}{N\mu}\varphi'(0) + \frac{2}{7}\left(1 - \frac{Z}{N}\right)\varepsilon_\mu + \varepsilon_\mu \tag{28}$$

erhält, wo φ' die Ableitung von φ nach x bezeichnet.

Wenn wir den Ionisationsgrad

$$q = \frac{Z - N}{Z} \tag{29}$$

einführen und beachten, dass für das hier zugrunde gelegte Thomas—Fermische Modell

$$\varepsilon_\mu = -\frac{(Z-N)e^2}{r_0} = -\frac{(Z-N)e^2}{\mu x_0} \tag{30}$$

ist, wo $r_0 = \mu x_0$ den Grenzradius des Modells bezeichnet, so ergibt sich

$$\bar{\varepsilon}_A = \frac{1}{N}\frac{2}{7}\frac{Z^2 e^2}{\mu}\left[\varphi'(0) - \frac{7}{2}\frac{q(1-q)}{x_0} + \frac{q^2}{x_0}\right]. \tag{31}$$

Für neutrale Atome, d. h. für $N = Z$, also $q = 0$ erhält man

$$\bar{\varepsilon}_A = \frac{2}{7}\frac{Ze^2}{\mu}\varphi_0'(0) = -0{,}5125\, Z^{4/3}\frac{e^2}{a_0}, \tag{32}$$

wo für neutrale Atome φ_0 anstelle φ und für $\varphi_0'(0)$ der Wert[9]

$$\varphi_0' = -1{,}588071 \tag{33}$$

gesetzt wurde.

In der Tabelle 1 sind die Werte von $\bar{\varepsilon}_A$ für die Atome K und Hg angegeben. In der Tabelle sind auch die aus den Hartreeschen Tabellen[10] ermittelten Werte von $\bar{\varepsilon}_A$ angeführt. Diese wurden aus der Formel

$$\bar{\varepsilon}_A = \frac{1}{N}\sum_i n_i \varepsilon_i \tag{34}$$

berechnet, die mit der Formel (25) aequivalent ist und aus dieser hervorgeht, wenn man von der kontinuierlichen Verteilung auf eine diskrete übergeht;

[9] S. KOBAYASHI, T. MATSUKUMA, S. NAGAI u. K. UMEDA, Journ. Phys. Soc. Japan **10**, 759, 1955.

[10] Für K: D. R. HARTREE u. W. HARTREE, Proc. Roy. Soc. London (A) **166**, 450, 1938; für Hg: D. R. HARTREE, Phys. Rev. **46**, 738, 1934 und D. R. HARTREE u. W. HARTREE, Proc. Roy. Soc. London (A) **149**, 210, 1935.

dementsprechend das Integral in (25) durch eine Summe zu ersetzen ist, in welcher ε_i die Hartreeschen Energieniveaus der Elektronen und n_i die Besetzungszahlen der Energieniveaus bezeichnen.

Tabelle 1

Werte von $\bar{\varepsilon}_A$ für das K- und Hg-Atom in e^2/a_0-Einheiten

	K	Hg
$\bar{\varepsilon}_A$ hier berechnet	−25,99	−176,7
$\bar{\varepsilon}_A$ nach HARTREE	−19,92	−140,0

Wie aus der Tabelle zu sehen ist, liegen unsere $\bar{\varepsilon}_A$ Werte bedeutend tiefer als die Hartreeschen, was darauf zurückzuführen ist, dass im ursprünglichen Thomas—Fermischen Atom die Elektronendichte am Ort des Kerns wie $1/r^{3/2}$ unendlich wird. Dies bewirkt, dass sich die Elektronenladung in der Umgebung des Kerns als zu gross und demzufolge die Energie der innersten Elektronen als zu tief ergibt.

Es sei hier noch erwähnt, dass man in Anschluss an BETHE und SOMMERFELD[11] eine mittlere Elektronenenergie im Atom auch als den geometrischen Mittelwert ε_M der Energien der einzelnen Elektronenzustände im Atom definieren kann. Für ε_M ergibt sich im Falle des neutralen Thomas—Fermischen Atoms[12]

$$\varepsilon_M = 0{,}0488\, Z^{4/3} \frac{e^2}{a_0}, \tag{35}$$

also ein cca 10-mal kleinerer Wert als der Mittelwert $\bar{\varepsilon}_A$, der das algebraische Mittel der Energieniveaus der Elektronen im Atom darstellt.

Wir wollen nun noch die gesamte Elektronenenergie E des Atoms berechnen. Diese erhält man, wenn man aus der Summe der Energien der einzelnen Elektronen im Atom, d. h. aus $N\bar{\varepsilon}_A$ die elektrostatische Wechselwirkungsenergie der Elektronen abzieht, da die Summe diese doppelt enthält. Für die elektrostatische Wechselwirkungsenergie E_p^e der Elektronen im Atom ergibt sich der Ausdruck[13]

$$E_p^e = -\frac{1}{2} e \int V_e \varrho \, dv = -\frac{1}{7} Ze\, V_e(0) + \frac{6}{7} N \varepsilon_\mu , \tag{36}$$

[11] H. BETHE, Zs. f. Phys. **76**, 293, 1932; Ann. d. Phys. (5) 5, 325, 1930; A. SOMMERFELD, Zs. f. Phys. **78**, 283, 1932.

[12] P. GOMBÁS, l. c., S. 181—183.

[13] P. GOMBÁS, l. c., S. 62.

den man mit Rücksicht auf (27), (29) und (30) in folgender Form schreiben kann

$$E_p^e = -\frac{1}{7}\frac{Z^2 e^2}{\mu}\left[\varphi'(0) + 7\frac{q(1-q)}{x_0} + \frac{q^2}{x_0}\right]. \tag{37}$$

Für die Gesamtenergie des Thomas—Fermischen Atoms erhält man also den Ausdruck

$$E = N\bar{\varepsilon}_A - E_p^e = \frac{3}{7}\frac{Z^2 e^2}{\mu}\left[\varphi'(0) + \frac{q^2}{x_0}\right], \tag{38}$$

der schon mehrfach auf verschiedenen anderen Wegen hergeleitet wurde.

§ 4. Energieverteilung und Energiemittelwerte von Elektronen mit vorgegebener Nebenquantenzahl

Zur gesonderten statistischen Behandlung der Elektronengruppen mit vorgegebener Nebenquantenzahl l im Atom teilt man den Impulsraum in der bekannten Weise in Zylinderschalen auf, deren Achsen zum Ortsvektor $\mathfrak{r}$ der Elektronen parallel sind.[14] Die Elektronen mit der Nebenquantenzahl l befinden sich dann in einer Zylinderschale, dessen innere und äussere Begrenzungsfläche je ein Zylinder vom Radius $p_l = lh/(2\pi r)$, bzw. vom Radius $p_{l+1} = (l+1)h/(2\pi r)$ bildet. Die Bildpunkte der Elektronen mit der Nebenquantenzahl l in der Volumeneinheit, deren radialer Impulsbetrag zwischen p_r und $p_r + dp_r$ fällt, füllen im Impulsraum in der besagten Zylinderschale ein Impulsraumvolumen von der Grösse

$$d\omega_l = (p_{l+1}^2 - p_l^2)\,\pi\, 2dp_r = 2(2l+1)\frac{h^2}{4\pi^2 r^2}\,dp_r \tag{39}$$

aus.

Für den Betrag des radialen Impulses p_r gilt der Ausdruck

$$p_r = \left[2m(Ve + \varepsilon) - \frac{h^2}{4\pi^2}\frac{k^2}{r^2}\right]^{1/2}, \tag{40}$$

wo k die azimutale Quantenzahl bezeichnet, für die wir in dieser halbklassischen Näherung in üblicher Weise $k = l + \frac{1}{2}$ setzen. Aus (40) folgt

$$dp_r = \frac{m}{p_r}\,d\varepsilon\,. \tag{41}$$

[14] Man vgl. z. B. P. GOMBÁS, Handb. d. Phys. **36/2**, S. 148 ff., Springer, Berlin—Göttingen—Heidelberg, 1956.

Mit diesem Ausdruck erhält man aus (39) am Ort $x = r/\mu$ pro Volumeneinheit für die Anzahl der Elektronen mit der Nebenquantenzahl l, deren Energie zwischen ε und $\varepsilon + d\varepsilon$, bzw. u und $u + du$ fällt

$$dn_l(u,x) = \frac{4(2l+1)}{h} \frac{m}{4\pi r^2} \frac{d\varepsilon}{p_r} =$$

$$= \frac{(2l+1)\alpha}{4\pi^2 \mu^3} \frac{1}{x^2} \frac{dv}{\left(\frac{\varphi}{x} + u - u_\mu - \frac{1}{\alpha^2} \frac{k^2}{x^2}\right)^{1/2}}, \tag{42}$$

wo

$$\alpha = \left(\frac{2Z\mu}{a_0}\right)^{1/2} \tag{43}$$

ist. Die Verteilungsfunktion hat natürlich nur in den Gebieten einen Sinn, in welchen in (42) der Ausdruck unter der Wurzel $\geqq 0$ ist.

Durch Integration über den Raum bekommt man hieraus für die Anzahl der Elektronen mit der Nebenquantenzahl l im ganzen Atom, deren Energie zwischen ε und $\varepsilon + d\varepsilon$, bzw. u und $u + du$ liegt

$$dN_l(u) = \frac{4(2l+1)}{h} \alpha \, d\varepsilon \int \frac{dr}{p_r} =$$

$$= \frac{(2l+1)\alpha}{\pi} du \int \frac{dx}{\left(\frac{\varphi}{x} + u - u_\mu - \frac{1}{\alpha^2} \frac{k^2}{x^2}\right)^{1/2}}, \tag{44}$$

wo die Integration nur auf solche Gebiete auszudehnen ist, für welche im Integranden der Ausdruck unter der Wurzel $\geqq 0$ ist.

Ganz ähnlich wie im vorangehenden Fall lässt sich durch Integration nach ε (bzw. u) von der tiefsten Energie ε_{l0} bis zu einer beliebigen Energie ε die Anzahl der Elektronen mit der Nebenquantenzahl l angeben, deren Energie zwischen die tiefste Energie ε_{l0} und die Energie ε fällt und zwar sowohl pro Volumeneinheit (n_l), wie für das ganze Atom (N_l). Die tiefste Energie ε_{l0} des Elektrons ergibt sich für den Wert 0 der radialen kinetischen Energie, d. h. für $p_r = 0$, woraus aus (40)

$$\varepsilon_{l0} = -Ve + \frac{h^2}{8\pi^2 m} \frac{k^2}{r^2} \tag{45}$$

folgt. Mit dieser Beziehung erhält man für n_l und N_l

$$n_l(u,x) = \frac{4(2l+1)}{h}\frac{p_r}{4\pi r^2} = \frac{(2l+1)a}{2\pi^2\mu^3}\frac{1}{x^2}\left(\frac{\varphi}{x} + u - u_\mu - \frac{1}{a^2}\frac{k^2}{x^2}\right)^{1/2}, \tag{46}$$

$$N_l(u) = \frac{4(2l+1)}{h}\int p_r\,dr = 2(2l+1)\frac{a}{\pi}\int\left(\frac{\varphi}{x} + u - u_\mu - \frac{1}{a^2}\frac{k^2}{x^2}\right)^{1/2} dx, \tag{47}$$

wo in (46) die Integration wieder nur auf solche Gebiete auszudehnen ist, für welche der Ausdruck im Integranden unter der Wurzel $\geqq 0$ ist.

Für $u = u_\mu$ ist $n_l(x, u)$ mit der Dichte der Elektronen mit der Nebenquantenzahl l am Ort x identisch, es ist also

$$n_l(x, u_\mu) = \varrho_l(x), \tag{48}$$

weiterhin folgt

$$N_l(u_\mu) = N_l, \tag{49}$$

wo N_l die Anzahl der Elektronen mit Nebenquantenzahl l im Atom bezeichnet.

Die Funktion $N_l(u)$ haben wir für das Hg-Atom für $l = 0$, 1, 2 und 3 berechnet und mit den Werten von $N_l(u)$ verglichen, die man mit der Methode des »self-consistent field« erhält.[15] Aus dieser Methode ergibt sich für $N_l(u)$ [geradeso wie für $N(u)$ in § 1] ein stufenweise abfallender Verlauf. Wie aus den Figuren 7, 8, 9 und 10 ersichtlich ist, werden diese stufenweise abfallenden Kurven durch unsere glatt verlaufenden Verteilungsfunktionen $N_l(u)$ im Mittel gut approximiert.

Mit dem Ausdruck (42) für dn_l kann man sofort den Mittelwert $\bar{\varepsilon}_l(x)$ der Energie eines Elektrons mit der Nebenquantenzahl l an einem Ort x im Atom bestimmen. Wir definieren $\bar{\varepsilon}_l(x)$ folgendermassen

$$\bar{\varepsilon}_l(x) = \frac{1}{\varrho_l}\int_{\varepsilon_0}^{\varepsilon_\mu} \varepsilon\,dn_l\,, \tag{50}$$

wo für die obere Grenze im Integral die von l unabhängige maximale Energie ε_μ eines Elektrons gesetzt wurde, was in dieser Näherung gerechtfertigt ist. Aus (50) findet man nach einfacher Rechnung

$$\begin{aligned}\bar{\varepsilon}_l &= -\frac{2}{3}\left(Ve - \frac{h^2}{8\pi^2 m}\frac{k^2}{r^2}\right) + \frac{1}{3}\varepsilon_\mu = \\ &= -\frac{2}{3}\frac{Ze^2}{\mu}\left(\frac{\varphi}{x} - \frac{1}{a^2}\frac{k^2}{x^2}\right) + \frac{Ze^2}{\mu}u_\mu.\end{aligned} \tag{51}$$

[15] D. R. HARTREE, Phys. Rev. **46**, 738, 1934 und D. R. HARTREE u. W. HARTREE, Proc. Roy. Soc. London (A) **149**, 210, 1935.

Die mittlere Energie $\bar{\varepsilon}_l^A$ eines Elektrons mit der Nebenquantenzahl l bezogen auf das ganze Atom erhält man folgendermassen

$$\bar{\varepsilon}_l^A = \frac{1}{N_l} \int \bar{\varepsilon}_l \varrho_l \, dv \,, \tag{52}$$

wo ϱ_l gemäss (48) und (46) durch den Ausdruck

$$\varrho_l = \frac{4(2l+1)}{h} \frac{p_r(\varepsilon_\mu)}{4\pi r^2} = \frac{2l+1}{2\pi^2 \mu^3} \frac{a}{x^2} \left(\frac{\varphi}{x} - \frac{1}{a^2} \frac{k^2}{x^2} \right)^{1/2} \tag{53}$$

dargestellt wird und das Integral in (52) nur auf solche Gebiete auszudehnen ist, für die der Ausdruck unter der Wurzel in ϱ_l grösser als 0 oder gleich 0 ist. Für N_l im Nenner von (52) hat man gemäss (49) $N_l(u_\mu)$ zu setzen.

Tabelle 2

Werte von $\bar{\varepsilon}_l^A$ ($l = 0, 1, 2, 3$) für das Hg-Atom in e^2/a_0-Einheiten

	0	1	2	3
$\bar{\varepsilon}_l^A$ hier berechnet	−712,4	−130,0	−37,95	−7,02
$\bar{\varepsilon}_l^A$ nach HARTREE	−562,4	−142,0	−32,87	−4,20

Wir haben $\bar{\varepsilon}_l^A$ für $l = 0$, 1, 2 und 3 im Falle des Hg-Atoms berechnet; die Resultate sind in der Tabelle 2 angegeben. Ausserdem haben wir $\bar{\varepsilon}_l^A$ für dieselben l-Werte für das Hg-Atom auch aus den Hartreeschen Tabellen[16] mit der Formel

$$\bar{\varepsilon}_l^A = \frac{1}{N_l} \sum_i n_{il} \varepsilon_{il} \tag{54}$$

berechnet, in welcher n_{il} die Anzahl der Elektronen im Energieniveau ε_{il} bezeichnet und die Summation auf alle besetzten Zustände mit der Nebenquantenzahl l auszudehnen ist. Formel (54) entspricht (52), wenn man in der letzteren von der kontinuierlichen Verteilung auf eine diskrete Verteilung übergeht und dementsprechend das Integral durch eine Summe ersetzt.

Wie man aus der Tabelle 2 sieht, ist der Unterschied zwischen den von uns berechneten $\bar{\varepsilon}_l^A$-Werten und den empirischen ziemlich gross. Dies dürfte in erster Linie darauf zurückzuführen sein, dass der Ausdruck (53) für ϱ_l nur eine grobe Näherung darstellt.

[16] D. R. HARTREE, Phys. Rev. **46**, 738, 1934 und D. R. HARTREE u. W. HARTREE, Proc. Roy. Soc. London (A) **149**, 210, 1935.

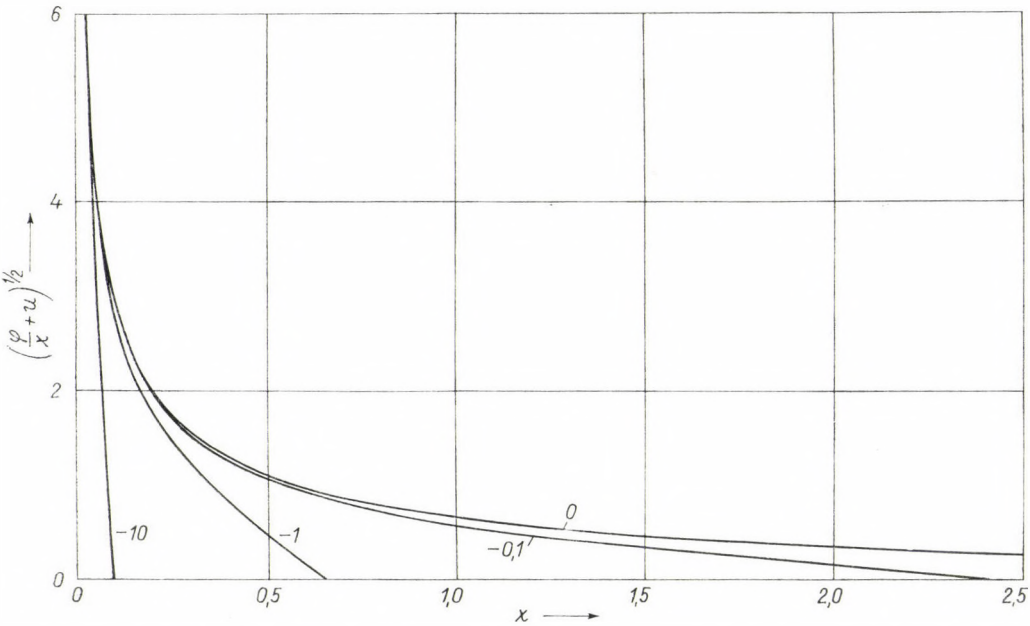

Fig. 1. $\frac{2}{3}-\frac{4\pi\mu^3}{Z}\frac{dn}{du}=\left(\frac{\varphi_0}{x}+u\right)^{1/2}$ als Funktion von x für mehrere festgehaltene u-Werte im Falle neutraler Atome. Die betreffenden u-Werte stehen neben den Kurven

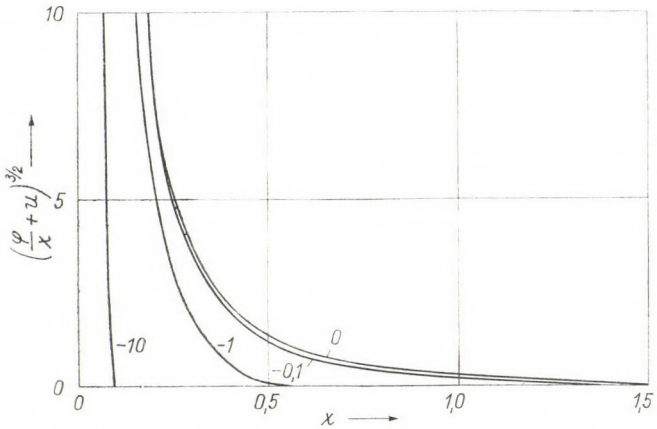

Fig. 2. $\frac{4\pi\mu^3}{Z}n=\left(\frac{\varphi_0}{x}+u\right)^{3/2}$ als Funktion von x für mehrere festgehaltene u-Werte im Falle neutraler Atome. Die betreffenden u-Werte stehen neben den Kurven

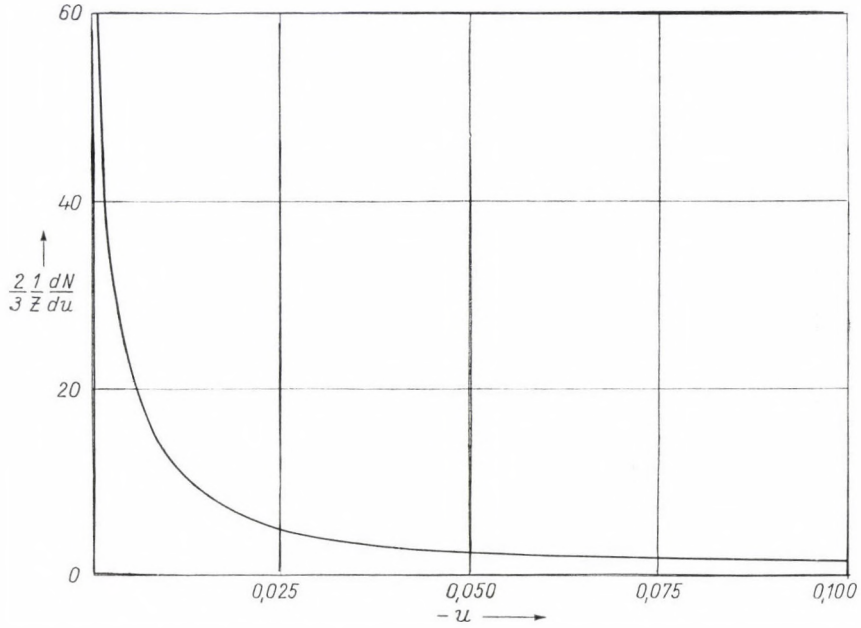

Fig. 3. $\frac{2}{3}\frac{1}{Z}\frac{dN}{du} = \int \left(\frac{\varphi_0}{x} + u\right)^{1/2} x^2\,dx$ als Funktion von u für neutrale Atome

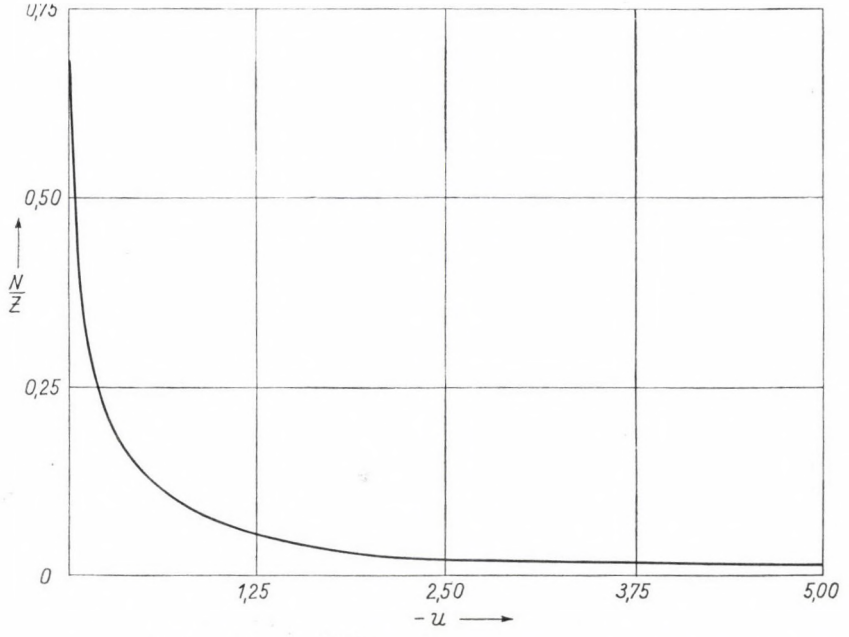

Fig. 4. $\frac{N(u)}{Z} = \int \left(\frac{\varphi_0}{x} + u\right)^{3/2} x^2\,dx$ als Funktion von u für neutrale Atome

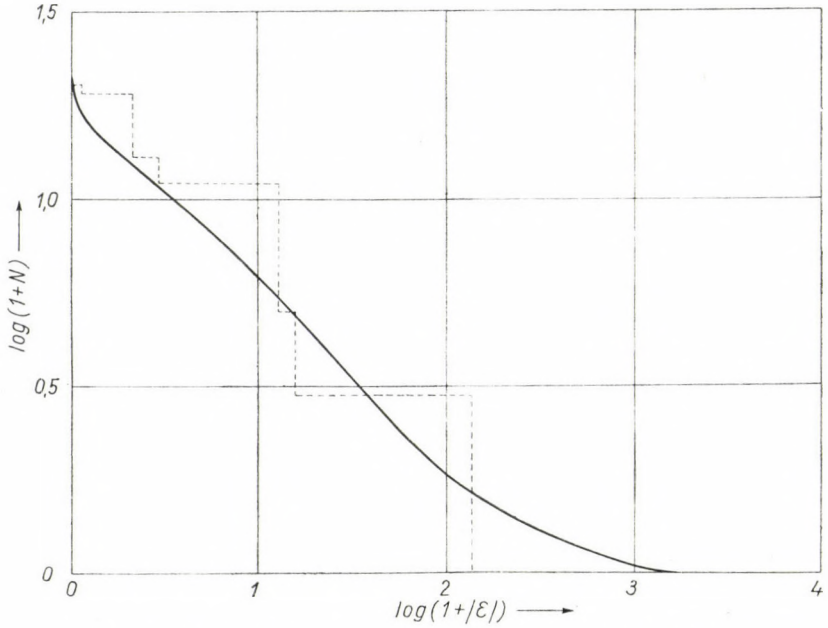

Fig. 5. N als Funktion von ε für das K-Atom. ε in e^2/a_0-Einheiten
——— hier berechnet,
- - - - - - - nach HARTREE

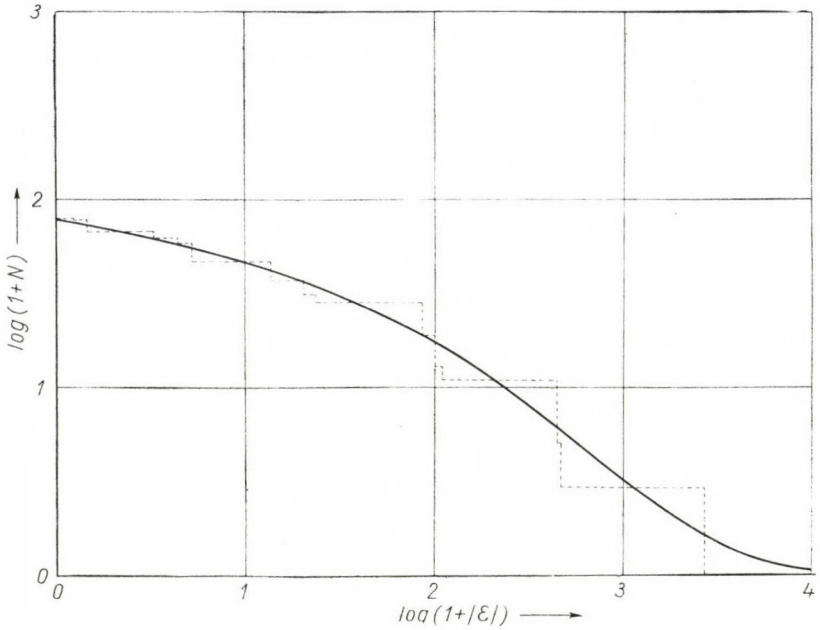

Fig. 6. N als Funktion von ε für das Hg-Atom. ε in e^2/a_0-Einheiten
——— hier berechnet,
- - - - - - - nach HARTREE

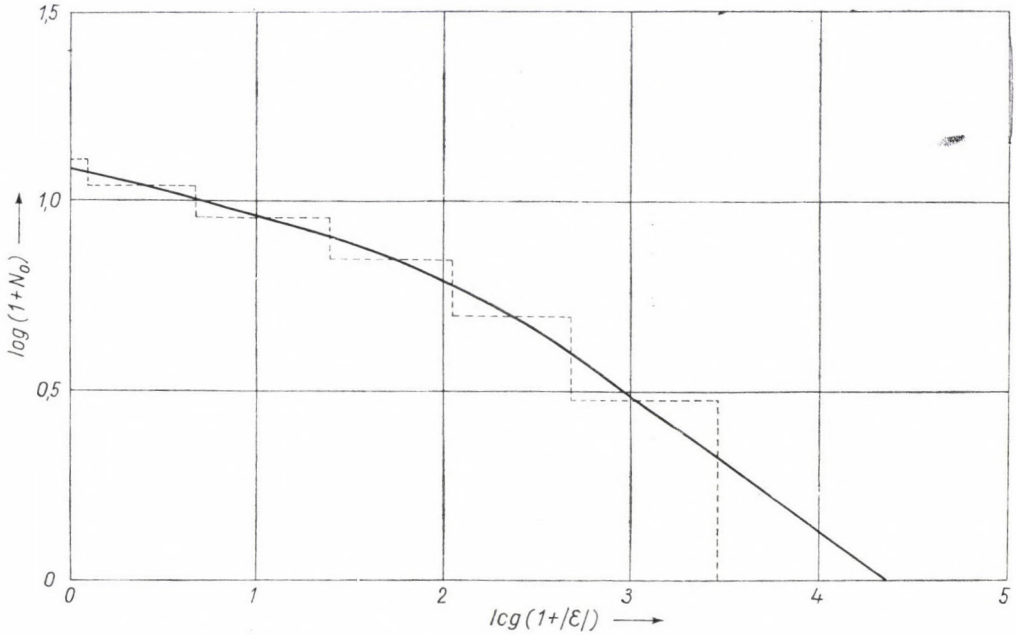

Fig. 7. N_0 als Funktion von ε für das Hg-Atom. ε in e^2/a_0-Einheiten
——— hier berechnet,
- - - - - - - nach HARTREE

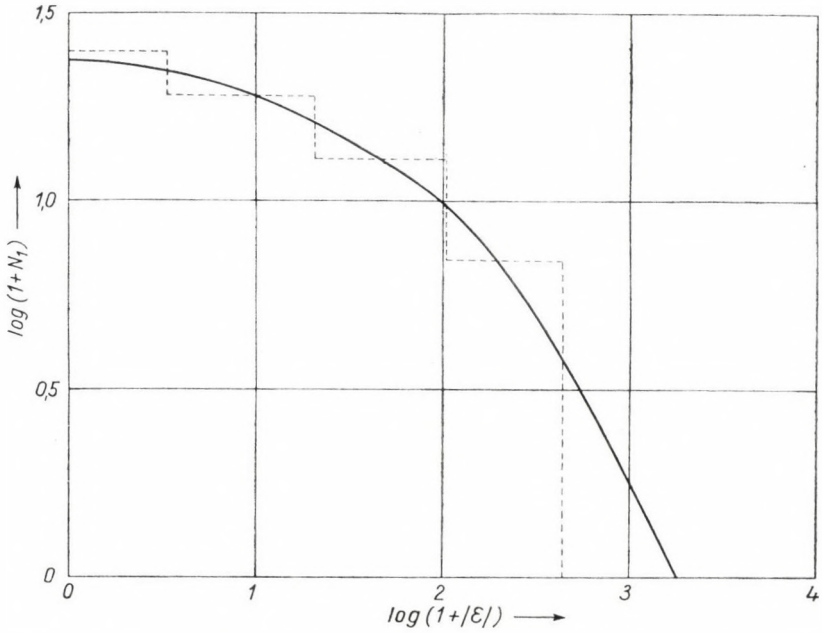

Fig. 8. N_1 als Funktion von ε für das Hg-Atom. ε in e^2/a_0-Einheiten
——— hier berechnet,
- - - - - - - nach HARTREE

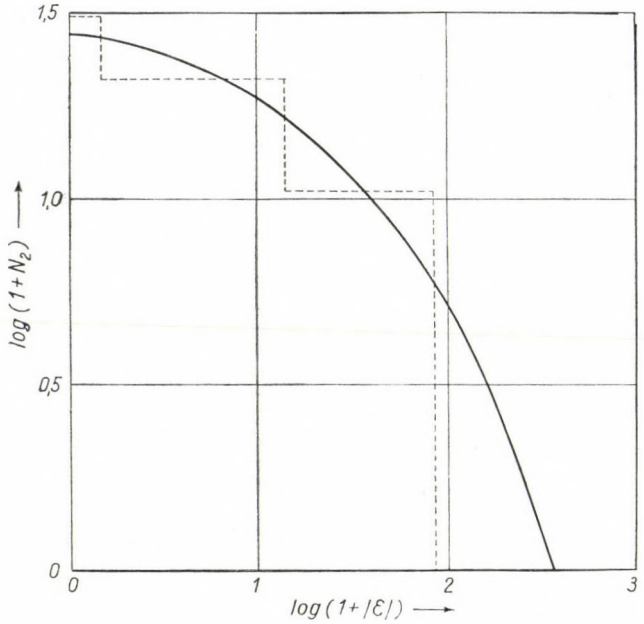

Fig. 9. N_2 als Funktion von ε für das Hg-Atom. ε in e^2/a_0-Einheiten
——— hier berechnet,
- - - - - - - nach HARTREE

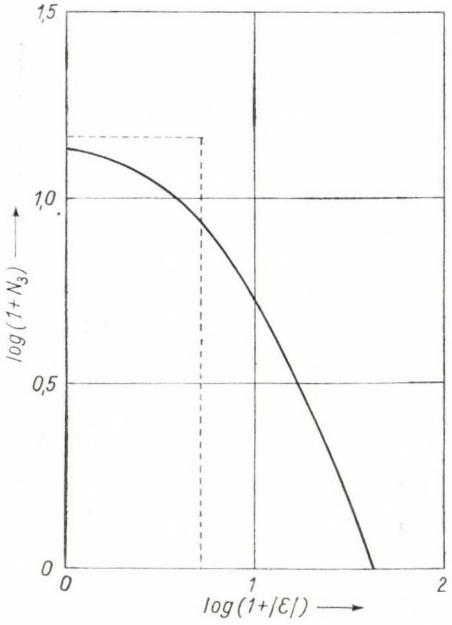

Fig. 10. N_3 als Funktion von ε für das Hg-Atom. ε in e^2/a_0-Einheiten
——— hier berechnet,
- - - - - - - nach HARTREE

Herrn Dr. T. Szondy danke ich für die Durchführung mehrerer Kontrollrechnungen und die sorgfältige Durchsicht des Manuskriptes. Frl. O. Kunvári verdanke ich die Durchführung der numerischen Rechnungen und die Zeichnung der Figuren.

О РАСПРЕДЕЛЕНИИ ЭНЕРГИИ ЭЛЕКТРОНОВ В СТАТИСТИЧЕСКОМ АТОМЕ

П. ГОМБАШ

Р е з ю м е

В работе выводятся формулы для распределения энергии электронов в статистически рассмотренном атоме как для случая общей трактовки электронов, так и для случая, когда электроны в атоме сгруппированы по побочным квантовым числам. В случае атома Hg результаты вычислений по распределению энергии электронов сравниваются с распределением, взятым по таблице Хартри. Оказывается, что результаты хорошо согласуются. Далее, на основе статистического распределения энергии электронов определяются средние значения энергии электронов в атоме. В этом случае результаты менее согласуются с квантово-механическими данными. Полученные в §§ 2 и 3 результаты могут распространяться на любые статистически рассмотренные системы.

INTERMEDIATE FIELDS WITHOUT PARTICLES

By

A. FRENKEL

CENTRAL RESEARCH INSTITUTE FOR PHYSICS OF THE HUNGARIAN ACADEMY OF SCIENCES, BUDAPEST

(Presented by L. Jánossy. — Received 11. V. 1965)

An extension of BOGOLIUBOV's S-matrix theory [1] to include intermediate fields with no corresponding particles in the initial and final states is proposed. The mathematical expression for the complete propagator of an intermediate field indicates that there may be cases when this propagator has the well-known analytic properties of a propagator of an unstable particle (or resonance). It is shown that if application of the formalism to the vector field is possible, a renormalizable theory of weak interactions with intermediate vector boson field can be constructed. In lowest order this theory leads to the same results for the weak decay processes as the usual FERMI theory.

Introduction

One of the advantages of BOGOLIUBOV's method for the construction of the S-matrix in quantum field theory [1] is that the problematical transformations from the SCHRÖDINGER (or HEISENBERG) picture to the interaction picture are avoided. Furthermore, the theory is constructed in a way which makes easy the investigation of the arbitrariness in the process of renormalization. For these reasons we closely adhere to the method of BOGOLIUBOV. In part I of this paper we briefly recapitulate the theory and illustrate it on hand of the well-known example of quantum-electrodynamics, without discussing special problems (infrared divergences, indefinite metric, gauge invariance). Nothing new is contained in this part of the paper, except perhaps for the remark at the end of it concerning the choice of the subtraction point when eliminating divergences from self energy parts. In part II we investigate the problem of the arbitrariness in the choice of the interaction Lagrangian $L(x)$ and give a detailed description of the effect caused by the introduction of a term $\tilde{m} : \bar{\psi}\,\psi :$ with a *finite* value of $\tilde{m}$. We find that the electrons are effectively eliminated from the initial and final states (see [1], § 31.2) and become resonance-like intermediate "particles". We conclude this part of the paper by remarking that the properties of unitarity and causality of the S-matrix must be reinvestigated for this case. We stress also that in order to verify these properties it seems desirable to find and example where the described situation with a resonance-like intermediate particle may have a physical background. Such is surely not to be found in quantum-electrodynamics which

serves here only as a model. A physically plausible example is given in part III where we propose to construct a renormalizable theory of weak interactions with an intermediate vector-boson field. Such a theory would lead to the same results as the Fermi theory for all processes with low momentum transfer, i. e. for all known β-decays.

I. As shown in [1] § 18, the most general form of the scattering operator $S \equiv \lim_{g \to 1} S(g)$ may be determined without reference to the Schrödinger equation. Indeed, the requirement of Lorentz-invariance, unitarity and causality lead to the formula

$$S(g) = 1 + i\int L(x_1; g)\, dx_1 + \ldots + \frac{i^n}{n!}\int T(L(x_1; g) \ldots L(x_n; g))\, dx_1 \ldots dx_n + \\ + \ldots \equiv T(\exp i\int L(x; g))\, dx, \tag{1}$$

where

$$L(x; g) = L(x)\, g(x) + \sum_{\nu \geq 2} \frac{1}{\nu!}\int A_\nu(x, y_1, \ldots y_{\nu-1})\, g(y_1) \ldots g(y_{\nu-1})\, dy_1 \ldots dy_{\nu-1}. \tag{2}$$

Here $0 \leqslant g(x) \leqslant 1$ is a classical function switching on and off the interaction and playing an important role in the derivation of (1); calculating the matrix elements of the S operator between free particle states, one may, however, put in the above formula $g(x) \equiv 1$ from the very beginning of the calculation.

The operator $L(x)$ is the interaction Lagrangean. It contains normal products of the operators of the fields under consideration, multiplied by appropriate coupling constants. The field operators obey free-field equations and free-field commutation relations. In order to have a Lorentz-invariant, unitary and causal S-operator, $L(x)$ must be scalar, Hermitean and local. Similarly, the A_ν-s must be scalar, Hermitean and quasi-local operators, and they may be chosen symmetric in all their arguments without loss of generality. Thus each $A_\nu(x_1, \ldots x_\nu)$ is a symmetrized sum of various normal products of an arbitrary number of field operators with arguments $x_1, x_2, \ldots, x_\alpha$; $\alpha \leqslant \nu$, each of these normal products being multiplied by a factor

$$Z\left(\ldots \frac{\partial}{\partial x_i} \ldots\right) \delta(x_1 - x_2)\, \delta(x_1 - x_3) \ldots \delta(x_1 - x_\nu) \tag{3}$$

ensuring the quasi-locality. Z is a polynom in $\frac{\partial}{\partial x_i}$, $i = 1, \ldots, \nu$ with arbitrary coefficients.

We see that in this most general form of the S operator of quantum field theory, we have to choose not only the interaction Lagrangean, but also

the infinite set of the highly arbitrary A_ν-s. Moreover, there is another arbitrariness in S, inherent in the fact that the time-ordered product

$$T(L(x_1)L(x_2)\ldots L(x_n))$$

is undetermined if two or more of its arguments are equal. It can be shown, however, that any change in $S(g)$ caused by a change in the definition of the T-products at $x_i = x_k = \ldots$ may also be expressed by changing some of the A_ν-s. Thus essentially we are left with one source of arbitrariness only, the other being redundant in the sense explained above.

At first sight it seems that the simplest way of constructing the S-operator would be the following. Since all the T-products are uniquely determined for $x_i \neq x_k$, extend the same expressions to $x_i = x_k = \ldots$ and put all $A_\nu \equiv 0$. Then one would have to choose only the interaction Lagrangian $L(x)$, and the free parameters of the theory would be the coupling constants and the masses, the latter entering into the S-matrix elements when expressing the T-products according to WICK's theorem. However, this simple procedure does not work, because the integrals $\int T\, dx_1 \ldots dx_n$ contained in (1) in general are divergent, and it is easy to show that the divergences arise just because of the simple extension of the T-product to $x_i = x_k$.[1] Thus one has to try, in order to obtain integrable expressions, to define the T-products for $x_i = x_k$ in some other way, or alternatively, (and that is what we shall do) to choose some of the A_ν-s different from zero. A detailed examination reveals the fact that — except for a few oversimplified model theories — in order to eliminate all the ultraviolet divergences[2] from all S-matrix elements one has to choose an infinite number of A_ν-s different from zero. Doing so one always succeeds in making all S-matrix elements finite, however, in general these matrix elements will contain an infinite number of arbitrary constants arising from the A_ν-s, and this clearly means that the theory is unacceptable. Only in a few cases can the elimination of all the divergences be accomplished in such a way that in spite of the infinite set of the A_ν-s the resulting S-matrix elements will contain only a *finite* number[3] of arbitrary parameters, which, together with the masses and the coupling constants originally contained in the theory, may be determined with the help of a finite number of experiments. The theories which turn out to be unacceptable in our scheme are called theories of the second kind (or non-renormalizable theories), while the "good" ones are the theories of the first kind (or renormalizable theories). The procedure of re-

[1] In special cases divergences from other causes occur, e.g. the infrared divergences in quantum electrodynamics. Such problems are irrelevant for us, and we simply disregard them. The divergences we are interested in are the ultraviolet divergences, which occur when $x_i - x_k \to 0$ (or $p_{ik} \to \infty$ if we transform to momentum space).

[2] See footnote 1.

[3] In some cases (e.g. in electrodynamics) this number turns out to be zero.

moving the divergences is called the renormalization, because in the original approach of DYSON and SALAM the divergences were formally compensated for by infinite charge and mass renormalization. It is important to realize that in BOGOLIUBOV's method the charge and mass parameters have *finite* (physical) values from the very beginning, and the divergences are disposed of with the help of the Λ_ν-s.

To illustrate the procedure for the elimination of the divergences in a theory of first kind, we turn to the well-known example of quantum electrodynamics. The interaction Lagrangean is

$$L(x) = e : \bar{\psi}(x)\, \gamma^\mu\, \psi(x) A_\mu(x) : \equiv e : \bar{\psi}(x) \hat{A}(x)\, \psi(x) : \tag{4}$$

where the electron and photon field operators satisfy the free field equations

$$\left(i \frac{\partial}{\partial x^a} \gamma^a - m \right) \psi(n) = 0\,; \qquad \Box A_\mu = 0 \tag{5}$$

and the corresponding free commutation relations. The parameters e and m are the electric charge and the electron mass, respectively. It can be shown that all the ultraviolet divergences[4] can be eliminated from the S-matrix elements with the help of operators $\Lambda_\nu(x_1, \ldots, x_\nu)$ of the following structure:

$$e^\nu \left\{ B_\nu\, \delta(x_1 - x_2) \ldots \delta(x_1 - x_\nu) \right\} : \bar{\psi}(x_i)\, \hat{A}(x_k)\, \psi(x_j) : \qquad (i \neq j;\ i \neq k;\ k \neq j) \tag{6}$$

for all odd ν-s starting with $\nu = 3$;

$$e^\nu \left\{ D_\nu \frac{1}{2} \left(\frac{\partial}{\partial x_i^\mu} \frac{\partial}{\partial x_j^\lambda} - g_{\mu\lambda} \frac{\partial}{\partial x_i^a} \frac{\partial}{\partial x_{ja}} \right) \delta(x_1 - x_2) \ldots \delta(x_1 - x_\nu) \right\} . \\ : A^\mu(x_i)\, A^\varkappa(x_j) : \qquad (i \neq j) \tag{7}$$

for all even ν-s starting with $\nu = 2$;

$$e^\nu : \bar{\psi}(x_l) \left\{ \left[F_\nu + G_\nu \frac{i}{2} \left(\frac{\hat{\partial}}{\partial x_i} - \frac{\hat{\partial}}{\partial x_j} \right) \right] \delta(x_1 - x_2) \ldots \delta(x_1 - x_\nu) \right\} \psi(x_j) : \quad (i \neq j) \tag{8}$$

for all even ν-s starting with $\nu = 2$. The derivations act on the variables x of the Dirac δ-functions only. We have here an infinite set of Λ_ν-s, but any operator product occurring in this set is at most trilinear, and any polynom Z in (3) is at most of second degree. The possibility of limiting both the linearity

[4] Except for the so-called vacuum divergences, which can be eliminated by dividing all the S-matrix elements by the vacuum expectation value of the S-operator.

of the operator products and the degree of the polynoms Z in the whole set of the A_ν-s is the necessary and sufficient condition for a theory to be renormalizable.

Symmetrizing the expressions (6)—(8) and inserting them into (2), we arrive after integration over the variables y at the effective Lagrangean ($g(x) \equiv 1$)

$$\begin{aligned} L(x;1) = {} & :\bar{\psi}(x)\hat{A}(x)\,\psi(x): + eB:\psi(x)\,\hat{A}(x)\,\psi(x): + \\ & + F:\bar{\psi}(x)\,\psi(x): + G\frac{i}{2}:\left(\psi(x)\,\gamma^a\frac{\partial\psi(x)}{\partial x^a} - \frac{\partial\bar{\psi}(x)}{\partial x^a}\gamma^a\psi(x)\right): - \\ & - D\frac{1}{2}:\frac{\partial A_\lambda(x)}{\partial x^a}\,\frac{\partial A^\lambda(x)}{\partial x_a} - \left(\frac{\partial A_a(x)}{\partial x_a}\right)^2: \end{aligned} \tag{9}$$

where

$$\begin{aligned} B &= \sum_{\nu=1}^{\infty}\frac{e^{2\nu}}{(2\nu)!}B_{2\nu+1}; & G &= \sum_{\nu=1}^{\infty}\frac{e^{2\nu}}{(2\nu)!}G_{2\nu}; \\ F &= \sum_{\nu=1}^{\infty}\frac{e^{2\nu}}{(2\nu)!}F_{2\nu}; & D &= \sum_{\nu=1}^{\infty}\frac{e^{2\nu}}{(2\nu)!}D_{2\nu}. \end{aligned} \tag{10}$$

For the complete proof of the statement that with suitably chosen series B, G, F, D all S-matrix elements become finite, the reader is referred to [1], § 30. Here we just perform the removal of the divergences in a simple case and indicate the general procedure. Let us try to calculate the S-matrix element between one-electron states

$$\begin{aligned} \langle\vec{p}',\, r\,|S|\,\vec{p},\, s\rangle = {} & \left\langle 0 \mid a_r^{(-)}(\vec{p}')\left\{1 + i\int L(x_1;1)\,dx_1 + \right.\right. \\ & \left.\left. + \frac{i^2}{2!}\int T(L(x_1;1)\,L(x_2;1)\,dx_1\,dx_2 + \ldots\right\} a_s^{*(+)}(\vec{p}) \mid 0\right\rangle \end{aligned} \tag{11}$$

up to second order in e. The terms omitted in (11) are of higher order, and from those written down we have the following contribution

$$\begin{aligned} & \left\langle 0 \mid a_r^{(-)}(\vec{p}')\left\{1 + \frac{e^2}{2}i\int\left[F_2:\bar{\psi}(x_1)\,\psi(x_1): + G_2\frac{i}{2}:\bar{\psi}(x_1)\frac{\hat{\partial}}{\partial x_1}\psi(x_1):\right]dx_1 + \right.\right. \\ & \left.\left. + \frac{i^2}{2}\int e^2\,T\,(:\bar{\psi}(x_1)\,\hat{A}(x_1)\,\psi(x_1)::\bar{\psi}(x_2)\,\hat{A}(x_2)\,\psi(x_2):)\,dx_1\,dx_2\right\} a_s^{*(+)}(\vec{p})|0\right\rangle \end{aligned} \tag{12}$$

Using the familiar Feynman rules given in [1] §§ 19—21, we find that up to second order in e

$$\langle \vec{p}', r \mid S \mid \vec{p}, s \rangle = \delta_{rs}\, \delta(\vec{p}' - \vec{p}) + (2\pi)^4\, i\, \delta\,(p' - p) \cdot$$
$$\cdot \frac{\bar{v}^{r+}(\vec{p})}{(2\pi)^{3/2}}\, e^2 \left[\frac{F_2}{2} + \frac{G_2}{2}\, \hat{p} + \Sigma^{(2)}(\hat{p}, m) \right] \frac{v^{s-}(\vec{p})}{(2\pi)^{3/2}}, \tag{13}$$

where the expression

$$\Sigma^{(2)}(\hat{p}, m) = \frac{1}{(2\pi)^4\, i} \int \frac{dk}{k^2 + i\varepsilon}\, \gamma^\alpha\, \frac{\hat{p} - \hat{k} + m}{(p-k)^2 - m^2 + i\varepsilon}\, \gamma_\alpha \equiv$$
$$\equiv \int R^2(\hat{p}, \hat{k}, m) dk \tag{14}$$

comes from the term of (12) containing the T-product. This T-product has been treated according to WICK's theorem, and the well-known expressions for the vacuum expectation value of the two-fold T-products

$$\langle 0 |\, T\big(\psi(x_1)\, \bar{\psi}(x_2)\big)\, | 0 \rangle = \frac{1}{(2\pi)^4\, i} \int \frac{m - \hat{p}}{m^2 - p^2 - i\varepsilon}\, e^{i(x_1 - x_2)p}\, dp,$$
$$\langle 0 |\, T\big(A_\mu(x_1)\, A_\nu(x_2)\big)\, | 0 \rangle = \frac{1}{(2\pi)^4\, i} \int \frac{g_{\mu\nu}}{k^2 + i\varepsilon}\, e^{i(x_1 - x_2)k}\, dk \tag{15}$$

have been used. These expressions are divergent for $x_1 - x_2 \to 0$ and this is why the integral in $\Sigma^{(2)}$ is also divergent for $k \to \infty$. The divergent second order

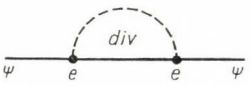

Fig. 1

term $e^2\, \bar{v}^+\, \Sigma^{(2)}\, v^-$ is illustrated by the Feynman diagram shown in Fig. 1. To see how the divergences occurring in $\Sigma^{(2)}$ can be compensated for by F_2 and G_2, we observe that the expression

$$\int \left[R^{(2)}(\hat{p}, \hat{k}, m) - R^{(2)}(0, \hat{k}, m) - \frac{\partial R^{(2)}(\hat{p}, \hat{k}, m)}{\partial \hat{p}} \bigg|_{\hat{p}=0} \cdot \hat{p} \right] dk \equiv$$
$$\equiv \hat{p}^2\, R_f^{(2)} \int (\hat{p}, \hat{k}, m) dk \tag{16}$$

is convergent. Thus if we choose in (13) F_2 and G_2 to be divergent in a well-defined manner,[5]

$$\frac{F_2}{2} = -\int R^{(2)}(0, \hat{k}, m)\, dk \equiv -\Sigma^{(2)}(0, m),$$

$$\frac{G_2}{2} = -\int \frac{\partial R(\hat{p}, \hat{k}, m)}{\partial \hat{p}}\bigg|_{\hat{p}=0} dk \equiv -\frac{\partial \Sigma^{(2)}(\hat{p}, m)}{\partial \hat{p}}\bigg|_{\hat{p}=0} \tag{17}$$

we are left with a finite remainder in (13)

$$e^2\left[\frac{F_2}{2} + \frac{G_2}{2}\hat{p} + \Sigma^{(2)}(\hat{p}, m)\right] = e^2\hat{p}^2\int R_f^{(2)}(\hat{p}, \hat{k}, m)\, dk \equiv e^2\Sigma_f^{(2)}(\hat{p}, m, 0). \tag{18}$$

We have introduced the third argument in $\Sigma_f^{(2)}$ to indicate that the latter depends on the point at which the expansion into Taylor series has been carried out.

Similar consderations lead to the compensation of the divergences in the second order vacuum polarization diagram (Fig. 2)

Fig. 2

and in the third order vertex diagram (Fig. 3),

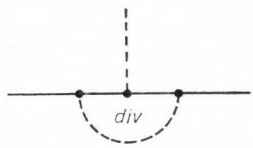

Fig. 3

when the divergent D_2 and B_3, respectively, are chosen suitably. Going then to fourth and fifth order in e, the constants F_4, G_4, D_4 and B_5 come into play and take care of the divergences of the fourth and fifth order graphs which eventually remain after the second and third order divergences have been eliminated from them with the help of the F_2, G_2, D_2 and B_3 already fixed. The procedure can be extended to arbitrarily high order in e, the essential point being that no such divergences occur that cannot be compensated for by the Λ_ν-s introduced in (6), (7) and (8).

[5] F_2 and G_2 are often said to be "divergent constants", to express the fact that they depend only on the electron mass and on the point at which the subtraction has been made, but not on the momentum variable p.

Let us come back to the second-order electron self-energy. We arrived at the finite remainder $\hat{p}^2 \Sigma_f^{(2)}(\hat{p}, m, 0)$ by subtracting from $R^{(2)}$ the first two terms of its Taylor series taken at the point $\hat{p} = 0$. It is easily seen that expanding $R^{(2)}$ at some other point $\hat{p} = m'$ we obtain another finite remainder. In an obvious shorthand notation we have

$$\Sigma^{(2)}(\hat{p}, m) = \Sigma^{(2)}(m', m) + \left.\frac{\partial \Sigma^{(2)}(\hat{p}, m)}{\partial \hat{p}}\right|_{\hat{p}=m'} (\hat{p} - m') + \\ + (\hat{p} - m')^2 \Sigma_f^{(2)}(\hat{p}, m, m'). \tag{19}$$

Now, by a slight modification of the corresponding A_ν-s we can get the compensating divergent constants. Indeed, it is enough to work instead of with (8) with the expression

$$e^\nu : \bar{\psi}(x_i) \left\{ \left[F_\nu + m' G_\nu + G_\nu \frac{i}{2} \left(\frac{\hat{\partial}}{\partial x_i} - \frac{\hat{\partial}}{\partial x_j} \right) - m' G_\nu \right] \cdot \right. \\ \left. \cdot \delta(x_1 - x_2) \ldots \delta(x_1 - x_\nu) \right\} \psi(x_j) : \qquad (i \neq j). \tag{8'}$$

This leads to the effective Lagrangean

$$L(x; 1) = e : \bar{\psi} \hat{A} \psi : + eB : \bar{\psi} \hat{A} \psi : + (F + m' G) : \bar{\psi} \psi : + \\ + G \left[\frac{i}{2} : \bar{\psi} \hat{\partial} \psi : - m' : \bar{\psi} \psi : \right] - D \frac{1}{2} : \partial_\alpha A_\lambda \partial^\alpha A^\lambda - (\partial^\alpha A_\alpha)^2 : \tag{9'}$$

with (10) formally unchanged. Repeating now the calculation which led from (11) to (13), we arrive at the expression

$$e^2 \left[\frac{1}{2} (F_2 + m' G_2) + \frac{1}{2} G_2 (\hat{p} - m') + \Sigma^{(2)}(\hat{p}, m) \right],$$

which reduces to

$$e^2 (\hat{p} - m')^2 \Sigma_f^{(2)}(\hat{p}, m, m') \tag{20}$$

if we put

$$\frac{1}{2} G_2 = - \left.\frac{\partial \Sigma^{(2)}(\hat{p}, m)}{\partial \hat{p}}\right|_{\hat{p}=m'}; \quad \frac{1}{2} (F_2 + m' G_2) = - \Sigma^{(2)}(m', m) \tag{17'}$$

The expression $e^2(\hat{p} - m')^2 \Sigma_f^{(2)}$ corresponds to the finite remainder (Fig. 4b) of the divergent diagram shown in Fig. 4a and enters into the various scattering

Fig. 4

amplitudes. E. g. the fourth order Compton scattering diagrams (Fig. 5) contain this element. Thus a new mass parameter m' appears in the theory. In many textbooks we may read that it is "convenient" to choose $m' = m$ because then all the radiative corrections to external and free electron lines are equal to zero, and also because then the pole of the complete electron propagator occurs at the electron mass m. It seems to us that the choice $m' = m$ is not

Fig. 5

Fig. 6

merely a matter of convenience. Let us examine the question of the radiative corrections to the external (e. g. ingoing) lines. The relevant factor corresponds to the part of a diagram shown in Fig. 6 and equals (except for immaterial factors 2π)

$$\frac{i}{\hat{p} - m} \frac{1}{i} e^2 (\hat{p} - m')^2 \Sigma_f^{(2)} (\hat{p}, m, m') v^-(\vec{p}) . \tag{21}$$

Taking into account that the spinor $v^-(\vec{p})$ satisfies the

$$(\hat{p} - m)v^-(\vec{p}) = 0$$

Dirac equation, we see that if $m' = m$ (21) gives

$$(\hat{p} - m) \Sigma_f^{(2)} (\hat{p}, m, m')v^-(\vec{p}) = 0$$

and the diagram with the radiative correction in the external line indeed does not contribute to the matrix element. However, if we put $m' \neq m$ (21) will be divergent because

$$(\hat{p} - m)^{-1} v^{-}(\vec{p}) = \infty$$

and the factor $(\hat{p} - m')^2$ will not counterbalance this. Similarly for a free electron line the propagator in the middle of the fourth order graph (Fig. 7)

Fig. 7

is easily seen to lead to divergence if $m' \neq m$, while for $m' = m$ we get zero as for the external lines. Thus for $m' \neq m$ the radiative corrections to the external and free lines make the S-matrix elements divergent, and therefore the choice $m' = m$ seems to be not only convenient, but necessary.

II. In the preceding section we have established that it is necessary to choose $m' = m$ in order to avoid infinities in the external and free electron lines. The result is of course easily extended to the self-energy graphs of the other particles, e. g. for the photon we have to carry out the expansion at the photon mass $m_f = 0$. The corresponding term with coefficient D in (9′) was written already in that form. For the vertex functions the choice of the subtraction point is probably not unambiguous in general, but in quantum electrodynamics gauge invariance imposes the condition $B_{2\nu+1} = G_{2\nu}$ and the problem is thereby resolved. Thus we arrive to the effective Lagrangean

$$\begin{aligned} L(x;1) = {} & e : \bar{\psi} \hat{A} \psi : + eB : \bar{\psi} \hat{A} \psi : - \delta m : \bar{\psi} \psi : + \\ & + G : \frac{i}{2} \bar{\psi} \hat{\partial} \psi - m \bar{\psi} \psi : - D \frac{1}{2} : \partial_\alpha A_\lambda \partial^\alpha A^\lambda - (\partial^\alpha A_\alpha)^2 : \end{aligned} \tag{9″}$$

where the notation $-\delta m = F + mG$ has been introduced.[6] Now the whole renormalization can be carried out without difficulty for the external and free lines.

Let us here recall to mind that up to now we have investigated the problem of removing the divergences from the S-matrix elements of a theory where the interaction Lagrangian was given by

$$L(x) = e : \bar{\psi} \hat{A} \psi : \tag{4}$$

[6] Notice the misprints in formula (30.45) of [1].

and the field operators ψ, A_μ satisfied the free field equations

$$(i\hat{\partial} - m)\psi = 0; \quad \Box A_\mu = 0 \tag{5}$$

and the corresponding free canonical commutation relations. Let us now ask what happens if we start from the same free field equations and commutation relations, but use the interaction Lagrangian

$$\tilde{L}(x) = e : \bar{\psi} \hat{A} \psi : + \tilde{m} : \bar{\psi} \psi : \equiv L(x) + \delta L(x), \tag{4'}$$

where $\tilde{m}$ is a new *finite* "coupling" constant, *independent* of e.

First of all let us remark that the introduction of the bilinear term $\tilde{m} : \bar{\psi} \psi :$ does not change the fact that all scattering processes, i. e. all processes where energy-momentum transfer between particles is possible, are due to the same trilinear operator terms as it was the case previously, since a bilinear term cannot lead to such processes.[7] Thus the structure of the basic interaction remains unchanged, and therefore we may hope that the renormalization can be carried out without essential changes in the A_ν-s. This is indeed the case, but, as pointed out at the end of § 31.2 in [1], the term $\tilde{m} : \bar{\psi}\psi :$ leads to a peculiar effect.[8] Namely, we shall see that this term modifies the free electron propagator $S^c(p)$ in the following way:

$$\frac{1}{i} S^c(p) \equiv \frac{i}{\hat{p} - m} \to \frac{i}{\hat{p} - (m + \tilde{m})} \tag{22}$$

and by the change

$$v^-(p) \longrightarrow \frac{\hat{p} - m}{\hat{p} - m - \tilde{m}} v^-(p) = 0 \tag{23}$$

makes all the graphs with external electron lines equal to zero. Thus the effect caused by the term $\tilde{m} : \bar{\psi} \psi :$ *is not equivalent* with a simple renormalization of the mass of the electron.

We shall show below that at the same time the finite remainders of the electron self-energy corrections take the form

$$e^{2\nu} (\hat{p} - m')^2 \Sigma_f^{(2\nu)} (\hat{p}, m + \tilde{m}, m') \tag{24}$$

and that in the present case no divergences arise when self-energy corrections are inserted in the external and free electron lines. Namely, we shall find that the mechanism leading to formulae (22)—(24) makes the corresponding graphs

[7] Of course other finite terms may also be introduced (see [1] § 32.), but we are not interested in them.

[8] We have written $\tilde{m}$ instead of δm in [1] to avoid confusion with the corresponding divergent constant in (9").

with external electron lines vanish with arbitrary m', while for free electron lines we have simply the contribution

$$\bar{v}^{r+}(\vec{p})\, v^{s-}(\vec{p}') = \delta_{rs}(\vec{p} - \vec{p}') \qquad (p^0 = p^{0\prime} = +\sqrt{\vec{p}^2 + m^2}). \tag{25}$$

The formulae (22)—(25) are obtained by inserting all the corrections coming from the $\tilde{m} : \bar{\psi}\psi :$ term in all simple electron lines of a Feynman graph

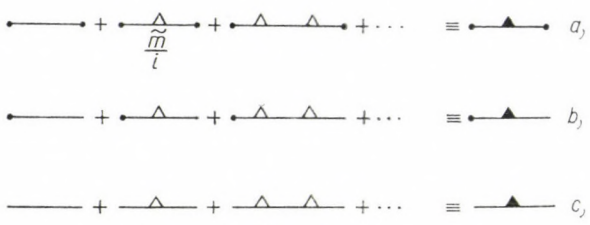

Fig. 8

and then eliminating all the divergences by appropriate choice of the divergent constants in the Λ_ν-s. Thus we obtain the following results:
for a propagator (Fig. 8a)

$$\frac{i}{\hat{p} - m} + \frac{i}{\hat{p} - m}\frac{\tilde{m}}{i}\frac{i}{\hat{p} - m} + \ldots = \frac{i}{\hat{p} - m}\left(1 + \frac{\tilde{m}}{\hat{p} - m} + \ldots\right) = \tag{22'}$$

$$= \frac{i}{\hat{p} - m}\frac{1}{1 - \dfrac{\tilde{m}}{\hat{p} - m}} = \frac{i}{\hat{p} - m - \tilde{m}};$$

for an external line (Fig. 8b)

$$\left[1 + \frac{i}{\hat{p} - m}\frac{\tilde{m}}{i} + \ldots\right] v^{-}(\vec{p}) = \frac{1}{1 - \dfrac{\tilde{m}}{\hat{p} - m}}\, v^{-}(\vec{p}) = \tag{23'}$$

$$= \frac{\hat{p} - m}{\hat{p} - m - \tilde{m}}\, v^{-}(\vec{p}) \longrightarrow 0 \qquad \text{for} \qquad p^2 \to m^2$$

for a free line (Fig. 8c)

$$\delta_{rs}(\vec{p} - \vec{p}') - (2\pi)^4 i\,\delta(p - p')\frac{\bar{v}^{r+}(\vec{p})}{(2\pi)^{3/2}}\left[\frac{\tilde{m}}{i} + \frac{\tilde{m}}{i}\frac{i}{\hat{p} - m}\frac{\tilde{m}}{i} + \ldots\right]\frac{v^{s-}(\vec{p})}{(2\pi)^{3/2}} =$$

$$= \delta_{rs}(\vec{p} - \vec{p}') + (2\pi)^4 i\delta(p - p')\frac{\bar{v}^{r+}(\vec{p})}{(2\pi)^{3/2}}\frac{\tilde{m}}{i}\frac{\hat{p} - m}{\hat{p} - m - \tilde{m}}\frac{v^{s-}(\vec{p})}{(2\pi)^{3/2}} \longrightarrow$$

$$\longrightarrow \delta_{rs}(\vec{p} - \vec{p}') + \delta(p - p') \cdot 0 \quad \text{for} \quad p^2 \to m^2 \tag{25'}$$

Of course, the geometrical series have been summed at such a value of p where they converge (such values of p surely exist for given m and $\tilde{m}$) and then the mass shell value $p^2 = m^2$ has been taken if needed. It is easily seen that it is *necessary* to carry out the summation over the *complete series*, because stopping at some finite order in $\tilde{m}$, we get divergent results on the mass shell.

We still have to show how (24) is obtained. Looking at the second-order formula (20), we see that it contains the divergent expression (14) $\Sigma^{(2)}(\hat{p}, m)$, in which the free electron propagator

$$\frac{i}{\hat{p} - \hat{k} - m}$$

occurs. According to (22) we have to put in it $m + \tilde{m}$ instead of m, i. e. we have to write $\Sigma^{(2)}(\hat{p}, m + \tilde{m})$ instead of $\Sigma^{(2)}(\hat{p}, m)$. To compensate the divergences we have evidently to choose

$$\frac{1}{2} G_2 = - \left. \frac{\partial \Sigma^{(2)}(\hat{p}, m + \tilde{m})}{\partial \hat{p}} \right|_{\hat{p} = m'} ; \quad \frac{1}{2} (F + m' G) = - \Sigma^{(2)}(m', m + \tilde{m}) \tag{17''}$$

Fig. 9

and we obtain the formula (24) for $\nu = 1$. It is now easily seen that no difficulty arises with the self-energy corrections to external and free lines. Indeed, while previously for an external line (Fig. 6) we had the formula

$$\frac{i}{\hat{p} - m} \frac{1}{i} e^2 (p - m')^2 \Sigma_f^{(2)}(\hat{p}, m, m') v^-(\vec{p}) = \begin{cases} \infty & \text{for } m' \neq m \\ 0 & \text{for } m' = m \end{cases}$$

we now have the case shown in Fig. 9, i. e.

$$\frac{i}{\hat{p} - m - \tilde{m}} \frac{1}{i} e^2 (\hat{p} - m')^2 \Sigma_f^{(2)}(\hat{p}, m + \tilde{m}, m') \frac{\hat{p} - m}{\bar{p} - m - \tilde{m}} v^-(\vec{p}) \to 0 \quad \text{if } p^2 \to m_2 \tag{26}$$

independently of the value of m'. Similar considerations show that all self-energy corrections to the free electron lines vanish and we therefore come to the expression (25). We see that the theory with the new Lagrangean $\tilde{L}(x)$ is renormalizable and that all the calculations may be carried out up to any given order in e. The structure of the basic interaction is the same as in the normal case $\tilde{m} = 0$, however, all the S-matrix elements with external spinor

lines are equal to zero. This means that the spinor field becomes an intermediate field, i. e. that the "electrons" take part in the scattering processes only as virtual particles. Free "electrons" may be present in the initial state, but they cannot interact and therefore they may be omitted without loss of generality.

Two problems arise in connection with these results. First, it is not sure that the procedure for the calculation of the new S-matrix elements leads to a unitary and causal S-matrix. We shall presently come back to this question. Second, even if these basic requirements are satisfied this does not necessarily mean that the theory corresponds to physical reality. In this connection it is enough to call to mind the well-known fact that present-day field theories are unfortunately much richer than necessary. E. g. a theory of quantum electrodynamics with electron mass and charge values different from the physical ones may mathematically be as good as a theory in which the true values have been used, but such a theory does not apply to nature. In the same way it is almost certain that even if the theory with intermediate electron field turns out to be not worse mathematically than the normal one, it should be rejected because there is no physical background for such a theory. In contrast to this, in part III of our paper we shall see that for weak interaction the case is different: while the normal ($\widetilde{M} = 0$) vector-boson theory of weak interaction is non-renormalizable, the introduction of a bilinear vector-boson term $-\frac{\widetilde{M}^2}{2} : B_\mu^* B^\mu :$ into the interaction Lagrangean makes the theory renormalizable. It is true that at the same time the vector boson becomes a purely intermediate field, but this is not in contradiction with any known experimental fact.

Let us now illustrate the problem of unitarity and causality on hand of example of quantum electrodynamics. The expression for the scattering operator $\tilde{S}$ with the new effective Lagrangean

$$\tilde{L}(x; 1) = L(x; 1) + \delta L(x)$$

according to (1) reads now:

$$\tilde{S} = 1 + i\int (L(1) + \delta L(1))\, d1 + \int \frac{i^2}{2!}\, T(L(1) + \delta L(1), L(2) + \delta L(2)) d1\, d2 + \ldots, \quad (27)$$

where 1 stands for x_1, $L(1)$ for $L(x_1; 1)$ and $\delta L(1) = \tilde{m} : \bar{\psi}(x_1)\, \psi(x_1) :$. A finite part of this series contains terms up to a finite order in $\tilde{m}$. However, we have seen that we must carry out the complete summation over $\tilde{m}$ for each electron line to avoid divergences in external and free lines [see formulae (23′) and (25′)]. This means that we have to rearrange the infinite series (27) in such a

way that for each given order in e we obtain an infinite series in $\tilde{m}$. To do this we have first to write down all the terms of zero order in $L(1)$ (i. e. in e), then all terms of first order in $L(1)$ and so on. (Of course, $L(1)$ contains the divergent constnats B, G, D, δm which themselves are infinite series in e, and in which only the terms up to the desired order are to be retained, just as in the normal case $\tilde{m} = 0$.) After trivial steps we arrive at the rearranged scattering operator

$$\tilde{\tilde{S}} = \sum_{n=0}^{\infty} \frac{i^n}{n!} \int T(\delta L(1) \ldots \delta L(n)) d1 \ldots dn +$$

$$+ \frac{i}{1!} \sum_{n=0}^{\infty} \frac{i^n}{n!} \int T(L(1') \, \delta L(1) \ldots \delta L(n)) \, d1' \, d1 \ldots dn + \ldots \equiv \tag{28}$$

$$\equiv \sum_{k'=0}^{\infty} \sum_{n=0}^{\infty} \frac{i^{k'}}{k'!} \frac{i^n}{n!} \int T(L(1') \ldots L(k') \, \delta L(1) \ldots \delta L(n)) \, d1' \ldots dk' d1 \ldots dn \,,$$

which has to be used if $\tilde{m} \neq 0$. Thus the rearrangement $\tilde{S} \to \tilde{\tilde{S}}$ must be considered as the necessary redefinition of the scattering operator for cases $\tilde{m} \neq 0$. Of course one cannot assert that $\tilde{\tilde{S}} = \tilde{S}$, because $\tilde{S}$ is not known to be absolutely convergent. Therefore all the properties of $\tilde{\tilde{S}}$ must be reinvestigated without reference to $\tilde{S}$ and it is in this connection that the problem of unitarity and causality arises. This problem, which is intimately related to the problem of the analytic structure of the Green's functions of the theory, will not be investigated in the present paper. Let us only remark that the two-point Green's function, i. e. the propagator of an intermediate field (with self-energy corrections included) has some encouraging properties. Indeed, formulae (22) and (24) indicte that this propagator is characterized by two mass parameters $m + \tilde{m}$ and m', and that the pole of the propagator

$$\frac{-1}{\hat{p} - (m + \tilde{m}) - (\hat{p} - m')^2 e^2 \Sigma_f^{(2)} (\hat{p}, m + \tilde{m}, m')} \tag{29}$$

including all second-order self-energy corrections may be shifted from the real axis. The important question is whether for suitably chosen mass parameters the pole will no longer be on the first Reimann sheet, as required by unitarity and causality.* The answer to this question may essentially depend on the concrete structure of the self-energy correction, determined by the basic interaction Lagrangean. Therefore we think that it would be useless to make a detailed investigation of these properties in quantum electrodynamics, where the case $\tilde{m} \neq 0$ is perhaps mathematically correct but surely not physical, and we turn now to a physically plausible case.

* See the note added in proof.

III. A possible application of the proposed scheme is the construction of a renormalizable theory of weak interactions with intermediate resonance-like vector boson.

It is well known that the vector boson theories with the trilinear interaction Lagrangean

$$L(x) = d : \bar{\psi}_1(x) \mathrm{O}^{\alpha} \psi_2(x) B_{\alpha}(x) : + h.c. \tag{30}$$

are in general non-renormalizable. The reason for this is the following. Let the free vector-boson field satisfy the KLEIN—GORDON equation[9]

$$(\Box - M^2) B_{\alpha}(x) = 0. \tag{31}$$

Then if the four components of B_{α} are quantized

$$[B_{\alpha}^{*}(x_1), B_{\beta}(x_2)]_{-} = g_{\alpha\beta} \frac{1}{(2\pi)^3} \int e^{ik(x_1 - x_2)} \varepsilon(k^0) \delta(k^2 - M^2) \, dk \tag{32}$$

we arrive at the following formula for the free vector boson propagator $D_{\alpha\beta}^{c}$:

$$\begin{aligned} \langle 0 | T(B_{\alpha}^{*}(x_1) B_{\beta}(x_2)) | 0 \rangle &\equiv \frac{1}{i} D_{\alpha\beta}^{c}(x_1 - x_2) = \\ &= \frac{i}{(2\pi)^4} \int g_{\alpha\beta} \frac{1}{k^2 - M^2 + i\varepsilon} e^{ik(x_1 - x_2)} \, dk \,. \end{aligned} \tag{33}$$

We see that the degrees of the fermion and boson propagators in momentum space and the topology of the Feynman graphs are the same as in quantum electrodynamics, and therefore the theory is formally renormalizable. However, because of the appearance of the metric tensor in the commutator (32), the free space state will be a vector space with indefinite metric, and negative probabilities occur in the theory. To remove this difficulty several methods are known, but except for the special case of conserved spinor currents, they all lead to non-renormalizable theories, essentially because in the boson propagator the factor

$$g_{\alpha\beta} (k^2 - M^2 + i\varepsilon)^{-1} \tag{34}$$

has to be changed to

$$\left(g_{\alpha\beta} - \frac{k_{\alpha} k_{\beta}}{M^2} \right) (k^2 - M^2 + i\varepsilon)^{-1} . \tag{35}$$

[9] More sophisticated equations for the vector boson have been proposed, but we shall not investigate them in the present paper.

Thus we have here a situation where the normal $\widetilde{M} = 0$ case turns out to be unacceptable in the framework of the renormalization program.

As a solution we propose to add the bilinear term $-\frac{\widetilde{M}^2}{2} : B_\mu^* (x)\ B^\mu (x) :$ to the interaction Lagrangian (30) and otherwise retain the formally renormalizable variant of the theory defined by the formulae (31)—(34). Going now over from $\tilde{S}$ to $\tilde{\tilde{S}}$, we arrive at a theory where free vector bosons cannot interact. The solution of the indefinite metric problem is then trivial. It is enough to demand that no vector boson be present in the initial states, because then they can never appear in the final states. More precisely, we split the vector space with indefinite metric into two orthogonal subspaces, a physical subspace (with positive definite norm) with no vector bosons and a subspace where bosons are present. The $\tilde{\tilde{S}}$-operator acting on physical states leads again to physical states and thereby no negative probabilities arise in the theory.

The applicability of this scheme to the construction of a renormalizable theory of weak interactions with purely intermediate vector-boson field is immediate. In lowest order this theory clearly leads to the results of the Fermi theory in all cases where $|k^2| \ll M^2 + \widetilde{M}^2$ i. e. for all β-decay processes, if we put

$$\frac{1}{\sqrt{8}} \frac{d^2}{M^2 + \widetilde{M}^2} = f = 1{,}4 \cdot 10^{-49}\ \mathrm{erg} \cdot \mathrm{cm}^3 ,$$

where d is the coupling constant of the vector boson to the weak currents. Comparison with the results of high-energy neutrino experiments could serve as a further experimental check on the theory, however, the theoretical uncertainties in the form factors together with the experimental ones make such a comparison probably premature.

In conclusion let us make the following remark. Usually field theories are expected to have structures in which each field operator gives rise to a particle which may be both external and virtual. However, we think that one need not consider this requirement as a necessary principle. Indeed, even for stable particles there may be special symmetry laws which eliminate some of the polarization states from the external lines but preserve them in the internal ones. A known example for this is the case of the electromagnetic field. A more general reason for doubt regarding the necessity of the above principle lies in the problem of the unstable particles (or resonances). At present it is an open question whether one has to introduce independent field operators for the unstable particles or whether one has to obtain them as composite systems of the stable particles. The second possibility is of course more satisfactory than the first, but up to now no such solution of the problem could be given. We may therefore adopt the first possibility and consider it as

a phenomenological approximation of the second. One then has to look for a mechanism which discards the unstable particles from the initial and final states of the scattering processes, because in a consistent S-matrix theory only stable particles should occur in those states. It may be that an extension of the procedure proposed in the present paper to all unstable particles may give such a mechanism.

Note added in proof. It is well-known that the propagator of a stable particle (including radiative corrections) may have and in many cases actually has a ghost pole. We are not concerned here with the elimination of the ghost, but rather with the elimination of the normal stable-particle pole. The detailed investigation of this problem for scalar and vector fields is in progress. The author expresses his thanks to Prof. I. Bialynicki—Birula for an interesting discussion on the subject. Valuable critical remarks of Prof. J. Rayski and I. Todorov are also greatly appreciated.

Acknowledgements

The author is deeply indebted to Dr. G. Domokos and Dr. K. L. Nagy for valuable discussions. Special thanks are due to P. Hraskó for continuous help and encouragement in all phases of this work.

REFERENCES

1. N. N. Bogoliubov and D. V. Shirkov, Introduction to the Theory of Quantized Fields. Interscience Publishers, New-York, London, 1959.

ПРОМЕЖУТОЧНЫЕ ПОЛЯ БЕЗ ЧАСТИЦ

А. ФРЕНКЕЛЬ

Р е з ю м е

Предлагается распространение теории S-матрицы Боголюбова [1] к описанию промежуточных полей без соответствующих частиц в начальном и конечном состояниях. Из математического выражения полной причинной функции Грина промежуточного поля видно, что могут быть случаи, когда эта функция обладает известными аналитическими свойствами пропагатора нестабильной частицы (или резонанса). Показано, что если предложенный формализм применим к полю векторного бозона, то можно построить перенормируемую теорию слабых взаимодействий с промежуточным полем векторного бозона. В низшем приближении теория ведет к тем же результатам, что и теория Ферми для всех слабых распадов.

THE HALF-LIFE OF THE SECOND EXCITED STATE IN Cs^{133}

By

T. SCHARBERT

INSTITUTE OF NUCLEAR RESEARCH OF THE HUNGARIAN ACADEMY OF SCIENCES, DEBRECEN

(Received 23. XI. 1964)

To obtain spins and parities of the levels of Cs^{133} many investigations were performed on the decay of both Ba^{133} and Xe^{133} [1]. It has been demonstrated that for three out of the first four excited states of Cs^{133} reliable spin and parity assignments [2] might be achieved. This is true especially for the first and the third excited levels where the values $5/2^+$ and $3/2^+$ are reliably established.

It is doubtless that the most problematic level is at 161 keV, i.e. the second excited level. According to certain measurements [3, 4] spin 3/2, while in others [2, 5, 6] 5/2 are supposed. The problem is even more interesting since Cs^{133} is near the double closed shells and the investigation of such kind of nuclei is very promising theoretically also.

It would be very useful in the given situation if there were any available experimental data referring to the lifetime of the 161 keV level. Unfortunately, up to now only the approximate estimation of BODENSTEDT et al. [5] has been known in literature according to which $T_{1/2} \leq 5 \cdot 10^{-10}$ sec.

That was the reason why we decided to measure the lifetime of the second excited state of this isotope.

The measuring instrument consisted of a time to amplitude converter with slow-fast system. The signals of two NaJ(Tl) crystals in connection with two 6810/A photomultipliers were connected with a fast coincidence circuit with tunnel diodes [7]. The slow part of the converter was the usual one, attached to a multichannel analyzer.

The resolving time of this instrument was $2\tau = 3{,}0 \cdot 10^{-9}$ sec for Co^{60} isotope.

Measuring the lifetime of the second excited level, the slow parts were set to the 161 keV and 276 keV energies, respectively. It is clear from the level scheme that no other cascades interfered in the measurement of this level. The transition being weak, the chance coincidences were reduced by placing a lead and tin shield between the source and the crystals. The lead shield made a cut off about 200 keV and the tin reduced the intensive 81 keV peak. We used Co^{60} isotope as a prompt gamma source.

The measurements were performed in five independent 24 hour periods. In each period the sources Co^{60} and Ba^{133} were changed 14 times to eliminate the drift of the instrument.

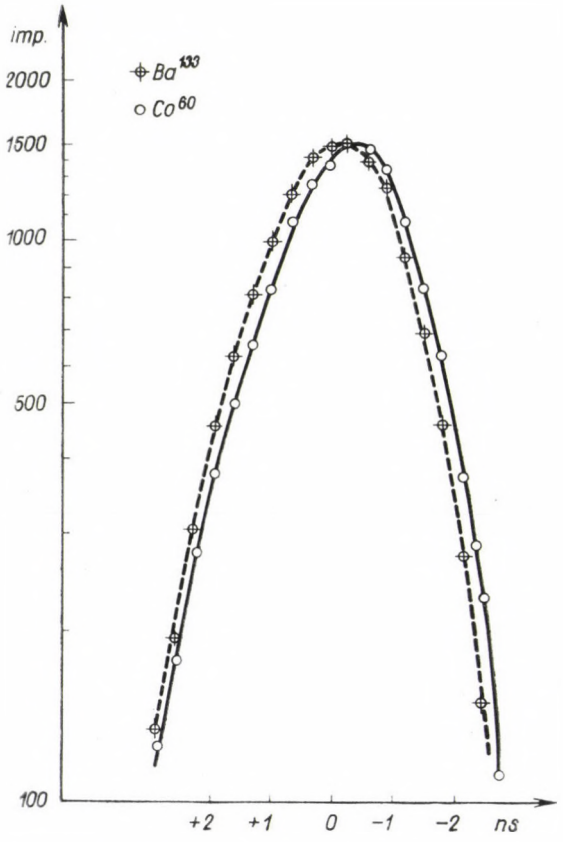

Fig. 1. Prompt and delayed coincidence resolution curves for Co^{60} and Ba^{133}

Evaluating the experimental curves (Fig. 1) by the centroid shift method the following value was received: $T_{1/2} = (9{,}7 \pm 2{,}6) \cdot 10^{-11}$ sec.

For the purpose of evaluating the measurement let us see Table 1:

Table 1

$I \to I'$	$1/2 \to 7/2^+$ $13/2 \to 7/2^+$		$3/2 \to 7/2^+$ $11/2 \to 7/2^+$		$5/2 \to 7/2^+$ $9/2 \to 7/2^+$		$7/2 \to 7/2^+$	
$\Delta\pi$	1	0	0	1	1	0	1	0
EL or ML	E3	M3	E2	M2	E1	M1	E1	M1
$T_{1/2}$ (W) sec	1	10^2	10^{-7}	10^{-5}	10^{-13}	10^{-12}	10^{-13}	10^{-12}

Here we obtained the values $T_{1/2}(W)$ according to the WEISSKOPF calculation from a nomogram given by WILKINSON [8].

It is clearly shown that on the basis of the one particle model among the values of $3/2^+$ and $5/2^+$ the assignment of $5/2^+$ seems to be the more probable (the columns with $\Delta\pi = 1$ can be eliminated on the basis of Coulomb excitation measurements). The deviation of the experimental value from the theoretical one can be explained by the appearance of collective effects and E2 mixture.

After we had finished our measurements, we received the paper by FLAUGER and SCHNEIDER [9]. They also measured the lifetime of this level but with the help of gamma-conversion electron coincidences, and they obtained $T_{1/2} = (0{,}85 \pm 0{,}16) \cdot 10^{-10}$ sec in close agreement with our value within the limits of errors.

I am indebted to Professor A. SZALAY for the excellent working conditions at this Institute and to Dr. D. BERÉNYI for stimulating advices.

LITERATURE

1. Nuclear Data Sheets (National Academy of Sciences, National Research Council,Washington) 61-2-91/92/93.
2. K. C. MANN and R. P. CHATURVEDI, Canadian Journal of Physics, **41**, 932, 1963.
3. M. G. STEWART and D. C. LU, Phys. Rev., **117**, 1044, 1960.
4. A. P. ARYA, Phys. Rev., **122**, 549, 1961.
5. E. BODENSTEDT, H. J. KÖRNER and E. MATTHIAS, Nucl. Phys., **11**, 584, 1959.
6. M. K. RAMASVAMY, W. L. SKEELAND and P. S. JASTRAM, Nucl. Phys., **19**, 299, 1960.
7. P. FRANZINI, Rev. Sci. Instr., **32**, 1222, 1961.
8. D. H. WILKINSON, in the book: Nuclear Spectroscopy (ed. by AJZENBERG-SELOVE), p. 852.
9. W. FLAUGER und H. SCHNEIDER: Atomkernenergie, **8**, H. 12, 1963.

ACTIVATION DEVICE FOR OBTAINING ACTIVE DEPOSIT OF THE THORON ON THIN WIRE

By

Cs. Ujhelyi and D. Berényi

INSTITUTE OF NUCLEAR RESEARCH OF THE HUNGARIAN ACADEMY OF SCIENCES, DEBRECEN

(Received 23. XII. 1964)

The ThB + C + C'' source provides a number of reliable standard calibration lines for beta-ray spectroscopy. To obtain active deposit on thin wire (~0,1 mm) two procedures are generally used: the wire together with the source-holder is placed into the activation device [1—3] or the wire itself is singly activated and then stretched (e.g. [4]). The disadvantage of the first procedure is that not only is the wire activated but the source-holder too. In the second procedure it is difficult to stretch the active wire on the source-holder.

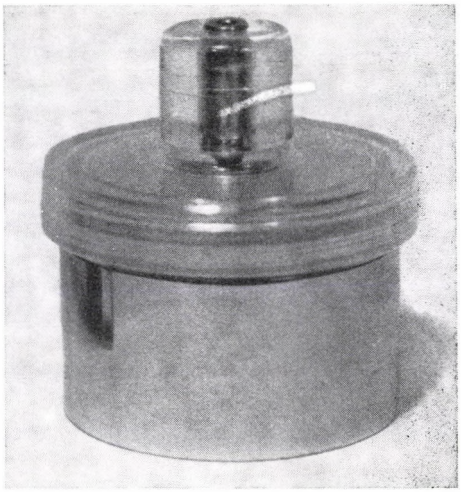

Fig. 1. General view of the activation device

In this short note an activation device designed for obtaining ThB + + C + C'' on thin wire is described. Here the thin wire stretched by a steel spring is activated and after activation the wire can be easily fixed on a suitable sourceholder.

The activation device is seen in Fig. 1. The device consists of the following parts: the stainless steel vessel containing the emanating preparation,

the wire stretched by the steel spring (bow), and the upper and lower parts of the unscrewable plexiglass plug (Fig. 2).

Before activation the plug is unscrewed and the wire stretched by a steel spring (the bow) is placed into the corresponding groove on the lower part of the plug. When the two parts of the plug are screwed up electric contact exists between the wire and the negative jack (Fig. 3).

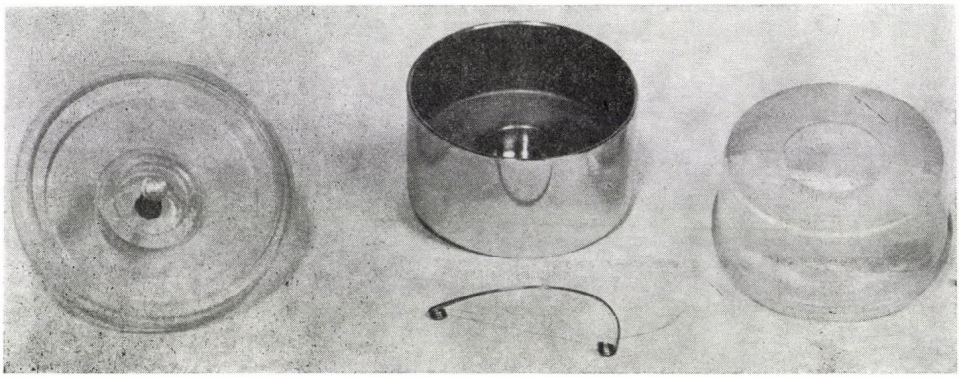

Fig. 2. Parts of the device

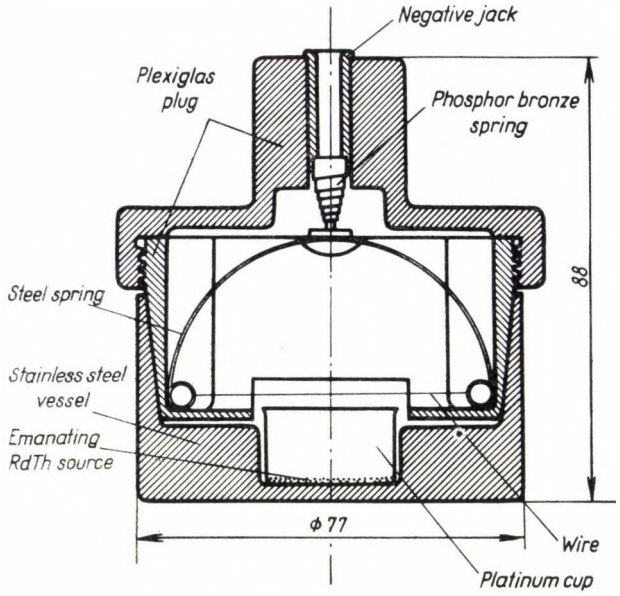

Fig. 3. Cross section of the device

The whole activation device is fastened to a metal disc supplied with a positive jack. The changeable lead shield surrounding the device is mounted on this disc.

According to our measurement the ThB + C + C'' activity deposited on the negatively charged wire shows a saturation at about 1000 V. With the increase of the voltage of 250 V to four times that value (1000 V) the activity of the wire increases by a factor of $\sim$ 1,5. (For an activation voltage of 1500 V the increase of the activity was not significant any more.) About 60% of ThB + C + C'' activity deposited on the plug and on the bow (steel spring + wire) is concentrated on that part of the wire just above the platinum cup containing the emanating RdTh source in hydrated ferric oxide preparation.

The authors are indebted to Dipl. Ing. J. SCHADEK for the technical design of the chamber.

REFERENCES

1. H. SLÄTIS, Ark. för Fysik, **6**, 417, 1953.
2. M. MLADJENOVIĆ and H. SLÄTIS, Ark. för Fysik, **8**, 67, 1954.
3. E. KARLSSON and K. SIEGBAHN, Nuclear Instruments, **7**, 123, 1960.
4. *В. И. Шумшуров*, private communication.

MESSUNG DER TOTALEN WIRKUNGSQUERSCHNITTE VON Cs UND Rb FÜR NEUTRONEN VON 14 MeV ENERGIE

Von

I. ANGELI und I. HUNYADI

INSTITUT FÜR KERNFORSCHUNG DER UNGARISCHEN AKADEMIE DER WISSENSCHAFTEN, DEBRECEN

(Eingegangen: 4. I. 1965)

Einleitung

Die Messung der totalen Wirkungsquerschnitte für schnelle Neutronen ist eine relativ einfache Aufgabe, und es wurden bereits eine ganze Reihe derartiger Messergebnisse veröffentlicht [1, 2, 3]. Es gibt jedoch noch etwa 20 Elemente, deren totale Wirkungsquerschnitte für Neutronen mit einer Energie von 14 MeV noch nicht gemessen wurden [4].

In dieser Arbeit sollen die experimentelle Anordnung für die Messung der Werte von σ_T bei Cs und Rb im Falle von 14 MeV-Neutronen und die bei der Messung erhaltenen Ergebnisse besprochen werden. Aus den Werten der gewonnenen Wirkungsquerschnitte erhält man auch eine Information über den Radius des Kerns von Cs^{133}, da das in der Natur vorkommende Cs nur das Isotop Cs^{133} enthält. Für den Radius von Rb kann daraus ein mittlerer Wert ermittelt werden.

Experimentelle Anordnung

Die Messung wurde bei einer »guten Geometrie« durchgeführt. Die Neutronen wurden von einem Neutronengenerator mit einer maximalen Beschleunigungsspannung von 110 KV [5] bzw. 300 KV [10] durch die Kernreaktion $T(d, n)He^4$ geliefert. Der Abstand der auszumessenden Probe vom Target betrug 30 cm und der des Neutronendetektors 60 cm; der letztere schloss im Falle von Cs mit dem Deuteronenstrahl einen Winkel von 90° ein, im Falle von Rb einen Winkel von 0°, d. h. wir erhielten Neutronen mit einer Energie von 14,08 MeV bzw. 14,69 MeV. Die Proben waren zylinderförmig und hatten Durchmesser von 3,9 bzw. 3,3 cm; sie enthielten 55 g CsCl bzw. 49 g RbCl. Als Neutronendetektor wurde ein organischer Kristall (Anthrazen, $\varnothing$ 3,8 cm $\times$ 1,2 cm) benutzt [11]. Die von den gestossenen Protonen hervorgerufenen Lichtimpulse gelangten in einen SEV (ФЭЧ — 19) und wurden durch die nachfolgende elektronische Anordnung registriert.

Der γ-Untergrund wurde mit Hilfe einer Impulsformdiskriminationsschaltung [6] beseitigt. Der von den gestreuten Neutronen herrührende Neutronenuntergrund konnte durch Amplitudendiskrimination im Zählinstrument im Falle von Cs auf 2,5%, im Falle von Rb auf 1,2% der gesamten Neutronenintensität herabgesetzt werden. Als Monitor wurde ein dem oben erwähnten Detektor ähnlicher Apparat benutzt.

Auswertung der Messergebnisse

Die Messergebnisse lieferten für die Wirkungsquerschnitte von CsCl und RbCl ohne Korrektion für Vorwärtsstreuung (»in-scattering«) die folgenden Werte:

$$\sigma'_T(\mathrm{Cs}) + \sigma'_T(\mathrm{Cl}) = 6{,}84 \pm 0{,}20 \text{ barn},$$

$$\sigma'_T(\mathrm{Rb}) + \sigma'_T(\mathrm{Cl}) = 5{,}81 \pm 0{,}09 \text{ barn}.$$

Mit $\sigma_T(\mathrm{Cl}) = 1{,}99 \pm 0{,}04$ barn [3] und $\left[\frac{\sigma_n(0^0)}{\sigma_T}\right]_{Cs} = 1{,}00 \pm 0{,}30$ str^{-1}, $\left[\frac{\sigma_n(0^0)}{\sigma_T}\right]_{Cl} = 0{,}70 \pm 0{,}17$ str^{-1}, $\left[\frac{\sigma_n(0^0)}{\sigma_T}\right]_{Rb} = 0{,}75 \pm 0{,}20$ str^{-1} (auf Grund der in [8] und [3] angegebenen Werte abgeschätzt) erhält man nach der Korrektion [7]:

$$\sigma_T(\mathrm{Cs}) = 4{,}96 \pm 0{,}21 \text{ barn} \qquad (E_n = 14{,}08 \text{ MeV}),$$

$$\sigma_T(\mathrm{Rb}) = 3{,}90 \pm 0{,}10 \text{ barn} \qquad (E_n = 14{,}69 \text{ MeV}).$$

In der theoretischen Arbeit [9] findet man $\sigma_T(\mathrm{Ba}) = 5{,}1$ b.

Auf die Radien der Kerne von Cs^{133} und Rb kann man aus der Formel $\sigma_T = 2\pi \cdot (R + \lambda)^2$ folgern [7]. In unserem Falle erhält man:

$$R(Cs^{133}) = 7{,}67 \pm 0{,}27 \text{ fermi} \qquad (E_n = 14{,}08 \text{ MeV}),$$

$$\overline{R}(\mathrm{Rb}) = 6{,}69 \pm 0{,}14 \text{ fermi} \qquad (E_n = 14{,}69 \text{ MeV}).$$

Die für 14 MeV-Neutronen näherungsweise gültige theoretische Formel $R_{th} = 1{,}5 \cdot A^{1/3}$ fermi liefert die Werte $R_{th}(\mathrm{Cs}) = 7{,}65$ fermi bzw. $R_{th}(\mathrm{Rb}) = 6{,}61$ fermi.

Die Verfasser sind Herrn B. Schlenk für seine Hilfe bei der Einstellung des Neutronendetektors zu Dank verpflichtet.

LITERATUR

1. D. J. HUGHES und R. B. SCHWARTZ, »Neutron Cross Sections« BNL 325, 2nd Ed., 1958, Brookhaven National Laboratory, Upton, New York.
2. D. W. GLASGOW und D. G. FOSTER, »Fast-Neutron Total Cross Sections of 44 Elements«, HW-SA-2875, Washington, 1963.
3. R. J. HOWERTON, »Tabulated Neutron Cross Sections 0,001—14,5 MeV«, Contract No W-7405-eng.-48., University of California Radiation Laboratory, 1958.
4. R. J. HOWERTON, »The Status of Experimental Neutron Cross Sections for Energies Between 0,5 and 14,5 MeV«; UCRL-5420, University of California Radiation Laboratory.
5. I. BERECZ, P. BORNEMISSZA und J. NAGY, Magyar Fizikai Folyóirat, **VI**, 431, 1958.
6. *В. Г. Бровченко, Г. В. Горлов:* Разделение нейтронного и гамма излучений по форме импульса в сцинтилляционном счетчике. Приборы и Техника Эксперимента, № 4, 49, 1961.
7. J. B. MARION und J. L. FOWLER, »Fast Neutron Physics II.«, S: 997, 1027, Interscience Publishers, New York, 1963.
8. M. D. GOLDBERG, V. M. MAY und J. R. STEHN, »Angular Distributions in Neutron-Induced Reactions« BNL-400, 2nd Ed., Sigma Center, Brookhaven National Laboratory, 1962.
9. D. WILMORE und P. E. HODGSON, Nuclear Physics, **55**, 673, 1964.
10. P. BORNEMISSZA, Atomki Közlemények, **VII**, No. 1, 47, 1965.
11. I. ANGELI und I. HUNYADI, Atomki Közlemények, **VII**, No. 2, 95, 1965.

ON THE HEISENBERG NONLINEAR SPINOR FIELD EQUATION IN THE PRESENCE OF GRAVITATION FOR A NONLOCAL SPIN CONNECTION

By

T. Toró

DEPARTMENT OF PHYSICS, THE UNIVERSITY OF TIMIŞOARA, RUMANIA

(Received in revised form 7. IV. 1965)

1. As is known, Heisenberg by formulizing his unitary theory of elementary particles starts from a nonlinear spinor field. The equation of the universal spinor field — as shown by W. Heisenberg and W. Pauli [1] may be put in the following form

$$\gamma_\mu \frac{\partial \psi}{\partial x_\mu} \pm l^2 \gamma_\mu \gamma_5 \psi(\bar{\psi} \gamma_\mu \gamma_5 \psi) = 0 . \tag{1}$$

If the idea of the fundamental spinor fields universality is correct, then the prospects of obtaining the whole usual matter based on this field raise the problem of including gravitation in this theory. The influence of the gravitational field on elementary particles constitues even today an interesting scope of research for those who deal with the theory of elementary particles. Since the establishment of Dirac's equations for electrons, many physicists [2—4] have tried to formulate a general covariant equation that is to give an account of the influence of gravitation on the electron.

Attempts to include gravitation in universal spinor theory have been made immediately after the outline of Heisenberg and Pauli's theory. We mention in this regard J. Rayski's [6], H. Kita's [7] and Rodichev's [8] attempt.

2. To write Heisenberg—Pauli's equation in the presence of the gravitational field, we first introduce the covariant derivative of the spinor in the following manner [2—4]

$$\nabla_\mu \psi = \frac{\partial \psi}{\partial x_\mu} - \Gamma_\mu \Psi. \tag{2}$$

The coefficients of affine spin connection Γ_μ are determined by the fundamental metric tensor $g_{\mu\nu}$ of the gravitational field and of the generalized Dirac matrices γ_μ which in this case are 4-dimensional coordinate functions $\gamma_\mu = \gamma_\mu(x_\mu)$. The relation between Γ_μ, $g_{\mu\nu}$ and γ_μ is as follows [5]

$$\frac{\partial \gamma_\nu}{\partial x_\mu} - \Gamma^\varrho_{\mu\nu} \gamma_\varrho - \Gamma_\mu \gamma_\nu + \gamma_\nu \Gamma_\mu = 0 , \tag{3}$$

where $\Gamma^{\varrho}_{\mu\nu}$ are Christoffel's symbols of the second kind. The matrices γ_μ by which the connection between space and spin is expressed satisfy the following anticommutation relations

$$\gamma_\mu \gamma_\nu + \gamma_\nu \gamma_\mu = 2 g_{\mu\nu} I \,. \tag{4}$$

With the aid of the spinor's covariant derivative, we shall transcribe HEISENBERG—PAULI's equation (1) for the nonlinear universal spinor field in the presence of gravitation as follows:

$$\gamma_\mu \nabla_\mu \psi \pm l^2 \gamma_\mu \gamma_5 \psi (\overline{\Psi} \gamma_\mu \gamma_5 \psi) = 0. \tag{5}$$

In this equation the spin connection coefficients depend on the point $\Gamma_\mu = \Gamma_\mu(\varkappa_\mu)$, thus this kind of connection is called *local.*

3. In the following we shall proceed to the establishment of HEISENBERG—PAULI's equation in the presence of gravitation in the case of nonlocal spin connection. Therefore we use the notion of nonlocal affine spin connection introduced in paper [9]:

$$\nabla_\mu \psi = \frac{\partial \psi}{\partial \varkappa_\mu} - \int T_\mu(\varkappa, \xi)\, \psi(\xi)\, d\,\xi \,, \tag{6}$$

The coefficients T_μ generalized the coefficients Γ_μ for the nonlocal case. If they are of the form

$$T_\mu (\varkappa, \xi) = \Gamma_\mu (\varkappa)\, \delta\, (\varkappa - \xi) + K_\mu\, (\varkappa, \xi), \tag{7}$$

where $\delta\,(\varkappa - \xi)$ is DIRAC's δ-function, then the spin connection is called *partially-local.* In this case the spinor's covariant derivative is written as

$$\nabla_\mu \psi = \frac{\partial \psi}{\partial \varkappa_\mu} - \Gamma_\mu (\varkappa)\, \psi - \int k_\mu\, (\varkappa, \xi)\, \psi(\xi)\, d\,\xi \,. \tag{8}$$

Using the expression (6) for the spinor's covariant derivative we shall write HEISENBERG—PAULI's equation in the presence of gravitation for the case of a nonlocal spin connection as

$$\gamma_\mu \left[\frac{\partial \psi}{\partial \varkappa_\mu} - \int T_\mu\, (\varkappa, \xi)\, \psi(\xi)\; d\,\xi \right] \pm l^2\, \gamma_\mu\, \gamma_5\, \psi(\overline{\psi}\, \gamma_\mu\, \gamma_5\, \psi) = 0 \,. \tag{9}$$

If we have a partially local spin connection, HEISENBERG—PAULI's equations becomes

$$\gamma_\mu \left[\frac{\partial \psi}{\partial x_\mu} - \Gamma_\mu(x)\,\psi - \int k_\mu(x,\xi)\,\psi(\xi)\,d\xi \right] \pm l^2\,\gamma_\mu\,\gamma_5\,\psi(\bar{\psi}\,\gamma_\mu\,\gamma_5\,\psi) = 0\,. \quad (10)$$

We may remark that in the case of nonlocal and partially-local spin connection equations (9) and (10) are integro-differential equations.

REFERENCES

1. W. HEISENBERG and W. PAULI, On the Isospin Group in the Theory of Elementary Particles. Preprint, 1958.
2. V. FOCK, Journ. de Phys. Rad., **10**, 392, 1929;
   H. WEYL, Zs. f. Phys., **56**, 330, 1929.
3. H. TETRODE, Zs. f. Phys., **50**, 336, 1928;
   E. SCHRÖDINGER, Sitzsb. Preuss. Akad. Wiss. Phys. Math. KI. XI. Berlin 105, 1932;
   V. BARGMANN, ibid, 346, 1932.
4. L. INFELD and B. L. VAN DER WAERDEN, ibid, 380, 474, 1933.
5. D. BRILL and J. WHEELER, Rev. Mod. Phys., **29**, 465, 1957.
6. J. RAYSKI, Nuovo Cim., **9**, 337, 1958.
7. H. KITA, Progr. of Theor. Phys., **19**, 454, 1958; ibid, Suppl., **9**, 5, 1959.
8. V. I. RODICHEV, JETF, **40**, 1469, 1961;
   A. PERES, Suppl. Nuovo Cim., **24**, 389, 1962.
9. T. TORÓ, Compt. Rendus, Paris **259**, 307, 1964; Nuovo Cim., **34**, 1391, 1964.

COMMENTS ON THE USE OF H_2^+ EIGENFUNCTIONS AS A BASIS SET FOR H_2 CALCULATIONS

By

JOHN R. RITER, Jr.

CHEMISTRY DEPARTMENT, UNIVERSITY OF DENVER, DENVER, COLORADO, USA

(Received 14. VI. 1965)

Some time ago LADIK [1] proposed the use of the exact eigenfunctions for the ground electronic state of H_2^+ as product orbitals in an approximate wave function for H_2. After splitting off the terms belonging to the hydrogen molecular-ion problem, he approximated the remaining electron repulsion integral by the known value using best MO-SCF functions of COULSON [2]. Not surprisingly, the calculated dissociation energy of 5,3 ev exceeds the true value by some 0,6 ev as the variation method was not called into play. This point was emphasized by LADIK.

The purpose of this note is to call attention to the earlier work of WALLIS and HULBURT [3] who computed the energy of H_2 using several types of trial functions built up from H_2^+-like functions with variable nuclear charges. Their most successful function, from the energy viewpoint, was

$$\psi(1, 2) = \psi_{1.0}(1)\,\psi_{0.5}(2) + \psi_{0.5}(1)\,\psi_{1.0}(2)\,,$$

where the subscripts 1.0 and 0.5 refer to the nuclear charges in the (homonuclear) one-electron diatomic problem. With the electron repulsion integrals evaluated analytically, the above trial function leads to a dissociation energy of 3,6834 ev, using the conversion factor 27,210 ev/a.u. This is somewhat better than the exact SCF bond energy of 3,6360 as determined by ROOTHAAN and KOLOS [4]. This is to be expected since the above is a valence-bond or HEITLER—LONDON type of function. Restricting themselves next to functions of the form

$$\psi(1, 2) = \psi_Z(1)\,\psi_Z(2)$$

WALLIS and HULBURT found bond energies of 2,0950 and 3,486 ev for $Z = 1{,}0$ and $Z = 0{,}7825$ (best value), respectively. The former calculation corresponds to that of LADIK [1] carried through analytically. All calculations were done with the internuclear distance 1,40 a.u., the experimental value.

It seems to us that a product function

$$\psi(1, 2) = [c_1 \psi_{1.0}(1) + c_2 \psi_{0.5}(1)] [c_1 \psi_{1.0}(2) + c_2 \psi_{0.5}(2)]$$

should yield a value of the energy very close to the SCF limit [4]; we are in the process of making such a calculation.

REFERENCES

1. J. LADIK, Acta Phys. Acad. Sci. Hung., **11**, 405, 1960.
2. C. A. COULSON, Proc. Cambridge Phil. Soc., **34**, 204, 1938.
3. R. F. WALLIS and H. M. HULBURT, J. Chem. Phys., **22**, 774, 1954.
4. W. KOLOS and C. C. J. ROOTHAAN. Rev. Mod. Phys., **32**, 219, 1960.

RECENSIONES

V. S. BURAKOV and A. A. YANKOVSKII:

Practical Handbook on Spectral Analysis

Pergamon Press Oxford, 1964

BURAKOV's and YANKOVSKII's book is essentially an introduction to the practice of emission spectral analysis. It treats in a condensed manner — in less than 200 pages — and in a simple and plain style the most important fundamental and indispensible bases of visual spectroscopy resp. emission spectrography for the industrial expert. From the structure of the book it is evident that the authors did not intend to explain the theoretical basis: they do, however, suggggest references for that purpose. Their aim is to acquaint the reader with the most important and indispensible instruments used in small and medium industrial spectro-analytical laboratories all over the Soviet Union, giving a short description of their operation and maintenance. In addition to this, the authors supply immediate help by introducing the analytical methods used for carrying out series analyses in plant laboratories, in the determination of the components, first of all, of the low and high alloy steels, cast iron and alloys with aluminium and copper base, since routine emission spectrum analysis is most widely employed in the field of metallurgy and in metal works.

Because of the increasing application of spectroscopic investigations in the field of metal, rock and mineral analysis, the authors treat the most important spectrographic methods for the determination of powder or solution. This part is supplemented by a description of a few fundamental methods, such as the additive method, the semiquantitative spectro-chemical analysis and the spectrographic examination of slags. The book omits spectro-metric, i.e. direct intensity measuring (so called direct reading) apparatus and methods owing to lack of space.

The greatest value of the book is that it covers the practical applications of both visual and photographic spectroscopy. No book of this kind has as yet been published. Visual spectroscopy is, apart from the Soviet Union, a rather neglected feature in spectroscopical books, although it is this field that is mainly dealt with by those employing spectroscopic methods in the testing of materials.

The closing part of the book, which deals with the planning, establishment, equipping, and even with the financial questions of spectroscopical laboratories, deserves special attention. The question might be raised, however, whether or not the editors are justified in confining themselves to Soviet instruments; in addition, out of the 90 references 89 are to the works of Soviet authors. We must not fail, however, to bear in mind that the original edition, written in Russian, was specially published for Soviet plants, and this explains the references, for the authors offer reference-books readily available to Soviet experts in their mother-tongue. That does not detract from the merits of the translation, since the instruments dealt with in the book may be found in a number of countries, particularly in the people's democracies; and where the products of other firms are more easily accessible, instruments analogous to those treated in the book may easily be employed as in most cases there is little or no difference in the optical and electrical principles, and after all, the present book is not supposed to serve as an instruction handbook. The analytical methods described in the book may be applied directly or with minor alterations.

The reasonable number of tables and the spectrum reproductions of the highest quality, which may well be used especially for photographic resp. visual spectral analysis, add greatly to the merits of the book.

Owing to lack of space, the authors had to refrain from detailed discussions and even from setting forth such time-honoured methods as trace analyses or quantitative analyses without standards although these fields are becoming more and more important in industry as well as for research.

Summarizing it can be concluded that the authors have fully achieved their aim in producing a useful reference-book primarily for the specialist in industrial spectroscopical laboratories. The careful translation should ensure a wide circulation for the book. The pleasing format of the book is a credit to the Pergamon Press.

K. ZIMMER

W. J. CASPERS:

Theory of Spin Relaxation

John Wiley and Sons, Inc., New York—London—Sydney, 1964.

Recently, the theory of spin relaxation has been widely developed. The publication of CASPERS' monograph is particularly significant because this book is the first work to cover the theory of spin-spin relaxation. Therefore this publication will be widely welcomed by all investigators in this field. This book will be of inestimable value both to practicising physicists and to students since the physical arguments are very clearly discussed in every chapter, while mathematical topics are treated in detail in the Appendices.

The book is divided into three chapters and an Appendix of six parts.

The first chapter outlines the general aspects of paramagnetic spin relaxation phenomena from a theoretical point of view. The author shows that paramagnetic spin relaxation phenomena are observed in paramagnetic crystals in a harmonically varying magnetic field and arise from the component of the magnetic moment parallel to the field and are best described in terms of susceptibility.

The second chapter deals with the description of a general theory of paramagnetic spin-spin relaxation. This takes up the greater part of the monograph. The author shows that the theoretical picture of KRONIG and BOUWKAMP cannot be correct, and in his own theory of spin-spin relaxation gives a more correct description in terms of the motion of the component in the direction of the external magnetic field of the total magnetic moment.

The third chapter gives a short survey of the theory of spin-lattice relaxation. The refinements of the CASIMIR—DU PRÉ picture in particular are treated by the author in some detail.

The Appendices at the end of the book contain all the important mathematical tools used by the author in the various chapters. These are as follows: Appendix I: the relation between $\chi(w)$ and $\varphi(t)$; Appendix II: the diagonal elements of the magnetic moment $\langle n| M_z | n\rangle$; Appendix III: irreducible tensor operators; Appendix IV: the number of independent hermitian operators for a spin moment S; Appendix V: classification of two-spin interaction terms according to their selection rules for crystal field energy; Appendix VI: determination of the operators $M_z(0)$ and $K'(0)$.

The value of the monograph is also increased by the extreme clarity of the author's treatment of his subject and also by the exemplary format of the volume.

F. BERENCZ

INDEX

COMMUNICATIONES BREVES

RECENSIONES

Printed in Hungary

A kiadásért felel az Akadémiai Kiadó igazgatója — Műszaki szerkesztő: Farkas Sándor

A kézirat nyomdába érkezett: 1965. VII. 12. — Terjedelem: 18 (A/5) ív, 71 ábra

66.61056 Akadémiai Nyomda, Budapest — Felelős vezető: Bernát György

The *Acta Physica* publish papers on physics, in English, German, French and Russian.
The *Acta Physica* appear in parts of varying size, making up volumes.
Manuscripts should be addressed to:

Acta Physica, Budapest 502, Postafiók 24.

Correspondence with the editors and publishers should be sent to the same address.
The rate of subscription to the *Acta Physica* is 110 forints a volume. Orders may be placed with "Kultúra" Foreign Trade Company for Books and Newspapers (Budapest I., Fő u. 32. Account No. 43-790-057-181) or with representatives abroad.

Les *Acta Physica* paraissent en français, allemand, anglais et russe et publient de travaux du domaine de la physique.
Les *Acta Physica* sont publiés sous forme de fascicules qui seront réunis en volumes.
On est prié d'envoyer les manuscrits destinés à la rédaction à l'adresse suivante:

Acta Physica, Budapest 502, Postafiók 24.

Toute correspondance doit être envoyée à cette même adresse.
Le prix de l'abonnement est de 110 forints par volume.
On peut s'abonner à l'Entreprise du Commerce Extérieur de Livres et Journaux «Kultúra» (Budapest I., Fő u. 32. — Compte-courant No. 43-790-057-181) ou à l'étranger chez tous les représentants ou dépositaires.

«*Acta Physica*» публикуют трактаты из области физических наук на русском, немецком, английском и французском языках.
«*Acta Physica*» выходят отдельными выпусками разного объема. Несколько выпусков составляют один том.
Предназначенные для публикации рукописи следует направлять по адресу:

Acta Physica, Budapest 502, Postafiók 24.

По этому же адресу направлять всякую корреспонденцию для редакции и администрации.
Подписная цена «*Acta Physica*» — 110 форинтов за том. Заказы принимает предприятие по внешней торговле книг и газет «*Kultúra*» (Budapest I., Fő u. 32. Текущий счет: № 43-790-057-181) или его заграничные представительства и уполномоченные.

All the reviews of the Hungarian Academy of Sciences may be obtained among others from the following bookshops:

ALBANIA

Ndermarja Shtetnore e Botimeve
Tirana

AUSTRALIA

A. Keesing
Box 4886, GPO
Sidney

AUSTRIA

Globus Buchvertrieb
Salzgries 16
Wien I.

BELGIUM

Office International de Librairie
30, Avenue Marnix
Bruxelles 5
Du Monde Entier
5, Place St. Jean
Bruxelles

BULGARIA

Raznoiznos
1Tzar Assen
Sofia

CANADA

Pannonia Books
2 Spadina Road
Toronto 4, Ont.

CHINA

Waiwen Shudian
Peking
P. O. B. Nr. 88.

CZECHOSLOVAKIA

Artia A. G.
Ve Smeckách 30
Praha II.
Postova Novinova Sluzba
Dovoz tisku
Vinohradska 46
Praha 2
Postova Novinova Sluzba
Dovoz tlace
Leningradska 14
Bratislava

DENMARK

Ejnar Munksgaard
Nörregade 6
Kopenhagen

FINLAND

Akateeminen Kirjakauppa
Keskuskatu 2
Helsinki

FRANCE

Office International de Documentation et Librairie
48, rue Gay Lussac
Paris 5

GERMAN DEMOCRATIC REPUBLIC

Deutscher Buch-Export und Import
Leninstraße 16.
Leipzig C. 1.
Zeitungsvertriebsamt
Clara Zetkin Straße 62.
Berlin N. W.

GERMAN FEDERAL REPUBLIC

Kunst und Wissen
Erich Bieber
Postfach 46
7 Stuttgart S.

GREAT BRITAIN

Collet's' Subscription Dept.
44—45 Museum Street
London W. C. 1.
Robert Maxwell and Co. Ltd.
Waynflete Bldg. The Plain
Oxford

HOLLAND

Swetz and Zeitlinger
Keizersgracht 471—487
Amsterdam C.
Martinus Nijhof
Lange Voorhout 9
The Hague

INDIA

Current Technical Literature
Co. Private Ltd.
Head Office:
India House OPP.
GPO Post Box 1374
Bombay 1.

ITALY

Santo Vanasia
71 Via M. Macchi
Milano
Libreria Commissionaria Sansoni
Via La Marmora 45
Firenze

JAPAN

Nauka Ltd.
2 Kanada-Zimbocho 2-chome
Chiyoda-ku
Tokyo
Maruzen and Co. Ltd.
P. O. Box 605
Tokyo
Far Eastern Booksellers
Kanada P. O. Box 72
Tokyo

KOREA

Chulpanmul
Korejskoje Obshchestvo po Exportu i Importu Proizvedenij Pechatij
Phenjan

NORWAY

Johan Grundt Tanum
Karl Johansgatan 43
Oslo

POLAND

Export und Import Unternehmen RUCH
ul. Wilcza 46.
Warszawa

ROUMANIA

Cartimex
Str. Aristide Briand 14—18.
Bucuresti

SOVIET UNION

Mezhdunarodnaja Kniga
Moscow
G—200

SWEDEN

Almquist and Wiksell
Gamla Brogatan 26
Stockholm

USA

Stechert Hafner Inc.
31 East 10th Street
New York 3 N. Y.
Walter J. Johnson
111 Fifth Avenue
New York 3. N. Y.

VIETNAM

Xunhasaba
Service d'Export et d'Import des Livres et Périodiques
19, Tran Quoc Toan
Hanoi

YUGOSLAVIA

Forum
Vojvode Misica broj 1.
Novi Sad
Jugoslovenska Kniga
Terazije 27.
Beograd

ACTA PHYSICA

ACADEMIAE SCIENTIARUM HUNGARICAE

REDIGIT
P. GOMBÁS

TOMUS XX FASCICULUS 3

AKADÉMIAI KIADÓ, BUDAPEST
1966

ACTA PHYS. HUNG.

ACTA PHYSICA

A MAGYAR TUDOMÁMYOS AKADÉMIA FIZIKAI KÖZLEMÉNYEI

SZERKESZTŐSÉG ÉS KIADÓHIVATAL: BUDAPEST V., ALKOTMÁNY UTCA 21.

Az *Acta Physica* német, angol, francia és orosz nyelven közöl értekezéseket a fizika tárgyköréből.

Az *Acta Physica* változó terjedelmű füzetekben jelenik meg: több füzet alkot egy kötetet.

A közlésre szánt kéziratok a következő címre küldendők:

Acta Physica, Budapest 502, Postafiók 24.

Ugyanerre a címre küldendő minden szerkesztőségi és kiadóhivatali levelezés.

Az *Acta Physica* előfizetési ára kötetenként belföldre 80 forint, külföldre 110 forint. Megrendelhető a belföld számára az Akadémiai Kiadónál (Budapest V., Alkotmány utca 21. Bankszámla 05-915-111-46), a külföld számára pedig a „Kultúra" Könyv- és Hírlap Külkereskedelmi Vállalatnál (Budapest I., Fő u. 32. Bankszámla 43-790-057-181 sz.), vagy annak külföldi képviseleteinél és bizományosainál.

Die *Acta Physica* veröffentlichen Abhandlungen aus dem Bereiche der Physik in deutscher, englischer, französischer und russischer Sprache.

Die *Acta Physica* erscheinen in Heften wechselnden Umfanges. Mehrere Hefte bilden einen Band.

Die zur Veröffentlichung bestimmten Manuskripte sind an folgende Adresse zu richten:

Acta Physica, Budapest 502, Postafiók 24.

An die gleiche Anschrift ist auch jede für die Redaktion und den Verlag bestimmte Korrespondenz zu senden.

Abonnementspreis pro Band: 110 Forint. Bestellbar bei dem Buch- und Zeitungs-Aussenhandels-Unternehmen »Kultúra« (Budapest I., Fő u. 32. Bankkonto Nr. 43-790-057-181) oder bei seinen Auslandsvertretungen und Kommissionären.

PERTURBED ANGULAR CORRELATION OF TRIPLE GAMMA CASCADE

By

GY. BENCZE and J. ZIMÁNYI

CENTRAL RESEARCH INSTITUTE FOR PHYSICS, BUDAPEST

(Presented by L. Jánossy. — Received 17. II. 1965)

The angular correlation function is derived for a triple gamma cascade perturbed by extranuclear field. Special cases are investigated for non-observed intermediate radiation and for static external magnetic field.

I. Introduction

It is known that the magnetic moment of excited nuclear states can be determined by investigating the directional correlation of gamma rays perturbed by extranuclear field. The perturbed correlation function for double gamma cascade is well known [1]. However, under some circumstances — owing to the shape of gamma spectra — it is possible to measure the correlation between the first and third member of a triple gamma cascade only [2]. The aim of the present work is to derive the perturbed correlation function needed for the evaluation of measurements in the latter case.

II. Formalism

The angular momenta of states will be denoted by Roman, the magnetic quantum numbers by the corresponding Greek letters. The decay scheme is illustrated in Fig. 1. The excited states with angular momenta a, b, and c decay through radiations of multipolarity L_1, L_2 and L_3, respectively, which are detected by delayed coincidence technique. The zero on the time scale is chosen to be the time at which the first radiation is observed. The second and third radiations are detected at times t_b and t. If the interaction between the nucleus and the extranuclear field is described by the operator K the evolution of nuclear states in time is governed by the unitary operator $U(t, t_0)$ which satisfies the equation [1]:

$$\frac{\partial}{\partial t} U(t, t_0) = -\frac{i}{\hbar} Kt, \qquad U(t_0, t_0) = 1, \qquad t \geqq t_0 . \tag{1}$$

If the operator K is time-independent (static field) Eq. (1) has the simple solution

$$U(t, t_0) = e^{-\frac{i}{\hbar}K(t-t_0)}. \tag{2}$$

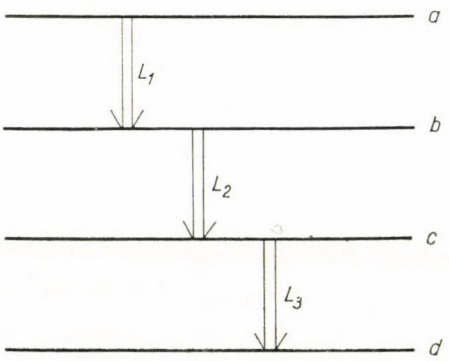

Fig. 1

Since the evolution of states with spins b and c in the time intervals $[0, t_b]$ and $[t_b, t]$ is described by $U(t, t_0)$ the perturbed correlation function has the form

$$W(\Omega_1, \Omega_2, \Omega_3, t, t_b) \sim \frac{1}{\hat{a}^2} \frac{1}{\tau_b \tau_c} e^{-\frac{t_b}{\tau_b}} e^{-\frac{t-t_b}{\tau_c}} \times$$

$$\begin{aligned}
&\Sigma \langle \Omega_3 \sigma_3, d\delta \,|H_3|\, c\,\gamma_2 \rangle \langle c\,\gamma_2 \,|U(t, t_b)|\, c\gamma_1 \rangle \langle \Omega_2 \sigma_2, c\gamma_1 \,|H_2|\, b\,\beta_2 \rangle \times \\
&\langle b\beta_2 \,|U(t_b, 0)|b\beta_1 \rangle \langle \Omega_1 \sigma_1\, b\beta_1 \,|H_1|a\alpha \rangle \langle b\beta_1' \,\Omega_1\, \sigma_1' \,|H_1|\, a\alpha \rangle^* \times \\
&\langle b\beta_2' \,|U(t_b, 0)|\, b\beta_1' \rangle^* \langle \Omega_2\, \sigma_2', c\gamma_1' \,|H_2|\, b\beta_2' \rangle^* \langle c\gamma_2' \,|U(t, t_b)|c\gamma_1' \rangle^* \times \\
&\langle \Omega_3\, \sigma_3', d\delta \,|H_3|\, c\gamma_2' \rangle^*,
\end{aligned} \tag{3}$$

where τ_b and τ_c are the lifetimes of the excited states with spins b and c, while H_1, H_2 and H_3 denote the electromagnetic interactions responsible for the emission of the first, second and third radiations, respectively. The summation extends over the indices

$$\sigma_1\, \sigma_1'\, \sigma_2\, \sigma_2'\, \sigma_3\, \sigma_3'\, \alpha\, \beta_1\, \beta_1'\, \beta_2\, \beta_2'\, \gamma_1\, \gamma_1'\, \gamma_2\, \gamma_2'\, \delta.$$

Let us express now the matrix elements of the electromagnetic interactions in terms of the matrix elements of multipole transitions as

$$\langle \Omega_1\, \sigma_1, b\beta_1 \,|H_1|\, a\alpha \rangle = \sum_{L_1 \pi_1 \lambda_1} \langle \Omega_1\, \sigma_1 \,|L_1\, \pi_1\, \lambda_1 \rangle \langle b\beta_1, L_1\, \pi_1\, \lambda_1 \,|H_1|\, a\alpha \rangle. \tag{4}$$

The expansion coefficient $\langle \Omega_1 \sigma_1 | L_1 \pi_1 \lambda_1 \rangle$ is transformed under rotations by the matrices D^{L_1}. Making use of this transformation property and applying the WIGNER—ECKART theorem, we can write

$$\langle \Omega_1 \sigma_1, b\beta_1 | H_1 | a\alpha \rangle = \sum_{L_1 \pi_1 \lambda_1 \mu_1} \langle 0 \sigma_1 | L_1 \pi_1 \lambda_1 \rangle (b\beta_1 L_1 \lambda_1 | a\alpha) \langle b \| L_1 \| a \rangle D^{L_1 *}_{\lambda_1 \mu_1}(R_1), \quad (5)$$

where $\langle b \| L_1 \| a \rangle$ is the reduced matrix element of the electromagnetic transition with multipolarity L_1, while R_1 denotes the rotation by which the quantisation axis is brought into the direction Ω_1. The matrix elements of H_2 and H_3 can be transformed in a similar way.

We introduce the perturbation factor by the definition [1]:

$$G^{\varkappa_1 \varkappa_2}_{k_1 k_2}(t, t_0) = \sum_{\mu_1 \mu_1' \mu_2 \mu_2'} (-1)^{I-\mu_1'} (I \ \mu_1 \ I - \mu_1' | k_1 \varkappa_1) (-1)^{I-\mu_2'} (I \ \mu_2 \ I - \mu_2' | k_2 \varkappa_2) \times$$
$$\langle I \ \mu_2 | U(t, t_0) | I \ \mu_1 \rangle \langle I \mu_2' | U(t, t_0) | I \mu_1' \rangle^*. \quad (6)$$

Finally we recall the definition of the particle parameter [3]:

$$C^*_{k\varkappa}(L, L') = \sum_{\sigma\sigma'\lambda\lambda'} (-1)^{L'-\lambda'} (L\lambda L' - \lambda' | k\varkappa) \langle 0\sigma | L\pi\lambda \rangle \langle 0\sigma' | L' \pi' \lambda' \rangle^*. \quad (7)$$

If the polarisations of the radiations are not observed only the particle parameters with $\varkappa = 0$ contribute to the correlation function. Taking into account (5), (6) and (7) and making use of the transformation properties of the rotation matrices, the correlation function (3) can be written in the case of unobserved polarisations as

$$W(\Omega_1, \Omega_2, \Omega_3, t, t_b) \sim \frac{1}{\hat{a}^2} \frac{1}{\tau_b \tau_c} e^{-\frac{t_b}{\tau_b}} e^{-\frac{t-t_b}{\tau_b}} \times$$

$$\Sigma R_{da} C^*_{k_1 0}(L_1, L_1') C^*_{k_2 0}(L_2, L_2') C^*_{k_3 0}(L_3, L_3') D^{L_1 *}_{\varkappa_1 0}(R_1) D^{L_2 *}_{\varkappa_2 0}(R_2) D^{L_3 *}_{\varkappa_3 0}(R_3) \times$$

$$(-1)^{L_1'-\lambda_1'} (L_1 \lambda_1 L_1' - \lambda_1' | k_1 \varkappa_1) (-1)^{L_2'-\lambda_2'} (L_2 \lambda_2 L_2' - \lambda_2' | k_2 \varkappa_2) (-1)^{L_3'-\lambda_3'} \times$$
$$\times (L_3 \lambda_3 L_3' - \lambda_3' | k_3 \varkappa_3) \times$$

$$(b \beta_1 L_1 \lambda_1 | a \alpha) (b\beta_1' L_1' \lambda_1' | a \alpha) (c\gamma_1 L_2 \lambda_2 | b\beta_2) (c\gamma_1' L_2' \lambda_2' | b\beta_2') (d\delta L_3 \lambda_3 | c\gamma_2) \times \quad (8)$$

$$(d \delta L_3' \lambda_3' | c\gamma_2') (-1)^{b-\beta_1'} (b \beta_1 b - \beta_1' | r_1 \varrho_1) (-1)^{b-\beta_2'} (b \beta_2 b - \beta_2' | r_2 \varrho_2)$$
$$(-1)^{c-\gamma_1'} (c \gamma_1 c - \gamma_1' | r_1' \varrho_1') \times$$

$$(-1)^{c-\gamma_2'} (c \gamma_2 c - \gamma_2' | r_2' \varrho_2') G^{\varrho_1 \varrho_2}_{r_1 r_2}(t_b, 0) G^{\varrho_1' \varrho_2'}_{r_1' r_2'}(t, t_b),$$

where the short notation

$$R_{da} = \langle d \parallel L_3 \parallel c\rangle\langle d \parallel L_3' \parallel c\rangle^* \langle c\| L_2\| b\rangle\langle c \parallel L_2'\| b\rangle^* \langle b \parallel L_1 \| a\rangle\langle b \parallel L_1' \| a\rangle^*$$

is used. The summation in (8) is to be performed over

$$\alpha\beta_1\beta_1'\beta_2\beta_2'\gamma_1\gamma_1'\gamma_2\gamma_2'\delta L_1\lambda_1 L_1'\lambda_1' L_2\lambda_2 L_2'\lambda_2' L_3\lambda_3 L_3'\lambda_3' k_1\varkappa_1 k_2\varkappa_2 k_3\varkappa_3 r_1\varrho_1 r_1'\varrho_1' r_2\varrho_2 r_2'\varrho_2'.$$

Performing the summation over the magnetic quantum numbers in (8) we obtain

$$W(\Omega_1, \Omega_2, \Omega_3, t, t_b) \sim \frac{1}{\tau_b\,\tau_c}\, e^{-\frac{t_b}{\tau_b}}\, e^{-\frac{t-t_b}{\tau_c}} \times$$

$$\Sigma\, R_{da}\,(4\pi)^{3/2}\,\hat{b}^2\,\hat{c}^2\,\frac{\hat{r}_1'}{\hat{k}^2\,\hat{k}^3}\, C^*_{k_10}(L_1, L_1')\, C^*_{k_20}(L_2, L_2')\, C^*_{k_30}(L_3, L_3') \times$$

$$(-1)^{a+d-b-c+k_3-L_1'+L_3}\, Y^*_{k_1\varkappa_1}(\Omega_1)\; Y_{k_2\varkappa_2}(\Omega_2)\; Y_{k_3\varkappa_3}(\Omega_3) \times$$

$$(r_1'\;\varrho_1'\;k_2\;\varkappa_2 \mid r_2\;\varrho_2)\, W(bb\,L_1\,L_1';\, k_1\,a)\; W(cc\,L_3\,L_3';\, k_3\,d) \begin{Bmatrix} c & c & r_1' \\ L_2 & L_2' & k_2 \\ b & b & r_2 \end{Bmatrix} \times \qquad (9)$$

$$G^{\varkappa_1\varrho_1'}_{k_1 r_1'}(t_b, 0)\; G^{\varrho_1'\varkappa_3}_{r_1' k_3}(t, t_b).$$

The summation extends over

$$L_1\,L_1'\,L_2\,L_2'\,L_3\,L_3'\,k_1\,\varkappa_1\,k_2\,\varkappa_2\,k_3\,\varkappa_3\,r_1'\,\varrho_1'\,r_2\,\varrho_2\,.$$

Expression (9) is the most general form of the perturbed correlation function. In the following this form will be applied to derive the correlation function for special cases.

III. Special cases

Let us recall some properties of the perturbation factor needed in the present treatment [1]. If the external perturbation disappears ($k = 0$), the operator $U(t, t_0)$ reduces to the unit operator. Then, as is apparent from the definition (6), we have

$$G^{\varkappa_1\varkappa_2}_{k_1k_2}(t, t_0) = \delta_{k_1k_2}\,\delta_{\varkappa_1\varkappa_2}. \qquad (10)$$

If the external field is a static magnetic field and the quantisation axis is taken in the direction of the magnetic field, then we have

$$G^{\varkappa_1\varkappa_2}_{k_1k_2}(t, t_0) = e^{-i\varkappa_1\omega(t-t_0)}\,\delta_{k_1k_2}\,\delta_{\varkappa_1\varkappa_2}, \qquad (11)$$

where ω is the Larmor-frequency of the intermediate state given by $\omega = -g\ \mu_N\ B/\hbar$. Here B is the strength of the magnetic field, μ_N is the nuclear magneton and g is the g-factor of the nuclear state.

Making use of the relation $\hat{d}\langle c \parallel L_3 \parallel d\rangle = (-1)^{c+L_3-d}\hat{c}\ \langle d \parallel L_3 \parallel c\rangle^*$ and by considering (11) the correlation function can be written in the form

$$W(\Omega_1, \Omega_2, \Omega_3, t, t_b) \sim \sum_{k_1 k_2 k_3} A_{k_1}(a, bb) A_{k_3}(cc,d)\ R_{k_1 k_2 k_3}(bb, cc)\ S_{k_1 k_2 k_3}(\Omega_1, \Omega_2, \Omega_3, t, t_b), \tag{12}$$

where we have introduced the notations used in [3]:

$$A_{k_1}(a,bb) = \sum_{L_1 L_1'} \langle b\|L_1\|a\rangle\langle b\|\ L_1'\|a\rangle^*\ C^*_{k_1 0}(L_1, L_1')\ \hat{b}(-1)^{a-b+k_1-L_1'} W(bb\ L_1 L_1'; k_1\ a) \tag{13a}$$

$$A_{k_3}(cc, d) = \sum_{L_3 L_3'} \langle c\|\ L_3\|d\rangle^*\ \langle c\|L_3'\|d\rangle\ C^*_{k_3 0}(L_3, L_3')\ \hat{c}(-1)^{d-c+k_3-L_3'} W(cc\ L_3 L_3'; k_3 d) \tag{13b}$$

$$R_{k_1 k_2 k_3}(bb, cc) = \sum_{L_2 L_2'} \langle c \parallel L_2 \parallel b\rangle\langle c \parallel L_2' \parallel b\rangle^*\ C^*_{k_2 0}(L_2\ , L_2')\ \frac{\hat{b}\hat{c}}{\hat{k}_3}\ (-1)^{k_3} \begin{Bmatrix} c & c & k_3 \\ L_2 & L_2' & k_2 \\ b & b & k_1 \end{Bmatrix}. \tag{13c}$$

The time and angle dependence is contained in the factor

$$S_{k_1 k_2 k_3}(\Omega_1, \Omega_2, \Omega_3, t, t_b) = \frac{1}{\tau_b\ \tau_c}\ e^{-\frac{t_b}{\tau_b}}\ e^{-\frac{t-t_b}{\tau_c}}\ . \tag{14}$$

$$\sum_{\varkappa_1 \varkappa_2 \varkappa_3} (4\pi)^{3/2}\ (k_1\ \varkappa_1\ k_2\ \varkappa_2 \mid k_3\ \varkappa_3)\ Y^*_{k_1 \varkappa_1}(\Omega_1)\ Y^*_{k_2 \varkappa_2}(\Omega^5)\ Y^*_{k_3 \varkappa_3}(\Omega_3)\ e^{-i[\varkappa_1 \omega_b t_b + \varkappa_3 \omega_c (t - t_b)]},$$

where ω_b and ω_c are the Larmor frequencies of the states with spins b and c. With vanishing external perturbation ($\omega_b = \omega_c = 0$), the well known form of triple correlation function is reproduced [3]. For unobserved intermediate radiation (14) has to be integrated over the directions Ω_2 and over the time t_b in the interval $[0, t]$. Then the correlation function for the unobserved intermediate radiation can be written

$$W(\Omega_1, \Omega_3, t) = (4\pi)^2 \sum_{k\varkappa} A_k(a, bb)\ A_k(cc, d)\ R_{k0k}(bb, cc)\ G^{\varkappa}(t)\ Y^*_{k\varkappa}(\Omega_1)\ Y_{k\varkappa}(\Omega_3), \tag{15}$$

where we used the short notation

$$G^{\varkappa}(t) = [(\tau_c - \tau_b) + i\ \varkappa(\omega_b - \omega_c)\ \tau_b\ \tau_c]^{-1} \left\{ e^{-(1 + i\varkappa\omega_c\tau_c)\frac{t}{\tau_c}} - e^{-(1 + i\varkappa\omega_b\tau_b)\frac{t}{\tau_b}} \right\}. \tag{16}$$

The correlation function becomes particularly simple if the detectors are placed in the plane normal to the direction of the magnetic field.

Making use of the relation

$$Y^*_{k\varkappa}\left(\frac{\pi}{2}, \varphi_1\right) Y_{k\varkappa}\left(\frac{\pi}{2}, \varphi_3\right) = C^{\varkappa}_k e^{i\varkappa(\varphi_3-\varphi_1)}, \tag{17}$$

where

$$C^{\varkappa}_k = \begin{cases} \dfrac{2k+1}{4\pi} \dfrac{(k-\varkappa)!\,(k+\varkappa)!}{[(k-\varkappa)!!\,(k+\varkappa)!!]^2} & \text{for } k+\varkappa \text{ even} \\ 0 & \text{for } k+\varkappa \text{ odd} \end{cases} \tag{18}$$

the correlation functions become

$$W(\varphi, t) = \sum_{\varkappa=-k_{\max}}^{k_{\max}} \frac{B_\varkappa}{[(\tau_c-\tau_b)^2 + \varkappa^2(\omega_b-\omega_c)^2\tau_b^2\tau_c^2]^{1/2}} \times$$
$$\times \left\{ e^{-\frac{t}{\tau_c}} e^{i\varkappa(\varphi-\varphi_0^{\varkappa}-\omega_c\tau_c)} - e^{-\frac{t}{\tau_b}} e^{i\varkappa(\varphi-\varphi_0^{\varkappa}-\omega_b\tau_b)} \right\}, \tag{19}$$

where we have introduced the simplifying notations

$$B_\varkappa = (4\pi)^2 \sum_{k=\varkappa}^{k_{\max}} C^{\varkappa}_k A_k(a, bb)\, A_k(cc, d)\, R_{k0k}(bb, cc),$$

$$\varphi_0^{\varkappa} = \frac{1}{\varkappa} \operatorname{arctg}\left[\frac{\varkappa(\omega_b-\omega_c)\tau_b\tau_c}{\tau_c-\tau_b}\right], \tag{20}$$

$$\varphi = \varphi_3 - \varphi_1 .$$

In actual experiments, if the time delay between the detection of the first and the third radiation is T and the resolving time of the coincidence circuit is τ_0 the observed correlation function is

$$W(\varphi, T, \tau_0) = \int_{T-\tau_0}^{T+\tau_0} W(\varphi, t)\, dt. \tag{21}$$

If the resolving time is much longer than the lifetimes of the intermediate states, the total time integrated correlation function is observed

$$\overline{W(\varphi, \infty)} = \int_0^{\infty} W(\varphi, t)\, dt. \tag{22}$$

The total time integrated correlation function from (19) can be written as

$$\overline{W(\varphi, \infty)} = \sum_{\varkappa=-k_{\max}}^{k_{\max}} \frac{B_\varkappa}{\left[(1+\varkappa^2\,\omega_b^2\,\tau_b^2)\,(1+\varkappa^2\,\omega_c^2\,\tau_c^2)\right]^{1/2}} e^{i\varkappa(\varphi-\varphi^\varkappa)}\,, \tag{23}$$

where

$$\varphi^\varkappa = \frac{1}{\varkappa}\,(\operatorname{arctg}\varkappa\omega_b\,\tau_b + \operatorname{arctg}\varkappa\omega_c\,\tau_c)\,. \tag{24}$$

The authors are indebted to Dr. L. Keszthelyi for suggesting the problem.

REFERENCES

1. R. M. Steffen and H. Fraunfelder, in Perturbed Angular Correlations, ed. E. Karlsson E. Matthias and K. Siegbahn (North Holland Publ. Co. Amsterdam, 1964).
2. L. Keszthelyi, to be published.
3. S. Devons and L. J. B. Goldfarb, Handbuch der Physik 42 (Springer-Verlag, Berlin, 1957) p. 362.

ВОЗМУЩЕННАЯ УГЛОВАЯ КОРРЕЛЯЦИЯ ТРОЙНОГО ГАММА-КАСКАДА

Д. БЕНЦЕ и Й. ЗИМАНИ

Р е з ю м е

Выводится функция угловой корреляции для тройного гамма-каскада, возмущенного экстраядерным полем. Исследуются специальные случаи, включающие в себе ненаблюдаемое промежуточное излучение и статическое внешнее магнитное поле.

ОТНОШЕНИЕ ВЕРОЯТНОСТЕЙ ε/β^+ ЭЛЕКТРОННОГО ЗАХВАТА И ПОЗИТРОННОЙ ЭМИССИИ В ПЕРЕХОДЕ С ОСНОВНОГО СОСТОЯНИЯ Co^{56} НА ВТОРОЙ ВОЗБУЖДЁННЫЙ УРОВЕНЬ Fe^{56}

Э. ВАТАИ

ИНСТИТУТ ЯДЕРНЫХ ИССЛЕДОВАНИЙ ВАН, ДЕБРЕЦЕН

(Представлено Ш. Салаи — Поступило 23. III. 1965)

Методом $4\pi\beta^+ - \gamma$ совпадений определена вероятность эмиссии позитрона в 1-запрещённом переходе с основного состояния $Co^{56}(4+)$ на второй возбуждённый уровень $Fe^{56}(4+)$. Результат $P_{\beta^+} = 0{,}899 \pm 0{,}142$ находится в хорошем согласии с результатами предыдущих измерений. Среднее взвешенное имеющихся результатов даёт $\varepsilon/\beta^+ = 0{,}117 \pm 0{,}089$. Эти результаты согласуются с теоретическими расчётами для разрешённого перехода. Эффективность 4π пропорционального счётчика определена из интенсивности аннигиляционного пика в одиночном и полном спектре гамма лучей, и в спектре совпадений.

1. Введение

Отношение ветвей ε/β^+ было определено в течение 1964-ого года в нашем Институте с двумя различными способами [1]. Там же даются отношения ветвей, рассчитанные по известным из литературы результатам. Учитывая повышенное значение ***log ft*** ($\sim 8{,}7$), по всей вероятности данный переход является ***l*** запретным (т. к. спин и чётность не меняются).

Сравнение экспериментальных и теоретических отношений ветвей ε/β^+ для переходов с l-запретом проведено в работе Д. Берени и Л. Казаи [1], и как это показано, знание точного экспериментального значения отношения ветвей ε/β^+ было бы желательно и в случае распада Co^{56}, для сравнения с расчётными данными. Однако, точность эксперимента ограничивается тем, что вероятность распада на второй уровень определяется из гамма интенсивностей с наиболее вероятной погрешностью 14%. Цель настоящей работы была подтвердить результаты ранее проведенных измерений при помощи независимого эксперимента.

Применённый в настоящей работе метод является, усовершенствованным и преобразованным к специфическим свойствам распада Co^{56}, вариантом методов Й. Конийна [2] и А. Уиллямся [3], которые использовали совпадения импульсов пропорционального счётчика и сцинтилляционного спектрометра для определения ε/β^+.

2. Экспериментальный метод

Схема распада Co^{56} показана на рис. 1. Она была составлена в настоящей форме Киэнле и сотрудниками [5] на основе измерения совпадений. Значения спинов и чётностей даны Дигенсом и др. [6], по результатам измерений угловой корреляции и поляризации гамма лучей. Интенсивности

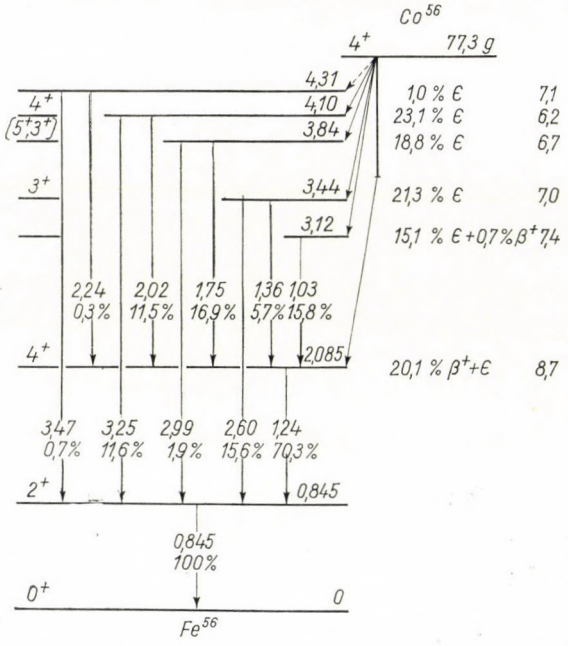

Рис. 1. Схема распада Co^{60}

гамма переходов в схеме распада даны по работе Кука и Томновека [4], которые указывают также точность результатов.

В настоящей работе определена вероятность перехода на второй возбуждённый уровень Fe^{56} путём испускания позитрона ($P_{\beta+}$), из которого, в свою очередь, можно определить отношение ветвей $\varepsilon/\beta^+ = P_\varepsilon/P_{\beta+}$ по следующим выражениям:

$$P_{\beta+} + P_\varepsilon = 1\,, \tag{1a}$$

$$\varepsilon/\beta^+ = \frac{1 - P_{\beta+}}{P_{\beta+}}\,, \tag{1b}$$

где P_ε вероятность перехода на второй возбужденный уровень путём захвата орбитального электрона на один распад Co^{56} на данный уровень.

Интегральный спектр позитронов был зарегистрирован в 4π пропорциональном счётчике, а спектр гамма лучей в сцинтилляционном спектрометре, расположенном рядом с пропорциональным счётчиком. Как это будет показано ниже, для определения P_{β^+} необходимо измерить:

а) интенсивности фотопиков с энергией 0,511; 0,845; 1,24 Мэв, и часть гамма спектра $E_\gamma > 1{,}24$ Мэв, последующаяся после чистого электронного захвата;

б) их интенсивность в спектре $\beta^+ - \gamma$ совпадений;

в) интенсивность аннигиляционного пика позитронов 0,511 Мэв, измеренная независимо от энергии позитронов.

Результаты по интенсивностям аннигиляционного излучения позитронов в различных измерениях дают возможность определить эффективность регистрации позитронов, а измерения при $E_\gamma > 1{,}24$ Мэв эффективность относительно рентгеновских лучей и Оже электронов. Снятие пиков с энергией 0,845 и 1,24 Мэв служит для повышения статистической точности, так как для обоих пиков можно вычислить P_{β^+}, учитывая, что вероятности этих переходов на один распад равны $n_\gamma\,(0{,}845) = 1{,}00$ и $n_\gamma\,(1{,}24) = 0{,}703$.

Число импульсов фотопика даётся следующим выражением:

$$N_\gamma = D n_\gamma S_\gamma\,, \tag{2}$$

где D — полное число распадов в источнике

S_γ — фотоэффективность сцинтилляционного спектрометра.

Число совпадений между импульсами пропорционального и сцинтилляционного спектрометров:

$$N_{\beta^+\gamma} = D\left[\varkappa P_{\beta^+} S_{\beta^+} + \varkappa P_\varepsilon S_\varepsilon + (n_\gamma - \varkappa) S_\varepsilon + n_{\beta^+} S_{\beta^+}\right] S_\gamma\,, \tag{3}$$

где S_{β^+} и S_ε — эффективности пропорционального счётчика по регистрации позитронов и излучений электронной оболочки после захвата (рентгеновских лучей и Оже электронов) соответственно.

$\varkappa$ — вероятность перехода (ε и β^+) на уровень 2,085 Мэв на один распад Co^{56}.

n_{β^+} — та часть β^+ распада на вышележащие уровни, которая даёт истинное совпадение с данным гамма переходом.

В третьем члене было учтено, что n_{β^+} намного меньше $\varkappa$, и таким образом $n_\gamma - n_{\beta^+} - \varkappa \sim n_\gamma - \varkappa$. Деля уравнение (3) на уравнение (2) и учитывая (1а), P_{β^+} даётся следующим выражением

$$P_{\beta^+} = \frac{n_\gamma}{\varkappa(S_{\beta^+} - S_\varepsilon)}\left[\frac{N_{\beta^+\gamma}}{N_\gamma} - S_\varepsilon - \frac{n_{\beta^+}}{n_\gamma} S_{\beta^+}\right]. \tag{4}$$

$\varkappa$ и n_γ могут быть рассчитаны по гамма интенсивностям, данным в работе [4], а $n_{\beta+}$ получается из β^+ интенсивностей работы [7].

Как видно из формулы (4), кроме числа одиночных счётов (N_γ) и числа совпадений ($N_{\beta+\gamma}$) необходимо определить также эффективности $S_{\beta+}$ и S_ε.

S_ε может быть определено по совпадениям импульсов пропорционального счётчика и таких гамма лучей, которые следуют за чистым электронным захватом. Таким свойством обладают все гамма лучи происходящие с уровней выше 3,119 Мэв, то есть $E_\gamma > 1{,}24$ Мэв. Число импульсов в сцинтилляционном спектрометре при этом даётся выражением:

$$N_\gamma = Dn_\gamma (> 1{,}24)\, S_\gamma \,. \tag{5}$$

Число совпадений для этих же импульсов, учитывая, что эффективность регистрации рентгеновских лучей и Оже электронов не изменяется:

$$N_{\varepsilon\gamma} = Dn_\gamma (> 1{,}24)\, S_\gamma S_\varepsilon \,. \tag{6}$$

Отношение этих даёт

$$S_\varepsilon = \frac{N_{\varepsilon\gamma}}{N_\gamma} \,. \tag{7}$$

Полученная таким образом эффективность учитывает полный (с K, L, M... оболочек) захват электронов.

Определение $S_{\beta+}$ в работе Конийна [2] проведена по измерениям распада Au^{198} с хорошо известной схемой распада, а в работе Уиллямса [3] по измерением на пике суммирования аннигиляционного и гамма квантов. Второй метод является более точным, но при бóльших энергиях позитронов и более сложных γ-спектров его применение затруднено по следующим причинам:

1) позитроны высокой энергии аннигилируют далеко от источника, и эффективность регистрации их квантов распада сильно зависит от энергии позитрона,

2) нельзя отделить пика суммирования от квантов более высоких энергий.

Ниже будет показана всзможность определения $S_{\beta+}$ по интенсивности аннигиляционного пика в спектре $\beta^+ - \gamma$ совпадений ($N_{\beta+\gamma 511}$), в спектре одиночных гамма лучей ($N_{\gamma 511}$) и в спектре гамма лучей, снятом поглотителем вокруг источника, в котором позитроны полностью замедляются.

Для расчёта $S_{\beta+}$ используем тот очевидный факт, что позитроны, которые не дают импульс на выходе интегрального дискриминатора при пороговом напряжении соответствующем 5—7 кэв, будут поглощены в источнике, в подложке или в непосредственной близости источника, и там же аннигилируют. Поэтому можно предполагать, что эффективность ($S^0_{\gamma 511}$)

сцинтилляционного спектрометра для этих квантов не зависит от места аннигиляции. Позитроны, дающие импульсы бóльшие порогового могут проходить значительное растояние, и эффективность для аннигиляционных квантов этих позитронов ($S^r_{\gamma 511}$) зависит от места аннигиляции. Учитывая это, число зарегистрированных квантов аннигиляции даётся следующим выражением:

$$N_{\gamma 511} = (D \varkappa P_{\beta^+}) \cdot (1 - S_{\beta^+}) \, S^0_{\gamma 511} + (D \varkappa P_{\beta^+}) \, S_{\beta^+} \, S^r_{\gamma 511} \,. \tag{8}$$

То же самое в спектре ($\beta^+ - \gamma$) совпадений:

$$N_{\beta^+ \gamma 511} = (D \varkappa P_{\beta^+}) \, S_{\beta^+} \, S^r_{\gamma 511} \,. \tag{9}$$

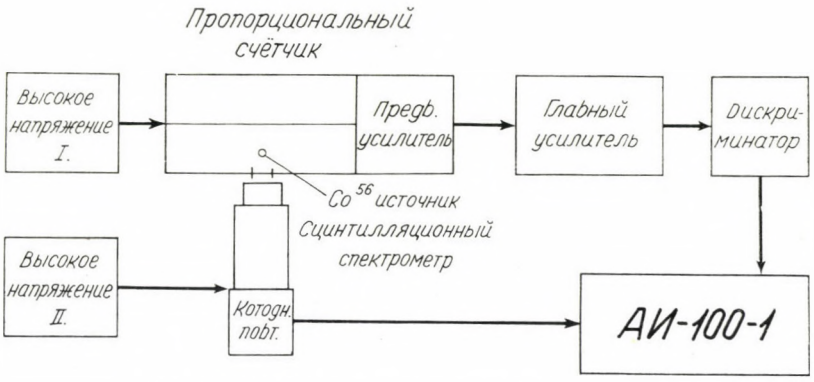

Рис. 2. Блок-схема измерительной аппаратуры

В спектре с поглотителем:

$$N^0_{\gamma 511} = (D \varkappa P_{\beta^+}) \, S^0_{\gamma 511} \, e^{-\mu x} \,, \tag{10}$$

где $e^{-\mu x}$ учитывает поглощение аннигиляционных квантов в поглотителе.

Деля разность (8) и (9) на уравнение (10) получаем:

$$S_{\beta^+} = 1 - \frac{N_{\gamma 511} - N_{\beta^+ \gamma 511}}{N^0_{\gamma 511} \, e^{+\mu x}} \,. \tag{11}$$

3. Измерения и результаты

Блок-схема аппаратуры показана на рис. 2. Источник Co^{56}, изготовленный методом электролиза, активности $\sim$0,2 мккюри, был расположен внутри пропорционального счётчика (телесный угол 4π). Препарат Co^{56} получен из Радиохимического Центра, Амершам. Пропорциональный счётчик напол-

нялся метаном до давления 280 мм. рт. ст., для уменьшения поглощения K рентгеновских лучей. После предварительного и главного усилителей импульсы поступали на вход интегрального дискриминатора, стандартные отрицательные импульсы которого управляли многоканальным анализатором АИ—100—1 во время измерений $\beta^+ - \gamma$ совпадений.

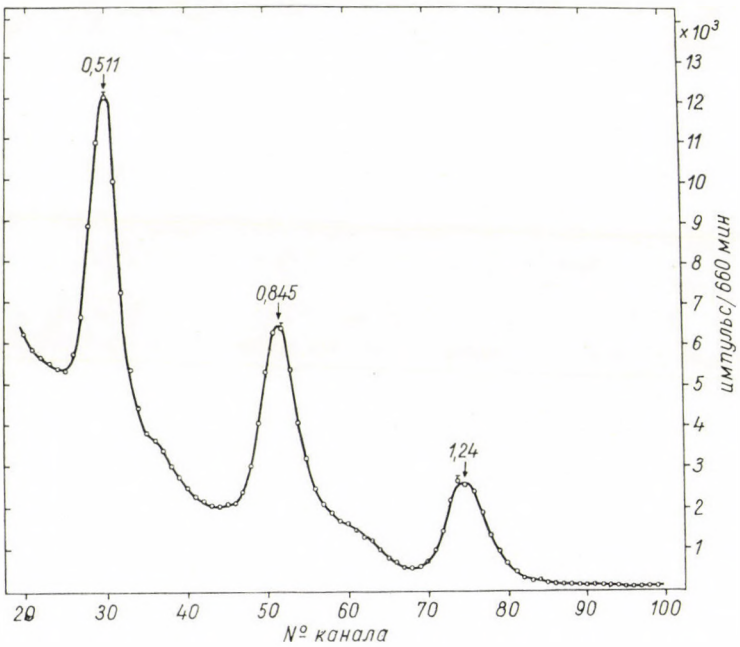

Рис. 3. Часть спектра $\beta^+ - \gamma$ совпадений Co^{60}. Случайные совпадения вычитанны

Гамма лучи попадались в сцинтилляционный спектрометр через окно с диаметром 15 мм, покрытое алюминиевой фольгой *Al* 10 мг/см². Импульсы сцинтилляционного спектрометра, после задержки на 2,2 мксек, необходимой для получения совпадений, подавались на вход анализатора. Измерения совпадений проводились с разрешением $2\tau = 2$ мксек.

При этих условиях были сняты спектры $\beta^+ - \gamma$ совпадений (рис. 3.) и одиночных гамма-лучей (рис. 4., кривая а.); также пик аннигиляционных гамма-лучей (рис. 4. кривая б.). В последнем случае источник был окружён **Cu** поглотителем толщиной 1 мм, в котором позитроны 1,5 Мэв полностью замедляются. Поглощение аннигиляционного кванта в поглотителе было учтено по коэффициентам поглощений, данных в [8]. Разложение спектра было проведено по близким гамма-линиям Na^{22}. Потеря импульсов из-за мёртвого времени анализатора $\sim 10^{-2}$ %. В нашем случае ей можно пренебречь.

Результаты измерений, на основе уравнения (7), дают следующее значение для S_ε:

$$S_\varepsilon = 0{,}0594 \pm 0{,}0015 .$$

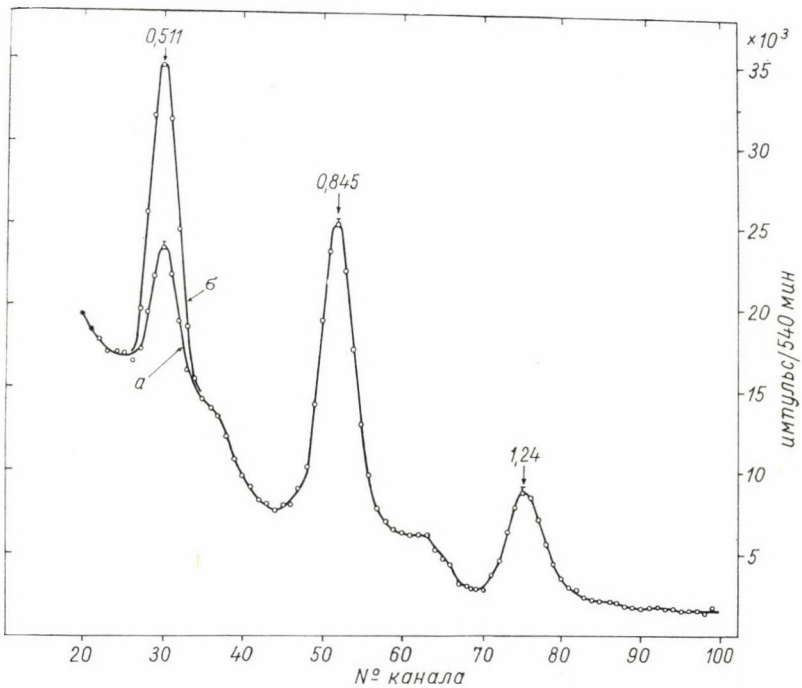

Рис. 4. а. Часть спектра γ лучей Co^{60}, после вычёта фона; б. Аннигиляционный пик, снятый с поглотителем позитронов и корректированный на поглощение γ-лучей

На основе (11) получаем для вероятности детектирования позитронов:

$$S_{\beta^+} = 0{,}892 \pm 0{,}028 .$$

В этом случае учтено возрастание эффективности из-за поглощения аннигиляционных квантов в пропорциональном счётчике (+0,27%-ная коррекция).

Используя S_ε, S_{β^+} и интенсивности соответствующих пиков, также усредняя результаты для пиков 0,845 и 1,24 Мэв, для P_{β^+} получаем:

$$P_{\beta^+} = 0{,}899 \pm 0{,}142 .$$

Как уже указали, погрешность $\varkappa$ является самым значительным. Кроме этого учитывали статистические погрешности и погрешности разложения.

Результаты, данные в работе [1] и результат настоящей работы собраны в таблице 1.

Среднее взвешенное результатов 2—5 даёт:

$$P_{\beta^+} = 0{,}895 \pm 0{,}072$$

или пересчитая по соотношению (1):

$$\varepsilon/\beta^+ = \frac{P_{K,L\ldots}}{P_{\beta^+}} = 0{,}117 \pm 0{,}089\,,$$

если учитываем захват с более высоких оболочек, следующее значение получается для отношения K захвата и эмиссии позитронов:

$$\varepsilon_k/\beta^+ = 0{,}107 \pm 0{,}081\,.$$

Эти результаты согласуются с теоретическим результатом для разрешённых переходов.

Таблица № I

№	Автор	Метод	P_{β^+}
1.	Скаи и др. [7]	Сц.сп.	0,719
2.	Кук и Томновек [4]	Сц.сп.	0,887 ± 0,148
3.	Берени и Казаи [1]	$\beta^+ - \gamma$ Совпад.	0,986 ± 0,148
4.	Берени и Казаи [1]	Спектр. и активность	0,810 ± 0,146
5.	Настоящая работа	Пропорциональный счётчик	0,899 ± 0,142
6.	Цвайфел [9]	Расчёт	0,907

* * *

Автор считает своим приятным долгом выразить благодарность профессору Ш. Салаи, директору Института за обеспечение хороших рабочих условий, д-ру Д. Берени за предложение темы, за полезные дискуссии и советы, которыми он помог провести эту работу, также физикам Д. Матэ и Т. Шарберт за помощь при разрешении проблем, связанных с электронной аппаратурой.

ЛИТЕРАТУРА

1. D. Berényi, L. Kazai, Nucl. Phys., **61**, 657, 1965.
2. H. L. Hagedoorn J. Konijn, Physica, **23**, 1069, 1957.
3. A. Williams, Nucl. Phys., **52**, 324, 1964.
4. C. S. Cook, F. M. Tomnovec, Phys. Rev., **104**, 1407, 1956.
5. P. Kienle, R. E. Segel, Phys. Rev., **114**, 1554, 1959.
6. A. N. Diddens, W. J. Huskamp, J. C. Severiens, A. R. Miedema, M. J. Steenland, Nucl, Phys., **5**, 58, 1958.
7. M. Sakai, J. L. Dick, W. S. Anderson, J. D. Kurbatov, Phys. Rev., **95**, 101, 1954.
8. *Ш. М. Дэйвиссон,* Коэффициенты поглощения γ-лучей. В книге, Бета и гамма спектроскопия, ред. К. Зигбан, Москва, 1959.
9. Van B. Nooijen, J. Konijn, A. Heyligers, et al. Physica **23**, 753, 1957.
10. A. H. Wapstra, G. J. Nijgh, Van R. Lieshout, Nuclear Spectroscopy Tables, North-Holland Publ. Co., Amsterdam, 1959.

ε/β^+ ELECTRON CAPTURE TO POSITRON EMISSION RATIO IN THE DECAY OF Co^{56} FOR THE SECOND EXCITED LEVEL OF Fe^{56}

By

E. VATAI

Abstract

Using the $4\pi\beta^+ - \gamma$ coincidence method the probability of positron emission had been determined in the 1-forbidden transition from the ground state of Co^{56} (4+) to the second excited state of Fe^{56} (4+). The result $P_{\beta^+} = 0{,}899 \pm 0{,}142$ is in good agreement with the previous measurements. The weighted average of the capture to positron emission ratio of the given results is $\varepsilon/\beta^+ = 0{,}117 \pm 0{,}089$. These are in agreement with the theoretical calculations for the allowed transition. The detection efficiency of proportional counter for positrons had been determined from the annihilation peak intensity in the single, coincidence and total spectra of the same source.

EXPERIMENTAL INVESTIGATION OF THE PROBABILITY OF $(n, \alpha n')$ REACTION IN NATURAL URANIUM

By

A. ÁDÁM, GABRIELLA PÁLLA and P. QUITTNER

CENTRAL RESEARCH INSTITUTE OF PHYSICS, BUDAPEST

(Presented by L. Jánossy — Received 8. IV. 1965)

Experiments have been undertaken to investigate whether the $(n, \alpha n')$ reaction is responsible for the anomaly observed in the small angle elastic scattering of 14 MeV neutrons by U^{238}. The results show the probability of this reaction, if it occurs at all, to be so low that its contribution cannot explain the anomaly in question. An estimate of the reaction cross-section gives a value of 0,5 mb in the upper limit.

Introduction

In a paper published simultaneously in this journal HRASKÓ and KÖVESY attempt to explain the anomaly observed in the elastic scattering of 14 MeV energy neutrons by uranium and thorium nuclei. The values of the differential cross-section for small angle scattering are found to be appreciably higher in the case of these nuclei than would be expected from diffranction scattering [1].

The authors assume a contribution from $(n, \alpha n')$ reaction to the measured elastic cross-section. This would be confirmed by experimental evidence on the existence of this reaction. The experiments performed to obtain this evidence are reported below.

The neutrons having the same energies as those elastically scattered are expected to be released by the assumed $(n, \alpha\, n')$ reaction at an angle of about 0°. The simultaneously produced α-particles may leave in any direction with the same energy as that of the α-particles emitted in radioactive decay. The problem now is to establish whether there are any systematic n-α coincidences, or more precisely, to find out whether α-particles actually do emerge simultaneously with the elastically scattered 14 MeV energy neutrons. To this end the neutrons have to be detected at 0° while the α-particles approximatively in the 0 to 2π angular range with respect to the direction of the bombarding neutrons.

Experimental

The experiment was performed on natural uranium target using the 14,7 MeV energy neutrons from $H^3(d, n)He^4$ reaction. The time and angle of neutron emergence as well as the neutron yield were evaluated from the de-

tected number of the recoil α-particles [2]. Time-of-flight technique was used for the acceptance of both neutrons and α-particles, analysing for the latter also the pulse height spectrum in the slow side channel. The target and detector arrangement is shown in Fig. 1, the electronic circuit diagram in Fig. 2.

For full exploitation of the reaction target and to have the optimum neutron solid angle, line-like source geometry (0,1 mm $\times$ 10 mm) was used. The 2,5 mg/cm^2 thick, U_2O_3 target on Al support of 1,5 mg/cm^2 thickness was

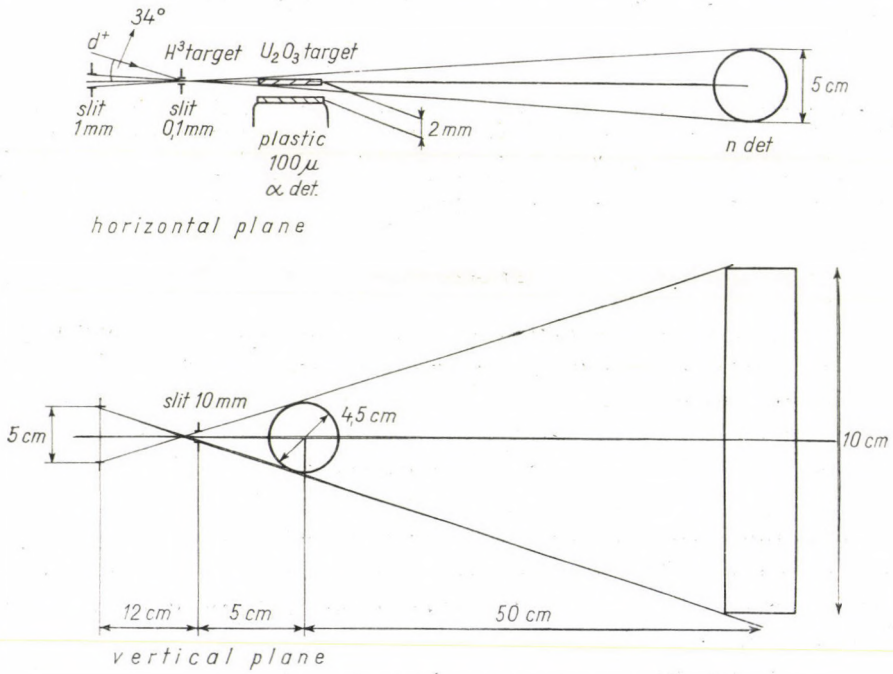

Fig. 1. Target and detector arrangement

placed into the α-solid angle of the detector delivering the start signal for the time-of-flight measurement. The charged particles arising from uranium were detected by a 100 μ plastic foil located outside the solid angle at 2 mm distance from the target and the neutrons by a 50 mm diameter plastic cylinder 10 cm long at 50 cm distance.

Let us first see how the questionable U^{238} $(n, \alpha n')$ reaction can be distinguished by the evaluation of the triple coincidences between start signal and reaction products, α-particles and neutrons.

a) Considering the results of DUKAREVICS [1] and assuming the difference between the measured and predicted values of the differential cross-section to be due to the reaction in question, the expected contribution is about 15 mb. This gives for the reaction probability, for the target used in the present experi-

ment, $5 \cdot 10^{-3}$. The bombarding neutron intensity was chosen so that random coincidences were of a negligible order compared with the systematical events. In the present case this intensity was $N_0 \sim 1{,}4 \cdot 10^8$ n/sec at which the number of triple coincidences as counted with the experimental setup shown in Fig. 1 is expected to be $N_{\text{syst}} \sim 400$ coinc/hour.

b) The most inconvenient background reaction is expected to be the 14 MeV neutron induced fission of U^{238} causing the same kind of systematical

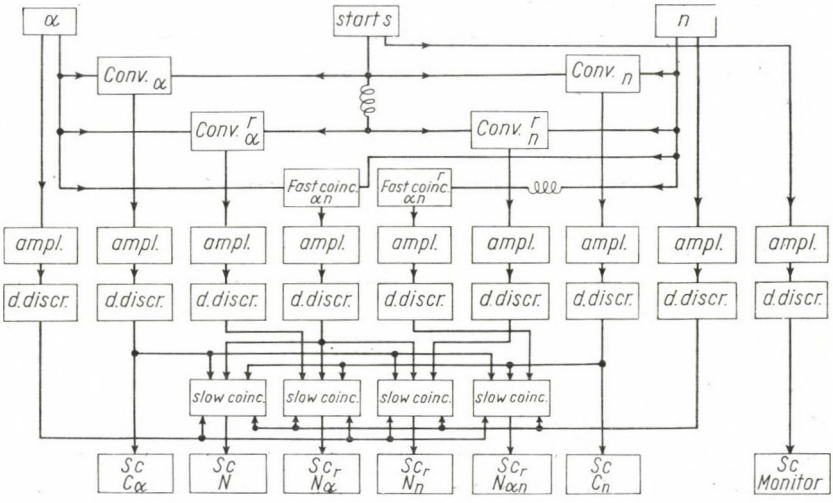

Fig. 2. Block diagram of the measuring apparatus

coincidences as the reaction to be investigated. For the present target, fission probability is estimated as $p_f = 0{,}18$ compared with a reaction probability of $5 \cdot 10^{-3}$ calculated above. The $(n, \alpha n')$ reaction can still be detected by reasoning as follows. First the frequency of neutrons with energies above 10 MeV in the energy spectrum of fission neutrons is not more than 10^{-2} while the time condition in the time-of-flight measurement was chosen to be such that only neutrons with energies between 10 and 22 MeV were being counted (this time gate excludes the fission γ-particles as well). Second, in contrast to the $(n, \alpha n')$ neutrons which, according to HRASKÓ and KÖVESY's theory, should emerge at about 0° only, the fission neutrons have no such forward peaking tendency and this is a decisive factor. Triple coincidences due to fission in the present experiments were found to be less than 1 coincidence/hour.

c) As already mentioned, at the intensities used in the experiments, the random coincidences could be kept negligible compared with the number of systematical coincidences. This does not apply, however, relative to the number of systematical fission coincidences. Random triple coincidences are due primarily to events which are simultaneous with a systematical coincidence between start signal and the α — or the neutron detector and a random

coincidence between the start signal and the other detector. Such events are caused in the first place by 14 MeV direct neutrons in random coincidence with α-particles emitted by the natural decay of U^{238}; second, by systematical coincidences between start signal and α-detector due to fission products or other charged particles from target reactions with a random simultaneous coincidence between start signal and the neutron detectors. Owing to the marked intensity dependence of random coincidences it seemed expedient to have them counted simultaneously with systematical events. This has been done by appropriate fast and slow coincidence units marked by C_a^r, C_n^r, C_{an}^r and N_a^r, N_n^r, N_{an}^r respectively, in Fig. 2.

Check of the measuring apparatus

The setting of the uranium foil position had to be controlled to 0,1 mm precision in order that the target should be inside the solid angle of the start signal detector, considering that the solid angle extent in the vertical plane is only about 0,4 mm at the target. The target position was set and checked on the basis of C_α (start signal $-\alpha$) coincidence counts. The solid angle between the target and neutron source was checked experimentally using the known value of the cross-section for charged particle reactions. The presence of support material was taken into account by the number of C_α coincidences measured in the absence of U_2O_3. The solid angle thus determined is satisfactory only if the target is everywhere uniformly and sufficiently thin to permit the emergence of fission products and 4 MeV α-particles. This was checked by the radioactive α counts from a known quantity of U_2O_3.

The time gate for coincidence units was set by making use of the charged particle from target reactions, and of the 14 MeV primary neutrons. The $\alpha - n$ fast coincidence circuit was biased by suitably delaying the neutron and α-pulses with respect to the start signal. The time resolution of the (start signal $- n$) coincidence stage was chosen to be $2\tau = 3{,}6$ mμ sec. This value is sufficiently large for the counting efficiency not to be reduced by the spread in the flight times of neutrons. This time gate corresponds to neutron energies from 10 to 22 MeV. In the C_α unit the time resolution was $2\tau = 10$ mμ sec so that, considering the maximum 5 cm flight path of the 4 MeV energy α-particles from U^{238}, there is no loss in counts even with an 80% loss in particle energy on their emergence from the target.

The measuring assembly was tested by the measurements of the known cross-section for fission of U^{238} bombarded with 14,7 MeV energy neutrons. The time gate in this case was set, of course, to cover the total energy spectrum of fission neutrons. The measured value seems to be in good agreement with that reported in the literature.

Results and conclusion

The measured value of triple coincidences $N = 140$ and $N^r = 137$. The similarity of the two values is not inconsistent with the expected number of systematical fission coincidences which has to be within the statistical error. It seems, however, to be in contradiction with the existence of the (n, $\alpha n'$) reaction. The double statistical error permits the maximum possible value of the reaction cross section to be estimated as 0,5 mb compared with 15 mb predicted by the theory. It follows that even if U^{238} (n, $\alpha n'$) reaction occurs at all, its contribution cannot explain the anomaly observed in the small angle scattering of fast neutrons by U^{238}.

The question now arises why the effect predicted by the dispersion theory by HRASKÓ and KÖVESY could not be observed in the present experiments.

Thanks are due to E. PÁSZTOR and I. VERESS as well as to other members of our group for the highly satisfactory operation of the accelerator and assistance in the experiment.

REFERENCES

1. JU. V. DUKAREVICS, A. N. GUMIN, JETF **44**, 130, 1963.
2. A. ÁDÁM, G. PÁLLA and P. QUITTNER, Acta Phys. Hung., **17**, 353, 1964.

ЭКСПЕРИМЕНТАЛЬНОЕ ИССЛЕДОВАНИЕ ВЕРОЯТНОСТИ РЕАКЦИИ (n, α n') В ЕСТЕСТВЕННОМ УРАНЕ

А. АДАМ, Г. ПАЛЛА и П. КВИТТНЕР

Резюме

Экспериментально исследуется, возможно ли истолковывать аномалию при упругом рассеянии нейтронов с энергией 14 МЭВ на малые углы реакций (n, α n') в U^{348}. Найдено, что реакция не имеет места, или если и протекает, то ей не обуславливается аномалия. Для эффективного поперечного сечения реакции — как верхний предел — получено значение 0,5 mb.

THE HYDRODYNAMICAL MODEL OF WAVE MECHANICS III

ELECTRON SPIN

By

L. JÁNOSSY and MARIA ZIEGLER-NÁRAY

CENTRAL RESEARCH INSTITUTE OF PHYSICS, BUDAPEST

(Received 22. VI. 1965)

The hydrodynamical model is extended to the problem of the electron as described by the Pauli equation. It appears that the Pauli equation can be transformed into a set of equations which have the form of the classical equations of motion describing an elastic medium which is inhomogeneously magnetized.

I. Basic conceptions

§ 1. In the present article we are concerned with the hydrodynamical model of an electron the motion of which is described by the Pauli equation, i. e. with the problem how far the procedure carried out in our previous articles (I and II see [1], [2]) can be extended to the case of the electron described by a two-component wave function

$$\psi = \begin{pmatrix} \psi_1 \\ \psi_2 \end{pmatrix} \qquad \text{and} \qquad \psi^* = (\psi_1^* \, \psi_2^*) \tag{1}$$

obeying the Pauli wave equation

$$i\hbar\dot{\psi} = \left[\frac{1}{2m}\left(-i\hbar\nabla - \frac{e}{c}\boldsymbol{A}\right)^2 + (e\varphi + V) - \mu(\boldsymbol{\sigma}\ \mathrm{rot}\ \boldsymbol{A})\right]\psi\,. \tag{2}$$

Here $\mu = \dfrac{e\hbar}{2mc}$ is the Bohr magneton; the components of the Pauli operator $\boldsymbol{\sigma}$ are*

$$\sigma_1 = \begin{pmatrix} 0 & 1 \\ 1 & 0 \end{pmatrix}, \qquad \sigma_2 = \begin{pmatrix} 0 & -i \\ i & 0 \end{pmatrix}, \qquad \sigma_3 = \begin{pmatrix} 1 & 0 \\ 0 & -1 \end{pmatrix}. \tag{3}$$

The potential V represents the non-electromagnetic outer forces, while $\boldsymbol{A}$ and Φ are the vector and scalar potentials, respectively, of the external electromagnetic field.

* In the following we shall denote the components x, y, z by 1, 2, 3 respectively.

The aim of the present paper is to show that equation (2) can be rewritten in terms of hydrodynamical variables into a system of equations which have the form of the classical equations of motion of an elastic medium. It should be emphasized that we endeavour to carry out a transformation resulting in the equations of motion of one elastic medium only and not in that of two, as might be expected from the fact that the wave function (1) has two components (see e. g. [3]).

In our previous papers we have described the medium corresponding to the particle by means of a density distribution ϱ and a velocity distribution $\boldsymbol{v}$. In the present paper we take the spin of the particle into consideration with the help of a further variable, i. e. we introduce the distribution of polarization of the medium. The new variables will thus be ϱ (or more precisely $\varrho_e = e\varrho$ and $\varrho_m = m\varrho$, respectively), $\varrho\boldsymbol{v}$ and the density of the polarization expressed by the vector $\boldsymbol{s}$.

§ 2. In order to account for the distribution of density and of velocity of flow in the medium representing the electron, we have to formulate the continuity equation. Multiplying (2) from the left by ψ and subtracting from it the conjugated equation multiplied from the right by ψ, and remembering that σ is a Hermitean operator we arrive at the continuity equation

$$\operatorname{div}(\varrho\,\boldsymbol{v}) + \frac{\partial\varrho}{\partial t} = 0\,, \tag{4}$$

where

$$\varrho = \psi^*\,\psi, \tag{5}$$

or explicitly

$$\varrho = \psi_1^*\,\psi_1 + \psi_2^*\,\psi_2 \tag{5a}$$

and the velocity distribution $\varrho\boldsymbol{v}$ might be put equal to $\varrho\boldsymbol{v}^0$ with

$$\varrho\boldsymbol{v}^0 = -\frac{i\hbar}{2m}(\psi^*\operatorname{grad}\psi - \operatorname{grad}\psi^*\cdot\psi) - \varrho\frac{e}{mc}\boldsymbol{A}\,, \tag{6}$$

if the only requirement were to satisfy equ. (4) mathematically.

However, as can be seen easily equ. (4) remains valid if we add the rotation of an arbitrary vector to the expression of the velocity given by (6). Thus (4) remains satisfied if we put

$$\varrho\,\boldsymbol{v} = \varrho\,\boldsymbol{v}^0 + \operatorname{rot}\boldsymbol{\chi}\,.$$

As will be shown later the correct hydrodynamical description of the spinning electron that corresponds to the experimental results is obtained if we choose

$$\chi = \alpha \frac{\hbar}{2m} \mathbf{s}$$

with

$$\alpha = \frac{1}{2} .$$

In the polarized elastic medium representing the electron we take therefore as the definition of the density of velocity of flow

$$\varrho_m \boldsymbol{v} = \varrho_m \boldsymbol{v}^0 + \alpha \frac{\hbar}{2} \operatorname{rot} \mathbf{s}, \tag{7}$$

or using (6), with $\alpha = \frac{1}{2}$ we have

$$\varrho_m \boldsymbol{v} = -\frac{i\hbar}{2} (\psi^* \operatorname{grad} \psi - \operatorname{grad} \psi^* \cdot \psi) - \frac{\varrho_e}{c} \boldsymbol{A} + \frac{\hbar}{4} \operatorname{rot} \mathbf{s} . \tag{7a}$$

For points in which $\varrho > 0$ we divide (7a) by ϱ_m and obtain the following explicit expression for $\boldsymbol{v}$:

$$\boldsymbol{v} = -\frac{i\hbar}{2m} \frac{1}{\varrho} (\psi^* \operatorname{grad} \psi - \operatorname{grad} \psi^* \cdot \psi) - \frac{e}{mc} \boldsymbol{A} + \frac{\hbar}{4m} \frac{1}{\varrho} \operatorname{rot} \mathbf{s} . \tag{8}$$

For points with $\varrho = 0$ the value of $\boldsymbol{v}$ is not defined, however, in such points its value is of no interest.

§ 3. Finally, the density of the polarization vector can be introduced by putting

$$\mathbf{s} = \psi^* \boldsymbol{\sigma} \psi. \tag{9}$$

The components of $\mathbf{s}$ are obtained with the help of (1) and (3) as

$$\begin{aligned} s_1 &= \psi_1^* \psi_2 + \psi_2^* \psi_1, \\ s_2 &= i(\psi_2^* \psi_1 - \psi_1^* \psi_2), \\ s_3 &= \psi_1^* \psi_1 - \psi_2^* \psi_2. \end{aligned} \tag{10}$$

Adding up the squares of the components of $\mathbf{s}$ we find with the help of (5a)

$$\mathbf{s}^2 = \varrho^2,$$

i. e. the length of the vector $\boldsymbol{s}$ is equal to the density ϱ. Therefore it seems to be convenient to introduce a unit vector $\boldsymbol{T}$ pointing into the direction of $\boldsymbol{s}$. This is done by writing

$$\varrho \boldsymbol{T} = \boldsymbol{s}, \tag{11}$$

or expressing ϱ and $\boldsymbol{s}$ by ψ

$$(\psi^* \psi)\, \boldsymbol{T} = \psi^* \boldsymbol{\sigma} \psi. \tag{11a}$$

The vector $\boldsymbol{T}$ can be regarded as giving the direction of polarization of the medium as function of the coordinates. Obviously, $\boldsymbol{T}$ can only be defined for points with $\varrho > 0$.

The hydrodynamical variables, the scalar density ϱ, the density of velocity of flow $\varrho \boldsymbol{v}$ and the density of the polarization vector $\varrho \boldsymbol{T}$, i. e. the quantities characteristic of the medium representing the spinning electron, can thus be expressed in terms of the wave function ψ with the help of equs. (5), (7a) and (11a).

II. Connection between hydrodynamical variables and the wave function

§ 4. In order to simplify the investigation of the relations between the hydrodynamical variables and the wave function let us represent the two complex components of ψ by four real functions of time t and coordinates $\boldsymbol{r}$:

$$R = R(\boldsymbol{r}, t); \qquad S = S(\boldsymbol{r}, t); \qquad \varphi = \varphi(\boldsymbol{r}, t); \qquad \vartheta = \vartheta(\boldsymbol{r}, t).$$

If the components of the wave function are expressed in terms of these auxiliary functions in the form

$$\begin{aligned} \psi_1 &= R \cos \frac{\vartheta}{2}\, e^{i\left(S - \frac{1}{2}\varphi\right)} \\ \psi_2 &= R \sin \frac{\vartheta}{2}\, e^{i\left(S + \frac{1}{2}\varphi\right)} \end{aligned} \tag{12}$$

R, S, ϑ and φ can be given clear physical meaning as will be shown later.

By means of equs. (12) the wave function ψ is unambiguously determined in terms of the variables R, S, ϑ and φ.

§ 5. Now we have to consider whether it is possible to associate values of R, S, ϑ, φ unambiguously with given values of ψ_1 and ψ_2; that means whether (12) can be reversed in an unambiguous way.

From equs. (12) it follows that the function $R(r, t)$ is obtained from given ψ_1 and ψ_2 as

$$R = \pm \sqrt{|\psi_1|^2 + |\psi_2|^2}\,.$$

When $\psi_1 \neq 0$ and $\psi_2 \neq 0$, we obtain for ϑ and φ with the help of equs. (12)

$$\vartheta = -\frac{i}{2}\ln z_1 \quad \text{and} \quad \varphi = -i\ln z_2\,, \tag{13a}$$

where

$$z_1 = \frac{i\dfrac{|\psi_1|^2 - |\psi_2|^2}{2|\psi_1\psi_2|} - 1}{i\dfrac{|\psi_1|^2 - |\psi_2|^2}{2|\psi_1\psi_2|} + 1} \qquad \text{and} \qquad z_2 = \frac{\psi_1^*\psi_2}{|\psi_2^*\psi_2|}\,.$$

These equations determine ϑ and φ uniquely in the intervals

$$0 \leq \vartheta \leq \pi \quad \text{and} \quad 0 \leq \varphi < 2\pi. \tag{13}$$

A physical interpretation of these restrictions will be given further below.

When $\psi_1 = \psi_2 = 0$ we have $R = 0$ and ϑ, φ can be chosen arbitrarily. For $\psi_1 = 0$, $\psi_2 \neq 0$ and $\psi_1 \neq 0$, $\psi_2 = 0$, respectively we have

$$R = |\psi_2|, \qquad \vartheta = \pi, \qquad S + \frac{1}{2}\varphi = -i\ln\frac{\psi_2}{|\psi_2|}\,,$$

and

$$R = |\psi_1|, \qquad \vartheta = 0\,, \qquad S - \frac{1}{2}\varphi = -i\ln\frac{\psi_1}{|\psi_1|}\,,$$

respectively. This means that in these cases φ remains indeterminated.

Finally, we find from (12)

$$S = -i\ln\frac{\psi_1}{|\psi_1|} + \frac{1}{2}\varphi\,,$$

where φ is to be inserted from (13a) in accordance with (13) and the logarithmus has to be chosen so as to restrict the values of S to the interval $0 \leq S < 2\pi$.

§ 6. Having shown that there exist essentially unambiguous relations between the components ψ_1 and ψ_2 of the wave functions and the functions R, S, ϑ and φ, we investigate now what kind of relations can be formulated between R, S, ϑ, φ and the hydrodynamical variables ϱ, $\boldsymbol{v}$, $\boldsymbol{T}$.

Let us begin with the density distribution. Inserting (12) into (5) we get

$$\varrho = R^2, \tag{14}$$

or

$$R = \pm\sqrt{\varrho}\,,$$

i.e. the scalar function $R(\boldsymbol{r}, t)$ introduced by the relations (12) corresponds to the square root of the density of the elastic medium.

§ 7. The physical meaning of the functions $\vartheta(\boldsymbol{r}, t)$ and $\varphi(\boldsymbol{r}, t)$ can also be seen easily. Introducing (12) into (10) we obtain with the help of (11)

$$T_1 = \sin\vartheta\cos\varphi, \quad T_2 = \sin\vartheta\sin\varphi, \quad T_3 = \cos\vartheta, \tag{15}$$

thus ϑ and φ are the polar angles of the vector $\boldsymbol{T}$. We note that T_1, T_2, T_3 just as ϑ, φ are functions of $\boldsymbol{r}$ and t.

From a short calculation the reversed relations between ϑ, φ and T_1, T_2, T_3 are obtained in the form

$$\vartheta = -\frac{i}{2}\ln\frac{\dfrac{iT_3}{\sqrt{1-T_3^2}} - 1}{\dfrac{iT_3}{\sqrt{1-T_3^2}} + 1} \quad \text{and} \quad \varphi = -i\ln\frac{T_1 + iT_2}{\sqrt{T_1^2 + T_2^2}}, \tag{16}$$

provided $\sqrt{T_1^2 + T_2^2} > 0$, which corresponds to the restrictions given in (13).

It remains to discuss the relations between S and the velocity vector $\boldsymbol{v}$.

§ 8. In order to express the velocity of flow in terms of the scalar functions $\boldsymbol{R}, \boldsymbol{S}, \vartheta$ and φ we substitute (12) in (8) and find as the result of a short calculation

$$\boldsymbol{v} = \frac{\hbar}{m}\operatorname{grad} S - \frac{\hbar}{2m}\cos\vartheta\ \operatorname{grad}\varphi - \frac{e}{mc}\boldsymbol{A} + \frac{\hbar}{4m}\frac{1}{\varrho}\operatorname{rot}\boldsymbol{s}. \tag{17}$$

Applying the operation rot to both sides of the above relation we obtain

$$\operatorname{rot}\boldsymbol{v} + \boldsymbol{W} = 0, \tag{18}$$

where we may write using (17)

$$\boldsymbol{W} = \frac{e}{mc}\operatorname{rot}\boldsymbol{A} - \frac{\hbar}{4m}\operatorname{rot}\left(\frac{1}{\varrho}\operatorname{rot}\boldsymbol{s}\right) + \frac{\hbar}{2m}\operatorname{rot}(\cos\vartheta\operatorname{grad}\varphi). \tag{18a}$$

Here we note that $\boldsymbol{W}$ is a vector quantity although its last term contains the rotation of the non covariant quantity $\xi = \cos\vartheta\operatorname{grad}\varphi$. Indeed, the rotation of ξ can be expressed by means of the vector $\boldsymbol{T}$ in the form

$$\operatorname{rot}\xi = \boldsymbol{T}\,\mathfrak{T}^*,$$

where $\mathfrak{T}^*$ is the tensor built up of the minors $(\mathfrak{T}^*)_{ik}$ of the matrix $\mathfrak{T}$ having as elements $T_{ik} = \dfrac{\partial T_i}{\partial x_k}$, i.e. in cases when $\det\mathfrak{T} \neq 0$ we have

$$(\mathfrak{T}^*)_{ik} = \frac{(\mathfrak{T}^+)_{ik}}{\det \mathfrak{T}},$$

where $(\mathfrak{T}^+)_{ik}$ are the elements of the matrix $(\mathfrak{T})^{-1}$.

From (17) we find

$$S = \frac{m}{\hbar} \int_{r_0}^{r} \left(\boldsymbol{v} + \frac{e}{mc} \boldsymbol{A} + \frac{\hbar}{2m} \cos \vartheta \operatorname{grad} \varphi - \frac{\hbar}{4m} \frac{1}{\varrho} \operatorname{rot} \boldsymbol{s} \right) d\boldsymbol{r} + S_0 , \quad (19)$$

where $\boldsymbol{r}_0$ is the coordinate vector of an arbitrary point. $S_0 = S_0(\boldsymbol{r}_0, t)$ is a quantity which depends on the choice of $\boldsymbol{r}_0$ but is independent of the vector $\boldsymbol{r}$; it may, however, depend on time. The path of integration has to be taken along a line connecting $\boldsymbol{r}_0$ with $\boldsymbol{r}$ in such a way that this avoids singular points. If the distribution of the hydrodynamical variables has no singularities and equ. (18) holds, the value of S becomes independent of the path of integration. In cases where there are singularities, the value of S as obtained from (19) depends on the path of integration and (19) defines a multi-valued function S.

However, we are primarily interested in the function ψ. It follows from (11) that ψ remains a single-valued function even if S is multivalued, provided the values of S in the same point differ by integer multiples of 2π only. This is the case if the integral on the right-hand side of (19) taken over any closed path is either zero or equal to an integer multiple of 2π; i.e. we have to require that integration of (19) along a closed path becomes

$$\oint \boldsymbol{v} d\boldsymbol{r} = 2\pi k \frac{\hbar}{m} + \oint \left[- \frac{e}{mc} \boldsymbol{A} - \frac{\hbar}{2m} \cos \vartheta \operatorname{grad} \varphi + \frac{\hbar}{4m} \frac{1}{\varrho} \operatorname{rot} \boldsymbol{s} \right] d\boldsymbol{r} \quad (20)$$

$$\text{with } k = 0, \pm 1, \pm 2, \ldots$$

The value of k depends on the particular choice of the path of integration. Applying Stokes' law we may also write

$$\oint \boldsymbol{v} d\boldsymbol{r} = 2\pi k \frac{\hbar}{m} + \int \boldsymbol{W} d\boldsymbol{f} . \quad (21)$$

It can be seen from equs. (21) and (18a) that in the case of a polarized medium the appearance of vortices is due not only to the external magnetic field but also to the polarization $\boldsymbol{T}$.

§ 9. Equ. (21) can be taken as an auxiliary condition for hydrodynamical variables. As we have shown above the hydrodynamical variables obtained uniquely from a given wave function satisfy condition (21) automatically.

On the other hand the distribution of the hydrodynamical variables defines a single-valued wave function (apart from a time-dependent phase factor $e^{iS_0(\boldsymbol{r}_0,t)}$) only if ϱ, $\boldsymbol{v}$ and $\boldsymbol{T}$ satisfy the auxiliary condition (21).

Further, it is usual to normalize the wave function by putting

$$\int \psi^* \, \psi \, d\tau = 1, \tag{22}$$

the corresponding condition in terms of the hydrodynamical density is

$$\int \varrho \, d\tau = 1.$$

Thus if we require (22a) to be valid for the wave function, in addition to the auxiliary condition (21) relating to ϱ, $\boldsymbol{v}$ and $\boldsymbol{T}$, we have to take into account the condition (22a) relating to the density distribution.

As conclusion of this section we thus state: From a given two-component normalized wave function ψ the hydrodynamical variables ϱ, $\boldsymbol{v}$ and $\boldsymbol{T}$ can be derived. The variables so obtained obey certain auxiliary conditions. Furthermore prescribing the hydrodynamical variables ϱ, $\boldsymbol{v}$ and $\boldsymbol{T}$ and satisfying the auxiliary conditions we can determine from them the normalized wave function ψ, apart from a constant phase factor.

III. Equations of motion

§ 10. In order to obtain the hydrodynamical equations of motion of the medium representing the electron we have to consider first the acceleration of a volume element. To obtain this we differentiate the expression for the velocity of flow given in (8) with respect to time and substitute the time derivatives of ψ^* and ψ with the help of the Pauli equation (2) by their spatial derivatives. With the help of equs. (5), (8) and (11) ψ and its spatial derivatives are then expressed by the hydrodynamical variables. In this way we obtain for the acceleration an expression containing, beside the hydrodynamical variables, only the field strengths $\boldsymbol{E}$ and $\boldsymbol{B}$ which are defined by the scalar and vector potentials

$$\boldsymbol{E} = -\operatorname{grad} \varphi - \frac{1}{c} \dot{\boldsymbol{A}} \, ,$$

$$\boldsymbol{B} = \operatorname{rot} \boldsymbol{A}.$$

The detailed calculation may be found in [4].

The equation of motion of the velocity vector of a volume element of the medium is obtained as the result of a lengthy calculation as

$$\varrho_m \frac{d\boldsymbol{v}}{dt} = \varrho\,(\boldsymbol{f}_0 + \boldsymbol{f}_i)\,, \tag{23}$$

where $\varrho \boldsymbol{f}_0$ is the density of the outer and $\varrho \boldsymbol{f}_i$ that of the inner force. For the density of the outer force we find

$$\varrho \boldsymbol{f}_0 = \varrho \operatorname{grad} V + \varrho \boldsymbol{f}_L + \varrho \boldsymbol{f}_B\,, \tag{24}$$

where

$$\varrho \boldsymbol{f}_L = \varrho_e \boldsymbol{E} + \frac{1}{c}\varrho_e [\boldsymbol{v} \times \boldsymbol{B}] \tag{24a}$$

is the well-known Lorentz force and

$$\varrho \boldsymbol{f}_B = \frac{1}{2}\mu \left\{(\boldsymbol{s}\operatorname{grad})\boldsymbol{B} + [\boldsymbol{s} \times \operatorname{rot} \boldsymbol{B}] + \operatorname{grad}(\boldsymbol{s}\boldsymbol{B}) - \operatorname{Div}(\boldsymbol{B} \circ \boldsymbol{s})\right\} \tag{24b}$$

represents the force derived for an outer magnetic field acting upon a polarized medium. To the physical interpretation of this expression we shall return later.

The inner force can be expressed, as is to be expected, as a tensor divergence

$$\varrho \boldsymbol{f}_i = \operatorname{Div} \mathfrak{R}, \tag{25}$$

where the tensor $\mathfrak{R}$ has the elements

$$\begin{aligned}(\mathfrak{R})_{ij} = &-\frac{\hbar^2}{4m}\varrho \frac{\partial^2 \ln \varrho}{\partial x_i \partial x_j} + \frac{\hbar}{4}(v_i \operatorname{rot}_j \boldsymbol{s} + \operatorname{rot}_i \boldsymbol{s} \cdot v_j) - \\ &- \frac{\hbar^2}{4m}\varrho \sum_{k=1}^{3} \frac{\partial T_k}{\partial x_i}\frac{\partial T_k}{\partial x_j} - \frac{\hbar^2}{16m}\frac{1}{\varrho}\operatorname{rot}_i \boldsymbol{s} \cdot \operatorname{rot}_j \boldsymbol{s} + (\mathfrak{k})_{ij}\end{aligned} \tag{25a}$$

and the tensor $\mathfrak{k}$ is defined by

$$\mathbf{Div}\ \mathfrak{k} = \operatorname{rot} \operatorname{Div} \mathfrak{g}, \tag{26}$$

i. e. the elements of the tensor $\mathfrak{k}$ are

$$\begin{pmatrix} 0 & \operatorname{Div}_3 \mathfrak{g} & -\operatorname{Div}_2 \mathfrak{g} \\ -\operatorname{Div}_3 \mathfrak{g} & 0 & \operatorname{Div}_1 \mathfrak{g} \\ \operatorname{Div}_2 \mathfrak{g} & -\operatorname{Div}_1 \mathfrak{g} & 0 \end{pmatrix},$$

where

$$(\mathfrak{g})_{kj} = -\frac{\hbar}{4}(s_k v_j) + \frac{\hbar^2}{16m}\frac{1}{\varrho} s_k \cdot \operatorname{rot}_j \boldsymbol{s} + \frac{\hbar^2}{8m}\varrho\left(T_l \frac{\partial T_m}{\partial x_j} - T_m \frac{\partial T_l}{\partial x_j}\right), \tag{26a}$$

here $j = 1, 2, 3$ and k, l, m are cyclic permutations of 1, 2, 3.

Thus for the acceleration of a volume element of the elastic medium representing the electron we have obtained an expression containing only quantities characteristic of the medium itself, such as ϱ, $\boldsymbol{v}$, $\boldsymbol{s}$ (or $\boldsymbol{T}$) and quantities characteristic of the outer field in which the medium moves (V, $\boldsymbol{E}$, $\boldsymbol{B}$).

§ 11. It remains to derive the equation of motion for the polarization vector $\boldsymbol{T}$.

In a way similar to that described above we obtain after some calculations (for details see [5]):

$$\varrho \frac{d\boldsymbol{T}}{dt} = \frac{2}{\hbar} \mu \varrho \, [\boldsymbol{T} \times \boldsymbol{B}] + \mathrm{Div}\, \mathfrak{G}, \tag{27}$$

where the k, j-th element of the tensor $\mathfrak{G}$ has the form

$$(\mathfrak{G})_{kj} = v_k s_j + \frac{\hbar}{4m} T_k \, \mathrm{rot}_j \, \boldsymbol{s} + \frac{\hbar}{2m} \varrho (T_l T_{mj} - T_m T_{lj}) \tag{27a}$$

(k, l, $m = 1, 2, 3$ in cyclic permutation), with the notation

$$T_{mj} = \frac{\partial T_m}{\partial x_j} .$$

§ 12. Equs. (23) and (27) together with the continuity equation (4) give a complete set of equations of motion. Indeed, if we give the values of ϱ, $\boldsymbol{v}$ and $\boldsymbol{T}$ at $t = 0$, i.e. if the state of the medium is characterized by the initial conditions

$$\boldsymbol{v}(\boldsymbol{r}, 0) = \boldsymbol{v}_0 (\boldsymbol{r}), \qquad \varrho(\boldsymbol{r}, 0) = \varrho_0 (\boldsymbol{r}), \qquad \boldsymbol{T}(\boldsymbol{r}, 0) = \boldsymbol{T}_0 (\boldsymbol{r}) \tag{28}$$

the motion is completely determined for any time $t > 0$.

We show further that relations (22a) and (21) if satisfied for $t = 0$ remain satisfied for any subsequent time.

Indeed, with the help of Gauss' law we find from (4)

$$\frac{d}{dt} \int \varrho \, d\tau = 0 , \qquad \text{i. e.} \qquad \int \varrho d\tau = \text{constant in time.}$$

Thus if the integral of the density extended over the whole space is equal to unity at $t = 0$ then it remains so at any later time.

We return to the auxiliary condition concerning the velocity vector $\boldsymbol{v}$ (21) and show that if the hydrodynamical variables given at $t = 0$ (ϱ_0, $\boldsymbol{v}_0$, $\boldsymbol{T}_0$) satisfy (21) for a given value of k then this equation remains satisfied for any ϱ, $\boldsymbol{v}$, $\boldsymbol{T}$ obtained by integrating the equations of motion starting from the given initial conditions for the same value of k.

From equ. (20) it follows that

$$\frac{d}{dt}\oint (\boldsymbol{v}+\boldsymbol{w})\,d\boldsymbol{r}=\frac{2\pi\hbar}{m}\frac{d}{dt}k\,,$$

where

$$\boldsymbol{w}=\frac{e}{mc}\boldsymbol{A}+\frac{\hbar}{2m}\cos\vartheta\,\mathrm{grad}\,\varphi-\frac{\hbar}{4m}\,\frac{1}{\varrho}\,\mathrm{rot}\,\boldsymbol{s}\,.$$

The left side of the above expression can be rewritten in the form

$$\frac{d}{dt}\oint (\boldsymbol{v}+\boldsymbol{w})\,d\boldsymbol{r}=\oint\frac{\partial}{\partial t}(\boldsymbol{v}+\boldsymbol{w})\,d\boldsymbol{r}-\oint[\boldsymbol{v}\times\mathrm{rot}\;(\boldsymbol{v}+\boldsymbol{w})]\,d\boldsymbol{r}\,. \quad (28a)$$

Introducing here from (17)

$$\boldsymbol{v}+\boldsymbol{w}=\frac{\hbar}{m}\,\mathrm{grad}\,S$$

it is seen that the second term of (28a) is zero.
The first integral on the right-hand side can be written in the following way

$$\oint\frac{\partial}{\partial t}(\boldsymbol{v}+\boldsymbol{w})\,d\boldsymbol{r}=\frac{\hbar}{m}\oint\mathrm{grad}\,\dot{S}\,d\boldsymbol{r}=0,$$

as grad $\dot{S}$, as we have shown in [4] can be substituted by grad ζ, where ζ is a single-valued function of $\boldsymbol{r}$ and t. I. e. we have thus proved

$$\frac{d}{dt}\oint(\boldsymbol{v}+\boldsymbol{w})\,d\boldsymbol{r}=0, \quad (28b)$$

which means that k is independent of time.

It must be emphasized, however, that the procedure followed here is justified only under the condition that no singularity crosses the path of integration in the course of the motion considered. So as to get rid of this condition, we may replace the fixed closed path of integration in (21) by the path moving together with the medium. If this avoids singular points at the time $t=0$ it will do so at any later time. It can be shown easily that equ. (28b) is valid taken with such a moving boundary. We see therefore that both auxiliary conditions (21) and (22a) if satisfied at $t=0$ will remain satisfied at any later time. The auxiliary conditions (21), and (22a) are automatically satisfied by the hydrodynamical variables determined from the equations of motion (4), (23) and (27) with the aid of given initial conditions.

§ 13. Finally, it remains to show that the hydrodynamical equations of motion are equivalent to the wave equation. With the help of equs. (12),

(14), (16) and (19) the wave function ψ can be expressed in terms of the hydrodynamical variables ϱ, $\boldsymbol{v}$, $\boldsymbol{T}$.

Introducing the explicit expression for $\psi = \psi(\varrho, \boldsymbol{v}, \boldsymbol{T})$ into the wave equation (2) it can be shown after a somewhat tedious calculation that the relation

$$H\psi(\varrho, \boldsymbol{v}, \boldsymbol{T}) = i\hbar \frac{\partial \psi(\varrho, \boldsymbol{v}, \boldsymbol{T})}{\partial t}$$

reduces to an identity provided ϱ, $\boldsymbol{v}$, $\boldsymbol{T}$ obey the hydrodynamical equs. (4), (23) and (27), and the constant of integration $S_0(\boldsymbol{r}_0, t)$ is taken to be

$$S_0(\boldsymbol{r}_0, t) = S^0 - \frac{1}{\hbar}\int_0^t \left[V + Q + e\Phi + \frac{1}{2}m\boldsymbol{v}^2\right]_{\boldsymbol{r}=\boldsymbol{r}_0} dt - \frac{1}{\hbar}\int_0^t [\eta(\boldsymbol{r}, t)]_{\boldsymbol{r}=\boldsymbol{r}_0} dt,$$

where S^0 is a real but otherwise arbitrary constant and $Q = -\frac{\hbar^2}{2m}\frac{\Delta \varrho^{1/2}}{\varrho^{1/2}}$. The function η contains besides the hydrodynamical variables the magnetic field vector $\boldsymbol{B}$; the explicit form of η was found to be

$$\begin{aligned}
\eta = &-\mu \frac{\boldsymbol{B}_1 T_1 + \boldsymbol{B}_2 T_2}{T_1^2 + T_2^2} + \\
&+ \frac{\hbar}{2} T_3 \left(\boldsymbol{v} \frac{T_1 \nabla T_2 - T_2 \nabla T_1}{T_1^2 + T_2^2} \right) - \frac{\hbar}{4}\frac{1}{\varrho}(\boldsymbol{v} \cdot \operatorname{rot} \boldsymbol{s}) + \\
&+ \frac{\hbar^2}{4m}\frac{T_3}{T_1^2 + T_2^2}\frac{1}{\varrho}\operatorname{div}(\varrho \nabla T_3) + \frac{\hbar^2}{32m}\frac{1}{\varrho^2}(\operatorname{rot} \varrho \boldsymbol{T})^2 + \\
&+ \frac{\hbar^2}{8m}(1 + T_3^2)\left[(\nabla T_1)^2 + (\nabla T_2)^2 + (\nabla T_3)^2\right] - \\
&- \frac{\hbar^2}{8m}\frac{1}{\varrho} T_3 \left(\operatorname{rot} \varrho \, \boldsymbol{T} \cdot \frac{T_1 \nabla T_2 - T_2 \nabla T_1}{T_1^2 + T_2^2} \right).
\end{aligned}$$

We intend to return to a detailed discussion of η in a later paper.

Summarizing, we conclude that a given set of hydrodynamical variables obeying the initial conditions (21) and (22) determines — apart from a constant phase factor e^{iS_0} — a wave function that satisfies the Pauli equation.

We can thus state that in the case of an electron the motion of which is described in quantummechanics by the Pauli equation there *is a one-to-one correspondence between the normalized solutions of the wave equation and the solutions of the hydrodynamical equations of motion satisfying the adequate initial conditions.* This means that the equations of motion in terms of the hydrodynamical variables are equivalent to the Pauli equation.

IV. Integral properties of closed systems

§ 14. So as to proceed with the discussion of our results let us consider the integral relations which can be derived from the equations of motion.

We see from (25) that the density of the inner force $\boldsymbol{f}_i$ can be obtained as the divergence of a tensor. Thus we have for the inner force of the elastic medium representing the electron

$$\boldsymbol{F}_i = \int \varrho \boldsymbol{f}_i \, d\tau = 0, \tag{29}$$

i. e. as is to be expected in a closed system, the inner forces have no resultant.

The moment of force produced by the inner forces can be written as

$$\boldsymbol{K}_i = \int \varrho [\boldsymbol{r} \times \boldsymbol{f}_i] \, d\tau = \int [\boldsymbol{r} \times \operatorname{Div} \mathfrak{R}] \, d\tau.$$

Integrating by parts we find, remembering that the divergence of the antisymmetric part of the tensor (25) can be written as a rotation of a vector which is the divergence of the tensor $\mathfrak{g}$ [see (26)]:

$$\boldsymbol{K}_i = 2 \int \operatorname{Div} \mathfrak{g} \, d\tau = 0, \tag{30}$$

i.e. the resultant moment of force produced by the inner forces is also zero.

§ 15. Thus, as was to be expected, the inner forces of the elastic medium representing the electron have no integral effects. At the same time we obtain by using (24) for the outer force acting on the system

$$\begin{aligned} \boldsymbol{F}_0 = & -\int \varrho \operatorname{grad} V \, d\tau + \int \varrho_e \left(\boldsymbol{E} + \frac{1}{c} [\boldsymbol{v} \times \boldsymbol{B}] \right) d\tau + \\ & + \int \frac{1}{2} \mu \left\{ (\boldsymbol{s} \operatorname{grad}) \boldsymbol{B} + [\boldsymbol{s} \times \operatorname{rot} \boldsymbol{B}] \right\} d\tau \end{aligned} \tag{31}$$

and for the moment of force produced by the outer forces:

$$\begin{aligned} \boldsymbol{K}_0 = & -\int [\boldsymbol{r} \times \varrho \operatorname{grad} V] \, d\tau + \\ & + \int [\boldsymbol{r} \times \varrho_e \boldsymbol{E}] \, d\tau + \frac{1}{c} \int [\boldsymbol{r} \times [\varrho_e \boldsymbol{v} \times \boldsymbol{B}]] \, d\tau + \\ & + \int \left[\boldsymbol{r} \times \frac{1}{2} \mu \left((\boldsymbol{s} \operatorname{grad}) \boldsymbol{B} + [\boldsymbol{s} \times \operatorname{rot} \boldsymbol{B}] \right) \right] d\tau + \int \frac{1}{2} \mu [\boldsymbol{s} \times \boldsymbol{B}] \, d\tau. \end{aligned} \tag{32}$$

These expressions may be given the following physical interpretation.

The dynamical behaviour of the electron described as a hydrodynamical system of density ϱ, velocity of flow $\boldsymbol{v}$ and polarization density $\boldsymbol{s}$, can be characterized by the average of the total momentum of the system

$$\boldsymbol{P} = \int \varrho_m \boldsymbol{v}\, d\tau, \tag{33a}$$

and by the total angular momentum

$$\boldsymbol{\Pi} = \int [\boldsymbol{r} \times \varrho_m \boldsymbol{v}]\, d\tau.$$

The rate of change of the momentum gives the force acting on the system, while that of the angular momentum is equal to the moment of force. Thus using (4), (23) and (29) we get for the total force acting on the electron

$$\boldsymbol{F} = \boldsymbol{F}_0 = \frac{d\boldsymbol{P}}{dt}, \tag{34}$$

and for the moment of force

$$\boldsymbol{K} = \boldsymbol{K}_0 = \frac{d\boldsymbol{\Pi}}{dt}. \tag{35}$$

Let us consider now the case when the external field in which the electron cloud moves can be described by functions changing slowly over the region covered by this cloud. In this case (34) has the form

$$\begin{aligned} \boldsymbol{F}_0 = &- (\overline{\nabla V}) + e\bar{\boldsymbol{E}} + \frac{e}{mc}[\boldsymbol{P} \times \bar{\boldsymbol{B}}] + \\ &+ \boldsymbol{M}_p (\overline{\nabla \circ \boldsymbol{B}}) + [\boldsymbol{M}_p \times \overline{\mathrm{rot}\, \boldsymbol{B}}], \end{aligned} \tag{36}$$

(The bar indicates average value.)

As one can see from (36) the outer force integrated over the whole medium representing the spinning electron corresponds to the force exercized by an external field of average field strength $\bar{\boldsymbol{E}}$, $\bar{\boldsymbol{B}}$ and $\overline{\nabla V}$ on a charged magnetic dipole of momentum

$$M_p = \frac{1}{2} \mu \boldsymbol{S}. \tag{37a}$$

where $\boldsymbol{S}$ is the total spin vector

$$\boldsymbol{S} = \int \varrho \boldsymbol{T}\, d\tau. \tag{37}$$

If we want to consider the moment of force exerted by the outer forces in a first approximation it is not sufficient to use the average value of the outer force acting in the region of the atom. So as to get the

first approximation of the moment of force we have to introduce the gradient of the outer force and express the moment of force in terms of the average value of this gradient. We do not give here the formula explicitely but note that the equations thus obtained have a certain similarity to the Euler's equations of motion of a top.

§ 16. From the equation of motion (27) of the polarization vector $\boldsymbol{T}$ we may obtain the time derivative of the spin vector $\boldsymbol{s}$ of a volume element. Integrating over the whole space and interchanging the order of operations we get

$$\frac{d}{dt}\int \boldsymbol{s}\, d\tau = \frac{e}{mc}\int [\boldsymbol{s}\times\boldsymbol{B}]\, d\tau\ . \tag{38}$$

Using here the same approximation as in § 15 and introducing the spin magnetic moment, by using (37), as:

$$\boldsymbol{M} = \frac{e\hbar}{2mc}\boldsymbol{S}$$

we get

$$\frac{d\boldsymbol{S}}{dt} = \frac{2}{\hbar}[\boldsymbol{M}\times\bar{\boldsymbol{B}}]$$

i.e. the rate of change of the spin vector is determined by the effect produced by the magnetic field on the spin magnetic moment.

Thus we see that all the actions expected in a classical picture appear in our relations.

V. The physical significance of the constant α

§ 17. Finally we return to the problem of the choice of the coefficient of the last term of expression (8) giving the velocity of flow. We show that only the choice $\alpha = \frac{1}{2}$, which we introduced in § 2 and used throughout our calculations leads to results which are in agreement with experience.

Indeed, in the model considered in this paper the total magnetic moment of the electron is taken to be built up of two parts: first, as can be seen from the expression of force (24b) as well as from equ. (36) the medium representing the electron has a permanent magnetic dipole moment of density

$$\boldsymbol{m}_p = \frac{1}{2}\mu\,\boldsymbol{s}.$$

This contributes to the magnetic moment of the electron

$$\boldsymbol{M}_p = \frac{1}{2}\mu\int \boldsymbol{s}\, d\tau\,.$$

Secondly, owing to its inner motion the electrically charged medium contains convection currents; the density of the magnetic moment of these currents can be obtained from the expression for the velocity of flow [equ. (8)], as (see [6]):

$$\boldsymbol{m}_c = \frac{1}{2}\mu\boldsymbol{s}\,.$$

Integrating over the whole of space we get

$$\boldsymbol{M}_c = \frac{1}{2}\mu\int \boldsymbol{s}\, d\tau\,. \tag{39}$$

Thus, for the total magnetic moment of the electron we have

$$\boldsymbol{M} = \boldsymbol{M}_p + \boldsymbol{M}_c = \mu\int \boldsymbol{s}\, d\tau\,. \tag{40}$$

This is in agreement with the fact that the magnetic moment of the electron in an s-state is one Bohr magneton.

We note, however, that the above result is independent of the choice of the parameter α. As a detailed calculation shows by changing the value of α we merely change the relative contributions of the convection current and the permanent magnetization to the total dipole moment, the value of the latter, however, is found to be independent of α.

An effect which does depend on α and therefore gives information on its correct value is described below.

According to classical mechanics a magnetized top when placed into an outside magnetic field will precess around the direction of the magnetic field with a frequency which is proportional to the moment of force and inversely proportional to the angular momentum, thus

$$\omega = \frac{|\boldsymbol{K}|}{|\boldsymbol{\Pi}|}\,. \tag{41}$$

In order to apply this result to an atom which we may compare to such a top we note that in that case we get for the moment of force independently of the choice of the value of α:

$$\boldsymbol{K} = \mu\,[\boldsymbol{S}\times\overline{\boldsymbol{B}}].$$

At the same time we obtain for the angular momentum given in (33b) with the help of the expression of the density of velocity of flow given in (8)

$$\boldsymbol{\Pi} = \alpha\hbar\, \mathbf{S}.$$

I.e. in our model the moment of force is proportional to the total magnetic moment, while the angular momentum is proportional to that part of the magnetic moment only which is produced by convection currents.

We get thus for the frequency of precession of the atom

$$\omega = \frac{\mu\,|\mathbf{S}|\cdot|\bar{\boldsymbol{B}}|}{\alpha\hbar\,|\mathbf{s}|} = \frac{1}{\alpha}\,\frac{e}{2mc}\,|\bar{\boldsymbol{B}}|\,. \tag{42}$$

The observed frequency, the so-called Larmour frequency in a magnetic field of strength B is known experimentally to be

$$\omega_L = \frac{e}{mc}\,B\,. \tag{43}$$

Comparing (42) with (43) we get for α the value $\alpha = \frac{1}{2}$ introduced in § 2.

A further remark must be made regarding the density of the electric current inside the cloud. The density of the convection current is given by

$$\boldsymbol{i}_c = \frac{1}{c}\,\varrho_e\,\boldsymbol{v}\,, \tag{44}$$

where we have to insert for $\boldsymbol{v}$ the value given by (8) corresponding to $\alpha = \frac{1}{2}$. However, in a magnetized medium an effective current $\boldsymbol{i}_{\text{eff}}$ can be defined (see e.g. [6]) the density of which is given by

$$\boldsymbol{i}_{\text{eff}} = \boldsymbol{i}_c + \operatorname{rot}\boldsymbol{M}\,, \tag{45}$$

where $\boldsymbol{M}$ is the density of magnetic polarization. In the case of the electron we may suppose

$$\boldsymbol{M} = \frac{1}{2}\,\mu\,\mathbf{s}\,. \tag{46}$$

Introducing (44) and (46) into (45) we obtain with the help of (8)

$$\boldsymbol{i}_{\text{eff}} = -\frac{ie\hbar}{2mc}(\psi^* \nabla\psi - \nabla\psi^* \cdot \psi) - \frac{e^2}{mc^2}\boldsymbol{A}\psi^*\psi + \frac{e\hbar}{2mc}\,\text{rot}\,(\psi^* \boldsymbol{\sigma} \psi)\,. \quad (47)$$

The latter expression is that usually given for the current density in quantum mechanical considerations.

We note that the density $\boldsymbol{i}_{\text{eff}}$ as given by expression (47) can be used to determine the field strength $\boldsymbol{B}$ produced by the magnetized system, i.e. $\boldsymbol{i}_{\text{eff}}$ can be regarded as a current density equivalent to one producing a magnetic field equal to the sum of the fields produced by the convection currents and the magnetic polarization.

The comparison of (7a) and (47) sheds also light upon the mechanism of the so-called anomalous magnetic moment of the electron. In the case when $\boldsymbol{v}^0 = 0$, i.e. in a system when only currents arising from the spin are present, we find

$$\boldsymbol{i}_{\text{eff}} = 2\boldsymbol{i}_c = \frac{e\hbar}{2mc}\,\text{rot}\,\boldsymbol{s}\,.$$

Thus the current intensity $\boldsymbol{i}_{\text{eff}}$ from which the magnetic moment can be derived is twice the intensity of the convection current density $\boldsymbol{i}_c$. Since the angular momentum is proportional to the momentum of the masses which are moving inside the atom, it is also proportional to the density $\boldsymbol{i}_c$ and thus the ratio of magnetic moment and angular momentum becomes twice the "normal" value, i.e. twice the value to be expected in the case of a system containing convection currents only.

REFERENCES

1. L. JÁNOSSY and M. ZIEGLER, Acta Phys. Hung. **16,** 37, 1963.
2. L. JÁNOSSY and M. ZIEGLER-NÁRAY, Acta Phys. Hung., **16,** 345, 1964.
3. T. TAKABAYASI, Progr. of Theor. Phys., **9,** 187, 1953.
4. L. JÁNOSSY and M. ZIEGLER-NÁRAY, Reports of the Central Research Institute of Physics.
5. Á. FODOR, L. JÁNOSSY and M. ZIEGLER-NÁRAY, Report of the Central Research Institute of Physics.
6. L. JÁNOSSY, Acta Phys. Hung., **20,** 67, 1966.

ГИДРОДИНАМИЧЕСКАЯ МОДЕЛЬ ВОЛНОВОЙ МЕХАНИКИ III

Спин электрона

Л. ЯНОШИ и МАРИЯ ЦИГЛЕР-НАРАИ

Р е з ю м е

Гидродинамическая модель волновой механики был распространен нами на проблему электрона, описанного уравнением Паули. Показано, что уравнения Паули могут быть преобразованы в систему уравнений, имеющую вид классического уравнения движения неоднородной намагниченной упругой среды.

DETERMINATION OF WAVE FUNCTIONS OF MOLECULAR SYSTEMS BY THE METHOD OF MOMENTS, II

By

ÉVA SZONDY

HUMAN SERUM AND VACCINE INSTITUTE, BUDAPEST

and

T. SZONDY*

RESEARCH GROUP FOR THEORETICAL PHYSICS OF THE HUNGARIAN ACADEMY OF SCIENCES, BUDAPEST

(Presented by A. Kónya — Received 6. VII. 1965)

Let H be the Hamiltonian operator of a molecular system, let $\varphi(\alpha_1, \alpha_2, \ldots, \alpha_n)$ be a variational wave function involving the set $\alpha_1, \alpha_2, \ldots, \alpha_n$ of variational parameters and let $u_0, u_1, \ldots, u_n$ be a set of arbitrary linearly independent functions depending on the same co-ordinates as φ.

In the special case

$$u_0 = \varphi; \quad u_i = \partial\varphi/\partial\alpha_i; \quad (i = 1, 2, \ldots, n)$$

the roots $\alpha_1, \alpha_2, \ldots, \alpha_n$ and ε of the set of equations

$$\langle u_k \mid H - \varepsilon \mid \varphi \rangle = 0; \quad (k = 0, 1, \ldots, n) \qquad (*)$$

coincide with the values of the variational parameters and the energy, respectively, obtained by the method of energy variation.

There is reason to expect that the roots of (*) are in many cases fairly insensitive to moderate deviations of the function u_0 from φ and of the functions u_i from $\partial\varphi/\partial\alpha_i$. Consequently if difficulties of integration prevent us from determining the α_i 's and ε by the method of energy variation it may be reasonable to solve the equations (*) approximately by replacing the functions u_k by some mathematically more convenient functions $v_0 \approx \varphi$ and $v_i \approx \partial\varphi/\partial\alpha_i$. This possibility seems to be an efficient tool for reducing difficulties of integration, and thus for extending the applicability of variational methods to problems which are — at least at the present stage of computer techniques — beyond the domain of applicability of the method of energy variation.

The present paper deals (a) with some practical aspects of the application of such an approach to problems of quantum chemistry, and (b) with questions concerning the reliability of the obtained results.

One of the most serious difficulties arising in the course of determining approximate wave functions of molecular systems is the calculation of certain integrals with very complicated integrands. It has been pointed out in the first paper of this series [1] that these difficulties can be significantly reduced if instead of determining the parameters of the variational wave functions by the method of energy variation (MEV) they are determined by the method of moments (MM). MM is a more general variational method than MEV in the sense that while every variant of MEV can be regarded as a definite special

* New address: Computer Center of the Chemical Industries, Budapest.

case of MM, there exist variants of MM of practical importance which are not equivalent to a MEV approximation.

In the present paper (a) the basic equations of MM will be re-formulated in a form which is more general and considerably more convenient for computational work than that considered in I, (b) the problem of the reliability of the results obtained by MM will be investigated in some detail, (c) the problem of obtaining an approximation to the energy of the system within the framework of MM will be discussed, and (d) some remarks will be made concerning the relation of MM to some other variational methods of quantum chemistry.

1. Introduction

The object of our investigations is a system consisting of a finite number of electrons and nuclei. It will be assumed that the system is in a stationary state. The system will be characterized by the (nonrelativistic) Hamiltonian operator H, the state by the wave function ψ and the corresponding energy eigenvalue E

$$H\psi - E\psi = 0, \tag{1}$$

$$\langle\psi|\psi\rangle = 1. \tag{2}$$

Our considerations will be confined to Hamiltonian operators which are real in the sense $H^* = H$, where H^* denotes the complex conjugate of H.

It should be noted that all our considerations are valid also for systems in which the nuclei are fixed (not necessarily at their equilibrium positions). In this case H, ψ and E denote the (nonrelativistic) electronic Hamiltonian operator, electronic wave function and electronic energy, respectively.

In order to make predictions concerning some property of the system we actually never need the wave function ψ itself, only certain matrix elements calculated from it. In order to have something definite before our eyes it will be assumed that we are interested in the expectation value $\langle\psi|P|\psi\rangle$ of an operator P, and any approximation φ to ψ will be called a "good approximation" if it satisfies the conditions

$$\langle\varphi \mid \varphi\rangle = 1, \tag{3}$$

$$|\langle\varphi| P \mid \varphi\rangle - \langle\psi \mid P \mid\psi\rangle| < \varepsilon_P, \tag{4}$$

and

$$\langle\eta \mid \eta\rangle < \varepsilon, \tag{5}$$

where η denotes the error in φ defined by

$$\eta = \varphi - \langle \psi \mid \varphi \rangle \psi, \tag{6}$$

while ε_P and ε denote preassigned small positive numbers. There is, in principle, no difficulty in generalizing our considerations to the cases (a) when we are interested in more than one expectation value, and (b) when we are interested in off-diagonal matrix elements. For the sake of simplicity we shall, however, not consider such cases explicitly.

Let $\varphi(\alpha)$ be a variational wave function depending on the same coordinates as ψ, being normalized

$$\langle \varphi(\alpha) \mid \varphi(\alpha) \rangle = 1, \tag{7}$$

and involving the set $\alpha \equiv \{\alpha_1, \alpha_2, \ldots, \alpha_n\}$ of variational parameters. MEV determines the values of the α_i 's [2] from the condition

$$\mathscr{E}(\alpha) = \langle \varphi(\alpha) \mid H \mid \varphi(\alpha) \rangle = \text{stationary}. \tag{8}$$

It will be convenient to start our considerations with the following assumptions:

(i) It will be assumed, that (8) has a root — denoted in the following by $\bar{\alpha}$ — for which $\varphi(\bar{\alpha})$ is a good approximation to ψ.

Such an assumption is based in practice always on an extrapolation of the experience obtained by performing calculations on a number of systems more or less related to that we investigate, using thereby variational wave functions of a type similar to or simpler than $\varphi(\alpha)$. The reliability of such an extrapolation can be significantly increased by certain qualitative or semiquantitative considerations such as an investigation of the "stability" of the wave function under suitably chosen perturbations (HALL [3], [4]), or investigations similar to those of KAPUY [5] concerning the range of applicability of wave functions built up from group orbitals. As, however, the reliability of such considerations is always limited, they do not diminish the importance of *a posteriori* tests of the accuracy of the approximate wave functions (cf. Sec. 3.).

(ii) It will be assumed, that $\varphi(\alpha)$ and H are so complicated that practical difficulties of integration prevent us from calculating the integral $\mathscr{E}(\alpha)$ (or at least the calculation is too tedious to pay off) and consequently we can not determine $\bar{\alpha}$.

(iii) It will be assumed that $\varphi(\alpha)$ can not be replaced by some other, mathematically more convenient variational wave function without risking an inadmissible loss of accuracy or an inadmissible decrease of the rate of convergence.

The problems which we shall discuss are (a) how to determine in a situation characterized by assumptions (i)—(iii) values $\tilde{\alpha}_i$ [2] of the variational parameters such, that it can still be expected that $\varphi(\tilde{\alpha})$ is a good ap-

proximation to ψ, or at least to $\varphi(\bar{\alpha})$ and (b) how to obtain in practice information about the accuracy of $\varphi(\bar{\alpha})$. Thus it will be attempted to extend the applicability of the variational methods to problems which are — at least at the present stage of computer techniques — beyond the domain of the practical applicability of MEV.

It seems almost certain that the application of MM to problems which can be easily dealt with by MEV is disadvantageous and in this sense MM will be probably always at a disadvantage against MEV.

It should be emphasized that the present paper provides hardly more than a list of possibilities which seem, after a careful consideration, worth testing. Our aim is by no means to give final answers to all the arising questions but rather to initiate further investigations.

2. The determination of $\bar{\alpha}$

Let us define a projection operator S by the following requirements: (a) S should act on functions depending on the same co-ordinates as ψ, and (b) S should project the function on which it acts onto that subspace of the Hilbert space the elements of which have the same symmetry properties as ψ with respect to both the permutation of the co-ordinates and spatial symmetry operations. Evidently $SH = HS$, $S^2 = S$ and it can be assumed without loss of generality, that $S\varphi(\alpha) = \varphi(\alpha)$.

In all the practically important cases $\varphi(\alpha)$ appears in the form

$$\varphi(\alpha) = N(\alpha)\, Su(\alpha), \tag{9}$$

where $N(\alpha)$ denotes the normalization factor $\langle Su(\alpha) \mid Su(\alpha)\rangle^{-1/2}$ and $u(\alpha)$ is a function — generally much simpler than $\varphi(\alpha)$ — depending on the same co-ordinates and variational parameters as $\varphi(\alpha)$. Introducing the notation

$$u(\alpha) \equiv u_0(\alpha);\quad \partial u(\alpha)/\partial\alpha_i = u_i(\alpha);\quad \mathscr{E}(\bar{\alpha}) = \bar{\alpha}_0, \tag{10}$$

it follows in a straightforward way that (8) is equivalent to the following set of equations [2], [6]

$$\langle u_k(\alpha) \mid H - \alpha_0 \mid \varphi(\alpha)\rangle = 0. \tag{11}$$

We now restrict our considerations to cases in which the stationary value of the integral (8) is a (local) extremum. This is certainly the case when ψ is the wave function associated with the ground state, but it is satisfied in many cases also for excited states. Then it can be easily verified, that in the neighbourhood of $\alpha = \bar{\alpha}$ and $\alpha_0 = \mathscr{E}(\bar{\alpha}) = \bar{\alpha}_0$

$$\det \left\| \frac{\partial}{\partial \alpha_l} \langle u_k(\alpha) | H - \alpha_0 | \varphi(\alpha) \rangle \right\| \neq 0. \tag{12}$$

In order to obtain an approximation $\tilde{\alpha}$ to $\bar{\alpha}$ we proceed in the following way:

Let us assume we succeeded in finding approximations $v_k(\alpha)$ to the $u_k(\alpha)$'s

$$v_k(\alpha) \approx u_k(\alpha) \tag{13}$$

such, that (a) the calculation of the integrals $\langle v_k(\alpha) | H | \varphi(\alpha) \rangle$ and $\langle v_k(\alpha) | \varphi(\alpha) \rangle$ is possible in practice (some aspects concerning the construction of such $v_k(\alpha)$'s are discussed in Appendix 1.), and (b) the property (12) of the integrals $\langle u_k(\alpha) | H - \alpha_0 | \varphi(\alpha) \rangle$ does not get lost by the changes $u_k(\alpha) \to v_k(\alpha)$, i.e. in the neighbourhood of $\alpha = \bar{\alpha}$ and $\alpha_0 = \bar{\alpha}_0$

$$\det \left\| \frac{\partial}{\partial \alpha_l} \langle v_k(\alpha) | H - \alpha_0 | \varphi(\alpha) \rangle \right\| \neq 0. \tag{14}$$

The integrals [2]

$$m_k(\alpha, \alpha_0) \equiv \langle v_k(\alpha) | H - \alpha_0 | \varphi(\alpha) \rangle \tag{15}$$

are, in general, not zero for $\alpha = \bar{\alpha}$ and $\alpha_0 = \bar{\alpha}_0$. However, whenever (14) holds, there always exist such changes of α_0 and the α_i's which simultaneously diminish the absolute values of all the $m_k(\alpha, \alpha_0)$'s. Evidently if the absolute values of the integrals $m_k(\bar{\alpha}, \bar{\alpha}_0)$ are sufficiently small, the set of equations

$$\langle v_k(\alpha) | H - \alpha_0 | \varphi(\alpha) \rangle = 0 \tag{16}$$

has a system of roots — to be denoted in the following by $\{\tilde{\alpha}, \tilde{\alpha}_0\}$ — such that $\varphi(\tilde{\alpha})$ is a good approximation to $\varphi(\bar{\alpha})$. It is also obvious that the values $|m_k(\bar{\alpha}, \bar{\alpha}_0)|$ can be reduced beyond every limit by reducing — at least in those regions of the configurational space which give significant contributions to the integrals $m_k(\alpha, \alpha_0)$ — the absolute values of the functions

$$\delta_k(\alpha) = v_k(\alpha) - u_k(\alpha). \tag{17}$$

Consequently if the $v_k(\alpha)$'s are "sufficiently good" approximations to the $u_k(\alpha)$'s the equations (16) provide a possible tool for approximately solving (8).

In the following the integrals $m_k(\alpha, \alpha_0)$ will be referred to as m o m e n t s of $(H - \alpha_0)\varphi(\alpha)$ with the w e i g h t f u n c t i o n s $v_k(\alpha)$ and the equations (16) will be regarded as the basic equations of MM [7].

Evidently the competitiveness of MM depends on two factors: (a) how can we decide in practice whether or not the approximate wave function $\varphi(\tilde{\alpha})$ obtained by an actual set of weight functions is a good approximation

to ψ (or least to $\varphi(\bar{\alpha})$), and (b) whether or not the root $\bar{\alpha}$ of (11) is sufficiently insensitive to changes $u_k(\alpha) \to v_k(\alpha)$ in practically important cases, that the requirement of obtaining a good approximation to ψ is compatible with $\delta_k(\alpha)$'s sufficiently large to make possible a significant reduction of the difficulties of integration. These problems will be dealt with in the next two sections.

3. Some possibilities for obtaining information about the accuracy of $\varphi(\tilde{\alpha})$

In this section we shall discuss some practical possibilities for deciding whether it is justified or not to expect that a wave function $\varphi(\tilde{\alpha})$ obtained by some actual set of weight functions is a good approximation to ψ (or at least to $\varphi(\bar{\alpha})$).

(i) The simplest possibility for obtaining information about the accuracy of $\varphi(\tilde{\alpha})$ is evidently to calculate some properties of the system from $\varphi(\tilde{\alpha})$ and compare the results with the experiment. This error estimate is an "absolute" one in the sense that it compares $\varphi(\tilde{\alpha})$ with ψ and not with $\varphi(\bar{\alpha})$. As this type of error estimate does not depend on the way $\varphi(\tilde{\alpha})$ has been obtained, we shall not discuss its problems in detail but refer to a review article dealing with this topic [8]. Only some remarks will be made on questions which are of a special interest for MM.

The difference between the expectation value $\mathscr{E}(\tilde{\alpha})$ and the empirical (nonrelativistic) value E of the energy is generally regarded as an important gauge of the accuracy of $\varphi(\tilde{\alpha})$. Although according to assumption (ii) made in Sec. 1. the calculation of $\mathscr{E}(\tilde{\alpha})$ may be prohibitively difficult, it must not be categorically excluded from among the practicable possibilities. Namely it is a much easier task to calculate $\mathscr{E}(\tilde{\alpha})$ for the one given set $\tilde{\alpha}$ of variational parameters than to calculate it several times in the course of the determination of $\tilde{\alpha}$.

The most serious shortcoming of the empirical error estimates certainly lies in the fact that they are limited to a fairly small proportion of the practically important problems, mainly to isolated atoms and small molecules in the ground state or some low-lying excited state. It is namely hardly possible in practice to carry out sufficiently accurate and clear-cut measurements on considerably more complicated systems, e.g. on a system consisting of an aggregate of interacting molecules with some prescribed nuclear arrangement. Unfortunately the quantumchemical methods are the most competitive just in those cases in which the experimental ones fail, and consequently purely theoretical error estimates are of a great practical importance even if they are mathematically not rigorous (in a similar sense as e. g. the error estimates of the Monte Carlo calculations). The main value of the empirical error estimates lies in the possibility of testing on simple problems the efficiency of different *types* of variational wave functions and error estimates.

(ii) In the case of MEV there is inevitably a considerable amount of arbitrariness in the choice of the variational wave function $\varphi(\alpha)$ and in the case of MM there is some additional arbitrariness in the choice of the weight functions $v_k(\alpha)$. It is evidently of importance to obtain information about the effect on the results of this latter source of arbitrariness and, as far as possible, to reduce this effect.

In order to obtain information about the order of magnitude of the changes $\bar{\alpha}_i \to \tilde{\alpha}_i$ we can make use of the fact that for given H and $\varphi(\alpha)$ the changes $\bar{\alpha}_i \to \tilde{\alpha}_i$ depend only on the magnitude and the shape of the functions $\delta_k(\alpha)$. Let us assume now that we have solved the equations (16) for more than one set of weight functions, say, for the sets $v_k^{(1)}(\alpha), v_k^{(2)}(\alpha), \ldots, v_k^{(f)}(\alpha)$, such, that the corresponding $\delta_k^{(h)}(\alpha)$'s $(h = 1, 2, \ldots, f)$ substantially differ from each other [9] and let us denote by $\tilde{\alpha}^{(h)}$ the root obtained by using the set $v_k^{(h)}(\alpha)$. Of course, it may — accidentally — happen that for some value of i two or more of the $(\tilde{\alpha}_i^{(h)} - \bar{\alpha}_i)$'s are approximately equal. The probability of *all* the $(\tilde{\alpha}_i^{(h)} - \alpha_i)$'s being approximately equal for some value of i decreases however, rapidly with the increase of f. It can be expected that even for rather low values of f the oscillations of the $\tilde{\alpha}_i^{(h)}$'s provide a fairly reliable estimate of the order of magnitude of the $|\tilde{\alpha}_i - \bar{\alpha}_i|$'s, where $\tilde{\alpha}_i$ denotes some average of the $\tilde{\alpha}_i^{(h)}$'s. Although this error estimate has the character of a "random sampling", we expect that if one obtains experience in its use its reliability will be sufficient for practical purposes.

There exists a very attractive variant of this error estimate. We start with a set $v_k^{(1)}(\alpha)$ which is a rough but possibly simple approximation to the set $u_k(\alpha)$, and continue with sets $v_k^{(2)}(\alpha), v_k^{(3)}(\alpha), \ldots$ which are better and better approximations to the set $u_k(\alpha)$. (E.g. if the $v_k^{(h)}(\alpha)$'s are obtained from the $u_k(\alpha)$'s by expanding certain constituents of them in terms of more convenient functions (as described in Appendix 1.), the subsequent sets $v_k^{(1)}(\alpha), v_k^{(2)}(\alpha), \ldots$ may be obtained by retaining more and more terms of the expansion.) It can be expected that in this case the subsequent $\tilde{\alpha}_i^{(h)}$'s tend to some definite values and the procedure can be ended after the changes of the $\tilde{\alpha}_i^{(h)}$'s do not exceed in the last steps some preassigned values.

It may turn out that this procedure is economical even from the point of view of computer times, as it means that the values of the $\tilde{\alpha}_i$'s are determined first roughly but in a relatively simple way and the more and more tedious steps serve only for refining the result obtained in the previous step. Evidently all the steps require in this case the running of a program of the same type.

(iii) A further possibility for obtaining information about the error in $\varphi(\tilde{\alpha})$ or rather in matrix elements of the type $\langle \varphi(\tilde{\alpha}) \mid P \mid \varphi(\tilde{\alpha}) \rangle$ is that proposed recently by CHEN and DALGARNO [10]. As to the details of the method we refer to the quoted paper and make here only a few remarks on problems of a specal interest for MM.

CHEN and DALGARNO have shown that under certain rather general conditions the integral

$$\Delta P \equiv 2\langle f\,\varphi(\tilde{a}) \mid H \mid \varphi(\tilde{a})\rangle \tag{18}$$

is of the same order of magnitude as the error in $\langle\varphi(\tilde{a}) \mid P \mid \varphi(\tilde{a})\rangle$, where f denotes a well-defined function determined in practice by minimizing a functional with respect to a selected trial form of f. The fact important for us is that this functional is so simple that it can be generally calculated without prohibitive difficulties even if this is not true for $\mathscr{E}(\alpha)$. Naturally the integral ΔP suffers from similar if not worse difficulties of integration as $\mathscr{E}(\alpha)$. However, having determined f we can approximate to $f\,\varphi(\tilde{a})$ by some more convenient function and thus calculate ΔP approximately. Taking into account that ΔP is generally only a small correction this latter neglection seems justified.

This error estimate is again an "absolute" one in the sense mentioned in (i). Although ΔP is not a rigorous error bound it can be expected that after gaining experience in the application of the method, its reliability will be sufficient for many purposes. Unfortunately the method fails if $\varphi(\tilde{a})$ is "stable" under the perturbation P in the sense defined by HALL [3], [4].

(iv) Information about the order of magnitude of the error in $\langle\varphi(\tilde{a})|P|\varphi(\tilde{a})\rangle$ may be obtained also in the following way [11]. At first we determine $\varphi(\tilde{a})$. Then we repeat the calculations with another variational wave function obtained from $\varphi(\tilde{a})$ by introducing some new variational parameters which have the effect of improving $\varphi(\tilde{a})$ particularly in those regions in which $|P\,\varphi(\tilde{a})|$ is large. The improvement in the expectation value of P, due to the introduction of the new parameters, can provide information about the order of magnitude of the error in $\langle\varphi(\tilde{a}) \mid P \mid \varphi(\tilde{a})\rangle$.

A possible form of such an "extended" variational wave function may be [11]

$$M(\beta)\left[1 + \beta_0 P + \sum_{h=1}^{H} \beta_h f_h P\right]\varphi(\tilde{a}), \tag{19}$$

where $M(\beta)$ denotes a normalization factor, $\beta_0, \beta_1, \ldots, \beta_H$ denote new variational parameters and the f_h 's denote suitably chosen functions depending on the co-ordinates of the particles comprising the system. The choice of the f_h 's is based on intuition and experience.

4. About the sensitivity of the approximate wave function to changes $u_k \to v_k$

We now discuss some aspects of the problem: how sensitive is the root $\bar{\alpha}$ of (11) to moderate changes $u_k(\alpha) \to v_k(\alpha)$. Unfortunately there seems to be little hope for finding a mathematically rigorous and yet practically useful

answer to this question and consequently we always must strongly rely on numerical experience. However, in order to justify the expectation that MM is a practically useful method and also to make it possible to draw conclusions from a much smaller amount of numerical results than would be possible by considering only the numerical results themselves, it seems useful to make some general investigations into this problem. E.g. it can be shown that even for weight functions $v_k(\alpha)$ strongly differing from the corresponding $u_k(\alpha)$'s the approximate wave function $\varphi(\tilde{a})$ satisfying (16) has certain important properties such that (a) no approximate wave function can be a good approximation to ψ if it does not, at least approximately, possess these properties, and (b) a wave function which is a bad approximation to ψ can only accidentally possess such properties.

As the moments are linear in the weight functions the roots of (16) remain unchanged if we replace the weight functions by $n+1$ linear combinations made up of them. Let us start by constructing such linear combinations $w_l(\tilde{a})$ of the $v_k(\tilde{a})$'s which are more convenient for our purposes than the $v_k(\tilde{a})$'s themselves. We write [2]

$$w_l(\tilde{a}) = \sum_{k=0}^{n} c_{lk} S v_k(\tilde{a}), \qquad (20)$$

$$(c_{lk} = \text{const}),$$

and determine the co-efficients c_{lk} in accordance with the requirements that (a) the $w_l(\tilde{a})$'s should be linearly independent, and (b) n of them, say $w_1(\tilde{a})$, $w_2(\tilde{a}), \ldots, w_n(\tilde{a})$, should satisfy the orthogonality relations [2]

$$\langle w_i(\tilde{a}) \mid \varphi(\tilde{a}) \rangle = 0. \qquad (21)$$

Although these conditions do not uniquely define the $w_l(\tilde{a})$'s, the remaining arbitrariness does not affect our following considerations.

The equations (16) can now be written for $\alpha = \tilde{a}$ and $\alpha_0 = \tilde{a}_0$ as

$$\langle w_l(\tilde{a}) \mid H - \tilde{a}_0 \mid \varphi(\tilde{a}) \rangle = 0. \qquad (22)$$

It is important to note that by (21) the integrals on the left hand side of the last n equations of (22) do not depend on the value $\tilde{a}_0$ and consequently they are equivalent to

$$\langle w_i(\tilde{a}) \mid H - \mathscr{E}(\tilde{a}) \mid \varphi(\tilde{a}) \rangle = 0. \qquad (23)$$

The equations (23) present a convenient starting point for our following considerations.

(i) Let us assume that the $w_i(\tilde{a})$'s are acceptable functions and let us consider the following variational wave function

$$\chi(\beta) \equiv (1 + \beta_0)\,\varphi(\tilde{a}) + \sum_{i=1}^{n} \beta_i\, w_i(\tilde{a}), \tag{24}$$

$$\langle \chi(\beta) \mid \chi(\beta) \rangle = 1, \tag{25}$$

where $\beta \equiv \{\beta_0, \beta_1, \ldots, \beta_n\}$ denotes a set of new variational parameters. The values of the β_k 's can be determined by MEV, and writing out the corresponding equations (cf. Sec. 2. of I) it can be easily verified that by (23) they are satisfied by the values $\beta_k = 0$, i.e. by this procedure we re-obtain $\varphi(\tilde{a})$. Consequently whenever the $w_i(\tilde{a})$'s are acceptable functions the approximate wave functions $\varphi(\tilde{a})$ satisfying (16) is always automatically also an exact solution to a well-defined MEV approximation to ψ. (It is essentially the functions w_i which have been called weight functions in I.)

Although there exist types of weight functions which are of considerable practical interest and do not satisfy the requirement that the $w_i(\tilde{a})$'s constructed from them should be acceptable functions, this requirement does not seem to cause a significant loss of generality. Namely in a majority of such cases the $w_i(\tilde{a})$'s are not acceptable because of their incorrect asymptotical behaviour which makes them unnormalizable. However, in these cases we can always think to have replaced these weight functions (without changing $\tilde{a}$) by such weight functions which are already acceptable but differ markedly from the old ones only in regions far enough to have no marked effect on the investigated properties of the system.

(ii) Let us recall a result derived by SCHWARTZ [12]. It is well known that if $\eta(\tilde{a})$ denotes the error in $\varphi(\tilde{a})$ as defined in (6) and P_i is an arbitrary operator associated with some physical property, the expectation value $\langle \varphi(\tilde{a}) \mid P_i \mid \varphi(\tilde{a}) \rangle$ generally differs from the exact value $\langle \psi \mid P_i \mid \psi \rangle$ by terms proportional to $\eta(\alpha)$, $\eta^2(\alpha)$ and higher powers of $\eta(\alpha)$. SCHWARTZ has shown that if we add to $\langle \varphi(\tilde{a}) \mid P_i \mid \varphi(\tilde{a}) \rangle$ the correction term

$$2Re\langle F_i\, \varphi(\tilde{a}) \mid H - \mathscr{E}(\tilde{a}) \mid \varphi(\tilde{a}) \rangle, \tag{26}$$

where the function F_i satisfies the equation

$$[F_i\ H - H\ F_i]\, \varphi(\tilde{a}) = [P_i - \langle \varphi(\tilde{a}) \mid P_i \mid \varphi(\tilde{a}) \rangle]\, \varphi(\tilde{a}), \tag{27}$$

the error in the corrected expectation value does not contain terms linear in $\eta(\tilde{a})$ and thus can be expected to be, in general, a significantly better approximation to $\langle \psi \mid P_i \mid \psi \rangle$ than is $\langle \varphi(\tilde{a}) \mid P_i \mid \varphi(\tilde{a}) \rangle$.

Now the equation

$$w_i(\tilde{a}) = F_i \varphi\ (\tilde{a}) \tag{28}$$

defines a function F_i, and by (23) for this F_i the correction term (26) vanishes. Consequently it can be expected that $\varphi(\tilde{a})$ is such an approximation to ψ which is particularly suitable for calculating expectation values of operators P which can be expressed as some linear combination of the operators P_i defined by (27) and (28). (Cf. ref. [16.].)

It is possible to obtain equations for the P_i 's directly in terms of the $w_i(\tilde{a})$'s instead of the F_i 's by multiplying (27) from the left by $\varphi(\tilde{a})$ and taking into account (28)

$$w_i(\tilde{a})\mathrm{H}\,\varphi(\tilde{a}) - \varphi(\tilde{a})\mathrm{H}\,w_i(\tilde{a}) = \varphi(\tilde{a})[P_i - <\varphi(\tilde{a}) \mid P_i \mid \varphi(\tilde{a})>]\,\varphi(\tilde{a}). \tag{29}$$

As follows from the results contained in HALL's paper [4] the vanishing of (26) is equivalent to the fact that $\varphi(\tilde{a})$ is "stable" under any perturbation P which can be expressed as some linear combination of the P_i 's.

(iii) The equations (16) have the property that if — accidentally — $\varphi(\bar{\alpha}) = \psi$, the values $\alpha = \bar{\alpha}$ and $\alpha_0 = \bar{\alpha}_0 = E$ satisfy them for a n y set of weight functions whatsoever.

(iv) As pointed out in Sec. 3 of I, for a number of large classes of weight functions strongly differing from each other and being arbitrary to a considerable extent, the results obtained by MM are equal to those obtained by other, more customary and probably highly reliable variational methods of quantum chemistry. This again strongly supports the expectation that the results of MM are not very sensitive to moderate changes of the weight functions.

5. Approximation to the energy

Finally we investigate some problems in obtaining an approximation to the energy of the system in the case when we cannot calculate $\mathscr{E}(\tilde{a})$.

Taking into account that the expectation value of the energy is generally fairly insensitive to a moderate increase of the error in the approximate wave function, the simplest but evidently not very attractive possibility is to carry out a MEV calculation with a variational wave function less accurate but mathematically more convenient than $\varphi(\alpha)$. If the $Sv_k(\tilde{a})$'s are acceptable functions, a possibility of this type is to regard the constants c_{0k} in the first equation of (20) as variational parameters and determine their values from the conditions

$$\langle w_0(\tilde{a}) \mid H \mid w_0(\tilde{a})\rangle = \text{stationary} \tag{30}$$

and

$$\langle w_0(\tilde{a}) \mid w_0(\tilde{a})\rangle = 1. \tag{31}$$

There exists, however, a possibility which seems to be in many respects a better one. It can be shown, namely, that (a) if E is the energy asso-

ciated with the ground state, (b) if we have any normalized acceptable approximation w to $\varphi(\tilde{a})$ for which we can calculate the integrals $\langle w \mid H \mid \varphi(\tilde{a})\rangle$ and $\langle w \mid \varphi(\tilde{a})\rangle$ and which satisfies the condition

$$|1 - \langle w \mid \varphi(\tilde{a})\rangle| \ll 1, \tag{32}$$

and (c) if there is some good reason to expect that $\mathscr{E}(\tilde{a})$ is a much better approximation to E than is $\langle w \mid H \mid w\rangle$, it is advantageous to use instead of $\langle w \mid H \mid w\rangle$ the value $Re\,\tilde{\mathfrak{E}}$

$$\tilde{\mathfrak{E}} \equiv \frac{\langle w| H |\varphi(\tilde{a})\rangle}{\langle w| \varphi(\tilde{a})\rangle} \tag{33}$$

as an approximation to E. (If $w = w_0\,(\tilde{a})$, $\tilde{\mathfrak{E}} = \tilde{a}_0$ and thus $\tilde{\mathfrak{E}}$ can be obtained without solving (30). In this case (13) may automatically ensure (32)).

Let us namely consider the following variational wave function

$$\xi(\gamma_0, \gamma_1) = \gamma_0\, \varphi(\tilde{a}) + \gamma_1\, w, \tag{34}$$

$$\langle \xi(\gamma_0, \gamma_1) \mid \xi(\gamma_0, \gamma_1)\rangle = 1, \tag{35}$$

where γ_0 and γ_1 denote variational parameters. Determining the values of γ_0 and γ_1 by MEV we obtain the secular equation

$$\begin{vmatrix} \langle \varphi(\tilde{a}) \mid H - \mathfrak{E} \mid \varphi(\tilde{a})\rangle & \langle \varphi(\tilde{a}) \mid H - \mathfrak{E} \mid w\rangle \\ \langle w \mid H - \mathfrak{E} \mid \varphi(\tilde{a})\rangle & \langle w \mid H - \mathfrak{E} \mid w\rangle \end{vmatrix} = 0. \tag{36}$$

Denoting by $\mathfrak{E}$ the lower root of (36) we have $E \leqq \mathfrak{E} \leqq \mathscr{E}(\tilde{a})$, and it follows from (32), (33) and (36) that

$$\begin{aligned} |Re\,\tilde{\mathfrak{E}} - \mathfrak{E}| \leqq |\tilde{\mathfrak{E}} - \mathfrak{E}| = |\langle w| \varphi(\tilde{a})\rangle|^{-1} \sqrt{[\mathscr{E}(\tilde{a}) - \mathfrak{E}]\,[\langle w|H|w\rangle - \mathfrak{E}]} \approx \\ \approx \sqrt{[\mathscr{E}(\tilde{a}) - \mathfrak{E}]\,[\langle w| H |w\rangle - \mathfrak{E}]}\,. \end{aligned} \tag{37}$$

Then — assuming (c) and taking into account that the more two positive quantities differ, relatively the closer is their geometrical mean to the smaller one — it immediately follows from (37) that the error in $Re\,\tilde{\mathfrak{E}}$ is much smaller than the error in $\langle w \mid H \mid w\rangle$. Evidently the worse an approximation $\langle w \mid H \mid w\rangle$ (as compared with $\mathscr{E}(\tilde{a})$) to E, the more advantageous is the use of $Re\,\tilde{\mathfrak{E}}$ instead of $\langle w \mid H \mid w\rangle$.

It should be noted that in the case of complicated systems the introduction of o n e s i n g l e variational parameter γ_1 (γ_0 is namely fixed by (35)) is not likely to give a drastic improvement in the energy. Then $\mathscr{E}(\tilde{a}) - \mathfrak{E} \ll$

$\leqslant \mathscr{E}(\tilde{a}) - E$ and this can by (37) have the effect that $Re\ \mathfrak{E}$ is a good approximation to $\mathscr{E}(\tilde{a})$ even if (32) is not fulfilled. In this case, however, the only possibility for obtaining information about the accuracy of $Re\ \mathfrak{E}$ seems to be a "random sampling" type estimate described in (ii) of Sec. 3.

6. Relations of MM to some other variational methods of quantum chemistry

Our aim has been to adapt MM as far as possible to the special needs of quantum echemistry, mainly in order to overcome difficulties of integration. Although MM is one of the standard methods for approximately solving complicated differential and integral equations [13] and it has been successfully used e.g. in the theory of elasticity, it appears to have found only a very few applications in quantum mechanics. Almost all these approaches deal with problems of solid-state physics and band spectra and differ so substantially from the method outlined in the present paper that further comment on this question seems unnecessary [14].

There exist, however, two further initiatives the relation of which to MM is of a considerable interest. Their discussion supplements similar considerations of Sec. 3. of I.

(i) Recently ARMSTRONG [15] has proposed to obtain a qualitative estimate of the error in an approximative wave function φ by comparing the values

$$\mathscr{E} = \frac{\langle 1|H|\gamma\rangle}{\langle 1|\varphi\rangle} \qquad \text{and} \qquad \mathscr{E} = \frac{\langle \varphi|H|\varphi\rangle}{\langle \varphi|\varphi\rangle}, \tag{38}$$

(provided that the denominator $\langle 1/\varphi\rangle$ differs from zero). By comparing (33) and (38) it can be seen that (33) is a straightforward generalization of the first equation of (38).

(ii) In a series of papers [16] HIRSCHFELDER, EPSTEIN, COULSON et. al. have considered the possibility of determining approximate wave functions of molecular systems from the requirement that these should satisfy so called hypervirial relations. The close relation of this approach to MM is evident from the relation of the two methods to MEV (cf. e.g. the quoted paper of EPSTEIN and HIRSCHFELDER). It seems probable that the two initiatives can supplement each other very satisfactorily as the hypervirial relations appear to be excellent tools for investigating problems of theoretical interest but seems less suited for reducing computational difficulties, while the opposite holds for MM.*

* *Note added in proof:* The reader's attention is drawn to a paper by C. A. COULSON, which has recently appeared in Quart.J. Math. (Oxford), **16**, 279,1965.; the results of the paper may prove very useful in eliminating difficulties of integration from calculations of wave functions associated with excited states.

1. Appendix

In the following some practical aspects will be discussed concerning the construction of the weight functions.

(i) Let us consider the equations (10), (13) and (16). In many cases when the relation $v_0(\alpha) \approx u_0(\alpha)$ holds in a large domain of the α_i 's also the relations

$$\partial v_0(\alpha)/\partial\alpha_i \approx \partial u_0(\alpha)/\partial\alpha_i \tag{39}$$

hold, and it may be reasonable to make the choice

$$v_i(\alpha) = \partial v_0(\alpha)/\partial\alpha_i. \tag{40}$$

The computational advantages of such a choice are obvious: (a) we have to approximate to only one function (namely to $u_0(\alpha)$) instead of approximating to $n+1$ ones, and (b) only integrals of the type

$$\langle v_0(\alpha') \mid H - \alpha_0 \mid \varphi(\alpha)\rangle \tag{41}$$

must be calculated for $\alpha' \approx \alpha$ as the integrals on the left hand side of equations (16) can be obtained from (41) by numerically differentiating with respect to the α_i' 's at $\alpha' = \alpha$. It should be noted that generally the calculation of the integrals (41) is not more difficult for $\alpha' \neq \alpha$ than for $\alpha' = \alpha$.

(ii) In some cases it may have advantages to determine at first an approximation to $\tilde{\alpha}$ and $\tilde{\alpha}_0$ from the condition

$$\alpha_0 = \frac{\langle v_0(\alpha)| H |\varphi(\alpha)\rangle}{\langle v_0(\alpha) \mid \varphi(\alpha)\rangle} = \text{stationary}, \tag{42}$$

and use the equations (16) only for refining this approximation. Equation (42) has practical advantages over (16) but it seems less satisfactory from the theoretical point of view.

(iii) The variational wave functions $u_0(\alpha)$ and their derivatives $u_i(\alpha)$ (Eqs. (10)) are in practice always constructed from simple "building elements" by simple operations (mainly multiplication of the building elements and constructing linear combinations of their products). The most frequently used building elements are (a) the cartesian co-ordinates of the particles making up the system, (b) powers and exponential functions of the distances from fixed points or from each other of the particles in the system, (c) exponential functions of linear or quadratic expressions of the cartesian co-ordinates of the particles, and (4) the well known spin functions. We shall denote the building elements occurring in the functions $u_k(\alpha)$ by $f_1, f_2, \ldots, f_P$. Evidently the $u_k(\alpha)$'s are definite functions of the f_p 's [2] and of the α_i 's

$$u_k(\alpha) = U_k(f_1, f_2, \ldots, f_P;\ \alpha_1, \alpha_2, \ldots, \alpha_n), \tag{43}$$

where the f_p 's themselves may depend on the α_i 's.

Now a very convenient way for constructing approximations $v_k(\alpha)$ to the $u_k(\alpha)$'s is to construct at first some mathematically more convenient approximations g_p to the f_p 's

$$g_p \approx f_p \tag{44}$$

and build up the $v_k(\alpha)$'s in the same way from the g_p 's as the $u_k(\alpha)$'s are built up from the f_p 's (cf. Appendix 2.)

$$v_k(\alpha) = U_k(g_1, g_2, \ldots, g_P;\ \alpha_1, \alpha_2, \ldots, \alpha_n). \tag{45}$$

The advantages of this procedure can be more easily seen from a simple illustrative example than from some general consideration. It is well known that the function $\exp(-r)$ can be approximated for not very large $r > 0$ by the polynomial $\sum_{h=0}^{S}{}' (-1)^h (h!)^{-1} r^h$. Now let us assume that some f_q occurring in $u_k(\alpha)$ has the form $\exp(-\alpha_j r)$. If we want to build up g_q in the form $\sum_{h=0}^{S}{}' a_h r^h$ (a_h = const.) we evidently can, in principle, determine the a_h 's e.g. from the condition

$$\langle v_k(\alpha) - u_k(\alpha) \mid v_k(\alpha) - u_k(\alpha) \rangle = \text{minimum}. \tag{46}$$

This procedure would be, however, an extremely tedious one as we had to determine simultaneously all the parameters in all the g_p 's (among them the a_h 's) for every value of k and even for every set of α_i 's anew. On the other hand by making the choice $g_q = \sum_{h=0}^{S}{}' (-1)^h (h!)^{-1} (\alpha_j r)^h$ the work of calculating the a_h 's is completely eliminated. This choice will probably pay off in most cases inspite of the fact that it does not provide the "absolute best" values of the a_h 's.

(iv) Let us finally list some types of functions which seem to have particular advantages if serving as building elements of weight functions [17]. This list is by far not complete and perhaps experience will teach us also other possibilities.

(a) At first we limit our considerations to cases when the wave function $\varphi(\alpha)$ consists of a linear combination of products of one-particle spin-orbitals and these spin-orbitals themselves are linear combinations of Slater-functions centered at arbitrary points and having integer principal quantum numbers. In this case it is natural to construct also the weight functions in the form of linear combinations of products of one-particle "spin-orbitals". The following types of functions seem to have advantages if serving as building elements of the one-particle "orbitals" comprising the weight functions:

(a/1) Polynomials of the cartesian co-ordinates of the particle. It can be easily verified that the most complicated integrals occurring in the moments are in this case two-center Coulomb integrals.

(a/2) Linear combinations of Boys-functions [18] depending on the co-ordinates of the particle. In this case the calculation of the moments can be easiliy performed by expanding also the Slater functions in $\varphi(\alpha)$ in terms of Boys-functions [19].

In practice such an expansion always means that we replace the Slater-functions in $\varphi(\alpha)$ by a finite linear combination of Boys-functions and thus in certain special cases this procedure simply coincides with carrying out a MEV approximation with a variational wave function built up from Boys-functions instead of Slater-functions. Yet the application of MM can provide considerable computational advantages because of the following reasons:

The obtaining of a good approximation to a Slater-function requires the use of a very high number of Boys-functions. Now evidently the number of Boys-functions used for expanding the Slater-functions in $\varphi(\alpha)$ is fixed by the required degree of accuracy and m u s t n o t be reduced. However, as it can be expected that the root $\bar{\alpha}$ of (11) is not very sensitive to moderate changes of the $u_k(\alpha)$'s, it can be expected, that the $v_k(\alpha)$'s can be constructed without a considerable loss of accuracy by expanding the Slater-functions in the $u_k(\alpha)$'s in terms of a much smaller number of Boys-functions than in $\varphi(\alpha)$. This leads to a very significant decrease in the number of integrals to be computed.

(a/3) Linear combinations of plane waves depending on the co-ordinates of the particle. In this case the situation is analogous to that discussed in (a/2), but the plane waves seem to be less advantageous for atomic and molecular problems apart perhaps from delocalized π-electron systems.

(b) Let us finally consider variational wave functions $\varphi(\alpha)$ consisting of a linear combination of products of (spin-) geminals which c a n n o t be reduced to a finite linear combination of products of one-particle spin-orbitals. In this case it seems advantageous to use weight functions consisting of a linear combination of products of o n e - p a r t i c l e "spin-orbitals". The advantages of this choice are: (a) no integrals involving inseparably the co-ordinates of more than four particles occur in the moments (in contrast to the case of MEV which requires the calculation of integrals in which the co-ordinates of a l l particles may occur inseparably), and (b) there exist possibilities of overcoming difficulties associated with the strong orthogonality conditions for the geminals [20].

2. Appendix

The following simple example can illustrate the main steps of an MM calculation [21], [22].

The electronic wave function associated with the ground state of the neutral helium atom can be approximated by the variational wave function

$$u_0(\alpha) = u_0(\alpha_1) = e^{-\alpha_1 r_1} e^{-\alpha_1 r_2}, \tag{47}$$

where r_1 and r_2 denote the distance from the nucleus of the electrons 1 and 2, respectively, and spin co-ordinates have been disregarded. $u_0(\alpha)$ can be regarded as being the product of the "building elements"

$$f_1 = e^{-\alpha_1 r_1};\ f_2 = e^{-\alpha_1 r_2}, \tag{48}$$

$$u_0(\alpha) = f_1 \cdot f_2 . \tag{49}$$

Now the function e^{-r} can be approximated by the function $0{,}473\, e^{-0{,}27 r^2}$ [23]. Consequently it can be attempted to make the choice

$$g_1 = 0{,}473\, e^{-0{,}27(\alpha_1 r_1)^2};\ g_2 = 0{,}473\, e^{-0{,}27(\alpha_1 r_2)^2}. \tag{50}$$

From (48), (49) and (50) we have in accordance with (45)

$$v_0(\alpha) = g_1 \cdot g_2 = 0{,}224\, e^{-0{,}27(\alpha_1 r_1)^2}\, e^{-0{,}27(\alpha_1 r_2)^2}. \tag{51}$$

For $v_1(\alpha)$ we make in accordance with (40) the choice

$$v_1(\alpha) = \partial\, v_0(\alpha)/\partial\alpha_1 . \tag{52}$$

Then equations (16) give the result

$$\tilde{\alpha}_0 = -2{,}766 \text{ at.u.}$$
$$\tilde{\alpha}_1 = \ \ 1{,}643 \text{ at.u.}$$

The corresponding MEV results are

$$\bar{\alpha}_0 = -2{,}848 \text{ at.u.}$$
$$\bar{\alpha}_1 = \ \ 1{,}688 \text{ at.u.}$$

Some further numerical examples can be found in Sec. 5. of I.

REFERENCES AND NOTES

1. T. Szondy, Acta Phys. Hung., **17**, 303, 1964. This paper will be referred to as I.

2. It will be tacitly assumed throughout the paper that the subscript i runs from 1 to n, the subscript p runs from 1 to P, and the subscripts k and l run from 0 to n.

3. G. G. Hall, Phil. Mag. (8), **6**, 249, 1961.

4. G. G. Hall, Accuracy of Calculated Atomic and Molecular Properties. [Advances in Quantum Chemistry, Vol. 1. (Edited by Per-Olov Löwdin.) Academic Press, New York—London, 1964.]

5. E. Kapuy, to be published in J. Chem. Phys.

6. (11) follows from (8) if we regard $Re\ a_i$ and $Im\ a_i$ as independent parameters. Otherwise (11) has to be replaced by

$$\langle u_k(a)\, |H - a_0|\, \varphi(a)\rangle + \langle \varphi(a)\, |H - a_0|\, u_k(a)\rangle = 0 .$$

All our considerations can be repeated by starting from these equations instead of (11).

7. This definition differs from the terminology used in I. As to the relation of the two terminologies cf. Sec. 4.

8. An excellent survey of this question has been given by H. PREUSS in Fortschritte der Physik, **10,** 271, 1962.

9. This implies that the sets $\delta_r^{(1)}(a)$, $\delta_k^{(2)}(a)$, ... must be linearly independent.

10. J. C. Y. CHEN and A. DALGARNO, Proc. Phys. Soc., **85,** 399, 1965.

11. G. G. HALL, refs. [3] and [4].

T. SZONDY and I. VÁGÓ, Z. Naturforschg., **18***a*, 263, 1963. The reader's attention is called to the fact that some results of the latter paper are already contained in the paper [3] of HALL. Unfortunately HALL's paper escaped our attention and we did not refer to it.

Cf. also H. PREUSS, Z. Naturforschg., **13***a*, 439, 1958; **16***a*, 598, 1961.

12. C. SCHWARTZ, Annals of Physics, **6,** 170, 1959. See also ref. [4].

13. See e.g. L. COLLATZ, Numerische und graphische Methoden. [Encyclopedia of Physics, Vol. II. Springer, Berlin—Göttingen—Heidelberg, 1955.].

14. The list of references we present here is by no means a complete one, but we expect that it can illustrate the main features of the other approaches: E. W. MONTROL, J. Chem. Phys., **10,** 218, 1942; **11,** 481, 1943; J. H. VAN VLECK, Phys. Rev., **74,** 1168, 1948; L. C. BROWN, P. M. PARKER, Phys. Rev., **100,** 1764, 1955; F. R. HALPERN, Phys. Rev., **107,** 1145, 1957; K. REBANE, O. SIL'D, "Semicoductor Physics Conference, Prague, 1960, p. 353; R. A. COLDWELL—HORSFALL, A. A. MARADUDIN, J. Math. Phys., **1,** 395, 1960; J. C. BRADLEY, Ann. Phys., **15,** 411, 1961.

15. B. H. ARMSTRONG, Bull. Am. Phys. Soc., *9*, 401, 1964. Cf. also R. J. DRACHMAN, Phys. Rev., **136***A*, 641, 1964.

16. J. O. HIRSCHFELDER, J. Chem. Phys., **33,** 1462, 1960. S. T. EPSTEIN and J. O. HIRSCHFELDER, Phys. Rev., **123,** 1495, 1961. J. O. HIRSCHFELDER and C. A. COULSON, J. Chem. Phys., **36,** 941, 1962. J. C. Y. CHEN, J. Chem. Phys., **40,** 615, 1964. S. I. VETCHINKIN, J. Chem. Phys., **41,** 1991, 1964. P. D. ROBINSON, Proc. Roy. Soc., *A***283,** 229, 1965. W. A. SANDERS and J. O. HIRSCHFELDER, J. Chem. Phys., **42,** 2904, 1965. and many other papers.

The investigations into the relation of MM and the method of SCHWARTZ were initiated by the closely related results of ROBINSON.

17. A part of these results is contained in Sec. 4. of I.

18. In analogy with the widely used term "Slater-functions" we shall call "Boys-functions" such functions which consist of a polynomial of the cartesian co-ordinates of certain particles (in our case of one particle) multiplied by an exponential function of a real, positive definite, second-order polynomial of the same co-ordinates. (Cf. ref. [19].)

19. S. F. BOYS, Proc. Roy. Soc. (Lond.), **258,** 402, 1960. K. SINGER, Proc. Roy. Soc. (Lond.), **258,** 412, 1960. R. KIKUCHI, J. Chem. Phys., **22,** 148, 1954.

20. Dr. E. KAPUY has been so kind as to call our attention to this possibility. The problems of orthogonality relations within the framework of MM will be investigated in detail in a subsequent paper.

21. As has been mentioned in Sec. 1., in so simple cases as that to be considered below the use of MM provides no computational advantages over MEV. The example is meant purely as an illustration of the m a i n s t e p s of an MM calculation.

22. Until some problems strongly affecting the computational work (e.g. the problems of orthogonality relations) are not investigated in detail, it appears better not to get involved into an extensive computation, as there is a significant danger of doing a great deal of useless extra work.

23. The function $0{,}473\ e^{-0{,}27r^2}$ has the same norm as e^{-r} and the scale factor 0,27 has been determined from the requirement that the Gaussian function should have a maximum overlap with the exponential one.

ОПРЕДЕЛЕНИЕ ВОЛНОВОЙ ФУНКЦИИ МОЛЕКУЛЯРНЫХ СИСТЕМ МЕТОДОМ МОМЕНТОВ, II.

Е. СОНДИ и Т. СОНДИ

Р е з ю м е

Пусть H — оператор Гамильтона молекулярной системы $\varphi(\alpha_1, \alpha_2, \ldots \alpha_n)$ — вариационная волновая функция, содержащая сеть вариационных параметров $\alpha_1, \alpha_2, \ldots \alpha_n$, далее $u_0, u_1, \ldots u_n$ — сеть произвольных линейно независимых функций, зависящих от тех же самых координат, что и φ.

В специальном случае

$$u_0 = \varphi \qquad u_i = \partial\varphi/\partial a_i\,; \qquad (i = 1,\ 2, \ldots n)$$

корни системы уравнений

$$< u_k \mid H - \varepsilon \mid \varphi > = 0 \qquad (k = 0,1, \ldots n) \qquad (*)$$

$a_1, a_2 \ldots a_n$ и ε совпадают со значениями вариационных параметров и энергии соответственно, полученными методом вариации энергии.

Есть основание предполагать, что корни выражения (*) во многих случаях довольно нечувствительны по отношению небольшого отклонения функции u_0 от φ и функций u_i от $\partial\varphi/\partial a_i$. Следовательно, целесообразным является решить уравнения приближенно, заменяя функции u_k некоторым, с математической точки зрения более подходящим приближением: $v_0 \approx \varphi$ и $v_i \approx \partial\varphi/\partial a_i$. Данная возможность оказывается эффективным приемом для уменьшения трудностей при интегрировании, и, таким образом, для расширения области применимости вариационного метода на смежные — при современном уровне вычислительной техники — области применимости метода вариации энергии.

В настоящей работе главным образом рассмотрены следующие вопросы: *а)* практическая сторона применения упомянутых приближенных приемов к проблемам квантовой химии; *б)* вопросы, касающиеся надежности полученных результатов.

THEORY OF CONGRUENCE IN GRAVITATIONAL FIELDS III.

SPACE INVERSION AND GRAVITATION

By

M. SÜVEGES

RESEARCH GROUP FOR THEORETICAL PHYSICS OF THE HUNGARIAN ACADEMY OF SCIENCES, BUDAPEST

(Presented by A. Kónya, — Received 31. VII. 1965)

The inversion part of the holonomy group, which is a good physical symmetry group locally, is investigated. It is shown that the existence of inversions depends on the topological properties of the gravitational field (supposed to be a Riemannian manifold M_n). Therefore M_n is defined to be a differentiable manifold and the Theorem on parallelism is extended to this case. It is shown that if M_n is orientable then Ψ is a subgroup of $SO(n)$ and if M_n is non-orientable then Ψ is a subgroup of $O(n)$. More precisely there exists a homomorphism $h : \pi_1(M_n) \to O(n)/SO(n)$, where $\pi_1(M_n)$ is the first homotopy group of M_n and the topologically invariant classification of gravitational fields according to factor groups of $\pi_1(M_n)$ is physically meaningful. Besides some simple examples space forms of zero and constant positive local curvature are classified. For example, there exists an infinity of 3-dimensional forms of positive curvature but local space inversion is not a good operation in either of them. It is also pointed out that physical space is not simply a Riemannian manifold M_n but a fibre bundle over M_n. Therefore the theory of fibre bundles with structure group over a differentiable manifold is used.

Introduction

In two previous papers [1, 2] it has been shown that the holonomy group (hg) Ψ of a gravitational field, assumed to be a Riemannian manifold M_n, is a good local physical symmetry group in the tangent space et each point of M_n. In a Riemannian manifold Ψ is a subgroup of the orthogonal group 0(n) and in [2] the identity component Ψ^0 (denoted previously by σ_x) of Ψ was discussed. It has been shown that the Lie-algebra of Ψ^0, the restricted hg, is given in terms of the Riemannian curvature tensor and its covariant derivatives. In particular, when M_n is of signature $+2$ then Ψ is a subgroup of the Lorentz group L and Ψ^0 is a subgroup of the restricted Lorentz group $L_+^\uparrow$. Physical consequences of this fact were discussed.

In the present paper we are going to deal with the discrete operations of Ψ. More precisely, given a gravitational field M_n we want to know whether its hg involves inversions or not. To grasp the nature of the problem consider the following simple example.

Suppose M_n is simply connected. Then every closed curve at any point $x \varepsilon M_n$ is homotopic to zero and hence the hg Ψ is equal to Ψ^0. Thus the hg of a simply connected M_n does not contain inversions and the possibility of inversions can happen only if M_n is not simply connected.

It is seen from this that the hg depends in a crucial way on the topological properties of the manifold. Therefore the rather loose term "Riemannian manifold" we used (and is usually used in classical relativity) up to now will not serve but must be made more precise by the introduction of topological properties into the concept of M_n.

This will be done by means of the concept of a Riemannian manifold as a differentiable manifold. Particular attention will be paid to the orientation of a differentiable manifold since, as will be seen, it plays a crucial role in the determination of the inversions in Ψ. In particular, for an orientable M_n Ψ is reduced to Ψ^0.

Before proceeding, however, to mathematical definitions we make one more remark. In usual geometrical theories of gravitation one is dealing with such objects as points, curves, geodesics, tensors. We have, however, seen that since the hg is a good physical symmetry group, each tangent space is provided with a structure defined by Ψ. So we have a superstructure at each point of the Riemannian manifold and we want to build this superstructure into the theory in a systematic way. This will be done by introducing the concept of a fibre bundle with a structure group over a differentiable manifold.

We first give the necessary mathematical definitions and theorems, then generalise the theorem of [1] and try to draw some consequences concerned with inversions in Ψ.

All the mathematical results needed in this paper are contained in standard books on global geometry such as those by LICHNEROWICZ [3], NOMIZU [4], KOBAYASHI and NOMIZU [5], and RINOW [6]. Since, however, they are scattered throughout these books we start by presenting them in an organised fashion most suitable for our purpose.

1. Differentiable manifolds, orientation

An n-dimensional manifold is a connected, separable topological space in which each point has a neighbourhood homeomorphic to some open set in Cartesian n-space R^n. A system S of differentiable coordinates, or atlas, in an n-manifold M_n is a family $\{U_\alpha\}$ of open sets covering M_n and for each α a homeomorphism

$$\varphi_\alpha : U_\alpha \to R^n_\alpha,$$

where R^n_α is an open set in R^n, such that the map

$$\varphi_\alpha \varphi_\beta^{-1} : \varphi_\beta (U_\alpha \cap U_\beta) \to \varphi_\alpha (U_\alpha \cap U_\beta) \tag{1}$$

is differentiable. The pairs $(U_\alpha, \varphi_\alpha)$ are called charts, or local coordinates in M_n. If such a map has continuous derivates of order r then S is said to be of

class C^r. If S and S' are two systems of coordinates in M_n of class C^r they are said to be r-equivalent if the composite families $\{U_\alpha, U'_\beta\}$, $\{\varphi_\alpha, \varphi'_\beta\}$ form a system of class C^r. A differentiable manifold M_n ([3], Chapitre I) of class C^r is an n-manifold M_n together with an r-equivalence of coordinate systems in M_n.

It should be noted that this definition of a differentiable manifold coincides with the more usual definition in terms of differentiable functions ([4], Chap. 1). The one given here is more convenient for geometry.

If $x \varepsilon U_\alpha \cap U_\beta$, let us denote the Jacobian $n \times n$ matrix of the coordinate transformation (1) by $a_{\beta\alpha}(x)$ at $\varphi_\beta(x)$. From the equation

$$a_{\alpha\gamma}(x)\, a_{\gamma\beta}(x) = a_{\alpha\beta}(x), x \varepsilon U_\alpha \cap U_\beta \cap U_\gamma$$

it immediately follows that $a_{\alpha\beta}(x)$ lies in $GL(n, R)$ and we have $a_{\alpha\beta} : U_\alpha \cap U_\beta \to \to GL(n, R)$.

An atlas S is called oriented if the determinant of $a_{\alpha\beta}(x)$ is positive for all α, β and $x \varepsilon U_\alpha \cap U_\beta$. If S and S' are two oriented systems, one can show that the Jacobian matrices of $\varphi'_\alpha \varphi_\beta^{-1}$ have determinants which are either positive for all α, β and $x \varepsilon U_\alpha \cap U_\beta$ or negative for all α, β and $x \varepsilon U_\alpha \cap U_\beta$. One says that S and S' are positively or negatively related. In this way oriented coordinate systems fall into two classes. Systems in the same class are positively related, systems in different classes negatively. Each class is called an orientation of the manifold M_n. If M_n admits an oriented system we say it is orientable. If this is not the case we say it is non-orientable. An oriented system has two orientations and orientation can be reserved by the transformation

$$(x^1, x^2, \ldots x^n) \to (-x^1, x^2, \ldots, x^n).$$

The transformation $\varphi_\alpha \varphi_\beta^{-1}$ at $x \varepsilon U_\alpha \cap U_\beta$ for every α and β induces a transformation in the tangent space at x of M_n. Since the induced transformations are given just by $a_{\alpha\beta}$, it is easy to see that the tangent spaces over an orientable differentiable manifold M_n fall naturally into two classes. Those in one class are arbitrarily described as right-handed and those in the other as left-handed.

2. Fibre bundles

Consider now the tangent space $T_x(M_n)$ at a point x of the differentiable manifold M_n.

A linear frame $u(x)$ at $x \varepsilon M_n$ is an ordered basis of the tangent space $T_x(M_n)$. Let $Q(x)$ be the set of all linear frames at $x \varepsilon M_n$ and let $L(M_n)$ be the set of all linear frames at all points of M_n

$$L(M_n) = \bigcup_{x \in M_n} Q(x).$$

$L(M_n)$ can now be made into a principal fibre bundle ([5], Chap. I): If a point in $L(M_n)$ is defined by the local coordinates x of the origin of the frame $u(x) \varepsilon L(M_n)$ at x and by the matrix defining u with respect to the natural frame at x and π is the projection which maps a linear frame u at x into x, then $L(M_n)$ is a fibre bundle over M_n with $GL(n, R^n)$ as structure group. This bundle is called the bundle of linear frames over M_n . The transition functions $\psi_{\alpha\beta}$ are in this case given by the Jacobian $a_{\alpha\beta}$ of the transformation (1)

$$\varphi_\alpha \varphi_\beta^{-1} : \varphi_\beta (U_\alpha \cap U_\beta) \to \varphi_\alpha (U_\alpha \cap U_\beta).$$

Since the linear group admits two components, there exist at a point $x \varepsilon M_n$ two arcwise-connected families of frames. The determinant associated with two frames in the same family is positive and with frames in different families is negative. Consequently, the bundle $L(M_n)$ either admits two arcwise-connected components or itself is arcwise-connected. Since the transition functions are given by a $a_{\alpha\beta}$ it is seen that in the first case the base manifold M_n is orientable and in the second case it is not. Conversely, if M_n is orientable then the first case is realised and if it is not orientable then the second.

If M_n is orientable then we denote by $L^0 (M_n)$ one of the components of $L(M_n)$. It is a principal bundle with structure group the identity component of the linear group.

Obviously, tensor bundles $T_r^s (M_n)$ of type (r, s) over M_n associated with $L(M_n)$ can be defined by regarding $GL(n, R)$ as a group of linear transformations of the tensor space T_r^s over the vector space R^n. The transition functions can again be constructed in straightforward way.

3. Connections, holonomy groups

Let $P(M_n, G)$ be a principal fibre bundle over a differentiable manifold M_n with structure group G. If $T(P)$ is the tangent space of P at $u \varepsilon P$, then a global connection Γ in P can be defined in the usual way by splitting up $T(P)$ into the direct sum of vertical and horizontal subspaces ([5], Chap. II) Given a connection Γ in P one can then define the connection form, which is a 1-form ω on P with values in the Lie-algebra k of G. This, in turn, can be expressed in terms of a family of local connection forms ω_α each defined on U_α for an open covering $\{U_\alpha\}$ of M_n. These k-valued local 1-forms are such that they satisfy for each intersection the transformation law

$$\omega_\alpha = (ad\, a_{\alpha\beta}^{-1})\, \omega_\beta + a_{\alpha\beta}^{-1}\, da_{\alpha\beta}$$

for each $x \varepsilon U_\alpha \cap U_\beta$, where $a_{\alpha\beta} \varepsilon G$.

By means of the connection Γ one can define parallel displacement of

fibres along any given curve τ in the base manifold. More precisely, let $\tau = x_t$, $0 \leqslant t \leqslant 1$, be a curve in M_n. A horizontal lift, or simply a lift of τ is a horizontal curve $\tau^* = u_t$, $a \leqslant t \leqslant b$, in $P(M_n, G)$ such that $\pi(u_t) = x_t$. A horizontal curve in P means now a curve whose tangent vectors are all horizontal. It can be shown that the lift τ^* of τ through $u_0 \varepsilon \pi^{-1}(x_0)$ is unique. Consider now τ^* through u_0 having end point u_1 such that $\pi(u_1) = x_1$. By varying u_0 in the fibre $\pi^{-1}(x_0)$ we get a mapping of the fibre $\pi^{-1}(x_0)$ onto the fibre $\pi^{-1}(x_1)$ which maps u_0 into u_1. This mapping will be denoted by the same letter τ and will be called the parallel displacement of the fibre along τ.

Consider now the loop space $C(x)$ at x. For each $\tau \varepsilon C(x)$ the parallel displacement along τ is an isomorphism of the fibre $\pi^{-1}(x)$ onto itself. The set of all isomorphisms forms a group which is the holonomy group of Γ with reference point x. The restricted hg Ψ^0 is defined similarly by means of the subset $C^0(x)$ of $C(x)$ consisting of loops homotopic to zero.

We now introduce the holonomy bundle which is important in our further work. This is made possible by the following theorem ([5], Chap. II), which in fact says that the holonomy bundle is a fibre bundle in its own right.

Theorem. (Reduction theorem.) Let $P(M_n, G)$ be a principal fibre bundle with a connection Γ, where M_n is connected and paracompact. Let u_0 be an arbitrary point of P. Denote by $P(u_0)$ the points in P which can be joined to u_0 by a horizontal curve. Then

(1) $P(u_0)$ is a reduced bundle with structure group $\Psi(u_0)$;

(2) The connection Γ is reducible to a connection in $P(u_0)$.

In other words the holonomy group defines a subbundle of $P(M_n, G)$ which will be called the holonomy bundle $P(u)$ at a point $u \varepsilon P$. It is obvious that $P(u) = P(v)$ if and only if u and v can be joined by a horizontal curve. Since the relation $\sim$ ($u \sim v$ if u and v can be joined by a horizontal curve) is an equivalence relation we have for any u and v of P that either $P(u) = Pv)$ or $P(u) \cap P(v)$ is empty. In other words P is decomposed into the disjoint union of the holonomy bundles. However, from the fact that every $a \varepsilon G$ maps each horizontal curve into a horizontal curve, it is easy to see that the holonomy bundles $P(u)$ are all isomorphic to each other.

It is an important fact that the holonomy groups can be defined in a different way as follows: The hg $\Psi(u)$ at $u \varepsilon P$ is the set of elements $a \varepsilon G$ such that u and ua can be connected by a horizontal curve ([5], Chap II). In this way the hg is realised as a Lie-subgroup of the structure group G which is an important fact: For example, for an orientable M_n G is the identity component of $GL(n; R^n)$ in $L(M_n)$ and thus Ψ cannot contain inversion.

However, to study inversions in Ψ it is often more advantageous to go over to the universal covering $\widetilde{M}_n$ of M_n (for covering manifolds see [6], Kap. 5) since this will give rise to a classification scheme which is physically meaningful.

That the hg of M_n can be studied on $\widetilde{M}_n$ can be seen as follows.

4. Holonomy and homotopy

First of all, the restricted hg Ψ^0 of M_n and the restricted hg $\widetilde{\Psi}^0$ of its universal covering $\widetilde{M}_n$ coincide. Roughly speaking, this follows from the fact that to loops based at x in M_n homotopic to zero there correspond loops at $\tilde{x}$ in $\widetilde{M}_n$ in the same equivalence class with respect to homotopy and vice versa. More precisely let M_n and M_n' be Riemannian manifolds with metrics g and g', respectively. If the mapping $f: M_n \to M_n'$ is isometric, i.e. if $g(X, Y) = g'(f_* X, f_* Y)$ for all $X, Y \varepsilon T_x(M_n)$, where $f_* : T_{x'}(M_n)$ then we have the following theorem [5].

Theorem. If f is an isometry of a Riemanniann manifold M_n onto another Riemannian manifold M_n', then the differential of f commutes with parallel displacement. More precisely, if τ is a curve (and the parallel displacement) from x to y in M_n, then the following diagram is commutative:

$$\begin{array}{ccc} T_x(M_n) & \xrightarrow{\tau} & T_y(M_n) \\ f_* \downarrow & & f_* \downarrow \\ T_{x'}(M_n') & \xrightarrow{\tau'} & T_{y'}(M_n') \end{array}$$

where $x' = f(x)$, $y' = f(y)$ and $\tau' = f(\tau)$.

The statement above follows by applying this theorem to the case when f is an isometric immersion of M_n into M_n'.

We now discuss the relationship between the inversion operations of Ψ and the first homotopy group π_1. Consider the loop space $C(x)$ based at x in the base manifold M_n and the horizontal curves constructed over $C(x)$. Take any two loops $C_1(x)$ and $C_2(x)$ which are in the same homotopy class. If the horizontal curves over $C_1(x)$ and $C_2(x)$ connect the points u to ua_1 and u to ua_2, respectively, $(a_1, a_2 \varepsilon \Psi)$ then the horizontal curve connecting u to $ua_2^{-1}a_1$ projects on the curve

$$C_2^{-1}(x)\, C_1(x),$$

which is homotopic to zero. Therefore it follows ([3], Chap. II) that $a_2^{-1}a_1 \varepsilon \Psi^0$ and it is easy to see that there exists a homomorphism h

$$h : \pi_1(x) \to \Psi(u)/\Psi^0(u),$$

where $\pi_1(x)$ is based at $x = \pi(u)$.

In other words Ψ/Ψ^0 is isomorphic to a factor group of the first homotopy group π_1 which is, in turn, isomorphic to a group of deck transformations ([6], Kap. 5) of $\widetilde{M}_n$ at least for locally simply connected and locally compact

M_n. Consider now the set D of all possible groups of discrete isometries acting freely on $\widetilde{M}_n$. Then each $d \varepsilon D$ is a deck transformation group of $\widetilde{M}_n$ and the factor spaces $\widetilde{M}_n/d$, $d \varepsilon D$, all have $\widetilde{M}_n$ as their universal covering. Moreover, the fundamental group $\pi_1(\widetilde{M}_n/d)$ of each factor space $\widetilde{M}_n/d$ is isomorphic to the corresponding group d.

Now all these factor spaces are topologically distinct. However, they can be divided into two large classes according to whether the homomorphism $h : \pi_1(\widetilde{M}_n/d) \to \Psi(\widetilde{M}_n/d)/\Psi^0(\widetilde{M}_n/d)$ is trivial or not. In the first class $\widetilde{M}_n/d$ is orientable and $\Psi(M_n/d)$ is reduced to $\Psi^0(M_n/d)$ that is Ψ does not contain inversion.

Obviously, the classification according to π_1 itself, rather than to its quotient groups, is more detailed and contains more information. It should also be noted that these classifications are topologically invariant ones since the fundamental group π_1 is a topological invariant.

For the sake of completeness we mention some well-known facts about Riemannian manifolds to show how these arise on a general differentiable manifold.

5. Riemannian manifolds

A Riemannian metric tensor of class C^V is defined to be a positive definite symmetric second order tensor of class C^V. If a differentiable manifold M_n of class C^u admits a Riemannian metric tensor of class C^V then it is said to be a Riemannian manifold of class C^V. According to a theorem of Whitney every differentiable manifold M_n of class C^u admits a Riemannian metric tensor of class C^{u-1}. In what follows we restrict attention to positive definite Riemannian metrics and always suppose differentiability sufficient for the purpose at hand.

Now every Riemannian metric tensor g defines an inner product in each tangent space $T_x(M_n)$ denoted by $g_x(X, Y)$, $X, Y \varepsilon T_x(M_n)$ and it is well known that there is a 1 : 1 correspondence between the set of Riemannian metrics and the set of reductions of the bundle $L(M_n)$ of linear frames to the bundle $O(M_n)$ of orthonormal (with respect to g) frames with structure group the orthogonal group $O(n)$.

In the principal fibre bundle $O(M_n)$ one can again introduce a connection. Given an open covering $\{U_\alpha\}$ of M_n and local sections of $O(M_n)$ over each U_α, the local connection is defined by an o-valued 1-form ω_α, on each U_α, where o is the Lie-algebra of the orthogonal group $O(n)$. These local 1-forms are then assembled by means of the transition functions: If $u_\alpha(x)$ is a representative of $O(M_n) \mid U_\alpha$ at $x \varepsilon U_\alpha$ and $c_{\alpha\beta}$ is an orthogonal matrix then

$$u_\alpha(x) = c_{\alpha\beta} u_\beta(x)$$

and for $x \varepsilon U_\alpha \cap U_\beta$ the matrices ω_α must satisfy

$$\omega_\alpha = (ad\, c_{\alpha\beta}^{-1})\, \omega_\beta + c_{\alpha\beta}^{-1}\, dc_{\alpha\beta}\,.$$

Obviously, if M_n is orientable then $O(M_n)$ admits two arcwise-connected components. If $O^0\,(M_n)$ is one of them then it is a principal fibre bundle with structural group $SO(n)$. If M_n is not orientable then $O(M_n)$ has only one arcwise connected component with structure group $O(n)$.

A linear connection Γ in the bundle of linear frames $L(M_n)$ is called a metric connection if it is determined by a connection in $O(M_n)$. The following two theorems ([5], Chap. IV.) settle the existence problem of Levi-Civita connections on M_n.

Theorem. A linear connection Γ of a Riemannian manifold M_n with metric g is a metric connection if and only if g is parallel with respect to Γ.

Theorem. Every Riemannian manifold admits a unique metric connection with vanishing torsion.

This the Levi-Civita connection. Other concepts in Riemannian geometry, such as covariant derivative, curvature tensor and the like can now be introduced. We, however, content ourselves by clarifying the above definitions and concepts on a few examples in terms of local coordinates. For example the Levi-Civita connection is just given by the Christoffel symbols $\Gamma_{\alpha\beta}^{\gamma}$. Or, for example the connection forms ω_α in $L(M_n)$ are of the form

$$\omega_j^i = Y_k^i\,(d\,X_j^k + \Gamma_{ml}^k\, X_j^l\, dx^m),$$

where Y_k^i is the dual of X_i^k and x^i is a local coordinate system in U_α. In particular, in the bundle $O(M_n)$ the X_k^i are orthonormal with respect to g and the ω_j^i are just the Ricci rotation coefficients. As a last example, the transition functions $\psi_{\alpha\beta}$ for $L(M_n)$ in terms of local coordinates are just given by

$$\psi_{\alpha\beta} = \frac{\partial x^i}{\partial \bar{x}^j}\,,$$

where x^i and $\bar{x}^j$ are local coordinates in two neighbourhoods U_α and U_β, respectively.

6. Extension of the Theorem on congruence and applications

In the introduction we mentioned the need for the incorporation of topological properties into the definition of gravitational fields. This will now be done by supposing gravitational fields to be described by differentiable manifolds M_n provided with Riemannian metric tensors (we restrict attention to positive definit metrics). In this case, however, one has to revise the proof of the Theorem on congruence.

Obviously, if M_n can be covered by one coordinate neighbourhood U the Theorem is valid and trouble arises only when this cannot be done. Suppose then that M_n is covered by a set of neighbourhoods $\{U_\alpha\}$ each provided with a local coordinate system x_α. Since the manifold M_n is supposed to be connected any two points can be connected by a curve C. Suppose C passes through the neighbourhoods U_1, U_2, . . . and denote by C_α the restriction $C \mid U_\alpha$ of C to U_α. It is obvious that in each U_α the proof can be carried through by introducing orthonormal frames which are parallel (with respect to the local connection Γ_α defined in U_α) along C_α. When this had been done one has only to assemble the frames in the intersections of U_1, U_2, . . . accroding to the transition functions $\psi_{\alpha\beta}(x)$ at $x \varepsilon U_\alpha \cap U_\beta$ for all intersections. In this way one can introduce a Fermi system all along C and with this the theorem is extended for arbitrary differentiable Riemannian manifolds.

The contents of the two previous papers can now be reformulated in terms of differentiable manifolds and fibre bundles. We content ourselves to enumerate some relevant theorems. First of all we note that the hg Ψ is a subgroup of the structure group G.

Theorem. (a) If $v = ua$, $a \varepsilon G$ and $v,u\varepsilon P(M_n,G)$, then $\Psi(v) = ad(a^{-1})\Psi(u)$ that is, the holonomy groups $\Psi(u)$ and $\Psi(v)$ are conjugate in G. Similarly, $\Psi^0(v) = ad(a^{-1})\Psi^0(u)$,

(b) If two points u and v of P can be joined by a horizontal curve, then $\Psi(u) = \Psi(v)$ and $\Psi^0(u) = \Psi^0(v)$.

Theorem. Let $P(M_n, G)$ be a principal fibre bundle whose base manifold M_n is connected and paracompact. Let $\Psi(u)$ and $\Psi^0(u)$, $u\varepsilon P$, be the holonomy group and the restricted holonomy group of a connection Γ with reference point u. Then

(a) $\Psi^0(u)$ is a connected Lie subgroup of G;

(b) $\Psi^0(u)$ is a normal subgroup of $\Psi(u)$ and $\Psi(u)/\Psi^0(u)$ is countable.

In the previous papers we were working with orthonormal frames defined in the tangent spaces of the Riemannian manifold M_n. Moreover each tangent space over M_n was provided with a structure defined by the holonomy group. In the introduction we mentioned the need for the incorporation of this superstructure into the theory. From the above results and sec. 3, it is obvious that this can be achieved by defining the holonomy bundle of orthonormal frames which is a sub-bundle of $O(M_n)$ with structure group the hg.

Using the above theorems and others on local and infinitesimal holonomy groups the restricted hg Ψ^0 can again be discussed as in the previous paper and we now turn to the inversion operations in Ψ.

The simplest thing for this purpose is to work in the orthogonal bundle $O(M_n)$ over M_n. Then the structure group G is the orthogonal group $O(n)$. From sec 2 it follows that for an orientable M_n $O(n)$ is reduced to the identity component $SO(n)$. Now the hg Ψ is a subgroup of the structure group

and we have the important result that for an orientable Riemannian manifold the hg is a subgroup of $SO(n)$ and for a non-orientable one it is a subgroup of $O(n)$. Hence the hg of an orientable manifold does not involve reflections. Therefore the concept of orientation is a crucial one and it is important to know whether a manifold is orientable or not.

Of course, the straightforward way would be that, given M_n, we cover it with a family of local coordinate systems x_α in U_α. Then we compute the Jacobians of the coordinate transformations in each intersection $U_\alpha \cap U_\beta$ to see their signs.

However, given M_n, it is more advantageous to go over to the universal covering $\widetilde{M}_n$ since in this way we will be able to classify large numbers of manifolds. Suppose, in fact, we have M_n with restricted $hg\,\Psi^0$ and universal covering $\widetilde{M}_n$. Let us determine the set D of all possible discrete isometries acting freely on $\widetilde{M}_n$. Then all factor spaces $\widetilde{M}_n/d$, $d \in D$, have same Ψ^0, but different topological properties, and can be classified according to sec. 4, where Ψ is now, in the orthonormal bundle, a subgroup of $O(n)$ and Ψ^0 is a subgroup of $SO(n)$.

7. Examples

As a first example we shall rather fully discuss a very simple case in order to illustrate concepts and method of classification.

We want to determine all (up to an isometry) 2-dimensional complete flat Riemannian (locally Euclidean) manifolds [6].

The problem is reduced to the determination of the discrete groups of motions acting freely on the Euclidean plane R^2, which is a simple task. We give the first homotopy group for each type by representing its action on the universal covering space, which is the Euclidean plane R^2, in terms of the Cartesian coordinate system (x, y).

(1) Euclidean plane (orientable)

$$\pi_1 : \text{identity};$$

(2) Ordinary cylinder (orientable)

$$\pi_1 : (x, y) \to (x + n, y) \qquad n = 0, \pm 1, \pm 2, \ldots;$$

(3) Ordinary torus (orientable)

$$\pi_1 : (x, y) \to (x + ma + n, y + mb),$$

a, b : real numbers, $b \neq 0$; $m, n = 0, \pm 1, \pm 2, \ldots$;

(4) Möbius band (edge removed) with infinite width (non-orientable)

$$\pi_1 : (x, y) \to (x + n, (-1)^n y) \qquad n = 0, \pm 1, \pm 2, \ldots;$$

(5) Klein bottle (non-orientable)

$$\pi_1 : (x, y) \to (x + n, (-1)^n y + bm)$$

b : non-zero real,

$$m, n = 0, \pm 1, \pm 2, \ldots .$$

Since the restricted hg Ψ^0 coincides with that of the universal covering, in each case Ψ^0 is the identity. In each case the kernel of the homomorphism

$$h : \pi_1 \to \Psi/\Psi^0$$

consists of pure translations N. Cases (2) and (3) together with (1) are orientable and the homomorphism h is trivial in each case. Consequently, the complete hg is the identity. Cases (4) and (5) are non-orientable and their holonomy groups contain reflection. Apart from the Euclidean plane, there is in each class one open and one closed manifold according to whether the pure translation part of π_1 is of one or of two dimensions, respectively. The concept of orientation is strikingly illustrated by the difference between the cylinder and the Möbius band.* When an oriented orthonormal frame is displaced parallel along the complete basis circle, orientation is preserved on the cylinder after coming back to the point of departure while orientation is reversed on the Möbius band. Of course, the classification according to π_1 rather than π_1/N is more detailed. For example (1) and (2) are in the same class with respect to π_1/N. Nevertheless the behaviour of geodesics, for example, is drastically different. In case (1) between two points there is only one geodesic while there is an infinity in case (2).

As an other example we consider spaces of constant curvature. These spaces are of some interest in cosmology since the constant-time sections of the Friedmann solutions are just of this type for dimension 3. The problem is the determination of all spaces which are locally Euclidean, spheric or hyperbolic. This is the well-known classical problem of the space forms and we do not go into detail.

The determination of all 3-dimensional locally Euclidean spaces proceeds along the same lines as in 2 dimensions in the preceeding example. There are 18 different types, 8 of which are open. Both in the open and closed classes there are orientable and non-orientable types. However, since these spaces are locally flat the restricted hg Ψ^0, which is now the group of proper rotations, is the identity.

The spherical spaces of constant positive local curvature, $K = +1$, have been fully discussed [6] in the mathematical literature. The even and odd dimensional cases must be treated separately.

* It is impossible to visualise the Klein bottle since it cannot be imbedded topologically in Euclidean 3-space.

There are exactly two spherical space forms of even dimensions n: the n-dimensional sphere S^n and the n-dimensional elliptic space. S^n is orientable, consequently its hg Ψ is a subgroup of $SO(n)$ and does not contain inversion. The elliptic space of even dimension is not orientable and its hg is a subgroup of $O(n)$. Thus these spaces fall naturally into two classes.

There is an infinity of odd-dimensional spherical space forms. For example if k is an integer then there is at least one form of odd dimensions whose first homotopy group is cyclic of order k. However, all odd-dimensional spherical forms are orientable. As a consequence the homomorphism $h : \pi_1 \to \to O(n)/SO(n)$ is trivial. In particular, the holonomy groups of 3-dimensional spherical space forms can never contain space inversion.

We are not going to deal with the hyperbolic cases since they have not been fully discussed, at least to the author's knowledge, in the mathematical literature.

The direct applicability of these results to observation is not quite clear. Obviously, one must consider four-dimensional spaces with indefinite metric. Indefinite metric, however, brings in some more complications and this problem will be dealt with in a separate paper.

The author is grateful to Professor P. GOMBÁS for his interest in the problems presented.

REFERENCES

1. MÁTÉ SÜVEGES, Acta Phys. Hung., **20**, 41, 1966.
2. MÁTÉ SÜVEGES, Acta Phys. Hung., **20**, 51, 1966.
3. A. LICHNEROWICZ, Théorie globale des connexions et des groupes d'holonomie, Roma 1962.
4. K. NOMIZU, Lie groups and differential geometry, Tokyo 1956.
5. S. KOBAYASHI and K. NOMIZU, Foundations of differential geometry Vol. 1., Interscience Publishers 1963.
6. W. RINOW, Die innere Geometrie der metrischen Räume, Springer-Verlag, Berlin, Göttingen, Heildelberg 1961.

ТЕОРИЯ ТОЖДЕСТВА В ГРАВИТАЦИОННЫХ ПОЛЯХ III.

Пространственная инверсия и гравитация

М. ШЮВЕГЕШ

Р е з ю м е

Исследуется инверсионная часть голономной группы Ψ, являющейся локально физической симметрической группой. Показывается, что существование инверсии зависит от топологических свойств гравитационного поля (предполагается, что гравитационное поле представляет собой множество Риманна M_n). С этой целью M_n определяется как дифференцируемое множество. Оказывается, что и в этом случае имеет место теорема параллелизма. Показывается далее, что если M_n — направляемое множество, то Ψ является подгруппой группы $SO(n)$ и если M_n — ненаправляемое, то Ψ является подгруппой группы $SO(n)$. Точнее, существует гомоморфизм h: $\pi_1(M_n) \to O(n)/SO(n)$, где $\pi_1(M_n)$ — первая гомотопная группа M_n и топологически инвариантная классификация гравитационных полей по отношению факторных групп группы $\pi_1(M_n)$ имеет физический смысл. Наряду с этим рассматриваются некоторые простые примеры пространственной формы нулевой и постоянной положительной локальной кривизны. Например, существует бесконечность трехмерной формы положительной кривизны, но локальная пространственная инверсия не является правильной операцией в любом из них. Показывается также, что физическое пространство нельзя считать просто множеством Риманна M_n, оно является волокнистым пучком над M_n. Поэтому применяется теория волокнистых пучков со структурной группой над дифференцируемом множеством.

COMMUNICATIONES BREVES

DIRECT PROCESSES ON RADIOACTIVE NUCLEI

By

P. HRASKÓ and ZS. KÖVESY

CENTRAL RESEARCH INSTITUTE FOR PHYSICS, BUDAPEST

(Received 16. II. 1965)

A theory of nuclear reactions, analogous to the dispersion theory of elementary particle processes was developed recently by I. S. SHAPIRO [1, 2]. The derivation of formulas for reaction amplitudes in this theory is based on the assumption that, because of the causality requirements, the amplitudes are analytic functions of the energy everywhere on the physical sheet except on the real axes, where the location of the singularities (poles and branch points) is determined by the unitarity condition. If in the unitarity condition one takes into account virtual states of certain type only, one gets the corresponding approximation to the amplitude.

The lowest order approximation consists in the restriction of the virtual states to the single particle states. In this case one finds that a pole of first order will be the only singularity of the amplitude and this pole approximation turns out to be equivalent to the BUTLER theory, when applied to the stripping reactions.

The location of the pole is completely determined by kinematic conditions. It is clear that the pole must not fall into the physical region of the kinematic variables, because in this case one would get an infinitely large cross section. The condition requiring the pole not to lie in the physical region implies the stability of all particles in the initial, final and virtual states. In other words the theory cannot be generalized to nuclei with spontaneous alpha decay.

Let us now consider the reaction

$$n + A \to B + \alpha' + n \tag{1}$$

on a hypothetical heavy nucleus. If the nuclei A and B are stable, the dispersion theory may be applied to compute the cross section which is supposed to be very small due to barrier effects. The pole approximation term of the reaction amplitude is represented graphically by the graph of Fig. 1, and the corresponding matrix element has the form (see [2] formula 2.47)

$$M \sim \frac{M(A \to B + \alpha) \cdot M^*(\alpha + n \to \alpha' + n')}{P_\alpha^2 - 2m_\alpha E_\alpha}, \tag{2}$$

where E_α and P_α, considering the energy and momentum conservation in vertices of the pole graph, are known functions of the kinetic energies and momenta in the initial or final state. It is clear that the "smallness" of the cross section is contained in the matrix element $M(A \to B + \alpha)$.

So far the nucleus has been considered as stable, satisfying therefore the mass relation

$$m_A < m_B + m_a. \tag{3}$$

Now, if we choose nuclei A with increasing mass, then for a certain nucleus A' the relation (3) will cease to hold. Therefore in the cases when $m_A > m_{A'}$ the pole of the amplitude M turns out to be inside the physical region for at least certain values of the kinematic variables, and so the theory cannot be applied in this case.

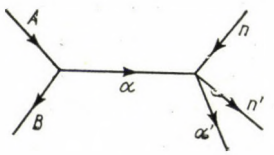

Fig. 1

It has to be pointed out that when $m_A < m_{A'}$ and the mass increases, the pole moves towards the physical region and in the usual interpretation the pole approximation becomes increasingly better. Nevertheless, when m_A reaches $m_{A'}$ the theory becomes in principle inapplicable.

On the other hand, it seems that there are no sharp differences between "almost stable" and "almost unstable" nuclei and this suggests that if the theory is true in the stable region, it can be modified to work at least at the onset of the unstable region too.

The simplest modification consists in including a small imaginary part $-i\gamma = -\frac{i\hbar}{2\tau}$ (τ is the lifetime of A) in the mass difference $Q = m_A - m_B - m_a$. As a result, the pole again turns out to lie outside the physical region and no infinite cross section arises. Nevertheless, owing to the smallness of γ, for real nuclei the pole will be very near to the physical region and will manifest itself in an unusually sharp and high peak. The shape of this peak cannot be resolved in detail experimentally since only the area under the peak is measurable.

The numerator of M contains the product of two matrix elements. Let us consider $M(A \to B + \alpha)$. When A is a stable nucleus, this matrix element has to be computed for non-physical negative kinetic energies of the decay products B and α. In our cases, however, $B + \alpha$ has positive kinetic energy equal to the decay energy Q. To understand this it is sufficient to note

that $M(A \to B + \alpha)$ has to be determined at the pole, i.e. where the denumerator of (2) vanishes. Therefore, the intermediate alpha particle is on its mass shell. The matrix element $M(A \to B + \alpha)$ can be computed for the nucleus A at rest. Considering the conservation of energy and momentum in the vertex $A \to$ $\to B + \alpha$, one concludes that precisely $M(A \to B + \alpha)$ is the matrix element for the real decay of A. The quantity $|M(A \to B + \alpha)|^2$ involved in the expression of the cross section will therefore be proportional to the observed decay probability γ. This quantity contains the reduced width and the barrier penetrability for the vertex $A \to B + \alpha$.

Similarly, $|M(\alpha + n \to \alpha' + n')|^2$ is proportional to the absolute square of the (n, α) elastic scattering amplitude $f(\varepsilon, q^2)$, which must be calculated for the momentum transfer $q^2 = (p_{n'} - p_n)^2$ and the relative energy

$$\varepsilon = \frac{m_\alpha + m_n}{2 m_\alpha m_n} \left[p_n - \frac{m_n}{m_\alpha + m_n} (p_{\alpha'} + p_{n'}) \right]^2 .$$

The differential cross section which can be obtained in the pole approximation is therefore:

$$d\sigma = (2\pi)^2 \left(\frac{m_n + m_\alpha}{m_\alpha} \right)^2 |f(\varepsilon, q^2)|^2 \sqrt{\frac{E_{\alpha'} E_{n'}}{Q E_n}} \times$$

$$\times \frac{\gamma}{\left[Q - \frac{1}{2 m_\alpha} (p_{n'} + p_{\alpha'} - p_n)^2 \right]^2 + \gamma^2} \delta(E_{n'} + E_{\alpha'} - E_n - Q) \, dE_{\alpha'} \, d\Omega_{\alpha'} \, dE_{n'} \, d\Omega_{n'} . \tag{4}$$

Since γ is an extremely small quantity, it is obvious that the characteristic features of the energy and angular distribution are determined by the factor

$$G = \frac{\gamma}{\left[Q - \frac{1}{2 m_\alpha} (p_{n'} + p_{\alpha'} - p_n)^2 \right]^2 + \gamma^2} \cong \pi \cdot \delta \left[Q - \frac{1}{2 m_\alpha} (p_{n'} + p_{\alpha'} - p_n)^2 \right] .$$

One may replace G by a delta-function, since the distributions observed experimentally are integrated over a range always much larger than γ.

Let us consider an experiment, when one fixes p_n and $p_{n'}$ and measures the angular distribution of α' particles with respect to the direction $p_{n'} - p_n$. The magnitude of E_α will be given by the energetic delta-function. Systematic coincidences between alpha-particles and neutrons may take place, when the angle β between $p_{\alpha'}$ and $p_{n'} - p_n$ equals β' which makes the argument of G to vanish. The existence of such a very sharp angular distribution may serve to decide on the existence of such a reaction mechanism as well. For the special case of $p_{n'} - p_n$ it has to be pointed out that when the arguments of the two

delta-functions in the expression of $d\sigma$ coincide after integration over the direction of $p_{\alpha'}$, $d\sigma$ contains a factor $\delta(0) \simeq 1/\gamma$. Therefore, for the angular distribution of elastically scattered high energy neutrons on nuclei, which are energetically unstable, an increased cross section in forward direction is expected as compared to the diffractive one.

An attempt to observe coincidences between alpha-particles and neutrons in the forward direction in the reaction $n+U \xrightarrow{238} Th^{234}+\alpha'+n'$ at $E_n=14$ MeV was made in [3]. No systematic coincidences were found although, according to (4), a cross section of the order of the (n, α) elastic cross section could be expected. Since the extension of the dispersion theory to the case of the "almost stable" nuclei was carried out in the most natural and usual way by replacing m_A by $m_A - i\gamma$ and considering that one expects the transition from stable to unstable cases to be smooth, the negative experimental result suggests some not yet clearly formulated limitations of the dispersion theory applied to nuclear reactions.

One of the authors (P.H.) is indebted to Professor Bosco for a discussion on the subject.

REFERENCES

1. *И. С. Шапиро*, ЖЕТФ **41**, 1616, 1961.
2. *И. С. Шапиро*, Теория прямых ядерных реакций, Москва, 1963.
3. A. ÁDÁM, G. PÁLLA and P. QUITTNER, Acta Phys. Hung., **20**, 227, 1966.

ON THE MOBILITY OF DISLOCATIONS IN Ge AT A TEMPERATURE RANGE BELOW THE TEMPERATURE LIMIT OF MACROSCOPICAL PLASTICITY

By

B. RÖSNER

RESEARCH INSTITUTE FOR TECHNICAL PHYSICS OF THE HUNGARIAN ACADEMY OF SCIENCES, BUDAPEST

(Received 18. II. 1965)

Recently, dislocation motion has been observed in Ge at room temperature as a result of indentation [1] and of bending [2]. These deformations have been carried out in etchants, because in this case the materials have an increased tendency to plasticity. We have investigated the dislocation mobility in Ge exposed to high stress at a temperature range below the limit temperature of macroscopical plasticity ($\sim$350°C [3]). Ge surface has been indented with a Vickers indenter at temperatures of 400°, 350°, 300°, 250°, 200°, 150°, 100°, 20°C and subsequently etched for 7 seconds in boiling Billig reagent. The material was loaded only for a few seconds: if the loading was applied for longer than 10 seconds, or was not carried out carefully enough, cracks arose and no dislocation etch pits could be observed. At temperatures below 250°C the diameters of indentations did not exceed 2 microns. The resulting etch pattern on the (111) Ge surface at 400°C (Fig. 1) displays arrays of dislocation etch pits aligned in (110) directions as previously observed in [1] and [4].

Indented at 100°C the etch pits near the indentation (large and flattened triangle) are due to the dislocations which have arisen and slipped in (110) direction. (Fig. 2.) (They have the same character as the etch pits of as-grown dislocations which can be seen elsewhere in the picture. These pits blurred after etching was continued for a few seconds. In the following calculation these shallow dislocations were supposed to be 60° type dislocations but we could not obtain any information about the mechanism of their motion or details of the dislocation structure owing to the limitations of the etching method. We obtained similar photographs for the etched indentations performed in the temperature range below 250°C.

The stress acting on dislocations in (110) direction near the surface ($z = 0$) was calculated according to the elasticity of the isotropic media in case of point load [5] taking into account the given geometrical situation. We obtained the following formula for this:

$$\tau = \frac{P(1-2\gamma)}{\pi\sqrt{6}} \frac{y^2 - x^2}{(y^2 + x^2)^2} \left[= \frac{P(1-2\gamma)}{\pi\sqrt{6}} \frac{\cos 2\varphi}{r^2} \right] \tag{1}$$

with P, γ, (x, y) the load, the Poisson-ratio and the coordinates, respectively. This stress was put in the dislocation velocity formula given by CHAUDHURY et al. [6]

$$v = B_m \tau^m \exp - \frac{U}{KT} \tag{2}$$

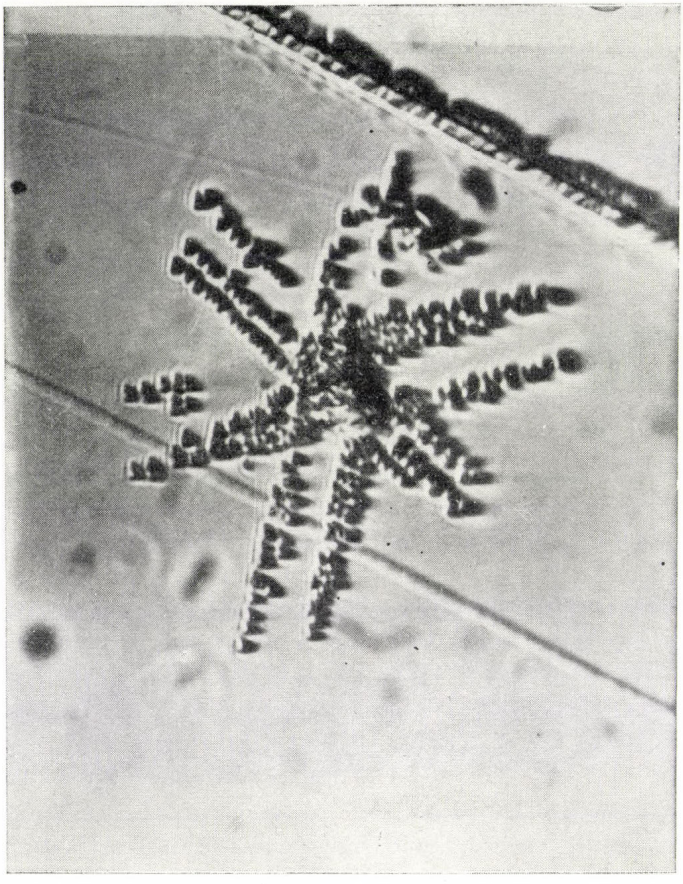

Fig. 1

with B_m, m constants. Table 1 shows the values of the average velocities over the replacement of dislocations.

Table 1

T	$\bar{\tau}$	$\bar{v}$ theoretical	$\bar{v}$ measured
100°C	57 kg/mm²	3×10^{-11} cm/sec	$1{,}7\times10^{-4}$ cm/sec
400°C	12 kg/mm²	$1{,}3\times10^{-4}$ cm/sec	$8{,}3\times10^{-4}$ cm/sec

According to Table 1, there is no difference in order of magnitude between the theoretical and measured dislocation mobilities at 400°C. The discrepancy is due to the approximate character of formula (1). However, the discrepancy between the theoretical and measured data increases in the temperature range below 250°C. Consequently the existing theory of dislocation mobility is not

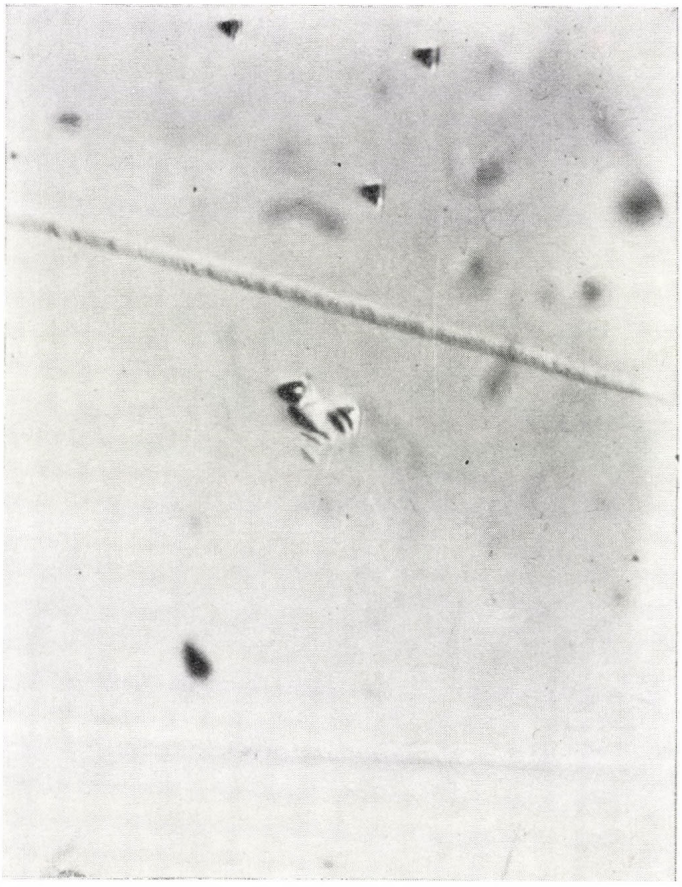

Fig. 2

valid for Ge over this temperature range and another theory is needed. The required new theory must account first of all for the temperature independence of dislocation mobility as demonstrated by our experimental results.

This conclusion may be supported qualitatively by microhardness measurements reported in [4]. According to this paper the measured microhardness does not increase with decreasing temperature as abruptly as would be expected from the existing dislocation velocity formulae in the low temperature range, although the relation between microhardness and dislocation

mobility cannot be as simple as assumed in [4] in view of the complexity of the indentation procedure.

The author is pleased to acknowledge the discussions with V. J. NIKITENKO and V. G. GOVORKOV.

LITERATURE

1. R. TRAMPOSCH and W. RINDNER, Appl. Phys. Letters, **3**, 42, 1963.
2. T. L. JOHNSTON, R. J. STOKES and C. H. LI, Acta Met., **6**, 713, 1958.
3. В. Г. Говорков, В. Р. Регель, ФТТ, **3**, 1324, 1961.
4. В. И. Трефилов, Ю. В. Мильман, Докл. Акад. Наук, **153**, 824, 1963.
5. М. М. Филоленко — Бородич, Теория упругости, Физматгиз, Москва 1959.
6. A. R. CHAUDHURY, J. R. PATEL and L. G. RUBIN, Journal of Applied Physics, **33**, 2736, 1962.

APPLICATION OF A MODIFIED EFFECTIVE-RANGE THEORY TO THE ELASTIC SCATTERING OF LOW-ENERGY ELECTRONS FROM HELIUM

By

O. J. ORIENT

DEPARTMENT OF ATOMIC PHYSICS, POLYTECHNICAL UNIVERSITY, BUDAPEST

(Received 31. III. 1965)

Introduction

RAMSAUER and KOLLATH [1], [2] have measured the total and differential scattering cross sections of low-energy electrons from helium, and NORMAND [3] has measured the total scattering cross-section.

MCDOUGALL [4] was the first to make theoretical calculations on the total scattering cross-section, by using the Hartree—Fock potential that applies to the helium atom. Significant discrepancies were found, between the computed total scattering cross-sections of low-energy electrons and measurement results particularly for differential cross-sections. MORSE and ALLIS [5] used the Hartree—Fock potential modified for exchange effect. Their results showed a better agreement with experimental data for the total scattering cross-section. Important discrepancies continued to exist at energies lower than a few eV. For low-energy electrons the agreement for differential cross sections was not satisfactory, either.

For neutral polarizable systems O'MALLEY, ROSENBERG and SPRUCH [6] have lately developed a theory of modified effective ranges. O'MALLEY [7] first applied this theory to the elastic scattering of electrons from helium. The author found a fair agreement with the measurement results of RAMSAUER and KOLLATH [1] for the total scattering cross-section, up to about 4 eV energy. The computation method he used did not permit more detailed investigations.

LA BAHN and CALLAWAY [8] in their computation took into consideration the polarisation effect produced by the electrons. The results obtained for the total scattering cross-sections displayed a fair accordance with the experimental data from 0 to 50 eV energy. The results for differential cross-sections, however, were at variance with the measurements of RAMSAUER and KOLLATH [2].

We have applied the theory of modified effective range to the scatter of low-energy electrons from helium, without following O'MALLEY's method. Our own method of handling the problem has resulted in a better agreement between computation results and measurement data for the total scattering cross-section in the range of 0 to 14 eV electron energy.

In addition, our results for the differential scattering cross-section are in better agreement with measurement data than are LA BAHN and CALLAWAY's computations [8].

Computation results

The pure theory of scattering of quantum mechanics, the method of partial waves, is used here. The formula for the total scattering cross-section is:

$$\sigma = \frac{4\pi}{k^2} \sum_{L=0}^{\infty} (2L+1) \sin^2 \eta_L \tag{1}$$

and for the differential cross-section:

$$\sigma(\vartheta) = \frac{1}{4k^2} \left\{ \left[\sum_{L=0}^{\infty} (2L+1)(\cos 2\eta_L - 1) P_L \right]^2 + \left[\sum_{L=0}^{\infty} (2L+1) \sin 2\eta_L P_L \right]^2 \right\}. \tag{2}$$

In the formulae $k^2 = \frac{2Em}{\hbar^2}$ (m is the mass of the electron, E the energy of the electron and η_L the phase shift corresponding to quantum number L.)

The modified effective-range theory [7] for η_L gives the following relationships:

$$\operatorname{tg} \eta_0 = -Ak - \frac{\pi}{3a_0} \alpha k^2 - \frac{4}{3a_0} \alpha A k^3 \ln (a_0 k) + 0(k^3), \tag{3}$$

$$\operatorname{tg} \eta_1 = \frac{\pi}{15a_0} \alpha k^2 - A_1 k^3 + 0(k^4), \tag{4}$$

$$\operatorname{tg} \eta_L = \frac{\pi}{(2L+3)(2L+1)(2L-1)} \alpha k^2 + 0(k^4); \quad L > 1; \tag{5}$$

here a_0 is the first Bohr radius, α = electric polarizability of the atom (for helium $\alpha = 1{,}36\, a_0^3$), A and A_1 are the scattering lengths for phase shifts S and P, respectively, $0(k^3)$ and $0(k^4)$ residuals containing k^3 and k^4 and terms of higher powers.

In the computation of the total scattering cross-section for helium O'MALLEY [7] worked with the following method: In formula (3) he determined A from the measurements of RAMSAUER and KOLLATH [1] by extrapolating for zero energy. This resulted in $A = 1{,}19\, a_0$. Instead of $0(k^3)$ he used the term Dk^3 and neglected the terms of higher powers. He determined the constant D equally from measurement data. In the computation of the total scattering

cross-section he assumed $\sin \eta_0 = \operatorname{tg} \eta_0$. Owing to this the computation is valid only for low values of η_0. In the energy range computed (0 to 4 eV) he discarded the values of η belonging to higher quantum numbers.

At variance with this method we have not made use of the simplified assumption that $\sin \eta_0 = \operatorname{tg} \eta_0$ and have not neglected η_1. In formula (3) we have used $A = 1{,}19 a_0$. We have determined D so as to obtain as good an agreement as possible, not only with the measurements of the total scattering cross-section of RAMSAUER and KOLLATH [1] and with NORMAND [3], but

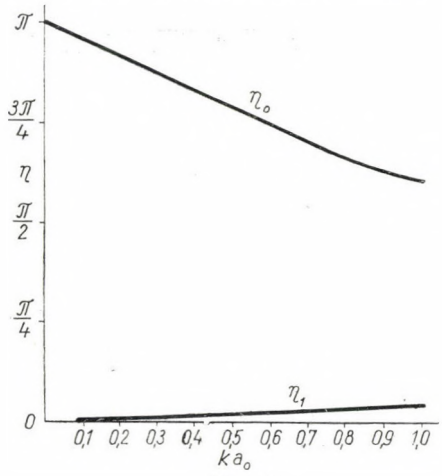

Fig. 1

also with the measurements of the differential cross-sections of RAMSAUER and KOLLATH [2]. We have followed a similar method in the determination of A_1. In equation (4) we have discarded the term $0(k^4)$. For η_0 and η_1 we have derived the following relationships:

$$\eta_0 = \operatorname{arc\,tg} [-1{,}190 a_0 k - 1{,}424 a_0^2 k^2 - 2{,}160 a_0^3 k^3 \ln (a_0 k) - 0{,}262 a_0^3 k^3], \quad (6)$$

$$\eta_1 = \operatorname{arc\,tg} [+0{,}285 a_0^2 k^2 - 0{,}163 a_0^3 k^3]. \quad (7)$$

η_0 and η_1 are represented in Figure 1 as functions of ka_0. With the phase shifts η_0 and η_1 the total scattering cross-sections have been calculated from relationship (1), throughout the range from 0 to 14 eV electron energy. In Figure 2 the continuous curve represents our computation results. The data marked with circles are those of RAMSAUER and KOLLATH [1], those marked with crosses those of NORMAND [3].

In a similar way, by using the values of η_0 and η_1, from equation (2) we have determined the differential cross-section. The computational results are represented in Figure 3 by a continuous curve. The data marked with circles are the measurement results of RAMSAUER and KOLLATH [2].

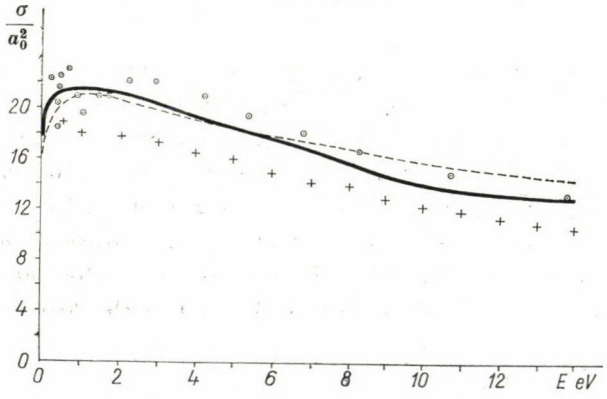
σ / a₀²
20
16
12
8
4
0
0
2
4
6
8
10
12
E eV

Fig. 2

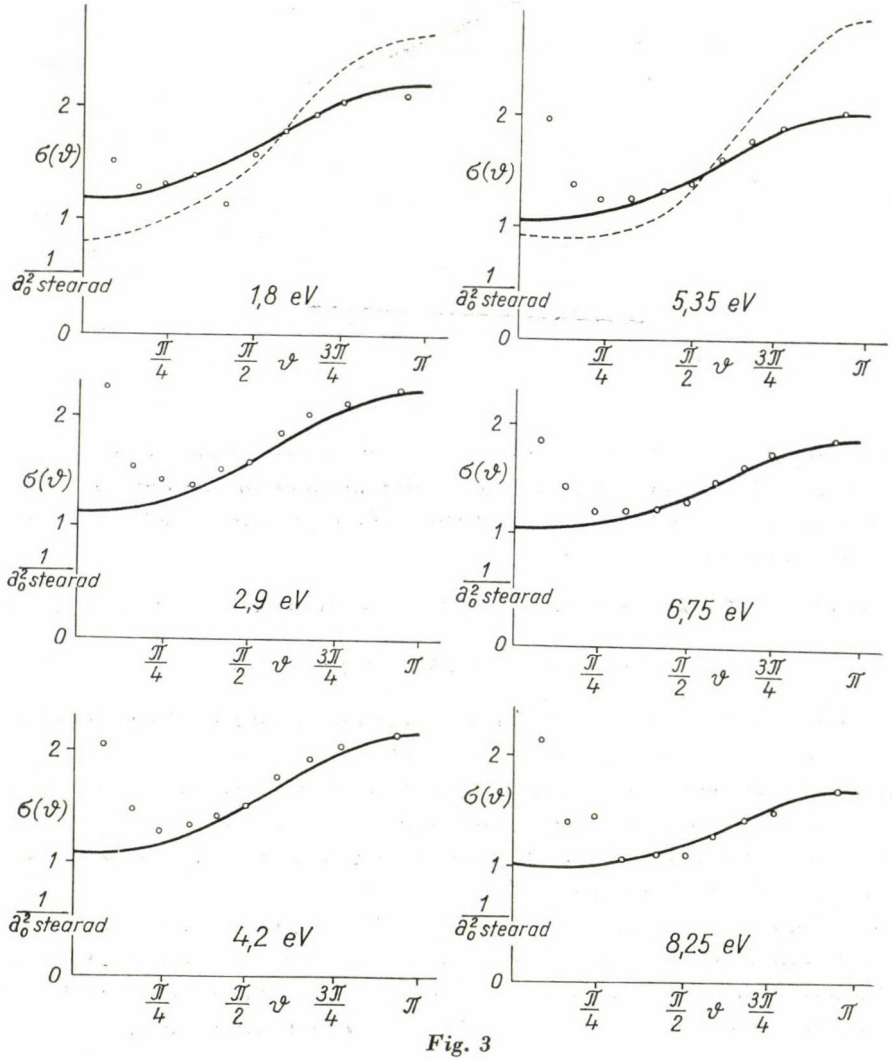
σ(ϑ)
1 / a₀² steard
1,8 eV
5,35 eV
2,9 eV
6,75 eV
4,2 eV
8,25 eV
π/4
π/2
ϑ
3π/4
π

Fig. 3

Conclusions

Our computations are in fair agreement with experimental results throughout the energy range represented in the figures. With energies higher than 14 eV, where $a_0 k > 1$ the discrepancy between computation and measurement results grows significant. (Computation results are higher than test results.) When $a_0 k > 1$ the error increases considerably because of the simplification in the term $0(k^3)$ and of the neglect of the term $0(k^4)$. According to our computations the neglect of the phase shifts belonging to higher quantum numbers in the energy range investigated does not produce any significant in accuracy.

Figure 2 also illustrates the computation results of LA BAHN and CALLAWAY [8] of the total scattering cross-section (dotted curve). The two calculated curves diverge at energies above 5 eV.

Our calculated differential cross-sections show a fair agreement with the measurement results at angles larger than $\vartheta = \frac{\pi}{4}$ from 1,8 to 8,25 eV energy. The comparison of measurement results for energies higher than 10 eV (not represented in the Figures) with our computations shows discrepancies. Similarly to the case of total scattering cross-sections, the discrepancies may be due to the simplifications regarding the terms $0(k^3)$ and $0(k^4)$.

LA BAHN and CALLAWAY's computations of differential cross-sections give less good agreement than do our own calculations from 1,8 eV to 8,75eV. In their computations the discrepancy increases with increasing energy. In Figure 3, at 1,8 eV and 5,35 eV the differential cross-sections determined by using the values η_0 and η_1 computed with their method are shown by dotted lines.

REFERENCES

1. C. RAMSAUER and R. KOLLATH, Ann. Physik, **3,** 536, 1929.
2. C. RAMSAUER and R. KOLLATH, Ann. Physik, **12,** 529, 1932.
3. C. E. NORMAND, Phys. Rev., **35,** 1217, 1930.
4. J. MCDOUGALL, Proc. Roy. Soc., A **136,** 549, 1932.
5. P. M. MORSE and W. P. ALLIS, Phys. Rev., **44,** 269, 1933.
6. T. F. O'MALLEY, L. SPRUCH and L. ROSENBERG, Phys. Rev., **125,** 1300, 1962.
7. T. F. O'MALLEY, Phys. Rev., **130,** 1020, 1963.
8. R. W. LA BAHN and J. CALLAWAY, Phys. Rev., **135,** A 1539, 1964.

ZUSAMMENHANG ZWISCHEN DER STRUKTUR UND DEN PHYSIKALISCHEN EIGENSCHAFTEN DES GLASES

V. ZUSAMMENHANG ZWISCHEN DICHTE UND LICHTBRECHUNG

Von

I. NÁRAY-SZABÓ

ZENTRALFORSCHUNGSINSTITUT FÜR CHEMIE DER UNGARISCHEN AKADEMIE DER WISSENSCHAFTEN, BUDAPEST

(Eingegangen: 15. VI. 1965)

Vor einigen Jahren hat TOLD [1] (1960) einen sehr einfachen Zusammenhang zwischen der Dichte und der Lichtbrechung von einer Reihe von optischen Gläsern nachgewiesen. Er fand bei 203 optischen Gläsern der Fa. Schott u. Gen., Jenaer Glaswerk (Mainz), dass — mit Ausnahme von 11 Gläsern — die folgende Gleichung mit einem maximalen Fehler von $\pm 2\%$ gültig ist:

$$n_D = \frac{d + 10{,}4}{8{,}6} .$$

Hier ist n_D die Brechungszahl für Na-Licht und d der Zahlenwert der Dichte. Die 11 Gläser, für die die obige Beziehung nicht gilt, sind lanthanhaltig oder stark bleihaltig (Flintgläser).

Die Parallelität der Dichte und der Lichtbrechungszahl ist selbst bei einer so geringen Genauigkeit wie der obigen interessant. Doch erhält man viel genauere Zusammenhänge, wenn man gewisse Reihen von Gläsern mit zwei oder drei Komponenten untersucht.

Für einfache Natriumsilikatgläser, d. h. für die Glieder der Reihe Na_2O-SiO_2 fand ich, dass folgende Gleichung Gültigkeit hat:

$$n_D = 0{,}143d + 1{,}1494. \tag{1}$$

Die experimentell gefundenen Brechungszahlen und Dichten sind nach MOREY [2] zusammen mit den nach Gl. (1) berechneten Brechungszahlen in Tab. 1 zusammengestellt.

Man sieht also, dass Gl. (1) einen durchschnittlichen Fehler von $2{,}4 \cdot 10^{-4}$ im Wert der Brechungszahl ergibt. Die Analysenfehler sind weitaus grösser, und man kann daher keineswegs eine bessere Übereinstimmung erwarten.

Es ist besonders bemerkenswert, dass für Natriumsilikatgläser mit Aluminiumoxidgehalt dieselbe Gleichung mit einer geringfügigen Änderung der additiven Konstante gültig bleibt:

$$n_D = 0{,}134\, d + 1{,}1508. \tag{1a}$$

In der Tab. 2 sehen wir die Messungsergebnisse von FAICK et al. [3] verglichen mit den nach Gl. (1a) berechneten Werten.

Die Abweichungen zwischen den berechneten und den gemessenen n_D-Werten betragen im Mittel $4 \cdot 10^{-4}$ und maximal $12 \cdot 10^{-4}$.

Nun kann man aber — wenn man ähnliche gute Übereinstimmung zwischen den berechneten und den gemessenen Brechungszahlen erreichen will, keine allgemein gültige Gleichung benützen, da mehr als zwei Variablen auftreten können. Man wird also eine Reihe von Gleichungen für ternäre Gläser erhalten, so z. B. für die wichtigen Na_2O-CaO-SiO_2-Gläser, deren Dichten und Brechungszahlen u. a. von PEDDLE [4] bestimmt wurden. Bleibt das Verhältnis $Na_2O : SiO_2$ konstant, so können wir für jedes solche Verhältnis eine Gleichung aufstellen, die mit sehr guter Annäherung den Zusammenhang zwischen der Dichte und der Brechungszahl angibt. Die Zusammensetzungen sind in Tab. 3 in Molverhältnissen angegeben.

Auch für K_2O-haltige Gläser können wir ähnliche Gleichungen formulieren, wie das aus der folgenden Tab. 4 zu ersehen ist.

Tabelle 1

Gefundene und berechnete Brechungszahlen sowie gefundene Dichten von Gläsern der Reihe Na_2O-SiO_2

No.	SiO_2 %	Na_2O %	Dichte g. cm^{-3}	$n_{D,\text{gem.}}$	$n_{D,\text{ber.}}$	$\Delta \cdot 10^4$
9	54,14	45,86	2,5475	1,5137	1,5137	0
11	57,45	42,55	2,5318	1,5112	1,5114	+ 2
15	59,97	40,03	2,5208	1,5099	1,5099	0
17	62,86	37,14	2,5044	1,5076	1,5075	− 1
18	63,06	36,94	2,5038	1,5075	1,5074	− 1
19	64,30	35,70	2,4890	1,5055	1,5053	− 2
20	65,32	34,68	2,4924	1,5055	1,5058	+ 3
22	67,14	32,86	2,4807	1,5042	1,5041	− 1
23	69,65	30,35	2,4644	1,5021	1,5016	− 5
24	70,21	29,79	2,4612	1,5014	1,5014	0
25	70,44	29,56	2,4603	1,5015	1,5012	− 3
26	72,15	27,85	2,4488	1,4993	1,4996	+ 3
30	75,29	24,71	2,4260	1,4965	1,4963	− 2
34	77,85	22,15	2,4007	1,4925	1,4927	+ 2
35	78,61	21,39	2,3935	1,4912	1,4917	+ 5
36	79,73	20,27	2,3813	1,4898	1,4899	+ 1
40	82,86	17,14	2,3536	1,4851	1,4861	+10

Für Na_2O-K_2O-CaO-SiO_2-Gläser können auch entsprechende Gleichungen aufgestellt werden, s. Tab. 5.

Will man solche Gleichungen für bleihaltige und bariumhaltige Gläser aufstellen, so werden die Differenzen zwischen den berechneten und den gefundenen Werten schon bedeutend höher, und sie können etwa 0,5% erreichen; deshalb wollen wir hier keine weiteren Berechnungen mitteilen.

Es ist interessant, den Zusammenhang zwischen der Brechungszahl und dem R-Werte (Sauerstoffionenzahl pro netzbildendes Ion) zu betrachten. Der R-Wert hängt von dem Verhältnis der Brückensauerstoffionen zu den nicht brückenbildenden Sauerstoffionen ab. Trägt man die Brechungszahl als Funktion von R in einem rechtwinkligen Koordinatensystem auf, so erhält man keine Gerade, sondern eine — zwar sehr schwach — gekrümmte Linie. Für die Brechungszahl ist zwar die Molrefraktion der Sauerstoffionen entscheidend, doch spielen auch die modifizierenden Kationen wie Na^+, K^+, Ca^{2+} usw. eine Rolle und das Gesamtergebnis ist die erwähnte nicht ganz

Tabelle 2

Gefundene und berechnete Brechungszahlen sowie gefundene Dichten von Gläsern der Reihe Na_2O-Al_2O_3-SiO_2

No.	SiO_2 %	Al_2O_3 %	Na_2O %	Dichte g · cm^{-3}	$n_{D,\text{gem.}}$	$n_{D,\text{ber.}}$	$\Delta \cdot 10^4$
101	50,32	2,86	46,82	2,5605	1,5162	1,5168	+ 6
102	50,57	7,00	42,43	2,5495	1,5164	1,5152	−12
103	50,86	6,71	42,43	2,5484	1,5155	1,5150	− 5
104	50,89	9,57	39,54	2,5410	1,5150	1,5140	−10
105	50,95	4,88	44,17	2,5533	1,5157	1,5157	0
106	55,25	9,83	34,92	2,5182	1,5116	1,5107	− 9
107	55,56	6,94	37,50	2,5259	1,5120	1,5118	− 2
108	55,66	9,68	34,66	2,5163	1,5110	1,5104	− 6
109	55,80	4,83	39,23	2,5304	1,5124	1,5124	0
110	55,86	4,83	39,23	2,5304	1,5124	1,5124	0
111	60,45	9,84	29,71	2,4897	1,5072	1,5066	− 6
112	60,68	4,86	34,46	2,5032	1,5088	1,5086	− 2
113	60,76	2,82	36,42	2,5111	1,5092	1,5097	+ 5
114	60,78	1,09	38,13	2,5168	1,5094	1,5105	+11
115	60,88	9,59	29,53	2,4891	1,5070	1,5065	− 5
116	60,97	6,57	32,46	2,4997	1,5073	1,5077	+ 4
117	64,78	1,02	34,20	2,4916	1,5059	1,5069	+10
118	65,10	9,96	24,94	2,4615	1,5032	1,5026	− 6
119	65,70	4,75	29,55	2,4749	1,5049	1,5045	− 4
120	65,88	9,43	24,69	2,4580	1,5025	1,5021	− 4

Tabelle 3

Gefundene und berechnete Brechungszahlen sowie gefundene Dichten von Gläsern der Reihe 100 SiO_2 : 40 Na_2O : x CaO

CaO Mole	Dichte g · cm^{-3}	$n_{D,\text{gem.}}$	$n_{D,\text{ber.}}$	$\Delta \cdot 10^4$	
5	2,512	1,5110	1,5132	+22	
10	2,533	1,5189	1,5187	− 2	
15	2,559	1,5259	1,5256	− 3	$n_D = 0{,}264\, d + 0{,}850$ (2)
20	2,584	1,5327	1,5322	− 5	
30	2,629	1,5442	1,5441	− 1	
40	2,667	1,5540	1,5541	+ 1	
Gläser der Reihe 100 SiO_2 : 20 Na_2O : x CaO					
5	2,412	1,4970	1,4975	+ 5	
10	2,458	1,5088	1,5088	0	
15	2,499	1,5192	1,5188	− 4	
20	2,537	1,5279	1,5280	+ 1	$n_D = 0{,}244\, d + 0{,}909$ (3)
30	2,603	1,5435	1,5441	+ 6	
40	2,659	1,5573	1,5578	+ 5	

Tabelle 4

Gefundene und berechnete Brechungszahlen sowie gefundene Dichten von Gläsern der Reihe 100 SiO_2 : 40 K_2O : x CaO

CaO Mole	Dichte g · cm^{-3}	$n_{D,\text{gem.}}$	$n_{D,\text{ber.}}$	$\Delta \cdot 10^4$	
5	2,488	1,5125	1,5115	−10	
10	2,513	1,5179	1,5178	− 1	
15	2,535	1,5229	1,5234	+ 5	$n_D = 0{,}253\, d + 0{,}882$ (4)
20	2,555	1,5277	1,5284	+ 7	
30	2,594	1,5379	1,5383	+ 4	
40	2,630	1,5475	1,5474	− 1	
Gläser der Reihe 100 SiO_2 : 20 K_2O : x CaO					
5	2,420	1,5011	1,5008	− 3	
10	2,450	1,5081	1,5087	+ 6	
15	2,478	1,5151	1,5160	+ 9	
20	2,505	1,5223	1,5231	+ 8	$n_D = 0{,}262\, d + 0{,}8663$ (5)
30	2,555	1,5355	1,5362	+ 7	
40	2,601	1,5491	1,5483	− 8	

Tabelle 5

Gefundene und berechnete Brechungszahlen sowie gefundene Dichten von Gläsern der Reihe 100 SiO_2 : 20 Na_2O : 20 K_2O : x CaO

CaO Mole	Dichte g · cm^{-3}	$n_{D,\text{gem.}}$	$n_{D,\text{ber.}}$	$\Delta \cdot 10^4$
5	2,502	1,5115	1,5115	0
10	2,529	1,5186	1,5187	+ 1
15	2,554	1,5255	1,5254	− 1
20	2,574	1,5314	1,5307	− 7
30	2,619	1,5428	1,5427	− 1
40	2,657	1,5528	1,5528	0
	Gläser der Reihe 100 SiO_2 : 10 NaO_2 : 10 K_2O : x CaO			
5	2,415	1,4992	1,4993	+ 1
10	2,450	1,5086	1,5082	− 4
15	2,485	1,5177	1,5710	− 7
20	2,523	1,5253	1,5258	+ 5
30	2,585	1,5401	1,5416	+15
40	2,626	1,5528	1,5520	− 8

$$n_D = 0{,}266\, d + 0{,}846 \qquad (6)$$

$$n_D = 0{,}254\, d + 0{,}886 \qquad (7)$$

lineare Kurve. Sind stark polarisierbare Kationen mit hoher Molrefraktion wie Ba^{2+}, Pb^{2+} usw. vorhanden, so wird die Krümmung noch stärker, und es ergibt sich keine Linearität. — Die netzbildenden Kationen, wie Si^{4+}, B^{3+} usw. üben dagegen sozusagen gar keinen Einfluss auf die Brechungszahl aus, was ihre starke Bindung bestätigt. In dieser Hinsicht verhält sich das Kation Al^{3+} ebenso, wie wir das aus der Gültigkeit der Gl. (2) schliessen können. Aluminium gehört also zu den netzbildenden Kationen mit tetraedrischer Koordination, obzwar das von einigen Autoren in Abrede gestellt wird.

Die mitgeteilten Gleichungen können einerseits als sehr gute Interpolationen für die Berechnung von Brechungszahlen für beliebige Glieder der angeführten Glasreihen dienen, andererseits ist es aber möglich, solche Gleichungen für andere Glasreihen auf Grund von zwei bis drei Messungen aufzustellen und somit Gläser mit vorausberechneter Brechungszahl herzustellen.

LITERATUR

1. F. Told, Glastechn. Ber., **33**, 303, 1960.
2. G. W. Morey, The properties of glass, 2nd Ed., Reinhold, New York 1954, p. 241. In den diesbezüglichen Arbeiten der National Bureau of Standards, Washington, haben Finn, Faick, Glaze und Young teilgenommen.
3. C. A. Faick, J. C. Young, D. Hubbard and A. N. Finn, J. Research Natl. Bur. Standards, **14**, 133, 1935.
4. C. J. Peddle, J. Soc. Glass Tech., **4**, 3; **20**; 46; **59**, 1920.

INDEX

COMMUNICATIONES BREVES

Printed in Hungary

A kiadásért felel az Akadémiai Kiadó igazgatója — Műszaki szerkesztő: Farkas Sándor

A kézirat a nyomdába érkezett: 1965. X. 11. — Terjedelem: 8,50 (A/5) ív. 13 ábra

65.61428 Akadémiai Nyomda, Budapest — Felelős vezető: Bernát György

The *Acta Physica* publish papers on physics, in English, German, French and Russian.
The *Acta Physica* appear in parts of varying size, making up volumes.
Manuscripts should be addressed to:

Acta Physica, Budapest 502, Postafiók 24.

Correspondence with the editors and publishers should be sent to the same address.
The rate of subscription to the *Acta Physica* is 110 forints a volume. Orders may be placed with „Kultúra" Foreign Trade Company for Books and Newspapers (Budapest I., Fő u. 32. Account No. 43-790-057-181) or with representatives abroad.

Les *Acta Physica* paraissent en français, allemand, anglais et russe et publient des travaux du domaine de la physique.
Les *Acta Physica* sont publiés sous forme de fascicules qui soront réunis en volumes.
On est prié d'envoyer les manuscrits destinés à la rédaction à l'adresse suivante:

Acta Physica, Budapest 502, Postafiók 24.

Toute correspondance doit être envoyée à cette même adresse.
Le prix de l'abonnement est de 110 forints par volume.
On peut s'abonner à l'Entreprise du Commerce Extérieur de Livres et Journaux «Kultúra» (Budapest I., Fő u. 32. — Compte-courant No. 43-790-057-181) ou à l'étranger chez tous les représentants ou dépositaires.

«*Acta Physica*» публикуют трактаты из области физических наук на русском, немецком, английском и французском языках.
«*Acta Physica*» выходят отдельными выпусками разного объема. Несколько выпусков составляют один том.
Предназначенные для публикации рукописи следует направлять по адресу:

Acta Physica, Budapest 502, Postafiók 24.

По этому же адресу направлять всякую корреспонденцию для редакции и администрации.
Подписная цена «*Acta Physica*» — 110 форинтов за том. Заказы принимает предприятие по внешней торговле книг и газет «*Kultúra*» (Budapest I., Fő u. 32. Текущий счет: № 43-790-057-181) или его заграничные представительства и уполномоченные.

All the reviews of the Hungarian Academy of Sciences may be obtained among others from the following bookshops:

ALBANIA

Ndermarja Shtetnore e Botimeve
Tirana

AUSTRALIA

A. Keesing
Box 4886, GPO
Sidney

AUSTRIA

Globus Buchvertrieb
Salzgries 16
Wien I.

BELGIUM

Office International de Librairie
30, Avenue Marnix
Bruxelles 5
Du Monde Entier
5, Place St. Jean
Bruxelles

BULGARIA

Raznoiznos
1Tzar Assen
Sofia

CANADA

Pannonia Books
2 Spadina Road
Toronto 4, Ont.

CHINA

Waiwen Shudian
Peking
P. O. B. Nr. 88.

CZECHOSLOVAKIA

Artia A. G.
Ve Smeckách 30
Praha II.
Postova Novinova Sluzba
Dovoz tisku
Vinohradska 46
Praha 2
Postova Novinova Sluzba
Dovoz tlace
Leningradska 14
Bratislava

DENMARK

Ejnar Munksgaard
Nörregade 6
Kopenhagen

FINLAND

Akateeminen Kirjakauppa
Keskuskatu 2
Helsinki

FRANCE

Office International de Documentation et Librairie
48, rue Gay Lussac
Paris 5

GERMAN DEMOCRATIC REPUBLIC

Deutscher Buch-Export und Import
Leninstraße 16.
Leipzig C. I.
Zeitungsvertriebsamt
Clara Zetkin Straße 62.
Berlin N. W.

GERMAN FEDERAL REPUBLIC

Kunst und Wissen
Erich Bieber
Postfach 46
7 Stuttgart S.

GREAT BRITAIN

Collet's' Subscription Dept.
44—45 Museum Street
London W. C. I.
Robert Maxwell and Co. Ltd.
Waynflete Bldg. The Plain
Oxford

HOLLAND

Swetz and Zeitlinger
Keizersgracht 471—487
Amsterdam C.
Martinus Nijhof
Lange Voorhout 9
The Hague

INDIA

Current Technical Literature
Co. Private Ltd.
Head Office:
India House OPP.
GPO Post Box 1374
Bombay I.

ITALY

Santo Vanasia
71 Via M. Macchi
Milano
Libreria Commissionaria Sansoni
Via La Marmora 45
Firenze

JAPAN

Nauka Ltd.
2 Kanada-Zimbocho 2-chome
Chiyoda-ku
Tokyo
Maruzen and Co. Ltd.
P. O. Box 605
Tokyo
Far Eastern Booksellers
Kanada P. O. Box 72
Tokyo

KOREA

Chulpanmul
Korejskoje Obshchestvo po Exportu Importu Proizvedenij Pechati
Phenjan

NORWAY

Johan Grundt Tanum
Karl Johansgatan 43
Oslo

POLAND

Export und Import Unternehmen RUCH
ul. Wilcza 46.
Warszawa

ROUMANIA

Cartimex
Str. Aristide Briand 14—18.
Bucuresti

SOVIET UNION

Mezhdunarodnaja Kniga
Moscow
G—200

SWEDEN

Almquist and Wiksell
Gamla Brogatan 26
Stockholm

USA

Stechert Hafner Inc.
31 East 10th Street
New York 3 N. Y.
Walter J. Johnson
111 Fifth Avenue
New York 3. N. Y.

VIETNAM

Xunhasaba
Service d'Export et d'Import des Livres et Périodiques
19, Tran Quoc Toan
Hanoi

YUGOSLAVIA

Forum
Vojvode Misica broj 1.
Novi Sad
Jugoslovenska Kniga
Terazije 27.
Beograd

ACTA PHYSICA

ACADEMIAE SCIENTIARUM HUNGARICAE

TOMUS XX FASCICULUS 4

AKADÉMIAI KIADÓ, BUDAPEST

1966

ACTA PHYS. HUNG.

ACTA PHYSICA

A MAGYAR TUDOMÁNYOS AKADÉMIA FIZIKAI KÖZLEMÉNYEI

SZERKESZTŐSÉG ÉS KIADÓHIVATAL: BUDAPEST V., ALKOTMÁNY UTCA 21.

Az *Acta Physica* német, angol, francia és orosz nyelven közöl értekezéseket a fizika tárgyköréből.

Az *Acta Physica* változó terjedelmű füzetekben jelenik meg: több füzet alkot egy kötetet.

A közlésre szánt kéziratok a következő címre küldendők:

Acta Physica, Budapest 502, Postafiók 24.

Ugyanerre a címre küldendő minden szerkesztőségi és kiadóhivatali levelezés.

Az *Acta Physica* előfizetési ára kötetenként belföldre 80 forint, külföldre 110 forint. Megrendelhető a belföld számára az Akadémiai Kiadónál (Budapest V., Alkotmány utca 21. Bankszámla 05-915-111-46), a külföld számára pedig a „Kultúra" Könyv- és Hírlap Külkereskedelmi Vállalatnál (Budapest I., Fő u. 32. Bankszámla 43-790-057-181 sz.), vagy annak külföldi képviseleteinél és bizományosainál.

Die *Acta Physica* veröffentlichen Abhandlungen aus dem Bereich der Physik in deutscher, englischer, französischer und russischer Sprache.

Die *Acta Physica* erscheinen in Heften wechselnden Umfanges. Mehrere Hefte bilden einen Band.

Die zur Veröffentlichung bestimmten Manuskripte sind an folgende Adresse zu richten:

Acta Physica, Budapest 502, Postafiók 24.

An die gleiche Anschrift ist auch jede für die Redaktion und den Verlag bestimmte Korrespondenz zu senden.

Abonnementspreis pro Band: 110 Forint. Bestellbar bei dem Buch- und Zeitungs-Aussenhandels-Unternehmen »Kultúra« (Budapest I., Fő u. 32. Bankkonto Nr. 43-790-057-181) oder bei seinen Auslandsvertretungen und Kommissionären.

INVESTIGATION OF THE GAMMA ACTIVITIES AND GAMMA SPECTRA OF SNOW SAMPLES

By

Á. TÓTH, T. ZSOLDOS and A. URBÁN

MÉV HEALTH SERVICE, PÉCS

(Presented by L. Pál — Received 18. II. 1965)

An analysis of the total gamma activities and the gamma spectra of 25 samples of snow and 1 of rainwater-snow collected in Hungary (between 16°—22° longitude and 46°—48° latitude) between 29th January and 22nd February 1963 revealed that *a)* the ^{137}Cs-equivalent total gamma activity is on the average $5{,}1 \cdot 10^{-7}$ μc/ml; *b)* the total beta concentration calculated from this is $\approx 1{,}2 \cdot 10^{-6}$ μc/ml; elements detected with great probability: ^{141}Ce, ^{144}Ce, ^{103}Ru, ^{7}Be, ^{137}Cs, ^{95}Zr and ^{95}Nb. Age of fission products: ranging from 50 to 80 days. ^{137}Cs and (^{95}Zr + ^{95}Nb)-concentrations have been estimated. Our total activity data agree well with those of other authors; the results of our selective determinations are of the order of the values obtained by other authors, differences being due to losses in collection and sample treatment. Our Szeged sample distinguished itself from the others by its anomalously high (approximately three times higher) radioactivity.

Introduction

Owing to atomic bomb explosion tests precipitation and falling dust inject fission products into the biosphere. On account of this man's external and internal radiation dose increases above the natural dose, and so does the radioactivity of the environment. This fact affects geophysical investigations and the determination of man's exposure to natural radioactive elements in the field, the investigations of the contamination of the environment and the measurement of low radioactivities. This accounts for the importance of analysis of precipitation for the presence of fission products.

In this country such measurements have been in progress at Debrecen, since 1952 [11, 12, 38, 39, 40]. The purpose of the present paper is to supplement these and other valuable Hungarian [37] and the many foreign data with some results of our own obtained by a preliminary informatory method. The improvement of the method employed is in progress.

Survey of the literature

Many excellent summaries of this problem have been published [10, 25, 28, 39, 51]. Several authors have dealt with the determination of fission product concentration in snow [1, 2, 3, 4, 14, 24], in rainwater [2, 3, 5, 9, 13, 14, 15,

17, 20, 24, 26, 27, 30, 31, 36, 37], in aerosols; and in snow, rainwater and in aerosols on the whole [6, 7, 8, 11, 12, 18, 22, 23, 29, 31, 38, 39, 44], as well as with the detection of the presence of these elements. The determinations are affected by the ^{7}Be [16, 32, 33, 44] and the ^{212}Pb [44], isotopes of natural origin and in the case of "hot" particles [58] by the phenomenon of fractionation [19].

Characteristic data for fission products in fall-out samples [8, 27, 34, 35, 42, 43] and assignments to atomic weapon tests carried out in 1962 have also been published [12, 21, 22, 23, 24].

Results of our investigations

The total gamma activities and gamma spectra of twenty-five snow samples and one rainwater-snow sample have been investigated. The samples were collected in the area between 16° and 22° longitude and 46°—48° latitude of this country (10 snow and 1 mixed rainwater-snow samples from Pécs, 2 snow samples from Maráza (Baranya County) and 1 snow sample from each of the following towns: Szigetvár, Szekszárd, Szombathely, Sopron, Kaposvár, Győr, Tapolca, Debrecen, Somoskőújfalu (Nógrád County), Miskolc, Szeged, Kecskemét and Budapest) between 29th January and 22nd February 1963. Although the reason for our choosing snow for the analysis was that it was simple to collect snow samples, later on, it appeared that snow was worth collecting also because its radioactivity was higher than that of rain [14, 24, 36]. On the other hand, the measurement of gamma activity and spectra is technically, preparationally and even informationally more advantageous than the observation of total beta activity detected after radiochemical treatment, although the disturbing element ^{7}Be cannot be separated from the 500 keV photopeak without radiochemical separation by means of the gamma spectrometrical instruments now avilable to us, and if at all, this can only be done by half-life estimation.

The snow was sampled from approx. $1 m^2$ area, to its full depth, without traces of soil. The melted snow mixed with rainwater was taken from the rainwater pipe. The volume of our samples prior to evaporation to dryness was 5000 ml, with one exception (sample marked F—18: 3000 ml). As no acids or carriers were added to the vessels when the snow samples were collected, melted and transported to the laboratory we did not use polyethylene vessels [14, 17, 19, 24, 26, 27] and did not record how long before collection the snow fell (leaching: [14]). Thus significant losses of fission products may have occurred.

After preliminary filtration the samples were boiled with nitric acid to the volume of 5—10 ml necessary for the measurement. The filtrate was also washed with nitric acid added to the filtered liquid. Thus, at this stage of the

work the adsorption can be assumed to be smaller [50], although it can still be very considerable [5], for carrier-free iodine, ruthenium and circonium. It has been shown that the adsorption loss can be decreased by rubbing with diatomaceous earth [26]. The solutions evaporated to approximately 9 ml were put into normal test tubes and measured in these with a single-channel recording spectrometer type 1820B, manufactured by Nuclear Chicago [52, 56] having a NaJ(Tl) detector of a bore-hole volume of 8,4 ml, and with scalers, types FH—49 and PSZ—20, connected to the spectrometer (their input sensitivities were 0,5 V and 3,0 V, respectively).

The three groups of our measurements (total gamma activity measurement, measurement of spectra by automatic continuous, and manual step method) are summarized in Table 1.

Our measurements of total gamma activity were carried out by the integral mode of operation above 80 keV, by scalers. Our equipment was calibrated by a point-like ^{137}Cs source for energy (linearity is fulfilled, see also Fig. 5) and for total efficiency. The values thus obtained: $e = 5{,}6 \cdot 10^5$ cpm/μc and $\eta_t = 25{,}4\%$ agree well with the results observed under different conditions ($6{,}1 \cdot 10^5$ cpm/μc and 27%, but with a 50 mV input sensitivity scaler [48]) or calculated [49] by others.

For a known fission product mixture, an efficiency of 39% was measured for photon energies above 60 keV [26]. This is substantially modified by the difference in the composition from that used in [26] and by the actual conditions of the measurement. The counting rates of our solutions with an average volume of 9 ml have been reduced to zero solution height, so that the corrections obtained by others [44, 45, 46, 47, 48] for NaJ(Tl)-crystals, the bore-hole of which was of a size similar to that of our detector, have been made universal by establishing the (sample/bore hole) — volume ratio. A curve has been plotted based also on the Operation Manual of our instrument [52].

The ^{137}Cs equivalent concentration shown in Table 1 has been calculated on the basis of the background-less counting rates M, the above data and the original volumes. The roughly approximate total beta concentration calculated from the ^{137}Cs equivalent concentration, as can be seen from Table 2, is in good agreement with the values of others for a similar period [37, 38]. As ^{90}Sr is also present in the samples [1, 20, 24, 37] our total beta value exceeds the level $1{,}0 \cdot 10^{-6}$ μc/ml fixed by ICPR (1959) by approximately 20%. This assertion is supported by the presence of ^{90}Sr actually detected by other authors in precipitations over the same period of collection, e. g. in Rumania [1], Canada [20], England [24] and even in this country [37]. The age of fission products on the basis of our total gamma measurements (see Table 1) is approximately 50—80 days. To obtain preliminary information as to composition we measured the spectra of our twenty six samples by automatic registration [52], four of which are shown in Figs. 1, 2, 3 and 4. These represent the spectra

of the remaining twenty two samples very well, apart from the 140 keV photopeak of the rainwater — melted snow sample, marked F—22, which is completely missing, and the 750 keV photopeak, which is scarcely visible

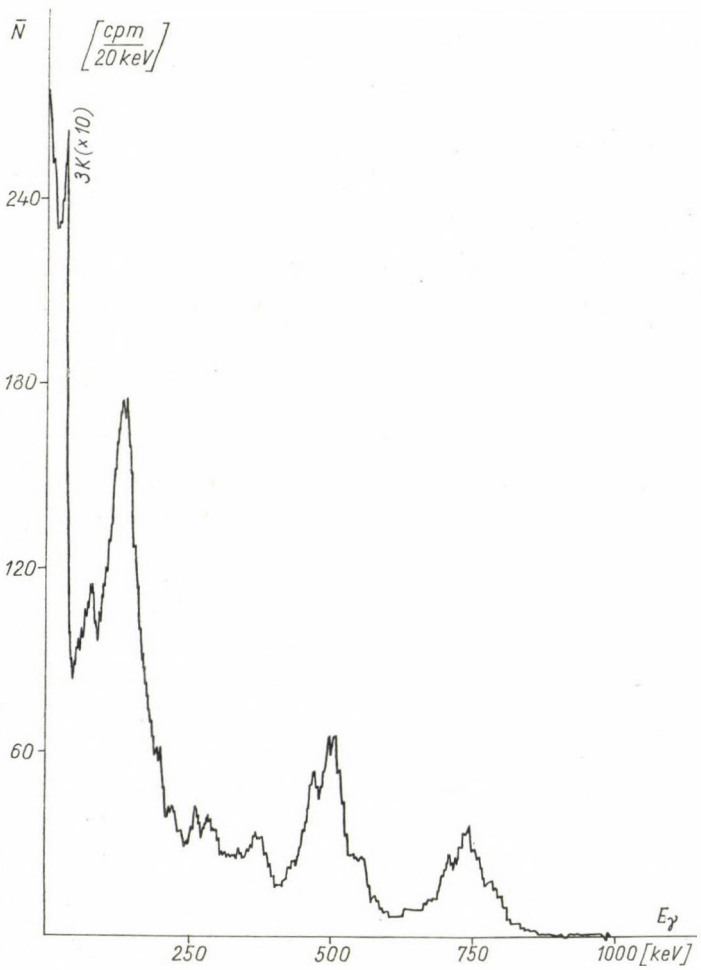

Fig. 1. Automatically recorded gamma spectrum of our Pécs sample. Sample mark: F-1' Site of collection: Pécs; Date of collection: 29.01.1963; Time and date of measurement: 16h; 19.02.1963; Volume of melted snow prior to evaporation: 5000 ml

(losses due to collection from the rainwater pipe). The figures in brackets indicate the values concerning the increased counting rate (cpm) — limits of measurement.

It is known [41] that the shape of spectra recorded by single-channel automatic analyzers with ratemeters is distorted (the photopeaks are flattened

Table I

Summary of the results of the measurements

Type of measurement		Total number of measurements and spectra taken of 26 samples	Arithmetic average of the time between collection and measurement (recording of spectra) Δt (day)	Arithmetic average and statistical error in % of integral, background-free counting rates M (cpm)	Average, approximate, ^{137}Cs-equivalent concentration calculated from M, not corrected for ^{7}Be, at the time of measurement C (μc/ml)	Arithmetic averages and statistical errors in % of some important, observed photopeak-heights and photopeak area ratios corrected for Compton scattering [27] and flattening [41]. (For error calculation see explanatory remarks 10. and 22.)						Average approximate age of fission products in the samples t_h (day)	Identification of elements by comparing the decay in time of an identical photopeak height (area) of a given sample and the Table of corrections for decay published in [57]				
						No. of measurements	$\left(\frac{500\text{ keV}}{140\text{ keV}}\right)$	No. of measurements	$\left(\frac{500\text{ keV}}{750\text{ keV}}\right)$	No. of measurements	$\left(\frac{750\text{ keV}}{140\text{ keV}}\right)$		sign of sample	140 keV	500 keV	662 keV	750 keV
Total gamma-counting rate measurements[1] (threshold: 80 keV)	I.	26 $(1)_2$	15 $(18)_2$	$1030 \pm 3\%$ $(3600 \pm 1{,}3\%)_2$	$5{,}09 \cdot 10^{-7}$ $(14{,}4 \cdot 10^{-7})_2$	—	—	—	—	—	—	$50 \pm 20_3$ or $80 \pm 10_4$	—	—	—	—	—
	II.	26 $(1)_2$	652 $(653)_2$	$73 \pm 14\%$ $(286 \pm 3{,}1\%)_2$	— —	—	—	—	—	—	—		—	—	—	—	
	II.	—	—	$(0{,}07 \pm 14{,}3\%)$ $(0{,}08 \pm 3{,}4\%)_2$	—	—	—	—	—	—	—		—	—	—	—	—
	I.																
Gamma spectra taken for preliminary information by automatic recording[5]		30_6	15	—	—	25_7	0,80 $\pm 17{,}5\%_{010}$	33 or 32_8	2,07 or $1{,}89_8$	22_9	0,41 $\pm 21{,}5\%_{010}$	between 45 and 65_{11} approx. 45_{12}	F-17$_{13}$	—	^{7}Be; ^{103}Ru?	—	^{95}Zr ^{95}Nb
													F-26	^{144}Ce ^{141}Ce	^{103}Ru ^{14}	—	—
Gamma spectra taken by the stepwise method[15]		17_{16}	22_{17} or 640_{10}	—	—	13_{19}	0,92 $\pm 53\%_{022}$	9_{20}	$2{,}44_{21}$ $\pm 55\%_{022}$	9	0,45 $\pm 47\%_{022}$	approx. 50_{23}	F-17$_{24}$	^{144}Ce? ^{141}Ce?	—	^{137}Cs$_{14}$	—
													F-26$_{25}$	^{144}Ce$_{14}$	—	^{137}Cs$_{14}$	—

Explanatory remarks:

[1] I: first series of measurements;
II: second series of measurements.

[2] Values for the anomalous Szeged sample marked: F-17.

[3] Based on 1030^{-1} and 73^{-1}.

[4] Based on $1030^{-0{,}83}$ and $73^{-0{,}83}$ [40].

[5] Duration of a run = 30 minutes; spectrum scanning speed = 0,555 keV/sec; recording paper speed = 30,5 cm/hour; window width = 2 Volts; counting rate, range in general: 0—150 cpm; rarely: between 0—300 cpm; charging time constant of the ratemeter for 0—300 cpm: of the order of 100 μsec [55]; integration time constant of the ratemeter: 40 sec [52]; equilibrium time calculated for the recording pen adjustment to the new average cpm with a probability of 50%, as well as for the difference between the cpm-s in the photopeaks and the "valleys" below the photopeaks for a time constant of 40 sec: approx. 100 sec [56]; energy range: from 0 to 1 MeV.

[6] Since we have taken four spectra altogether for the sample F-1, two spectra for the sample F-2 and two spectra for the sample F-17, the automatic spectrum of F-5 was not recorded at all owing to instrument fault.

[7] Owing to distortion it was not possible to evaluate the 140 keV photopeak several times.

[8] Without the anomalous value of (7,84) obtained for F-26.

[9] For the February 1963 measurements which could be evaluated.

[10] Photopeak heights graphically corrected for the average, distorted, total background, in [cpm/20 keV] — units, for 140, 500 and 750 keV: $\bar{N}_i = 51$, 47 and 24. The relative statistical errors of the observations of $\bar{N}_i$ (assuming an equilibrium time of approx. 100 sec and that the differential background is zero; we know, however, that these assumptions are not satisfied) are for the time constant $\tau_2 = 40$ sec on the basis of the formulas

$$\delta = \pm \left(100 \Big/ \sqrt{\frac{2\,\bar{N}_i \cdot \tau_2}{60}}\right) \quad \text{and} \quad \delta = \pm (87/\sqrt{\bar{N}_i}) \qquad [\%]$$

of the values: $\pm 12{,}2$; $\pm 12{,}7$; $\pm 17{,}8\%$. The errors in the ratios have been calculated by the square law of the propagation of error.

[11] From the comparison of the shapes of our spectra and those in [51b].

[12] For the ratio of value 0,41, as well as for the conditions of measurement given in [51a], assuming ^{235}U-fission products.

[13] See Fig. 3.

[14] Certainly.

[15] Window width = step distance = 2 Volts = 20 keV; energy-range: 0 to 1 MeV; observation by scaler; durations of observations (t_1: sample + background; t_2: background): for the sample F-17 early in 1963: $t_1 = 2'$; $t_2 = \varnothing$' (the ten times smaller background-cpm was neglected); late in 1964: $t_1 = t_2 = 3'$. For the sample F-26 early 1963: $t_1 = t_2 = 2'$; late in 1964: $t_1 = t_2 = 4'$. Errors of the respective observations: F-17, 1963, in the neighbourhood of 750 keV: $\pm 11\%$; 500 keV: $\pm 7\%$; 140 keV: $\pm 5\%$; F-17, 1964, 660 keV: approx. $\pm 30\%$; F-26, 1963, 750 keV: $\pm 25\%$; 500 keV: $\pm 10\%$; 140 keV: $\pm 8\%$. F-26, 1964, 660 keV: approx. $\pm 30\%$.

[16] For the samples F-17 and F-21 the number of partial spectra recorded in the neighbourhood of 660 keV is not included here.

[17] For the 11 measurements carried out in March 1963.

[18] For the 6 measurments carried out in 1964.

[19] The 500 keV photopeak already decayed in three cases, while for the sample F-22 the 140 keV photopeak was missing.

[20] The 750 keV photopeak was missing in 8 spectra.

[21] For the relation $t_h = 50$ to 60 days, and for the assumptions of [18] this photopeak area ratio is only approx.: 0,5. According to [42] this ratio for $t_h = 42$ days, when it is just maximum, is only of the value: 1,33. As the ratios observed by us are much larger, thus in our case it is either due to the disturbing effect of the element ^{7}Be that the area of the 500 keV photopeak is larger, or it is due to losses in collection and treatment that the area of the 750 keV photopeak is smaller, or in our case the assumption in [18] about the fission of ^{238}U by fast neutrons can no longer be maintained. As the errors of our ratios are about 20% and 50%, these can only be used for estimation.

[22] The error of the photopeak area ratios has been calculated in the following way: *a)* the own relative statistical errors of the values of measurements determining the area of the photopeak have been established; *b)* for simplicity the arithmetic average of the errors so obtained has been taken for the significant photopeaks of each sample: *c)* finally the arithmetic average of the average errors referred to in *b)* has been taken for the given identical photopeak energy of each sample (i.e. separately for the 140 keV, 500 keV and 750 keV energies.) For the estimable 140 keV peak of 16 we have thus obtained an error of $\pm 32\%$, for the 500 keV of 14 an error of $\pm 42\%$, and for the 750 keV of 10 an error of $\pm 35\%$. The errors of photopeak area ratios have been calculated by the square law of the propagation of error. These errors, as can be seen in the Table, are approximately 50%.

[23] According to the photopeak area ratio of approx. 0,45 and [51*a*] (see remark 12).

[24] See Fig. 7.

[25] See Fig. 8.

and shifted, resolving power decreases.) For the conditions of our measurements [55, 52, 56] we have determined the distortions (at 140, 500 and 750 keV: *a)* flattening of photopeak 27, 16 and 12%, respectively; correction factors 1,27, 1,16 and 1,12; *b)* decrease of resolving power: at least 28, 11 and 10%, correction factors: 1,28; 1,11 and 1,10; *c)* photopeak shift towards small energies: 15, 17 and 19 keV), for the automatic spectrum obtained for ^{137}Cs

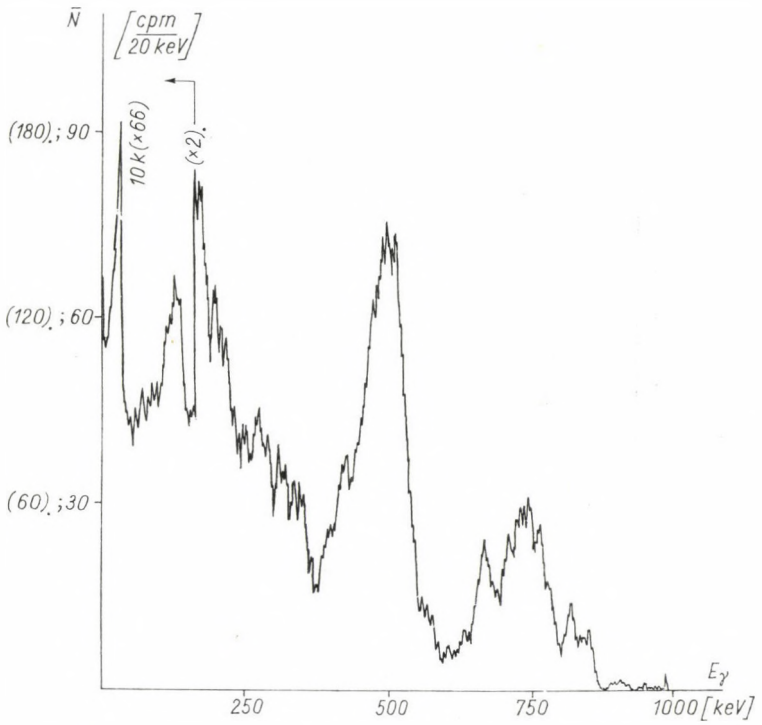

Fig. 2. Automatically recorded gamma spectrum of our Somoskőújfalu sample. Sample mark: F-14; Site of collection: Somoskőújfalú (Nógrád County); Date of collection: 12.02.1963; Date of measurement: 22.02.1963; Volume of melted snow prior to evaporation: 5000 m

(the resolution is 13,75%; and by dividing this by the correction at least 1,11 for 660 keV, the undistorted resolution gives 12,4%, while in the stepwise operation (see later) it is 11,6%. Thus the correction is good within the 7% error mentioned in [41].)

After graphical Compton correction [27] the rough photopeak heights have been corrected according to [41] and the ratios of the corrected values are given in Table 1. Figs. 1—4 and Table 1 show that expressed photopeaks appear mainly in the neighbourhood of 140, 500 and 750 keV (thus, at places

distant from one another in this country the distribution of fission products is approximately identical) the heights of which, except for the 140 keV peaks, always exceed the values of the total background (below them). Owing to

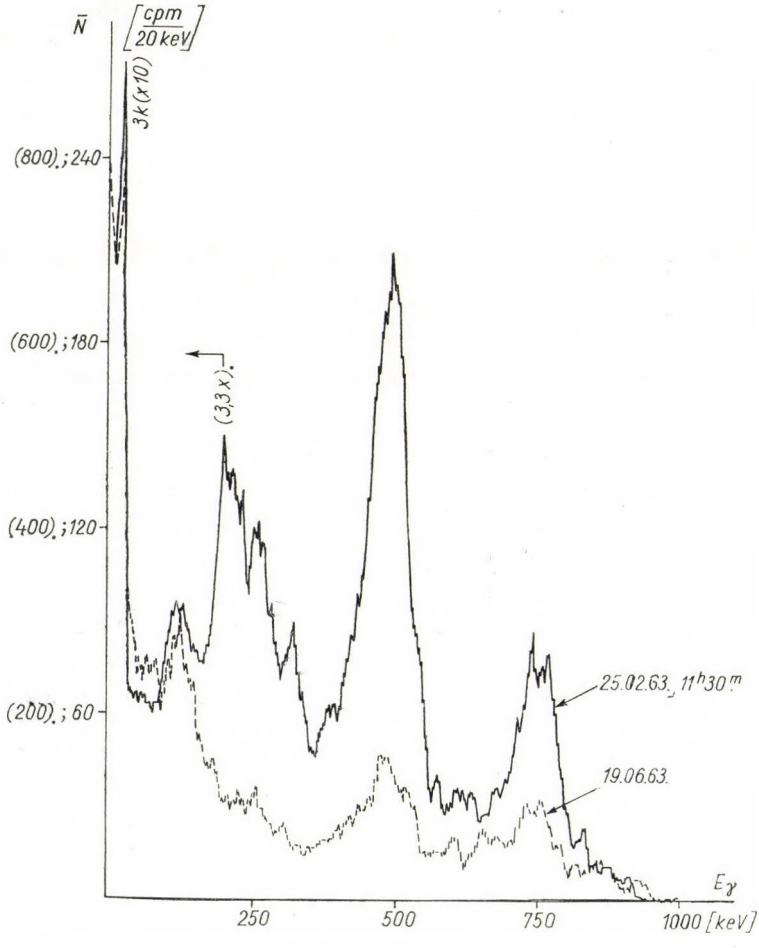

Fig. 3. Automatically recorded gamma spectra of our Szeged sample showing an activity much higher than the average. The second spectrum was recorded approx. four months later. Sample mark: F-17; Site of collection: Szeged; Date of collection: 07.02.1963; Volume of melted snow prior to evaporation: 5000 ml

errors [41] it would be unreasonable to regard smaller protrusions as "photo-peaks" or to assign them to specific elements.

Based on automatic recordings, Table 1 also contains age and element-identification estimations (45—60 days, ^{141}Ce, ^{144}Ce, ^{7}Be, ^{103}Ru, ^{95}Zr and ^{95}Nb).

The presence of ^{144}Ce is confirmed by the fact that after more than one and a half years it can still be detected in the stepwise spectra (see Figs. 7 and 8). On the other hand, the presence of the other elements (except for ^{7}Be) is sug-

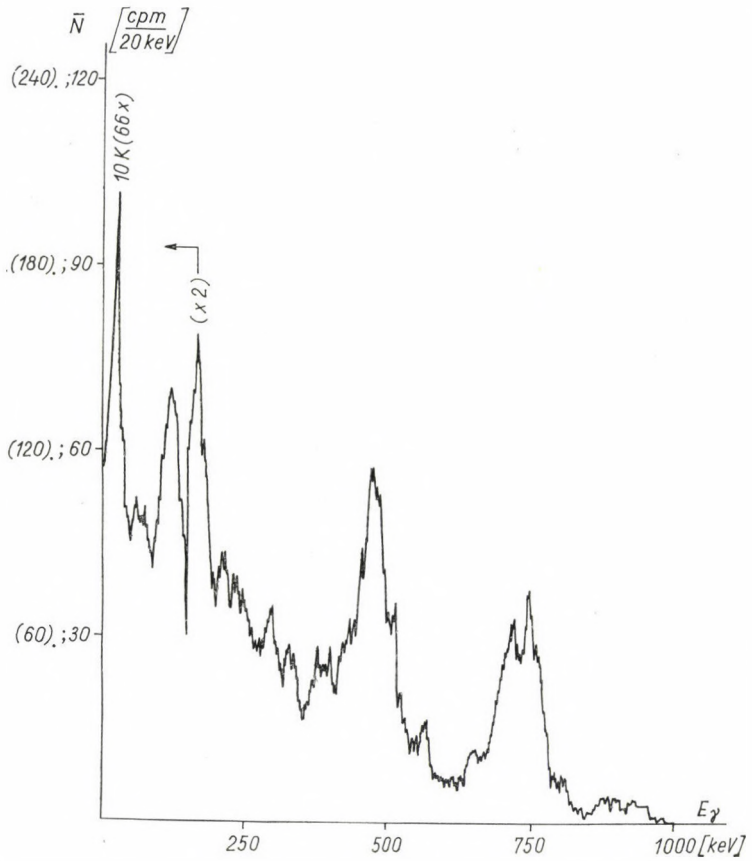

Fig. 4. Automatically recorded gamma spectrum of our Kecskemét sample. Sample mark: F-21; Site of collection: Kecskemét; Date of collection: 14.02.1963; Date of measurement: 26.02. 1963; Volume of melted snow prior to evaporation: 5000 ml

gested by the fact that they were also detected in neighbouring countries during the period of our collections (see Table 2).

The manual stepwise spectra of a few samples (measurements with scalers) were taken directly after the automatic recordings, and (to detect ^{137}Cs) again much later, in order to decrease statistical and distortion errors. (Unfortunately, owing to the restricted duration of the measurements we failed to obtain a smaller statistical error).

Table 2

Presence and concentration of fission products in precipitations

Isotope	Medium	Date and site of collection	Date of measurement	Concentration C (μc/ml)	Trend in time of C	Literature
^{144}Ce	s	21.12.1962—10.01.1963 Bucharest, Rumania	?	?; ce	?	[1]
	r	30.04.1962—01.01.1963 Vienna, Austria	11.05.1962—04.01.1963	?; ce	?	[5]
	$(r + s)^x$	12.1962 London	?	$2{,}5 \cdot 10^{-7}$; co	i	[24]
		01.1963 London	?	$7{,}0 \cdot 10^{-7}$; co	max	
		02.1963 England	?	$3{,}5 \cdot 10^{-7}$; co	d	
	r	03.1963 England	?	$3{,}0 \cdot 10^{-7}$; co	d	
	s	29.01.1963—22.02.1963 Hungary	After $\sim$ 15 and 640 days	?; ce (Table 1)	?	o
^{141}Ce	r	16.07.1962—15.08.1962 Sydney, Australia	?	$2{,}7 \cdot 10^{-7}$	i	[13]
^{103}Ru	s	17.02.1963 Budapest, Hungary	28.02.1963 and 19.06.1963	?; ce (Table 1)	?	o
	s	11—13.03.1962 Seibersdorf, Austria	21—22.03.1962	$< 0{,}68 \cdot 10^{-7}$; co	?	[2]
^{106}Ru	r	05—07.11.1961 Seibersdorf, Austria	27—28.11.1961	?; ce	?	[2]
+ ^{106}Rh	s	11—13.03.1962 Seibersdorf, Austria	21—22.03.1962	?; ce	?	
^{106}Ru	r	30.04.1962—01.01.1963 Vienna, Austria	11.05.1962—04.01.1963	?; ce	?	[5]
^{140}Ba	r, s	11.1961 and 03.1962 Seibersdorf, Austria	11.1961 and 03.1962	?; ce	?	[2]

^{140}Ba	$(r + s)^x$	12.1962 } London 01.1963 } London 02.1963 } England	? ? ?	$1{,}1 \cdot 10^{-7}$; co $5{,}5 \cdot 10^{-7}$; co $1{,}2 \cdot 10^{-7}$; co	i max d	[24]
	r	03.1963 } England	?	$1{,}2 \cdot 10^{-8}$; co	d	
^{140}La	s	21.12.1962—10.01.1963 Bucharest, Rumania	?	?; pr.	?	[1]
	r	05.11.1961—07.11.1961 Seibersdorf, Austria	27--28.11.1961	$0{,}8 \cdot 10^{-7}$; co	?	[2]
	r	16.07.1962—15.08.1962 Sydney, Australia	?	$9{,}3 \cdot 10^{-8}$	?	[13]
^{137}Cs	s	21.12.1962—10.01.1963 Bucharest, Rumania	?	?; ce	?	[1]
	$(r + s)^x$	12.1962 } London 01.1963 } London 02.1963 } England	? ?	$8{,}0 \cdot 10^{-9}$; co $5{,}0 \cdot 10^{-8}$; co	i max	[24]
	r	03.1963 } England	?	$4{,}0 \cdot 10^{-8}$; co $3{,}5 \cdot 10^{-8}$; co	d d	
	s	03, 14 and 17.02.1963 Hungary	after $\sim$ 670 days	$> (6{,}0 \cdot 10^{-9})$; a; j	?	o
	s	07.02.1963 Szeged, Hungary	after 690 days	$> (1{,}1 \cdot 10^{-8})$; a; l	?	o
^{95}Zr	r	30.04.1962—01.01.1963 Vienna, Austria	11.05.1962— 04.01.1963	?; ce	?	[5]
	$(r + s)^x$	12.1962 } London 01.1963 } London 02.1963 } England	? ?	$1{,}0 \cdot 10^{-6}$; co —	max. (d)	[24]
	r	03.1963) } England	? ?	$5{,}0 \cdot 10^{-7}$; co $2{,}7 \cdot 10^{-7}$; co	d d	
^{95}Zr + ^{95}Nb	s	21.12.1962—10.01.1963 Bucharest, Rumania	?	?; pr	?	[1]
	s	11—13.03.1962 Seibersdorf, Austria	21—22.03.1962	?; ce	?	[2]

Table 2 (continued)

Isotope	Medium	Date and site of collection	Date of measurement	Concentration C (μc/ml)	Trend in time of C	Literature
	r	16.07—15.08.1962 Sydney, Australia	?	$2{,}1 \cdot 10^{-7}$	i	[13]
	s	02.03.11, 12, 17, 22. 02.1963, Hungary	after $\sim$ 12 days	$> (3{,}0 \cdot 10^{-8})$; a; p	?	o
	s	07.02.1963, Szeged, Hungary	after 18 days	$> (1{,}3 \cdot 10^{-7})$; a; l	?	o
^{91}Y	r	05.1963 London, England	?	$2{,}0 \cdot 10^{-7}$; co	max.	[24]
^{147}Pm	r	07.1963 London, England	?	$2{,}0 \cdot 10^{-7}$; co	c	[24]
^{90}Sr	s	21.12.1962—10.01.1963 Bucharest, Rumania	?	?; ce	?	[1]
	(r + s)	1955—1962, Deep River, Canada	?	$4{,}2 \cdot 10^{-9}$	?	[20]
	r	Spring 1962 Deep River, Canada	?	$3{,}0 \cdot 10^{-8}$	max.	
	r	Late 1962 Deep River, Canada	?	$5{,}0 \cdot 10^{-9}$	d	
	$(r + s)^x$	12.1962 London 01.1963 London 02.1963 England	? ? ?	$6{,}0 \cdot 10^{-9}$; co $3{,}0 \cdot 10^{-8}$; co $2{,}0 \cdot 10^{-8}$; co	i max d	[24]
	r	03.1963 England	?	$2{,}0 \cdot 10^{-8}$; co	c	
	r	12.1962 Budapest 01.1963 Budapest 02.1963 Hungary 03.1963 Hungary	after 3 weeks	$3{,}2 \cdot 10^{-9}$ $4{,}8 \cdot 10^{-9}$ $1{,}2 \cdot 10^{-9}$ $1{,}1 \cdot 10^{-8}$	i i d max	[37]
	s	03, 14, and 17.02.1963 Hungary	calculated from Cs-137 value; e	$> (3{,}6 \cdot 10^{-9})$; a; j	?	o

	s	07.02.1963 Szeged, Hungary	calculated from ^{137}Cs value; e	$> (6{,}6 \cdot 10^{-9})$; a; l	?	o
^{7}Be; n	s	19.02.1956 01.03.1956 } Uppsala 03.03.1956 } Sweden	?	$1{,}31 \cdot 10^{-8}$ $1{,}61 \cdot 10^{-8}$ $2{,}64 \cdot 10^{-8}$	i i i	[32] [33]
	r	20.06.1958 11.09.1958 } Bombay 14.07.1958 } India	?	$1{,}87 \cdot 10^{-8}$ (average of 19 samples) $4{,}3 \cdot 10^{-8}$	 max.	[16] [33]
480 keV peak $^{7}Be + {}^{103}Ru$ deducting ^{140}La	r	16.07.1962—15.08.1962 Sydney, Australia	?	$4{,}00 \cdot 10^{-7}$	max.	[13]
Total beta	r	01.1963 02.1963 } Budapest 03.1963 } Hungary	after 3 weeks?	$2{,}6 \cdot 10^{-6}$ $1{,}1 \cdot 10^{-6}$ $1{,}7 \cdot 10^{-6}$	i, ? d i	[37]
	r + s + + y	01.1963 02.1963 } Debrecen 03.1963 } Hungary	after 2 days at least	$0{,}88 \cdot 10^{-6}$ $0{,}67 \cdot 10^{-6}$ $0{,}82 \cdot 10^{-6}$	c d i	[38]
	s	29.01.1963—22.02.1963 Hungary	~ 15 days	$< (1{,}17 \cdot 10^{-6})$ f;	?	o
	r + s + + y	05—12.02.1963	~ 2 days	$0{,}56 \cdot 10^{-6}$	—	[38]
	s	11.02.1963 Debrecen, Hungary	11 days	$< (0{,}85 \cdot 10^{-6})$ g;	—	o

Explanatory remarks to Table 2

r = rain
s = melted snow
r + s = melted snow mixed with rainwater
co = corrected for the date of collection
i = increasin
d = decreasin g
max = maximum
min = minimum
c = approximately constant
ce = certainly present
pr = probably present
? = not published, undeterminable value of C given in cpm/ml only
x = between 11.01.1963 and 08.02.1963 only snow, for [24]
o = our investigations
a = approximate, neglecting sampling and concentration losses, calculating in a rough approximation for the volume-dependence of photopeak-efficiency, taking (^{95}Zr + ^{95}Nb) with the efficiency of [27] at the date of measurement (not corrected for decay !)
e = obtained from eight pairs of data [24, 14], converted with the average value (^{90}Sr/^{137}Cs) = = 0,6
y = "dry" fall-out on precipitation-free days
f = calculated for our conditions by a multiplying factor of $\sim$(2,3) [26] from the approximate total gamma concentration in Table 1, determined in ^{137}Cs-equivalent and not corrected for ^{7}Be, neglecting losses and with a rough correction for the volume-dependence of the ^{137}Cs total-efficiency; average value applicable to all 26 samples. The multiplying factor $\sim$(2,3) can be applied under the following assumptions [26]: *a)* the fission products in our samples are due to the fission of ^{235}U by slow neutrons; *b)* the measurement was made not earlier than 100 days after the fission. With a known fission product mixture [26] and with an unknown geometry the mean integral counting efficiency is 0,39 and 0,33 for 60 keV and 140 keV threshold, respectively. For 80 keV and an unknown geometry of measurement approximately 0,38 can be taken. The authors calculated for point-like Cs-137, for 80 keV and other, known conditions of measurement with an integral counting efficiency of

$$\eta_t = 0{,}254\ [\text{impulse}/^{137}\text{Cs disintegration}] \doteq 0{,}31 \left[\frac{\text{impulse}}{661\ \text{keV-photon}}\right].$$

The deviation is in percentage of the value 0,38: —18,4%, appropriate for estimation, still acceptable.
n = element of natural origin, affecting the determination of fission products
g = see f, but only for our sample, marked: F-15.
j = for the samples marked: F-5, 6, 9, 21 and 26
l = for the sample marked: F-17
p = for the samples marked- F-4, 10, 15, 16, 18, 24, 25 and 26
> = greater than
< = smaller than

As shown in Fig. 5 the energy linearity of our apparatus is satisfied between $\sim$ 140 and 1280 keV. Below 100 keV linearity is not guaranteed for our instrument by the manufacturer [52]. The energy-dependence of energy

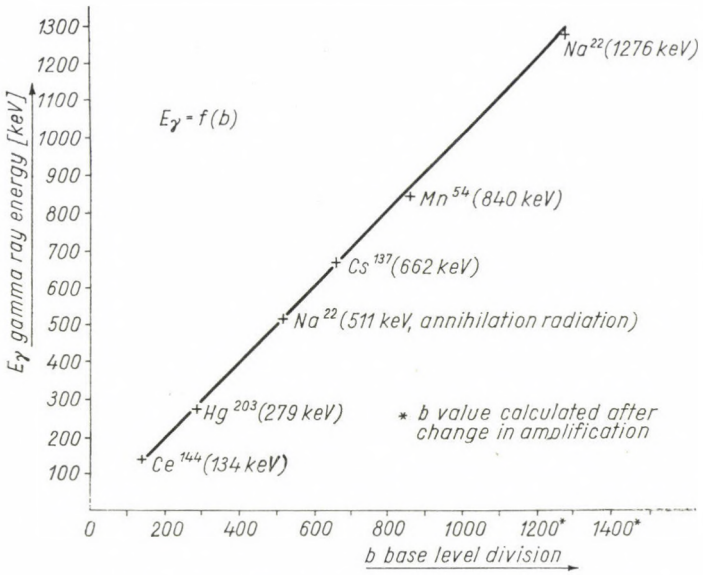

Fig. 5. Energy linearity of our gamma-spectrometer

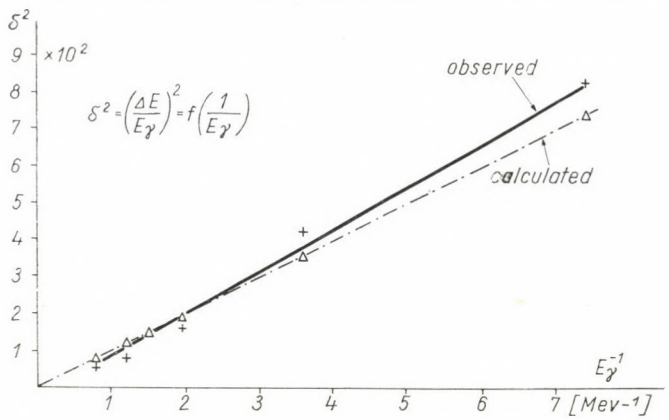

Fig. 6. Energy-dependence of the energy resolution of our gamma-spectrometer

resolution is shown approximately in Fig. 6, where the extrapolated straight line obtained from observation — apparently owing to equalization errors — does not intersect the ordinate [54].

Energy calibration measurements were carried out with non-pointlike sources (solutions). For pointlike ^{137}Cs in the stepwise mode of operation the

half value width is 76 keV (in automatic recording 91 keV), the resolution is 11,6%, and the photopeak efficiency calculated from the area of the photopeak: $P_{662} = 13{,}8\%$. The latter value is in good agreement with values obtained by other authors: 14% and 15% [2, 53].

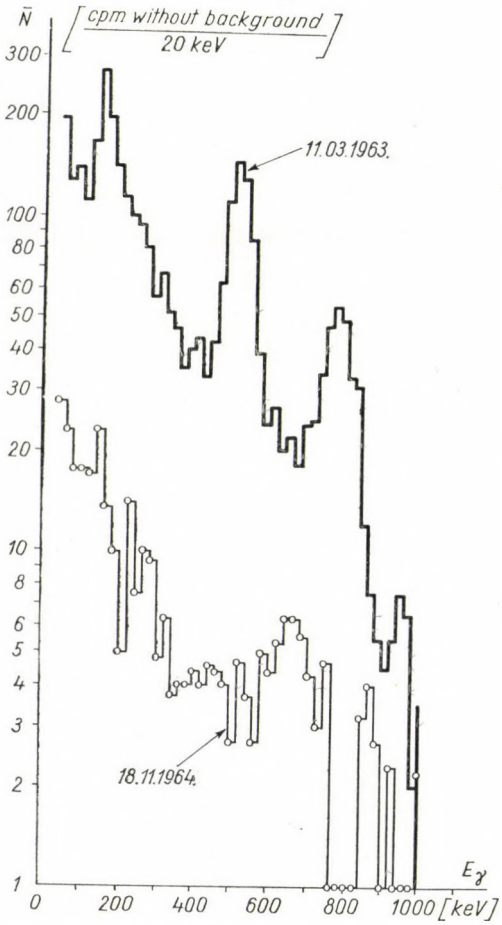

Fig. 7. Gamma spectra recorded by the stepwise method, by scaler, of our Szeged sample. The second spectrum, in which the peak appearing in the vicinity of 660 keV refers to the existence of ^{137}Cs, was recorded 20 months later. Sample mark: F-17; Site of collection: Szeged; Date of collection: 07.02.1963; Volume of melted snow prior to evaporation: 5000 ml

Table 1 as well as Figs. 7 and 8 show the results of our stepwise spectra obtained at two subsequent time-intervals for the samples F—17 and F—26. At this time too, outstanding peaks appear at 140, 500 and 750 keV, except for two samples of the remaining twenty two (F—22: peak appears only at 500 keV; F—23: the 750 keV peak is missing; but when observed automatically,

soon after collection, it was barely visible). For at least one and a half year after collection the 140 keV (^{144}Ce) peak can still be found in the spectra, the 500 keV peak can scarcely be observed and since the 750 keV peak and its Compton continuum have already decayed, the 662 keV peak of ^{137}Cs also

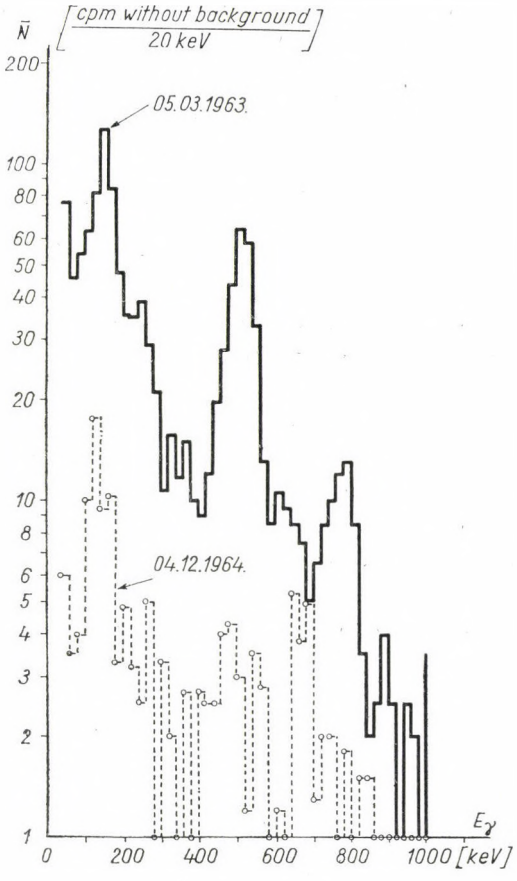

Fig. 8. Gamma spectra recorded by the stepwise method of our Budapest sample. The peak appearing in the vicinity of 660 keV in the spectrum recorded approx. 21 months later refers to the presence of ^{137}Cs. Sample mark: F-26; Site of collection: Budapest; Date of collection: 17.02.1963; Volume of melted snow prior to evaporation: 5000 ml

appears. The areas of the significant photopeaks have been determined from linear scale graphs by means of the graphical correction already mentioned [27]. The ratios of the areas are shown in Table 1. Although with a large error ($\pm$ 82, 68, 88, 23, 74, 46%) ^{137}Cs has been detected in the samples marked F—5, F—6, F—9, F—17, F—21 and F—26 one and a half year after collection, with the greatest probability in the F—17 sample ($\pm$ 23% statistical error).

From the resulting ^{137}Cs concentrations, ^{90}Sr concentration for the above six samples has also been estimated by means of the conversion factor mentioned in remark *d)* to Table 2 (see Table 2).

The ^{137}Cs concentrations (see Table 2) have been calculated on the basis of zero solution height corrections and the $P_{662} = 13{,}8\%$ photopeak efficiency. As the value of P_{662} agrees with the one in [27] and as in [27] the 750 keV photopeak efficiency (for $^{95}Zr + {}^{95}Nb$) is $P_{750} = 12\%$, based on the latter we have estimated ($^{95}Zr + {}^{95}Nb$)-concentration from the 750 keV photopeak areas. This is relatively simple, as a single gamma photon of given energy is emitted in the decay of each of these elements. As for ^{137}Cs, calculations have also been made for point source geometry assuming a 100% recovery of the element, although we know that this is not true. Table 2 shows the estimated ($^{95}Zr + {}^{95}Nb$)-concentration, just as the ^{137}Cs concentration, marked by the "greater than" sign before the bracket.

According to Table 2 our approximate values agree quite well with those of other authors (for total beta activity) or are of the same order of magnitude (owing to loss of material).

Owing to the dependence of fall-out concentration on latitude and season [24, 28, 29] and to possible fractionation [10, 19, 22] it is difficult to assign the fission product age of approximately 2 months obtained from the three types of measurements (see Table 1) to any particular nuclear explosion test, although snow normally contains younger fission products than does rain[36].

Our preliminary investigations have revealed that the surface of this country is also contaminated by fission products in snow and that some local anomalies occur (F—17 sample collected at Szeged, being approximately 3-times higher than the average). Improvements in our techniques are in progress.

Acknowledgements

Thanks are due to Prof. DÁNIEL VÖDRÖS, for his valuable comments, to the County KÖJÁL Organizations, for collecting and dispatching some of the samples, and to Mrs. K. FILUS, Mr. and Mrs. J. PÉTER, for treating and measuring the samples.

REFERENCES

1. I. I. GEORGESCU et al., Acad. Rep. Populare Romine, Studii si Cercetari de Fizica, **XIV**, 805, 1963.
2. G. M. TISLJAR—LENTULIS, Atompraxis, **9**, 214, 1963.
3. C. B. SENVAR and U. YÜCELIK, ibidem, 222.
4. F. SCHEFFER and F. LUDWIEG, Atompraxis, **9**, 75, 1963.
5. E. SCHMIED et al., Mikrochimica Acta, Heft **3**, 552, 1963.

6. A. KAUL and U. NAY, Die Naturwissenschaften, **50**, 615, 1963.
7. H. J. GRÜTER, Staub, **23**, 278, 1963.
8. H. J. GRÜTER, Staub **23**, 416, 1963.
9. M. LESIGANG and F. HECHT, Monatshefte für Chemie, **93**, 369, 1962.
10. B. RAJEWSKY et al., Atompraxis, **8**, 237, 1962.
11. A. SZALAY and A. KOVÁCS, Acta Phys. Hung., **18**, 281, 1961.
12. A. SZALAY and A. KOVÁCH, Acta Phys. Hung., **16**, 321, 1964.
13. D. R. DAVY and R. M. GREEN, Nature, **198**, 77, 1963.
14. N. G. STEWART et al., AERE(HP)R 2790, 10, 1959.
15. T. FLORKOWSKI et al., Nukleonika, **V**, 629, 1960.
16. D. LAL et al., Journ. Geophys. Research, **65**, 669, 1960.
17. E. M. R. FISHER et al., AERE — M 1010, 17, 1962.
18. M. SEDLACEK, Staub **22**, 87, 1962.
19. T. MAMURO et al., Nature, **197**, 964, 1963.
20. W. E. GRUMMITT and J. E. GUTHRIE, Canad. Journ. Phys., **42**, 287, 1964. AECL — 1873.
21. G. KISTNER, Die Naturwissenschaften, **51**, 109, 1964.
22. A. SITTKUS and L. LEHMANN, Die Naturwissenschaften **51**, 352, 1964.
23. P. F. GUSTAFSON et al., Nature, **203**, 470, 1964.
24. R. WOOD et al., Nature, **203**, 617, 1964.
25. V. P. SVEDOV and Sz. I. SIROKOV, Ragyioaktivnüje zagrjaznyenyija vnyesnyej szredü, Goszatomizdat, Moszkva, 1962, p. 275.
26. T. SCHÖNFELD and K. LIEBSCHER, Mitt. d. Anorg. u. phys. Chem. Inst. d. Univ. Wien, 8, 1959.
27. K. LIEBSCHER et al., Atompraxis, **7**, 94, 1961.
28. V. HAVLOVIC, Kernenergie, **7**, 49, 1964.
29. W. MARQUARDT, Kernenergie, **7**, 680, 1964.
30. A. AARKROG et al., Risö Report No. 63, 147, 1963.
31. A. AARKROG et al., Risö Report No. 64, 29, 1963.
32. R. NILSSON et al., Arkiv för Fysik, **11**, 445, 1957.
33. I. R. KAROL and Sz. G. MALACHOV, Voproszü jagyernoj meteorologiji, Goszatomizdat, Moszkva, 1962, p. 12.
34. C. E. CROUTHAMEL, Applied Gamma-Ray Spectrometry, Pergamon Press, Oxford, 1960.
35. O. I. LEJPUNSZKIJ, Gamma Izlucsenyije Atomnovo Vzrüva, Izd. Gl. Upr. Iszp. At. En. Moszkva, 1959, p. 137.
36. A. AARKROG, Nature, **204**, 771, 1964.
37. E. BAKÁCS—POLGÁR and I. KURCZ—CSIKY, Nature, **204**, 1057, 1964.
38. A. KOVÁCH (MTA-ATOMKI, Debrecen), communication by letter, 1964.
39. A. SZALAY and D. BERÉNYI, Proc. 2nd UN Geneva Conference, **18**, 570, 1958.
40. A. KOVÁCH and S. SZALAY, ATOMKI Közlemények, **II**, 229, 1960.
41. K. H. BERGER, Kernenergie, **4**, 181, 1961.
42. C. S. COOK, Health Physics, **4**, 42, 1960.
43. P. J. DOLAN, Gamma Spectra of Uranium — 235 Fission Products at Various Times after Fission, AFSWP 524, 1959.
44. V. N. LAVRENCSIK, "Izmerenyije γ i β-aktivnosztyi aerozolej", p. 150, Fig. 7; in "Tyechnika izmerenyii ragyioaktivnüch preparatov", Goszatomizdat, Moszkva, 1962. Pod. red. Bocskarjev.
45. L'Instrumentation Nucléaire, ACEC B. P. Charleroi, Belgium.
46. Zs. MAKRA (ed.), "Measuring methods for protection against radiation hazard", (in Hungarian), K. F. K. I., Budapest, 1964.
47. K. JORDAN, Die Atomwirtschaft, **3**, 499, 1958.
48. K. WAECHTER, "Metrology of Radionuclides", IAEA Symposium, Session 5, 375, 1959, Vienna.
49. U. C. MISHRA et al., Calculation of the Gamma-Ray Detection Efficiency of Annular and Well-type Sodium-Iodide Crystals, TID-17630, p. 28, 1962.
50. B. LENGYEL and J. PROSZT, General and Inorganic Chemistry (in Hungarian), Tankönyvkiadó, Budapest, p. 776, 1959.
51. "Radioaktyivnüje csaszticü v Atmoszfere", Szbornyik sztatyej, Goszatomizdat, Moszkva, 1963.
    a) H. D. SCHULZ and W. KOLB, p. 75, Fig. 3.
    b) R. MAY and H. SCHNEIDER, p. 56, Figs. 2, 6, 7.
52. Operation and Maintenance Manual of Model 1820 B Recording Spectrometer, Nuclear Chicago Corporation, p. 21.
53. D. REDON et al., Nucl. Intr. and Meth., **26**, 18, 1964.

54. L. KESZTHELYI, "Scintillation Counters" (in Hungarian), Műszaki Könyvkiadó Új technika sorozat, Budapest, 1964, p. 82.
55. E. VÁLÓCZY, private communication (11. I. 1965.).
56. Operation and Maintenance Manual of Model 1620 B Analytical Counting Ratemeter, Nuclear Chicago Corporation, pp. 11—19.
57. G. J. HUNTER and V. F. MITCHELL, "Tables of Factors for Correcting for Radioactive Decay, AERE" — R 4237, p. 3, Table 27, 1963.
58. J. A. SCHEDLING and W. A. MÜLLER, Zur Frage der Grösse und des Aufbaus der heissen Teilchen. Strahlenschutz, 1963. XII. (Bundesministerium für Atomkernenergie und Wasserwirtschaft).

ИССЛЕДОВАНИЕ ГАММА-АКТИВНОСТИ И ГАММА-СПЕКТРА СНЕЖНЫХ ОБРАЗЦОВ

А. ТОТ, Т. ЖОЛДОШ, и А. УРБАН

Резюме

Исследуя суммарную гамма-активность и гамма-спектр 25 снежных образцов и 1 образца дождевой воды, накопленных в периоде от 29 января по 22 февраля 1963 года на территории Венгрии (16°—22° меридианов и 46°—48° северной широты), выясняется, что а) эквивалентная суммарная гамма-активность Cs—137 составляет в среднем $5{,}1 \cdot 10^{-7}$ μc/ml; б) суммарная бета-концентрация, определенная на основе этого, равна $\approx 1{,}2 \cdot 10^{-6}$ μc/ml; с большой вероятностью встречаются элементы Ce—141, Ce—144, Ru—103, Be—7, Cs—137, Zr—95 и Nb—95. Возраст продуктов распада составляет 50—80 суток. Оценивается концентрация Cs—137 и (Zr—95 + Nb—95). Данные суммарной активности хорошо совпадают с результатами других исследователей, результаты селективного определения вследствие потерь при взятии проб и обработке образцов по порядку величины согласуются с данными других работ. Образец, взятый в г. Сегед, отличается от других аномальной радиоактивностью, примерно в три раза большей.

POTENTIAL FIELD AND FORCE CONSTANTS OF PHOSPHORUS AND ARSENIC TRICYANIDES

By

G. NAGARAJAN*

DEPARTMENT OF CHEMISTRY, UNIVERSITY OF MARYLAND, COLLEGE PARK, MARYLAND, U. S. A.

(Presented by A. Kónya. — Received 8. VI. 1965)

An orthonormalized set of symmetry coordinates satisfying the transformation properties has been constructed for a pyramidal $X(YZ)_3$ molecular model following the WILSON's group theoretical method. The F and G matrices relating to the potential and kinetic energies have been derived. The recent vibrational and structural data of phosphorus and arsenic tricyanides have been applied and in each case nine valence force constants evaluated.

Introduction

The infrared absoprtion spectrum of phosphorus tricyanide was studied and only four bands were observed by STAATS and MORGAN [1]. Later, GOUBEAU, HAEBERLE and ULMER [2] studied the Raman spectrum in solid and solution states and the infrared absorption spectrum in solid state and assigned the fundamental frequencies on the basis of a pyramidal configuration. Recently, MILLER, FRANKISS and SALA [3] studied the Raman and infrared absorption spectra of phosphorus and arsenic tricyanides in both solution and solid states and assigned the fundamental frequencies on the basis of a C_{3v} symmetry. X-ray diffraction studies by EMERSON and BRITTON [4, 5] favour a pyramidal configuration for these two molecules. It is aimed here to evaluate the force constants of these two molecules on the basis of the WILSON's group theoretical method [6] with help of the recent vibrational and structural data [3—5].

Symmetry and selection rules

In a molecule of the $X(YZ)_3$ type possessing the symmetry point group C_{3v}, the X atom lies on the symmetry axis and the three YZ groups lie in the planes passing through the symmetry axis; each plane bisecting the angle formed by the other two planes. The equilibrium configuration adopted for this molecule is given in Figure 1. The six covering operations of the point group C_{3v} pertaining to this system have been classified as follows: — an

* Permanent address: Kalyanapuram, Thanjavur District, Madras State, India.

identity operation E, rotations by $+ 2\pi/3$ around the symmetry axis $2C_3(z)$ and reflections in the three planes with respect to the symmetry axis $3\sigma_v$. The characters and other relevant features [7] of the point group C_{3v} pertaining to this system reveal that there are fifteen vibrational degrees of freedom constituting only ten fundamental frequencies. They are distributed under the various irreducible representations as follows: $-4A_1 + A_2 + 5E$, where the vibrations of A_1 symmetry species are nondegenerate and symmetric with respect to $C_3(z)$, the vibration of A_2 species is nondegenerate and asymmetric with respect to $C_3(z)$ and the vibrations of E species are degenerate. During the oscillations of A_1 species the molecule remains always a symmetric pyramid,

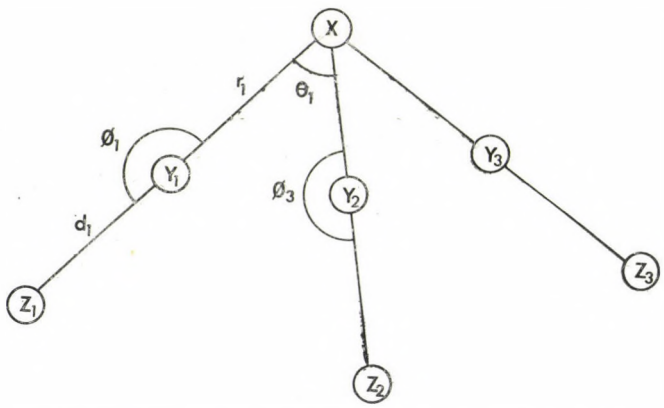

Fig. 1. Geometric illustration of the internal coordinates for a pyramidal $X(YZ)_3$ molecule. The symbols denote the values at the equilibrium configuration

but it does not during the oscillations of E species. There are no genuine vibrations of A_2 species, but the rotation about the symmetry axis has this type. A schematic representation of the normal modes of oscillation for a molecule of the present investigation has already been given by FRITZ and MANCHOT [8]. The fundamental frequencies ν_1, ν_2, ν_3 and ν_4 under the symmetry species A_1 are of totally symmetrical $Y-Z$ stretching, $X-Y-Z$ bending and XY_3 deformation vibrations; ν_5 under the A_2 species is of an asymmetrical $X-Y-Z$ bending; ν_6, ν_7, ν_8, ν_9 and ν_{10} under the E species are of asymmetrical $Y-Z$ stretching, $X-Y$ stretching, $X-Y-Z$ bending, $X-Y-Z$ bending and XY_3 deformation vibrations. All the vibrations are active in both Raman and infrared absorption spectra except the one under the A_2 species which is inactive in both. The vibrations coming under the A_1 species are polarized in the Raman spectrum, whereas those coming under the species E are depolarized in the Raman spectrum, and similarly the former are parallel and the latter perpendicular in the infrared absorption spectrum.

Symmetry coordinates

Fifteen internal coordinates as the deviations from the equilibrium interbond distances and interbond angles have been selected here to describe the fifteen vibrational degrees of freedom and they are given as follows: — Δr_1, Δr_2 and Δr_3 are the $X-Y$ stretching coordinates; Δd_1, Δd_2 and Δd_3 are the $Y-Z$ stretching coordinates; $\Delta\Theta_1$, $\Delta\Theta_2$ and $\Delta\Theta_3$ are the $Y-X-Y$ bending coordinates; and $\Delta\Phi_1$, $\Delta\Phi_2$, $\Delta\Phi_3$, $\Delta\Phi_4$, $\Delta\Phi_5$ and $\Delta\Phi_6$ are the $X-Y-Z$ bending coordinates. On the basis of the principle postulated by WILSON [6], a set of symmerty coordinates (linear combination of internal coordinates) satisfying the conditions of normalization, orthogonality and transformations of the concerned vibration species has been well constructed with help of the internal coordinates described above and given in the following: For the A_1 type vibrations:

$$S_1 = (\Delta r_1 + \Delta r_2 + \Delta r_3)/\sqrt{3},$$
$$S_2 = (\Delta d_1 + \Delta d_2 + \Delta d_2)/\sqrt{3},$$
$$S_3 = (\Delta\Theta_1 + \Delta\Theta_2 + \Delta\Theta_2)/\sqrt{3},$$
$$S_4 = (\Delta\Phi_1 + \Delta\Phi_2 + \Delta\Phi_3 + \Delta\Phi_4 + \Delta\Phi_5 + \Delta\Phi_6)/\sqrt{6}.$$

For the A_2 type vibration:

$$S_5 = (\Delta\Phi_1 - \Delta\Phi_2 + \Delta\Phi_3 - \Delta\Phi_4 + \Delta\Phi_5 - \Delta\Phi_6)/\sqrt{6}.$$

For the E type vibrations:

$$S_{6a} = (2\Delta r_1 - \Delta r_2 - \Delta r_3)/\sqrt{6},$$
$$S_{6b} = (\Delta r_2 - \Delta r_3)/\sqrt{2},$$
$$S_{7a} = (2\Delta d_1 - \Delta d_2 - \Delta d_3)/\sqrt{6},$$
$$S_{7b} = (\Delta d_2 - \Delta d_3)/\sqrt{2},$$
$$S_{8a} = (2\Delta\Theta_2 - \Delta\Theta_1 - \Delta\Theta_3)/\sqrt{6},$$
$$S_{8b} = (\Delta\Theta_1 - \Delta\Theta_3)/\sqrt{2},$$
$$S_{9a} = (2\Delta\Phi_1 - \Delta\Phi_3 - \Delta\Phi_5)/\sqrt{6},$$
$$S_{9b} = (\Delta\Phi_3 - \Delta\Phi_5)/\sqrt{2},$$
$$S_{10a} = (2\Delta\Phi_2 - \Delta\Phi_4 - \Delta\Phi_6)/\sqrt{6},$$
$$S_{10b} = (\Delta\Phi_4 - \Delta\Phi_6)/\sqrt{2}.$$

Potential energy matrices

In the most general harmonic potential energy expression for a molecule of the present study, the number of force constants is twenty four, but the available number of observed fundamental frequencies is only nine. Even if the fundamental frequencies of isotopic species are available, it is not possible to evaluate uniquely all the twenty four valence force constants. Hence most of the interaction constants of higher order were neglected in this case by retaining only eight prominent valence force constants. The adopted potential energy expression is given as follows:

$$2V = f_r \sum_{i=1} (\Delta r_i)^2 + f_d \sum_{i=1} (\Delta d_i)^2 + f_\Theta r^2 \sum_{i=1} (\Delta\Theta_i)^2 + f_\Phi rd \sum_{i=1} (\Delta\Phi_i)^2 +$$
$$+ 2f_{rr} \sum_{i=1} (\Delta r_i)(\Delta r_{i+1}) + 2f_{dd} \sum_{i=1} (\Delta d_i)(\Delta d_{i+1}) +$$
$$+ 2f_{\Theta\Theta} r^2 \sum_{i=1} (\Delta\Theta_i)(\Delta\Theta_{i+1}) + 2f_{\Phi\Phi} rd \sum_{i=1} (\Delta\Phi_i)(\Delta\Phi_{i+1}) +$$
$$+ 2f_{\Phi\Phi'} rd \sum_{i=1} (\Delta\Phi_i)(\Delta\Phi_{i+2}),$$

where f_r is the $X-Y$ stretching force constant, f_d the $Y-Z$ stretching force constant, f_Θ the $Y-X-Y$ bending constant, f_Φ the $X-Y-Z$ bending constant and f_{rr}, f_{dd}, $f_{\Theta\Theta}$, $f_{\Phi\Phi}$, and $f_{\Phi\Phi'}$ are the respective interaction constants. In the above potential energy expression the angle displacements are multiplied by the equilibrium interbond distances r and d in order to keep the dimensions of the force constants referring to the angle bending the same as those of the force constants due to the interbond distances.

The F matrix elements for the various irreducible representations were obtained by means of proper matrix multiplications according to WILSON [6] and they are given as follows: $F_{11} = f_r + 2f_{rr}$, $F_{22} = f_d + 2f_{dd}$, $F_{33} = r^2(f_\Theta - 2f_{\Theta\Theta})$, $F_{44} = rd(f_\Phi + f_{\Phi\Phi} + f_{\Phi\Phi'})$, $F_{66} = f_r - f_{rr}$, $F_{77} = f_d - f_{dd}$, $F_{88} = r^2(f_\Theta - f_{\Theta\Theta})$, $F_{99} = rd(f_\Phi - f_{\Phi\Phi'})$ and $F_{1010} = rd\, f_\Phi$. Since the vibration corresponding to the frequency ν_5 is forbidden in both Raman and infrared absorption spectra, the expression for the symmetrized force constant F_{55} in terms of the valence force constants (f) has not been given here. All the off-diagonal elements involving the interaction force constants have been neglected for the sake of convenience in solving the secular equations.

Kinetic energy matrices

Assuming unit vectors along the chemical bonds of the molecular system, the inverse kinetic energy matrices were obtained according to WILSON [6]

and they are given as follows under the various irreducible representations: For the A_1 type vibrations:

$$G_{11} = \mu_x + \mu_y, \quad G_{22} = \mu_y + \mu_z, \quad G_{33} = (2/r^2)(2\mu_x + \mu_y),$$
$$G_{44} = 2[(1/d^2)\mu_z + \{(1/r) + (1/d)\}^2 \mu_y], \quad G_{12} = -\mu_y,$$
$$G_{13} = -(2/r)\mu_x, \quad G_{14} = G_{23} = G_{24} = G_{34} = 0 .$$

For the E type vibrations:

$$G_{66} = \mu_x + \mu_y, G_{77} = \mu_y + \mu_z, \quad G_{88} = (1/r^2)(\mu_x + 2\mu_y),$$
$$G_{99} = \{(1/r) + (1/d)\}^2 \mu_y + (1/d^2)\mu_z, \quad G_{1010} = \{(1/r) + (1/d)\}^2 \mu_y + (1/d^2)\mu_z,$$
$$G_{67} = -\mu_y, \quad G_{68} = (1/r)\mu_x, \quad G_{910} = \{(1/r) + (1/d)\}^2 \mu_y + (1/d^2)\mu_z,$$
$$G_{69} = G_{610} = G_{78} = G_{79} = G_{89} = G_{810} = 0 ,$$

where μ_x, μ_y and μ_z are the reciprocal masses of the atoms X, Y and Z, respectively. Here the matrices are symmetrical ones. As in the cases of valence force constants not given in the expression for the symmetrized force constant under the A_2 species, the expression for the inverse kinetic energy matrix element G_{55} has not been derived here. The off-diagonal elements of the kinetic energy matrices are to be included in constructing the secular equations as they are not cancelled in the product equations though the off-diagonal elements of the potential energy matrices are neglected.

Results

The observed fundamental frequencies of phosphorus and arsenic tricyanides [3] in cm^{-1} are given in Table 1. The X-ray diffraction studies [4, 5] yield the following values of molecular parameters: $P-C = 1{,}78$ Å, $C\equiv N = 1{,}15$ Å and $C-\hat{P}-C = 93°$ for phosphorus tricyanide and $As-C = 1{,}88$ Å, $C\equiv N = 1{,}15$ Å and $C-\hat{As}-C = 92°$ for arsenic tricyanide. The equation $|FG - E\lambda| = 0$ postulated by WILSON [6] has been adopted in the present study, where E is the unitary matrix and $\lambda = 4\pi^2 c^2 \nu^2$. Here c is the velocity of light in vacuum and ν the observed fundamental frequency in wave number. On the basis of the above equation the secular equations giving the normal frequencies in terms of the valence force constants were constructed with help of the F and G matrices, fundamental frequencies in cm^{-1} given in Table 1 and the molecular parameters given above. All the off-diagonal elements were for the sake of convenience and brevity neglected and only the diagonal elements evaluated by keeping only nine valence force constants. The obtained

Table 1

Fundamental frequencies of phosphorus and arsenic tricyanides in cm^{-1}

Species	Frequency	Schematic description	$P(CN)_3$	$As(CN)_3$
	ν_1	$Y-Z$ symmetrical stretching	2206	2199
	ν_2	$X-Y$ symmetrical stretching	620	415
A_1	ν_3	$X-Y-Z$ symmetrical bending	468	140
	ν_4	XY_3 symmetrical deformation	145	106
A_2	ν_5	$X-Y-Z$ asymmetrical bending	—	—
	ν_6	$X-Z$ asymmetrical stretching	2202	2210
	ν_7	$X-Y$ asymmetrical stretching	581	451
E	ν_8	$X-Y-Z$ asymmetrical bending	452	280
	ν_9	$X-Y-Z$ asymmetrical bending	314	122
	ν_{10}	XY_3 asymmetrical deformation	159	80

Table 2

Valence force constants of phosphorus and arsenic tricyanides in 10^5 dynes/cm

Constant	Phosphorous tricyanide	Arsenic tricyanide
f_r	4,638	3,924
f_d	17,853	17,514
f_θ	1,446	1,243
f_Φ	1,105	0,896
f_{rr}	1,214	1,085
f_{dd}	2,846	2,168
$f_{\theta\theta}$	0,779	0,547
$f_{\Phi\Phi}$	0,532	0,495
$f_{\Phi\Phi'}$	0,245	0,179

values of the valence force constants in 10^5 dynes/cm are given in Table 2 for phosphorus and arsenic tricyanides.

The force constants in general are slightly in the decreasing order from phosphorus tricyanide to arsenic tricyanide. This indicates that the replacement of the apex atom by an atom of higher atomic weight causes lower fundamental frequencies (see Table 1) and correspondingly lower force constants. The $Si-C$ stretching force constant in silyl acetylene [9] is $3{,}3 \times 10^5$ dynes/cm and $S-C$ stretching force constant in thiocyanate ion [10] is $5{,}3 \times 10^5$ dynes/cm. The increase in the $Si-C$, $P-C$ and $S-C$ stretching force constants is not a li-

near one but the increase from $Si-C$ to $P-C$ is much greater than it is from $P-C$ to $S-C$ bond. The values of the $C\equiv N$ stretching force constants obtained in the present study are well comparable with those obtained in other related systems having similar chemical bonds such as hydrogen cyanide [11], halogen cyanides [7, 10, 12—13], halogenated methyl cyanides [14, 15], cyanogen [7] etc. The force constant due to $Y-X-Y$ bending is slightly greater than that of the $X-Y-Z$ bending. The force constants due to the interaction of stretchings are similarly slightly greater than those of the bendings. The reliable data are not available to compare the other constants of the present study. The data obtained here would be very helpful to evaluate the vibrational frequencies in other related systems having similar chemical bonds with nearly identical internuclear distances.

REFERENCES

1. P. A. Staats and H. W. Morgan, Appl. Spectroscopy, **13**, 79, 1959.
2. J. Goubeau, H. Haeberle and H. Ulmer, Z. anorg. allgm. Chem., **311**, 110, 1961.
3. F. A. Miller, S. G. Frankiss and O. Sala, Spectrochimica Acta, **21**, 775, 1965.
4. K. Emerson and D. Britton, Acta Cryst., **17**, 1134, 1964.
5. K. Emerson and D. Britton, Acta Cryst., **16**, 113, 1963.
6. E. B. Wilson, Jr., J. Chem. Phys., **7**, 1047, 1939; **9**, 76, 1941.
7. G. Herzberg, Infrared and Raman Spectra of Polyatomic Molecules, D. Van Nostrand Company, New York, 1960.
8. H. P. Fritz and J. Manchot, Spectrochimica Acta, **18**, 171, 1962.
9. J. L. Duncan, Spectrochimica Acta, 20, 1807, 1964.
10. Landolt—Börnstein, Tabellen. Atom und Molekularphysik. 2 Teil. Molekeln I (Kerngerüst), Berlin, Springer, 1951.
11. W. S. Richardson and E. B. Wilson, Jr., J. Chem. Phys., **18**, 694, 1950.
12. E. E. Aynsley and R. Little, Spectrochimica Acta, **18**, 667, 1962.
13. W. J. Jones, W. J. Orville—Thomas and U. Opik, J. Chem. Soc., 1625, 1959.
14. S. C. Wait, Jr and G. J. Janz, J. Chem., Phys., **26**, 1554, 1957.
15. S. L. N. G. Krishnamachari., Indian J. Phys., **28**, 463, 1954.

ПОТЕНЦИАЛЬНОЕ ПОЛЕ И СИЛОВЫЕ КОНСТАНТЫ ФОСФОРНОГО И АРЗЕННОГО ТРИЦИАНИДОВ

Г. НАГАРАЯН

Резюме

Применением группово-теоретического метода Вильсона для $X(YZ)_3$ молекулярнох модели пирамидальной формы сконструируется ортонормальная сеть симметричны-координат, удовлетворяющих свойствам преобразования. Выводятся матрицы F и G, от носящиеся к потенциальной и кинетической энергиям. Новейшие вибрационные и струк турные данные фосфорного и арзенного трицианидов используются и в каждом случае определяется девять валентных сильных констант.

ELECTRONIC CONFIGURATION, MOLECULAR POLARIZABILITY, MEAN AMPLITUDES OF VIBRATION AND THERMODYNAMIC FUNCTIONS OF DISULPHUR MONOXIDE

By

G. NAGARAJAN*

DEPARTMENT OF CHEMISTRY, UNIVERSITY OF MARYLAND, COLLEGE PARK, MARYLAND U. S. A.

(Presented by A. Kónya. — Received 1. VII. 1965)

An electronic configuration for the ground state of disulphur monoxide possessing an asymmetrical structure with the symmetry point group C_s is given. Molecular polarizability is calculated by the LIPPINCOTT—STUTMAN method employing the delta-function model of chemical binding. Mean amplitudes of vibration at the room temperature are computed by the CYVIN method utilizing the symmetry coordinates. The molar thermodynamic functions for the temperature range 100—6000°K are calculated on the basis of a rigid rotator, harmonic oscillator model. The results are briefly discussed.

Introduction

The infrared absorption spectrum of sulphur monoxide was studied and the bands were observed at 679 cm^{-1} and 1165 cm^{-1} by JONES [1]. The ultraviolet spectrum was also studied and a ground state vibration frequency of 679 cm^{-1} was deduced from a partial analysis of the electronic absorption band system. It was concluded that the molecule cannot be diatomic SO but the formula S_2O_2 as suggested by KONDRAT'EVA and KONDRAT'EV [2]. The microwave spectrum of the product resulting from the passage of an electrical discharge through a mixture of sulphur and sulphur dioxide was examined by MESCHI and MYERS [3] and the product, usually called, "sulphur monoxide" was found to have a microwave spectrum which was assigned to disulphur monoxide with a bent asymmetrical structure; and on the basis of which the fundamental frequencies were assigned from the existing infrared absorption data. It is the aim of the present investigation to present a most stable electronic configuration in the ground state, evaluate the molecular polarizability by the LIPPINCOTT—STUTMAN method [4] employing the delta-function model of chemical binding, calculate the mean amplitudes of vibration by the CYVIN method [5] utilizing the symmetry coordinates and compute the molar thermodynamic functions on the basis of a rigid rotator, harmonic oscillator model.

* Permanent address: Kalyanapuram, Thanjavur District, Madras State, India.

Electronic configuration

LEWIS [6] was the first to propose all the electronic formulae on the "group of eight" which was later described by LANGMUIR [7] as the "octet". The very importance of the "pairing of electrons" in the "group of two" was also stressed by LEWIS; sometimes shared, sometimes unshared (lone). However, the stability of the molecules (or radicals) was not fully explained by LEWIS, [8] but PAULING [9] by introducing the concept of resonance and also the existence of the one and three-electron bonds. When the resonance was accepted, the concept of the electron pair was retained; accordingly, better descriptions of the electronic configurations of certain molecules could be given by a combination of canonical structures of the type proposed by LEWIS [6, 8]. On the basis of the LEWIS-LANGMUIR octet rule [6, 7] and the concept of resonance proposed by PAULING [9], disulphur monoxide could be represented as a resonance hybrid of the pair of structure I and II given in Figure 1. However, both of these structures do not actually represent the stable configuration of disulphur monoxide in the ground state. MESCHI and MYERS [3] proposed the structures III and IV given in Figure 1 from the usual resonance picture for disulphur monoxide. Both of these structures make the end atoms negative with respect to the apex sulphur atom. Because of the difference in electronegativities and on the basis of the calculated bond moments, the structure III is more favoured over IV. These two also do not represent the stable configuration of the molecule in the ground state.

Recently, LINNETT [10] modified the LEWIS-LANGMUIR octet rule [6, 7] as a double-quartet of electrons rather than as four pairs; accordingly each group of four electrons will tend to have a disposition round the nucleus which is approximately that of the corners of a regular tetrahedron [11—14]. On the basis of the octet as two groups of four electrons (the quartets being strongly correlated within the group but the two groups being loosely correlated the one with the other), it is proposed here the structure *V* given in Figure 1 as the most stable configuration for disulphur monoxide in the ground state, where the "dots" represent the electrons with spin quantum number of $+1/2$ and the "crosses" the electrons with spin quantum number of $-1/2$ or vice versa. The electrons are more widely separated in *V* than they are in other structures. Moreover, both spin sets of nine electrons would favour a bent configuration for this molecule in accordance with the results of microwave studies. The two sets of four round each nucleus can be treated uncorrelated spatially relative to one another. As far as the spatial correlation of the two sets is concerned, the electrostatic repulsion and the Pauli Principle effect cancel one another.

The structures from I to IV give a high probability to configurations in which two electrons are in one bond and four in the other or vice versa, whereas the structure *V* gives a high probability to configurations in which there are

three electrons simultaneously in both bond regions. Resonance between I and II or III and IV can result in the mean electron density in each bond region being three, but it gives a completely different measure of the instantaneous configurations from that denoted by the structure *V*; hence the inter-electron

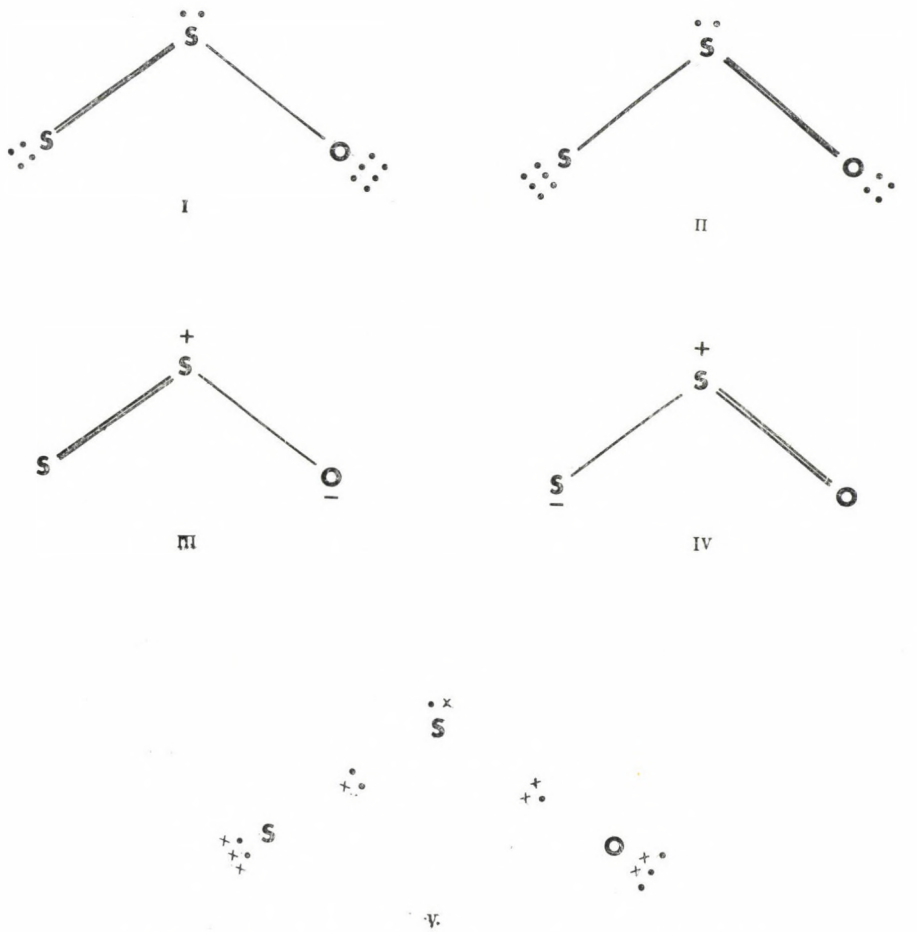

Fig. 1. Electronic configurations of disulphur monoxide

effects for the conventional resonance hybrid (I and II or III and IV) will be different from what they would be for the structure *V*. Since the structure *V* would appear to reduce inter-electron repulsion in comparison with the other structures, it will provide a more satisfactory description of the ground state of disulphur monoxide than will a resonance hybrid of the structures I and II or III and IV.

Molecular polarizability

Several investigations have been made in recent years and developed in many ways to compute the atomic and molecular polarizability values on the basis of quantum mechanical models for many molecules and ions in order to test how far the polarizability could be a useful criterion for testing the accuracy of wave functions adopted. Of the various potential models developed, the most recent one is the delta-function potential initiated by FROST [15] and developed by LIPPINCOTT [16]. LIPPINCOTT and STUTMAN [4] applied this semi-empirical model to develop a method of generating component polarizabilities in order to compute the molecular or average polarizabilities. This model gives explicit expressions for the parallel and perpendicular components and mean polarizabilities for diatomic as well as polyatomic molecules. The molecular polarizability is composed mainly of bond parallel components obtainable from molecular delta-function model and bond perpendicular components obtainable from the atomic delta-function polarizabilities. The polarizability contributions from the bond region electrons and those from the nonbond region electrons are clearly distinguished. In addition, corrections to the parallel and perpendicular components are made to compensate for polarity effects. The same method has been adopted and hence one may refer to LIPPINCOTT and STUTMAN [4] for the detailed theoretical considerations and calculations.

The delta-function strengths A's in atomic units, atomic polarizabilities α's in 10^{-25} cm^3 and c's in atomic units adopted from earlier work [4] for disulphur monoxide are as follows: $A_S = 0{,}688$, $A_0 = 1{,}00$, $\alpha_S = 18{,}20$, $\alpha_0 = 5{,}92$, $c_S = 4{,}128$ and $c_0 = 4{,}899$. The c value for the apex sulphur atom was obtained in the manner described by LIPPINCOTT and DAYHOFF [17] for a bond of polyatomic system and used in the calculation. The internuclear distances $S \div S = 1{,}884$ Å and $S \div S = 1{,}465$ Å and the interbond angle $S \div \hat{S} \div O = 118°$ from microwave studies by MESCHI and MYERS [3] were used for such calculations. The assumed bond order 3/2 is slightly lower for the sulphur-sulphur bond whereas it is fully satisfied for the sulphur-oxygen bond in accordance with the results in other similar systems [18].

The contribution to the parallel component by the bond region electrons is calculated using a linear combination of atomic delta-functions representing the two nuclei in the bond and analytically expressed as $\alpha||_b = 4nA_{12}\ (1/a_0)\ (<x^2>)^2$ where A_{12} is the root mean-square delta-function strength of the two nuclei, n the bond order, a_0 the radius of the first Bohr orbit of atomic hydrogen and $<x^2>$ the mean-square position of a bonding electron which may be expressed as $<x^2> = (R^2/4) + (1/2\ c_{R_{12}}{}^2)$, where R is the internuclear distance at the equlibrium configuration. The calculated values of the polarizabilities in 10^{-25} cm^3 for the $S \div S$ and $S \div O$ bonds are 59,403 and 27,073, respectively. The total value of the polarizability contribution to the parallel component from the bond region electrons is obtained as $\Sigma\alpha||_b = 86{,}476 \times 10^{-25}$ cm^3.

The nonbond region electron contribution to the parallel bond component $\alpha||_n$ is calculated from the fraction of the electrons in the valence shell of each atom not involved in bonding and its respective atomic polarizability; and the basis for such calculation is the LEWIS-LANGMUIR octet rule [6, 7] modified by LINNETT [10] as a double-quartet of electrons. Disulphur monoxide has an even number of electrons in the valence shell. Since five of six electrons in the valence shell of the end sulphur as well as oxygen atoms and two of six electrons in the valence shell of the apex sulphur atom are not involved in bonding (structure V in Fig. 1), the polarizability contribution to the parallel component from the nonbond region electrons is obtained as $\Sigma\alpha||_n = \Sigma f_j\alpha_j = (7/6)\alpha_S + (5/6)\alpha_O =$ $= 26{,}167 \times 10^{-25}$ cm^3. Here f_j is the fraction of electrons in the valence shell of the jth atom not involved in bonding and α_j the atomic polarizability of the jth atom obtainable from the delta-function strength A_j.

The perpendicular component of a diatomic molecule was assumed to be the sum of the two atomic polarizabilities, i. e. $\alpha_\perp = 2\alpha_A$ for a non-polar diatomic A_2 molecule $= 2\ (X_A^2\alpha_A + X_B^2\alpha_B)/(X_A^2 + X_B^2)$ for an $A-B$ molecule, where X refers to the electronegativity of the atom on the Pauling scale. This principle was extended to polyatomics and the derived equation for the sum of the perpendicular components of all the bonds in the molecule is given as $\Sigma 2\alpha_\perp = n_{df}$ $(\Sigma X_j^2\alpha_j)/(\Sigma X_j^2)$, where n_{df} is the number of residual atomic degrees of freedom, X_j the electronegativity of the jth atom and α_j the atomic polarizability of the jth atom. n_{df} is obtained directly from a consideration of the structure of the molecule and the assumption that each atom, if it were not bonded, would possess three degrees of atomic polarizability freedom. If an atom forms one bond, one degree of freedom is lost. i. e., a diatomic molecule has four residual atomic degrees of freedom. If an atom forms two bonds which are linear, only one degree of freedom is lost. i. e., carbon dioxide has only six residual atomic degrees of freedom. If an atom forms two bonds which are non-linear, two degrees of freedom are lost. i. e., disulphur monoxide has only five residual atomic degrees of freedom. The calculated value of the sum of the perpendicular components for the bonds of disulphur monoxide is given as $\Sigma 2\alpha_\perp = 60{,}610 \times$ $\times 10^{-25}$ cm^3. Hence the average molecular polarizability is obtained in terms of the parallel bond, nonbond region electron and perpendicular bond contributions as follows: —

$$\alpha_M = (1/3)(\Sigma\alpha||_b + \Sigma\alpha||_n + \Sigma 2\alpha_\perp) =$$
$$= (1/3)(86{,}476 + 26{,}167 + 60{,}610) \times 10^{-25}\ \text{cm}^3 =$$
$$= 57{,}751 \times 10^{-25}\ \text{cm}^3.$$

There are no experimental values of dielectric constant, index of refraction etc. available to derive the molecular polarizability and make a comparison here.

However, the bond parallel components may be compared with those of other molecular systems having chemical bonds with same as well as different bond orders. The bond parallel components were calculated for the S_2 and H_2S_2 molecules from the existing structural data [18]. The values of the bond parallel components in 10^{-25} cm^3 are 55,358 for the $S-S$ bond in H_2S_2, 59,403 for the $S-S$ bond in S_2O and 80, 041 for the $S = S$ bond in S_2. Similar argument may be extended to the sulphur-oxygen bond. This shows that the bond parallel component of the polarizability increases with the increase in the bond order. Thus the delta-function model gives explicit expressions for the parallel and perpendicular components and the mean polarizabilities for any molecular system and these are in accordance with the investigations of DENBIGH [19] in which the molar refraction of a molecule is assumed to be the sum of the refractions of all the bonds in the molecule and similarly, the molecular polarizability is assumed to be the sum of the bond polarizabilities. The sum of the perpendicular components of all the bonds in a molecule is a linear combination of atomic polarizabilities and is independent of the internuclear distance, whereas the bond parallel component is dependent on the internuclear distance and hence the perpendicular component will always be transferable from one molecular system to another but such transfer in the case of parallel component would be possible only when the internuclear distances are nearly identical in the two different molecules.

Mean amplitudes of vibration

Disulphur monoxide possessing an asymmetrical structure with the point group C_s gives rise, according to the relevant symmetry considerations and selection rules [20] to three vibrational degrees of freedom constituting only three fundamental frequencies, namely, ν_1 the frequency corresponding to the sulphur-sulphur stretching vibration, ν_2 to the sulphur-oxygen stretching vibration and ν_3 to the bending of the molecule. All are allowed in both the infrared absorption and Raman spectra. The equilibrium interbond distances $S-S$ and $S-O$ are being represented by the symbols r and d, respectively and similarly the interbond angle $S-\hat{S}-O$ by the symbol Θ. On the basis of the principle postulated by WILSON [21], the following symmetry coordinates under the symmetry species A' are formed: — $S_1 = \Delta d$, $S_2 = \Delta r$ and $S_3 = (rd)^{1/2}\,\Delta\Theta$. Here the angle displacement is multiplied by the equilibrium bond lengths in order to keep the dimensions of the mean-square amplitude quantities referring to the angle bending the same as those of the bonded atom pairs. On the basis of the symmetry coordinates, the derived G matrix elements related to the kinetic energy under the symmetry species A' are given as follows:

$$G_{11} = \mu_S + \mu_O,$$

$$G_{12} = G_{21} = \mu_S \cos\Theta,$$

$$G_{13} = G_{31} = -\mu_S \sin\Theta,$$

$$G_{22} = 2\mu_S,$$

$$G_{23} = G_{32} = -(r/d)\ \mu_S \sin\Theta,$$

$$G_{33} = \mu_S \{2 + (r/d)^2 - 2\ (r/d) \cos\Theta\} + (r/d)^2\ \mu_O,$$

where μ_S and μ_O are the reciprocal masses of the atom S and O, respectively.

The fundamental frequencies used for the present investigation are, according to MESCHI and MYERS [3], as follows: $\nu_1 = 1165$ cm^{-1}, $\nu_2 = 679$ cm^{-1} and $\nu_3 = 387$ cm^{-1}. The structural data were also taken from microwave studies [3]. From the secular equation $|\Sigma G^{-1} - E\Delta| = 0$ postulated by CYVIN [5], the secular equations giving the normal frequencies in terms of the mean-square amplitude quantities were constructed at the room temperature with help of the Σ and G matrices and the vibrational and structural data [3]. The G matrix elements were calculated, the inverse of those elements derived and introduced into the secular equations. The symmetrized mean-square amplitude matrices Σ_{11}, Σ_{22}, Σ_{33}, Σ_{12}, Σ_{13} and Σ_{23} are directly related to the mean-square amplitude quantities σ_b, σ_r, σ_Θ, σ_{rd}, $\sigma_{d\Theta}$ and $\sigma_{r\Theta}$, respectively. Since there are three equations with six symmetrized mean-square amplitude matrices, it is not possible to solve them uniquely unless the fundamental frequencies of the possible isotopic species are available. Hence all the off-diagonal elements were neglected for the sake of brevity and convenience and only the diagonal elements alone were evaluated. The evaluated values of the mean-square amplitude quantities in Å^2 at the room temperature are given as follows: $\sigma_r = 0{,}0023619$, $\sigma_d = 0{,}0019272$ and $\sigma_\Theta = 0{,}0098465$. The quantity due to the bending of the molecule is very much greater than those of the bonded atom pairs. The situation is reversed in the cases of corresponding force constants. The calculated values of the mean amplitudes of vibration in Å are given as follows: 0,0486 for the $S \cdots S$ bond and 0,0439 for the $S \div S$ bond. These values would be very useful for the interpretation of the electron diffraction studies when undertaken for this molecule.

Thermodynamic functions

The statistical thermodynamic functions such as heat content, free energy, entropy and heat capacity of disulphur monoxide were calculated using the vibrational and structural data [3] for the temperature range 100—6000° K. A rigid rotator, harmonic oscillator model was assumed and all the

Table 1

Heat content, free energy, entropy and heat capacity of disulphur monoxide for the ideal gaseous state at one atmospheric pressure*

T(°K)	$(H_0 - E_0°)/T$	$-(F_0 - E_0°)/T$	$S°$	$C_p°$
100	7,990	45,869	53,859	8,196
150	8,150	49,134	57,284	8,780
200	8,387	51,510	59,897	9,421
273,16	8,783	54,184	62,967	10,284
298,16	8,919	54,957	63,876	10,543
300	8,927	55,011	63,938	10,556
400	9,452	57,657	67,109	11,421
500	9,914	59,820	69,734	12,043
600	10,302	61,654	71,956	12,474
700	10,633	63,261	73,894	12,783
800	10,920	64,704	75,624	13,010
900	11,165	66,013	77,178	13,177
1000	11,363	67,183	78,546	13,297
1100	11,547	68,277	79,824	13,397
1200	11,711	69,319	81,030	13,473
1300	11,844	70,239	82,083	13,532
1400	11,962	71,109	83,071	13,580
1500	12,077	71,961	84,038	13,621
1600	12,171	72,727	84,898	13,654
1700	12,261	73,472	85,733	13,682
1800	12,344	74,188	86,532	13,707
1900	12,422	74,885	87,307	13,728
2000	12,476	75,471	87,947	13,742
2200	12,604	76,724	89,328	13,772
2400	12,693	77,785	90,478	13,792
2600	12,784	78,831	91,615	13,810
2800	12,851	79,735	92,586	13,822
3000	12,910	80,575	93,485	13,833
3200	12,979	81,506	94,485	13,843
3400	13,031	82,303	95,334	13,850
3600	13,066	82,944	96,010	13,855
3800	13,110	83,662	96,772	13,861
4000	13,545	84,411	97,956	13,866
4200	13,190	85,089	98,279	13,870
4400	13,217	85,621	98,838	13,872
4600	13,253	86,295	99,548	13,877
4800	13,271	86,776	100,038	13,878
5000	13,289	87,303	100,592	13,880
5200	13,316	87,790	101,106	13,883
5400	13,344	88,440	101,784	13,884
5600	13,362	88,888	102,250	13,886
5800	13,371	89,235	102,606	13,887
6000	13,399	89,865	103,264	13,889

* T is the temperature in degrees Kelvin; the other quantities are in cal. deg^{-1}.mole^{-1} and E_0 is the energy of one mole of perfect gas at absolute zero temperature.

quantities were calculated for a gas in the thermodynamic standard gaseous state of unit fugacity (one atmosphere). The standard formulae and tables of functions for the harmonic oscillator contributions given by PITZER [22] were used. The principal moments of inertia were calculated from microwave data [3] and their values are given as follows:

$$I_{aa} = 13{,}7811 \text{ AMU Å}^2 \ (22{,}8922 \times 10^{-40} \text{ g cm}^2),$$

$$I_{bb} = 98{,}5735 \text{ AMU Å}^2 \ (163{,}7434 \times 10^{-40} \text{ g cm}^2),$$

$$I_{cc} = 112{,}3546 \text{ AMU Å}^2 \ (186{,}6356 \times 10^{-40} \text{ g cm}^2).$$

Assumed in the calculations were a symmetry number of 1, singlet ground electronic state and chemical atomic weights. Neglected in the calculations were the contributions due to the centrifugal distortion, isotopic mixing and nuclear spins. The calculated values of the thermodynamic functions in cal. deg^{-1}. mole^{-1} for disulphur monoxide are given in Table 1. No calorimetric data are available in the literature to make interpretation and comparison with the results of the present investigation.

REFERENCES

1. A. V. JONES, J. Chem. Phys., **18,** 1263, 1950.
2. E. KONDRAT'EVA and V. KONDRAT'EV, J. Chem. Phys. U. S. S. R., **14,** 1528, 1940.
3. D. J. MESCHI and R. J. MYERS, J. Mol. Spectroscopy, **3,** 405, 1959.
4. E. R. LIPPINCOTT and J. M. STUTMAN, J. Phys. Chem., **68,** 2926, 1964.
5. S. J. CYVIN, Spectrochimica Acta, **15,** 828, 1959.
6. G. N. LEWIS, J. Am. Chem. Soc., **38,** 762, 1916.
7. I. LANGMUIR, J. Am. Chem. Soc., **38,** 2221, 1916.
8. G. N. LEWIS, Valence and the Structure of Atoms and Molecules, The Chemical Catalog Company, New York, 1923.
9. L. PAULING, The Nature of the Chemical Bond, Cornell University Press, Ithaca, New York, Third Edition, 1960.
10. J. W. LINNETT, J. Am. Chem., **83,** 2643, 1961.
11. H. K. ZIMMERMANN and P. VAN RYSSELBERGHE, J. Chem. Phys., **17,** 598, 1949.
12. J. W. LINETT and A. J. POE, POE, Trans. Farad. Soc. **47,** 1033, 1951.
13. R. DAUDEL and C. VROELANT, C. R. Acad. Sci. Paris **236,** 78, 1953.
14. C. E. MELLISH and J. W. LINNETT, Quart. Rev. Chem. Soc., **11,** 291, 1957.
15. A. A. FROST, J. Chem. Phys., **22,** 1613, 1954; **23,** 985, 1955; **25,** 1150, 1956.
16. E. R. LIPPINCOTT, J. Chem. Phys., **23,** 603, 1955; **26,** 1678, 1957.
17. E. R. LIPPINCOTT and M. O. DAYHOFF, Spectrochimica Acta, **16,** 807, 1960.
18. L. E. SUTTON, Tables of Interatomic Distances and Configurations in Molecules and Ions, The Special Publication No. 11, The Chemical Society, London, 1958.
19. K. G. DENBIGH, Trans. Farad. Soc., **36,** 936, 1940.
20. G. HERZBERG, Infrared and Raman Spectra of Polyatomic Molecules., D. Van Nostrand Company, New York, 1960.
21. E. B. WILSON, Jr., J. Chem. Phys., **7,** 1047, 1939; **9,** 76, 1941.
22. K. S. PITZER., Quantum Chemistry, Prentice-Hall, Inc., New York, 1953, P. P. 457.

ЭЛЕКТРОННАЯ КОНФИГУРАЦИЯ, МОЛЕКУЛЯРНАЯ ПОЛЯРИЗУЕМОСТЬ, СРЕДНИЕ АМПЛИТУДЫ ВИБРАЦИОННЫХ И ТЕРМОДИНАМИЧЕСКИХ ФУНКЦИЙ ДИСУЛЬФИДНОЙ ОДНООКИСИ

Г. НАГАРАЯН

Р е з ю м е

Дается электронная конфигурация для основного состояния дисульфидной однооокиси, имеющей несимметричную структуру с симметричной основной группой C_s. Молекулярная поляризуемость определяется методом Липпинкотта—Статмена, использующим модель дельта-функции химической связи. Средние амплитуды вибрации при комнатной температуре вычисляются методом Сайвина, использующим симметричные координаты. Молярные термодинамические функции в интервале температур 100—6000 К° определяются на базе моделей жесткого ротатора, гармонического осциллятора. Коротко объясняются результаты.

OPTICAL DIAGRAMS FOR ELECTROSTATIC LENSES APPLIED IN HIGH VOLTAGE ACCELERATORS

By

E. KOLTAY and S. CZEGLÉDY

INSTITUTE OF NUCLEAR RESEARCH OF THE HUNGARIAN ACADEMY OF SCIENCES, DEBRECEN

(Presented by A. Szalay. — Received 17. VIII. 1965)

Optical data for two similar electrode configurations generally used as electrostatic lenses in high current cascade generators are presented in the form of P—Q diagrams and cardinal characteristic obtained by the application of the GANS' method.

1. Introduction

Several theoretical works can be found in the literature devoted to the ion-optical description of acceleration tubes with a non-uniform field [1] [2] [3] generally used in open-air high voltage accelerators. Although results obtained in this way are very important in the general solution of this question, simple methods using optical diagrams have great utility and are very frequently applied in practical construction work. Graphs summarizing the ion-optical parameters for a number of simple electrode configurations partly used as gaps in acceleration tubes are presented in a book by K. R. SPANGENBERG [4]. The possibilities of their application, however, are limited to a few cases of simple configurations by the fact that effects connected with the presence of secondary electrons in the tube necessitate the application of more complicated systems of electrodes.

In the present article graphs, similar to those of SPANGENBERG, obtained by the application of GANS' method [5] [6], are given for two different cases of electrode gaps with cylindrical lens shields, which are generally used in cascade generators of high ion current [7].

2. Electrode configurations and potential distributions

The shape and relative dimensions of the two different gaps treated are defined in Figs. 1a and 1b. The cylindrical lens shield electrodes are used to prevent the gap from viewing the insulator walls of the acceleration tube. In the case of Fig. 1a the tube sections are closed with apertures preventing

secondary electrons from crossing more than one gap along their trajectory [7]. In the case of toroidal closure as shown in Fig. 1b similar apertures can only be placed inside the tube at a distance from the gap in order to minimize their influence on the potential distribution within the gap.

As a first step for the determination of the optical characteristics, the potential distribution and the axial potential curve were measured in an electrolytic trough for the cases shown in Figs. 1a and 1b. The strong effect of

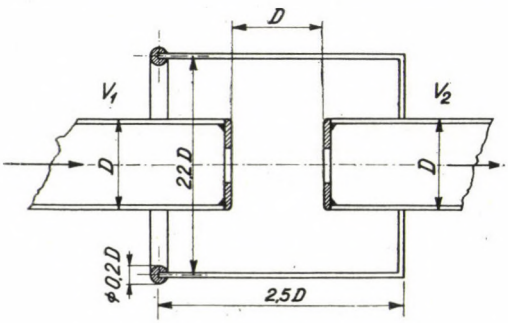

Fig. 1a

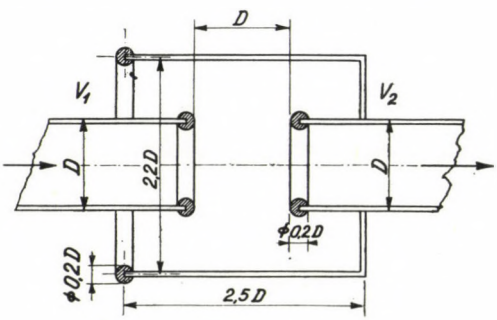

Fig. 1b

the shield on the potential distribution is clearly demonstrated in Fig. 2 for the case of toroidal closures. The equipotential line corresponding to the half value of the potential difference on the lens is moved towards the tube entering the shield (left in the Figure) in comparison with its position in the field of a symmetrical two-tube immersion lens. Consequently, a stronger converging and a weaker diverging effect will be obtained (if accelerating the beam from left to right), i. e. the presence of the shield results in shortening the focal distances.

For calculation an analytical expression of the axial potential curve is required. In Fig. 3 the measured curves $V_a(Z)$ and $V_b(Z)$ i. e. the axial potential curves for the cases of Figs. 1a and 1b, respectively, are compared with $V_0(Z)$, i. e. with that for the symmetrical two-tube immersion lens. As follows from the evaluation of the measurements, $V_a(Z)$ and $V_b(Z)$ can be expressed by means of appropriate transformations of the formula [8]

$$V_0(Z) = \frac{V_1 + V_2}{2} + \frac{V_2 - V_1}{b} \int_0^Z \exp\left[-\left(\frac{\pi}{b^2}\right)Z^2\right] dZ, \tag{1}$$

where

$$b = D\left[0{,}73 + 0{,}53\left(\frac{S}{D}\right)^2\right],$$

D = the tube diameter,

S = the width of the gap.

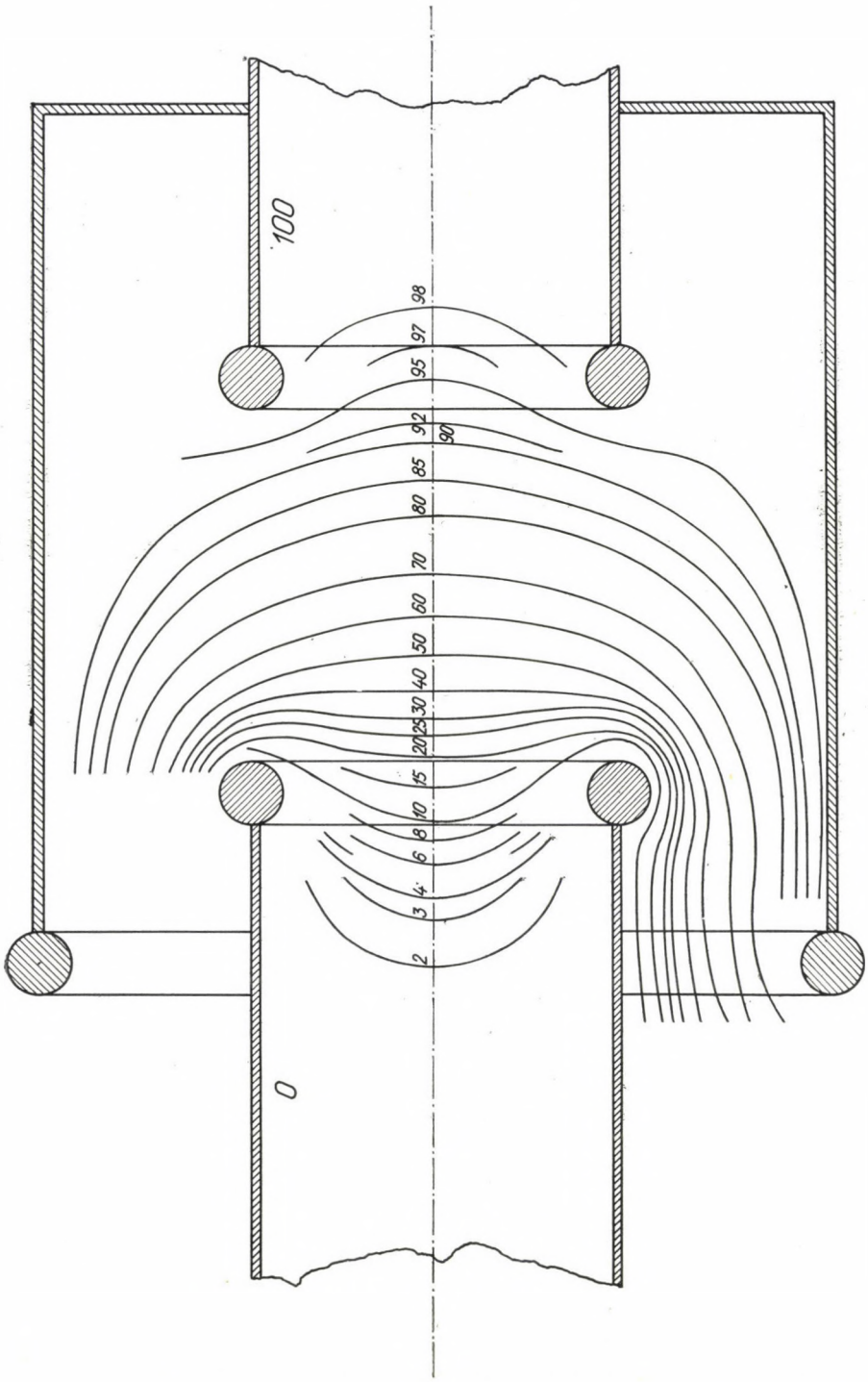

Fig. 2

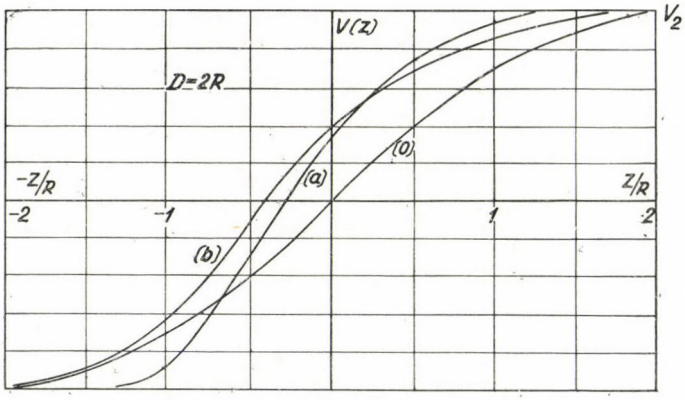

Fig. 3

V_1 and V_2 are the voltages on the first and second electrodes, respectively. In this way, we obtained the following expressions for our cases with $S = D$:

$$V_a(Z) = V_0(\zeta) \tag{2}$$

with

$$\zeta = 0{,}720\left(\frac{Z}{R}\right)^3 - 0{,}296\left(\frac{Z}{R}\right)^2 + 2{,}330\left(\frac{Z}{R}\right) + 0{,}75 \tag{2'}$$

and

$$V_b(Z) = V_0(Z) + \begin{cases} 0{,}75\ \exp\left[-\left(\frac{Z}{R} + 0{,}075\right)^2/0{,}537\right] \text{ for } \frac{Z}{R} < -0{,}075, \\ 0{,}75\ \exp\left[-\left(\frac{Z}{R} + 0{,}075\right)^2/1{,}68\right] \text{ for } \frac{Z}{R} > -0{,}075. \end{cases} \tag{3}$$

The transformation (2′) and the second term of Equation (3) are shown in Figs. 4a and 4b, respectively, together with the corresponding data from the measurements. In Fig. 4b both linear and Gaussian scales [9] are used. The validity of the expressions (2), (2′) and (3) is verified by the excellent fit of the curves to the experimental points.

3. Procedure

The method used in the present calculations is based upon the approximate integration of the paraxial equation for systems of axial symmetry

$$\frac{d^2 r}{dZ^2} + \frac{V'}{2V}\frac{dr}{dZ} + \frac{V''}{4V} r = 0 \tag{4}$$

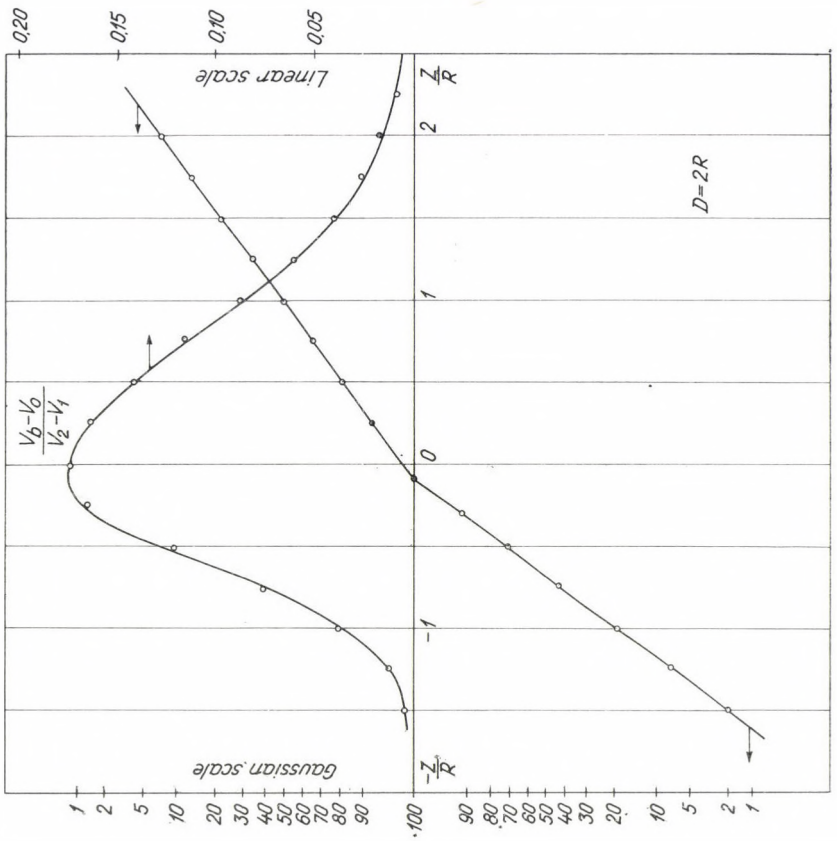
0,20
0,15
0,10
0,05
Linear scale
$\frac{V_2-V_0}{V_2-V_1}$
Gaussian scale
$\frac{z}{R}$
$-\frac{z}{R}$
D=2R
2
1
0
-1
100
90
80
70
60
50
40
30
20
10
5
2
1

Fig. 4b

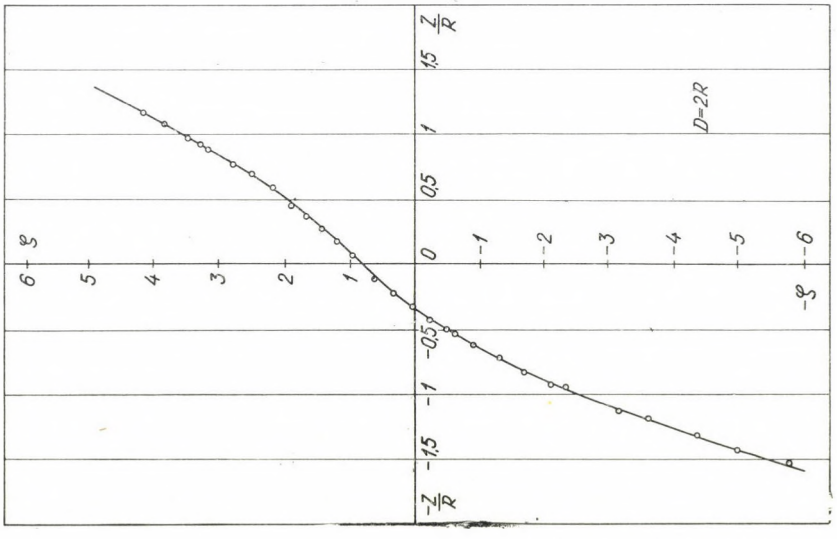
$\frac{z}{R}$
$-\frac{z}{R}$
D=2R
1,5
1
0,5
0
-0,5
-1
-1,5
6
5
4
3
2
1
-1
-2
-3
-4
-5
-6
S
-S

Fig. 4a

by replacing the $V(Z)$ axial distribution of the potential by a broken line as proposed by GANS. A description of the method can be found in various articles and books on electron optics (see for example [5] [6] [10]).

By the application of this method, the $r = r(Z)$ trajectory and its $r' = r'(Z)$ slope were computed under different initial conditions. As a result, the associated object and image distances (P and Q, respectively, measured in the units of tube diameter from the reference plane of the lens) and the corresponding angular magnifications (m) were obtained for the different values of the voltage ratio (V_2/V_1).

The cardinal elements and lateral magnifications were deduced from the following expressions using the above data

$$M \cdot m \frac{\sqrt{V(Q)}}{\sqrt{V(P)}} = 1 ; \tag{5}$$

$$f_1 = \frac{P_1 - P_2}{\frac{1}{M_2} - \frac{1}{M_1}} ; \quad f_2 = \frac{Q_1 - Q_2}{M_2 - M_1} ; \tag{6a, 6b}$$

$$F_1 = \frac{P_1 M_2 - P_2 M_1}{M_2 - M_1} ; \quad F_2 = \frac{\frac{Q_1}{M_2} - \frac{Q_2}{M_1}}{\frac{1}{M_2} - \frac{1}{M_1}} , \tag{7a, 7b}$$

where F_i and f_i denote focal distances measured from the lens reference plane and from the i-th principal plane, respectively,

$i = 1$ and $i = 2$ denote elements for the object side and image side, respectively, M denotes the lateral magnification,

P_j, Q_j and M_j $(j = 1,2)$ indicate values of P, Q and M for two different values of P at a given voltage ratio, respectively and

a sign convention denoting distances measured towards the object with negative, those in opposite direction with positive sign is used.

4. Results

The optical characteristics of both lenses defined in Figs. 1a and 1b are presented in the form of $P-Q$ curves showing the associated object and image distances for given values of the voltage ratio and the curves of constant lateral magnification in Figs. 5a and 5b. Similarly, Figs. 6a and 6b show the plot of the

position of principal planes and focal points as functions of the voltage ratio (cardinal characteristics).

For the sake of comparison, the trajectories computed according to the procedure described in 3. (curve *a)* and that given by the graphical method of

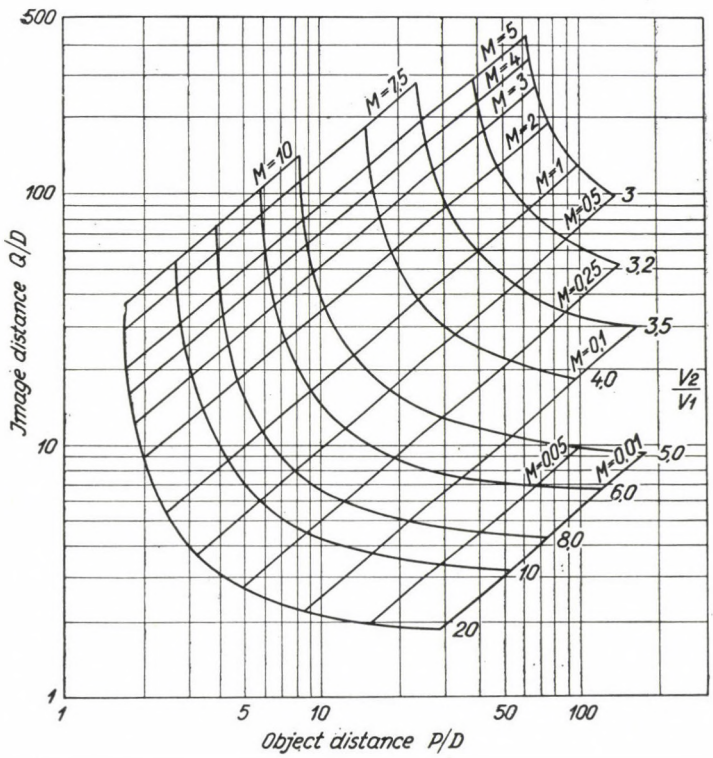

Fig. 5a

Hepp [11] (curve *b)* are presented in Fig. 7. The focal points, principal planes and lens reference plane are also indicated together with the simple construction of the image using the cardinal elements. It can be seen that the graphical method results in a fairly good approximation of the trajectory obtained by making use of the more accurate numerical method.

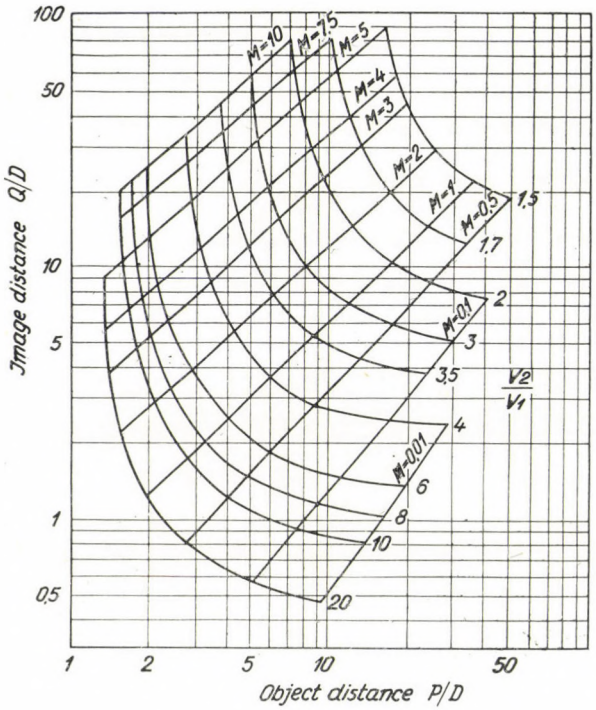

Fig. 5b

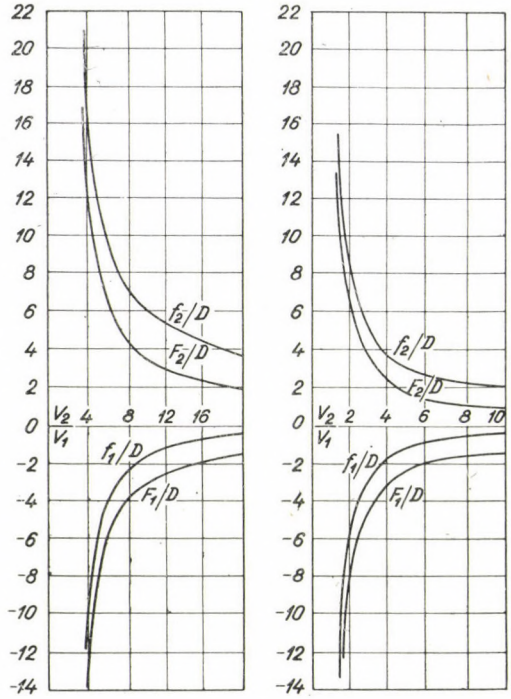

Fig. 6a and b

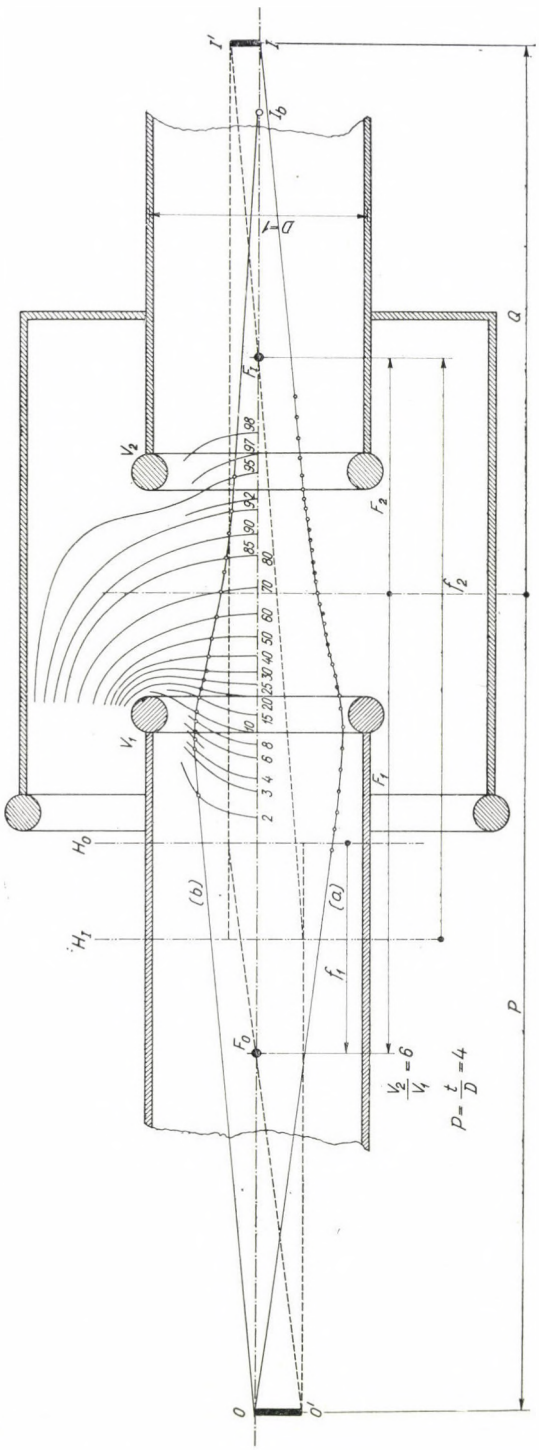

Fig. 7

5. Acknowledgement

Thanks are due to Prof. A. SZALAY, Doctor of Physical Sciences, for his continued interest in this work.

REFERENCES

1. U. TIMM, Z. Naturforsch., **10a**, 1036, 1955.
2. M. MORIKAWA, Nucl. Instr. & Meth., **15**, 282, 1962.
3. P. CROITORU, Nucl. Instr. & Meth., **33**, 39, 1965.
4. K. R. SPANGENBERG, Vacuum Tubes, McGraw Hill, 1948.
5. A. A. RUSTERHOLZ, Elektronenoptik I. Verlag Birkhäuser, Basel, 1950.
6. E. KOLTAY, Nucl. Instr. & Meth., **6**, 45, 1960.
7. F. A. HEIJN and A. BOUWERS, Phil. Techn. Rundschau, **6**, 46, 1941.
   E. W. TITTERTON, Nucleonics, **10**, No. 5, 28, 1952.
8. P. KIRKPATRIK and J. G. BECKERLEY, Rev. Sci. Instr., 7, 25, 1936.
9. P. ONNO, Rev. Sci. Instr., **32**, 1253, 1961.
10. V. K. ZWORYKIN, et al. Electron Optics and Electron Microscopy, John Wiley Inc. New York, 1948.
11. G. HEPP, Phil. Techn. Rundschau, **4**, 235, 1939.

ОПТИЧЕСКИЕ ДИАГРАММЫ ДЛЯ ЭЛЕКТРОСТАТИЧЕСКИХ ЛИНЗ, ИСПОЛЬЗОВАННЫХ В УСКОРИТЕЛЯХ ВЫСОКОГО НАПРЯЖЕНИЯ

Э. КОЛТАИ и Ш. ЦЕГЛЕДИ

Р е з ю м е

Даются оптические данные для двух подобных электродных конфигураций, использованных обычно в качестве электростатических линз в каскадных генераторах сильного тока, в форме $P—Q$ диаграмм и характеристик главных плоскостей, полученные применением метода Ганса.

INFLUENCE OF TEMPERATURE ON ELECTRONIC SPECTRA OF DYESTUFF SOLUTIONS*

By

J. HEVESI and L. KOZMA

INSTITUTE OF EXPERIMENTAL PHYSICS, JÓZSEF ATTILA UNIVERSITY, SZEGED

(Presented by Á. Budó. — Received 28. IX. 1965)

Analytical formulas based on investigation concerning the influence of temperature on electronic spectra of different luminescent systems are given to describe the change of the shape of spectra due to temperature. It is shown that a simple relation exists between the constants in the formulas and the temperature. The experimental values for the systems examined are in very good agreement with those calculated from the formulas. The changes in the spectra are interpreted by the supposition that the influence of temperature on the distribution of vibrational energy is different for the ground state and the excited state.

1. In studying the laws of luminescent radiation it proves useful to examine the temperature dependence of the parameters of luminescence, e. g. of absorption and emission spectra. Earlier investigations, performed mainly in the temperature range 7°K to 300°K, showed changes in the structure of spectra as well as in the yield of absorption and emission with changing temperature. The interpretation of experimental results cannot yet be considered as satisfactory. Several authors (e. g. [1]—[3]) derived formulas on the basis of general physical laws, in an attempt to describe the shape of spectra and their change with temperature, using simplified models instead of luminescent centra. These formulas could not provide satisfactory solutions of the problem, either on account of the complexity of the relations or because of the simplifying suppositions used in deriving them.

An empirical approach to the solution of the problem was given by TARASOVA [4], who proved by many experiments that the maximal values of the absorption coefficient k_T and of the emission spectrum f_m (more exactly that of the spectral yield) for a given temperature T can be described with the formulas

$$\frac{k_T}{k_{T_0}} = \text{const } [1-d_1 \exp(-\Delta E_1/kT)] \tag{1}$$

and

$$\frac{f_T}{f_{T_0}} = \text{const } [1-d_2 \exp(-\Delta E_2/kT)] , \tag{2}$$

* Delivered at the 8th European Congress on Molecular Spectroscopy in Copenhagen 1965.

where k_{T_0} and f_{T_0} are corresponding values for temperature T_0. (d_1, d_2, ΔE_1 and ΔE_2 are empirical constants.) TARASOVA showed that the values of ΔE_1 and ΔE_2, having the character of energies, are equal to the activation energy for dielectric relaxation of the solvent in the cases examined. The relations (1) and (2) give an adequate description of the temperature dependence of k_T and f_T, as was ascertained by our own investigations. On the other hand, they are not suitable for describing the changes in the shape of spectra due to temperature.

DOMBI et al. [5], taking the general equations describing the connection between the absorption spectra $k(\nu)$ and the luminescence spectra $f_q(\nu)$ as a starting point, obtained the relations

$$k(\nu) = A_1 \nu \exp(b\nu) \operatorname{sech}[a_1(\nu_{01}-\nu)] \tag{3}$$

and

$$f_q(\nu) = A_2 \nu^3 \exp(-b\nu) \operatorname{sech}[a_2(\nu_{02}-\nu)], \tag{4}$$

which give a satisfactory agreement with experimental results for many cases with empirically determined values of a_1 and a_2. (A_1 and A_2 in the formulas are normalizing factors, ν_{01} and ν_{02} are values near ν_0, the pure electron transition frequency, and $b = h/2kT^*$, where T^* is the effective temperature or vibration temperature of the molecule. The latter can be calculated on the basis of the spectra with the method given in [6]).

According to our experimental results, relations (3) and (4) proved to be adequate for describing the changes in the shape of spectra caused by temperature if the dependence of a_1 and a_2 on temperature could be determined. One of our most important results was to give this relation.

2. From relations (1) and (2) giving the intensity of spectra, as well as (3) and (4) describing the changes of their shape with temperature, it can be concluded that the absorption and emission spectra of a luminescent system at temperature T can be given in the following form:

$$\frac{k(\nu, T)}{k(\nu_{\max}, T_0)} = \frac{1 - d_1 \exp(-\Delta E_1/kT)}{1 - d_1 \exp(-\Delta E_1/kT_0)} \cdot \frac{\nu \exp(b\nu) \operatorname{sech}[a_1(\nu_{01}-\nu)]}{\max\{\nu \exp(b\nu) \operatorname{sech}[a_1(\nu_{01}-\nu)]\}} \tag{5}$$

and

$$\frac{f_q(\nu, T)}{f_q(\nu_{\max}, T_0)} = \frac{1 - d_2 \exp(-\Delta E_2/kT)}{1 - d_2 \exp(-\Delta E_2/kT_0)} \cdot \frac{\nu^3 \exp(-b\nu) \operatorname{sech}[a_2(\nu_{02}-\nu)]}{\max\{\nu^3 \exp(-b\nu) \operatorname{sech}[a_2(\nu_{02}-\nu)]\}}, \tag{6}$$

where $k(\nu_{\max}, T_0)$ and $f_q(\nu_{\max}, T_0)$ denote the values belonging to the frequencies $\nu_{\max}$ of the spectra measured at temperature T_0.

These relations are suitable for calculating the spectra, because the constants can be determined from relatively few experimental data.

3. In the course of our experiments the spectra of six luminescent systems listed in Table I were measured in the temperature range 262 to 338°K. For measuring the absorption spectra a grating spectrophotometer Optica

Table I

No	Fluorescent material (concentration) (mole/l)	Solvent	T (°K)	$b \cdot 10^{14}$ (s)	absorption spectra		emission spectra	
					$a_1 \cdot 10^{14}$ (s)	$\nu_{01} \cdot 10^{-14}$ (s^{-1})	$a_2 \cdot 10^{14}$ (s)	$\nu_{02} \cdot 10^{-14}$ (s^{-1})
1	Fluorescein $(1 \cdot 10^{-4})$	NaOH (1%) C_2H_5OH	262	9,099	12,006	5,915	11,283	5,875
			338	6,478	9,625	5,882	8,059	5,850
2	Eosine $(5 \cdot 10^{-5})$	NaOH $(5 \cdot 10^{-3}$ m/l) C_2H_5OH	262	7,336	10,822	5,660	10,711	5,625
			338	6,004	9,256	5,639	8,612	5,620
3	Erythrosine $(5 \cdot 10^{-5})$	NaOH $(5 \cdot 10^{-3}$ m/l) C_2H_5OH	262	6,678	10,247	5,680	9,441	5,650
			338	5,229	8,405	5,661	7,599	5,640
4	Rose Bengale $(5 \cdot 10^{-5})$	NaOH $(5 \cdot 10^{-3}$ m/l) C_2H_5OH	262	6,792	9,947	5,360	10,500	5,390
			338	5,787	8,934	5,350	8,882	5,370
5	Aurophosphine $(1 \cdot 10^{-4})$	HCl $(3 \cdot 10^{-3}$ m/l) C_2H_5OH	262	6,472	8,750	6,320	7,944	6,190
			338	5,000	7,000	6,320	6,150	6,190
6	Flavophosphine $(5 \cdot 10^{-5})$	HCl $(3 \cdot 10^{-3}$ m/l) (C_2H_5OH) glycerol (10%)	262	7,160	10,000	6,260	9,000	6,190
			338	6,588	9,000	6,260	8,400	6,190

Milano CF—4 was used with a supplementary device for regulation of temperature, suitable for measuring layer thicknesses up to 20 cm [7]. In the case of luminescence spectra the solution was placed in a box with double walls serving to regulate the temperature. The windows of this box were placed in front of the entrance slit of the spectrophotometer. The layer thickness of the solution was chosen according to the method given in [8] in order to keep the influence of secondary luminescence within the limits of experimental error. Reabsorption in the system was taken into account in the usual way [9]. The temperature was held constant within ± 1°K. A high pressure Xenon-lamp (Osram XBO 500) and a Hg-lamp (Osram HBO 500) served as light source. The nearly monochromatic exciting beam was obtained with a double monochromator or a metal interference filter SIF from the light of the lamps.

4. The results show that the changes in the spectra due to temperature are of identical character for all systems. The height of *absorption spectra* decreases with increasing temperature, but the shape of the spectra is also subject to changes at the same time. The greatest change in height can be observed in the neighbourhood of the maxima, while the changes in the short wave region are considerably less. In the long wave region the decrease of the absorption coefficients is not only less than that found near the maxima, but even an increase can be found in some cases. In the *emission spectra* a shift towards longer wavelengths can be observed with increasing temperature, evidently due to an increase in the relative transition frequency of emission belonging to longer wave-lengths.

Figs. 1 and 2 show the measured absorption and emission spectra of fluorescein and aurophosphine, respectively. (The units are chosen in such a way as to give spectra of the same height for all solutions). It can be seen from the figures that an increase of temperature resulted in a broadening of the spectra. Aurophosphine exhibits a somewhat different behaviour in so far as no significant broadening in the absorption spectra occurs even in the anti-Stokes region. It should be noted that for this dyestuff the quantum yield function shows no significant temperature dependence, either [10].

According to the present results and our earlier investigations [10] concerning the dependence of quantum yield on the wave-length of exciting light, the similar temperature dependence of quantum yield and of absoprtion spectrum can be ascribed to the fact that the population in higher vibrational levels of the ground state is altered by changes of temperature. The relatively increasing frequency of transitions with low energy in the emission spectra indicates that the changes in the vibrational configurations of molecules produced by the changing temperature are different for ground state and excited state. This possibility as well as the influence of vibrational energy distribution on the shape of spectra has been referred to by several authors [11]—[13] in earlier papers. The constants in relations (5) and (6) were determined from experimental absorption and emission spectra with the methods given in [4] and [5].

Values of the activation energy ΔE_1 in relation (5) were found to be nearly equal for all systems examined and were calculated to $\Delta E_1 \approx 2 \cdot 10^{-13}$ erg/particle, in good accordance with the dielectric relaxation time of ethanol which was used as a solvent. The divergence between the calculated values is less than $\pm$ 3%. It is to be noted that these values of ΔE_1 are based on temperature dependence of the maxima of spectra.

The value of the "mirror frequency" ν_0 in the formulas was determined in the usual way from the intersection of the spectra. Calculation from the extreme values of function $\varphi(\nu)$ given in [5] leads practically to the same results. Our calculations show that relation (5) is fulfilled in a very good

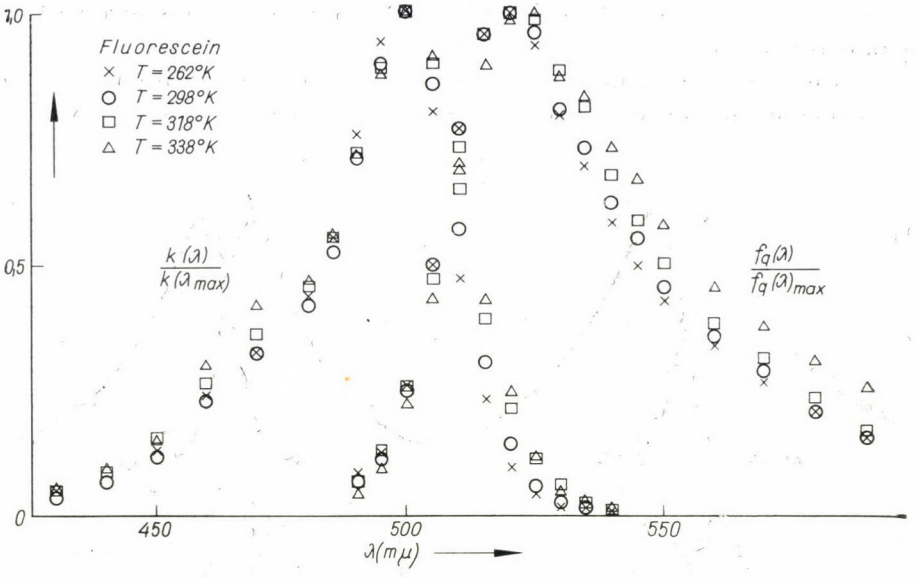

Fig. 1

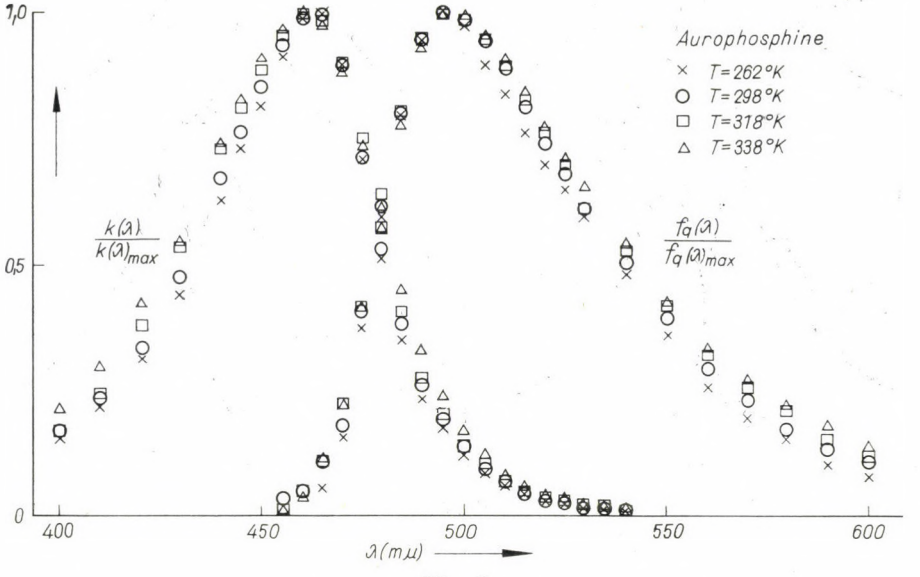

Fig. 2

approximation using these values of ν_0. However, the emission spectra $f_q(\nu,T)$ calculated with the same values on the basis of formula (6) show significant divergences from the measured values. For most of the systems examined (except Bengali Red) the values of frequency had to be taken with $\nu_{02} < \nu_{01}$

($=\nu_0$) (see columns 7. and 9. of Table I) to obtain a good accordance with the experimental results.

In the Table the luminescent dyestuffs, their concentrations, and the composition of the solvent as well as the values of constants playing a role in

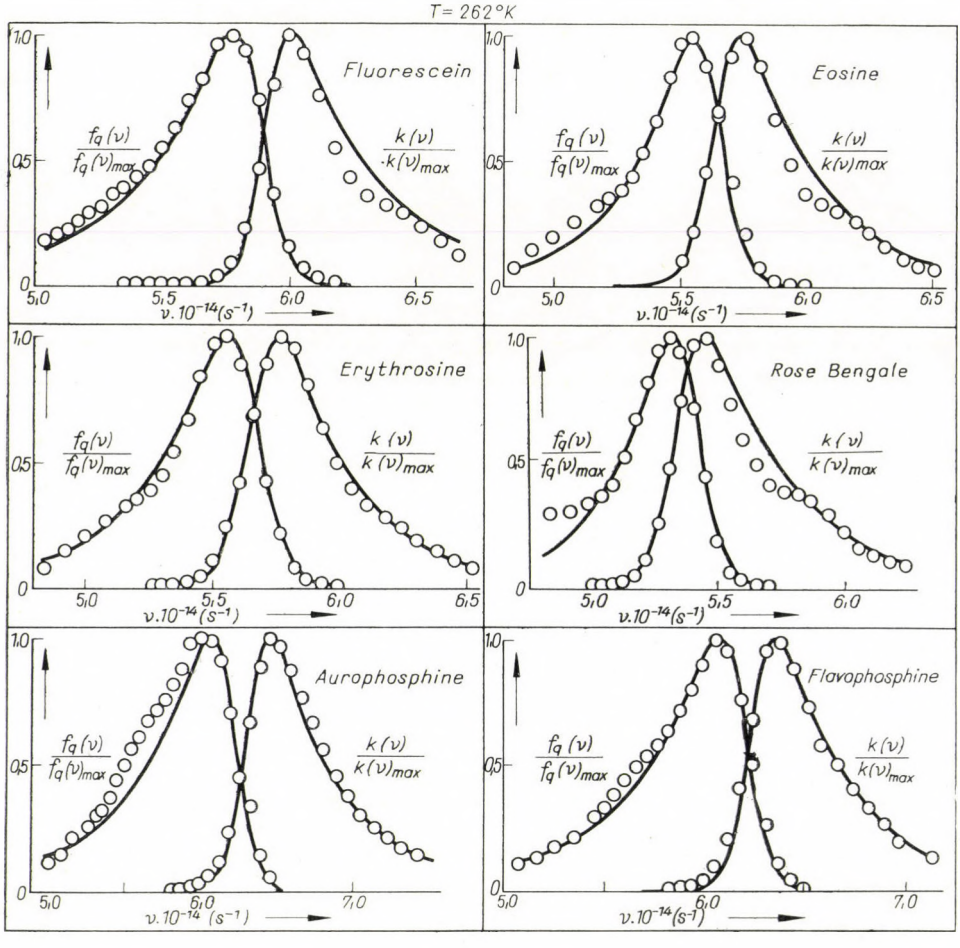

Fig. 3

relations (5) and (6) are given only for two temperatures, though measurements were also made at $T = 298°K$ and $T = 318°K$.

One of the possible explanations of the fact that in calculating the emission spectra the frequency ν_{02} had to be taken less than ν_{01} is to be found in the supposition that the energy system of complex luminescent molecules can be described with the three level term-scheme suggested by NEPORENT [14]. It can

be easily understood on the basis of this scheme that greater pure electronic transition frequencies ν_0 will belong to absorption processes than those belonging to emission acts.

Factors a_1 and a_2 were determined from experimental data with the method given in [5]. One of the main results of our investigations was to

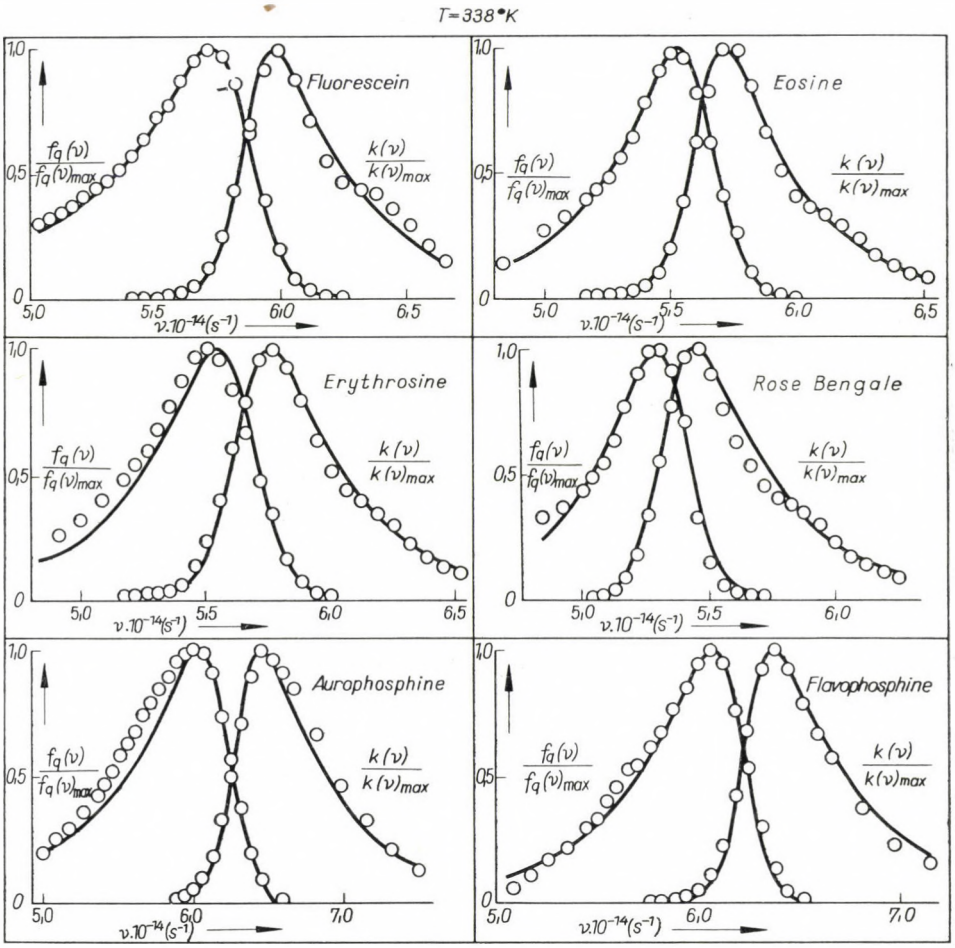

Fig. 4

give the temperature dependence of the factors a_1 and a_2, which was not known earlier. Our results show that a_1 and a_2 are inversely proportional to the temperature, i. e. $a_1 = c_1/T^*$ and $a_2 = c_2/T^*$, where c_1 and c_2 are constants characteristic of the luminescent system.

Emission and absorption spectra for temperatures $T = 262°K$ and $T = 338°K$ are shown in Figs. 3 and 4. The spectra calculated with the values

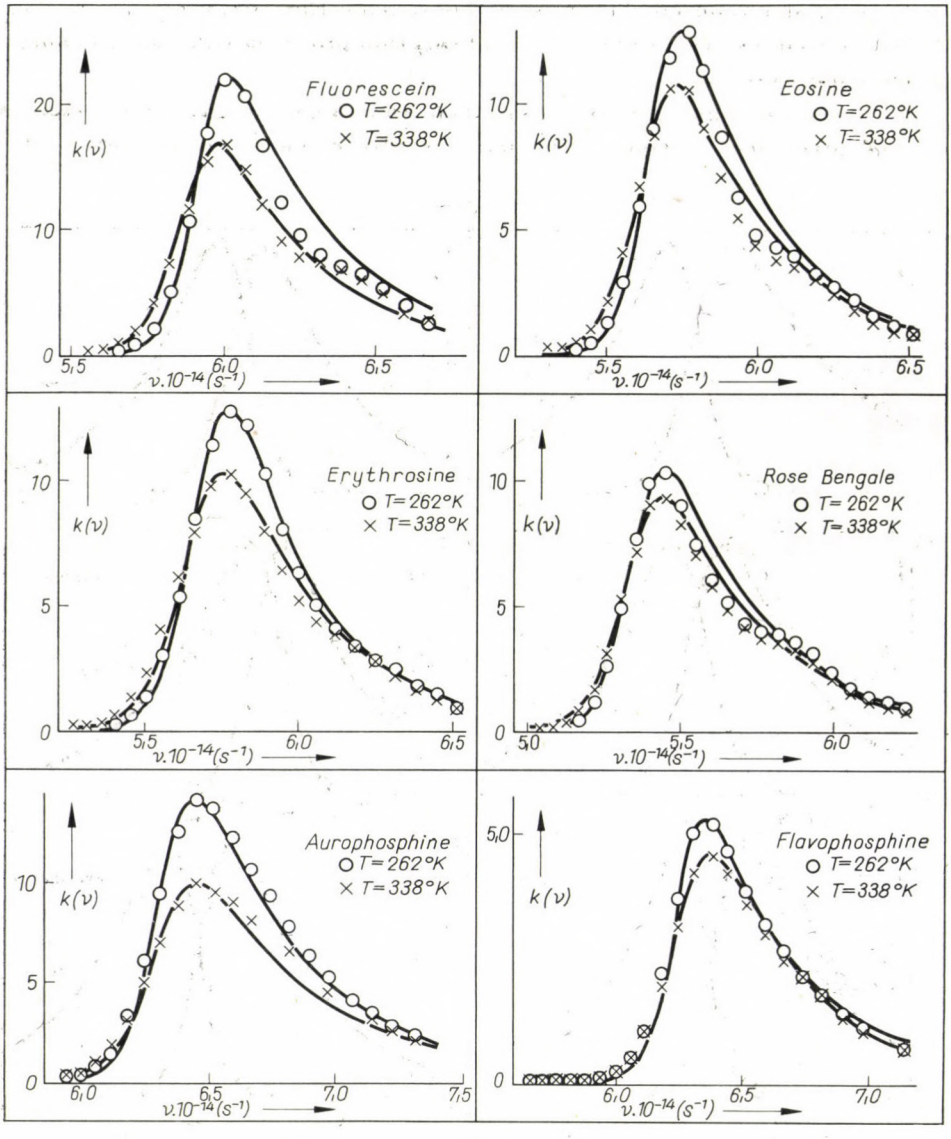

Fig. 5

a, b and ν_0 given in Table I are indicated by solid lines, while measured spectra are indicated by small circles. The spectra are plotted in arbitrary units. As can be seen from the figures the values calculated with the formulas are in very good accordance with the experimental data.

The values of $k(\nu)$, both measured and calculated with formula (5) using the activation energy ΔE_1, are plotted in Fig. 5 in order to show the tempera-

ture dependence of the real conditions of intensity. It can be seen that the changes both in the shape of the spectra and in their intensity, due to the influence of temperature are very well described by relation (5).

The authors are indebted to Prof. Dr. Á. Budó, Member of the Hungarian Academy of Sciences, to whom they offer their sincere thanks for most valuable discussions and advice during this work.

REFERENCES

1. B. I. Stepanov, Lumineszcencia szlozsnüh molekul (Minszk, Izd. A. Nauk BSSR 1956.)
2. Sz. I. Kubarev, Optika i Spektr., Tom. I. (Izd. A. Nauk USSR, Moszkva—Leningrád 1963.)
3. J. Horváth, Acta Phys. et Chem. Szeged, **11,** 3, 1965.
4. T. M. Tarasova, ZSETF., **21,** 189, 1951.
5. J. Dombi, I. Ketskeméty and L. Kozma, Acta Phys. et Chem. Szeged, **10,** 15, 1964; Optika i Spektr., **18,** 710, 1965.
6. M. N. Alencev, Optika i Spektr., **4,** 690, 1958; I. Ketseméty, J. Dombi and R. Horvai, Ann. Phys., **8,** 342, 1961.
7. J. Hevesi, Dissertation, Szeged, 1965.
8. Á. Budó and I. Ketskeméty, Acta Phys. Hung., **7,** 207, 1957.
9. Th. Förster, Fluoreszenz organischer Verbindungen (Göttingen 1951.)
10. J. Hevesi and L. Kozma, Optika i Spektr., **19,** 434, 1965.
11. A. N. Nikitina, G. S. Ter-Sarkisjan, B. M. Mikhailov and L. E. Minchenkova, Acta Phys. Polon. Sci., **24,** 483, 1964; Optika i Spektr., **14,** 655, 1963.
12. J. B. Birks and D. J. Dyson, Proc. Roy Soc., **A275,** 135, 1963.
13. J. Horváth, Magyar Fizikai Folyóirat, **13,** 195, 1965.
14. B. Sz. Neporent, Izv. A. Nauk. USSR, **22,** 1372, 1958.

ВЛИЯНИЕ ТЕМПЕРАТУРЫ НА ЭЛЕКТРОННЫЕ СПЕКТРЫ РАСТВОРОВ ОГРАНИЧЕСКИХ КРАСИТЕЛЕЙ

Е. ХЕВЕШИ и Л. КОЗМА

Резюме

На основании исследований о влиянии температуры на электронные спектры разных люминесцирующих систем выводятся аналитические формулы, дающие возможность для описания изменения вида спектров в зависимости от температуры. Показывается, что существует простое соотношение между постоянными в формулах и температурой. Экспериментальные результаты для исследованных систем удовлетворительно согласуются с данными, вычисленными на основе полученных формул. Изменения в спектре объясняются с предположением, что влияние температуры на распределение вибрационной энергии различно для основного и для возбужденного состояний.

ELECTRON GROUPS IN THE THOMAS-FERMI ATOM ACCORDING TO THE RADIAL QUANTUM NUMBER

By

A. KÓNYA

RESEARCH GROUP FOR THEORETICAL PHYSICS, HUNGARIAN ACADEMY OF SCIENCES, BUDAPEST

(Received 1. XI. 1965)

A method is given for the decomposition of the electron cloud in the THOMAS—FERMI atom into electron groups which correspond to the groups of electrons with equal radial quantum numbers in the wave mechanical atom. The number of electrons with given values of the radial quantum number is calculated numerically as function of the atomic number. The results agree quite well with those of wave mechanics.

1. Introduction

If we want to use the THOMAS-FERMI (TF) statistical theory of atoms in the interpretation of atomic properties depending on the shell structure, one must introduce the concept of quantum numbers in this theory as it was initiated by ALFRED [1] and by GOMBÁS [2] or to seek for continuous quantities corresponding to these numbers in the TF model.

The problem of the angular quantum number was solved by FERMI in the following manner [3]. In the statistical theory the electrons $\varrho(r)dv$ in a volume element dv of the atom are treated as totally free, their states being fully characterized by the momentum vector $\bar{p}$ with radial component p_r and azimuthal component $p_\perp$.

The maximal value of p is

$$P(r) = (3\pi^2)^{1/3}\ \hbar\ \varrho^{1/3}(r),$$

the radius of the FERMI sphere in the momentum space. The energy E of an electron with the momentum $\bar{p}$ is

$$E = \frac{p^2}{2m} - e_0 V(r)$$

and the absolute value of the angular momentum is

$$M = rp_\perp$$

(m is the electronic mass, e_0 the elementary charge, $V(r)$ the potential resulting from the nucleus and the electron cloud).

The continuous quantity k^* corresponding to the azimuthal quantum number k of the quantum theory is, according to Fermi, given by

$$k^* = \frac{M}{\hbar}. \tag{1}$$

The wave mechanical states with angular quantum number l are described by the states in the TF model with the values k^* obtained from the relation [4, 5]

$$k^* = l + 1/2, \quad l = 0, 1, 2, \ldots \tag{2}$$

Starting from these statements FERMI has defined the electrons with

$$l \leqq k^* \leqq l + 1 \tag{3}$$

as the electrons with angular quantum number l in the TF atom. The prescription (3) to form the groups of electrons with equal values l was investigated by several authors [6, 7, 8] and was found to be the most suitable one for the statistical treatment.

The continuous quantity n_r^* corresponding to the radial quantum number n_r of the quantum theory was defined by KÓNYA on the basis of the BOHR-SOMMERFELD quantization rule [9]. After this definition the quantity

$$n_r^* = \frac{1}{\pi\hbar} \int_{r_1}^{r_2} \left[2\, m\, e_0\, V(r) + 2\, m\, E - \frac{M^2}{r^2} \right]^{1/2} dr \tag{4}$$

can be assigned to the electron with the energy E and angular momentum M. Here r_1 and r_2 are the lower and upper bounds of the range where the integrand is real.

The states in the TF atom for which

$$n_r^* = n_r + 1/2, \quad n_r = 0, 1, 2, \ldots \tag{5}$$

correspond to the wave mechanical states with the radial quantum number n_r in close analogy to the relation (2).

In earlier papers the author has defined the quantity

$$n^* = n_r^* + k^* \tag{6}$$

corresponding to the principal quantum number n of wave mechanics and has interpreted some properties of the periodic system of the elements by investigating the possible values of n^* [9, 10]. In the present work we will investigate the quantity n_r^* defined in (4), on the basis of which we deduce a method for decomposing the total electron density of the TF atom into partial densities of electrons with equal values n_r (Section 2). The numerical computations were performed for several values of the atomic number Z. From the partial densities we easily obtain the number of electrons with given values n_r and the dependence of these numbers on the atomic number (Section 3).

2. Decomposition of the total electron density of the TF atom according to the radial quantum number

In the following we deal only with the case of free neutral TF atom. Introducing the FERMI function $\varphi(x)$ the expression (4) may be written as

$$n_r^* = \left(\frac{3}{4\pi^2}\right)^{1/3} Z^{1/3}\, \Phi(\alpha,\beta). \tag{7}$$

This value belongs to all the electrons in the volume dv at $r = \mu x$, which have the momentum components

$$p_r = \frac{4}{(6\pi)^{1/3}} \frac{\hbar}{a_0} Z^{2/3} \left[\frac{\varphi(x)}{x} - \beta - \frac{\alpha^2}{x^2}\right]^{1/2}, \tag{8}$$

$$p_\perp = \frac{4}{(6\pi)^{1/3}} \frac{\hbar}{a_0} Z^{2/3} \frac{\alpha}{x}, \tag{9}$$

when the momentum value $p = (p_r^2 + p_\perp^2)^{1/2}$ is lying inside the FERMI sphere. The notations

$$\Phi(\alpha, \beta) = \int_{x_1}^{x_2} \left[x\varphi(x) - \beta x^2 - \alpha^2\right]^{1/2} \frac{dx}{x},$$

$$\alpha = \frac{k^*}{\left(\frac{3\pi}{4}\right)^{1/3} Z^{1/3}}$$

and

$$\beta = -\frac{(6\pi)^{2/3}}{8\, Z^{4/3}} \frac{a_0}{e_0^2} E$$

are the same as in [9], where numerical tables for the function $\Phi(\alpha, \beta)$ are also given. For the meaning of the notation see [11].

As follows from (2) and (5), which express the relation between the wave mechanical and statistical states, one must choose the same intervals for n_r^* for defining the n_r groups of the TF atom, as FERMI has done for k^* in the case of the l groups. Therefore we define the electrons of the TF atom with

$$n_r \leqq n_r^* \leqq n_r + 1, \qquad n_r = 0,\ 1,\ 2, \ldots \tag{10}$$

as those corresponding to the electrons with the radial quantum number n_r in the wave mechanical atom.

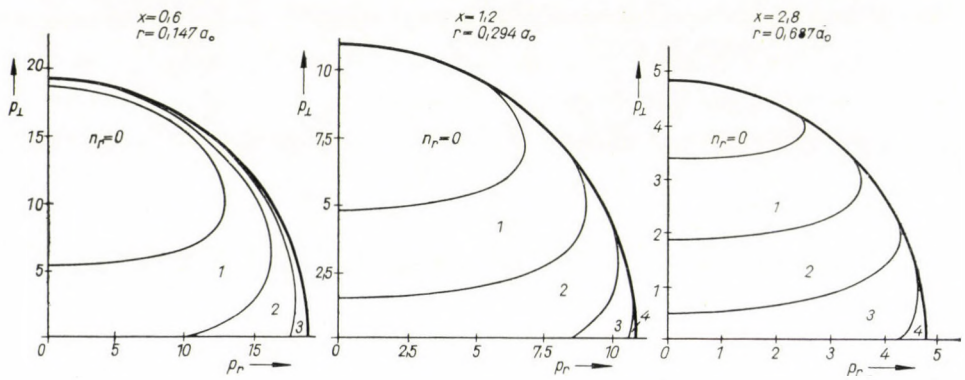

Fig. 1. Decomposition of the volume of the Fermi sphere into the partial volumes $\omega_{n_r}(r)$ occupied by the electrons of the n_r groups in the case of the TF model for the Ag atom

We determine the density of the electrons in the n_r groups in the following way. In a volume dv at the arbitrary distance $r = \mu x$ all electrons are characterized by some value n_r^* according to (7). With the help of the Tables for $\Phi(\alpha, \beta)$ given in [9] one may find those values of the parameters α and β for which $n_r^* = 0, 1, 2, \ldots$ By the equations (8) and (9) we get further the momentum vectors having integer values of n_r^*. These momentum vectors define a series of surfaces inside the FERMI sphere. To a given integer value of n^* there belongs a surface of this kind.

The partial volume $\omega_{n_r}(r)$ between the neighbouring surfaces $n_r^* = n_r$ and $n_r^* = n_r + 1$ is occupied by the electrons of the TF atom which belong, according to (10), to the group with quantum number n_r. Accordingly the density of this group at the place $r = \mu x$ is

$$\varrho_{n_r}(r) = \frac{\omega_{n_r}(r)}{4\pi^3 \hbar^3}\,. \tag{11}$$

Examples for the decomposition of the FERMI sphere into the partial volumes $\omega_{n_r}(r)$ are shown in Fig. 1 for the Ag atom ($Z = 47$). The boundary surfaces possess rotational symmetry around the p_r-axis and reflection symmetry with the symmetry plane perpendicular to this axis through the origin of the momentum space. After having computed numerically the components

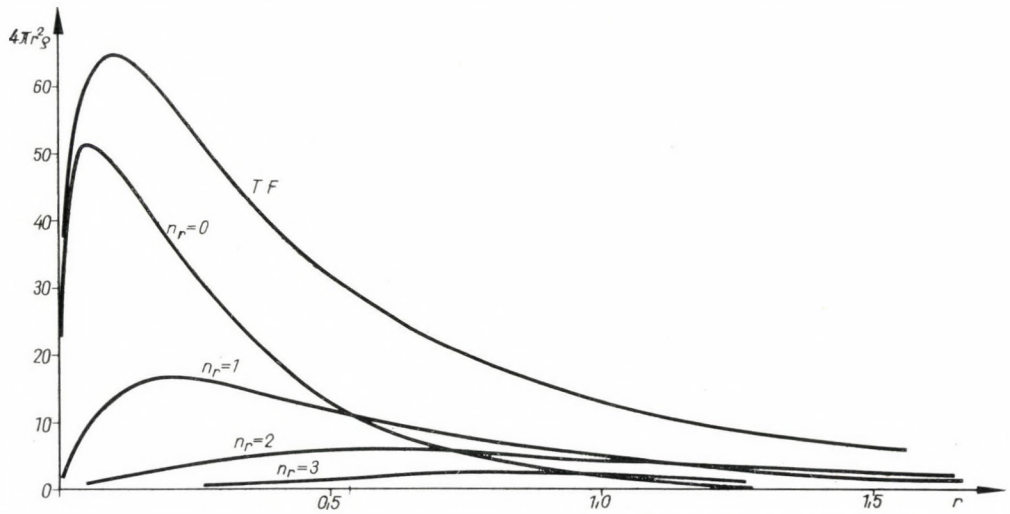

Fig. 2. The total radial density and the partial radial densities of the electron groups with $n_r = 0, 1, 2$ and 3 in the TF model of the Ag atom

p_r and $p_\perp$ of the points lying on the boundary surfaces, one can calculate the partial volumes $\omega_{n_r}(r)$ by numerical integration.

The partial densities obtained with this method are shown for the case of the Ag atom in Figs. 2, 3 and 4. In Fig. 2 one may see how the total radial density $4\pi r^2\varrho(r)$ of the TF atom is decomposed into the partial radial densities $4\pi r^2\varrho_{n_r}(r)$.

In most cases the TF model has also a group with greater radial quantum number than those occurring in the wave mechanical atom. In the case of the Ag atom for example the TF model has electrons with $n_r = 4$ too (the partial density of this group is small to be shown in Fig. 2). The reason for this is, that the maximal value of n_r^* in the TF model is greater than the maximal radial quantum number in the wave mechanical atoms.

In Figs. 3 and 4 the partial radial densities $4\pi r^2\varrho_{n_r}(r)$ are compared with the results obtained by GÁSPÁR for the wave mechanical Ag atom [12]. The partial densities of the TF atom approach to the curves of the wave mechanical atom in the same manner as it is the case for the total densities. The maxima of the wave mechanical curves are smoothed out by the statistical curves. One

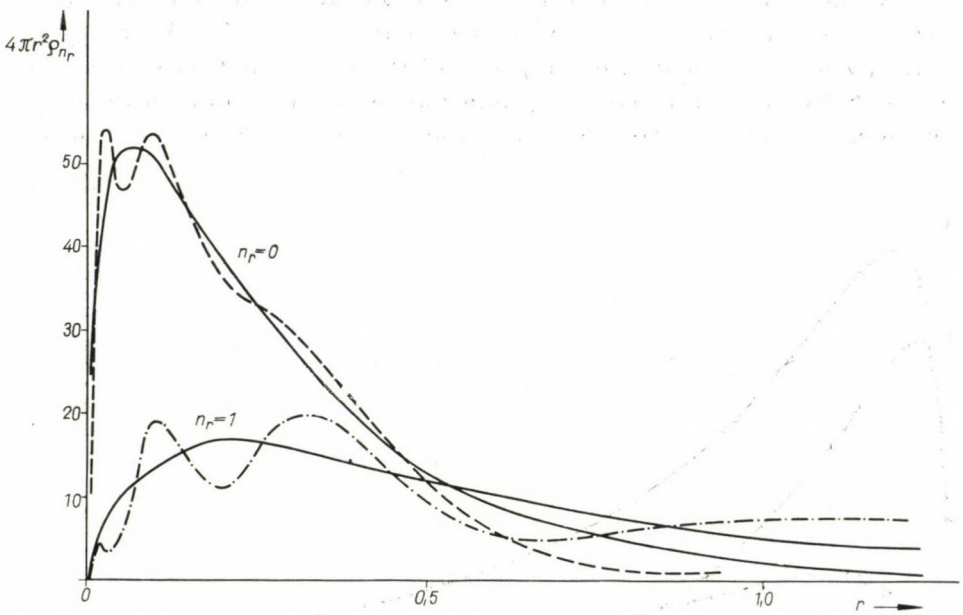

Fig. 3. The partial radial densities for $n_r = 0$ and 1 in the TF model and in the wave mechanical shell model of the Ag atom. —— TF model, — — — — wave mechanical atom

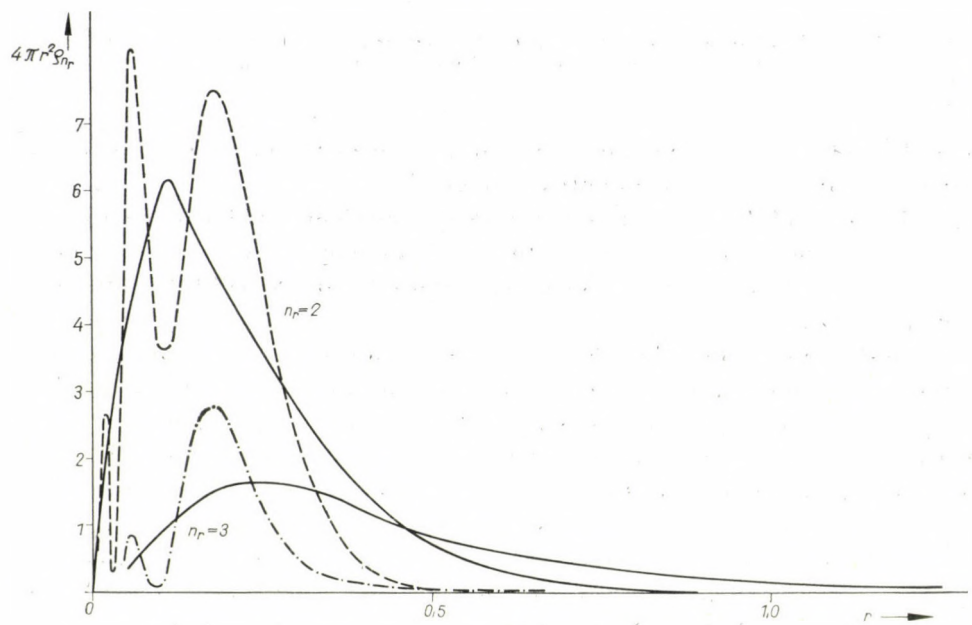

Fig. 4. The partial radial densities for $n_r = 2$ and 3 in the TF model and in the wave mechanical shell model of the Ag atom. —— TF model, — — — — wave mechanical atom

obtains from the TF model in average a good description of the general behaviour of the partial densities. The regions with maximal densities are nearly the same.

In comparing these curves one must take into account — as we shall see it in detail in the next section — that the wave mechanical and the statistical curves belonging to the same values of n_r are not normalized to the same electron number.

3. The number of electrons with given values of n_r in the periodic system of the elements

Having obtained the partial radial densities (11) one can get at once the number of electrons with radial quantum number n_r in the TF atom by numerical integration

$$N_{n_r} = \int_0^\infty 4\pi r^2 \varrho_{n_r}(r)\, dr\,. \tag{12}$$

The numerical computations were made for the atoms Ne, Ag and Hg ($Z = 10, 47$ and 80, respectively). The results together with the data taken from the periodic system of the elements are shown in Figs. 5 and 6. As can be seen, the curves for the TF atom describe very well the general behaviour of the wave mechanical curves with abrupt changes.

Beginning from $Z \sim 75$ the TF model has also a group with $n_r = 6$. The number of the few electrons in this group may be computed numerically with relatively great error, thus we have not shown it in Fig. 5.

In some cases there are relatively very great differences between the values N_{n_r}, taken from the TF model and from the periodic system. This is caused by the following fact. The successive filling of the electronic states with increasing atomic number Z occurs in the wave mechanical atom in the way that in some intervals of Z there is only one n_r group in which the number of electrons increases, in all other groups the N_{n_r}'s remain constants. This is contrary to the behaviour of the TF model, where all values N_{n_r} increase continuously with increasing atomic number Z.

It follows from the basic conceptions of the TF theory that it is unable to describe the individual shell properties of the atoms but it gives a description of the average behaviour. This is the case according to Figs. 5 and 6 also for the change of the values N_{n_r} in the periodic system.

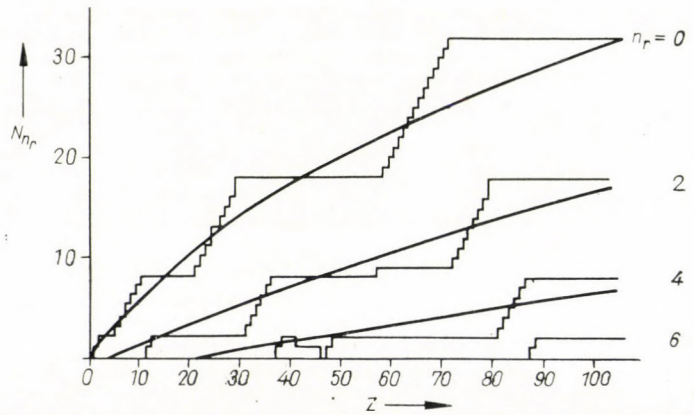

Fig. 5. The number of electrons in the groups with $n_r = 0, 2, 4$ and 6 as functions of the atomic number according to the TF model and to the wave mechanical shell model

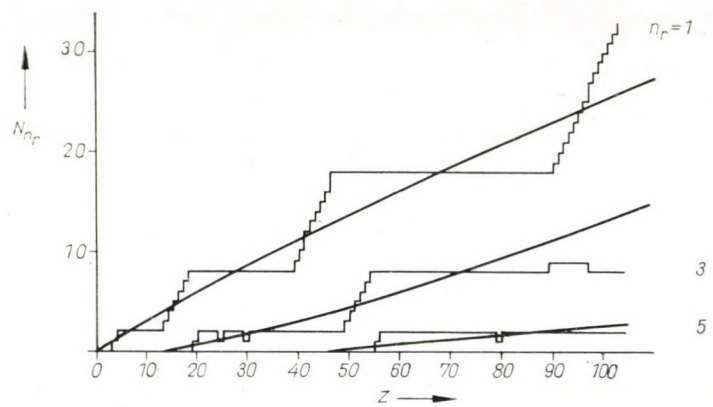

Fig. 6. The number of electrons in the groups with $n_r = 1, 3$ and 5 as functions of the atomic number according to the TF model and to the wave mechanical shell model

The approximation of the TF theory to the wave mechanical atom in determining the values N_{n_r} is the same as it is for the number of electrons in the l groups determined earlier by FERMI [3], THEISS [7] and OLIPHANT [8].

Thanks are due to Mrs. J. HUSZÁR and Miss É. SZABÓ for carrying out the numerical calculations and for drawing the figures.

REFERENCES

1. L. C. R. ALFRED, Phys. Rev., **125,** 214, 1962.
2. P. GOMBÁS and K. LADÁNYI, Acta Phys. Hung., **5,** 313, 1955; **7,** 255, 1957; **7,** 263 1957; **8,** 301, 1958; Zs. f. Phys., **158,** 261, 1960; P. GOMBÁS and T. SZONDY, Acta Phys. Hung. **14,** 335, 1962.

3. E. FERMI, Zs. f. Phys., **48,** 73, 1928.
4. H. A. KRAMERS, Zs. f. Phys., **39,** 828, 1926.
5. R. E. LANGER, Phys. Rev., **51,** 669, 1937.
6. J. H. D. JENSEN and J. M. LUTTINGER, Phys. Rev., **86,** 907, 1952.
7. W. R. THEIS, Zs. f. Phys., **140,** 1, 1955.
8. T. A. OLIPHANT, Jr., Phys. Rev., **104,** 954, 1956.
9. A. KÓNYA, Acta Phys. Hung., **18,** 39, 1964.
10. A. KÓNYA, Acta Phys. Hung., **18,** 129, 1964.
11. P. GOMBÁS, Statistische Behandlung des Atoms, Hb. d. Phys. Vol. XXXVI, Springer, Berlin—Göttingen—Heidelberg, 1956.
12. R. GÁSPÁR, Acta Phys. Hung., **6,** 105, 1956.

ЭЛЕКТРОННЫЕ ГРУППЫ ПО РАДИАЛЬНОМУ КВАНТОВОМУ ЧИСЛУ В АТОМЕ ТОМАСА—ФЕРМИ

А. КОНЯ

Р е з ю м е

В работе излагается метод для разделения электронного облака в атоме Томаса—Ферми на электронные группы, содержащие электроны с одинаковым радиальным кван товым числом квантовомеханического атома. Численным методом определяется число электронов с данным значением радиального квантового числа как функция от порядкового номера. Результаты удовлетворительно согласуются с соответствующими данными квантовой механики.

COMMUNICATIONES BREVES

DISPERSION RELATION FOR THE CAUSAL TRANSFORM AND ITS CORRESPONDENCE WITH A ONE DIMENSIONAL DYNAMICAL SYSTEM

By

P. K. Biswas

DEPARTMENT OF THEORETICAL PHYSICS, INDIAN ASSOCIATION FOR THE CULTIVATION OF SCIENCE, JADAVPUR, CALCUTTA—32, INDIA

(Received 22. VI. 1965)

Let two functions $u(t)$ and $v(t)$ be the Hilbert transforms of each other so that

$$u(t) = \frac{1}{\pi} P \int_{-\infty}^{\infty} \frac{v(t')}{t'-t}\, dt' , \qquad v(t) = -\frac{1}{\pi} P \int_{-\infty}^{\infty} \frac{u(t')}{t'-t}\, dt' . \tag{1}$$

Further let q and p be defined by

$$u(t) = \frac{dq}{dt} , \qquad v(t) = \frac{dp}{dt} . \tag{2}$$

We have shown in a recent work [1] that q and p satisfy certain relations which are similar to the partial differential equations of Hamilton's canonical form

$$\frac{dq}{dt} = \frac{\partial H}{\partial p} , \qquad \frac{dp}{dt} = -\frac{\partial H}{\partial q} , \tag{3}$$

where H is a suitable function*, not necessarily unique, of q and p. We shall look at this result as a sort of mapping of (u, v) on to a set of families of trajectories defined by the partial differential equations (3). Further this mapping seems interesting since there is a large class of physical quantities (called the *causal transforms* [2] in the dispersion theory), whose real and imaginary parts

* The function is given by (9) of [1]. Any two functions $q(t)$ and $p(t)$ define a trajectory that can always be represented as in (3), where $H(q, p)$ is some function of q and p and may be non-unique. What is new in our result is the *restriction of* $H(q,p)$ *to the explicit form* (9) *of* [1] *due to the constraint* (1) *between* $u(t)$ *and* $v(t)$. Constraint (1) is in fact a type of causality condition in physical cases.

are Hilbert transforms of each other. Below we consider such a quantity, namely the complex refractive index $N(\omega)$ considered as a function of the frequency ω of light*. Strictly speaking (Ch. I, [2])it is $N(\omega) - 1$ and not $N(\omega)$, which is a causal transform (we consider scattering of light by bound electrons). We shall also go through some necessary manipulations so as to make the families of trajectories look like the dynamical ones, for the sake of elegance. The result is the correspondence of $N(\omega)$ with a set of one-dimensional dynamical systems. This is possible because of the similarity of the differential eqs. (3) with the canonical forms of the equations of motion. Let us come back to the index $N(\omega)$. Both its real and imaginary parts are pure numbers. We have the following relations from dispersion theory (p. 3, [2]).

$$\begin{aligned} Re\,[N(\omega) - 1] &= \frac{1}{\pi} P \int_{-\infty}^{\infty} \frac{Im\,[N(\omega') - 1]}{\omega' - \omega}\, d\omega', \\ Im\,[N(\omega) - 1] &= -\frac{1}{\pi} P \int_{-\infty}^{\infty} \frac{Re\,[N(\omega') - 1]}{\omega' - \omega}\, a\omega'. \end{aligned} \tag{4}$$

Let us define $$\omega = C_0[T^{-2}]t, \tag{5}$$

where C_0 is a constant and its dimension is indicated in the parentheses. The variable t has the dimension of time so that we may call it the time variable. Let us put $N(\omega)-1 = N(c_0t)-1 = u(t) + iv(t)$,

so that $$Re[N(\omega)-1] = u(t),$$

and $$\mathrm{Im}[N(\omega)-1] = v(t);$$

and so changing the variable from ω to t (4) becomes formally identical to the relation (1). Now we define q and p having the dimension of co-ordinate (space co-ordinate) and momentum respectively and consistent dimensionally by

$$u(t) = C_1[L^{-1}T] \cdot \frac{dq}{dt}, \qquad v(t) = C_2[M^{-1}L^{-1}T^2] \cdot \frac{dp}{dt}, \tag{2'}$$

where C_1 and C_2 have dimensions as indicated and each** $\equiv 1$. We note that

* $N(\omega) = n(\omega) + ic/2\omega\,\alpha(\omega)$, where $n(\omega)$ is the index of refraction of light of frequency ω, and $\alpha(\omega)$ is the absorption co-efficient of the medium for ω. The factor $c/2\omega$ is introduced to make $Im\ N(\omega)$ dimensionless.

** This is possible by choosing suitable of units.

$u(t)$ and $v(t)$ are dimensionless. Thus the relations (2′) are the same as (2). So we have an $H(q, p)$, or a set of $H(q, p)$'s (given by (9) of [1]) satisfying.

$$\frac{dq}{dt} = \frac{\partial H}{\partial p}, \qquad \frac{dp}{dt} = -\frac{\partial H}{\partial q}. \tag{3′}$$

With q and p as defined in (2′) and t as in (5), we see that $H(q, p)$ has the dimension of energy and may be called the Hamiltonian of a one-dimensional dynamical system, with q and p as co-ordinate and momentum respectively, and whose trajectories are determined by the canonical equations (3′).

We thus associate with a refractive index $N(\omega)$ a classical (one dimensional) dynamical system. It may also be looked at as a type of correspondence (one to many in case $H(q, p)$ is not unique) between a system consisting of a photon + an electron bound to an atom of type A (for specification) and a family of one-dimensional dynamical systems via the intermediation of the complex refractive index $N(\omega)$.

Similar correspondence is also possible for a quantum mechanical system. Consider a scattering process in the system. By virtue of the *principle of causality* it will have a causal transform (see Chapter VII, [2]), and this can be mapped on to a (or a set of)one-dimensional dynamical system as in the preceding example.

Thanks are due to Professor D. Basu, Ph. D. for kind encouragement.

REFERENCES

1. Paresh Kumar Biswas, Acta Phys. Hung., **18**, 263, 1965.
2. P. Roman, Lecture Notes "An Introduction to Dispersion Relation Techniques", The Institute of Mathematical Sciences, Madras, India.

THE STATISTICAL TREATMENT OF MANY-BODY SYSTEMS UNDER CONSIDERATION OF THE CENTRIFUGAL POTENTIAL

By

P. RENNERT

INSTITUTE OF THEORETICAL PHYSICS OF THE TECHNICAL UNIVERSITY, DRESDEN, DDR

(Received 17. VIII. 1965)

When investigating systems comprising a large number of particles such as electrons in atom shells good results can be obtained by statistical approximation. So, the THOMAS-FERMI method [1] gives a smooth curve of electron density in which, as opposed to the HARTREE-FOCK method, only the finer curvature of electron density as well as a correct asymptotic falling-off for $r \to 0$ and $r \to \infty$ cannot be found.

In the THOMAS-FERMI approximation the electron density $\varrho(\mathfrak{r})$ at $\mathfrak{r}$ is determined by the value of the potential $V(r)$ at point $\mathfrak{r}$ only. Recently, some improved methods have been developed and assessed [2]—[16]. With these methods, the influence of the whole potential form on density distribution is taken into consideration, and density curves are obtained which show the finer curvature also. For $r \to \infty$ the density shows the exact exponential falling-off, but for $r \to 0$, the singularity of the centrifugal potential still results in a wrong asymptotical form. Therefore, a method has been developed which contains completely the centrifugal potential as follows:

In [9] from the density matrix

$$\varrho(\mathfrak{r}, \mathfrak{r}') = \sum_{\text{occ.}} \psi(\mathfrak{r})\psi^*(\mathfrak{r}') = \Theta\big(E_A - H(\mathfrak{r})\big) \quad \delta(\mathfrak{r}-\mathfrak{r}')$$

$$\int \mathrm{d}\mathfrak{r}\varrho(\mathfrak{r}) = A \qquad H = \frac{\mathfrak{p}^2}{2\,m} + V(r) \tag{1}$$

the density $\varrho(\mathfrak{r}) = \varrho(\mathfrak{r}, \mathfrak{r})$ in an external potential $V(r)$ is obtained for a system of A particles in this potential by suitable approximation for the derivations of the potential with regard to the evaluation of the Hamiltonian, H. In the one-dimensional case a standard density $\varrho_0(q)$ is obtained. This is the exact solution for a linearly increasing potential $V_0(x) = a\,|x|$ so that by a transformation $q(x)$ (I, 1.5) determined by the particularly interesting potential $V(x)$ the density can be calculated as follows:

$$\varrho(x) = \frac{|k(x)|}{q^{1/3}(x)}\,\varrho_0[q(x)]\,, \quad k(x) = \sqrt{\frac{2\,m}{\hbar^2}\,(E_A - V(x))}\,. \tag{2}$$

Consider now the radial density distribution $D^l(r)$ as well as the radial density matrix $D^l(r, r')$ for the angular momentum l (I, 1.6) and the occupied levels $n = 0.1 \ldots N_1$:

$$\varrho_l = \sum_{n=0}^{N_l} \psi_{nl}(\mathfrak{r})\, \psi^*_{nl}(\mathfrak{r}'),$$

$$D^l(r, r') \equiv \int d\Omega\, rr'\, \varrho_l(r, \zeta, \varphi\,; r', \zeta, \varphi),$$

$$D^l(r, r') = (2\,l + 1)\, \Theta(E_A - H_l)\, \delta(r - r'), \quad D^l(r) = D^l(r, r), \tag{3}$$

$$\int dr\, D^l(r) = (2\,l + 1)\,(N_l + 1), \quad H_l = -\frac{\hbar^2}{2\,m}\,\frac{d^2}{dr^2} + \frac{\hbar^2 l(l+1)}{2\,mr^2} + V(r).$$

Then, the centrifugal potential $\hbar^2 l(l + 1)/2mr^2$ occurs additionally which leads to the above mentioned errors. To correct these errors a potential $V_1(r)$ is sought for which the exact density $D^l_1(r)$ can be calculated in a closed form.

This may be practicable for the harmonic oscillator $V_1(r) \equiv V_{osc}(r) = m\omega^2 r^2/2$. The eigenfunctions contain Laguerre's polynominals $L_n^{(\alpha)}$

$$\psi_{nl}(\mathfrak{r}) = \sqrt{\frac{2\,\lambda^{l+3/2}}{\Gamma\left(l + \frac{3}{2}\right)\binom{n + l + 1/2}{n}}}\, r^l\, e^{-\lambda r^2/2}\, L_n^{(l+1/2)}(\lambda r^2) \times$$

$$\times \sqrt{\frac{2\,l + 1}{4\,\pi}\,\frac{(l - m)!}{(l + m)!}}\, P_l^m(\zeta)\, e^{im\varphi}, \tag{4}$$

where $\lambda = m\omega/\hbar$, and for the radial density matrix and the radial density of the harmonic oscillator, they lead to:

$$D^l_{osc}(r, r') = (2l+1) \sum_{n=0}^{N_l} \frac{2\,\lambda^{1/2}}{\Gamma(\alpha+1)\binom{n+\alpha}{n}}\, (yy')^{(l+1)/2}\, e^{-(y+y')/2}\, L_n^{(\alpha)}(y)\, L_n^{(\alpha)}(y') =$$

$$= (2l+1)\,\frac{2\lambda^{1/2}(N_l+1)}{\Gamma(\alpha+1)\binom{N_l+\alpha}{N_l}}\, (yy')^{(l+1)/2} e^{-(y+y')/2}\, \frac{L^{(\alpha)}_{N_l}(y)\, L^{(\alpha)}_{N_l+1}(y') - L^{(\alpha)}_{N_l+1}(y) L^{(\alpha)}_{N_l}(y')}{y - y'} \tag{5}$$

$$D^l_{osc}(r) = (2\,l+1)\,\frac{2\,\lambda^{1/2}(N_l+1)!}{(N_l+\alpha)!}\, y^{l+1} e^{-y} \left[L^{(\alpha)}_{N_l+1}(y)\,\frac{d}{dy}\, L^{(\alpha)}_{N_l}(y) - \right.$$

$$\left. - L^{(\alpha)}_{N_l}(y)\,\frac{d}{dy}\, L^{(\alpha)}_{N_l+1}(y) \right],$$

where $\alpha = l + 1/2$ and $y = \lambda r^2$.

By means of a transformation $q = q_{osc}(r)$ $r = q_{osc}^{-1}(q)$ from (5), a standard density $\varrho_{osc}(q)$

$$\varrho_{osc}(q) = \left(\frac{q_{osc}^{1/3}(r)}{|k_{osc}(r)|} D_{osc}^{l}(r) \right)_{r=q_{osc}^{-1}(q)} = \frac{q^{1/3} D_{osc}^{l}[q_{osc}^{-1}(q)]}{|k_{osc}[q_{osc}^{-1}(q)]|} \tag{6}$$

is obtained which in approximation (2) is equal to the standard density $\varrho_0(q)$. Consequently, for any potential $V(r)$ the radial density $D^l(r)$ can be calculated by means of two successive transformations $q_{osc}^{-1}(q)$ and $q(r)$, and

$$D^{l}(r) = \frac{|k(r)|}{q^{1/3}(r)} \varrho_{osc}[q(r)] = \frac{|k(r)| D_{osc}[q_{osc}^{-1}(q(r))]}{|k_{osc}[q_{osc}^{-1}(q(r))]|} \tag{7}$$

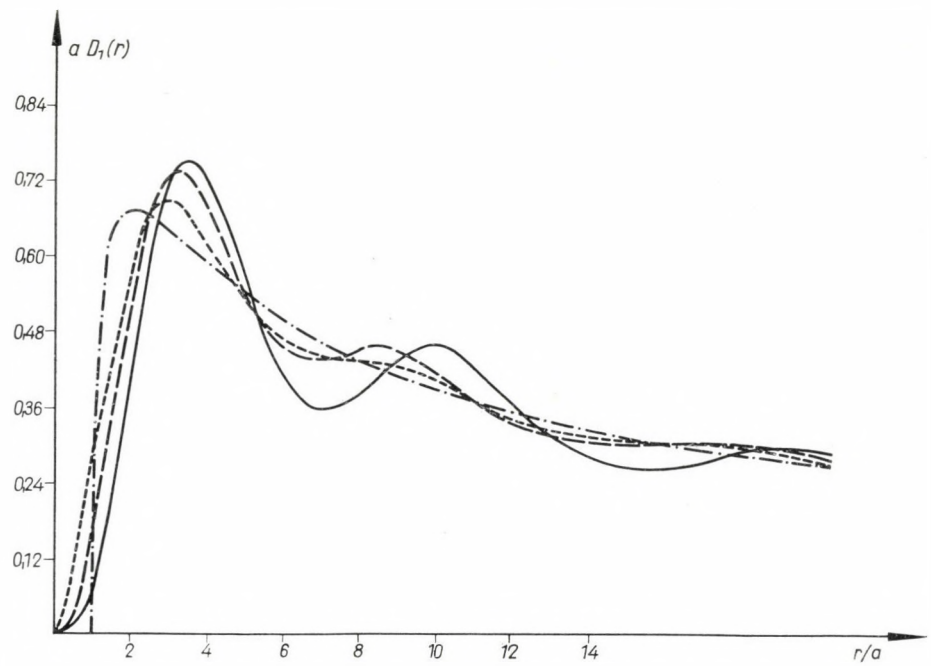

Fig. 1. The radial density distribution $D^l(r)$ for a Coulomb potential $V(r) = -Ze^2/r$ to angular momentum $l = 1$, the levels $n = 0$ to $n = 5$ being occupied ($a = \hbar^2/mZe^2$). Comparison of approximation (7) — — — with the exact solution ———, approximation (*I*) - - - - - - - -, and Thomas—Fermi approximation —.—.—.

is obtained in the same approximation (2), where the function $\varrho_{osc}(q)$ need not be determined. For $r \to 0$ the density computed in this way falls off with the correct power r^{2l+2} because with a small r the centrifugal potential forms the main part of the potential in H_l (3), consequently $q_{osc}(r) = q(r)$ and, therefore, $q_{osc}^{-1}[q(r)] = r$.

It is no disadvantage that owing to these two transformations the quantum mechanical approximation (the approximation concerning treatment of the derivations of $V(r)$ by the evaluation of the operators comprising the Hamiltonian) is done twice. As the total error is of the same size the errors may partially compensate one another. With $q(r) \equiv q_{osc}(r)$, the function D^l_{osc} (r) is obtained for $D^l(r)$, i. e. the exact solution.

Now, these considerations are applied to the Coulomb potential $V(r) = -Ze^2/r$. The Coulomb potential may be considered as a test for the quality of statistical approximation because owing to its singularity relatively large errors appear. On the other hand the Coulomb potential is one of the most interesting potentials. The Figure shows the density distribution for $18(Nl=5)$ particles without interaction to angular momentum $l = 1$ in the Coulomb potential. The HARTREE solution, the THOMAS-FERMI approximation and the approximation (I, 1.5) are compared with approximation (7), $D_{osc}(r)$ being the starting point. For $r \to 0$ the calculated density (7) has the correct falling-off, viz. r^4; it approaches the HARTREE solution more closely than the other approximations.

I am indebted to Prof. W. MACKE for helpful discussions, to Dr. DEMKOV of the University of Leningrad for reference to the representation of the harmonic oscillator density, and to Dipl.-Ing. A. SCHUBERT for the performance of numerical calculations.

REFERENCES

1. P. GOMBÁS, Die statistische Theorie des Atoms, Springer, Vienna, 1949.
2. S. GOLDEN, Phys. Rev., **107,** 1283, 1957.
3. D. A. KIRZHNITZ, J. Exp. Theor. Phys., Moscow, **32,** 115, 1957.
4. S. GOLDEN, Rev. Mod. Phys., **32,** 322, 1960.
5. L. ALFRED, Phys. Rev., **121,** 1275, 1961; **125,** 214, 1962.
6. G. A. BARAFF, Phys. Rev., **123,** 2087, 1961.
7. G. A. BARAFF and S. BOROWITZ, Phys. Rev., **121,** 1704, 1961.
8. M. J. STEPHEN and K. ZALEWSKI, Proc. Roy. Soc. *A* **270,** 435, 1962.
9. W. MACKE and P. RENNERT, Ann. Phys. (Leipzig) **12,** 84, 1963. (This paper is referred to as I.)
10. H. PAYNE, Phys. Rev., **132,** 2544, 1963.
11. N. L. BALAZS, Phys. Rev., **134,** A 841, 1964.
12. K. J. LE COUTEUR, Proc. Phys. Soc., **84,** 837, 1964.
13. P. HOHENBERG and W. KOHN, Phys. Rev., **136,** B 864, 1964.
14. H. PAYNE, J. Chem. Phys., **41,** 3650, 1964.
15. K. S. VISWANATHAN, and B. N. N. ACHAR, Can. J. Phys., **42,** 2332, 1964.
16. W. KOHN and L. J. SHAM, Phys. Rev., **137,** A 1697, 1965.

MÖSSBAUER EFFECT IN Tb^{159}

By

T. Czibók, I. Dézsi and L. Keszthelyi

CENTRAL RESEARCH INSTITUTE FOR PHYSICS, BUDAPEST

(Received 31. VIII. 1965)

The Mössbauer effect was studied on the 58 keV energy first excited state of Tb^{159} nucleus by Dézsi and Keszthelyi [1]. In this first work only the existence of the Mössbauer effect was stated. The aim of the present investigation was a more careful study of the effect.

The source was prepared by irradiating $Gd(NO_3)_3$ (enriched to 92% in Gd^{158}) in reactor, then by heating at 800°C to produce Gd_4O_7 policrystalline material. The half life of Gd^{159} is 18 hours [2] it decays in 24% to the 58 keV state of Tb^{159}. The absorber was 50 mg/cm^2 Tb^{159} in Tb_4O_7 compound. The source and absorber were at about −190°C temperature in the same cryostat cooled by liquid nitrogen.

The γ-spectrum measured by a krypton-filled proportional counter (Fig.1) is very complicated and the intensity of the 58 keV line is small because of the high internal conversion ($\alpha = 10{,}4 \pm 1$ [2]). The discriminator channel was set to the 58 keV peak.

The half life ot the 58 keV state was measured by Berlovich et al [3] to be $(1{,}4 \pm 0{,}3).\ 10^{-10}$ sec, but Meiling [4] found that $T/2 < 10^{-10}$ sec. In any case the line width is large and we had to reach large velocities (~10 cm/sec) in movement. Therefore the source was attached to the moving coil of a loudspeaker and was moved by sinusoidal voltage of different amplitudes. The counting rate was measured as a function of the amplitude. The calibration was made with the help of Fe^{57} Mössbauer effect. By such method the possible isomer shift causes an increased line width but taking into account the large line width this error may probably be neglected. The form of the line in the case of a Lorentz curve of width Γ is

$$I(B) \sim \frac{1}{B\Gamma\sqrt{1+\frac{\Gamma^2}{B^2}}},$$

where B is the amplitude of the sinusoidal voltage. The result of the measurment (corrected for background) is shown in Fig. 2. The fitting gives $\Gamma = (11{,}5 \pm \pm 0{,}6)$cm/sec. The maximum of the nuclear absorption is $(15 \pm 1)\%$. If we

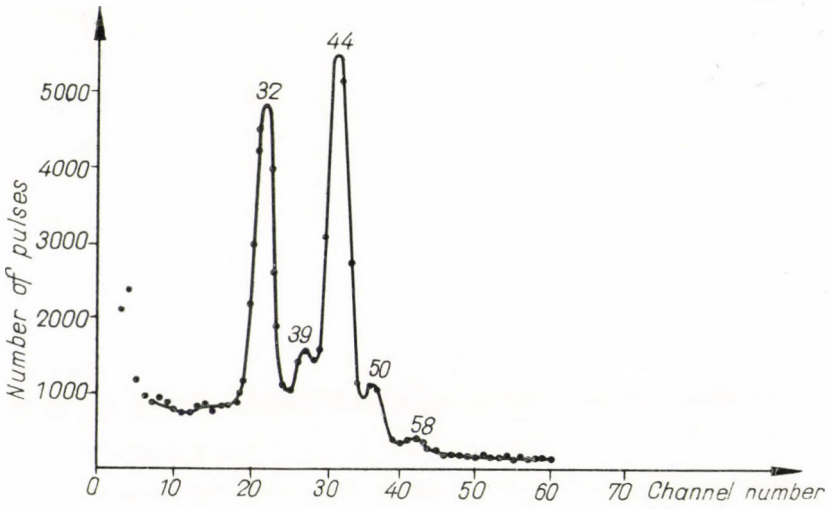

Fig. 1. γ-spectra measured by a krypton-filled proportional counter

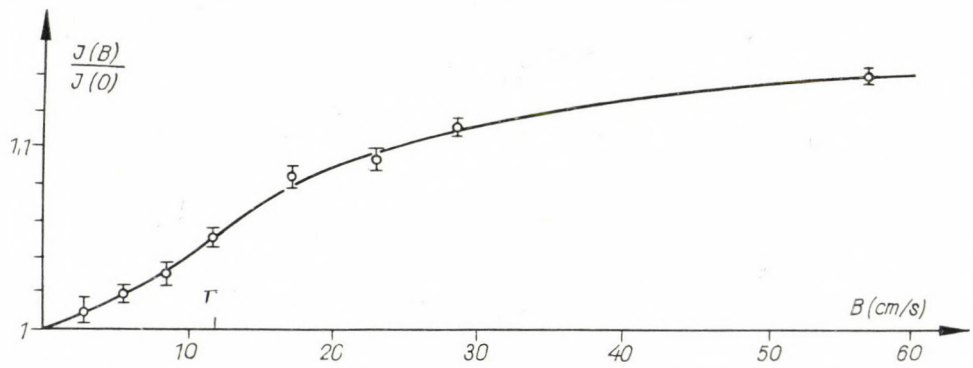

Fig. 2. Result of the absorption measurement

assume that the Debye-Waller factors of the source and the absorber are equal then $f(T) = f'(T) = 0{,}19 \pm 0{,}02$, the Debye-temperature $\Theta_D = (225 \pm \pm 10)°\mathrm{K}$ and the line width after correcting for finite thickness of absorber is $(7{,}7 \pm 0{,}9)$ cm/sec. This gives the lower limit for the half life of the 58 keV state of Tb^{159} as $\frac{T}{2} = (3 \pm 0{,}3).\ 10^{-11}$ sec. At this moment it is impossible to see if there is an isomer shift or some splitting of line both of which cause an apparent shorter life time.

We are indebted to Mr. B. MOLNÁR for producing the sources.

REFERENCES

1. И. Дежи и Л. Кестхели, Материялы Рабочего Совещания по Эффекту Мессвауеру, Дубна, 1963.
2. D. S. Dzelepow, L. K. Peker and V. O. Sergejev, Decay Schemes of Radioactive Nuclei, Academy of Sciences of the USSR Press, Moscow, Leningrad 1963.
3. Э. Е. Берлович, М. П. Бониц и М. К. Никитин, ЖЭТФ, 40, 749, 1961.
4. K. Meiling, private communication.

ON THE CURRENT CONSUMPTION OF THE AUXILIARY ELECTRODES OF DISCHARGES

By

J. Bitó

INDUSTRIAL RESEARCH INSTITUTE FOR TELECOMMUNICATION TECHNIQUE, BUDAPEST

(Received 31. VIII. 1965)

The power consumption of the nickel plates used as auxiliary electrodes was determined in a Hg—A discharge, under d.c. and a.c. conditions. The nickel plates used were radially movable, 1,0 mm thick, 7 mm wide and 12 mm long. They were arranged parallel to each other and to the electrode axes, and extended into the electrode space. The electrodes of the glass-walled discharge tube with an inner diameter of 36 mm were formed of tungsten spirals coated with an electronemitting substance, and of wholly uniform design. The spirals were spaced at 1090 mm. The discharge space contained argon at a pressure of 3 mm Hg, and about 50 mg of mercury. The latter ensured a vapour pressure of $6 \pm 0{,}5 \times 10^{-3}$ mm Hg during the measurements. For both the a.c. and d.c. tests a discharge current of 430 amps was applied, and the cathode was heated only by the discharge. The current of the auxiliary electrodes was measured with reference to the spiral ends.

The power consumption of the auxiliary electrodes extending into the cathode space during the d. c. measurements is shown in Fig. 1. In this case there was a constant distance of 17 mm between the auxiliary electrode I and the spiral. There was no current variation concomitant with the change of position or the current of the other auxiliary electrode moving on the opposite side of the spiral. To enable the current conditions to be followed more clearly only the curve for the auxiliarry electrode I has been plotted in Fig. 1. The subscript f for the cases i_I and i_{II} indicates the situation when the auxiliary electrode was tied to the spiral end nearer the cathode spot. For both auxiliary electrodes, in the given position, the current consumption was higher in this instance. As a matter of fact the potential of the spiral end next to the cathode spot was lower than that of the other end. Consequently, on account of this lower potential the auxiliary electrodes could attract a larger number of ions and, therefore, the current consumed by them was higher. At the same time it may be seen that for the given comparable situation, for a distance of 17 mm, there was an appreciable difference between the currents of the two auxiliary electrodes. According to complementary optical measurements, this was attributable to the asymmetric arrangement of the cathode spot. In the case

investigated here the cathode spot was arranged on the spiral surface asymmetrically to the spiral axis, and was shifted in the direction of the auxiliary electrode II. Consequently a corresponding change took place in the power consumption of the auxiliary electrodes. That is the electrode with the cathode

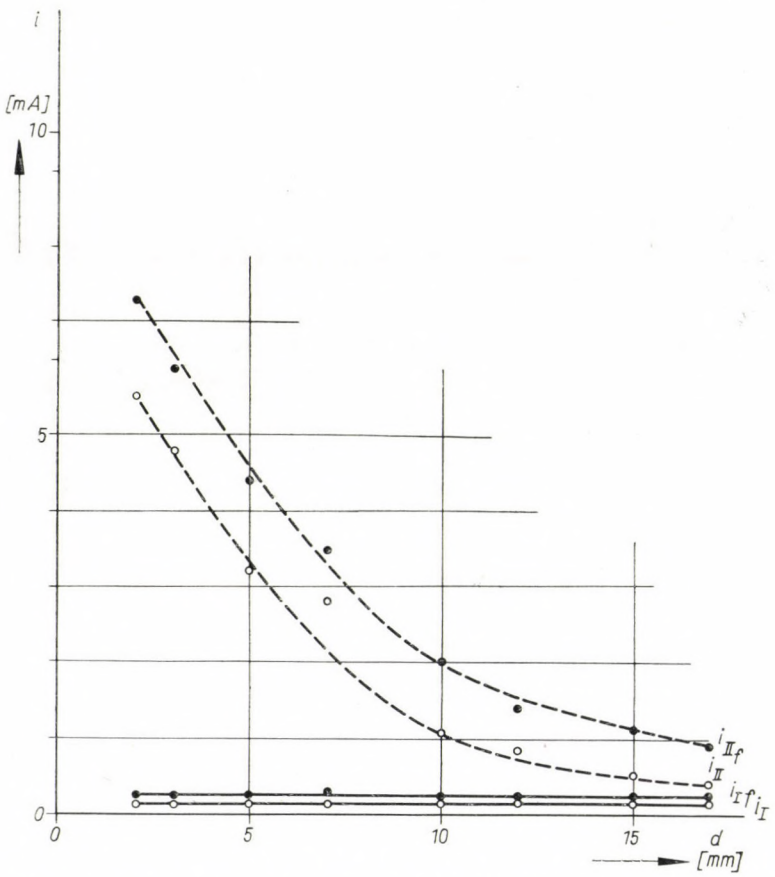

Fig. 1. Currents i_{II} and i_I, respectively, consumed by the auxiliary electrode II moving in the cathode space of the d. c. discharge and by the non-moving auxiliary electrode I, as a function of the distances measured from the axis of the cathode spiral. The subscript f denotes the auxiliary electrode connected to the spiral end next to the cathode spot, whereas the notation without subscript stands for the auxiliary electrode having the potential of the other spiral tip

spot and its accompanying range of a high concentration of charge carriers closer by, consumed more current, although otherwise in an identical geometrical position. Furthermore, the measurements disclose that irrespective of whether the two auxiliary electrodes were connected to the same spiral end, or to two different ends, the sum total of the current was, in all instances, smaller than the total of the currrents consumed by each electrode separately. For

reasons of greater convenience in the study of the plots this relation is not shown. However, when due consideration is given to the distribution of the specific superficial current densities, the effect noticed here can be very easily confirmed theoretically. From the trend of the curves it appears that on approaching the spiral, the current of the electrically coupled auxiliary electrodes tended to rise rapidly, but even so the electrodes did not modify the processes in the cathode space to any appreciable extent, as the power consumed by the electrodes was extremely small. Consequently their influence on the cathode drop was only slight [1]. Further results obtained in this connection [1] were in good agreement with the relations of the distances obtained and presented here.

Fig. 2 shows the current consumption of the auxiliary electrodes in a similar manner under d. c. conditions, but in this case for electrodes moving in the anode space. From the current values obtained here it is incontrovertibly evident that for all auxiliary electrode arrangements and connections the current density of the auxiliary electrodes was substantially greater here than was the case in the cathode space. Consequently the electrodes influenced the phenomena in the anode space to a greater extent than those in the cathode space. The notations used in Fig. 2 correspond to those in Fig. 1. What was striking was that, in this case, the current of the non-moving auxiliary electrode at 17 mm from the spiral end did not remain constant either when connected to the anode spot or to the other end of the anode, and with the approach of the auxiliary electrode II and the rise in its current, the current of the auxiliary electrode I also rose, although its position remained constant. Here, the auxiliary electrode II behaved with respect to the auxiliary electrode I, so to say, as a charge reflector, a phenomenon highly current-dependent. Apparently it was due to this property of electrode II that with cathodic interference, this phenomenon escaped observation owing to the extremely low currents consumed there. The basic effect may be traced to the modification of the anode glow space caused by the radially moving auxiliary electrode II.

The third set of curves in Fig. 2 has not yet been mentioned. They describe the overall currents. When these curves were plotted auxiliary electrode II was moving in the direction of the spiral, whereas auxiliary electrode I was at a distance of 17 mm from the spiral. Both electrodes were simultaneously electrically connected, alternately to the anode end close to the anode spot (position subscript f), and to the spiral end far from the anode spot (no subscript position) Even in this case the overall current consumed by the electrodes simultaneously and jointly was smaller than the sum total of the currents consumed by the electrodes *seriatim*.

Experiments with an alternating current of 50 c/s were conducted under similar conditons and with similar methods. Here the auxiliary electrodes extended into the space of a preferred electrode which alternately performed

the functions of the anode and the cathode. On the auxiliary electrodes approaching the spiral their previous constant current density began to increase at a distance of about 10 mm from the spiral. When the electrodes approached the spiral their alternating current consumption began to rise appreciably. However

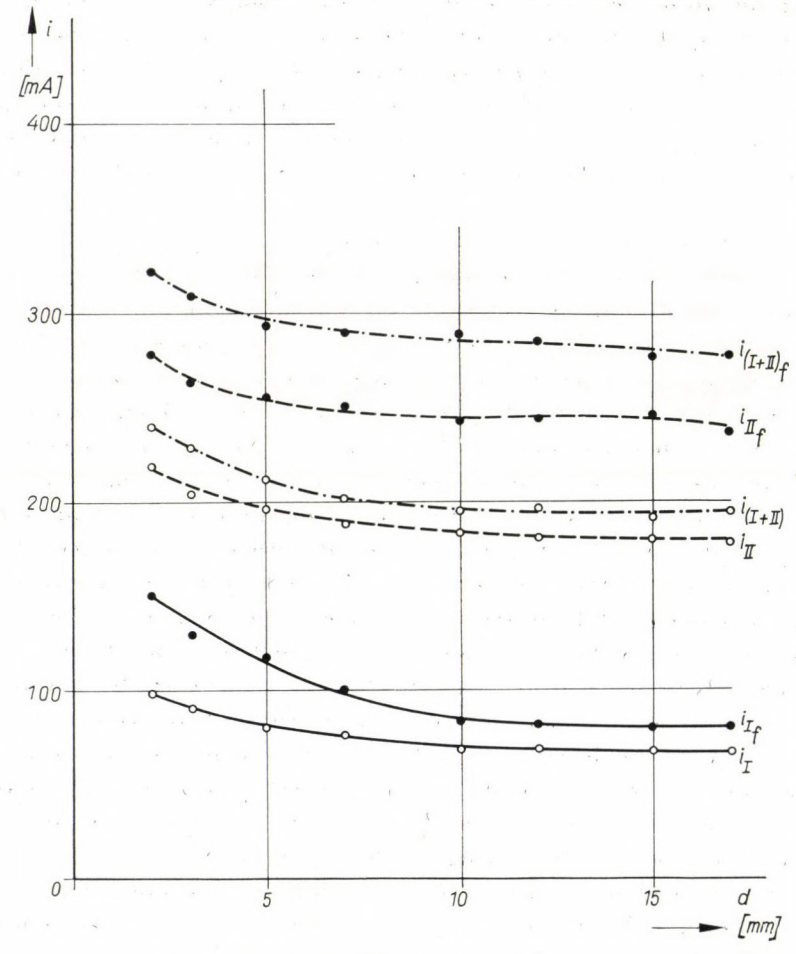

Fig. 2. Currents i_{II} and i_I, respectively, consumed by the auxiliary electrode II moving in the anode space of the d. c. discharge and the non-moving auxiliary electrode I, together with their total current $i_{(I+II)}$ referred to the spiral end close to the ande spot (with subscript f) and to the other spiral end (without subscript)

it fell short of that observed for d. c. plate interference. Even so, the value of the current consumption was by an order of magnitude in excess of that for d. c. cathode interference. In this case, too, the "reflector" effect was noticed. In fact, the current of the extension at rest also increased with that of the opposing moving extension. Furthermore, in this case, too, the sum total of the indivi-

dually consumed currents exceeded the total simultaneously consumed current. Since the shapes of the curves plotted for a. c. discharge tests conform essentially to those plotted for d. c. discharge tests, no separate diagrams have been drawn.

In conclusion, it can be stated that the spaces of the discharge electrodes can be changed appreciably by introducing auxiliary electrodes of appropriate arrangement into these spaces. In an earlier paper HINMAN and FOX [2] made it clear that the superficial dimensions of these auxiliary electrodes substantially affected the phenomena taking place round the electrodes. In addition to the observations made by these authors it is evident from the data presented here that even the arrangement of the auxiliary electrodes will effect the conditions round the electrodes appreciably. The auxiliary electrodes may abstract charge carriers from the environment of the main electrodes, and by this process influence the characteristics of the corresponding fields. In this way, the auxiliary electrodes will influence the anode and cathode fall, the temperature of the anode and cathode spots, and further, through these, the tube voltage of the discharge. From the plots presented it may be expected that under d. c. discharge conditions, the auxiliary electrodes will influence the phenomena round the anode to a greater extent than those in the cathode space.

LITERATURE

1. J. BITÓ, Lecture given at the 3rd Czechoslovak Conference on Electronic and Vacuum Physics, Prague, September, 1965.
2. D. D. HINMAN and R. S. FOX, Ill. Eng., **56,** 222, 1961.

MIGRATION OF ELECTRONIC EXCITATION ENERGY IN SOLUTIONS*

By

L. SZALAY and L. KOZMA

INSTITUTE OF EXPERIMENTAL PHYSICS, JÓZSEF ATTILA UNIVERSITY, SZEGED

(Received 28. IX. 1965)

The electronic excitation energy — as is well known — may be transferred over several molecular diameters from the excited molecules to the unexcited neighbours by means of radiationless processes. The quantitative treatment of the energy transfer leads to a characteristic distance[1] ([1], p. 176)

$$R_0 = \left(\frac{9\,\varkappa^2 \ln 10\, c^4 \tau}{128\,\pi^5\, n^4\, N'\, \tau_e} \int_0^\infty \varepsilon(\nu) f_q(\nu)\, \frac{d\nu}{\nu^4} \right)^{1/6}, \tag{1}$$

for which excitation transfer and spontaneous deactivation are of equal probability. Here ν is the frequency, $\varepsilon(\nu)$ the molar decadic extinction coefficient, $f_q(\nu)$ the quantum emission spectrum, $\varkappa^2$ an orientation factor ($=2/3$ for random directional distribution), $\tau/\tau_e = \eta_Q$ the absolute quantum yield of fluorescence, n the refractive index of the solvent, $N' = 6{,}02 \cdot 10^{20}$, $c = 3 \cdot 10^{10}$ cms^{-1}. Eq. (1) is valid for any thermal equilibrium distribution over the vibrational levels of both molecules, provided the spectra are taken at the corresponding temperature, but it is not valid when energy transfer occurs before thermal equilibrium is established. According to [2] an equilibrium would not be expected even in liquids when, due to strong interaction, the transfer is very rapid. In these cases, the transfer may take place directly from the vibrational level obtained by excitation and depends, therefore, on the exciting wavelength.

Though the interaction process between the excited solute and the solvent is generally supposed to take place in a very short period (in 10^{-13}—10^{-12}s) compared to the mean life time of the excited state (10^{-9} — 10^{-8}s) and the thermal equilibrium is expected to be practically established by the instant of emission, some recent investigations show the existence of a slow interaction process completed in about 10^{-8}s. This process results in a vibrational temperature of the excited solute higher than the bulk temperature of the solution. In

* Delivered at the 8th European Congress on Molecular Spectroscopy in Copenhagen, 1965.

[1] π^5 has to be taken as π^6, see [8].

proper systems this phenomenon is revealed in the dependence of the emission spectrum on the frequency of exciting light [3] or in an increased rotational depolarization of fluorescence [4]. For such systems eq. (1) does not hold because the absorption spectrum corresponds to a temperature lower than the vibrational temperature to which the emission spectrum belongs.

According to [5], and [6] respectively, the quantum emission spectrum may be given as

$$f_q(\nu) = \frac{8\pi\nu^2 \ln 10\, n^2(\nu)\,\eta_Q(\nu)\,\tau\varepsilon(\nu)}{N' c^2\,\eta_Q(\nu)_{\max}} \exp\left[-h(\nu-\nu_0)/kT\right], \qquad (2)$$

where $\eta_Q(\nu)$, $n(\nu)$, ν_0, T, h and k are the quantum yield, the refractive index, the frequency of pure electronic transition, the temperature, the Planck and Boltzmann constant, respectively. Eq. (2) has been found to be valid in a very wide sense for vapours, liquids and solids, in the majority of cases, however, only for temperatures $T^* > T$ obtained from the slope of the function $F(\nu) = 2 \ln \nu - \ln[f_q(\nu)/\varepsilon(\nu)] = h(\nu-\nu_0)/kT + \text{const.}$, giving a straight line in a considerable spectral region (even if the variation of $n(\nu)$ and $\eta_Q{}^{(\nu)}$ is neglected). Considering T^* as the vibrational temperature at which the emission occurs, substituting T^* for T in eq. (2) and introducing $f_q(\nu)$ from eq. (1) with $\tau/\tau_e = \eta_Q$, we have

$$R_{0,T}{}^* = \left\{5{,}07 \cdot 10^{-23}\, \frac{\tau}{n^2\,\eta_{Q,\max}} \int_0^\infty \left[\frac{\eta_Q(\nu)\,\varepsilon(\nu)}{\nu}\right]^2 \exp\left[-h(\nu-\nu_0)/kT^*\right]\right\}^{1/6}, \qquad (3)$$

which — provided $\varepsilon(\nu)$ has been taken at the proper temperature — yields the correct value of the critical distance for the temperature T^*. An acceptable approximate value of $R_{0\,T^*}$ might be given with $\varepsilon(\nu)$ measured at temperature T and for some cases with $\eta_Q(\nu) = 1$.

Our experiments have been carried out in luminescent systems under circumstances described in [7] and with the same methods. In Fig. 1 two examples are shown for the variation of spectra with the temperature. Table 1 exhibits the results for glycerol solutions. Eq. (1) and eq. (3) yield very similar results when taking the spectra at the proper temperatures (see upper and lower figures, respectively). Note that the differences are not large.

Table 2 shows the approximate values of R_{0,T^*} at different temperatures T for glycerol solutions. Decay times were taken from [1] (p. 155). As the frequency of radiationless transitions is given by $n_{AB} = R_0^6/\tau R^6$ (where R is the average distance of the fluorescent solute particles), the frequency of radiationless transitions decreases with the temperature in all cases investigated due to the decrease of R_{0,T^*} under constant concentration (neglecting a decrease

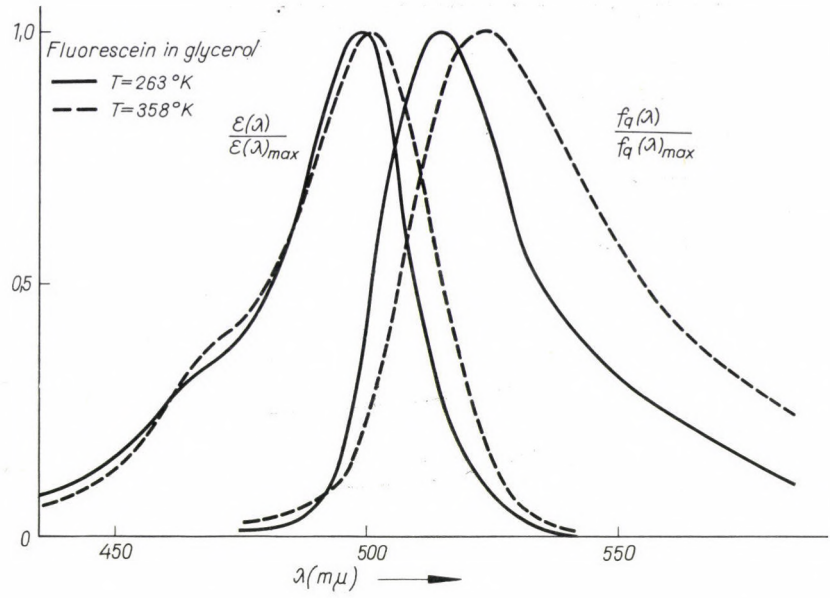
1,0
0,5
0
Fluorescein in glycerol
T=263 °K
T=358°K
ε(λ)/ε(λ)max
fq(λ)/fq(λ)max
450
500
550
λ(mμ)

Fig. 1a

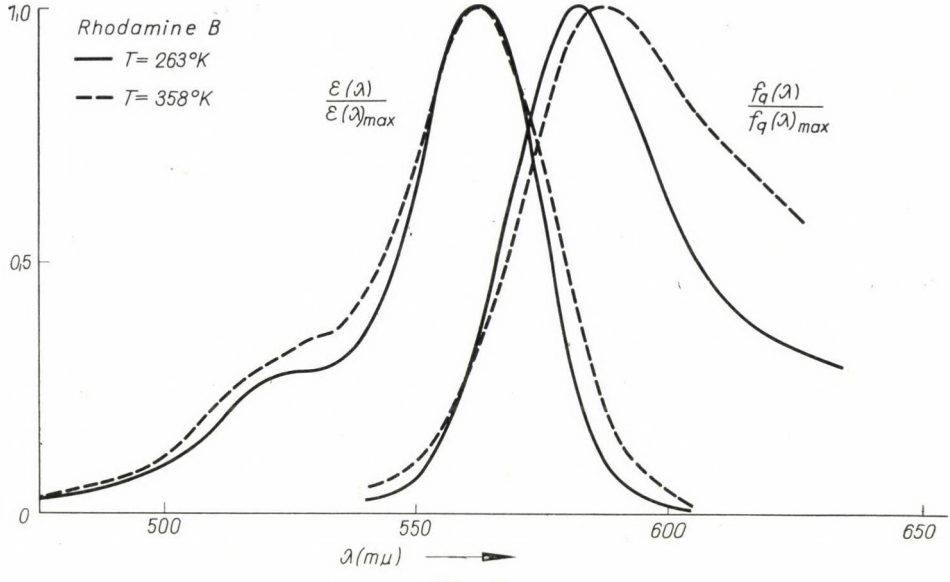
1,0
0,5
0
Rhodamine B
T= 263°K
T= 358°K
ε(λ)/ε(λ)max
fq(λ)/fq(λ)max
500
550
600
650
λ(mμ)

Fig. 1b

Table I

	T^* (°K)	R_0 (Å)	τ (*ns*)
Fluorescein	338	52,7 54,6	4,4
Trypaflavine	358	45,2 46,7	4,4
Rhodamine B	318	60,5 61,1	4,1

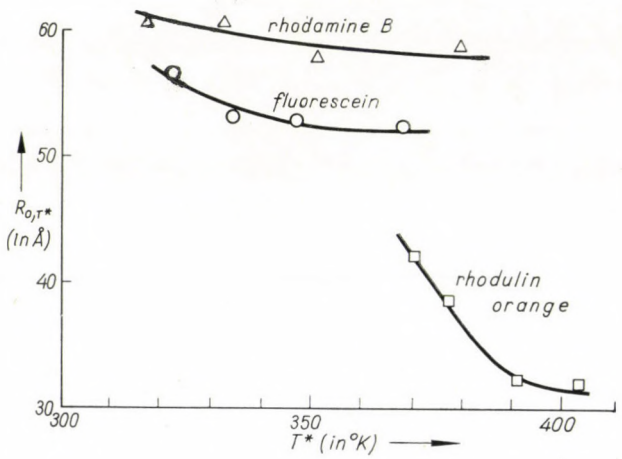

Fig. 2

TabIe II

Fluorescein	T^* (°K)	322	334	347	368
	R_0 (Å)	56,7	53,3	53,0	52,6
	τ (ns)	4,4	4,4	4,4	4,4
Rhodulin orange	T^* (°K)	370	377	391	403
	R_0 (Å)	42,2	38,8	32,4	32,2
	τ (ns)	4,3	3,7	3,0	2,0
Rhodamine B	T^* (°K)	317	332	351	379
	R_0 (Å)	60,8	60,8	58,0	58,8
	τ (ns)	4,2	4,2	4,1	3,5

of concentration of less than 5 per cent due to the thermal expansion which causes an increase of R less than 2 per cent in glycerol solutions). Fig. 2 shows the decrease of R_{0,T^*} with the vibrational temperature T^* (the actual temperatures T are somewhat smaller, but the general line of the variation of R_{0,T^*} with T is the same).

Similar results may be obtained if the variation of R_{0,T^*} with the frequency of exciting light is studied. In solutions of trypaflavine in glycerol where the quantum yield (and consequently very probably the decay time) is practically constant in the wavelength range of 436—375 $m\mu$, R_{0,T^*} may be given as the function of the wavelength of exciting light as follows: at 436, 455 and 475 mμ, R_{0,T^*} is 46,9, 47,6 and 49,2, respectively. The corresponding values of T^* are 361, 347 and 336°K (see [3] b), Table III).

As a final conclusion of our investigations we may state:

a) Eq. (3) seems to be useful for calculating the critical distance characteristic of energy migration in systems where the thermal equilibrium between solvent and solute molecules has not been established by the instant of emission.

b) The critical distance (except in some cases, e. g. rhodulin orange solution) is practically the same, independently of whether energy migration is completed before or after termal equilibrium between solute and solvent is established.

The authors are indebted to Prof. Dr. A. Budó, member of the Hungarian Academy of Sciences for most valuable discussions and advices during the work.

REFERENCES

1. Th. Förster: Fluoreszenz Organischer Verbindungen, Göttingen. Vandenhoeck und Ruprecht, 1951.
2. Th. Förster, Disc. Farad. Soc., **27,** 7, 1959.
3. *a)* A. Kawski, Bull. Acad. Polon., **11,** 567, 1963.
   b) L. Kozma, L. Szalay and J. Hevesi, Acta Phys. et Chem. Szeged, **10,** 67, 1964.
4. A. Jablonski, Acta Phys. Polon., **26,** 427, 1964.
   E. Lisicki, Bull. Acad. Polon., **11,** 665, 1963.
5. B. I. Stepanov, Izv. Akad. Nauk. USSR, **112,** 839, 1957.
6. B. S. Neporent, Izv. Akad. Nauk. USSR, **22,** 1372, 1958; Dokl. Akad. Nauk. USSR, **119,** 682, 1958.
7. J. Hevesi and L. Kozma, Acta Phys. Hung., **20,** 451, 1966.
8. I. Ketskeméty, Z. Naturforschg., **17***a*, 666, 1962.

RECENSIONES

RICHARD J. WEISS:

Solid State Physics for Metallurgists

Pergamon Press, Oxford, 1963, 410 pages, 84s.

The book appeared as the 6th Volume of the International Series of Monographs on Metal Physics and Physical Metallurgy. It is concerned mainly with problems of interest to engineers and experimental physicists working in solid state research, metallurgy or related fields.

The author approaches the subject from the experimental point of view giving only a short summary of the theoretical foundations in the first four chapters of the book, approximately a hundred pages. This first part entitled Theory outlines the most essential results of the theory of the atom (Chapter I) and the binding of molecules and the cohesion of solids (Chapter II). Chapter III entitled Temperature and Pressure gives some insight into the mechanical and thermal properties of crystals, while Chapter IV briefly reviews some facts connected with nuclei. This first part of the book is intended primarily for reference, as the author notes, to enable the student to orientate himself for studying this material.

The second part entitled Experiment consists of eight chapters (Chapters V—XII) covering almost three times as many pages as the first part. In an introductory chapter (Chapter V, Experimental Techniques) the author deals with some general problems related to the experimental techniques used normally in solid state physics. This is followed by a fairly thorough description of many important diffraction experiments and techniques in Chapter VI, including X-ray, neutron and electron diffraction equipment as well as the methods of use of these techniques and the results obtained. Chapter VII reports on the spectroscopy of solids. The remaining five chapters are devoted to some of the most common basic aspects of solid state research. Chapter VIII summarizes the experiments and experimental methods used in the investigation of transport properties of the solid. Chapter IX deals with the experimental procedures required for the investigation of the thermal behaviour of the solid. Chapters X and XI are concerned with the experimental methods of magnetic and nuclear measurements. Chapter XII outlines some aspects of problems in the synthesis of the various experimental results.

Three Appendices containing thermodynamic table (I), nuclear tables (II) and some references, constants and conversion factors, etc. (III) are given.

The book is written in a clear style. Every chapter includes problems which are, in many cases, very illuminating. The special attitude of the authors in approaching the subject from the experimental side may be of value for those seeking a medium sized summary of the experimental techniques used in everyday work in solid state research.

Edited by Pergamon Press, the book reflects the usual high standard.

J. ANTAL

Signal Detection and Recognition by Human Observers

arranged and edited by *John A. Swets* ; John Wiley and Sons, Inc., New York—London—Sydney, 1964, 702 + XI pages.

About a hundred years ago G. T. FECHNER, in his *Elemente der Psychophysik* (1860), by his famous law relating thresholds focussed attention on problems in psychophysics, problems in signal detection and recognition increasingly approached vital realistic decision problems. In spite of the importance of modern detection theory applied to human observers, until now there has been a lack of a comprehensive textbook in this field. The present book tries to build a bridge over this broad field of various sciences, until such a textbook becomes

available. This book consists of thirty three collected articles by the most prominent authorities on visual and auridoty detection, recognition, sensory physiology, auditory frequency analysis, vigilance, memory and speech communication fields.

Nowadays, even in the tendency towards complete automation, practical reasons suggest that a complex process is most valuable in which, among the automata, the human servo also plays some role. In this regard, the most objective treatment possible of the behaviour of a human observer is very important in order to find those characteristics which are useful in plamning a complex system involving man. This book indicates a giant step in this direction.

The first four articles discuss elementary notions and the basic experiments both on visual and auditory phenomena, discuss the necessity of reforming FECHNER's notion of the threshold, and show the interdependence of statistical decision theory and human observation.

The next four articles relate the parameters of a measurement to some operating characteristics in visual and auditory observations.

The next seven articles discuss observation in the presence of noise, and in some respects expand the old notion of threshold.

Three articles then follow in which the physiological applications for the sensory systems are discussed.

An important point is emphasized in the next four articles. The role of recognition is discussed. The authors develop clearly that a hungary man is much more likely to see food as fata morgana than a well-fed man. In this sens the mechanism of subjective evaluation is placed under the microscope of objective investigation.

The next seven articles discuss the interrelation between frequency analysis, noise, and masking effects, primarily in relation to auditory signals.

The last four articles deal with special applications to speech communication, articulation, vocabulary size and related subjects.

An appendix with tabulated material and another tih a comprehensive bibliography on the application of detenction theory in psychophysics widens the value of this pioneering book.

This well edited book deserves to be studied not only by psychologists, physiologists and biophysicists, but also by engineers, cyberneticians and scientists in other fields who have to include human sensory organs in their system design.

T. A. HOFFMANN

Printed in Hungary

A kiadásért felel az Akadémiai Kiadó igazgatója Műszaki szerkesztő: Farkas Sándor

A kézirat nyomdába érkezett: 1966. I. 19 — Terjedelem: 8,25 (A/5) ív, 37 ábra, 1 melléklet

66.61846 Akadémiai Nyomda, Budapest — Felelős vezető: Bernát György

INDEX

COMMUNICATIONES BREVES

RECENSIONES

PERIODICAL PUBLICATIONS

OF THE INSTITUTE OF PHYSICS AND THE PHYSICAL SOCIETY

Proceedings of the Physical Society

A monthly publication containing papers describing original work in basic physics

£8 *per volume*
3 *volumes in* 1966

Reports on Progress in Physics

An annual publication containing comprehensive reviews

£6 (1965)

British Journal of Applied Physics

A monthly publication containing papers describing new applications of physics and physical principles

£12 *per annum*

Journal of Scientific Instruments

A monthly publication dealing with physical instruments, instrumental and general experimental techniques developed in the course of research work in pure or applied physics

£8 *per annum*

The above publications (UNESCO coupons can be accepted) are available from:

The Institute of Physics and The Physical Society,
47 Belgrave Square, London S.W.1.

The *Acta Physica* publish papers on physics, in English, German, French and Russian.

The *Acta Physica* appear in parts of varying size, making up volumes.

Manuscripts should be addressed to:

Acta Physica, Budapest 502, Postafiók 24.

Correspondence with the editors and publishers should be sent to the same address.

The rate of subscription to the *Acta Physica* is 110 forints a volume. Orders may be placed with "Kultúra" Foreign Trade Company for Books and Newspapers (Budapest I., Fő u. 32. Account No. 43-790-057-181) or with representatives abroad.

Les *Acta Physica* paraissent en français, allemand, anglais et russe et publient de travaux du domaine de la physique.

Les *Acta Physica* sont publiés sous forme de fascicules qui seront réunis en volumes.

On est prié d'envoyer les manuscrits destinés à la rédaction à l'adresse suivante:

Acta Physica, Budapest 502, Postafiók 24.

Toute correspondance doit être envoyée à cette même adresse.

Le prix de l'abonnement est de 110 forints par volume.

On peut s'abonner à l'Entreprise du Commerce Extérieur de Livres et Journaux «Kultúra» (Budapest I., Fő u. 32. — Compte-courant No. 43-790-057-181) ou à l'étranger chez tous les représentants ou dépositaires.

«*Acta Physica*» публикуют трактаты из области физических наук на русском, немецком, английском и французском языках.

«*Acta Physica*» выходят отдельными выпусками разного объема. Несколько выпусков составляют один том.

Предназначенные для публикации рукописи следует направлять по адресу:

Acta Physica, Budapest 502, Postafiók 24.

По этому же адресу направлять всякую корреспонденцию для редакции и администрации.

Подписная цена «*Acta Physica*» — 110 форинтов за том. Заказы принимает предприятие по внешней торговле книг и газет «*Kultúra*» (Budapest I., Fő u. 32. Текущий счет: № 43-790-057-181) или его заграничные представительства и уполномоченные.

24,— Ft

All the reviews of the Hungarian Academy of Sciences may be obtained among others from the following bookshops:

ALBANIA

Ndermarja Shtetnore e Botimeve
Tirana

AUSTRALIA

A. Keesing
Box 4886, GPO
Sidney

AUSTRIA

Globus Buchvertrieb
Salzgries 16
Wien I

BELGIUM

Office International de Libraire
30, Avenue Marnix
Bruxelles 5
Du Monde Entier
5, Place St. Jean
Bruxelles

BULGARIA

Raznoiznos
1Tzar Assen
Sofia

CANADA

Pannonia Books
2 Spadina Road
Toronto 4, Ont.

CHINA

Waiwen Shudian
Peking
P. O. B. Nr. 88.

CZECHOSLOVAKIA

Artia A. G.
Ve Smeckách 30
Praha II.
Postova Novinova Sluzba
Dovoz tisku
Vinohradska 46
Praha 2
Postova Novinova Sluzba
Dovoz tlace
Leningradska 14
Bratislava

DENMARK

Ejnar Munksgaard
Nörregade 6
Kopenhagen

FINLAND

Akateeminen Kirjakauppa
Keskuskatu 2
Helsinki

FRANCE

Office International de Documentation et Librairie
48, rue Gay Lussac
Paris 5

GERMAN DEMOCRATIC REPUBLIC

Deutscher Buch-Export und Import
Leninstraße 16.
Leipzig C. 1.
Zeitungsvertriebsamt
Clara Zetkin Straße 62.
Berlin N. W.

GERMAN FEDERAL REPUBLIC

Kunst und Wissen
Erich Bieber
Postfach 46
7 Stuttgart S.

GREAT BRITAIN

Collet's' Subscription Dept.
44—45 Museum Street
London W. C. 1.
Robert Maxwell and Co. Ltd.
Waynflete Bldg. The Plain
Oxford

HOLLAND

Swetz and Zeitlinger
Keizersgracht 471—487
Amsterdam C.
Martinus Nijhof
Lange Voorhout 9
The Hague

INDIA

Current Technical Literature
Co. Private Ltd.
Head Office:
India House OPP.
GPO Post Box 1374
Bombay I

ITALY

Santo Vanasia
71 Via M. Macchi
Milano
Libreria Commissionaria Sansoni
Via La Marmora 45
Firenze

JAPAN

Nauka Ltd.
2 Kanada-Zimbocho 2-chome
Chiyoda-ku
Tokyo
Maruzen and Co. Ltd.
P. O. Box 605
Tokyo
Far Eastern Booksellers
Kanada P. O. Box 72
Tokyo

KOREA

Chulpanmul
Korejskoje Obschestvo po Exportu i Importu Proizvedenij Pechati
Phenjan

NORWAY

Johan Grundt Tanum
Karl Johansgatan 43
Oslo

POLAND

Export und Import Unternehmen RUCH
ul. Wilcza 46.
Warszawa

ROUMANIA

Cartimex
Str. Aristide Briand 14—18.
Bucuresti

SOVIET UNION

Mezhdunarodnaja Kniga
Moscow
G—200

SWEDEN

Almquist and Wiksell
Gamla Brogatan 26
Stockholm

USA

Stechert Hafner Inc.
31 East 10th Street
New York 3 N. Y.
Walter J. Johnson
111 Fifth Avenue
New York 3. N. Y.

VIETNAM

Xunhasaba
Service d'Export et d'Import des Livres et Périodiques
19, Tran Quoc Toan
Hanoi

YUGOSLAVIA

Forum
Vojvode Misica broj 1.
Novi Sad
Jugoslovenska Kniga
Terazije 27.
Beograd